Reaktivität und Selektivität anellierter, verbrückter und tertiärer Sauerstoff-Radikale

---

Vom Fachbereich Chemie der Universität Kaiserslautern

zur Verleihung des akademischen Grades

„Doktor der Naturwissenschaften“

genehmigte Dissertation

D386

Tag der wissenschaftlichen Aussprache: 10.07.2015

Prüfungsvorsitzender: Prof. Dr. Markus Gerhards

Erstgutachter und Betreuer: Prof. Dr.-Ing. Jens Hartung

Zweitgutachter: Prof. Dr. Stefan Kubik

vorgelegt von

Diplom-Chemikerin **Christine Schur**

Kaiserslautern 2015

Für meine Eltern,

meine drei coolen Schwestern

und natürlich meinen Schatz!!!

Die vorliegende Arbeit wurde in der Zeit von Februar 2009 bis Mai 2015 im Fachbereich Chemie (Organische Chemie) der Technischen Universität Kaiserslautern durchgeführt.

Herrn Prof. Dr.-Ing. Jens Hartung danke ich, neben der Aufnahme in seinen Arbeitskreis, für die Bereitstellung meines Promotionsthemas.

Für das Zweitgutachten danke ich Prof. Dr. Stefan Kubik und für den Vorsitz der Prüfungskommission Prof. Dr. Markus Gerhards.

Dr. Harald Kelm danke ich für die bereitwillige Übernahme der Protokollführung.

Prüfungskommission:

Vorsitzender: Prof. Dr. Markus Gerhards

Erstgutachter: Prof. Dr.-Ing. Jens Hartung

Zweitgutachter: Prof. Dr. Stefan Kubik

Die Ergebnisse der vorliegenden Dissertation wurden in den folgenden begutachteten Arbeiten veröffentlicht oder sind zur Veröffentlichung vorgesehen.

Kapitel 1 und 2

[1] *Efficiency of alkoxyl radical product formation from 5-substituted 3-alkoxy-4-methylthiazole-2(3H)-thiones*. Jens Hartung, Christine Schur, Irina Kempter, Thomas Gottwald, *Tetrahedron* **2010**, *66*, 1365–1374.

[2] *Discussion Addendum for: N-Hydroxy-4-(p-chlorphenyl)thiazole-2(3H)-thione*. Christine Schur, Irina Kempter, Jens Hartung, *Organic Syntheses* **2012**, *89*, 409–419.

Kapitel 3

[3] *Annulated and Bridged Tetrahydrofurans from Alkenoxyl Radical Cyclization.* Christine Schur, Harald Kelm, Thomas Gottwald, Arne Ludwig, Rainer Kneuer, Jens Hartung, *Organic & Biomolecular Chemistry* **2014**, *12*, 8288–8307.

Kapitel 4

[4] *Tertiary Alkoxyl Radicals from 3-Alkoxythiazole-2(3H)-thiones.* Christine Schur, Nina Becker, Uwe Bergsträßer, Thomas Gottwald, Jens Hartung, *Tetrahedron* **2011**, *67*, 2338–2347.

Kapitel 5

[5] *Heterocyclic O-(tert*-Butyl) *Thiohydroxamates*. Christine Schur, Manuel Zimmer, Harald Kelm, Markus Gerhards, Jens Hartung, *Manuskript in Vorbereitung.*

Eidesstattliche Erklärung

Hiermit erkläre ich ehrenwörtlich, dass ich die vorliegende Arbeit selbständig angefertigt und keine anderen als die angegebenen Quellen und Hilfsmittel benutzt habe.

Ich erkläre außerdem, dass diese Dissertation weder in gleicher noch in ähnlicher Form bereits in einem anderen Prüfungsverfahren vorgelegen hat und ich, außer den mit dem Zulassungsgesuch urkundlich vorgelegten Graden, keine weiteren akademischen Grade erworben habe oder zu erwerben versucht habe.

Kaiserslautern, den 19.05.2015

_____

Christine Schur

Erläuterungen

Die vorliegende Arbeit besteht aus einer Zusammenfassung, einer Einleitung (Kapitel 1), einem Kenntnisstand mit Aufgabenstellung (Kapitel 2), drei voneinander unabhängigen Ergebnisteilen (Kapitel 3−5), sowie einem Anhang. Forschungsartikel sind jedem Kapitel als Unterpunkt beigefügt, wobei dazugehörige Zusatzinformationen (*Supporting Information*), wie experimentelle Daten, Methoden, verwendete Arbeits- und Messgeräte im Anhang zu finden sind. Für jedes Kapitel wurde ein separates Literaturverzeichnis erstellt, wobei mehrfach zitierte Referenzen in jedem Kapitel neu berücksichtigt wurden.

Abbildungen, Tabellen und Schemata sind im jeweiligen Kapitel fortlaufend nummeriert. Die Nummerierung der Strukturformeln in den Ergebnisteilen beginnt stets neu und stimmt nicht zwingend mit der Nummerierung in den Forschungsartikeln überein. Strukturformeln mit Keilschreibweise bezeichnen, wenn nicht anders angegeben, relative und nicht absolute Konfigurationen.

Die Hierarchie von Substituenten zur Benennung von Verbindungen folgt in einigen Fällen nicht der IUPAC-Hierarchie, falls inhaltliche Zusammenhänge innerhalb homologer Reihen durch alternative Molekülnamen didaktisch einfacher nachvollziehbar werden.

Inhaltsverzeichnis

Zusammenfassung

In der vorliegenden Arbeit wurde die Reaktivität und Selektivität anellierter, verbrückter und tertiärer *O*-Radikale, in drei Teilprojekten, untersucht. Die zur Erzeugung primärer und sekundärer *O*-Radikale benötigten Thiohydroxamsäure-*O*-ester stammen aus Reaktionen von Cyclopentenyltosylaten mit 3-Hydroxy-4-methylthiazol-2(3*H*)-thion-Tetraethylammoniumsalz (Salz-Methode). Für tertiäre Thiohydroxamsäure-*O*-ester hat sich die Umsetzung tertiärer *O*-Alkylisoharnstoffe mit 3-Hydroxy-4-methylthiazol-2(3*H*)-thionen bewährt (Isoharnstoff-Methode). Die anschließende Freisetzung der *O*-Radikale, aus den *O*-Alkylthiohydroxamaten, erfolgte photochemisch oder thermisch unter pH-neutralen und nicht oxidativen Bedingungen in Gegenwart von Bromtrichlormethan. Relative Reaktivitäten der *O*-Radikale in Sauerstoff-Elementarreaktionen beruhen auf Abschätzungen mit Hilfe unimolekularer Vergleichsreaktionen (*Radikaluhr Konzept*). Beobachtete Selektivitäten und Stabilitäten wurden anhand theoretischer Analyseverfahren (Twist-Modell, Dichtefunktional-Rechnungen und Møller-Plesset-Störungsrechnung 2. Ordnung), in Kooperation mit Jens Hartung, interpretiert und quantifiziert. Die synthetisierten β-bromierten, bicyclischen, tricyclischen sowie tertiären Tetrahydrofurane erweitern die bis dato auf primäre und sekundäre Monocyclen beschränkte Vielfalt der 5-Ring-Strukturen über Sauerstoff-Radikalreaktionen. Beispiele für Synthesen mittels intermolekularer *O*-Radikaladditionen liefern funktionalisierte Bromalkoxybicyclo[2.2.1]heptane und *tert*-Butoxybromalkane.

Durch Variation (1,2-Cyclopentyl und 1,2-Cyclohexyl) und Permutation (Kohlenstoff-Atome C1 und C2 / C2 und C3 / C3 und C4) der Anellierung, sowie durch verbrückte Reste (C2 und C5 / C3 und C5) am 4-Penten-1-oxyl-Gerüst gelang es, im ersten Teilprojekt, diastereomerenreine primäre und sekundäre *O*-Radikalvorläufer für eine systematische Untersuchung der Stereoselektivität in 5-*exo*-*trig*-Reaktionen zu synthetisieren. Umsetzungen der *O*-Radikalvorläufer zeigten Regelmäßigkeiten im Produktbild, die in Form von Richtlinien für zukünftige Syntheseplanungen zusammengefasst wurden: *(I)* Für sterisch und elektronisch vergleichbare Substituenten in direkter Nachbarschaft (zum Beispiel C1 und C2) ist der stereochemische Einfluss des Substituenten größer, der der Doppelbindung näher ist (hier Substituent an C2). Die relative Konfiguration der beiden anellierten Substituenten zueinander wirkt sich auf den Stereoselektivitätsgrad aus, wobei *trans*-anellierte 4-Penten-1-oxyl-Radikale stereoselektiver cyclisieren als *cis*-konfigurierte Isomere. Hauptprodukte der 1,2- und 2,3-cyclohexyl-anellierten 4-Penten-1-oxyl-Radikale sind 2,4-*cis*- und 2,3-*trans*-

substituierte Tetrahydrofurane. (*II*) Ist die Flexibilität der Sauerstoffatom-tragenden Seitenkette konformell eingeschränkt, cyclisieren anellierte (C3 und C4) sowie verbrückte (C2 und C5 / C3 und C5) 4-Penten-1-oxyl-Radikale 2,3- und 2,4-*cis*-spezifisch an *endo*- und *exo*-cyclische π-Bindungen. Theoretische Berechnungen diesbezüglich haben gezeigt, dass der 2,3-*trans*-Ringschluss des Modell-Radikals 1-(Cyclohexen-3-yl)-2-ethoxylradikal aufgrund sterischer Effekte eine deutlich höhere Barriere besitzt (89.5 kJ/mol) als der 2,3-*cis*-Ringschluss (35.4 kJ/mol).

Die Herstellung tertiärer 3-Alkyloxy- und 3-Cumyloxy-5-(4-methoxyphenyl)thiazol-2(3*H*)-thione und die Untersuchung der Reaktivitäten daraus erzeugter tertiärer *O*-Radikale in Elementarreaktionen waren Schwerpunkte des zweiten Themengebiets. Experimentell bestimmte relative Geschwindigkeitskonstanten für die δ-H-Abstraktion ($k^{\text{Subst}} = 10^7–10^8\ \text{s}^{-1}$), die 5-*exo*-*trig*-Cyclisierung ($k^{5\text{-}exo} = 10^8–10^9\ \text{s}^{-1}$) und die intermolekulare Addition ($k^{\text{Add}} = 10^7\ \text{M}^{-1}\text{s}^{-1}$) demonstrieren, dass tertiäre *O*-Radikale trotz größerer sterischer Hinderung eine ähnliche (Substitution) oder höhere Reaktivität (5-*exo*-Reaktion) als vergleichbare primäre und sekundäre Analoga aufweisen. Der 5-*exo*-Rinschluss des 2-Phenyl-5-hexen-2-oxyl-Radikals erfolgt 2,5-*cis*-selektiv. Intermolekulare Additionen der *tert*-Butoxyl-, Cumyloxyl- oder *p*-Chlorcumyloxyl-Radikale an Norbornen verlaufen *exo*-spezifisch. Dichtefunktional Berechnungen zufolge sind Torsionsspannungen im 2,5-*trans*-Übergangszustand der 5-*exo*-*trig*-Cyclisierung und im *endo*-Übergangszustand der intermolekularen Addition für die beobachtete Selektivität verantwortlich.

Im dritten Projekt wurden *O*-(*tert*-Butyl)thiohydroxamate aus *O*-(*tert*-Butyl)-*N*,*N*-diisopropylisoharnstoff und dem 3-Hydroxy-4-methylthiazol-2(3*H*)-thion sowie dem 3-Hydroxy-4-methyl-5-(4-nitrophenyl)thiazol-2(3*H*)-thion hergestellt. Die gleiche Reaktion zeigt bei Verwendung des 1-Hydroxypyridin-2(1*H*)-thions eine spontane Umlagerung des *O*-(*tert*-Butyl)thiohydroxamats zum *O*-(*tert*-Butyl)pyridin-2-sulfenat. Stabilitätsunterschiede der tertiären Thiohydroxamat-Klassen lassen sich der Molekülorbital-Theorie folgend auf drei unterschiedliche, π-artige Wechselwirkungen der N,O-Bindung mit dem Thiohydroxamat-Kern und dem *O*-Alkyl-Rest im Grundzustand zurückführen, die die N,O-Bindung insgesamt stärken. Tertiäre 3-Alkoxythiazolthione erfahren dabei eine größere Stabilisierung als vergleichbare Pyridinthione. Photochemische Umsetzungen der *tert*-Butoxythiazolthione liefern *tert*-Butoxyl-Radikale, die durch Addition an 5,5-Dimethylpyrrolidin *N*-Oxid (DMPO) und Styrol nachgewiesen wurden.

1. Einleitung

1.1 Struktur und Reaktivität sauerstoffzentrierter Radikale

Als reaktive Zwischenstufen[1] organischer Synthesen weisen Sauerstoff-Radikale eine zwei bis drei Größenordnungen höhere Reaktivität auf als vergleichbare Kohlenstoff-Radikale.[2,3] In atmosphärischen[4,5] und biochemischen Prozessen[6–9] spielen *O*-Radikale eine wichtige Rolle bei Abbaureaktionen und zur Knüpfung von C,O-Bindungen.[10–12] Außergewöhnlich hohe Selektivitäten bei Additionen an Mehrfachbindungen[10,13–15], H-Abstraktionen[16–17], β-C,C-Fragmentierungen[18–19] oder Umlagerungsreaktionen[20–21] tragen dazu bei, dass *O*-Radikalreaktionen zunehmend an Bedeutung gewinnen. Mechanistische Untersuchungen der vergangenen Jahre haben gezeigt, dass die Reaktivität und Selektivität von Sauerstoff-Radikalen maßgeblich durch den Substituenten R beeinflusst wird (Abb. 1.1).[22]

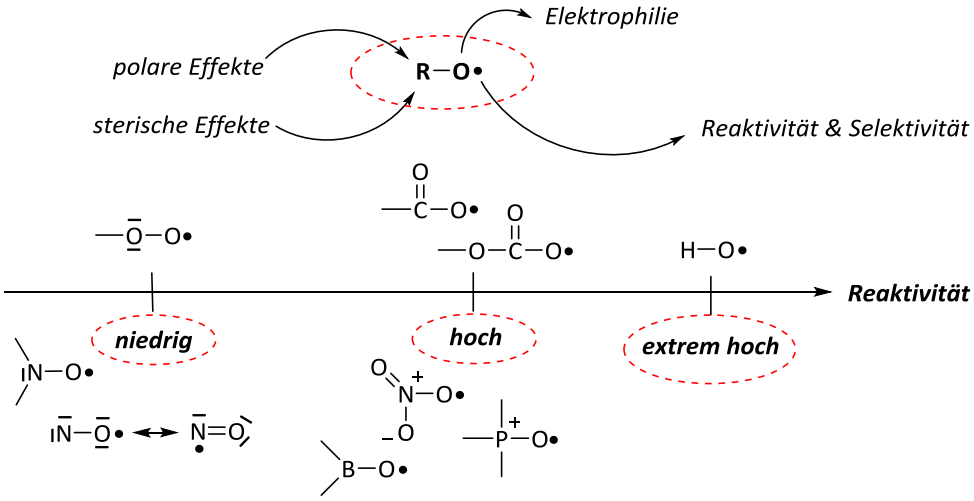

Abbildung 1.1. Struktur und Reaktivität sauerstoffzentrierter Radikale.[22]

Sauerstoff-Radikalreaktionen sind im Allgemeinen stark exotherme Prozesse mit hohen Aktivierungsenergien für Rückreaktionen. Additionen, H-Abstraktionen und Umlagerungen verlaufen kinetisch kontrolliert unter Bildung starker C,O- bzw. O,H-Bindungen. Für Fragmentierungen ist die Energiedifferenz der Aktivierungsbarrieren zwischen Hin- und Rückreaktion deutlich kleiner. Rückreaktionen werden experimentell dennoch selten beobachtet, da der anschließende Radikaleinfang durch Wasserstoffatom- oder Halogenatom-Donoren meist deutlich schneller erfolgt (Schema 1.1).[22]

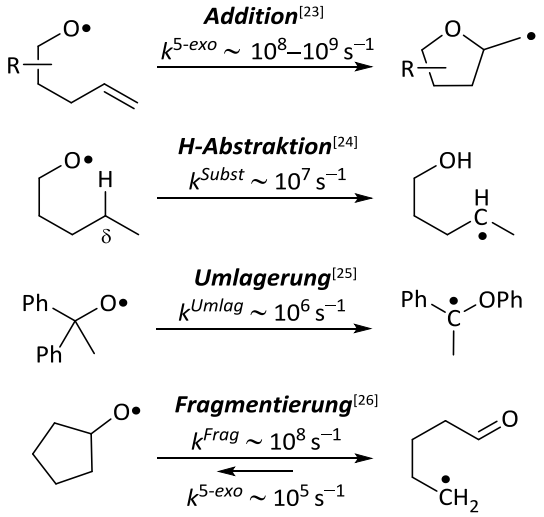

Schema 1.1. Elementarreaktionen sauerstoffzentrierter Radikale mit charakteristischen Geschwindigkeitskonstanten. R = H, Alkyl, Aryl.[23–26]

Die hohe Reaktivität und die ausgeprägte thermochemische Triebkraft von Sauerstoff-Radikalen bildet sich dem Hammond-Postulat[27] folgend in der Position von Übergangszuständen auf den dazugehörigen Reaktionskoordinaten ab. Geometrien früher Übergangszustände ähneln dabei strukturell den Startmaterialien, so dass deren Grenzorbitale zur Beschreibung von Reaktivitäten und Selektivitäten herangezogen werden können.[28,29,30] Günstige Wechselwirkungen ergeben sich dabei zwischen dem höchsten besetzten Orbital (HOMO, *engl*. Highest Occupied Molecular Orbital) eines nukleophilen oder dem tiefsten unbesetzten Orbital (LUMO, *engl*. Lowest Unoccupied Molecular Orbital) eines elektrophilen Reaktionspartners mit dem einfach besetzten Orbital (SOMO, *engl.* Singly Occupied Molecular Orbital) des *O*-Radikals. Je ähnlicher die Energien der wechselwirkenden Grenzorbitale sind, desto stärker ist nach dem Klopman-Theorem die Stabilisierung des Ensembles. In den meisten Reaktionen zeigen *O*-Radikale überwiegend elektrophile Reaktivität, das heißt die SOMO/HOMO-Wechselwirkung ist effektiver als die SOMO/LUMO-Wechselwirkung (Abb. 1.2, rechts). Bei Additionen an Alkene, die mit starken Akzeptorgruppen substituiert sind, reagieren Sauerstoff-Radikale aber auch als Nukleophile. In diesem Fall dominiert die SOMO/LUMO-Wechselwirkung gegenüber der SOMO/HOMO-Wechselwirkung (Abb. 1.2, links).[31]

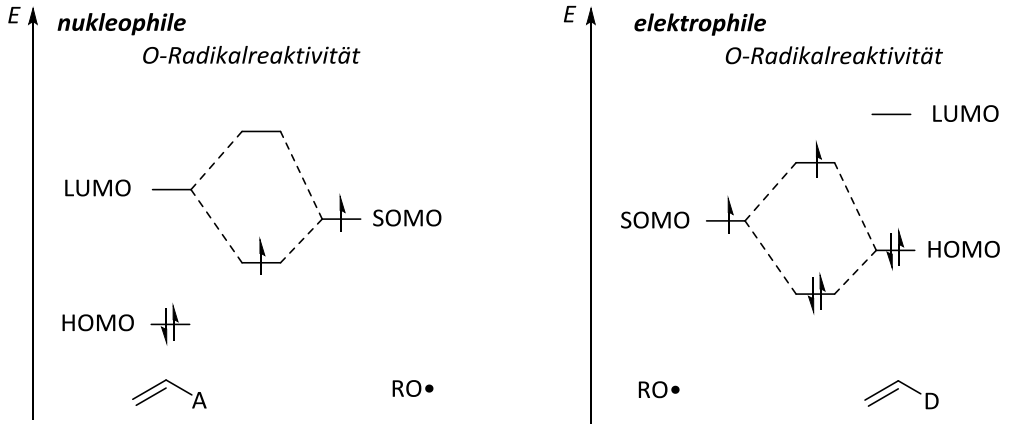

Abbildung 1.2. Grenzorbitalwechselwirkungen eines Akzeptor-substituierten Alkens (A = CO_2Me, CN) mit einem nukleophilen *O*-Radikal (RO•, links) und eines Donor-substituierten Alkens (D = OCH_3, CH_3, Ph) mit einem elektrophilen *O*-Radikal (RO•, rechts). R = Alkyl, Aryl.[31]

1.2 Stereo- und Regioselektivitäten substituierter 4-Penten-1-oxyl-Radikale

Im Verlauf der letzten 20 Jahre zeichneten sich deutliche synthetische Fortschritte bei intramolekularen *O*-Radikaladditionen ab. 4-Penten-1-oxyl-Radikalcyclisierungen stellen in diesem Zusammenhang die wichtigste Gruppe dar.[10,15,22–24,32,33] Die in diesen Reaktionen entstehenden Tetrahydrofuranylmethyl-Radikale lassen sich mit Wasserstoff- oder Halogenatomen zu präparativ nützlichen Syntheseprodukten abfangen (Schema 1.2).[24,34–36] Aufgrund elektrophiler Eigenschaften der Alkoxyl-Radikale in Additionen an terminale oder Donor-substituierte π-Bindungen verlaufen *O*-Radikaladditionen häufig mit komplementärer Stereo- und Regioselektivität, im Vergleich zu Elektrophil-induzierten, ionischen 4-Pentenol-cyclisierungen (nukleophiles Sauerstoffatom).[35,37,38] Der präparative Wert der *O*-Radikal-cyclisierungen leitet sich, neben interessanten Chemoselektivitäten, aus vorhersagbaren Stereoselektivitäten ab.[24,32] Alkyl- und *ortho*-Methyl-substituierte Arylsubstituenten in Position 1 sowie Alkyl- und Arylsubstituenten in Position 3 dirigieren die 5-*exo*-*trig* Reaktion 2,5-*trans*-selektiv, während Alkyl- und Arylsubstituenten in Position 2 Produkte mit *cis*-Konfiguration favorisieren. Annähernd äquivalente *cis*/*trans*-Mischungen resultieren aus der Umsetzung von 4-Penten-1-oxyl-Radikalen mit *para*- oder unsubstituierten Phenylresten in Position 1.[39] Der stereochemische Einfluss von Steuergruppen in 5-*exo*-*trig*-Reaktionen steigt mit sinkendem Abstand zur π-Bindung. Terminale Methylgruppen beschleunigen durch einen polaren Effekt den Angriff eines elektrophilen *O*-Radikals und üben für Alkyl-

und Arylsubstituenten in den Positionen 1 und 3 einen Diastereoselektivität-steigernden Effekt aus (Schema 1.2).[24,32,36]

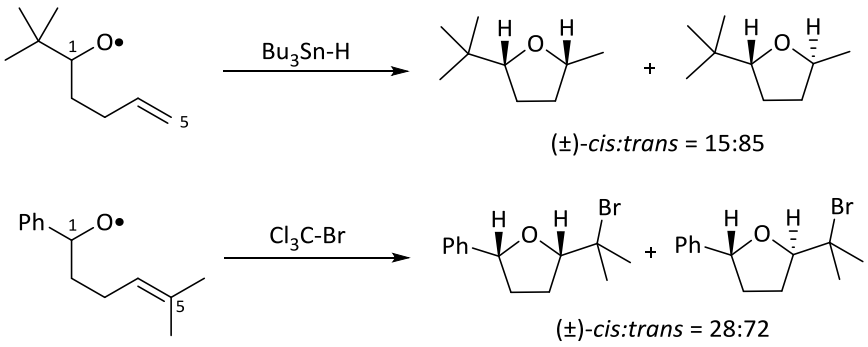

Schema 1.2. Diastereoselektivitäten bei der intramolekularen 5-*exo*-Addition substituierter 4-Penten-1-oxyl-Radikale in Gegenwart von Bu_3SnH (oben) und $BrCCl_3$ (unten).[24, 35]

Die beobachteten Selektivitäten lassen sich mit einem stereochemischen Modell (Twist-Modell, Schema 1.3)[40] beschreiben. Es wurde mit dem Ziel entwickelt, Stereoselektivitäten experimentell nicht durchgeführter Reaktionen in Syntheseplanungen vorherzusagen. Dem Twist-Modell zufolge greift das Sauerstoff-Radikal aus stereoelektronischen Gründen die π-Bindung orthogonal zur Alkenebene an. Die Vinyl-Gruppe und das Kohlenstoff-Atom C3 nehmen aus sterischen Gründen bevorzugt entgegengesetzte Positionen entlang der Ebene ein, die von den Atomen O1, C5 und C4 definiert wird. Substituenten im konformell flexiblen Teil sind, aufgrund sterischer Effekte (Torsionsspannungen), vorzugsweise äquatorial (C2, C3) oder *pseudo*-äquatorial (C4) angeordnet. Die Bildung von cis/trans-Isomeren resultiert aus einer 180°-Rotation der terminalen Vinyl-Gruppe um die C4-C5-Bindung.

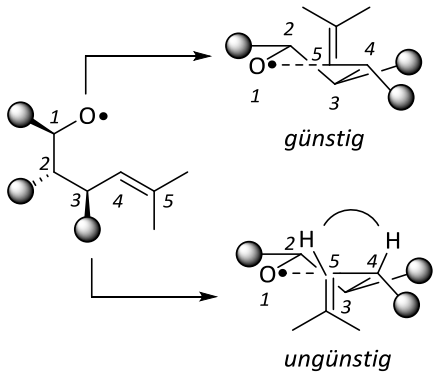

Schema 1.3. Twist-Modell-Übergangsstrukturen zur Beschreibung von Stereoselektivitäten in 5-*exo*-Cyclisierungen substituierter 4-Penten-1-oxyl-Radikale.[40] Kugeln = Alkyl, Aryl.

4-Penten-1-oxyl-Radikalcyclisierungen verlaufen nicht nur stereoselektiv, sondern weisen zudem eine ausgeprägte Regioselektivität auf.[24,41] Radikale, die in Position 4 der 4-Penten-1-oxyl-Radikalkette ein Wasserstoffatom tragen, liefern ein charakteristisches 98:2-Verhältnis an 5-*exo* und 6-*endo*-Cyclisierungsprodukten. Entlang der Reihe der Substituenten Wasserstoff, Methyl, *tert*-Butyl und Phenyl in Position 4 steigt der Anteil an 6-*endo*-Cyclisierungsprodukt auf 7:93 (Abb. 1.3). Regioselektivitätsänderungen basieren auf einer Balance zwischen Grenzorbitalwechselwirkungen und Torsionsspannungen im Übergangszustand.[41]

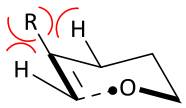

Abbildung 1.3. 6-*endo*-*trig*-Übergangsstruktur substituierter 4-Penten-1-oxyl-Radikale. R = H, Methyl (*exo*:*endo* = 69:31), *tert*-Butyl (*exo*:*endo* = 46:54), Phenyl (*exo*:*endo* = 7:93).[41]

Mit der sich entwickelnden Vielfalt der bisher untersuchten 5-*exo*-Reaktionen ist die Zeit gekommen, Synthesen komplexerer Tetrahydrofuran-Naturstoffe, die aus substituierten Monocyclen oder aus Bi- und Tricyclen bestehen, durch Ringschlussreaktionen tertiärer und anellierter 4-Penten-1-oxyl-Radikale aufzubauen (Abb. 1.4). Dabei wäre zu hinterfragen, inwieweit stereochemische Richtlinien für die Synthese von Monocyclen (Twist-Modell) auf die Darstellung anspruchsvollerer Molekülstrukturen übertragen werden können und ob tertiäre 4-Penten-1-oxyl-Radikale überhaupt für derartige Synthesezwecke eingesetzt werden können. Mit diesen Fragestellungen beschäftigt sich die vorliegende Dissertation.

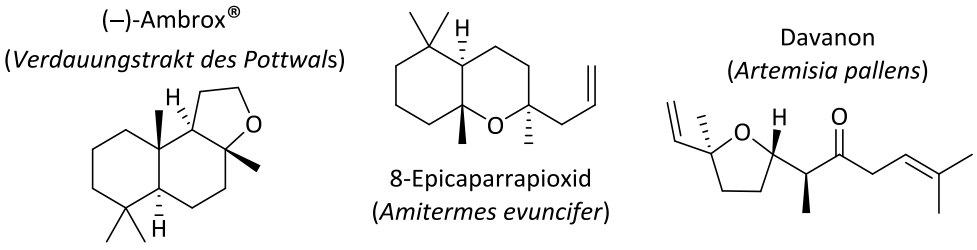

Abbildung 1.4. Tetrahydrofuran- und Tetrahydropyran-abgeleitete Naturstoffe mit tertiären Ether- und polycyclischen Grundgerüsten.[42–46]

1.3 Literaturverzeichnis

[1] P. Gray, A. Williams, *Chem. Rev*. **1959**, *59*, 239–328.

[2] D. P. Curran, *Synthesis* **1988**, 417–439 und 489–513.

[3] C. P. Jasperse, D. P. Curran, T. L. Fevig, *Chem Rev*. **1991**, *91*, 1237–1286.

[4] R. Atkinson, J. Arey, *Chem. Rev.* **2003**, *103*, 4605–4638.

[5] R. Atkinson, *Atmos. Environ*. **2007**, *41*, 8468–8485.

[6] D. J. Betteridge, *Metabolism* **2000**, *49*, 3–7.

[7] E. Niki, *Free Radical Biol. Med.* **2014**, *66*, 3–12.

[8] B. Halliwell, J. M. C. Gutteridge, Free Radicals in Biology and Medicine, 3rd ed., Oxford University Press: Oxford **1999**.

[9] M. Möller, W. Adam, S. Marquardt, C. R. Saha-Möller, H. Stopper, *Free Radical Biol. Med.* **2005**, *39*, 473–482.

[10] M. Rueda-Becerril, J. C. T. Leung, C. R. Dunbar, G. M. Sammis, *J. Org. Chem*. **2011**, *76*, 7720–7729.

[11] M. Bietti, A. Calcagni, D. O. Cicero, R. Martella, M. Salamone, *Tetrahedron Lett*. **2010**, *51*, 4129–4131.

[12] I. Kempter, B. Frensch, T. Kopf, R. Kluge, R. Csuk, I. Svoboda, H. Fuess, J. Hartung, *Tetrahedron* **2014**, *70*, 1918–1927.

[13] J.-M. Surzur, M.-P. Bertrand, R. Nougier, *Tetrahedron Lett*. **1969**, 4197–4200.

[14] J. Hartung in *Radicals in Organic Synthesis*; P. Renaud, M. P. Sibi, Eds.; Wiley-VCH-Weinheim, **2001**, Vol. 2, Kapitel 5.2, 427–439.

[15] M. Zlotorzynska, H. Zhai, G. M. Sammis, *Org. Lett*. **2008**, *10*, 5083–5086.

[16] Z. Čeković, *J. Serb. Chem. Soc*. **2005**, *70*, 287–318.

[17] M. Salamone, R. Amorati, S. Menichetti, C. Viglianisi, M. Bietti, *J. Org. Chem*. **2014**, *79*, 6196–6205.

[18] E. Suárez, M. S. Rodriguez in *Radicals in Organic Synthesis*; P. Renaud, M. P. Sibi, Eds.; Wiley-VCH, Weinheim, **2001**, Vol. 2, Kapitel 5.3, 440–454.

[19] D. Hernández-Guerra, M. S. Rodriguez, E. Suárez, Eur. *J. Org. Chem.* **2014**, 5033–5055.

[20] H. Wieland, *Chem. Ber.* **1911**, *44*, 2550–2556.

[21] A. Studer, M. Bossart, *Tetrahedron* **2001**, *57*, 9649–9667.

[22] J. Hartung, T. Gottwald, K. Špehar, *Synthesis* **2002**, *11*, 1469–1498.

[23] A. L. J. Beckwith, B. P. Hay, *J. Am. Chem. Soc.* **1989**, *111*, 230–234.

[24] J. Hartung, F. Gallou, *J. Org. Chem*. **1995**, *60*, 6706–6716.

[25] J. H. Horner, S. Y. Choi, M. Newcomb, *Org. Lett.* **2000**, *2*, 3369–3372.

[26] J. T. Banks, J. C. Scaiano, *J. Phys. Chem*. **1995**, *99*, 3527–3531.

[27] G. S. Hammond, *J. Am. Chem. Soc.* **1955**, *77*, 334–338.

[28] I. Flemming in *Grenzorbitale und Reaktionen organsicher Verbindungen,* Wiley-VCH-Weinheim, **1979**.

[29] B. Giese, J. He, W. Mehl, *Chem. Ber.* **1988**, *121*, 2063–2066.

[30] K. Heberger, H. Fischer, *Int. J. Chem. Kin.* **1993**, *25*, 249–263.

[31] I. Kempter, A. Groß, J. Hartung, *Tetrahedron* **2012**, *68*, 10378–10390.

[32] J. Hartung, *Eur. J. Org. Chem.* **2001**, 619–632.

[33] H. Zhu, J. G. Wickenden, N. E. Campbell, J. C. T. Leung, K. M. Johnson, G. M. Sammis, *Org. Lett.* **2009**, *11*, 2019–2022.

[34] J. Hartung, R. Kneuer, *Eur. J. Org. Chem.* **2000**, 1677–1683.

[35] J. Hartung, R. Kneuer, S. Laug, P. Schmidt, K. Špehar, I. Svoboda, H. Fuess, *Eur. J. Org. Chem.* **2003**, 4033–4052.

[36] J. Hartung R. Kneuer, T. M. Kopf, P. Schmidt, *C. R. Acad. Sci. Paris, Chimie/Chemistry,* **2001**, 649–666.

[37] T. Gottwald, M. Greb, J. Hartung, *Synlett* **2004**, *1*, 65–68.

[38] J. Hartung, R. Kneuer, *Tetrahedron: Asymmetry* **2003**, *14*, 3019–3031.

[39] J. Hartung, M. Hiller, P. Schmidt, *Liebigs. Ann*. **1996**, 1425–1436

[40] J. Hartung, K. Daniel, C. Rummey, G. Bringmann, *Org. Biomol. Chem*. **2006**, *4*, 4089–4100.

[41] J. Hartung, R. Kneuer, C. Rummey, G. Bringmann, *J. Am. Chem. Soc*. **2004**, *126*, 12121–12129.

[42] *Ambrox:* M. Stoll, M. Hinder, *Helv. Chim. Acta*, **1950**, *33*, 1251–1261.

[43] *Ambrox*: J. M. Castro, S. Salido, J. Altarejos, M. Nogueras, A. Sanchez, *Tetrahedron* **2002**, *58*, 5941–5949.

[44] *Caparrapioxid*: M. Uyanik, K. Ishihara, H. Yamamoto, *Bioorg. Med. Chem*. **2005**, *13*, 5055–5065.

[45] *Davanon*: L. N. Misra, A. Chandra, R. S. Thakur, *Phytochemistry* **1991**, *30*, 549–552.

[46] *Davanon*: H. Jork, M. Nachtrab, *Arch. Pharm.* (Weinheim) **1979**, *312*, 435–445.

2. Kenntnisstand und Aufgabenstellung

2.1 Erzeugung von *O*-Radikalen

Sauerstoff-Radikale entstehen durch homolytische Spaltung schwacher Bindungen, die aus einem Sauerstoff- und einem Heteroatom wie beispielsweise Chlor, Stickstoff, Sauerstoff oder Schwefel bestehen (Abb. 2.1).[1–17] Mechanistische und synthetische Studien profitieren dabei von pH-neutralen, nicht oxidativen Bedingungen zur Sauerstoff-Radikalerzeugung, da so unerwünschte Produkte aus Oxidationsprozessen ausbleiben. Für die anschließende *O*-Radikalreaktion sind unverzweigte Kettenreaktionen vorteilhaft, da diese es erlauben, stationäre und niedrige Radikalkonzentrationen aufrecht zu erhalten, in denen Radikal-Molekülreaktionen über Radikal-Radikalreaktionen dominieren (Schema 2.1).[18,19] Nach dem Quasistationaritätsprinzip von M. Bodenstein[20,21] liegen solche Bedingungen dann vor, wenn eine reaktive Zwischenstufe langsam gebildet und schnell umgesetzt wird, was sich experimentell durch einen Überschuss an Radikalabfangreagenzien realisieren lässt. In verzweigten Kettenreaktionen nimmt die Radikalkonzentration bei Umsetzung eines Stoffes stetig zu, so dass in der Regel große Mengen unerwünschter Nebenprodukte gebildet werden.[18,19]

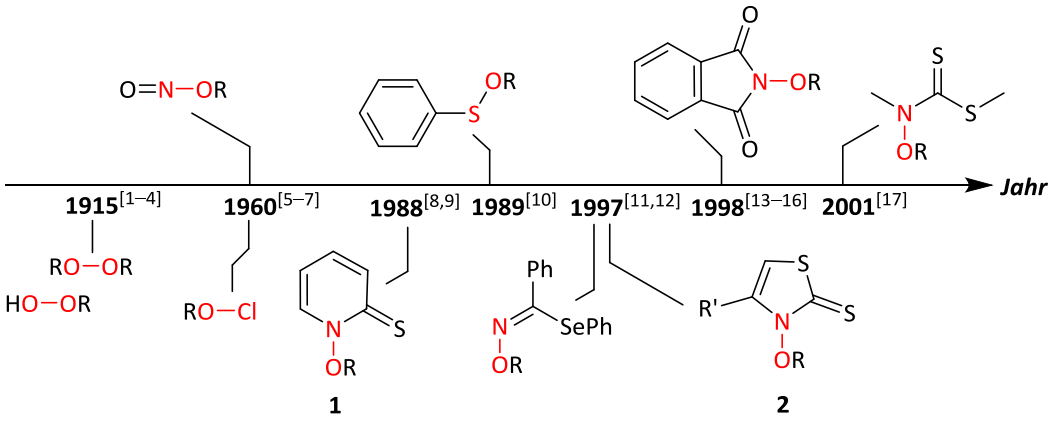

Abbildung 2.1. Auswahl sauerstoffzentrierter Radikalvorläufer des letzten Jahrhunderts. R = R'= Alkyl, Aryl. [1–17]

Die Technik zur Erzeugung von *O*-Radikalen mit Hilfe unverzweigter Kettenreaktionen stammt aus den Jahren 1988–1997 (Abb. 2.1), in denen die cyclischen Thiohydroxamsäureester **1** und **2** für diese Zwecke entwickelt wurden. Mechanistisch entstehen *O*-Radikale (RO•) aus *O*-Alkylthiohydroxamaten durch homolytische Spaltung der schwachen N,O-Bindung. Ursache des N,O-Bindungsbruchs ist der Angriff des kettentragenden Radikals Y• am

Thiocarbonylschwefel (Schema 2.1). Das Radikal Y• stammt aus einem Mediator X–Y und wird photochemisch (25 °C) ohne Radikalstarter oder thermisch (80 °C), unter Zuhilfenahme von Initiatormolekülen wie Azobis(isobutyronitril) (AIBN), erzeugt. Aus den Sauerstoff-Radikalen (RO•) entstehen, den Elementarreaktionen folgend, stabilere Kohlenstoff-Radikale (R•), die durch den Mediator X–Y unter Bildung des kettentragenden Radikals Y• abgefangen werden. Für die Kettenfortsetzung ist entscheidend, dass Y• schneller an den Thiocarbonyl-schwefel addiert als jedes andere an der Reaktion beteiligte Radikal. Geringe Radikal-konzentrationen (< 0.01 M) verhindern einen vorzeitigen Kettenabbruch durch Dispropor-tionierung oder Rekombination.[22,23]

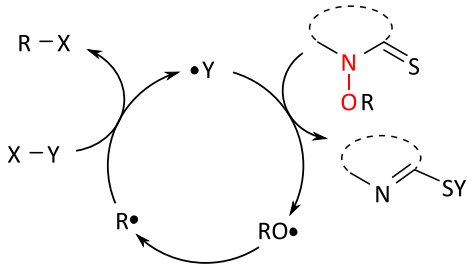

Schema 2.1. Unverzweigte Kettenreaktion Thiohydroxamat-abgeleiteter *O*-Radikale. X–Y = $BrCCl_3$, CCl_4, IC_4F_9, Bu_3SnH, HSC_8H_9, $HSi(SiMe_3)_3$. R = Alkyl, Alkenyl.[22]

Als Mediatoren für Synthesen mit Sauerstoff-Radikalen eignen sich insbesondere Halogenatom-[24–27] oder Wasserstoffatom-[23,24]Donoren. Während letztere zu reduktiv ter-minierten Produkten führen, eignen sich erstere zur Funktionalisierung der Reaktions-produkte für Folgereaktionen. Für die Auswahl des Mediators sind Toxizität, Funktionalisie-rung, aber auch die Geschwindigkeit des Radikaleinfangs ausschlaggebend. Als wirkungs-voller Mediator zur Bromierung von Radikalen hat sich Bromtrichlormethan ($k^{Br} \sim 10^8\ M^{-1}s^{-1}$) bewährt.[26,27]

2.2 Herstellung und Reaktivität cyclischer Thiohydroxamsäure-*O*-ester

Aufgrund der günstigen Kombination aus präparativer Zugänglichkeit, Lagerstabilität und chemischer Reaktivität in unverzweigten Kettenreaktionen stellen 3-Alkoxythiazol-2(3*H*)-thione zur Zeit die vermutlich praktikabelsten Vorläufer zur Erzeugung von Sauerstoff-Radikalen unter „Zinn-freien“ sowie pH-neutralen, nicht-oxidativen Bedingungen in präpara-

tiven und mechanistischen Studien dar.[23–28] Primäre und sekundäre 3-Alkoxythiazol2(3*H*)-thione können aus Alkoholen mit Hilfe des Mitsunobu-Verfahrens[29] oder aus Alkylhalogeniden und Alkyltosylaten durch nukleophile Substitution mit einem Thiohydroxamat-Salz (Salz-Methode, Schema 2.2)[30] dargestellt werden. Für sekundäre *O*-Alkylthiohydroxamate erfolgt die C,O-Bindungsknüpfung unter Inversion der Konfiguration.

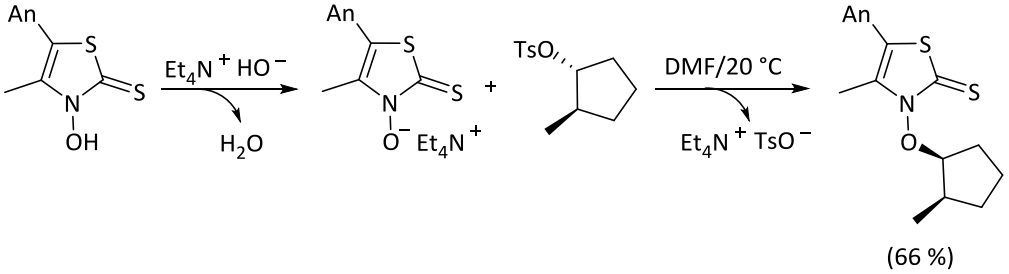

Schema 2.2. Synthese eines Thiohydroxamsäure-*O*-esters aus dem 3-Hydroxy-5-(4-methoxyphenyl)-4-methylthiazol-2(3*H*)-thion (An = Anisyl) über das Tetraethylammonium-Salz der Thiohydroxamsäure und einem Alkyltosylat in einer S_N2-Reaktion (Salz-Methode).[30]

Tertiäre Thiohydroxamsäure-*O*-ester können aus *O*-Alkylisoharnstoffen[29,30] (Isoharnstoff-Methode) und Thiohydroxamsäuren hergestellt werden, wobei die Synthese dieser Verbindungen bislang nur in Ansätzen untersucht ist (Schema 2.3).[9,33,34]

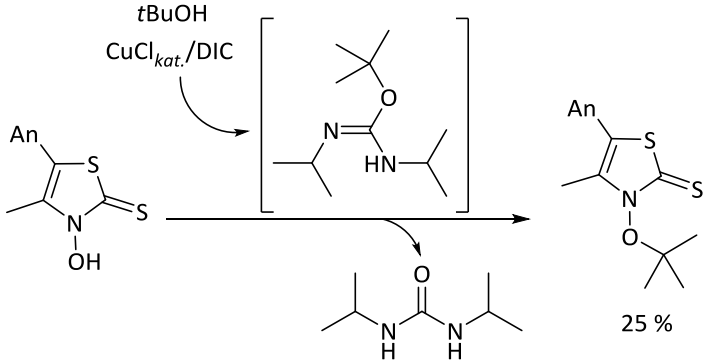

Schema 2.3. *O*-Alkylierung des 3-Hydroxy-5-(4-methoxyphenyl)-4-methylthiazol-2(3*H*)-thions mit *tert*-Butanol, Diisopropylcarbodiimid (DIC) und katalytischen Mengen Cu(I)Cl.[33,34]

Das größte Anwendungsgebiet primärer und sekundärer 3-Alkoxythiazol-2(3*H*)-thione als Vorläufer von Sauerstoff-Radikalen liegt in der stereoselektiven Synthese monocyclischer Tetrahydrofurane.[23,26–28,30,35,36] Zu Beginn dieser Arbeit existierten kaum Ergebnisse zum Aufbau bi-, tri- oder polycyclischer Ether über dem Sauerstoff-Radikale. Eine Erweiterung des

Sauerstoff-Radikal-Verfahrens um die genannten Stoffklassen würde die Synthesechemie durch das Erschließen neuer Grundstrukturen bereichern.

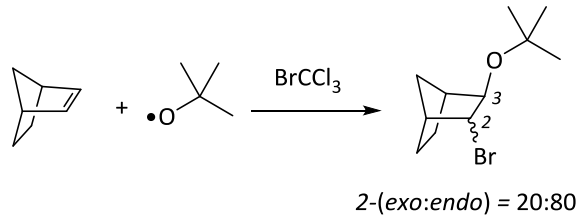

2-(*exo*:*endo*) = 20:80

Schema 2.4. Intermolekulare Addition des *tert*-Butoxyl-Radikals an Norbornen.[37]

Reaktionen tertiärer Alkoxyl-Radikale sind aufgrund der eingeschränkten Verfügbarkeit der Radikalvorläufer bis dato auf intermolekulare Additionen an Norbornen beschränkt (Schema 2.4).[37] Da die Verwendung tertiärer *O*-Radikale in Radikalcyclisierungen neue Synthesewege zu einer Vielzahl von Naturstoffen eröffnen würde, ist die systematische Untersuchung solcher Radikale von besonderem Interesse (Schema 2.5).

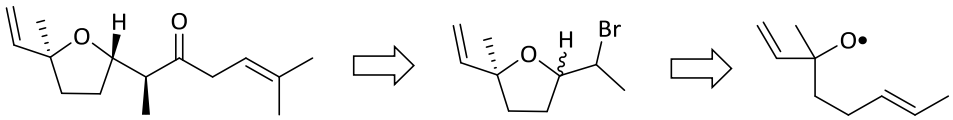

Davanon *trans-selektiv*

Schema 2.5. Retrosynthese von Davanon über das Sauerstoff-Radikal-Verfahren.

2.3 Aufgabenstellung

Vor dem Hintergrund des dargelegten Forschungsstands widmet sich die vorliegende Arbeit folgenden Themenfeldern der Sauerstoffradikalchemie:

- Synthese anellierter und verbrückter *O*-Alkylthiohydroxamate und Untersuchung der Selektivität in 4-Penten-1-oxyl-Radikalcyclisierungen beim Aufbau bicyclischer und tricyclischer Tetrahydrofurane.
- Weiterentwicklung der Isoharnstoff-Methode zur Darstellung einer größeren strukturellen Vielfalt tertiärer *O*-Radikalvorläufer im präparativen Maßstab.
- Untersuchung der Reaktivität tertiärer *O*-Radikale in intra- und intermolekularen Additionsreaktionen sowie der δ-H-Abstraktion.

2.4 Literaturverzeichnis

[1] H. J. H. Fenton, *J. Chem. Soc. Trans*. **1894**, *65*, 899–910.

[2] H. Wieland, *Chem. Ber.* **1911**, *44*, 2550–2556.

[3] H. Wieland, *Naturwissenschaften* **1915**, *3*, 594–596.

[4] P. Gray, A. Williams, *Chem. Rev*. **1959**, *59*, 239–328.

[5] D. H. R. Barton, J. M. Beaton, L. E. Geller, M. M. Pechet, *J. Am. Chem. Soc.* **1960**, *82*, 2640–2641.

[6] C. Walling, A. B. B. Jacknow, *J. Am. Chem. Soc.* **1960**, *82*, 6108–6112.

[7] C. Walling, A. J. Padawa, *J. Am. Chem. Soc.* **1963**, *85*, 1593–1597.

[8] B. P. Hay, A. L. J. Beckwith, *J. Am. Chem. Soc*. **1988**, *110*, 4415–4416.

[9] B. P. Hay, A. L. J. Beckwith, *J. Org. Chem.* **1989**, *54*, 4330–4334.

[10] A. L. J. Beckwith, B. P. Hay, G. M. Williams, *J. Chem. Soc*., *Chem. Commun*. **1989**, 1202–1203.

[11] S. Kim, T. A. Lee, *Synlett* **1997**, *8*, 950–952.

[12] J. Hartung, M. Schwarz, *Synlett* **1997**, 848–850.

[13] J. Hartung, M. Schwarz, I. Svoboda, H. Fueß, M.-T. Duarte, *Eur. J. Org. Chem.* **1999**, 1275–1290.

[14] S. Kim, T. Au Lee, Y. Song, *Synlett*, **1998**, *5*, 471–472.

[15] M. Zlotorzynska, H. Zhai, G. M. Sammis, *Org. Lett.* **2008**, *10*, 5083–5086.

[16] M. Rueda-Becerril, J. C. T. Leung, C. R. Dunbar, G. M. Sammis, *J. Org. Chem*. **2011**, *76*, 7720–7729.

[17] S. Kim, C. J. Lim, S.–E. Song, H.–Y. Kang, *Synlett* **2001**, *5*, 688–690.

[18] V. N. Kondratiev in *Comprehensive chemical kinetics: The Theory of Kinetics*; C. H. Bamford, C. F. H. Tripper Eds.; Elsevier Scientific Publishing Company, Amsterdam, **1969**, Vol. 2, Kapitel 2, 81–183.

[19] N. N. Semenov, *Z. Phys. Chem.* **1929**, *B2*, 161.

[20] M. Bodenstein, *Z. Phys. Chem.* **1913**, *85*, 329–397.

[21] G. Wedler in *Lehrbuch der physikalischen Chemie*; G. Wedler, Ed.; Wiley-VCH-Weinheim, **1997**, 4. Auflage, Kapitel 6.2, 865–873.

[22] J. Hartung, T. Gottwald, K. Špehar, *Synthesis* **2002**, *11*, 1469–1498.

[23] J. Hartung, *Eur. J. Org. Chem.* **2001**, 619–632.

[24] J. Hartung, F. Gallou, *J. Org. Chem*. **1995**, *60*, 6706–6716.

[25] J. Hartung, R. Kneuer, *Eur. J. Org. Chem.* **2000**, 1677–1683.

[26] J. Hartung, R. Kneuer, S. Laug, P. Schmidt, K. Špehar, I. Svoboda, H. Fuess, *Eur. J. Org. Chem.* **2003**, 4033–4052.

[27] J. Hartung, R. Kneuer, T. M. Kopf, P. Schmidt, *C. R. Acad. Sci. Paris, Chimie/ Chemistry,* **2001**, 649–666.

[28] C. Schur, I. Kempter, J. Hartung, *Org. Synth*. **2012**, 228–235.

[29] J. Hartung, T. Gottwald, R. Kneuer, *Synlett* **2001**, 749–751.

[30] J. Hartung, C. Schur, I. Kempter, T. Gottwald, *Tetrahedron* **2010**, *66*, 1365–1374.

[31] L. J. Mathias, *Synthesis* **1979**, 561–576.

[32] M. Mikołajczyk, P. Kiełbasiński, *Tetrahedron* **1981**, *37*, 233–284.

[33] T. Gottwald, *Dissertation* **2004**, Julius-Maximilians-Universität Würzburg.

[34] N. Schneiders, *Dissertation* **2008**, Technische Universität Kaiserslautern.

[35] I. Kempter, A. Groß, J. Hartung, *Tetrahedron* **2012**, *68*, 10378–10390.

[36] I. Kempter, B. Frensch, T. Kopf, R. Kluge, R. Csuk, I. Svoboda, H. Fuess, J. Hartung, *Tetrahedron* **2014**, *70*, 1918–1927.

[37] J. Hartung, N. Schneiders, T. Gottwald, *Tetrahedron Lett.* **2007**, *48*, 6027–6030.

3 Bi- und tricyclische Tetrahydrofurane aus substituierten 4-Penten-1-oxyl-Radikalen

3.1 Zusammenfassung

Bei 1,2- und 2,3-anellierten 4-Penten-1-oxyl-Radikalen steuert der näher zur π-Bindung lokalisierte Substituent, als primärer Induktor, den stereochemischen Verlauf der 5-*exo*-trig-Cyclisierung 2,4-*cis*- bzw. 2,3-*trans*-selektiv. Der Substituent mit größerer Distanz zur Doppelbindung fungiert als sekundärer Induktor. Seine relative Konfiguration zum primären Induktor erhöht die Diastereoselektivität im Falle einer *trans*-Konfiguration und senkt sie, wenn beide Substituenten *cis* zueinander angeordnet sind. 3,4-Anellierte sowie 2,5- und 3,5-verbrückte 4-Penten-1-oxyl-Radikale mit eingeschränkter konformeller Flexibilität der Sauerstoffatom-tragenden Seitenkette cyclisieren 2,3-*cis*- bzw. 2,4-*cis*-spezifisch. Der 2,3-*cis*-spezifische Ringschluss eines Verbenylethoxyl-Radikals liefert zwei β-bromierte, tricyclische Tetrahydrofurane. Theoretischen Berechnungen zufolge sind Torsionsspannungen dafür verantwortlich, dass die Aktivierungsbarriere der 2,3-*trans*-Cyclisierung 55 kJ/mol höher ist als die Barriere für den 2,3-*cis*-Ringschluss, weshalb 2,3-*trans*-Produkte des Verbenylethoxyl-Radikals experimentell nicht beobachtet werden

3.2 Wissenschaftlicher Hintergrund, Zielsetzung und Strategie

Eine Extrapolation von Richtlinien[1] zur Beschreibung von Selektivitäten beim Aufbau monocyclischer Verbindungen ist in den seltensten Fällen auf bicyclische Zielmoleküle übertragbar, da transannulare und andere Spannungseffekte in kaum vorhersagbarer Weise überlagern. Einflüsse cyclischer Substrukturen auf Stereoselektivitäten von 4-Penten-1-oxyl-Radikalcyclisierungen in der Synthese bicyclischer Tetrahydrofurane lassen sich jedoch durch systematische Permutation des Verbrückungsschemas (Typ **A**–**E**, Abb. 3.1) erfassen und zur Weiterentwicklung stereochemischer Richtlinien nutzen.[2,3]

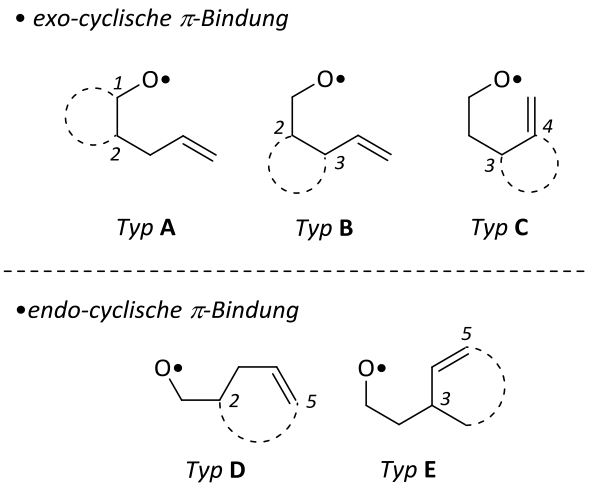

Abbildung 3.1. Anellierte (Typ **A**–**C**) und verbrückte (Typ **D**–**E**) 4-Penten-1-oxyl-Radikale. Gestrichelte Linie: cyclischer Rest / Verbrückung.

Dem dargelegten Hintergrund folgend, hatte das Projekt zum Ziel,

- den dominierenden stereochemischen Einfluss des Substituenten zu identifizieren, der die Selektivitäten von 1 und 2 (Typ **A**), 2 und 3 (Typ **B**) sowie 3 und 4 (Typ **C**) cycloalkylverbrückter 4-Penten-1-oxyl-Radikale in 5-*exo*-Cyclisierungen steuert und
- die Systematik von Stereoselektivitäten in 5-*exo*-Cyclisierungen von 4-Penten-1-oxyl-Radikalen mit *endo*-cyclischen Doppelbindungen zu untersuchen (Typ **D**–**E**).

3.3 Ergebnisse und Diskussion

3.3.1 Synthese und Eigenschaften anellierter und verbrückter *O*-Alkylthiohydroxamate

Die Synthese der Thiohydroxamsäure-*O*-ester **1a–1h** für die experimentell angestrebten Untersuchungen erfolgte durch selektive *O*-Alkylierung des 3-Hydroxy-4-methyl-thiazol-2(3*H*)-thion Tetraethylammonium-Salzes mit substituierten 4-Pentenyltosylaten (Salz-Methode, Schema 3.1). Sekundäre *O*-Alkylthiohydroxamate (*cis*/*trans*-**1a–1c**) reagieren unter Inversion der Konfiguration zu stereochemisch homogenen Produkten.[4]

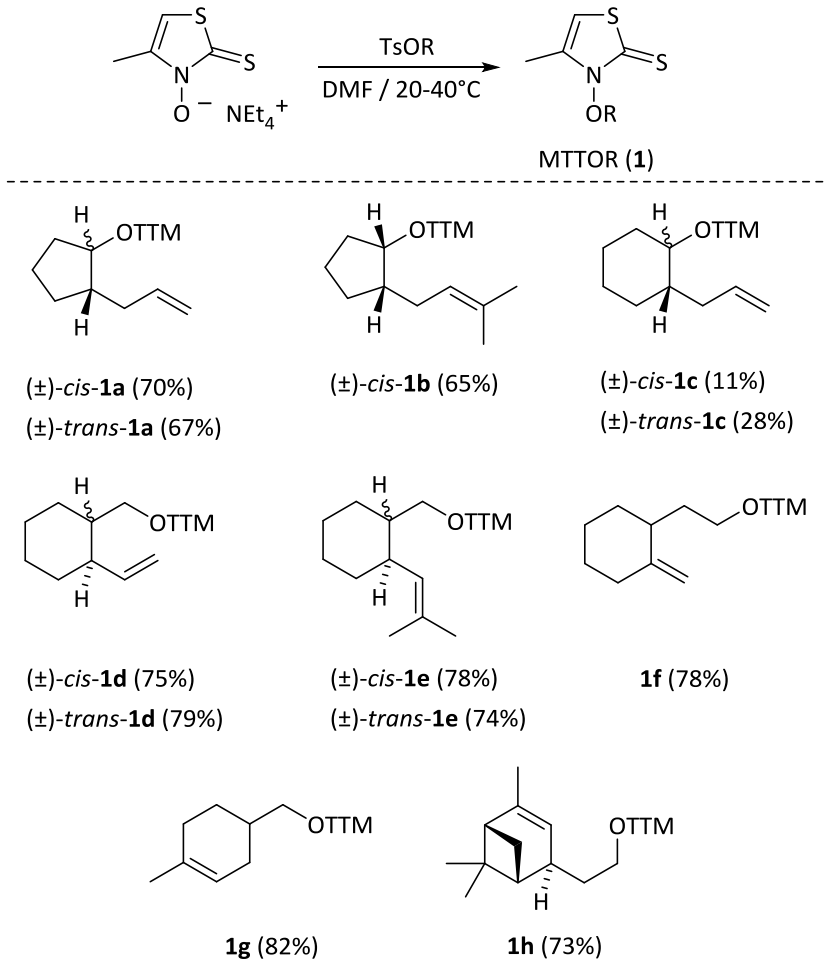

Schema 3.1. Salz-Methode (oben) zur Herstellung der anellierten und verbrückten Thiohydroxamsäure-*O*-ester **1a–1h** (unten).

Die *O*-Radikalvorläufer wurden als farblose bis blassgelbe Öle (**1a–b,** *cis*-**1c**, **1f**) oder als farblose Feststoffe (*trans*-**1c**, **1d–e**, **1g**, **1h**) isoliert. Für 3-[(1-Methylcyclohex-1-en-4-yl)-methoxy]-4-methylthiazol-2(3*H*)-thion (**1g**) zeigte die Kristallstrukturanalyse zwei Diastereomere entlang der stereogenen Achse [N3–O1] (Abb. 3.2). Beide nehmen eine Konformation ein, die aus dynamischen NMR-Studien von 3-Isopropoxy-4-methylthiazol-2(3*H*)-thion bekannt ist.[5] Um Abstoßungen durch die Thiocarbonyl- [C2,S2] und die Methyl-Gruppe [C6] auszuweichen, stehen Heterocyclus und Hexenyl-Rest dabei nahezu orthogonal zueinander [C2–N3–O1–C7 = 91.0(2)°].

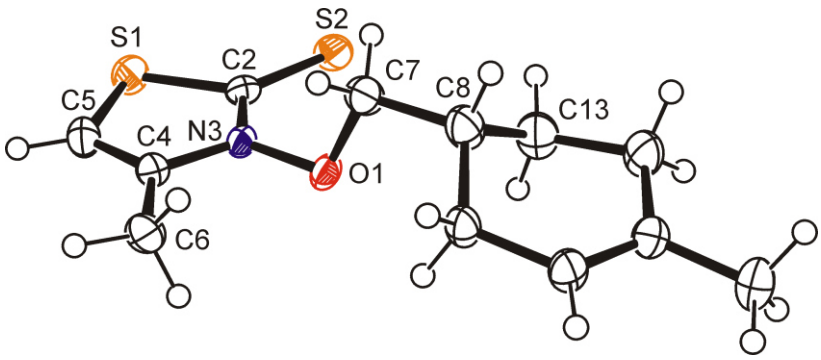

Abbildung 3.2. Ellipsoid Graphik (50% Wahrscheinlichkeit) des Hauptdiastereomers von 3-[(1-Methylcyclohex-1-en-4-yl)-methoxy]-4-methylthiazol-2(3*H*)-thion (**1g**) im Kristall (150 K). Wasserstoffatome: farblose Kreise (willkürlicher Radius); Sauerstoff: rot, Stickstoff: blau, Schwefel: orange. C2–S2 = 1.666(1) Å, C2–N3 = 1.358(2) Å, N3–O1 = 1.386(2) Å.

Die *O*-Alkylthiohydroxamate **1a–1h** absorbieren UV/Vis-Licht im Bereich von 317−319 nm und zeigen charakteristische ^{13}C-NMR-Verschiebungen für den Thiocarbonyl-Kohlenstoff (C2: 180 ppm), den Kohlenstoff in Position 5 des Thiazol-2(3*H*)-thion-Kerns (C5: 102 ppm) und die Ester-Kohlenstoffe (C7: 74.8–92.1 ppm), wobei *trans*-konfigurierte Ester **1a**−**1e** einen stärkeren Tieffeld-Shift für Sauerstoff-gebundene Kohlenstoffe (C7) zeigen als die *cis*-Stereoisomere.[6]

3.3.2 Typ A: 1,2-anellierte *O*-Alkylthiohydroxamate

Thermische und photochemische Reaktionen der 1,2-Cyclopentyl-anellierten Thiohydroxamsäure-*O*-ester **1a**−**1b** mit Bromtrichlormethan liefern nur geringe Mengen der β-bromierten Oxabicyclen **2a**−**2b** (Tabelle 3.1). Als Hauptprodukte entstehen die δ-Bromaldehyde **3a**−**3b**. Die 1,2-Cyclohexyl-anellierten-Analoga *cis*/*trans*-**1c** cyclisieren selektiv zu den Tetrahydrofuranen *cis*/*trans*-**2c** und bilden nur bei thermischen Reaktionsbedingungen das δ-Bromaldehyd **3c** als Nebenprodukt (Tabelle 3.2).

Tabelle 3.1. Produkte thermischer und photochemischer Umsetzungen der 1,2-Cyclopentyl-anellierten Thiohydroxamsäure-*O*-ester *cis*/*trans*-**1a** und *cis*-**1b** mit Bromtrichlormethan

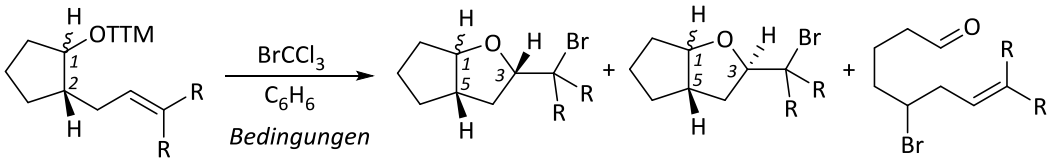

(±)-**1a/b** (±)-3,5-*cis*-**2a/b** (±)-3,5-*trans*-**2a/b** **3a/b**

Eintrag	**1**[a]	R	Bedingungen	**2** / % (3,5-*cis*:*trans*)	**3** / %	**2**:**3** / %	k^{rel}
1	*cis*-**1a**	H	*hν* / 25 °C	**2a**: 10 (70:30)	**3a**: 60	14:86	0.17
2	*cis*-**1a**	H	AIBN / 80 °C	**2a**: 8 (71:29)	**3a**: 54	13:87	0.15
3	*cis*-**1b**	CH_3	*hν* / 25 °C	**2b**: 49 (64:36)	**3b**: 31	61:39	1.55
4	*cis*-**1b**	CH_3	AIBN / 80 °C	**2b**: 34 (56:44)	**3b**: 35	49:51	0.97
5	*trans*-**1a**	H	*hν* / 25 °C	– [b]	**3a**: 44	–	–
6	*trans*-**1a**	H	AIBN / 80 °C	– [b]	**3a**: 73	–	–

[a] Stereodeskriptor für relative Konfiguration der Anellierung, [b] nicht beobachtet (GC, NMR).

Tabelle 3.2. Produkte thermischer und photochemischer Umsetzungen der 1,2-Cyclohexyl-anellierten Thiohydroxamsäure-*O*-ester *cis*/*trans*-**1c** mit Bromtrichlormethan

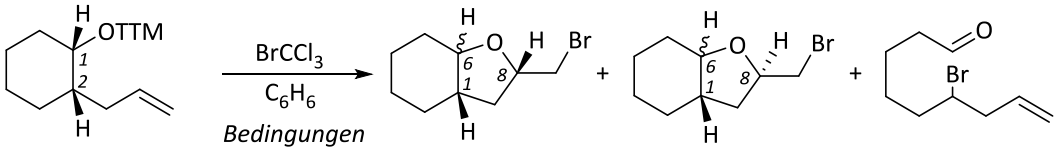

(±)-**1c** (±)-1,8-*cis*-**2c** (±)-1,8-*trans*-**2c** **3c**

Eintrag	**1c**[a]	Bedingungen	**2c** / % (1,8-*cis*:*trans*)	**3c** / %	**2:3** / %	k^{rel}
1	*cis*-**1c**	*hν* / 25 °C	45 (89:11)	– [b]	–	–
2	*cis*-**1c**	AIBN / 80 °C	61 (68:32)	12	84:16	5.08
3	*trans*-**1c**	*hν* / 25 °C	49 (92:08)	– [b]	–	–
4	*trans*-**1c**	AIBN / 80 °C	70 (87:13)	8	90:10	8.75

[a] Stereodeskriptor für relative Konfiguration der Anellierung, [b] nicht beobachtet (GC, NMR).

Typ-**A**-anellierte 4-Penten-1-oxyl-Radikale (*cis*/*trans*-**1c**) cyclisieren 2,4-*cis*-selektiv und demonstrieren damit, dass der dominierende Stereoinduktor für Ringschlussreaktionen

der Substituent in Position 2 ist. Betrachtungen mit Hilfe eines erweiterten Twist-Modells zeigen, dass die 2,4-*cis*-Cyclisierungen aufgrund von Abstoßungen in den *trans*-Übergangszuständen bevorzugt wird (Abb. 3.2).

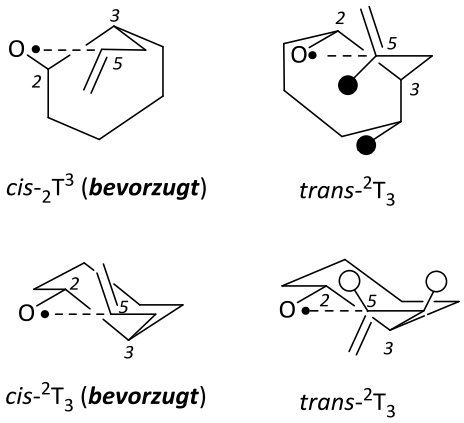

Abbildung 3.2. 5-*exo*-Übergangszustände cyclohexyl-anellierter Typ-**A**-Radikale (schwarze Kreise: räumlich nahe H-Atome; weiße Kreise ekliptisch angeordnete H-Atome).

1,2-Cyclopentyl-anellierte 4-Penten-1-oxyl-Radikale fragmentieren aufgrund der signifikanten Cyclopentylspannung[12] in hohem Maße (Tabelle 3.1). Mengen an Cylisierungsprodukten steigen dabei für *cis*-konfigurierte Radikalvorläufer (*cis*-**1a**) sowie in Gegenwart terminaler Methylgruppen (*cis*-**1b**). Mit einem 60:40-Verhältnis zwischen Cyclisierung und Fragmentierung ist für 4-Penten-1-oxyl-Radikale mit dem gespannten Fünfring das beste Resultat erreicht (Tabelle 3.1, Eintrag 3).

Die relative Reaktivität zwischen Addition ($k^{5\text{-}exo}$) und Fragmentierung (k^{Frag}) der Radikale **Ia**–**Ic** ($c_{Ia–Ic}$ = 0.167 M, Schema 3.2) spiegelt sich in den Ausbeuteverhältnissen der Produkte [**2**]/[**3**] wider, da für beide Reaktionen kinetische Kontrolle sowie Bedingungen *pseudo*-erster Ordnung (c_{Br} = 1.67 M) vorliegen.[7,8] Für die Fragmentierung basiert diese Näherung auf der höheren effektiven Geschwindigkeitskonstante des Bromeinfangs (k^{Br}_{eff} = 4.3×10^8 s^{-1}) der Radikale **IIIa**–**c** im Vergleich zur 5-*exo*-Cyclisierung des 4-Formylbutyl-Radikals ($k^{5\text{-}exo}$ = 8.7×10^5 s^{-1}, 80 °C).[9] k^{Br}_{eff} wurde aus der Bromtrichlormethan-Konzentration c_{Br} und der Geschwindigkeitskonstante des Bromatomeinfangs k^{Br} des Hept-6-en-2-yl-Radikals (k^{Br} = 2.6×10^8 M^{-1} s^{-1}, 26 °C)[10] abgeschätzt. Das Verhältnis zwischen 4-Penten-1-oxyl-Radikalcyclisierung ($k^{5\text{-}exo}$ = 5.2×10^8 s^{-1}, 26 °C)[11] und Cyclopentoxyl-Radikalfragmentierung (k^{Frag} = 4.8×10^8 s^{-1}, 80 °C)[9] erlaubt als Referenzsystem Rückschlüsse auf absolute Geschwindigkeitskonstanten für die Reaktion der Radikale **Ia**–**Ic**.

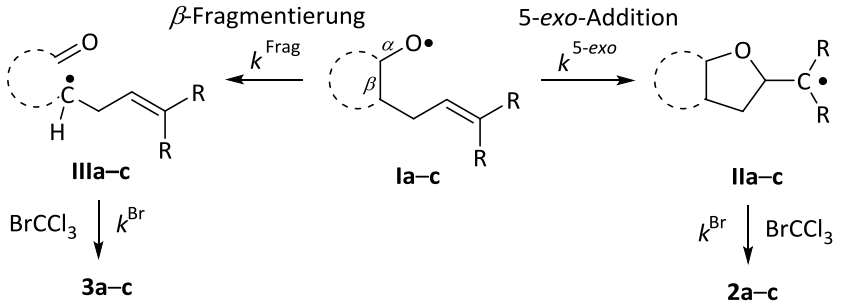

Schema 3.2 Konkurrenzkinetische Betrachtung der Fragmentierung (k^{Frag}) und 5-*exo*-Addition ($k^{5\text{-}exo}$) der Typ-**A**-Radikale **Ia–c** für die mechanistische Interpretation der Reaktivität und Chemoselektivität.

3.3.3 Typ B: 2,3-anellierte *O*-Alkylthiohydroxamate

Die 2,3-Cyclohexyl-anellierten Thiohydroxamate *cis*/*trans*-**1d** reagieren in photochemischen und thermischen Umsetzungen mit Bromtrichlormethan zu diastereomeren Mischungen der anellierten-Tetrahydrofurane *cis*/*trans*-**2d**. Als Nebenprodukte entstehen die Tetrahydropyrane *cis*/*trans*-**4d** (Tabelle 3.3, Eintrag 1–4). Die Prenyl-abgeleiteten Typ-**B**-Derivate *cis*/*trans*-**1e** cyclisieren innerhalb der NMR- und GC/MS-Nachweisgrenze stereo- und regiospezifisch zum 5-*exo*-Bicyclus 6,7-*trans*-**2e**.

Tabelle 3.3. Produkte thermischer und photochemischer Cyclisierungen der 2,3-anellierten Thiohydroxamate *cis*/*trans*-**1d**–**1e** mit Bromtrichlormethan

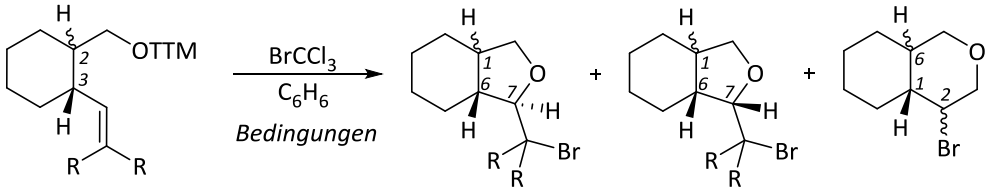

(±)-**1d/e** (±)-6,7-*trans*-**2d/e** (±)-6,7-*cis*-**2d/e** (±)-**4d/e**

Eintrag	**1**[a]	Bedingungen	R	**2** / % (6,7-*cis*:*trans*)	**4** / % (1,2-*cis*:*trans*)	*exo*:*endo*
1	*cis*-**1d**	$h\nu$ / 25 °C	H	**2d**: 70 (20:80)	**4d**: 3 (95:5)[b]	96:4
2	*cis*-**1d**	AIBN / 80 °C	H	**2d**: 81 (21:79)	**4d**: 5 (95:5)[b]	94:6
3	*trans*-**1d**	$h\nu$ / 25 °C	H	**2d**: 57 (7:93)	**4d**: 10 (50:50)	85:15
4	*trans*-**1d**	AIBN / 80 °C	H	**2d**: 70 (10:90)	**4d**: 17 (41:59)	80:20
5	*cis*-**1e**	$h\nu$ / 25 °C	CH_3	**2e**: 80 (5:95)[b]	**4e**: –[c]	–
6	*cis*-**1e**	AIBN / 80 °C	CH_3	**2e**: 95 (5:95)[b]	**4e**: –[c]	–
7	*trans*-**1e**	$h\nu$ / 25 °C	CH_3	**2e**: 81 (5:95)[b]	**4e**: –[c]	–
8	*trans*-**1e**	AIBN / 80 °C	CH_3	**2e**: 94 (5:95)[b]	**4e**: –[c]	–

[a] Stereodeskriptor für relative Konfiguration der Anellierung, [b] innerhalb der GC/MS- und NMR-Nachweisgrenze nur ein Isomer detektiert, [c] nicht beobachtet (NMR, GC/MS).

Der 2,3-*trans*-selektive Ringschluss 2,3-anellierter 4-Penten-1-oxyl-Radikale (Typ-**B**) verdeutlicht, dass die Stereochemie maßgeblich durch den Substituent bestimmt wird, der näher zur Doppelbindung steht (Position 3). Ursache der 2,3-*trans*-Selektivität ist, dem erweiterten Twist-Modell zufolge (Abb. 3.3), die sterische Hinderung zwischen den H-Atomen der π-Bindung und der Cyclohexyl-Einheit während des 2,3-*cis*-Ringschlusses. Für terminale Methyl-Gruppen nimmt die räumliche Abstoßung zu.

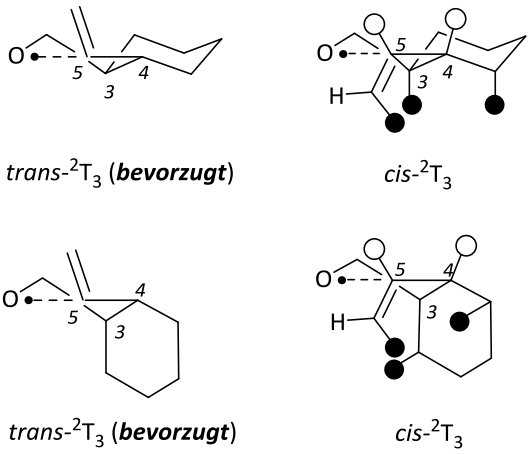

Abbildung 3.3. Übergangszustände der Typ-**B**-Vorläufer **1d/e** (schwarze Kreise: H-Atome, die an 1,3-diaxialen Abstoßungen beteiligt sind; weiße Kreise: ekliptisch angeordnete H-Atome).

3.3.4 Typ C: 3,4-anelliertes *O*-Alkylthiohydroxamat

Das 3,4-Cyclohexyl-anellierte Thiazol-2(3*H*)-thion **1f** cyclisiert in Gegenwart von Bromtrichlormethan, photochemisch wie thermisch, unter stereospezifischer Bildung des Oxabicyclus (±)-*cis*-**2f** (Tabelle 3.4). Darüber hinaus entsteht mit einem relativen Anteil von maximal 47% das 6-*endo*-Produkt 1-Bromo-3-oxabicyclo[4.4.0]decan (**4f**).

Tabelle 3.4. Produkte des Typ-**C**-Vorläufers **1f** der thermischen und photochemischen Umsetzungen mit Bromtrichlormethan

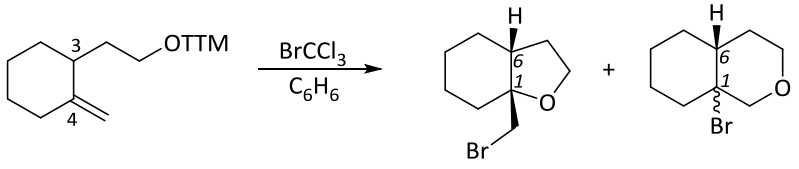

1f (±)-*cis*-**2f** (±)-**4f**

Eintrag	Bedingungen	*cis*-**2f** / %	**4f** / % (1,6-*cis*:*trans*)	*exo*:*endo*
1	*hν* / 25 °C	24	21 (19:81)	53:47
2	AIBN / 80 °C	35	22 (32:68)	61:39

Der 5-*exo*-Ringschluss des 3,4-anellierten 4-Penten-1-oxyl-Radikals **If** kann aufgrund der eingeschränkten Flexibilität der Seitenkette nur 2,3-*cis*-spezifisch erfolgen (Schema 3.3).

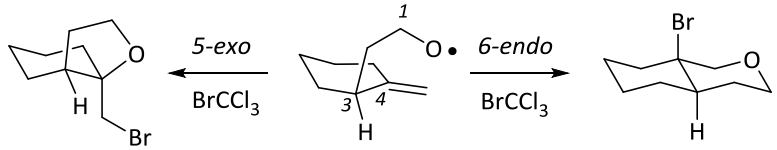

(±)-*cis*-**2f** **If** (±)-*trans*-**4f**

Schema 3.3. Stereo- und regiochemischer Verlauf der *exo*- bzw. *endo*-Addition des Typ-**C**-Radikalvorläufers **1f** in Gegenwart von Bromtrichlormethan.

3.3.5 Typ D: 2,5-verbrücktes *O*-Alkylthiohydroxamat

Intramolekulare Additionen des 2,5-verbrückten Thiohydroxamsäure-*O*-esters **1g** liefern für thermische und photochemische Reaktionen mit Bromtrichlormethan die Bicyclen cis/trans-**2g** (Tabelle 3.5).

Tabelle 3.5. Produkte der 5-*exo*-Additionen des Cyclohexenyl-substituierten Thiohydroxamsäure-*O*-esters **1g** in Gegenwart von Bromtrichlormethan

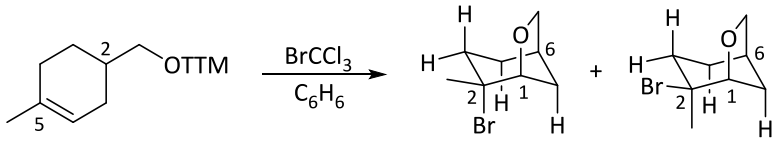

1g (±)-*trans*-**2g** (±)-*cis*-**2g**

Eintrag	Bedingungen	*trans*-**2g** / %	*cis*-**2g** / %	1,2-*cis*:*trans*
1	$h\nu$ / 25 °C	46	18	28:72
2	AIBN / 80 °C	58	14	19:81

Der 2,4-*cis*-stereospezifische 5-*exo*-Ringschluss des Typ-**D**-anellierten 4-Penten-1-oxyl-Radikals **Ig** ist das Resultat der eingeschränkten Flexibilität der Sauerstoffatom-tragenden Seitenkette (Schema 3.4).

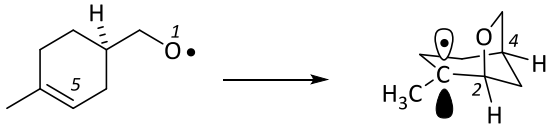

Ig **IIg**

Schema 3.4. 5-*exo*-*trig*-Cyclisierung des Radikals **Ig**.

3.3.6 Typ E: 3,5-verbrücktes *O*-Alkylthiohydroxamat

Die photochemische Umsetzung des 3,5-verbrückten Verbenol-abgeleiteten Thiohydroxamats **1h** mit Bromtrichlormethan bildet als Hauptprodukt den bromierten Oxatricyclus **5** neben geringen Mengen des Isomer **6** (Schema 3.5).

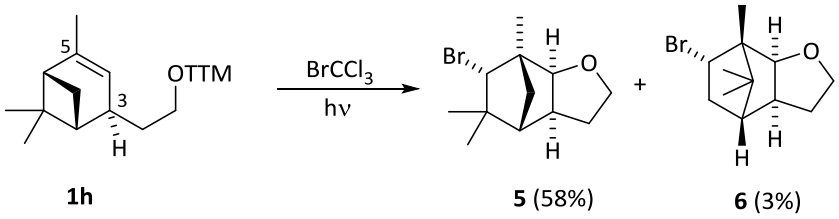

1h **5** (58%) **6** (3%)

Schema 3.5. Produkte der photochemischen Umsetzung des 3,5-verbrückten Verbenol-Radikalvorläufers **1h** in Gegenwart von Bromtrichlormethan.

Die erhaltenen Tricyclen **5** und **6** entstehen durch Folgereaktionen der 5-*exo*-*trig*-Cyclisierung (**Ih**→**IIh**). Zum Abbau von Ringspannung lagert die Cyclobutyl-Einheit in **IIh** um, sodass die stabileren Radikale **V** und **VI** gebildet werden. Der anschließende Radikaleinfang mit Bromtrichlormethan liefert die Produkte **5** und **6** (Schema 3.6).

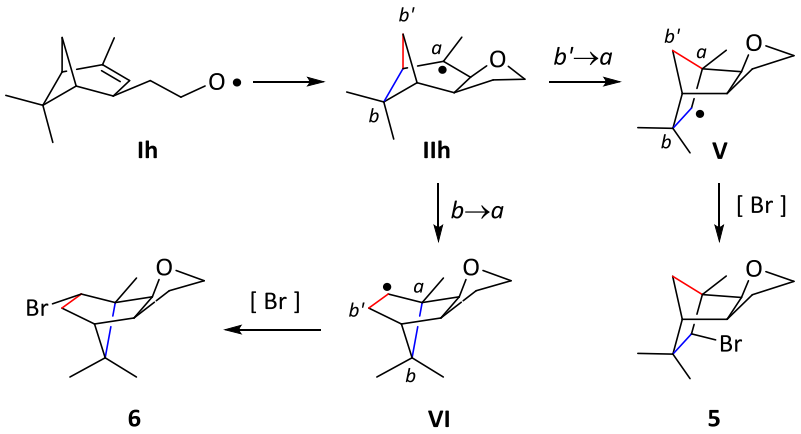

Schema 3.6. Reaktionskaskade aus Cyclisierung, Umlagerung und Bromatomeinfang des Radikals **Ih** bei der Bildung der Tricyclen **5** und **6**.

Typ-**E**-anellierte 4-Penten-1-oxyl-Radikale cyclisieren 2,3-*cis*-spezifisch, da die Flexibilität der Seitenkette eingeschränkt ist.

Um Barrieren abschätzen zu können, die mit dem *cis*- und *trans*-Ringschluss von **1h** verbunden sind, wurden in Kooperation mit Jens Hartung Energien für den *cis*- und *trans*-spezifischen Ringschluss des Modell-Radikals 1-(Cyclohexen-3-yl)-2-ethoxyl-Radikal **Ii**,

berechnet.[13,14] Die bekannten Energien der 5-*exo*-Reaktion des 4-Penten-1-oxyl-Radikals **Ij** wurden für den intramolekularen Vergleich herangezogen, während der energetisch ungünstige Angriff des Methoxyl-Radikals **Ik** an das interne Kohlenstoffatom (C2) von Propen aus struktureller Analogie zu den Radikalen **Ii** und **Ij** der Gegenüberstellung der intermolekularen Addition diente (Tabelle 3.6).[15,16]

Stark exotherme Reaktionsverläufe ($\Delta_R E$) der betrachteten Radikale verdeutlichen eine kinetische Reaktionskontrolle mit frühen Übergangszuständen (Hammond-Postulat)[17] – Fakten, die sich bereits in früheren Studien mit der B3LYP/6-31+G**-Methode ausreichend beschreiben ließen.[18,19] Die Berechnungen liefern die Übergangsstrukturen *cis*-**IIi** (ax), *cis*-**IIi** (eq) und *trans*-**IIi**, sowie die zugehörigen Reaktions- ($\Delta_R E$) und Aktivierungsenergien ($\Delta E^{\ddagger}$) (Tabelle 3.6).

Tabelle 3.6. Berechnete Übergangzustände und Energien (B3LYP/6-31+G**-Methode) der Alkoxyl-Radikale *pe*-**Ii**, *pa*-**Ii, Ij** und **Ik**

Sauerstoff-Radikal	Kohlenstoff-Radikal	$\Delta_R E$ /kJ mol^{-1}	$\Delta E^{\ddagger}$ /kJ mol^{-1}	$\Delta E^{\ddagger}_{i}$ /kJ mol^{-1}	$\Delta E^{\ddagger}_{TD}$ /kJ mol^{-1}
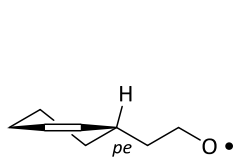 *pe*-**Ii**	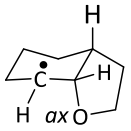 *cis*-**IIi** (*ax*)	–44.1	16.7	35.4	–18.6
	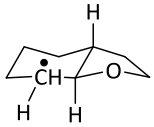 *trans*-**IIi**	–34.5	73.1	89.5	–16.4
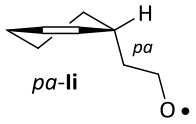 *pa*-**Ii**	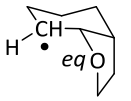 *cis*-**IIi** (*eq*)	–46.8	17.4	37.1	–19.7
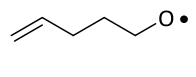 **Ij**	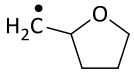 **IIj**	–40.5	19.8	37.3	–17.5
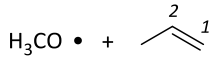 **Ik**	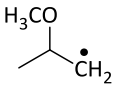 **III**	–53.8	20.5	43.2	–22.7

Unter Verwendung der Marcus-Theorie[20–22] (Gleichungen 1 und 2) können die berechneten Werte für $\Delta_R E$ und $\Delta E^{\ddagger}$ Informationen über Energien der Bindungsbildung bzw. -lösung ($\Delta E^{\ddagger}_{TD}$) und über sterische Effekte ($\Delta E^{\ddagger}_{i}$) liefern. Die Berechnungen zeigen, dass der 2,3-*cis*-Ringschluss von **Ii** (**1h**) energetisch deutlich günstiger ist als die 2,3-*trans*-Cyclisierung.

Eine intrinsische Barriere ($\Delta E^{\ddagger}_{i}$) von fast 90 kJ/mol ist dafür verantwortlich, dass 2,3-*trans* Produkte experimentell nicht entstehen (Tabelle 3.6).

$$\Delta E^{\ddagger} = \Delta E^{\ddagger}_{i} + \Delta E^{\ddagger}_{TD} \qquad \text{(Gleichung 1)}$$

$$\Delta E^{\ddagger}_{i} = \frac{\Delta E^{\ddagger} - \frac{\Delta_R E}{2} + \sqrt{(\Delta E^{\ddagger})^2 - (\Delta_R E)(\Delta E^{\ddagger})}}{2} \qquad \text{(Gleichung 2)}$$

3.4 Fazit und Ausblick

Anellierte und verbrückte 4-Penten-1-oxyl-Radikale cyclisieren in stereochemisch vorhersagbarer Weise. Für anellierte Substrate des Typs **A** und **B** dominiert der näher zur Doppelbindung befindliche Substituent (primärer Induktor) über die Stereochemie der 5-*exo*-Reaktion, sofern es sich um gleiche Reste handelt. Die relative Konfiguration beider Substituenten zueinander verbessert (*trans*) oder verschlechtert (*cis*) die Stereoselektivität. Verbindungen mit konformell eingeschränkter Seitenkette cyclisieren *cis*-spezifisch an *exo*- und *endo*-cyclische π-Bindungen (Typen **C**–**E**). Daraus lässt sich ableiten, dass 4-Penten-1-oxyl-Radikale mit drei gleichen Induktoren in den Positionen 1, 2 und 3 vermutlich der hier erkennbaren stereochemischen Prioritätsabstufung folgen, wonach der Einfluss der Induktoren mit zunehmendem Abstand zur Doppelbindung sinkt. Denkbar ist darüber hinaus, dass Substituenten größerer Sterik (z.B. *tert*-Butyl) in Positionen mit geringerem stereochemischen Einfluss (z.B. Position 2) Induktoren höherer Hierarchie (z.B. Methyl in Position 3) zu übersteuern vermögen und der Übersteuerungseffekt durch Substituenten unterschiedlicher Polarität beeinflusst werden kann. Diese Hypothesen sind Ziele zukünftiger Arbeiten und tragen dazu bei, die derzeitige Vielfalt Tetrahydrofuran-abegleiteter Derivate in der Synthesechemie um weitere bi-, tri- oder sogar polycyclische Teilstrukturen zu bereichern.

3.5 Literaturverzeichnis

[1] J. Hartung, *Eur. J. Org. Chem.* **2001**, 619–632.

[2] R. Kneuer, *Dissertation* **2001**, Julius-Maximilians-Universität Würzburg.

[3] T. Gottwald, *Dissertation* **2004**, Julius-Maximilians-Universität Würzburg.

[4] J. Hartung, C. Schur, I. Kempter, T. Gottwald, *Tetrahedron* **2010**, *66*, 1365–1374.

[5] J. Hartung, R. Kneuer, M. Schwarz, M. Heubes, *Eur. J. Org. Chem.* **2001**, 4733–4736.

[6] J. Hartung, R. Kneuer, M. Schwarz, I. Svoboda, H. Fueß, *Eur. J. Org. Chem.* **1999**, 97–106.

[7] D. Griller, K. U. Ingold, *Acc. Chem. Res.* **1980**, *13*, 317–323.

[8] M. Newcomb in *Radicals in Organic Synthesis*; P. Renaud, M. P. Sibi, Eds.; Wiley-VCH-Weinheim, **2001**, Vol. 1, Kapitel 3.1, 317–324.

[9] A. L. J. Beckwith, B. P. Hay, *J. Am. Chem. Soc.* **1989**, *111*, 230–234.

[10] J. Hartung, B. Hertel, F. Trach, *Chem. Ber.* **1993**, *126*, 1187–1191.

[11] J. Hartung, F. Gallou, *J. Org. Chem*. **1995**, *60*, 6706–6716.

[12] K. S. Pitzer, W. E. Donath, *J. Am. Chem. Soc*. **1959**, *81*, 3213–3218.

[13] Gaussian 03, Revision E.01, M. J. Frisch, G. W. Trucks, H. B. Schlegel, G. E. Scuseria, M. A. Robb, J. R. Cheeseman, J. A. Montgomery, Jr., T. Vreven, K. N. Kudin, J. C. Burant, J. M. Millam, S. S. Iyengar, J. Tomasi, V. Barone, B. Mennucci, M. Cossi, G. Scalmani, N. Rega, G. A. Petersson, H. Nakatsuji, M. Hada, M. Ehara, K. Toyota, R. Fukuda, J. Hasegawa, M. Ishida, T. Nakajima, Y. Honda, O. Kitao, H. Nakai, M. Klene, X. Li, J. E. Knox, H. P. Hratchian, J. B. Cross, V. Bakken, C. Adamo, J. Jaramillo, R. Gomperts, R. E. Stratmann, O. Yazyev, A. J. Austin, R. Cammi, C. Pomelli, J. W. Ochterski, P. Y. Ayala, K. Morokuma, G. A. Voth, P. Salvador, J. J. Dannenberg, V. G. Zakrzewski, S. Dapprich, A. D. Daniels, M. C. Strain, O. Farkas, D. K. Malick, A. D. Rabuck, K. Raghavachari, J. B. Foresman, J. V. Ortiz, Q. Cui, A. G. Baboul, S. Clifford, J. Cioslowski, B. B. Stefanov, G. Liu, A. Liashenko, P. Piskorz, I. Komaromi, R. L. Martin, D. J. Fox, T. Keith, M. A. Al-Laham, C. Y. Peng, A. Nanayakkara, M. Challacombe, P. M. W. Gill, B. Johnson, W. Chen, M. W. Wong, C. Gonzalez, J. A. Pople, Gaussian, Inc., Wallingford CT, **2004**.

[14] J. B. Foresman, Æ. Frisch, *Exploring Chemistry with Electronic Structure Methods*, 2nd ed. **1996**, Gaussian Inc., Pittsburgh, PA.

[15] J. Hartung, K. Daniel, C. Rummey, G. Bringmann, *Org. Biomol. Chem*. **2006**, *4*, 4089–4100.

[16] C. Schur, N. Becker, U. Bergsträßer, T. Gottwald, J. Hartung, *Tetrahedron* **2011**, *67*, 2338–2347.

[17] G. S. Hammond, *J. Am. Chem. Soc.* **1955**, *77*, 334–338

[18] A. D. Becke, *J. Chem. Phys.* **1993**, *98*, 5648–5652.

[19] C. Lee, W. Yang, R. G. Parr, *Phys. Rev.* **1988**, *B37*, 785–789.

[20] R. A. Marcus, *J. Phys. Chem*. **1968**, *72*, 891–899.

[21] W. J. Albery, *Ann. Rev. Phy. Chem.* **1980**, *31*, 227–263.

[22] L. H. Gade in *Koordinationschemie*, Wiley-VCH, Weinheim, 1998, 1. Auflage, 443–479.

3.6 Forschungsartikel

Annulated and Bridged Tetrahydrofurans from Alkenoxyl Radical Cyclization

Christine Schur, Harald Kelm, Thomas Gottwald, Arne Ludwig, Rainer Kneuer, Jens Hartung

Organic & Biomolecular Chemistry **2014**, *12*, 8288–8307.

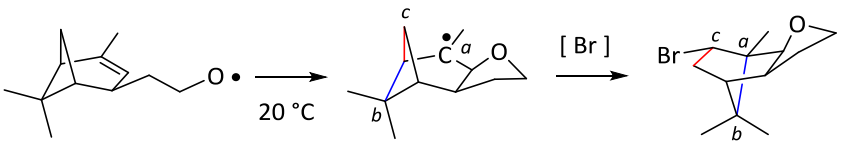

addition *rearrangement and homolytic substitution*

Organic & Biomolecular Chemistry

PAPER

View Article Online
View Journal | View Issue

Cite this: Org. Biomol. Chem., 2014, 12, 8288

Annulated and bridged tetrahydrofurans from alkenoxyl radical cyclization†‡

Christine Schur,[a] Harald Kelm,[a] Thomas Gottwald,[b] Arne Ludwig,[b] Rainer Kneuer[b] and Jens Hartung*[a]

Received 17th June 2014,
Accepted 12th August 2014

DOI: 10.1039/c4ob01266f

www.rsc.org/obc

4-Pentenoxyl radicals sharing two or more carbon atoms with a cycloalkane cyclize in a predictable manner stereoselectively and regioselectively to afford in solutions of bromotrichloromethane cycloalkyl-fused or -bridged 2-bromomethyltetrahydrofurans in up to 95% yield. Stereoselectivity in alkenoxyl radical ring closures arises from cumulative steric effects. The substituent positioned the closest to the alkene carbon, which is being attacked by the oxygen radical, exerts the strongest stereodirecting effect. This principal inductor guides 5-*exo*-cyclization 2,3-*trans*- or 2,4-*cis*-selectively. The substituent located further from the attacked π-bond is the secondary inductor. A secondary inductor in the relative *trans*-configuration enhances stereodifferentiation by the primary inductor; a *cis*-configured secondary inductor decreases this effect. A secondary inductor is not able to overrule the guiding effect of a similar sized primary inductor. Intramolecular 4-pentenoxyl radical additions to a cyclohexene-bound *exo*-methylene group or to endocyclic double bonds proceed *cis*-specifically, as exemplified by synthesis of a diastereomerically pure bromobicyclo[2.2.1]heptyl-annulated tetrahydrofuran from the verbenylethyloxyl radical. According to theory, the experimental 2,3-*cis*-specificity in alkoxyl radical cyclization to an endocyclic π-bond arises from strain associated with the 2,3-*trans*-ring closure.

1. Introduction

4-Pentenoxyl radicals add intramolecularly to the inner alkene carbon with rate constants of 10^8 per second and above.[1–6] Alkyl or *ortho*-substituted aryl groups in position 1 exert a stereodirecting effect, leading to 2,5-*trans*-configured tetrahydrofurans as principal products. Carbon substituents at positions 2 and 3 direct 4-pentenoxyl radical cyclization 2,4-*cis*- and 2,3-*trans*-selectively.[7–9] Stereodifferentiation by alkyl or aryl groups arises from steric effects, which gradually increases as the distance between a controlling substituent and the attacked π-bond shortens, for example from a 15/85-*cis*/*trans*-ratio at room temperature to <2/98 by shifting a *tert*-butyl group from position 1 to position 3.[8] In synthesis, 5-*exo*-cyclized 4-pentenoxyl radicals are preferentially trapped by a heteroatom atom donor,[10,11] for introducing halogen,[12–14] alkylsulfanyl,[15] or other synthetically useful functional groups.[16]

The model to explain stereodifferentiation by a carbon substituent in 4-pentenoxyl radical cyclization predicts that the intramolecular addition proceeds *via* a distorted twist-conformer of tetrahydrofuran as the favored transition structure (twist-model),[8,17] differing from the cyclohexane-based Beckwith–Houk-model for carbon radical cyclization.[18,19] Application of the alkoxyl radical approach to synthesis of more demanding targets, for example biologically active terpene-, acetogenin-, and fatty acid-derived cycloalkyl-fused tetrahydrofurans,[20–22] requires to extend the model in order to predict the selectivity for constructing bicyclic compounds.[7,23] Lessons from carbon radical chemistry have taught that stereodifferentiation in synthesis of bicyclic compounds is difficult to extrapolate by transferring results from monocycle to bicycle formation, since transannular and other strain effects may superimpose in an unpredictable manner.[24,25] To find out whether embedding two carbons of a 4-pentenoxyl radical into a cycloaliphatic framework conserves or changes guidelines for stereoselective tetrahydrofuran synthesis, we examined in this study bromocyclization of *cis*/*trans*-cycloalkyl-bridged alkenoxyl

[a]Fachbereich Chemie, Organische Chemie, Technische Universität Kaiserslautern, Erwin-Schrödinger-Straße, D-67663 Kaiserslautern, Germany. E-mail: hartung@chemie.uni-kl.de; Fax: +49-631-205-3921; Tel: +49-631-205-2431
[b]Institut für Organische Chemie, Universität Würzburg, Am Hubland, 97074 Würzburg, Germany

†Dedicated to the memory of Athelstan (Athel) L. J. Beckwith in recognition of his pioneering and creative contributions to the chemistry of free radicals in general and to free radical cyclizations in particular. We will miss his humor and his intellectual approach to chemical science.

‡Electronic supplementary information (ESI) available: Standard instrumentation, the protocol for ESI containing instrumentation, synthesis of 4-pentenols, *O*-pentenyl tosylates, carbon-13 spectra of selected compounds, calculated atomic coordinates and energies of transition structures and radicals. CCDC 1008593. For ESI and crystallographic data in CIF or other electronic format see DOI: 10.1039/c4ob01266f

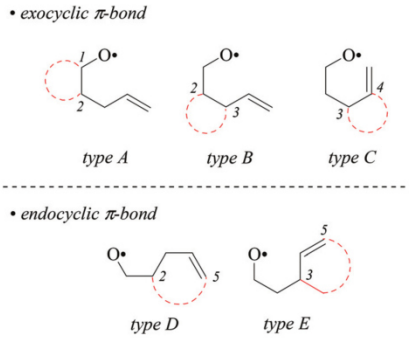

Fig. 1 Classification of cycloalkyl-bridged 4-pentenoxyl radicals (type A–C) and alkenoxyl radicals having an endocyclic carbon–carbon double bond (type D–E; dotted red lines symbolize alkyl bridging).

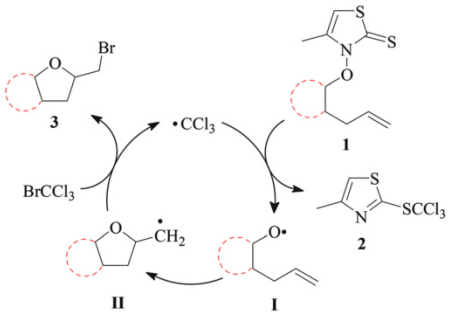

Scheme 1 Chain mechanism for synthesis of annulated bromomethyltetrahydrofuran **3** from 3-alkenoxy-4-methylthiazole-2(3*H*)-thione **1** and $BrCCl_3$ (the red dotted line symbolizes an alkyl-bridge; *cf.* Fig. 1 and Scheme 2).

radicals, having the carbon–carbon double bond located in a conformationally flexible side chain (types A and B), in the *exo*-position of cyclohexane (type C), or incorporated into an alicyclic core (types D and E, Fig. 1).

The most important finding from the study shows that cycloalkyl-bridged 4-pentenoxyl radicals cyclize in a predictable manner stereoselectively and regioselectively, to afford in solutions of bromotrichloromethane cycloalkyl-annulated or -bridged bromomethyltetrahydrofurans in up to 95% yield. The principal stereoinductor is the substituent attached the closest to the carbon–carbon double bond, which is being attacked by the radical oxygen. A principal inductor guides 5-*exo*-cyclization 2,3-*trans*- or 2,4-*cis*-selectively. The substituent bound further from the attacked π-bond is the secondary inductor. A *trans*-arranged secondary inductor enhances stereocontrol of the primary inductor, and a *cis*-configured secondary inductor decreases this effect. A secondary inductor of similar steric size, located further from the attacked π-bond is not able to overrule the directing effect of the principal inductor. Oxygen radicals attached *via* a methylene- or an ethylene-spacer to cyclohexene cyclize *cis*-specifically, as exemplified by synthesis of a diastereomerically pure bromobicyclo[2.2.1]-heptyl-annulated tetrahydrofuran from a type-E radical. The propensity of cyclohexenylethyloxyl radicals to cyclize 2,3-*cis*-specifically arises from strain associated with the 2,3-*trans*-ring closure, as derived by a Marcus analysis of density functional-calculated reaction energies and barriers.

2. Results and interpretation

2.1 Alkenoxyl radicals from 3-alkenoxy-4-methylthiazole-2(3*H*)-thiones

2.1.1 Alkenoxyl radical generation, intramolecular addition, and chain reaction. In extension to previous studies, we used derivatives of 3-alkenoxy-4-methylthiazole-2(3*H*)-thione (MTTOR) **1** as progenitors for generating oxygen radicals under non-oxidative and pH-neutral conditions.[11,26,27] MTTORs (*e.g.* **1**) are heterocyclic *O*-alkenyl thiohydroxamates, liberating oxygen radicals in an addition/fragmentation sequence involving a mediator radical. The intermediate formed by adding, for example, the trichloromethyl radical to the thione sulfur of MTTOR **1** dissociates into 2-(trichloromethylsulfanyl)-4-methylthiazole **2** and oxygen radical **I** (Scheme 1).[14] 4-Pentenoxyl radicals cyclize by intramolecularly adding with rate constants of 10^8–10^9 s^{-1} at room temperature to a terminal double bond, providing tetrahydrofuranylmethyl radicals, for example **II**, in a fingerprint 5-*exo*/6-*endo*-regioselectivity of 98 : 2.[17] Trapping of carbon radical **II** by bromotrichloromethane yields bromomethyltetrahydrofuran **3** as a target product, and the trichloromethyl radical for propagating the chain reaction.

2.1.2 Preparation and properties of 3-alkenoxy-4-methylthiazole-2(3*H*)-thiones (MTTORs). The standard approach to synthesis of *O*-alkenyl thiohydroxamate **1** is substitution of a leaving group from a carbon electrophile by the 4-methyl-2-thiooxothiazole-2(3*H*)-3-oxido ion ($MTTO^-$; Scheme 2).[26] In the present study we used *O*-alkenyl tosylates as carbon electrophiles, obtained in 69–96% yield from an alkenol,[28–31] *p*-toluenesulfonyl chloride, and 1,4-diazabicyclo-[2.2.2]octane for buffering *in situ*-liberated hydrogen chloride (ESI‡).[32] Some alkenol syntheses required modification of the original instruction, for example for preparing *cis*- and *trans*-isomers of 2-(2-methylprop-1-enyl)-cyclohexylmethanol (for **1e**)[33,34] and β-verbenylethanol (for **1h**; ESI‡).[35] Treating *O*-pentenyl tosylates at room temperature in solutions of dimethyl formamide with the tetraethylammonium salt of $MTTO^-$ furnished MTTORs **1a**, **1b**, and **1d–h** in yields between 65% and 82% (Scheme 2). In position 2 substituted cyclohexyl tosylates gave stereochemically pure target products *cis*-**1c** and *trans*-**1c**, although in comparatively low yields. We explain this observation by steric shielding of the electrophilic carbon in 2-substituted cyclohexyl tosylates toward the incoming nucleophile, the $MTTO^-$-anion, in a S_N2-reaction.[36]

3-Alkenoxyl-4-methylthiazole-2(3*H*)-thiones obtained as described above are oils (**1a–b**, *cis*-**1c**, **1f**) or crystalline solids (*trans*-**1c**, **1d–e**, **1g**, **1h**), stable for months when stored in vials at room temperature. Recrystallizing 3-(methylcyclohexenyl)-

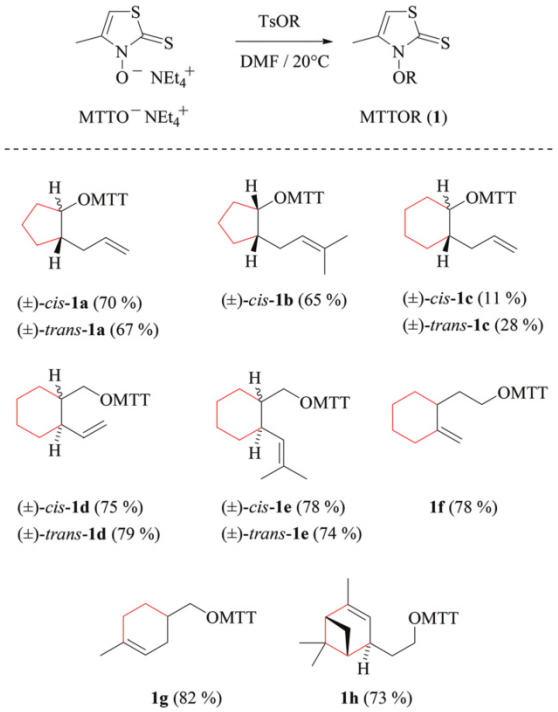

Scheme 2 Indexing, yields, and structure formulas of MTTORs **1a–h** prepared from *O*-alkenyl tosylates and 3-hydroxy-4-methylthiazole-2(3*H*)-thione tetraethylammonium salt (segments drawn in red refer to subunits represented by dotted lines in Fig. 1 and in Scheme 1).

methyloxy-thiazolethione **1g** removed a regioisomer, which had been formed with 5/95-selectivity as a by-product from the [4 + 2]-cycloaddition between isoprene and methyl acrylate, in the first step of the synthesis for constructing the 1,4-disubstituted cyclohexenyl nucleus.[37,38]

3-Alkenoxy-4-methylthiazole-2(3*H*)-thiones **1a–h** show diagnostic carbon-13 chemical shifts for the thiocarbonyl carbon (180–181 ppm) and the thiohydroxamate-bound carbon (74.8–92.1 ppm). The compounds absorb in solutions of methanol UV-light, leading to absorption-maxima at λ = 316–319 nm ($\lg \varepsilon \sim 3.10$–$3.19$ m^2 mol^{-1}). Photoexciting the tail end of this absorption band with 350 nm light causes the nitrogen–oxygen bond in **1** to break homolytically, liberating oxygen radicals without an externally added initiator.[39]

In solution, 3-alkoxy-4-methylthiazole-2(3*H*)-thiones show the phenomenon of hindered rotation about the nitrogen–oxygen bond, becoming apparent in nuclear magnetic resonance spectra of, for example, 3-isopropoxy-4-methyl-thiazole-2(3*H*)-thione by signal coalescence at −60 °C, and a twofold set of resonances below this temperature.[40] The lowest in energy conformer has the ester carbon C7 offset by almost 90 degrees from the thiohydroxamate plane, to prevent close contacts with the thione sulfur and methyl group in position 4 of the heterocyclic core.[41] The structure of 3-alkenyloxythiazolethione **1g** in the solid state corresponds to the predicted minimum

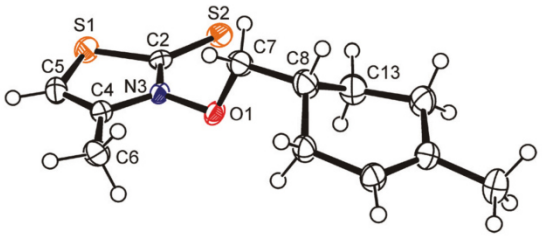

Fig. 2 Ellipsoid graphic of 3-[(1-methylcyclohex-1-en-4-yl)-methyloxy]-4-methylthiazole-2(3*H*)-thione (**1g**) in the solid state [major diastereomer at 150 K; the (*R*,*P*)-isomer was arbitrarily chosen from the racemate (*R*,*P*)/(*S*,*M*)-**1g** for presentation (50% probability level); hydrogen atoms are drawn as circles of an arbitrary radius; oxygen is depicted in red, nitrogen in blue, and sulfur in orange; for depiction of the minor diastereomer (*S*,*P*)/(*R*,*M*)-**1g**, see the ESI‡].

conformation of thiazolethione-derived *O*-alkyl thiohydroxamates in solution and in the gas phase. The crystals available for determining the structure of compound **1g** were systematically disordered showing, according to the model used for solving and refining the structure, a 78/22-ratio of diastereomers at crystallographic independent sites.§ The diastereomers differ with respect to the configuration at C8/C8a (ESI‡) and the helicity at the nitrogen–oxygen bond, showing both the characteristic offset of thiohydroxamate bound carbon 7 from the heterocyclic plane [major diastereomer (ds): C2–N3–O1–C7 = 91.0(2)°; minor ds: C2–N3a–O1a–C7a = 59.8(6)°] and bond lengths which are diagnostic for primary *O*-alkyl thiohydroxamates [major ds (Fig. 2): C2–S2 = 1.666(1) Å, C2–N3 = 1.358(2) Å, N3–O1 = 1.386(2) Å; minor ds (ESI‡): C2–N3a = 1.366(6) Å, N3a–O1a = 1.373(4) Å].[42]

2.1.3 Numbering of atom positions in *O*-alkenyl thiohydroxamates, alkenoxyl radicals, and cyclized products. Oxygen and carbon differ in priority for systematically naming open chain and heterocyclic organic compounds according to the IUPAC convention. For the stereochemical discussion in this article we numbered the 4-pentenyl chain in *O*-radical progenitor **1** and alkenoxyl radical **I** as recommended by IUPAC for aliphatic compounds.[43] A transition structure (TS)-**I** for 5-*exo*-cyclization in the twist model is a derivative of tetrahydrofuran, and thus numbered, similar to cyclized carbon radical **II**, according to the Hantzsch–Widman notation for heterocyclic compounds.[44,45] For numbering positions in bicyclic bromocyclization product **3**, we used the von Baeyer convention (Fig. 3).[46,47]

2.2 Alkenoxyl radical addition to exocyclic double bonds

2.2.1 1,2-Annulation – 2-allylcycloalkyl-1-oxyl radical reactions. For elucidating principles of stereocontrol exerted by a cycloalkane fused in positions 1 and 2 to the 4-pentenoxyl radical we investigated the size effect of the cycloaliphatic ring,

§Crystallographic data (excluding structure factors) for the structure in this paper are deposited with the Cambridge Crystallographic Data Centre as supplementary publication [CCDC 1008593 (compound **1g**)].

View Article Online
Organic & Biomolecular Chemistry Paper

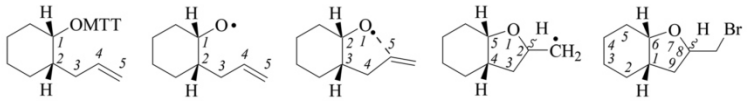

Fig. 3 Convention used in this article for numbering atoms in product classes associated with alkoxyl radical reactions, exemplified for alkenoxythiazolethione *cis*-**1c**, derived 4-alkenoxyl radical *cis*-**Ic**, the transition structure for the 5-*exo*-cyclization TS-*cis*-**Ic**, 5-*exo*-cyclized carbon radical *cis*-**IIc**, and bicyclic bromocyclization product *cis*-**3c**.

Table 1 Products formed from 3-(*cis*-2-allylcyclopentyloxy)-thiazolethiones *cis*-**1a–b** and $BrCCl_3$

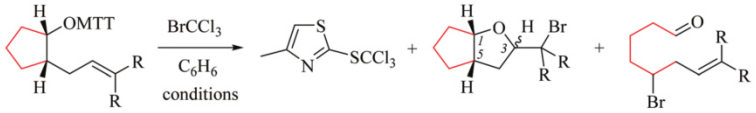

Entry	*cis*-**1**	R	Conditions	**2**/%	*cis*-**3a–b**/% (1,3-*cis* : *trans*)	**4**/%
1	**1a**	H	*hν*/25 °C	85	**3a:** 10 (70 : 30)	**4a:** 60
2	**1a**	H	AIBN/80 °C	87	**3a:** 8 (71 : 29)	**4a:** 54
3	**1b**	CH_3	*hν*/25 °C	73	**3b:** 49 (64 : 36)	**4b:** 31
4	**1b**	CH_3	AIBN/80 °C	75	**3b:** 34 (56 : 44)	**4b:** 35

Table 2 Products formed from 3-(*trans*-2-allylcyclopentyloxy)-thiazolethione *trans*-**1a** and $BrCCl_3$

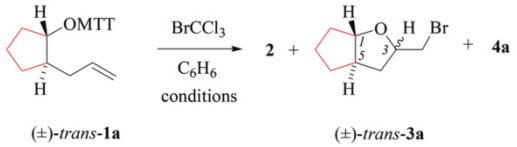

Entry	Conditions	**2**/%	*trans*-**3**/% (1,3-*cis* : *trans*)	**4a**/%
1	*hν*/25 °C	56	—[a]	44 (14)[b]
2	AIBN/80 °C	85	—[a]	73 (14)[b]

[a] Not detected (NMR). [b] Figures in brackets refer to the yield of 5,7-dibromo-9,9,9-trichlorononanal.

Table 3 Products formed from 3-(*cis*-2-allylcyclohexyloxy)-thiazolethione *cis*-**1c** and $BrCCl_3$

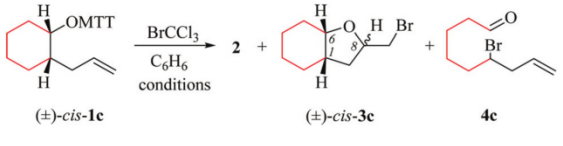

Entry	Conditions	**2**/%	*cis*-**3c**/% (6,8-*cis* : *trans*)	**4c**/%
1	*hν*/25 °C	73	45 (89 : 11)	—[a]
2	AIBN/80 °C	74	61 (68 : 32)	12

[a] Not detected (NMR).

Table 4 Products formed from 3-(*trans*-2-allylcyclohexyloxy)-thiazolethione *trans*-**1c** and $BrCCl_3$

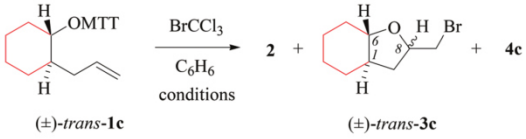

Entry	Conditions	**2**/%	*trans*-**3c**/% (6,8-*cis* : *trans*)	**4**/%
1	*hν*/25 °C	92	49 (8 : 92)	—[a]
2	AIBN/80 °C	80	70 (13 : 87)	8

[a] Not detected (NMR).

the relative configuration of substituents, and substitution at the terminal alkene carbon on reactivity and selectivity of type-A alkenoxyl radicals (Tables 1–4).

(*i*) *Methods of alkenoxyl radical generation and product analysis*. Photolyzing solutions of *O*-alkenyl thiohydroxamates **1a–c** in benzene containing 10 equivalents (1.67 M) of bromotrichloromethane, using Rayonet® chamber apparatus equipped with 350 nm illuminants, quantitatively consume the starting material within 30 minutes, as determined by thin layer chromatography. Reaction mixtures from photochemical experiments tended to turn turbid and yellow. A gas chromatogram (GC) recorded by the end of the reaction time provided information on the original product pattern and distribution.

Column chromatography furnished samples of purified 2-(trichloromethylsulfanyl)-4-methyl-1,3-thiazole (**2**), 5-*exo*-bromocyclized products **3a–c**, and β-fragmented unsaturated 5-bromoaldehydes **4a–b**, for collecting analytical data (Tables 1–4, and Experimental). Solutions from thermally initiated reactions were in addition charged with 15 mole percent of azo-α,α-bis-(isobutyronitrile) (AIBN) as the initiator. Such mixtures remained clear but tended to turn yellow by the end of the reaction.

(*ii*) *Product pattern and kinetic interpretation*. Reactions between *O*-(2-allylcycloalkyl) thiohydroxamates *cis*-**1a–c** and bromotrichloromethane furnish bromomethyltetrahydrofurans *cis*-**3a–c**, with the yields gradually decreasing for thermally initiated reactions from 61% for *cis*-**3c** through 34% for *cis*-**3b** to 8% for *cis*-**3a** (Table 1, entries 2 and 4; Table 3, entry 2). The reactions gave bromoaldehydes **4a–c** as co-products in yields increasing from 12% for **4c**, through 35% for **4b** to 54% to **4a**. Photolyzing or heating *O*-(2-allylcyclopentyl) thiohydroxamate *trans*-**1a** in the presence of bromotrichloromethane provided bromooctanal **4a**, but no bromomethyltetrahydrofuran *trans*-**3a** as secured by independent analysis of an authentic sample of the compound (ESI‡). The ratio of the bromocyclized product *trans*-**3c** and bromoaldehyde **4c** obtained from *O*-cyclohexylallyl ester *trans*-**1c** is similar to the ratio of *cis*-**3c** and **4c** obtained from the stereoisomer *cis*-**1c** (entry 2 in Tables 3 and 4). The pattern of products obtained from radical reactions conducted at 80 °C in summary is similar, except for bromoaldehyde **4c**, which did not form in the room temperature experiments. None of the reactions furnished 2-allylcycloalkanols or 2-allylcycloalkanones in verifiable amounts (GC-MS).

In kinetically controlled reactions, the quotient between bromomethyltetrahydrofuran **3** and bromoaldehyde **4** is equivalent to the relative rate constant for the addition (k^{add}) *versus* β-fragmentation (k^{β}) (Scheme 3). Kinetic control for oxygen radical addition to terminal double bonds is documented.[8] For the following reason we suggest that the sequence leading to bromoaldehyde **4** under conditions chosen in this study also is kinetically controlled. In 1.67 molar solution of bromotrichloromethane, the effective rate constant for bromine atom trapping by secondary alkyl radicals, such as **III**, is approximately 4.3×10^8 s^{-1}, based on k^{Br} for the 6-hepten-2-yl radical (2.6×10^8 M^{-1} s^{-1}; 26 °C)[48] as a reference. The rate constant k^{add} for the 4-formylbutyl radical 5-*exo*-cyclization (8.7×10^5 s^{-1}; 80 °C),[49] serving as a reference for the reaction **III** → **I**, is by almost three orders of magnitude slower than the effective rate of bromine atom transfer from bromotrichloromethane to the secondary carbon radical **III**.

For comparing rates of 5-*exo*-cyclization to rates of β-fragmentation for intermediates **Ia–c**, we standardized reactant concentrations and used a tenfold molar excess of bromotrichloromethane. Under such conditions, the ratio of bromide **3** to **4** corresponds to the quotient k^{add}/k^{β}, gradually increasing along the series of radicals *trans*-**Ia** (k^{rel} = 0), *cis*-**Ia** (0.2), *cis*-**Ib** (1.0) to *cis*/*trans*-**Ic** (k^{rel} = 5–9). Dividing k^{add} for the 4-pentenoxyl radical cyclisation (5.2×10^8 s^{-1}; 26 °C) by k^{β} for the cyclopentoxyl radical β-fragmentation (4.7×10^8 s^{-1}; 80 °C) for

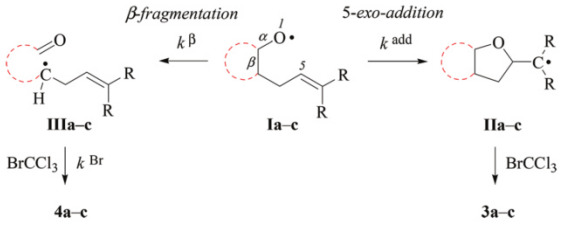

Scheme 3 Competing reaction pathways for mechanistically interpreting the origin and yields of 5-*exo*-cyclization- *versus* β-fragmentation-products from 2-allylcycloalkyloxyl radicals **Ia–c** (R = H, CH_3; for details associated with rate constants k^{β}, k^{Br}, and k^{add}, see the text).

calibrating the competition system with the aid of absolute rate constants leads to a similar order of magnitude for the k^{add}/k^{β} ratio.[2,49]

The propensity of cyclopentane-fused 4-pentenoxyl radicals to provide β-fragmented products, such as bromoaldehydes **4a–b**, arises from strain, being ~20 kJ mol^{-1} higher for cyclopentane than for cyclohexane.[50] Substituting methyl for hydrogen at the terminal alkene carbon increases the fraction of the 5-*exo*-cyclized product from *cis*-**3a** to *cis*-**3b**, which we address to a rate enhancing polar effect of the methyl group in oxygen radical additions.[51]

(*iii*) *Stereochemical guidelines*. 1,2-Cycloalkyl-bridged 4-pentenoxyl radicals **Ia–c** cyclize 2,4-*cis*-selectively showing that the substituent in position 2 is the principal stereoinductor for 5-*exo*-cyclization of type-A radicals. A *trans*-arranged secondary inductor in position 1 enhances the directing effect of the principal inductor; a *cis*-configured secondary inductor decreases this effect.

(iv) *On the origin of 2,4-cis-selectivity in 5-exo-cyclization of type-A 4-pentenoxyl radicals*. To understand the origin of 2,4-*cis*-selectivity, we modelled transition structures (TS) of 2-allylcyclohexyl-1-oxyl radical 5-*exo*-cyclization **Ic** → **IIc**, using assessed electronic structure methods.[14,52]

For stereochemical analysis, we considered transition structures for 2,4-*cis*-(TS^1) and 2,4-*trans*-cyclization (TS^2) of allylcyclohexyloxyl radicals *cis*/*trans*-**Ic** (Fig. 4 and ESI;‡ see also section 2.4). Transition structure searches according to an established methodology[17] (ESI‡) led to twist (T)-conformers of tetrahydrofuran (Fig. 4), similar to intermediates modelled for 5-*exo*-cyclization of monosubstituted 4-pentenoxyl radicals.[8] The radical oxygen in transition structures $TS^{1,2}$-*cis*/*trans*-**Ic** lies for stereoelectronic reasons in a plane defined by inner alkene carbon (C5) and the allylic carbon (C4). Carbons 2 and 3 are offset into opposite directions from this plane, leading to $^2T_3$-(TS^2-*cis*-**Ic**, TS^1-*trans*-**Ic**, and TS^2-*trans*-**Ic**) and $_2T^3$-conformers of tetrahydrofuran (TS^1-*cis*-**Ic**). *cis*/*trans*-Diastereodifferentiation, in this model, occurs by rotating the vinyl substituent by 180 degrees about the bond between carbons 4 and 5. Positioning the vinyl group and carbon 3 on opposite sides of the twist plane prevents eclipsing of hydrogens at carbons 4 and 5, thus favoring transition structures TS^1-*cis*-**Ic** and TS^1-*trans*-**Ic**. Favored transition structures furthermore have the cyclohexyl-

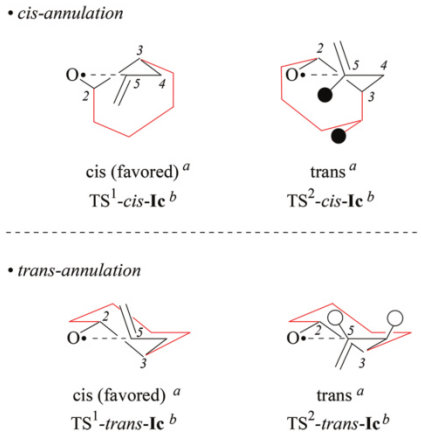

Fig. 4 Modelled transition structures for 2,4-*cis* (TS^1) and 2,4-*trans* (TS^2)-cyclization of alkenoxyl radicals *cis*-**Ic** (top) and *trans*-**Ic** (bottom). Black circles represent hydrogens experiencing close contacts ($d_{H,H}$ = 2.423 Å; B3LYP/6-31+G**), open circles symbolize eclipsed hydrogens (H–C4–C3–H = 2.1°). [a]Stereodescriptor referring to the configuration at carbons 2 and 4 in cyclized radical **IIc** (*cf.* Fig. 3). [b]Stereodescriptor referring to the configuration at carbons 2 and 3 in TS-**Ic**.

substituent in position 3 bound equatorially to the distorted tetrahydrofuran nucleus (Fig. 4). Positioning the cyclohexyl-substituent at carbon 3 axially leads to transannular repulsion between the hydrogen attached to carbon 5 and one of the axial cyclohexane hydrogens (TS^2-*cis*-**Ic**). The lowest in energy transition structure modelled for the 2,4-*trans*-ring closure of *trans*-**Ic** (TS^2-*trans*-**Ic**; Fig. 4, bottom right) shows an eclipsing of hydrogens at carbons 4 and 5.

2.2.2 2,3-Annulation – 2-(vinylcyclohexyl)-methyloxyl radical reactions. For elucidating principles controlling the stereoselectivity in cyclization of 2,3-cyclohexyl-bridged 4-pentenoxyl radicals (type B), we investigated bromocyclization of 2-vinyl- and 3-(2-dimethylvinylcyclohexylmethyloxy)-thiazolethiones *cis*/*trans*-**1d–e** (Tables 5 and 6).

(*i*) *Methods of alkenoxyl radical generation and product analysis*. Thermally induced reactions between *O*-(2-vinylcycloalkyl-1-methyloxy) thiohydroxamates *cis*-**1d**/**e** and bromotrichloromethane furnish 81% of 7-bromomethyltetrahydrofuran *cis*-**3d** and 95% of bromoisopropyl derivative *cis*-**3e** (entry 2 in Tables 5 and 6). The former reaction provided in addition 5% of the diastereomerically pure 6-*endo*-cyclized product *cis*-**5d**, which was not obtained from dimethylvinyl-congener *cis*-**1e** (GC-MS).

Heating *O*-(2-vinylcycloalkyl-1-methyloxy) thiohydroxamate *trans*-**1d** in the presence of bromotrichloromethane furnishes an 80/20-mixture of 5-*exo*/6-*endo*-bromocyclized products *trans*-**3d** and *trans*-**5d**, whereas *O*-[2-(dimethylvinyl)-cyclohexyl-methyl] ester *trans*-**1e** affords bromopropyltetrahydrofuran *trans*-**3e** as a single diastereomer (Tables 5 and 6, entry 4). Photochemical reactions gave 13–20% lower yields of bromocyclization products **3** and **5** taken together, and 8–19% less thiazole **2**, than thermally initiated reactions (entries 1 and 3 in Tables 5 and 6).

(*ii*) *Effect of methyl substitution at the terminal alkene carbon*. Substituting two hydrogens at the terminal alkene carbon by methyl improves the stereoselectivity and regioselectivity in cyclization of type-B 4-pentenoxyl radicals (Tables 5 and 6). Terminal methyl groups furthermore improve the regioselectivity of the intramolecular addition, occurring with 80/20-selectivity for *trans*-**Id**, 94/6 for *cis*-**Id**, and 5-*exo*-specifically for *cis*/*trans*-**Ie** (GC-MS; Table 5, entries 2 and 4, and Table 6).

Table 6 Products formed from 3-{[(2-methylpropenyl)-cyclohexyl]-methyloxy}-thiazolethione **1e** and $BrCCl_3$

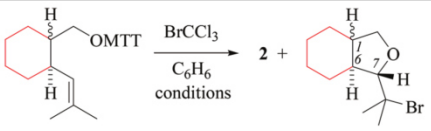

(±)-**1e** (±)-**3e**

Entry	**1e**	Conditions	**2**/%	**3e**/% (6,7-*cis* : *trans*)
1	*cis*	*hν*/25 °C	82	1,6-*cis*: 80[a] (>99 : 1)
2	*cis*	AIBN/80 °C	90	1,6-*cis*: 95[a] (>99 : 1)
3	*trans*	*hν*/25 °C	79	1,6-*trans*: 81[a] (>99 : 1)
4	*trans*	AIBN/80 °C	98	1,6-*trans*: 94[a] (>99 : 1)

[a] Single diastereomer, according to proton-NMR- and GC-MS-data.

Table 5 Bromocyclization products formed from 3-[(2-vinylcyclohexyl)methyloxy]-thiazolethione **1d** and $BrCCl_3$

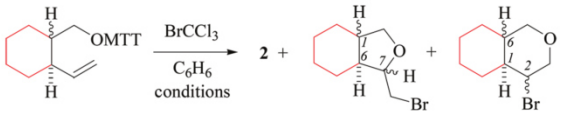

(±)-**1d** (±)-**3d** (±)-**5d**

Entry	**1d**	Conditions	**2**/%	**3d**/% (6,7-*cis* : *trans*)	**5d**/% (1,2-*cis* : *trans*)
1	*cis*	*hν*/25 °C	71	1,6-*cis*[a]: 70 (20 : 80)	1,6-*cis*[a]: 3 (99 : 1)
2	*cis*	AIBN/80 °C	88	1,6-*cis*[a]: 81 (21 : 79)	1,6-*cis*[a]: 5 (99 : 1)
3	*trans*	*hν*/25 °C	78	1,6-*trans*[a]: 57 (7 : 93)	1,6-*trans*[a]: 10 (50 : 50)
4	*trans*	AIBN/80 °C	97	1,6-*trans*[a]: 70 (10 : 90)	1,6-*trans*[a]: 17 (41 : 59)

[a] Stereodescriptor referring to the configuration of bridgehead carbons in products **3d** and **5d**.

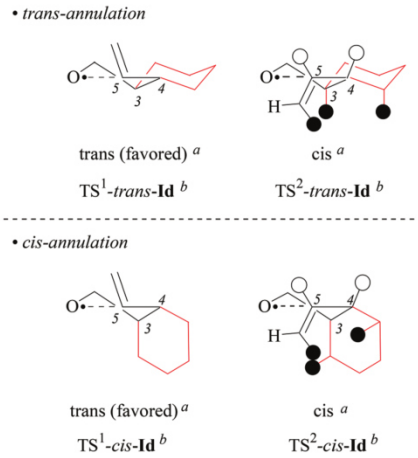

Fig. 5 Transition structure models for explaining the origin of 2,3-*trans*-stereoselectivity in 5-*exo*-cyclization type-B pentenoxyl radicals, exemplified by favored intermediates TS^1-*cis*/*trans*-**Id** and disfavored intermediates TS^2-*cis*/*trans*-**Id**. Hydrogen atoms drawn as black circles give rise to 1,3-diaxial repulsion, ecliptically arranged hydrogens are drawn as open circles. [a]Stereodescriptor referring to the configuration at carbons 2 and 3 in cyclized radical **IId** (*cf.* Fig. 3). [b]Stereodescriptor referring to the configuration at carbons 3 and 4 in TS-**Id**.

(*iii*) *Stereochemical guidelines*. 2,3-Cycloalkyl-bridged 4-pentenoxyl radicals **Id–e** cyclize 2,3-*trans*-selectively, indicating that the principal stereoinductor in cyclization of type-B radicals is the substituent in position 3 of the radical. Fusing 4-pentenoxyl radicals in relative *trans*-positions of cyclohexane enhances stereodifferentiation by the principal inductor.

(*iv*) *On the origin of 2,3-trans-selectivity in 5-exo-cyclization of type-B 4-pentenoxyl radicals*. Models built as instructed in section 2.1 show that type-B cyclohexyl-bridged 4-pentenoxyl radicals *cis*/*trans*-**Id–e** cyclize 2,3-*trans*-selectively, because steric constraints disfavor the 2,3-*cis*-mode of ring closure. In transition structures for 2,3-*cis*-cyclization, van der Waals repulsion between the (*E*)-positioned alkene substituent and the axially arranged hydrogens raises conformational free energy. The second aspect raising conformational free energy thus disfavoring a transition structure is eclipsing of hydrogens bound to carbons 4 and 5 (for TS^2-*trans*-**Id** and TS^2-*cis*-**Id**; Fig. 5). Extending the size of the (*E*)-substituent from hydrogen to methyl raises transannular repulsion, explaining the stereodirecting effect of a terminal substituent in cyclization of *cis*/*trans*-**Ie**.

2.2.3 3,4-Annulation – 2-(2-methylenecyclohexyl)-1-ethyloxyl radical reactions. To explore the selectivity in intramolecular addition of a 3,4-cyclohexyl-bridged 4-pentenoxyl radical (type C), we investigated photochemical and thermal reactions between 3-[2-(2-methylenecyclohexyl)-ethyloxy]-thiazolethione **1f** and bromotrichloromethane (Table 7).

(*i*) *Methods of alkoxyl radical generation and product analysis*. 3-[2-(2-methylenecyclohexyl)-ethyloxy]-thiazolethione **1f** furnishes the 5-*exo*-bromocyclized product *cis*-**3f** as a single diastereomer, bridgehead brominated oxadecalin **5f**, and 2-(trichloromethylsulfanyl)-thiazole **2**, when heated in the presence of bromotrichloromethane at 80 °C (Table 7, entry 2). The photochemical reaction provides a similar product pattern, although lower yields of compounds **2** and *cis*-**3f**. The fraction of bromotetrahydropyran **5f** remained almost unchanged (Table 7, entry 1).

Table 7 Products formed from 3-[2-(2-methylenecyclohexyl)-ethyl-1-oxyl]-thiazolethione **1f** and $BrCCl_3$

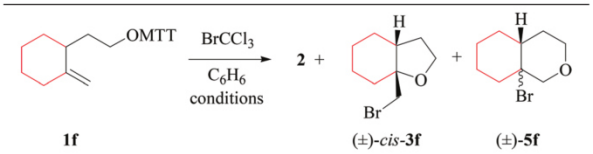

Entry	Conditions	**2**/%	*cis*-**3f**/%	**5f**/% (*cis* : *trans*)
1	*hν*/25 °C	54	24	21 (19 : 81)
2	AIBN/80 °C	80	35	22 (32 : 68)

The 5-*exo*/6-*endo*-selectivity of radical **If** (53 : 47) at room temperature falls below the value reported for the 4-methyl-4-pentenoxyl radical (69 : 31) and is higher than the regioselectivity determined for the 4-*tert*-butyl-4-pentenoxyl radical (46 : 54).[17] Regioselectivity in 4-pentenoxyl radical cyclization originates from a balance between FMO attractions, torsional strain, and steric shielding. A carbon substituent in position 4 lowers the barrier for 6-*endo*-addition based on favorable frontier molecular orbital (FMO) interactions for the C,O-addition to the terminal carbon. Steric blocking of the incoming oxygen radical gradually lowers the rate of 5-*exo*-addition as the size of the carbon substituent in position 4 increases. The fraction tetrahydropyranyl radical **IVf** obtained from 6-*endo*-cyclization of **If** is in line with the general mechanistic interpretation.[17] Homolytic bromination of tetrahydropyranyl radical **IVf** occurs for steric reasons preferentially from the axial side (Scheme 4), similar to bromination of structurally related cyclohexyl radicals.[53]

(*ii*) *Stereochemical guideline*. Methylenecyclohexylethoxyl radical **If** cyclizes 2,3-*cis*-specifically (Scheme 4).

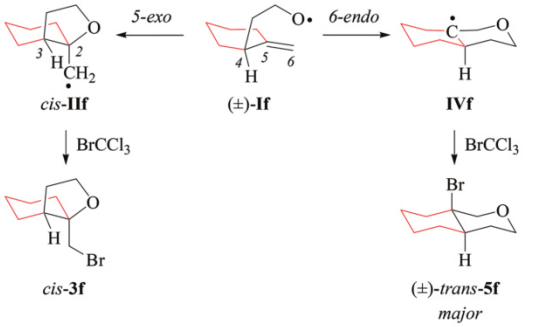

Scheme 4 Stereoselectivity in cyclization of the 1-methylenecyclohexyl-2-ethyloxyl radical **If** (type C).

Table 8 Products formed from 3-[(1-methylcyclohex-1-en-4-yl)-methyloxy]-thiazolethione **1g** and $BrCCl_3$ and diagnostic proton-NMR shift values of bromocyclization product **3g**[a]

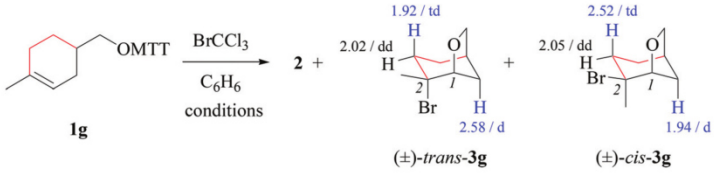

Entry	Conditions	**2**/%	**3g**/% (1,2-*cis* : *trans*)
1	*hν*/25 °C	69	64 (28 : 72)
2	AIBN/80 °C	76	72 (19 : 81)

[a] Protons experiencing deshielding by changing the position of the carbon–bromine bond from *anti* to *syn*, and *vice versa*, are printed in blue.

2.3 Cyclization onto endocyclic double bonds

For investigating the stereoselectivity in intramolecular addition to endocyclic double bonds we examined bromocyclization of 3-[2-(2-methylenecyclohexyl)-ethyloxy]-thiazolethione **1g** (type D; section 3.1) and verbenylethanol-derived thiohydroxamate **1h** (type E; section 3.2).

2.3.1 The (cyclohexen-4-yl-)-methyloxyl radical cyclization. (*i*) *Methods of alkoxyl radical generation and product analysis*. Photochemical and thermal reactions between 3-[(1-methylcyclohex-1-en-4-yl)-methyloxy]-thiazolethione **1g** and bromotrichloromethane furnish the 5-*exo*-bromocyclized product **3g** and substituted thiazole **2** (Table 8, entries 1 and 2).

Bicyclic tetrahydrofuran **3g** forms at 80 °C as a 19/81-mixture of 1,2-*cis*/*trans*-stereoisomers. Resonances of protons in β- and γ-positions to the carbon–bromine bond experience a shift dispersion by ~0.5 ppm upon changing orientation of the bromosubstituent from anticlinal *or* antiperiplanar to synclinal (Table 8). We address this phenomenon to magnetic anisotropy induced by the carbon–bromine bond, possibly in combination with three nonbonding electron pairs at bromine.[54]

(*ii*) *Stereochemical guideline*. Cyclohexenylmethyloxyl radical **1g** cyclizes 2,4-*cis*-specifically (Scheme 5).

2.3.2 The verbenylethyloxyl radical cyclization. (*i*) *Products from photochemical activation*. Verbenylethanol-derived thiohydroxamate **1h** furnishes tricyclic bromides **6** and **7** in a total yield of 61%, besides 79% of 2-(trichloromethylsulfanyl)-4-methylthiazole **2**, when photolyzed in the presence of bromotrichloromethane (Scheme 6).

(*ii*) *Stereochemical guideline*. Cyclohexenylethyloxyl radical **Ih** cyclizes *cis*-specifically (Scheme 7).

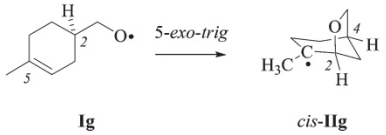

Scheme 5 2,4-*cis*-cyclization of alkenoxyl radical **Ig** (type D; from **1g**).

(*iii*) *Verbenylethyloxyl radical chemistry*. In extension to the chemistry summarized in this article, we propose that tricyclic products **6** and **7** arise from a sequence composed of intramolecular addition **Ih** → *cis*-**IIh**, ring-opening of cyclobutylmethyl radical *cis*-**IIh**, and bromine atom trapping by rearranged radicals **V** and **VI** (Scheme 7). 1,2-Shifting of the methylene bridge releases cyclobutyl strain in radical *cis*-**IIh**, leading to the secondary carbon radical **V**. For steric reasons, we expect trapping of the bicyclic radical **V** by bromotrichloromethane to occur from the concave face due to shielding of the convex side with the vicinal *exo*-oriented methyl group. The minor product **7**, according to the proposed model, results from 1,2-shifting of the dimethylmethylene bridge *cis*-**IIh** → **VI** and subsequent homolytic bromination.

2.4 Strain effects in alkoxyl radical additions

For estimating differences in energy barriers associated with 2,3-*cis*- and 2,3-*trans*-cyclization of type-E alkenoxyl radicals, we modelled energetics associated with 5-*exo*-cyclization using electronic structure methods.[55,56] The 2-(cyclohexen-3-yl)-ethyloxyl radical **Ii**, in this approach, served as a truncated model for the verbenyl-4-ethyloxyl radical **Ih**, while the 4-pentenoxyl radical 5-*exo*-cyclization **Ij** → **IIj** and the methoxyl radical addition to the inner carbon of propene served as references (Schemes 8 and 9).

(*i*) *Density functional theory*. For computing ground state energies of radicals and energies of transition structures, we used Becke's three parameter Lee–Young–Parr-hybrid functional (B3LYP)[57,58] and Becke's half and half Lee–Young–Parr hybrid functional (BHandHLYP)[59] in combination with 6-31+G**- and 6-311G**-basis sets.[56] All selected density functional/basis set-combinations reproduce experimental stereo- and regioselectivity for oxygen radical addition to carbon–carbon double bonds with a precision coming close to the accuracy for determining experimental selectivity.[8,14,17,52,60]

(*ii*) *Theoretical approach*. For calculating equilibrium structures of conformational flexible molecules and transition structures associated with radical addition to carbon–carbon double bonds we used an established strategy.[8,14] According to theory, the 2-(cyclohexen-3-yl)-ethyloxyl radical **Ii** favors

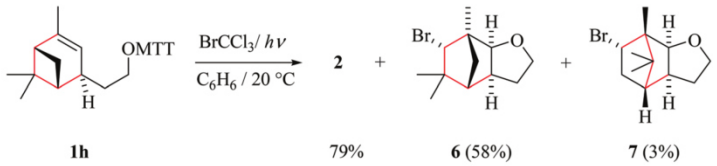

Scheme 6 Formation of bicyclic products from 3-(verbenylethyloxy)-thiazole-2(3*H*)-thione **1h**.

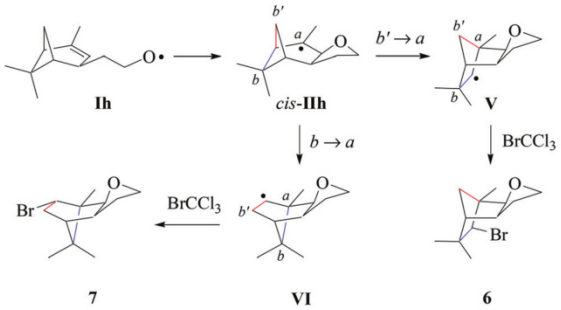

Scheme 7 Proposed pathways for product formation from verbenylethyloxyl radical **Ih** (type E; from **1h**).

pseudo-equatorial (pe) positioning of the ethyloxyl radical side to pseudo-axial (pa), as expressed by a modelled 90/10-mixture of pe/pa-conformers of **Ii** at 298 K (B3LYP/6-31+G**; ESI‡). Both conformers served as starting points for modeling 5-*exo*-cyclizations.

Equilibrium structures of propene, alkoxyl radicals **Ii–k**, cyclized radicals **IIi–j**, and the addition product **VIII** lack in negative eigenvalues of second derivatives of energy-minimized wavefunctions. Transition structures TS-**I** and TS-**VII** show one imaginary frequency *i*, describing the trajectory of oxygen radical addition to the inner alkene carbon (Table 9).[61]

Attempts to localize a transition structure for the *trans*-5-*exo*-cyclization of conformer pa-**Ii** led to TS^1-*trans*-**Ii**, already available from conformer pe-**Ii**.

(*iii*) *Quality of the models*. Computed wavefunctions characterizing equilibrium structures show expectation values for the spin operator $\langle S^2 \rangle$ close to 0.75 for oxygen and carbon radicals (ESI‡), as expected for doublet states. Wavefunctions describing transition structures show $\langle S^2 \rangle$-values of ~0.77 for B3LYP-calculated intermediates and 0.82–0.84 for BHandHLYP-calculated transition structures (ESI‡). The effect of spin contamination in BHandHLYP-calculated transition structures was discussed previously, but is not considered relevant for attaining reasonable precision in determining computed relative energies.[52]

(*iv*) *Methoxyl radical addition to propene*. Theory predicts a lower barrier for methoxyl radical addition to the terminal carbon than for addition to the inner carbon of propene (ΔG^{298} = −5.0 to −8.5 kJ mol^{-1}; ESI‡). The decision to compare structure and energetics from the disfavored mode of addition to data obtained for monocycle and bicycle formation was guided by structural similarity between TS-**Ii–j** and TS-**VII** on one side, and derived addition products **IIi–j**, **VIII** on the other (Table 9, Schemes 8 and 9).

(*v*) *Thermochemistry*. Cyclization of the 2-(cyclohexen-3-yl)-ethyloxyl radical **Ii** → **IIi**, according to zero-point energy corrected reaction energies (B3LYP/6-31+G**), is for all considered

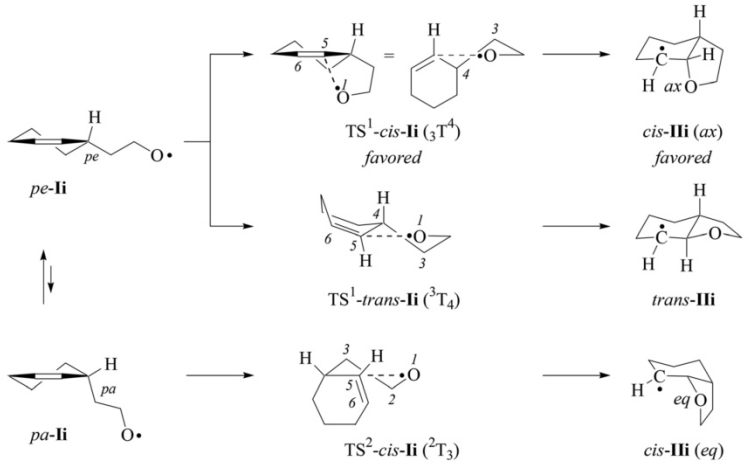

Scheme 8 Structure formulas of radicals and intermediates associated with the 1-(cyclohexen-3-yl)-ethyl-2-oxyl radical 5-*exo*-cyclization (pe = pseudo-equatorial; pa = pseudo-axial; ax = axial; eq = equatorial).

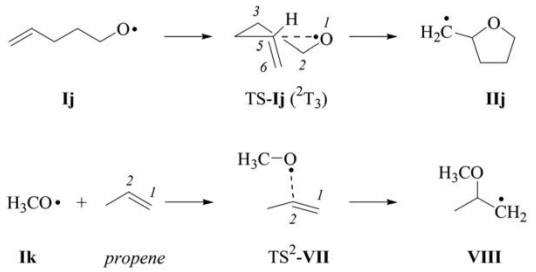

Scheme 9 Structure formulas of radicals and intermediates associated with the 4-pentenoxyl radical 5-*exo*-cyclization (top) and methoxyl radical addition to the inner carbon of propene (bottom; for discussion of TS^1-VII, refer to the text and the ESI‡).

Table 9 Selected geometrical parameters of transition structures TS^{1,2}-*cis*/*trans*-Ii, TS-j and TS-VII[a]

I	i[b]/cm^{-1}	d = O1–C5[c]/Å	α = O1–C5–C6[d]/°	ω = H5–C4–C5–C6[e]/°
TS^1-*cis*-**Ii** ($_3$T^4)	−342	2.077	103.5	161.6
	(−496)	(2.024)	(103.9)	(159.4)
	[−529]	[2.018]	[103.0]	[158.5]
TS^1-*trans*-**Ii** (^{3}T$_4$)	−397	2.042	122.7	152.9
	(−547)	(2.003)	(121.6)	(152.2)
	[−575]	[1.986]	[121.3]	[151.5]
TS^2-*cis*-**Ii** (^{2}T$_3$)	−353	2.058	100.8	−160.5
	(−500)	(2.010)	(101.5)	(−158.6)
	[−531]	[1.990]	[101.6]	[−157.6]
TS-**Ij**	−382	2.046	99.1	162.1
	(−531)	(1.996)	(100.4)	(159.9)
	[−558]	[1.997]	[100.5]	[159.0]
TS^2-**VII**[f]	−334	2.061	98.3	161.2
	(−489)	(1.999)	(100.6)	(158.6)
	[−517]	[1.979]	[100.8]	[157.8]

[a] B3LYP/6-31+G**-calculated values; numbers in parentheses arise from BHandHLYP/6-31+G**-calculations and values in brackets from BHandHLYP/6-311G**-calculations. [b] i = imaginary mode of vibration. [c] O–C2 for TS^2-**VII**. [d] O–C2–C1 for TS^2-**VII**. [e] C–C2–H2–C1 for TS^2-**VII**. [f] For the transition structure TS^1-**VII**, refer to the ESI.

pathways strongly exothermic ($\Delta_R E$ = −35 to −47 kJ mol^{-1}), pointing to a notable barrier for the reverse reaction, the β-fragmentation. Computed energetics for the addition **Ii** → **IIi** are similar to the values calculated for the 4-pentenoxyl radical ring closure **Ij** → **IIj** ($\Delta_R E$ = −41 kJ mol^{-1}), and are less exothermic than the methoxyl radical addition to the inner carbon of propene ($\Delta_R E$ = −53 mol^{-1}). BHandHLYP-calculations provide similar trends for reaction energies, except for a stronger driving force for the intermolecular addition (Table 10).

(*vi*) *Transition structures*. The distance d between the radical oxygen and the attacked carbon, as predicted by B3LYP theory for transition structures of cyclohexenylethyloxyl radical cyclization (2.04–2.08 Å), 4-pentenoxyl radical cyclization (2.05 Å) and methoxyl radical addition to propene (2.06 Å), is marginally wider than those obtained from BHandHLYP-calculations (1.98–2.02 Å; Table 9). Values for the angle α describing oxygen radical attack to the inner alkene carbon are grouped for all calculated transition structures in the range between 98 and 104 degrees, being more acute than the angle calculated for the highest in the energy transition structure TS-*trans*-**Ii** (^{3}T$_4$) (121–122 degrees; Table 9). Absolute values of improper torsion angles ω for transition structures TS-**Ii**, TS-**Ij**, and TS-**VIII**, according to B3LYP- and BHandHLYP-theory, are close to 160 degrees, indicating the hybridization change at the attacked carbon from sp^2 (ω = 180° for propene) toward sp^3 (122° for propane).

Superimposing atomic coordinates of 4-pentenoxyl radical cores illustrates that density functional-calculated favored transition structures for the cyclohexenylethyloxyl radical cyclization and the 4-pentenoxyl radical ring closure are nearly identical (Fig. 6). A $_3$T^4-conformation, as predicted by theory for TS-*cis*-**Ii** ($_3$T^4), is separated by only 36 degrees from a ^{2}T$_3$-conformer in TS-**Ij** (^{2}T$_3$) on the pseudorotatory cycle of tetrahydrofuran.[62]

(*vii*) *Energy barriers*. The barrier for 2,3-*cis*-cyclization of cyclohexenylethyloxyl radical **Ii** ($\Delta E^{\ddagger}$ = 17 kJ mol^{-1}) is similar to the barrier predicted by B3LYP-theory for the 4-pentenoxyl radical 5-*exo*-cyclization (20 kJ mol^{-1}) and the methoxyl radical addition to propene (21 kJ mol^{-1}). BHandHLYP-computed barriers for 2,3-*cis*-cyclization of **Ii** and 5-*exo*-cyclization of **Ij** are higher, but generally show the same trends (Table 10).

The computed relative Gibbs free energy of activation for the 2,3-*trans*-mode of cyclization is 55 kJ mol^{-1} above the value for the lowest in the energy pathway of 2,3-*cis*-ring closure (B3LYP; 58 kJ mol^{-1} for BHandHLYP calculations using either the 6-31+G** or the 6-311G** basis set; ESI‡). A Gibbs free activation energy difference of 55 kJ mol^{-1} translates for a kinetically controlled reaction and a temperature of 298.15 K into a relative rate constant of 4 × 10^9 in favor of the 2,3-*cis*-cyclization. Detecting a 2,3-*trans*-bromocyclized product with such a precision was beyond the capability of analytic instruments used in the study.

(*viii*) *Marcus analysis*. For analyzing strain and electronic effects on barriers of 5-*exo*-alkenoxyl radical cyclization, we split zero-point vibrational energy-corrected electronic barriers ($\Delta E^{\ddagger}$) into an intrinsic ($\Delta E^{\ddagger}_i$) and a thermodynamic term ($\Delta E^{\ddagger}_{TD}$), using Marcus theory (Fig. 7, Table 10, eqn (1)–(3)).[63–65] The intrinsic part describes contributions of strain and steric repulsion in a thermoneutral degenerated reaction to the barrier $\Delta E^{\ddagger}_i$ in a transition structure located half way on the reaction coordinate ($x^{\ddagger}$ = 0.5) between reactant(s) (x = 0) and product(s) (x = 1; Fig. 7). The thermodynamic part of the barrier $\Delta E^{\ddagger}_{TD}$ describes energy changes arising from incipient bond forming and bond breaking in a transition structure.

$$\Delta E^{\ddagger}_i = \frac{\Delta E^{\ddagger} - \frac{\Delta_R E}{2} + \sqrt{(\Delta E^{\ddagger})^2 - (\Delta_R E)(\Delta E^{\ddagger})}}{2} \quad (1)$$

$$x^{\ddagger} = \frac{1}{2}\left(1 + \frac{\Delta_R E}{4\Delta E^{\ddagger}}\right) \quad (2)$$

$$\Delta E^{\ddagger} = \Delta E^{\ddagger}_i + \Delta E^{\ddagger}_{TD} \quad (3)$$

(*ix*) *Localizing transition structures – the $x^{\ddagger}$-value*. According to Marcus theory, reaction energies and barriers obtained from

Table 10 Zero-point vibrational energy-corrected activation energies ($\Delta E^{\ddagger}$), reaction energies ($\Delta_R E$), intrinsic energy barriers ($\Delta E^{\ddagger}_i$), thermodynamic contribution $\Delta E^{\ddagger}_{TD}$ to $\Delta E^{\ddagger}$, free energy differences [$\Delta G^{298} = G^{298}$(I) − G^{298}(II) or $\Delta G^{298} = [G^{298}$(Ik) + G^{298}(propene)] − G^{298}(VIII)] and approximated transition location $x^{\ddagger}$ for alkoxyl radical additions (Schemes 8 and 9, eqn (1)–(3))

Reaction	Method	$\Delta E^{\ddagger}$/kJ mol^{-1}	$\Delta_R E$/kJ mol^{-1}	$\Delta E^{\ddagger}_i$/kJ mol^{-1}	$\Delta E^{\ddagger}_{TD}$/kJ mol^{-1}	$x^{\ddagger}$
pe-**Ii** → *cis*-**IIi** (ax)	B3LYP/6-31+G**	16.7	−44.1	35.4	−18.6	0.2
	BHandHLYP/6-31+G**	39.3	−46.4	60.3	−21.0	0.4
	BHandHLYP/6-311G**	40.6	−44.7	60.9	−20.3	0.4
pe-**Ii** → *trans*-**IIi**	B3LYP/6-31+G**	73.1	−34.5	89.5	−16.4	0.4
	BHandHLYP/6-31+G**	99.1	−35.7	116.3	−17.2	0.5
	BHandHLYP/6-311G**	100.7	−33.7	116.9	−16.2	0.5
pa-**Ii** → *cis*-**IIi** (eq)	B3LYP/6-31+G**	17.4	−46.8	37.1	−19.7	0.2
	BHandHLYP/6-31+G**	39.5	−50.4	62.2	−22.7	0.3
	BHandHLYP/6-311G**	40.9	−49.0	63.1	−22.1	0.4
Ij → **IIj**	B3LYP/6-31+G**	19.8	−40.5	37.3	−17.5	0.2
	BHandHLYP/6-31+G**	41.0	−43.5	60.8	−19.8	0.4
	BHandHLYP/6-311G**	41.7	−41.8	60.8	−19.1	0.4
Ik + propene → **VIII**	B3LYP/6-31+G**	20.5	−53.8	43.2	−22.7	0.2
	BHandHLYP/6-31+G**	37.3	−61.2	64.2	−27.0	0.3
	BHandHLYP/6-311G**	36.3	−61.0	63.1	−26.8	0.3

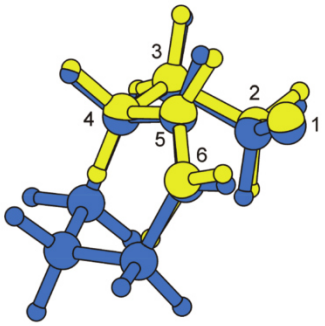

Fig. 6 Match plot of B3LYP/6-31+G**-computed transition structures TS-*cis*-**Ii** ($_3T^4$) (blue) and TS-**Ij** ($^2T_3$) (yellow).

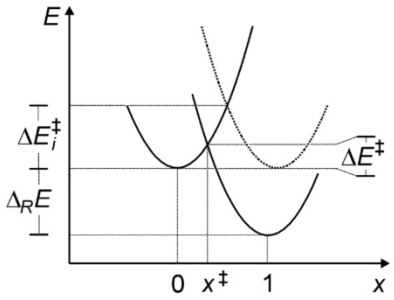

Fig. 7 Potential energy curves $E(x)$ for reaction associated with an energy change $\Delta_R E$ across a barrier $\Delta E^{\ddagger}$, having an intrinsic barrier $\Delta E^{\ddagger}_i$, according to Marcus-theory, and harmonic potentials of the identical curvature for the initial (x = 0) and final state (x = 1).

B3LYP-calculations translate into a $x^{\ddagger}$-value of 0.2 for positioning transition structures on the respective reaction coordinates for C,O-addition (eqn (2)). Transition structures predicted from BHandHLYP-calculated energies are positioned later on the same reaction coordinate ($x^{\ddagger}$ = 0.3–0.5), due to higher barriers $\Delta E^{\ddagger}$. Considering the magnitude of the experimental rate constant $k^{add} = 5 \times 10^8$ s^{-1} for the 4-pentenoxyl 5-*exo*-cyclization **Ij** → **IIj**[2] and computed significant reaction energies, we expect transition structures of alkoxyl radical additions in extension to the Hammond-postulate[66] to be localized early on a reaction coordinate, rather than midway between reactant **I** and product **II**.

(*x*) *The role of the thermodynamic barrier*. In transition structures associated with alkoxyl radical addition to alkenes, incipient carbon–oxygen bond formation and carbon–carbon π-bond breaking in summary is exothermic, lowering the intrinsic barrier by a thermodynamic contribution of −19 to −20 kJ mol^{-1}. This thermodynamic barrier $\Delta E^{\ddagger}_{TD}$ is surprisingly similar for 2,3-*cis*- and 2,3-*trans*-ring cyclization of cyclohexenylethyloxyl radical **Ii** (−16 to −20 kJ mol^{-1}), the 4-pentenoxyl radical 5-*exo*-cyclization **Ij** → **IIj** (−18 kJ mol^{-1}; B3LYP/6-31+G**), and the barrier for methoxyl radical addition to the inner carbon of propene (−23 kJ mol^{-1}). BHandHLYP-computed energies lead to more negative thermodynamic barriers, but show otherwise similar trends. From the data we concluded that the thermodynamic barrier is not the key parameter for explaining the experimental 2,3-*cis*-specificity of verbenylethyloxyl radical cyclization.

(xi) *The role of the intrinsic barrier*. Intrinsic barriers modelled for 2,3-*cis*-cyclization of cyclohexenylethyloxyl radical **Ii** ($\Delta E^{\ddagger}_i$ = 35–37 kJ mol^{-1}, B3LYP; for BHandHLYP-calculated values, refer to Table 10) and 5-*exo*-cyclization of 4-pentenoxyl radical **Ij** (37 kJ mol^{-1}) are marginally smaller than the intrinsic barrier for methoxyl radical addition to the inner carbon of propene (43 kJ mol^{-1}). An intrinsic barrier of 90 kJ mol^{-1} predicted for 2,3-*trans*-cyclization of the cyclohexenylethyloxyl radical **Ii** exceeds the value for the barriers of all other investigated oxygen radical additions in the study by far. From this information we concluded that the experimentally observed 2,3-*cis*-stereospecificity of the verbenylethyloxyl radical cycliza-

View Article Online
Organic & Biomolecular Chemistry Paper

tion originates from a large intrinsic barrier associated with the 2,3-*trans*-ring closure.

3. Concluding remarks

Cycloalkyl-fused and -bridged 4-pentenoxyl radicals provide bicyclic and tricyclic tetrahydrofurans by 5-*exo*-cyclizations. The selectivity determining step is the intramolecular oxygen radical addition to the carbon–carbon double bond, occurring in most instances with notable stereochemical preference. From the observed stereoselectivities we concluded that a system exists, which can be summed up by two new directives for predicting the stereochemical outcome of similar cyclizations not exemplified in this article. The new guidelines supplement the set of existing directives, developed for predicting the major products in synthesis of monocyclic disubstituted tetrahydrofurans by the oxygen radical method.[7,14,67]

The first of the new guidelines ranks the hierarchy of two similarly sized stereoinductors by the distance between the alkyl group and the alkene carbon which is being approached by the oxygen radical. This guideline states that the substituent positioned the closest to the attacked alkene carbon is the principal (primary) inductor, guiding 5-*exo*-cyclization 2,3-*trans*- and 2,4-*cis*-selectively. The substituent bound further from the attacked π-bond is the secondary inductor, enhancing stereodifferentiation exerted by the principal inductor in the case of the *trans*-configuration, and decreasing this effect in the case of the *cis*-configuration. A secondary inductor is not able to overrule the guiding effect of a similarly sized primary inductor. The first guideline applies to 5-*exo*-cyclization of type-A and type-B 4-pentenoxyl radicals (Fig. 1).

The second new directive states that 4-pentenoxyl radical 5-*exo*-cyclization to a cyclohexene-bound *exo*-methylene group or an endocyclic double bond occurs *cis*-specifically. The second guideline refers to intramolecular addition of type-C–E radicals (Fig. 1).

From the hierarchy of similar-sized inductors we expect a substituent located in position 3 to also control the stereoselectivity in 5-*exo*-cyclization of 4-pentenoxyl radicals having similar sized substituents attached to carbons 1, 2, and 3. According to the first new guideline, a group in position 2 will be secondary and a group in position 1 the least effective, the tertiary inductor. From today's point of view we expect the stereoisomer of a 1,2,3-substituted 4-pentenoxyl radical corresponding to an all-*trans*-configured type-A and type-B radical to cyclize with notable 2,3-*trans*-, 2,4-*cis*-, and 2,5-*trans*-selectivity, possibly providing a single diastereomer. In the same model, a sterically more demanding substituent in position 2, for example *tert*-butyl, should be able to overrule the effect of a smaller group in position 3, such as methyl. Stereochemical questions of this kind attracted our attention and are being pursued at the moment in our laboratory, with the aim to provide new solutions to synthesis of functionalized ethers from oxygen radical addition to alkenes.

4. Experimental

4.1. General

For general laboratory practice and instrumentation see ref. 42 and the ESI.‡

4.2. General methods

4.2.1 3-Hydroxy-4-methylthiazole-2(3*H*)-thione tetraethylammonium salt (MTTO$^-$NEt$_4^+$). A solution of 3-hydroxy-4-methylthiazole-2(3*H*)-thione (MTTOH; 1.3 mmol) in methanol (2 mL) was treated at 20 °C with a 1.5 M solution of tetraethylammonium hydroxide in methanol (0.87 mL, 1.3 mmol) and stirred for 1 hour. The solvent was removed under reduced pressure and the residue was freeze-dried for 12–14 hours.

4.2.2 Synthesis of *O*-alkenylthiohydroxamates. A suspension of 3-hydroxy-4-methylthiazole-2(3*H*)-thione tetraethylammonium salt (1.3 mmol) in anhydrous dimethyl formamide (1 mL) was treated at 20 °C with a solution of an alkenyl *p*-toluenesulfonate (1 mmol) in anhydrous dimethyl formamide (1 mL) for the time span specified in section 3. The resulting solution was stirred at 20 °C or 40–50 °C (for specific information, see synthetic procedures in section 4.3) diluted with dichloromethane (10 mL) and washed with an aqueous 2 M solution of sodium hydroxide (10 mL) and water (3 × 10 mL). The organic layer was separated, dried ($MgSO_4$), and concentrated under reduced pressure to leave a residue, which was purified by chromatography (SiO_2) or crystallized (solvent specification in section 4.3).

4.3 3-Alkenyloxy-4-methylthiazole-2(3*H*)-thiones

4.3.1 3-[*cis*-2-(Prop-2-en-1-yl)-cyclopent-1-yloxy]-4-methylthiazole-2(3*H*)-thione *cis*-(1a). From *trans*-2-(prop-2-en-1-yl)-cyclopent-1-yl 4-toluenesulfonate (4.22 g, 15.1 mmol); reaction time: 72 hours at 20 °C, the eluent used for chromatography: dichloromethane–pentane = 2 : 1 (v/v), R_f = 0.51. Yield: 2.67 g (10.5 mmol, 70%), colorless oil.[36] ^{1}H-NMR ($CDCl_3$, 600 MHz) δ 1.60–1.75 (m, 3 H), 1.80–1.84 (m, 1 H), 1.87–1.93 (m, 2 H), 2.03–2.06 (m, 1 H), 2.22 (d, J = 1.2 Hz, 3 H), 2.22–2.27 (m, 1 H), 2.67–2.71 (m, 1 H), 4.99–5.01 (m, 1 H), 5.08 (dq, J_d = 17.0, J_q = 1.7 Hz, 1 H), 5.74–5.77 (m, 1 H), 5.98–6.05 (m, 1 H), 6.16 (q, J = 0.9 Hz, 1 H). ^{13}C-NMR ($CDCl_3$, 150 MHz) δ 13.8, 21.8, 29.2, 29.3, 30.1, 45.2, 88.2, 102.9, 115.4, 137.9, 139.2, 181.0. UV (methanol): λ_{max} (lg ε/m^2 mol^{-1}) 319 nm (3.14), 210 nm (3.05). Anal. Calcd for $C_{12}H_{17}NOS_2$ (255.40): C, 56.43; H, 6.71; N, 5.48; S, 25.11; Found: C, 56.48; H, 6.56; N, 5.68; S, 25.27.

4.3.2 3-[*trans*-2-(Prop-2-en-1-yl)-cyclopent-1-yloxy]-4-methylthiazole-2(3*H*)-thione *trans*-(1a). From *cis*-2-(prop-2-en-1-yl)-cyclopent-1-yl 4-toluenesulfonate (1.85 g, 6.60 mmol); reaction time: 1 hour at 45 °C; the eluent used for chromatography: diethyl ether–pentane = 1 : 1 (v/v), R_f = 0.38. Yield: 1.13 g (4.42 mmol, 67%), yellow oil.[36] ^{1}H-NMR ($CDCl_3$, 400 MHz) δ 1.28–1.37 (m, 1 H), 1.67–1.84 (m, 3 H), 1.86–1.93 (m, 1 H), 1.98–2.09 (m, 1 H), 2.21–2.30 (m, 2 H), 2.24 (d, J = 1.2 Hz, 3 H), 2.22–2.27 (m, 1 H), 4.97–5.05 (m, 2 H), 5.43–5.46 (m, 1 H), 5.78 (ddt, J_d = 17.0, 10.2, J_t = 6.8 Hz, 1 H), 6.16 (q, J = 1.4 Hz, 1 H). ^{13}C-NMR ($CDCl_3$, 100 MHz) δ 14.1, 23.2, 30.4, 30.6, 37.6, 43.7,

92.1, 102.9, 116.3, 136.4, 138.8, 181.0. UV (methanol): λ_{max} (lg ε/m^2 mol^{-1}) 319 nm (3.17), 208 nm (3.09). Anal. Calcd for $C_{12}H_{17}NOS_2$ (255.40): C, 56.43; H, 6.71; N, 5.48; S, 25.11; Found: C, 56.49; H, 6.85; N, 5.46; S, 24.96.

4.3.3 3-[*cis*-2-(3-Methylbut-2-en-1-yl)-cyclopent-1-yloxy]-4-methylthiazole-2(3*H*)-thione *cis*-(1b). From [*trans*-2-(3-methylbut-2-en-1-yl)-cyclopent-1-yl] 4-toluenesulfonate (2.48 g, 8.04 mmol); reaction time: 21 hours at 20 °C; the eluent used for chromatography: diethyl ether–pentane = 1 : 2 (v/v), R_f = 0.30. Yield: 1.49 g (5.26 mmol, 65%), colorless oil. ^{1}H-NMR ($CDCl_3$, 400 MHz) δ 1.59–1.76 (m, 3 H), 1.64 (s, 3 H), 1.71 (s, 3 H), 1.77–2.03 (m, 4 H), 2.18–2.30 (m, 1 H), 2.23 (d, J = 1.4 Hz, 3 H), 2.47–2.59 (m, 1 H), 5.33 (ddt, J_d = 7.9, 6.5, J_t = 1.5 Hz, 1 H), 5.72 (td, J_t = 4.5, J_d = 1.7 Hz, 1 H), 6.15 (d, J = 1.4 Hz, 1 H). ^{13}C-NMR ($CDCl_3$, 100 MHz) δ 13.8, 17.9, 21.9, 25.8, 27.1, 29.1, 29.4, 46.0, 88.5, 102.8, 123.5, 132.0, 139.2, 181.0. UV (methanol): λ_{max} (lg ε/m^2 mol^{-1}) 318 nm (3.14), 205 nm (3.16). Anal. Calcd for $C_{14}H_{21}NOS_2$ (283.45): C, 59.32; H, 7.47; N, 4.94; S, 22.62; Found: C, 59.33; H, 7.38; N, 5.03; S, 22.47.

4.3.4 3-[*cis*-2-(Prop-2-en-1-yl)-cyclohex-1-yloxy]-4-methylthiazole-2(3*H*)-thione *cis*-(1c). From [*trans*-2-(prop-2-en-1-yl-cyclohex-1-yl] 4-toluenesulfonate (6.30 g, 21.4 mmol); reaction time: 13 days at 40 °C; the eluent used for chromatography: diethyl ether–pentane = 1 : 2 (v/v), R_f = 0.28. Conversion 84%. Yield: 637 mg (2.36 mmol, 11%), colorless oil. ^{1}H-NMR ($CDCl_3$, 600 MHz) δ 1.23–1.49 (m, 4 H), 1.54–1.83 (m, 4 H), 2.09–2.38 (m, 2 H), 2.25 (s, 3 H), 2.55–2.62 (m, 1 H), 4.99–5.08 (m, 2 H), 5.25–5.32 (m, 1 H), 5.73–5.84 (m, 1 H), 6.16 (d, J = 1.2 Hz, 1 H). ^{13}C-NMR ($CDCl_3$, 150 MHz) δ 14.2, 20.4, 23.8, 26.1, 26.7, 30.5, 37.5, 85.2, 102.8, 116.1, 137.2, 139.1, 180.7. UV (methanol): λ_{max} (lg ε/m^2 mol^{-1}) 318 nm (3.18), 210 nm (3.12). Anal. Calcd for $C_{13}H_{19}NOS_2$ (269.42): C, 57.96; H, 7.11; N, 5.20; S, 23.80; Found: C, 57.94; H, 7.34; N, 5.47; S, 23.73.

4.3.5 3-[*trans*-2-(Prop-2-en-1-yl)-cyclohex-1-yloxy]-4-methylthiazole-2(3*H*)-thione *trans*-(1c). From [*cis*-2-(prop-2-en-1-yl)-cyclohex-1-yl] 4-toluenesulfonate (1.63 g, 5.54 mmol); reaction time: 3 hours at 45 °C; the eluent used for chromatography: diethyl ether–pentane = 1 : 2 (v/v), R_f = 0.32. Yield: 412 mg (1.53 mmol, 28%), colorless oil, which crystallizes on standing at 20 °C. M.p. = 62–63 °C. ^{1}H-NMR ($CDCl_3$, 400 MHz) δ 1.03–1.13 (m, 1 H), 1.14–1.30 (m, 2 H), 1.32–1.44 (m, 1 H), 1.61–1.73 (m, 2 H), 1.73–1.84 (m, 2 H), 1.87–1.96 (m, 1 H), 2.13 (dt, J_d = 14.3, J_t = 8.3 Hz, 1 H), 2.24 (d, J = 1.2 Hz, 3 H), 2.83 (dddd, J = 14.1, 4.8, 3.4, 1.9 Hz, 1 H), 4.94–5.15 (m, 3 H), 5.79–5.97 (m, 1 H), 6.15 (d, J = 1.2 Hz, 1 H). ^{13}C-NMR ($CDCl_3$, 100 MHz) δ 14.1, 24.2, 25.0, 30.19, 30.23, 36.4, 41.8, 86.0, 102.8, 116.3, 136.8, 139.2, 180.7. UV (methanol): λ_{max} (lg ε/m^2 mol^{-1}) 318 nm (3.14), 211 nm (3.04). Anal. Calcd for $C_{13}H_{19}NOS_2$ (269.42): C, 57.96; H, 7.11; N, 5.20; S, 23.80; Found: C, 58.16; H, 7.16; N, 5.19; S, 23.67.

4.3.6 3-[*cis*-2-(Eth-1-en-1-yl)-cyclohex-1-ylmethyloxy]-4-methylthiazole-2(3*H*)-thione *cis*-(1d). From [*cis*-2-(eth-1-en-1-yl)-cyclohex-1-ylmethyl] 4-toluenesulfonate (1.50 g, 5.10 mmol); reaction time: 3 hours at 50 °C; the eluent used for chromatography: diethyl ether–pentane = 1 : 2 (v/v), R_f = 0.33. Yield: 1.03 g (3.81 mmol, 75%), colorless oil, which crystallizes on standing at −18 °C. M.p. = 61–62 °C. ^{1}H-NMR ($CDCl_3$, 400 MHz) δ 1.34–1.65 (m, 6 H), 1.67–1.79 (m, 2 H), 2.16–2.22 (m, 1 H), 2.23 (d, J = 1.2 Hz, 3 H), 2.50 (dq, J_d = 8.3, J_q = 4.1 Hz, 1 H), 4.18 (dt, J_d = 23.0, J_t = 7.1 Hz, 2 H), 4.98–5.12 (m, 2 H), 6.02 (ddd, J = 17.1, 10.4, 8.4 Hz, 1 H), 6.14 (d, J = 1.2 Hz, 1 H). ^{13}C-NMR ($CDCl_3$, 100 MHz) δ 13.5, 22.2, 24.3, 25.5, 30.5, 38.5, 40.9, 78.2, 102.6, 115.8, 137.7, 138.4, 180.2. UV (methanol): λ_{max} (lg ε/m^2 mol^{-1}) 316 nm (3.19), 206 nm (3.11). Anal. Calcd for $C_{13}H_{19}NOS_2$ (269.42): C, 57.96; H, 7.11; N, 5.20; S, 23.80; Found: C, 57.89; H, 6.94; N, 5.20; S, 23.44.

4.3.7 3-[*trans*-2-(Eth-1-en-1-yl)-cyclohex-1-ylmethyloxy]-4-methylthiazole-2(3*H*)-thione *trans*-(1d). From [*trans*-2-(eth-1-en-1-yl)-cyclohex-1-ylmethyl] 4-toluenesulfonate (650 mg, 2.20 mmol); reaction time: 3 h at 40 °C; the eluent used for chromatography: diethyl ether–pentane = 1 : 2 (v/v), R_f = 0.33. Yield: 466 mg (1.73 mmol, 79%), yellow oil, which crystallizes from diethyl ether to afford colorless crystals. M.p. = 51–52 °C. ^{1}H-NMR ($CDCl_3$, 400 MHz) δ 1.14–1.41 (m, 4 H), 1.65–1.82 (m, 4 H), 1.84–1.96 (m, 1 H), 2.14–2.29 (m, 1 H), 2.24 (d, J = 1.0 Hz, 3 H), 4.10 (t, J = 7.6 Hz, 1 H), 4.41 (dd, J = 7.3, 3.4 Hz, 1 H), 4.97–5.04 (m, 2 H), 5.71 (ddd, J = 17.2, 10.0, 9.1 Hz, 1 H), 6.13 (d, J = 0.7 Hz, 1 H). ^{13}C-NMR ($CDCl_3$, 100 MHz) δ 13.5, 25.4, 25.6, 29.5, 33.5, 41.0, 44.6, 79.3, 102.6, 114.9, 137.7, 142.2, 180.3. UV (methanol): λ_{max} (lg ε/m^2 mol^{-1}) 317 nm (3.13), 208 nm (3.05). Anal. Calcd for $C_{13}H_{19}NOS_2$ (269.42): C, 57.96; H, 7.11; N, 5.20; S, 23.80; Found: C, 57.92; H, 7.05; N, 5.20; S, 23.70.

4.3.8 3-[*cis*-2-(2-Methylprop-1-en-1-yl)-cyclohex-1-ylmethyloxy]-4-methylthiazole-2(3*H*)-thione *cis*-(1e). From [*cis*-2-(2-methylprop-1-en-1-yl)-cyclohex-1-ylmethyl] 4-toluenesulfonate (1.06 g, 3.28 mmol); reaction time: 4 hours at 50 °C; the eluent used for chromatography: diethyl ether–pentane = 1 : 2 (v/v), R_f = 0.31. Yield: 761 mg (2.56 mmol, 78%), colorless oil, colorless crystals on standing at 20 °C. M.p. = 78 °C. ^{1}H-NMR ($CDCl_3$, 400 MHz) δ 1.29–1.56 (m, 6 H), 1.62 (d, J = 1.5 Hz, 3 H) 1.67–1.81 (m, 2 H), 1.71 (d, J = 1.5 Hz, 3 H), 2.11–2.25 (m, 1 H), 2.21 (d, J = 1.4 Hz, 3 H), 2.71–2.80 (m, 1 H), 4.15 (d, J = 6.8 Hz, 2 H), 5.35 (ddt, J_d = 9.8, 3.0, J_t = 1.5 Hz, 1 H), 6.13 (q, J = 1.4 Hz, 1 H). ^{13}C-NMR ($CDCl_3$, 100 MHz) δ 13.1, 18.0, 21.9, 24.8, 25.0, 26.2, 31.8, 34.3, 38.9, 78.9, 102.5, 123.5, 132.9, 137.8, 180.3. UV (methanol): λ_{max} (lg ε/m^2 mol^{-1}) 316 nm (3.10), 204 nm (3.18). Anal. Calcd for $C_{15}H_{23}NOS_2$ (297.48): C, 60.56; H, 7.79; N, 4.71; S, 21.55; Found: C, 60.43; H, 7.68; N, 4.76; S, 21.43.

4.3.9 3-[*trans*-2-(2-Methylprop-1-en-1-yl)-cyclohex-1-ylmethyloxy]-4-methyl-thiazole-2(3*H*)-thione *trans*-(1e). From [*trans*-2-(2-methylprop-1-en-1-yl)-cyclohex-1-ylmethyl] 4-toluenesulfonate (2.72 g, 8.44 mmol); reaction time: 2 hours at 45 °C; the eluent used for chromatography: diethyl ether–pentane = 1 : 2 (v/v), R_f = 0.31. Yield: 1.86 g (6.25 mmol, 74%), yellow oil, which was crystallized from ethyl acetate to afford a colorless solid. M.p. = 47–48 °C. ^{1}H-NMR ($CDCl_3$, 400 MHz) δ 1.01–1.15 (m, 1 H), 1.20–1.40 (m, 3 H), 1.54–1.86 (m, 4 H), 1.57 (d, J = 1.0 Hz, 3 H), 1.67 (d, J = 0.7 Hz, 3 H), 1.98–2.11 (m, 1 H), 2.14–2.29 (m, 1 H), 2.22 (d, J = 1.2 Hz, 3 H), 4.07 (t, J = 7.6 Hz, 1 H), 4.35 (dd, J = 7.3, 3.2 Hz, 1 H), 4.97 (dt, J_d = 9.3, J_t =

1.5 Hz, 1 H), 6.12 (d, J = 1.5 Hz, 1 H). ^{13}C-NMR ($CDCl_3$, 100 MHz) δ 13.2, 18.1, 25.6, 25.7, 25.8, 29.9, 33.4, 38.7, 42.1, 79.5, 102.5, 128.8, 131.7, 137.8, 180.2. UV (methanol): λ_{max} ($\lg \varepsilon$/m^2 mol^{-1}) 317 nm (3.13), 209 nm (3.02). Anal. Calcd for $C_{15}H_{23}NOS_2$ (297.48): C, 60.56; H, 7.79; N, 4.71; S, 21.55; Found: C, 60.41; H, 7.73; N, 4.74; S, 21.47.

4.3.10 3-[2-(1-Methylenecyclohex-2-yl)-eth-1-yl-2-oxy]-4-methylthiazole-2(3*H*)-thione (1f). From [2-(1-methylenecyclohex-2-yl)-ethyl] 4-toluenesulfonate (3.60 mg, 12.2 mmol); reaction time: 1 hour at 50 °C; the eluent used for chromatography: diethyl ether–pentane = 1 : 1 (v/v), R_f = 0.39. Yield: 2.57 g (9.54 mmol, 78%), yellow oil. ^{1}H-NMR ($CDCl_3$, 400 MHz) δ 1.25–1.38 (m, 1 H), 1.42–1.55 (m, 2 H), 1.56–1.74 (m, 2 H), 1.76–1.89 (m, 2 H), 2.03 (ddd, J = 13.0, 8.5, 4.5 Hz, 1 H), 2.14 (td, J_t = 14.1, J_d = 7.2 Hz, 1 H), 2.20–2.39 (m, 2 H), 2.27 (d, J = 1.2 Hz, 3 H), 4.38 (q, J = 7.3 Hz, 1 H), 4.45 (q, J = 7.3 Hz, 1 H), 4.60 (s, 1 H), 4.70 (s, 1 H), 6.15 (d, J = 1.2 Hz, 1 H). ^{13}C-NMR ($CDCl_3$, 100 MHz) δ 13.4, 24.1, 28.6, 30.0, 34.0, 34.7, 39.4, 74.8, 102.6, 106.1, 137.7, 151.6, 180.3. UV (methanol): λ_{max} ($\lg \varepsilon$/m^2 mol^{-1}) 316 nm (3.18), 206 nm (3.10). Anal. Calcd for $C_{13}H_{19}NOS_2$ (269.42): C, 57.96; H, 7.11; N, 5.20; S, 23.80. Found: C, 57.74; H, 7.12; N, 5.14; S, 23.93.

4.3.11 3-[(1-Methylcyclohex-1-en-4-yl)-methyloxy]-4-methylthiazole-2(3*H*)thione (1g). From [(1-methylcyclohex-1-en-4-yl)-methyl] 4-toluenesulfonate (4.20 g, 15.0 mmol); reaction time: 75 hours at 20 °C or 2 hours at 40 °C. Yield: 3.13 g (12.3 mmol, 82%), yellow oil, which was crystallized from methanol–ethyl acetate [2/1 (v/v)] to afford colorless crystals. M.p. 99–100 °C. ^{1}H-NMR ($CDCl_3$, 400 MHz) δ 1.40–1.49 (m, 1 H), 1.63 (s, 3 H), 1.86–2.02 (m, 4 H), 2.09–2.25 (m, 2 H), 2.26 (d, J = 1.2 Hz, 3 H), 4.22–4.32 (m, 2 H), 5.34–5.44 (m, 1 H), 6.16 (d, J = 1.2 Hz, 1 H). ^{13}C-NMR ($CDCl_3$, 100 MHz) δ 13.4, 23.5, 25.5, 28.1, 29.0, 32.5, 74.8, 102.7, 119.1, 134.0, 137.7, 180.3. UV (methanol): λ_{max} ($\lg \varepsilon$/m^2 mol^{-1}) 317 nm (3.11), 206 nm (3.06). Anal. Calc. for $C_{12}H_{17}NOS_2$ (255.39): C, 56.43; H, 6.71; N, 5.49; S, 25.11; Found: C, 56.34; H, 6.69; N, 5.46; S, 25.26. X-ray crystallography. T = 150(2) K, λ = 0.71073 Å, monoclinic, $P2_1/n$, a = 9.1980(3) Å, b = 13.3225(3) Å, c = 10.6301(3) Å, β = 100.318(3)°, Z = 4, μ = 0.395 mm^{-1}, completeness 99.6% (2θ = 57.0), goodness-of-fit on F^2 = 1.009; final R indices [$I > 2\sigma(I)$]: R_1 = 0.0373, wR_2 = 0.0891.

4.3.12 3-[{(1*S*,4*S*,5*R*)-2,6,6-Trimethyl-bicyclo[3.1.1]-hept-2-en-4-yl}eth-1-yl-2-oxy]-4-methylthiazole-2(3*H*)-thione (1h). From [2-{(1*S*,4*S*,5*R*)-2,6,6-trimethylbicyclo-[3.1.1]hept-2-en-4-yl]}-ethyl] 4-toluenesulfonate (686 mg, 2.05 mmol); reaction time: 20 hours at 20 °C; the eluent used for chromatography: diethyl ether–pentane = 1 : 2 (v/v), R_f = 0.28. Yield: 463 mg (1.50 mmol, 73%) colorless oil, which crystallizes on standing at 20 °C. $[\alpha]_D^{25}$ = −52.9 (c = 1.02/ethanol). ^{1}H-NMR ($CDCl_3$, 600 MHz) δ 0.86 (s, 3 H), 1.15 (d, J = 9.0 Hz, 1 H), 1.29 (s, 3 H), 1.67 (t, J = 1.7 Hz, 3 H), 1.79 (dq, J_d = 14.0, J_q = 7.0 Hz, 1 H), 1.89 (dq, J_d = 13.8 Hz, J_q = 6.9 Hz, 1 H), 1.95–2.05 (m, 2 H), 2.21 (dt, J_d = 8.8, J_t = 5.6 Hz, 1 H), 2.28 (d, J = 1.0 Hz, 3 H), 2.48–2.57 (m, 1 H), 4.41–4.52 (m, 2 H), 5.19 (d, J = 0.8 Hz, 1 H), 6.15 (d, J = 1.0 Hz, 1 H). ^{13}C-NMR ($CDCl_3$, 150 MHz) δ 13.5, 20.4, 22.9, 26.5, 27.8, 31.6, 36.4, 40.8, 45.1, 47.6, 75.0, 102.7, 119.3, 137.7, 145.5, 180.4. Anal. Calcd for $C_{16}H_{23}NOS_2$ (309.49): C, 62.09; H, 7.49; N, 4.53; S, 20.72; Found: C, 61.81; H, 7.51; N, 4.56; S, 21.09.

4.4 Alkoxyl radical reactions

4.4.1 Photochemical reactions. A solution of 3-alkoxythiazolethione **1** (1.00 mmol, c_1^0 = 0.17 M) and $BrCCl_3$ (10 mmol, c^0_{BrCCl3} = 1.67 M) in dry C_6H_6 (6 mL) was photolyzed at ~25 °C in a Rayonet® chamber reactor equipped with twelve 350 nm illuminants, until the starting material was completely consumed (~30 min, tlc). The solution was concentrated under reduced pressure (10 mbar, 40 °C) to leave an oil, which was purified by chromatography (SiO_2).

4.4.2 Thermal reactions. A solution of 3-alkoxythiazolethione **1** (1.00 mmol, c_1^0 = 0.17 M), $BrCCl_3$ (10 mmol, c^0_{BrCCl3} = 1.67 M), and AIBN (25 mol%) in dry C_6H_6 (6 mL) was heated to 80 °C for 30 min. After complete consumption of **1** (tlc), the solvent was removed under reduced pressure (10 mbar, 40 °C) to leave a residue, which was purified by chromatography (SiO_2).

4.4.3 Conversion of 3-[*cis*-2-(prop-2-en-1-yl)-cyclopent-1-yloxy]-4-methylthiazole-2(3*H*)-thione *cis*-(1a). *Photochemical reaction*. *cis*-**1a** 528 mg (2.07 mmol); the eluent used for column chromatography: diethyl ether–pentane = 1 : 5 (v/v). *3-Bromomethyl-2-oxabicyclo[3.3.0]octane cis*-(**3a**). Yield: 42.3 mg (206 μmol, 10%), yellow liquid, 70/30-mixture of 1,3-*cis*/*trans*-isomers, *i.e.* *rel*-(1*S*,3*S*,5*S*)-**3a**/*rel*-(1*S*,3*R*,5*S*)-**3a**. R_f = 0.48 for diethyl ether–pentane = 1 : 5 (v/v). Anal. Calcd for $C_8H_{13}BrO$ (205.09): C, 46.85; H, 6.39; Found: C, 46.73; H, 6.40. *rel*-(1*S*,3*S*,5*S*)-**3a**: ^{1}H-NMR ($CDCl_3$, 400 MHz) δ 1.37–1.47 (m, 1 H), 1.50–1.68 (m, 3 H), 1.69–1.92 (m, 3 H), 1.98 (ddd, J = 12.8, 8.7, 7.2 Hz, 1 H), 2.68–2.75 (m, 1 H), 3.29–3.36 (m, 1 H), 3.36–3.42 (m, 1 H), 4.23 (quin, J = 6.2 Hz, 1 H), 4.60 (t, J = 4.8 Hz, 1 H). ^{13}C-NMR ($CDCl_3$, 100 MHz): δ 24.6, 32.8, 34.7, 35.5, 38.4, 42.8, 78.8, 85.7. *rel*-(1*S*,3*R*,5*S*)-**3a**: ^{1}H-NMR ($CDCl_3$, 400 MHz) δ 1.16–1.30 (m, 1 H), 1.37–1.47 (m, 1 H), 1.50–1.68 (m, 3 H), 1.69–1.92 (m, 2 H), 2.22–2.35 (m, 1 H), 2.65–2.78 (m, 1 H), 3.44 (d, J = 5.5 Hz, 2 H), 3.89 (dq, J_d = 10.3, J_q = 5.3 Hz, 1 H), 4.45 (t, J = 6.3 Hz, 1 H). ^{13}C-NMR ($CDCl_3$, 100 MHz). δ 23.3, 33.2, 33.8, 34.6, 39.3, 42.9, 78.8, 85.8. *4-Methyl-2-(trichloromethylsulfanyl)-thiazole* (**2**). Yield: 438 mg (1.76 mmol, 85%), yellow liquid. R_f = 0.40 for diethyl ether–pentane = 1 : 5 (v/v). ^{1}H-NMR ($CDCl_3$, 400 MHz) δ 2.57 (s, 3 H), 7.30 (s, 1 H). ^{13}C-NMR ($CDCl_3$, 100 MHz) δ 17.3, 96.9, 122.6, 153.2, 155.8. Anal. Calcd for $C_5H_4NCl_3S_2$ (248.57): C, 24.16; H, 1.62; N, 5.64; S, 25.80. Found: C, 24.17; H, 1.82; N, 5.70; S, 25.50. *5-Bromoct-7-enal* (**4a**). Yield: 253.6 mg (1.24 mmol, 60%), yellow liquid. R_f = 0.28 for diethyl ether–pentane = 1 : 5 (v/v). ^{1}H-NMR ($CDCl_3$, 600 MHz) δ 1.71–1.97 (m, 4 H), 2.43–2.54 (m, 2 H), 2.62 (t, J = 6.6 Hz, 2 H), 3.91–4.11 (m, 1 H), 5.10–5.18 (m, 2 H), 5.84 (ddt, J_d = 17.0, 10.3, J_t = 6.9 Hz, 1 H), 9.78 (t, J = 1.6 Hz, 1 H). ^{13}C-NMR ($CDCl_3$, 100 MHz) δ 20.1, 37.5, 43.0, 43.2, 55.3, 118.1, 134.5, 201.8. HRMS (EI$^+$) m/z 204.0149/206.0124 (M$^+$); calculated mass for $C_8H_{13}OBr^+$: 204.0150/206.0129. *Thermal reaction*. *cis*-**1a** 526 mg (2.06 mmol). Eluent used for column chromatography: diethyl ether–pentane = 1 : 5 (v/v). *3-Bromomethyl-2-oxabicyclo[3.3.0]octane cis*-(**3a**). Yield: 33.4 mg

(163 μmol, 8%), yellow liquid, 71/29-mixture of 1,3-*cis*/*trans*-isomers, *i.e.* *rel*-(1*S*,3*S*,5*S*)-**3a**/*rel*-(1*S*,3*R*,5*S*)-**3a**. *4-Methyl-2-(trichloromethylsulfanyl)-thiazole* (**2**). Yield: 446 mg (1.80 mmol, 87%), yellow liquid. *5-Bromoct-7-enal* (**4a**). Yield: 230 mg (1.12 mmol, 54%), yellow liquid.

4.4.4 Conversion of 3-[*trans*-2-(prop-2-en-1-yl)-cyclopent-1-yloxy]-4-methylthiazole-2(3*H*)-thione *trans*-(1a). *Photochemical reaction*: *trans*-**1a** 203 mg (795 μmol); eluent used for column chromatography: diethyl ether–pentane = 1 : 5 (v/v). *4-Methyl-2-(trichloromethylsulfanyl)-thiazole* (**2**). Yield: 110 mg (443 μmol, 56%), yellow liquid. *5-Bromoct-7-enal* (**4a**). Yield: 72.5 mg (354 μmol, 44%), yellow liquid. *Unlike*-5,7-*dibromo-9,9,9-trichlorononanal*. Yield: 9.3 mg (23.1 μmol, 3%), yellow liquid. R_f = 0.22 for diethyl ether–pentane = 1 : 5 (v/v). ^{1}H-NMR ($CDCl_3$, 400 MHz) δ 1.72–2.05 (m, 4 H), 2.40–2.67 (m, 4 H), 3.23 (dd, J = 15.9, 4.8 Hz, 1 H), 3.47 (dd, J = 16.0, 5.3 Hz, 1 H), 4.18–4.29 (m, 1 H), 4.37 (ddt, J_d = 8.0, 6.6, J_t = 5.1 Hz, 1 H), 9.80 (t, J = 1.5 Hz, 1 H). ^{13}C-NMR ($CDCl_3$, 100 MHz) δ 19.6, 35.8, 42.9, 44.8, 48.3, 51.9, 62.3, 96.6, 201.5. HRMS (EI^+) m/z 400.8288/402.8250 (M − H); calculated mass for $C_9H_{12}OCl_3Br_2^+$: 400.8291/402.8261. *Like*-5,7-*dibromo-9,9,9-trichlorononanal*. Yield: 36.8 mg (91.2 μmol, 11%), yellow liquid. R_f = 0.20 for diethyl ether–pentane = 1 : 5 (v/v). ^{1}H-NMR ($CDCl_3$, 600 MHz) δ 1.75–2.01 (m, 4 H), 2.23 (ddd, J = 15.3, 11.6, 2.1 Hz, 1 H), 2.46–2.61 (m, 3 H), 3.24 (dd, J = 15.7, 6.2 Hz, 1 H), 3.57 (dd, J = 15.7, 4.6 Hz, 1 H), 4.21–4.35 (m, 1 H), 4.70 (dddd, J = 11.2, 6.5, 4.4, 2.4 Hz, 1 H), 9.80 (t, J = 1.2 Hz, 1 H). ^{13}C-NMR ($CDCl_3$, 100 MHz) δ 20.0, 38.2, 42.9, 47.5, 48.0, 54.4, 62.6, 96.6, 201.5. HRMS (EI^+) m/z 400.8314/402.8297/404.8233 (M − H); calculated mass for $C_9H_{12}OCl_3Br_2^+$: 400.8300/402.8312/404.8232. *Thermal reaction*. *trans*-**1a** 250 mg (979 μmol); eluent used for column chromatography: diethyl ether–pentane = 1 : 5 (v/v). *4-Methyl-2-(trichloromethylsulfanyl)-thiazole* (**2**). Yield: 208 mg (836 μmol, 85%), yellow liquid. *5-Bromoct-7-enal* (**4a**). Yield: 145.5 mg (709 μmol, 73%), yellow liquid. *Unlike-5,7-dibromo-9,9,9-trichlorononanal*. Yield: 19.2 mg (47.6 μmol, 5%), yellow liquid. *Like-5,7-dibromo-9,9,9-trichlorononanal*. Yield: 34.1 mg (84.5 μmol, 9%), yellow liquid.

4.4.5 Conversion of 3-[*cis*-2-(3-methylbut-2-en-1-yl)-cyclopent-1-yloxy]-4-methylthiazole-2(3*H*)-thione *cis*-(1b). *Photochemical reaction*. *cis*-**1b** 296 mg (1.04 mmol); eluent used for column chromatography: diethyl ether–pentane = 1 : 5 (v/v). *3-(2-Bromoprop-2-yl)-2-oxabicyclo[3.3.0]octane cis*-**3b**. Yield: 119 mg (510 μmol, 49%), 64/36-mixture of 1,3-*cis*/*trans*-isomers, *i.e.* *rel*-(1*S*,3*S*,5*S*)-**3b**/*rel*-(1*S*,3*R*,5*S*)-**3b**, pale yellow oil. R_f = 0.56 for diethyl ether–pentane = 1 : 5 (v/v). HRMS (EI^+) m/z 231.0399/233.0372 (M − H); calculated mass for $C_{10}H_{16}OBr^+$: 231.0385/233.0364. *rel*-(1*S*,3*S*,5*S*)-**3b**: ^{1}H-NMR ($CDCl_3$, 400 MHz) δ 1.35–1.51 (m, 2 H), 1.51–1.67 (m, 3 H), 1.71 (s, 3 H), 1.75 (s, 3 H), 1.78–1.86 (m, 1 H), 1.91 (dd, J = 13.1, 6.0 Hz, 1 H), 2.21 (ddd, J = 12.3, 9.5, 5.5 Hz, 1 H), 2.63–2.75 (m, 1 H), 3.62 (dd, J = 10.5, 5.4 Hz, 1 H), 4.45 (t, J = 6.3, Hz, 1 H). ^{13}C-NMR ($CDCl_3$, 100 MHz) δ 23.5, 30.3, 30.6, 33.4, 33.9, 37.1, 42.4, 67.0, 85.3, 86.7. *rel*-(1*S*,3*R*,5*S*)-**3b**: ^{1}H-NMR ($CDCl_3$, 400 MHz) δ 1.35–1.51 (m, 1 H), 1.51–1.76 (m, 6 H), 1.69 (s, 3 H), 1.73 (s, 3 H), 2.12 (dt, J_d = 12.9, J_t = 8.5 Hz, 1 H), 2.63–2.75 (m, 1 H), 3.91 (dd, J = 8.0, 6.6 Hz, 1 H), 4.61–4.67 (m, 1 H). ^{13}C-NMR ($CDCl_3$, 100 MHz) δ 24.9, 30.1, 30.8, 33.0, 34.9, 36.8, 43.5, 69.3, 86.7, 87.2. *4-Methyl-2-(trichloromethylsulfanyl)-thiazole* (**2**). Yield: 190 mg (764 μmol, 73%), pale yellow liquid. *5-Brom-8-methylnon-7-enal* (**4b**). Yield: 75.6 mg (324 μmol, 31%), pale yellow liquid. R_f = 0.25 for diethyl ether–pentane = 1 : 5 (v/v). ^{1}H-NMR ($CDCl_3$, 400 MHz) δ 1.62 (s, 3 H), 1.72 (s, 3 H), 1.76–2.02 (m, 4 H), 2.37–2.68 (m, 4 H), 3.93–4.03 (m, 1 H), 5.17 (t, J = 7.0 Hz, 1 H), 9.78 (s, 1 H). ^{13}C-NMR ($CDCl_3$, 150 MHz) δ 18.1, 20.3, 25.8, 37.5, 37.8, 43.1, 56.9, 120.5, 134.8, 201.9. HRMS (EI^+) m/z 232.0463/234.0452 (M^+); calculated mass for $C_{10}H_{17}OBr^+$: 232.0463/234.0442. *Thermal reaction*. *cis*-**1b** 292 mg (1.03 mmol); eluent used for column chromatography: diethyl ether–pentane = 1 : 5 (v/v). *3-(2-Bromoprop-2-yl)-2-oxoabicyclo[3.3.0]octane cis*-**3b**. Yield: 81.8 mg (351 μmol, 34%), 56/44-mixture of 1,3-*cis*/*trans*-isomers, *i.e.* *rel*-(1*S*,3*S*,5*S*)-**3b**/*rel*-(1*S*,3*R*,5*S*)-**3b**, yellow oil. *4-Methyl-2-(trichloromethylsulfanyl)-thiazole* (**2**). Yield: 193 mg (776 μmol, 75%), yellow liquid. *5-Brom-8-methylnon-7-enal* (**4b**). Yield: 84.2 mg (361 μmol, 35%), yellow liquid.

4.4.6 Conversion of 3-[*cis*-(2-prop-2-en-1-yl)-cyclohex-1-yloxy]-4-methylthiazole-2(3*H*)-thione *cis*-(1c). *Photochemical reaction*: *cis*-**1c** 137 mg (508 μmol); eluent used for chromatography: diethyl ether–pentane = 1 : 10 (v/v). *8-(Bromomethyl)-7-oxabicyclo[4.3.0]nonane cis*-(**3c**). Yield: 50.2 mg (229 μmol, 45%), 89/11-mixture of 6,8-*cis*/*trans*-isomers *i.e.* *rel*-(1*S*,6*S*,8*S*)-**3c**/*rel*-(1*S*,6*S*,8*R*)-**3c**, colorless liquid. R_f = 0.44 for diethyl ether–pentane = 1 : 10 (v/v). Anal. Calcd for $C_9H_{15}BrO$ (219.12): C, 49.33; H, 6.90. Found: C, 49.46; H, 6.80. *rel*-(1*S*,6*S*,8*S*)-**3c**. ^{1}H-NMR ($CDCl_3$, 400 MHz) δ 1.21–1.29 (m, 1 H), 1.31–1.37 (m, 1 H), 1.38–1.45 (m, 1 H), 1.47–1.56 (m, 3 H), 1.57–1.70 (m, 2 H), 1.76–1.85 (m, 1 H), 2.12–2.20 (m, 2 H), 3.40 (dd, J = 10.0, 6.7 Hz, 1 H), 3.53 (dd, J = 10.0, 5.9 Hz, 1 H), 3.91 (q, J = 5.0 Hz, 1 H), 4.15 (quin, J = 6.7 Hz, 1 H). ^{13}C-NMR ($CDCl_3$, 100 MHz) δ 21.4, 23.5, 28.5, 29.0, 36.4, 36.5, 37.6, 77.8, 78.3. *rel*-(1*S*,6*S*,8*R*)-**3c**. ^{1}H-NMR ($CDCl_3$, 400 MHz) δ 1.17–1.70 (m, 7 H), 1.76–1.85 (m, 1 H), 1.87–1.94 (m, 2 H), 2.06–2.12 (m, 1 H), 3.39 (dd, J = 6.6, 10.0 Hz, 1 H), 3.47 (dd, J = 10.0, 5.0 Hz, 1 H), 4.05 (q, J = 3.8 Hz, 1 H), 4.37–4.43 (m, 1 H). ^{13}C-NMR ($CDCl_3$, 100 MHz) δ 20.5, 24.0, 27.6, 28.1, 37.2, 37.8, 38.4, 76.4, 77.7. *4-Methyl-2-(trichloromethylsulfanyl)-thiazole* (**2**). Yield: 92.8 mg (373 μmol, 73%), colorless liquid. R_f = 0.36 for diethyl ether–pentane = 1 : 10 (v/v). *Thermal reaction*. *cis*-**1c** 81.6 mg (303 μmol); eluent used for chromatography: diethyl ether–pentane = 1 : 10 (v/v). *8-(Bromomethyl)-7-oxabicyclo[4.3.0]-nonane cis*-(**3c**). Yield: 40.6 mg (185 μmol, 61%), 68/32-mixture of 6,8-*cis*/6,8-*trans*-isomers, *i.e.* *rel*-(1*S*,6*S*,8*S*)-**3c**/*rel*-(1*S*,6*S*,8*R*)-**3c**, colorless liquid. *4-Methyl-2-(trichloromethylsulfanyl)-thiazole* (**2**). Yield: 55.9 mg (225 μmol, 74%), colorless liquid. *6-Bromo-8-nonenal* (**4c**). Yield: 7.8 mg (36.0 μmol, 12%), yellow oil.

4.4.7 Conversion of 3-[*trans*-(2-prop-2-en-1-yl)-cyclohex-1-yloxy)]-4-methylthiazole-2(3*H*)-thione *trans*-(1c). *Photochemical reaction*. *trans*-**1c** 139 mg (516 μmol); eluent used for chromatography: light petroleum–diethyl ether = 5 : 1 (v/v). *8-(Bromomethyl)-7-oxabicyclo[4.3.0]nonane*[28] *trans*-(**3c**). Yield: 55.0 mg (251 μmol, 49%), 8/92-mixture of 6,8-*cis*/6,8-*trans*-isomers,

i.e. rel-(1*R*,6*S*,8*S*)-**3c**/*rel*-(1*R*,6*S*,8*R*)-**3c**, colorless liquid. R_f = 0.50 for diethyl ether–pentane = 1 : 5 (v/v). *rel*-(1*R*,6*S*,8*S*)-**3c**: ^{1}H-NMR ($CDCl_3$, 400 MHz) δ 1.04–1.58 (m, 6 H), 1.67–2.13 (m, 5 H), 3.11 (dt, J_d = 3.7 Hz, J_t = 10.4 Hz, 1 H), 3.34 (dd, J = 6.7, 10.1 Hz, 1 H), 3.42 (dd, J = 4.9, 10.1 Hz, 1 H), 4.20–4.24 (m, 1 H). ^{13}C-NMR ($CDCl_3$, 100 MHz) δ 24.2, 25.7, 28.9, 31.2, 35.3, 36.3, 43.9, 76.7, 84.5. *rel*-(1*R*,6*S*,8*R*)-**3c**: ^{1}H-NMR ($CDCl_3$, 400 MHz) δ 1.08–1.53 (m, 6 H), 2.18–2.24 (m, 1 H), 1.69–2.12 (m, 4 H), 3.23 (dt, J_d = 4.0 Hz, J_t = 10.4 Hz, 1 H), 3.41 (dd, J = 6.5, 10.1 Hz, 1 H), 3.50 (dd, J = 5.3, 10.1 Hz, 1 H), 4.24–4.30 (m, 1 H). ^{13}C-NMR ($CDCl_3$, 100 MHz) δ 24.2, 25.5, 28.8, 31.3, 36.7, 37.1, 46.3, 77.3, 83.3. *Thermal reaction*. *cis*-**1c** 111 mg (412 µmol); eluent used for chromatography: diethyl ether–pentane = 1 : 5 (v/v). *8-(Bromomethyl)-7-oxabicyclo[4.3.0]nonane trans*-(**3c**). Yield: 63.1 mg (288 µmol, 70%), 13/87-mixture of 6,8-*cis*/*trans*-isomers, *i.e. rel*-(1*R*,6*S*,8*S*)-**3c**/*rel*-(1*R*,6*S*,8*R*)-**3c**, pale yellow liquid. *4-Methyl-2-(trichloromethylsulfanyl)-thiazole* (**2**). Yield: 81.8 mg (329 µmol, 80%), yellow liquid. *6-Bromo-8-nonenal* (**4c**). Yield: 7.4 mg (33.8 µmol, 8%), yellow oil. ^{1}H-NMR ($CDCl_3$, 400 MHz) δ 1.36–1.52 (m, 1 H), 1.54–1.74 (m, 3 H), 1.76–1.90 (m, 2 H), 2.47 (dt, J_d = 7.1, J_t = 1.8 Hz, 2 H), 2.61 (tt, J = 6.7, 1.3 Hz, 2 H), 4.02 (dtd, J_d = 8.2, 4.9, J_t = 6.5, Hz, 1 H), 5.09–5.19 (m, 2 H), 5.75–5.93 (m, 1 H), 9.78 (t, J = 1.6 Hz, 1 H). ^{13}C-NMR ($CDCl_3$, 100 MHz) δ 21.4, 27.1, 38.0, 43.3, 43.7, 55.8, 118.0, 134.7, 202.3. HRMS (EI^+) *m*/*z* 218.0296/220.0282 (M^+); calculated mass for $C_9H_{15}OBr^+$: 218.0306/220.0286.

4.4.8 Conversion of 3-[*cis*-2-(eth-1-en-1-yl)-cyclohex-1-ylmethyloxy]-4-methylthiazole-2(3*H*)-thione *cis*-(1d). *Photochemical reaction*. Yield of *cis*-**1d**: 131 mg (487 µmol); eluent used for chromatography: diethyl ether–pentane = 1 : 10 (v/v). *2-Bromo-4-oxabicyclo[4.4.0]decane cis*-(**5d**). Yield: 3.5 mg (16.0 µmol, 3%), *i.e. rel*-(1*S*,2*S*,6*R*)-**5d**, yellow liquid. R_f = 0.46 for diethyl ether–pentane = 1 : 10 (v/v). ^{1}H-NMR ($CDCl_3$, 600 MHz) δ 1.18–1.53 (m, 6 H), 1.63–1.89 (m, 2 H), 1.97–2.07 (m, 1 H), 2.09–2.23 (m, 1 H), 3.47 (t, J = 10.8 Hz, 1 H), 3.57–3.65 (m, 1 H), 3.67–3.76 (m, 1 H), 4.14 (dd, J = 11.1, 4.7 Hz, 1 H), 4.34 (td, J_t = 10.6, J_d = 4.5 Hz, 1 H). ^{13}C-NMR ($CDCl_3$, 150 MHz, −37.3 °C) δ 19.7, 25.1, 25.9, 28.5, 39.4, 42.2, 49.5, 73.3, 73.6. HRMS (EI^+) *m*/*z* 218.0307/220.0286 (M^+); calculated mass for $C_9H_{15}OBr^+$: 218.0306/220.0286. *7-Bromomethyl-8-oxabicyclo[4.3.0]nonane cis*-(**3d**). Yield: 75.1 mg (343 µmol, 70%), colorless liquid, 20/80-mixture of 6,7-*cis*/6,7-*trans*-isomers, *i.e. rel*-(1*R*,6*S*,7*R*)-**3d**/*rel*-(1*R*,6*S*,7*S*)-**3d**. R_f = 0.31 for diethyl ether–pentane = 1 : 10 (v/v). Anal. Calcd for $C_9H_{15}BrO$ (219.12): C, 49.33; H, 6.90. Found: C, 49.24; H, 6.88. *rel*-(1*R*,6*S*,7*R*)-**3d**. ^{1}H-NMR ($CDCl_3$, 400 MHz) δ 1.13–1.22 (m, 2 H), 1.23–1.39 (m, 1 H), 1.46–1.56 (m, 1 H), 1.57–1.67 (m, 3 H), 1.72–1.80 (m, 1 H), 2.12 (dq, J_d = 10.7, J_q = 5.4 Hz, 1 H), 2.48–2.60 (m, 1 H), 3.30–3.37 (m, 1 H) 3.37–3.46 (m, 1 H), 3.80 (dd, J = 11.1, 7.8 Hz, 1 H), 3.87–3.93 (m, 1 H), 4.15 (td, J_t = 7.2, J_d = 4.2 Hz, 1 H). ^{13}C-NMR ($CDCl_3$, 100 MHz) δ 20.7, 20.8, 23.6, 24.4, 30.8, 38.1, 40.4, 69.4, 82.7. *rel*-(1*R*,6*S*,7*S*)-**3d**. ^{1}H-NMR ($CDCl_3$, 400 MHz) δ 1.23–1.36 (m, 1 H), 1.39–1.49 (m, 3 H), 1.52–1.60 (m, 2 H), 1.61–1.70 (m, 2 H), 2.14 (quin, J = 6.0 Hz, 1 H), 2.20–2.30 (m, 1 H), 3.33–3.40 (m, 1 H), 3.42–3.49 (m, 1 H), 3.66 (dd, J = 8.1, 4.4 Hz, 1 H) 3.89 (dd, J = 8.0, 5.9 Hz, 1 H) 3.98–4.06 (m, 1 H). ^{13}C-NMR ($CDCl_3$, 100 MHz) δ 22.4, 23.5, 25.4, 25.9, 35.9, 38.4, 41.8, 72.8, 80.6. *4-Methyl-2-(trichloromethylsulfanyl)-thiazole* (**2**). Yield: 85.3 mg (343 µmol, 71%), colorless liquid. *Thermal reaction*. *cis*-**1d** 136 mg (505 µmol); eluent used for chromatography: diethyl ether–pentane = 1 : 10 (v/v). *2-Bromo-4-oxabicyclo[4.4.0]decane cis*-(**5d**). Yield: 5.6 mg (25.6 µmol, 5%), *i.e. rel*-(1*S*,2*S*,6*R*)-**5d**, yellow liquid. 6,7-*cis*-*7-Bromomethyl-8-oxabicyclo[4.3.0]nonane cis*-(**3d**). Yield: 19.0 mg (86.7 µmol, 17%), *rel*-(1*R*,6*S*,7*R*)-**3d** colorless liquid. 6,7-*trans*-*7-Bromomethyl-8-oxabicyclo[4.3.0]nonane cis*-(**3d**). Yield: 70.5 mg (322 µmol, 64%), *i.e. rel*-(1*R*,6*S*,7*S*)-**3d** colorless liquid. *4-Methyl-2-(trichloromethylsulfanyl)-thiazole* (**2**). Yield: 111 mg (446 µmol, 88%), colorless liquid.

4.4.9 Conversion of 3-[*trans*-2-(eth-1-en-1-yl)-cyclohex-1-ylmethyloxy]-4-methylthiazole-2(3*H*)-thione *trans*-(1d). *Photochemical reaction*. *trans*-**1d** 276 mg (1.02 mmol); eluent used for chromatography: diethyl ether–pentane = 1 : 10 (v/v). *2-Bromo-4-oxabicyclo[4.4.0]decane trans*-(**5d**). Yield: 11.8 mg (53.9 µmol, 5%), *rel*-(1*S*,2*S*,6*S*)-**5d** colorless liquid. R_f = 0.46 for diethyl ether–pentane = 1 : 10 (v/v). ^{1}H-NMR ($CDCl_3$, 400 MHz) δ 0.84–1.04 (m, 2 H), 1.24–1.42 (m, 3 H), 1.44–1.55 (m, 2 H), 1.73–1.84 (m, 2 H), 2.13–2.23 (m, 1 H), 3.13 (t, J = 10.9 Hz, 1 H), 3.43–3.57 (m, 1 H), 3.70–3.88 (m, 2 H), 4.12 (dd, J = 11.1, 4.7 Hz, 1 H). ^{13}C-NMR ($CDCl_3$, 100 MHz) δ 25.75, 25.83, 27.6, 30.7, 44.1, 49.7, 54.4, 73.2, 73.7. Anal. Calcd for $C_9H_{15}BrO$ (219.12): C, 49.33; H, 6.90. Found: C, 48.88; H, 6.86. HRMS (EI^+) *m*/*z* 218.0298/220.0277 (M^+); calculated mass for $C_9H_{15}OBr^+$: 218.0306/220.0286. *4-Methyl-2-(trichloromethylsulfanyl)-thiazole* (**2**). Yield: 199 mg (801 µmol, 78%), colorless liquid. 93/7-mixture of *exo*/*endo*-isomers *7-Bromomethyl-8-oxabicyclo[4.3.0]nonane trans*-(**3d**) and *2-Bromo-4-oxabicyclo-[4.4.0]-decane trans*-(**5d**). Yield: 137 mg (624 µmol, 61%), 7/93-mixture of 6,7-*cis*/*trans*-isomers, *i.e. rel*-(1*S*,6*S*,7*R*)-**3d**/*rel*-(1*S*,6*S*,7*S*)-**3d** and *rel*-(1*S*,2*R*,6*S*)-**5d**, colorless liquid. R_f = 0.25 for diethyl ether–pentane = 1 : 10 (v/v). Anal. Calcd for $C_9H_{15}BrO$ (219.12): C, 49.33; H, 6.90. Found: C, 49.04; H, 6.93. *rel*-(1*S*,6*S*,7*S*)-**3d**. ^{1}H-NMR ($CDCl_3$, 400 MHz) δ 1.03–1.19 (m, 2 H), 1.20–1.38 (m, 3 H), 1.66–1.97 (m, 5 H), 3.36–3.45 (m, 2 H), 3.52–3.58 (m, 1 H), 3.71 (ddd, J = 9.7, 5.5, 4.2 Hz, 1 H), 3.96 (t, J = 7.3 Hz, 1 H). ^{13}C-NMR ($CDCl_3$, 100 MHz) δ 25.3, 25.5, 27.4, 27.7, 35.3, 46.3, 49.7, 72.3, 81.6. *rel*-(1*S*,6*S*,7*R*)-**3d**. ^{1}H-NMR ($CDCl_3$, 400 MHz) δ 0.98–1.11 (m, 1 H), 1.14–1.28 (m, 3 H), 1.62–1.72 (m, 2 H), 1.75–1.97 (m, 4 H), 3.15–3.24 (m, 1 H), 3.25–3.34 (m, 2 H), 3.97–4.04 (m, 1 H), 4.21–4.29 (m, 1 H). ^{13}C-NMR ($CDCl_3$, 100 MHz) δ 25.4, 26.0, 26.2, 27.8, 33.9, 42.7, 48.0, 72.7, 79.6. HRMS (EI^+) *m*/*z* 125.0940 (M − CH_2Br); calculated mass for $C_8H_{13}O^+$: 125.0966. *rel*-(1*S*,2*R*,6*S*)-**5d**. ^{1}H-NMR ($CDCl_3$, 400 MHz) δ 1.03–1.38 (m, 3 H), 1.49–1.56 (m, 2 H), 1.66–1.97 (m, 5 H), 3.05 (t, J = 11.1 Hz, 1 H), 3.80–3.86 (m, 2 H), 4.11–4.16 (m, 2 H). ^{13}C-NMR ($CDCl_3$, 100 MHz) δ 25.2, 25.7, 27.5, 31.4, 36.4, 45.4, 57.0, 73.5, 73.8. HRMS (EI^+) *m*/*z* 218.0304/220.0287 (M^+); calculated mass for $C_9H_{15}OBr^+$: 218.0306/220.0286. *Thermal reaction*. *cis*-**1d** 270 mg (1.00 µmol); eluent used for chromatography: diethyl ether–pentane = 1 : 10 (v/v). *2-Bromo-4-oxabicyclo[4.4.0]decane trans*-(**5d**). Yield: 21.7 mg (99.0 µmol, 10%), *rel*-(1*S*,2*S*,6*S*)-**5d** yellow

liquid. *4-Methyl-2-(trichloromethylsulfanyl)-thiazole* (**2**). Yield: 243 mg (977 μmol, 98%), colorless liquid. 91/9-mixture of *exo*/*endo*-isomers *7-Bromomethyl-8-oxabicyclo[4.3.0]nonane trans*-(**3d**) and *2-Bromo-4-oxabicyclo[4.4.0]decane trans*-(**5d**). Yield: 168 mg (767 μmol, 77%), 10/90-mixture of 6,7-*cis*/6,7-*trans*-isomers, *i.e. rel*-(1*S*,6*S*,7*R*)-**3d**/*rel*-(1*S*,6*S*,7*S*)-**3d** and *rel*-(1*S*,2*R*,6*S*)-**5d**, pale yellow liquid.

4.4.10 Conversion of 3-[*cis*-2-(2-methylprop-2-en-1-yl)-cyclohex-1-ylmethyloxy]-4-methylthiazole-2(3*H*)-thione *cis*-(1e). *Photochemical reaction*. *cis*-**1e** 161 mg (541 μmol); eluent used for chromatography: diethyl ether–pentane = 1 : 10 (v/v). *7-(2-Bromoprop-2-yl)-8-oxabicyclo[4.3.0]nonane cis*-(**3e**). Yield: 107 mg (433 μmol, 80%), *i.e. rel*-(1*R*,6*S*,7*S*)-**3e**, pale yellow liquid. R_f = 0.48 for diethyl ether–pentane = 1 : 10 (v/v). ^{1}H-NMR ($CDCl_3$, 600 MHz) δ 1.32–1.43 (m, 2 H) 1.45–1.55 (m, 3 H) 1.59–1.67 (m, 2 H) 1.68–1.76 (m, 7 H) 2.25–2.33 (m, 2 H) 3.63–3.69 (m, 2 H) 3.91 (dd, J = 8.2, 5.9 Hz, 1 H). ^{13}C-NMR ($CDCl_3$, 100 MHz) δ 23.1 (2C, HMQC), 25.2, 28.1, 30.1, 30.9, 38.6, 40.3, 69.9, 72.6, 90.1. Anal. Calcd for $C_{11}H_{19}BrO$ (247.17): C, 53.45; H, 7.75; Found: C, 53.32; H, 7.59. *4-Methyl-2-(trichloromethylsulfanyl)-thiazole* (**2**). Yield: 110 mg (443 μmol, 82%), pale yellow liquid. *Thermal reaction*: *cis*-**1e** 151 mg (508 μmol); eluent used for chromatography: diethyl ether–pentane = 1 : 10 (v/v). *7-(2-Bromoprop-2-yl)-8-oxabicyclo[4.3.0]nonane cis*-(**3e**). Yield: 119 mg (481 μmol, 95%), *i.e. rel*-(1*R*,6*S*,7*S*)-**3e**, pale yellow liquid. *4-Methyl-2-(trichloromethylsulfanyl)-thiazole* (**2**). Yield: 114 mg (460 μmol, 90%), colorless liquid.

4.4.11 Conversion of 3-[*trans*-2-(2-methylprop-2-en-1-yl)-cyclohex-1-ylmethyloxy]-4-methylthiazole-2(3*H*)-thione *trans*-(1e). *Photochemical reaction*. *trans*-**1e** 140 mg (471 μmol); eluent used for chromatography: diethyl ether–pentane = 1 : 10 (v/v). *7-(2-Bromoprop-2-yl)-8-oxabicyclo[4.3.0]nonane trans*-(**3e**). Yield: 94.4 mg (382 μmol, 81%), *i.e. rel*-(1*S*,6*S*,7*S*)-**3e**, colorless liquid. R_f = 0.39 for diethyl ether–pentane = 1 : 10 (v/v). ^{1}H-NMR ($CDCl_3$, 400 MHz) δ ppm 1.04–1.35 (m, 4 H) 1.46–1.58 (m, 1 H) 1.68–1.91 (m, 4 H), 1.74 (s, 3 H), 1.77 (s, 3 H), 2.06–2.14 (m, 1 H), 3.37 (dd, J = 11.3, 7.4 Hz, 1 H), 3.44 (d, J = 9.2 Hz, 1 H), 3.92 (t, J = 7.1 Hz, 1 H). ^{13}C-NMR ($CDCl_3$, 150 MHz) δ 25.3, 25.9, 27.3, 30.5, 30.7, 31.0, 47.2, 47.8, 69.3, 72.1, 89.4. Anal. Calcd for $C_{11}H_{19}BrO$ (247.17): C, 53.45; H, 7.75; Found: C, 53.62; H, 7.82. *4-Methyl-2-(trichloromethylsulfanyl)-thiazole* (**2**). Yield: 92.4 mg (372 μmol, 79%), colorless liquid. *Thermal reaction*. *trans*-**1e** 147 mg (495 μmol); eluent used for chromatography: diethyl ether–pentane = 1 : 10 (v/v). *7-(2-Bromoprop-2-yl)-8-oxabicyclo[4.3.0]nonane trans*-(**3e**). Yield: 115 mg (465 μmol, 94%), *i.e. rel*-(1*S*,6*S*,7*S*)-**3e**, colorless liquid. *4-Methyl-2-(trichloromethylsulfanyl)-thiazole* (**2**). Yield: 120 mg (483 μmol, 98%), colorless liquid.

4.4.12 Conversion of 3-[2-(1-methylenecyclohex-2-yl)-ethyloxy]-4-methylthiazole-2(3*H*)-thione (1f). *Photochemical reaction*. **1f** 275 mg (1.02 mmol); eluent used for chromatography: diethyl ether–pentane = 1 : 10 (v/v). *cis-(1-Bromo)-3-oxabicyclo-[4.4.0]decane cis*-(**5f**). Yield: 8.2 mg (37.4 μmol, 4%), yellow liquid. R_f = 0.46 for diethyl ether–pentane = 1 : 10 (v/v). ^{1}H-NMR ($CDCl_3$, 400 MHz, 22.2 °C) δ 1.31–1.59 (m, 4 H), 1.62–1.90 (m, 3 H), 1.96–2.25 (m, 3 H), 2.34 (ddd, J = 14.7, 12.1, 4.2 Hz, 1 H), 3.51 (br. t, J = 10.0 Hz, 1 H), 3.78 (d, J = 11.4 Hz, 1 H), 3.92 (d, J = 11.6 Hz, 1 H), 4.01 (br. d, J = 10.0 Hz, 1 H). ^{1}H-NMR ($CDCl_3$, 600 MHz, −39.7 °C) δ 1.35–1.45 (m, 3 H), 1.46–1.53 (m, 1 H), 1.65–1.72 (m, 2 H), 1.73–1.82 (m, 1 H), 2.03–2.13 (m, 2 H), 2.15–2.21 (m, 1 H), 2.26–2.33 (m, 1 H), 3.46–3.52 (m, 1 H), 3.78 (d, J = 11.2 Hz, 1 H), 3.91 (d, J = 11.2 Hz, 1 H), 4.03 (dd, J = 11.3, 4.8 Hz, 1 H). ^{13}C-NMR ($CDCl_3$, 150 MHz, −39.7 °C) δ 19.3, 22.7, 27.3, 29.4, 32.1, 42.0, 68.7, 72.9, 78.4. Anal. Calcd for $C_9H_{15}BrO$ (219.12): C, 49.33; H, 6.90; Found: C, 49.58; H, 6.83. *cis-(1-bromomethyl)-9-oxabicyclo[4.3.0]-nonane cis*-(**3f**). Yield: 53.6 mg (245 μmol, 24%), pale yellow liquid. R_f = 0.36 for diethyl ether–pentane = 1 : 10 (v/v). ^{1}H-NMR ($CDCl_3$, 600 MHz) δ 1.27–1.33 (m, 1 H), 1.34–1.44 (m, 2 H), 1.47–1.56 (m, 2 H), 1.61 (m, 1 H), 1.73 (m, 1 H), 1.78–1.85 (m, 2 H), 2.09 (m, 1 H), 2.26 (quin, J = 6.6 Hz, 1 H), 3.35 (d, J = 10.6 Hz, 1 H), 3.46 (d, J = 10.6 Hz, 1 H), 3.90 (td, J_t = 8.7, J_d = 5.6 Hz, 1 H), 3.97 (td, J_t = 8.5, J_d = 6.5 Hz, 1 H). ^{13}C-NMR ($CDCl_3$, 100 MHz) δ 22.0, 22.5, 27.3, 30.8, 30.9, 39.2, 39.8, 65.4, 81.6. Anal. Calcd for $C_9H_{15}BrO$ (219.12): C, 49.33; H, 6.90; Found: C, 49.17; H, 6.79. *4-Methyl-2-(trichloromethylsulfanyl)-thiazole* (**2**). Yield: 137 mg (551 μmol, 54%), pale yellow liquid. *trans-(1-Bromo)-3-oxabicyclo[4.4.0]decane trans*-(**5f**). Yield: 37.1 mg (169 μmol, 17%), yellow liquid. R_f = 0.28 for diethyl ether–pentane = 1 : 10 (v/v). ^{1}H-NMR ($CDCl_3$, 400 MHz) δ 1.12 (tt, J = 11.4, 3.6 Hz, 1 H), 1.22–1.36 (m, 2 H), 1.37–1.51 (m, 3 H), 1.63–1.71 (m, 1 H), 1.73–1.87 (m, 2 H), 1.90–2.06 (m, 2 H), 3.35 (d, J = 12.1 Hz, 1 H), 3.50 (td, J_t = 12.0, J_d = 2.5 Hz, 1 H), 3.98 (d, J = 12.3 Hz, 1 H), 4.07 (dd, J = 11.5, 4.7 Hz, 1 H). ^{13}C-NMR ($CDCl_3$, 150 MHz) δ 21.8, 25.6, 29.0, 29.8, 36.3, 45.2, 68.8, 76.9, 78.4. Anal. Calcd for $C_9H_{15}BrO$ (219.12): C, 49.33; H, 6.90; Found: C, 49.33; H, 7.02. *Thermal reaction*. **1f** 270 mg (1.00 mmol); eluent used for column chromatography: diethyl ether–pentane = 1 : 10 (v/v). *cis-1-Bromo-3-oxabicyclo[4.4.0]-decane cis*-(**5f**). Yield: 14.8 mg (67.5 μmol, 7%), yellow liquid. *cis-(1-Bromomethyl)-9-oxabicyclo[4.3.0]nonane cis*-(**3f**). Yield: 76.7 mg (350 μmol, 35%), pale yellow liquid. *trans-1-Bromo-3-oxabicyclo[4.4.0]decane trans*-(**5f**). Yield: 33.5 mg (153 μmol, 15%), yellow liquid. *4-Methyl-2-(trichloromethylsulfanyl)-thiazole* (**2**). Yield: 199 mg (801 μmol, 80%), pale yellow liquid.

4.4.13 Conversion of 3-[(1-methylcyclohex-1-en-4-yl)-methyloxy]-4-methylthiazole-2(3*H*)-thione (1g). *Photochemical reaction*: **1g** 536 mg (2.10 mmol); eluent used for column chromatography: diethylether–acetone–pentane = 1 : 1 : 15 (v/v/v). *rel-(1R,4R,5R)-4-Bromo-4-methyl-6-oxabicyclo[3.2.1]octane trans*-(**3g**). Yield: 213 mg (1.04 mmol, 50%), pale yellow liquid. R_f = 0.46 for diethyl ether–acetone–pentane = 1 : 1 : 15 (v/v/v). ^{1}H-NMR ($CDCl_3$, 400 MHz) δ 1.48–1.57 (m, 1 H), 1.77 (s, 3 H), 1.79–1.89 (m, 2 H), 1.90–1.96 (m, 1 H), 1.97–2.06 (m, 1 H), 2.33–2.39 (m, 1 H), 2.58 (d, J = 11.9 Hz, 1 H), 3.73–3.88 (m, 2 H), 4.10 (d, J = 5.8 Hz, 1 H). ^{13}C-NMR ($CDCl_3$, 100 MHz) δ 26.8, 32.3, 33.9, 35.4, 36.4, 67.9, 72.3, 83.0. Anal. Calcd for $C_8H_{13}BrO$ (205.09): C, 46.85; H, 6.39; Found: C, 46.74; H, 6.36. *4-Methyl-2-(trichloromethylsulfanyl)-thiazole* (**2**). Yield: 358 mg (1.44 mmol, 69%), pale yellow liquid. R_f = 0.35 for diethyl ether–acetone–pentane = 1 : 1 : 15 (v/v/v). *rel-(1R,4S,5R)-4-Bromo-4-methyl-6-oxabicyclo[3.2.1]octane cis*-(**3g**). Yield: 62.0 mg

(302 μmol, 14%), pale yellow liquid. R_f = 0.22 for diethyl ether–acetone–pentane = 1 : 1 : 15 (v/v/v) ^{1}H-NMR ($CDCl_3$, 600 MHz) δ 1.51–1.62 (m, 2 H), 1.72–1.82 (m, 1 H), 1.78 (s, 3 H), 1.94 (d, J = 12.0 Hz, 1 H), 2.05 (dd, J = 13.6, 5.9 Hz, 1 H), 2.42–2.46 (m, 1 H), 2.51 (td, J_t = 13.2, J_d = 7.0 Hz, 1 H), 3.85 (ddd, J = 8.1, 4.4, 1.4 Hz, 1 H), 3.93 (d, J = 7.9 Hz, 1 H), 4.31 (d, J = 6.1 Hz, 1 H). ^{13}C-NMR ($CDCl_3$, 100 MHz): δ 28.7 (2C, HMQC), 34.1, 34.4, 37.5, 71.4, 71.5, 84.9. Anal. Calcd for $C_8H_{13}BrO$ (205.09): C, 46.85; H, 6.39. Found: C, 46.87; H, 6.37. *Thermal reaction*. **1g** 513 mg (2.00 mmol); eluent used for column chromatography: diethyl ether–acetone–pentane = 1 : 1 : 15 (v/v/v). *rel-(1R,4R,5R)-4-Bromo-4-methyl-6-oxabicyclo[3.2.1]octane trans-*(**3g**). Yield: 238 mg (1.16 mmol, 58%), pale yellow liquid. *4-Methyl-2-(trichloromethylsulfanyl)-thiazole* (**2**). Yield: 377 mg (1.52 mmol, 76%), pale yellow liquid. *rel-(1R,4S,5R)-4-Bromo-4-methyl-6-oxabicyclo[3.2.1]octane cis-*(**3g**). Yield: 57.2 mg (279 μmol, 14%), pale yellow liquid.

4.4.14 Conversion of 3-[{(1*S*,4*S*,5*R*)-2,6,6-trimethylbicyclo-[3.1.1]-hept-2-en-4-yl}-ethyloxy]-4-methylthiazole-2(3*H*)-thione (1h). *Photochemical reaction*. **1h** 305 mg (985 μmol); eluent used for chromatography: diethyl ether–pentane = 1 : 4 (v/v). *rel-(1R,2S,6S,7S,9S)-9-bromo-1,8,8-trimethyl-3-oxatricyclo[5.2.1.0^{2,6}]-decane* (**6**). Yield: 148.2 mg (58%), yellow liquid. $[\alpha]_D^{25}$ = 36.6 (c = 0.85/ethanol). ^{1}H-NMR ($CDCl_3$, 600 MHz): δ 1.08 (s, 3 H), 1.10 (s, 3 H), 1.15 (s, 3 H), 1.33 (dd, J = 11.1, 1.7 Hz, 1 H), 1.35–1.41 (m, 1 H), 1.55 (dd, J = 11.3, 1.3 Hz, 1 H), 1.60 (s, 1 H), 2.04 (dddd, J = 12.1, 9.5, 5.8, 1.3 Hz, 1 H), 2.60–2.66 (m, 1 H), 3.40 (ddd, J = 11.1, 8.6, 5.9 Hz, 1 H), 3.79 (s, 1 H), 3.88–3.97 (m, 2 H). ^{13}C-NMR ($CDCl_3$, 100 MHz): δ 15.4, 25.9, 30.3, 31.8, 34.9, 40.5, 41.8, 50.9, 53.4, 67.9, 72.1, 83.4. HRMS (EI$^+$) m/z 258.0612 (M^+); calculated mass for $C_{12}H_{19}OBr^+$: 258.0442 260. *4-Methyl-2-(trichloromethylsulfanyl)-thiazol* (**2**). Yield: 193 mg (774 μmol, 79%), colorless liquid. *rel-(1S,2S,6S,7S,9S)-9-bromo-1,10,10-trimethyl-3-oxatricyclo[5.2.1.0^{2,6}]-decane* (**7**). Yield: 7.7 mg (3%). ^{1}H-NMR ($CDCl_3$, 400 MHz) δ 0.93 (s, 3 H), 1.05 (s, 6 H), 1.81–2.04 (m, 4 H), 2.32–2.42 (m, 1 H), 3.01 (ttd, J_t = 9.7, 4.7, J_d = 1.4 Hz, 1 H), 3.85–3.93 (m, 1 H), 4.30 (ddd, J = 11.2, 5.8, 1.7 Hz, 1 H), 4.35–4.44 (m, 2 H). ^{13}C-NMR ($CDCl_3$, 100 MHz) δ 13.8, 20.4, 20.5, 26.0, 31.2, 43.0, 47.2, 51.8, 53.2, 53.8, 71.7, 91.2. HRMS (EI$^+$) m/z 258.0612/260.0612 (M^+); calculated mass for $C_{12}H_{19}OBr^+$: 258.0619/260.0599.

Acknowledgements

This work is part of Ph.D. theses of C. S., T. G., and R. K., and an undergraduate research project of A. L. We express our gratitude to the State Rheinland-Pfalz (scholarship for C. S. and equipment for computational chemistry), and the Deutsche Forschungsgemeinschaft (grant Ha1705/5-2) for financial support.

Notes and references

1 A. L. J. Beckwith and B. P. Hay, *J. Am. Chem. Soc.*, 1988, **110**, 4415–4416.
2 J. Hartung and F. Gallou, *J. Org. Chem.*, 1995, **60**, 6706–6716.
3 M. Rueda-Becerril, J. C. T. Leung, C. R. Dunbar and G. M. Sammis, *J. Org. Chem.*, 2011, **76**, 7720–7729.
4 J. M. Surzur, M. P. Bertrand and R. Nougier, *Tetrahedron Lett.*, 1969, 4197–4200.
5 J. M. Surzur and M. P. Bertrand, *Bull. Soc. Chim. Fr.*, 1973, 1861.
6 R. D. Rieke and N. A. Moore, *J. Org. Chem.*, 1972, **37**, 413–418.
7 J. Hartung, T. Gottwald and K. Špehar, *Synthesis*, 2002, 1469–1498.
8 J. Hartung, K. Daniel, C. Rummey and G. Bringmann, *Org. Biomol. Chem.*, 2006, **4**, 4089–4100.
9 For stereodirecting effects of amino- or silyloxy groups see: M. Zlotorzynska, H. Zhai and G. M. Sammis, *J. Org. Chem.*, 2010, **75**, 864–872.
10 J. Hartung, R. Kneuer, S. Laug, P. Schmidt, K. Špehar, I. Svoboda and H. Fuess, *Eur. J. Org. Chem.*, 2003, 4033–4052.
11 J. Hartung, T. Gottwald and M. Greb, *Synlett*, 2004, 65–68.
12 J. Hartung and R. Kneuer, *Tetrahedron: Asymmetry*, 2003, **14**, 3019–3031.
13 N. Schneiders, T. Gottwald and J. Hartung, *Eur. J. Org. Chem.*, 2009, 799–801.
14 C. Schur, N. Becker, U. Bergsträßer, T. Gottwald and J. Hartung, *Tetrahedron*, 2011, **67**, 2338–2347.
15 P. Fries, M. K. Müller and J. Hartung, *Org. Biomol. Chem.*, 2013, **11**, 2630–2637.
16 P. Fries and J. Hartung, *J. Am. Chem. Soc.*, 2011, **133**, 3906–3912.
17 J. Hartung, R. Kneuer, C. Rummey and G. Bringmann, *J. Am. Chem. Soc.*, 2004, **126**, 12121–12129.
18 A. L. J. Beckwith and C. H. Schiesser, *Tetrahedron*, 1985, **41**, 3925–3941.
19 K. N. Houk, M. N. Paddon-Row, D. C. Spellmeyer, N. G. Rondan and S. Nagase, *J. Org. Chem.*, 1986, **51**, 2874–2879; D. C. Spellmeyer and K. N. Houk, *J. Org. Chem.*, 1987, **52**, 959–974.
20 M. Stoll and M. Hinder, *Helv. Chim. Acta*, 1950, **33**, 1251–1261; J. M. Castro, S. Salido, J. Altarejos, M. Nogueras and A. Sanchez, *Tetrahedron*, 2002, **58**, 5941–5949.
21 R. R. Gadikota, A. I. Keller, C. S. Callam and T. L. Lowary, *Tetrahedron: Asymmetry*, 2003, **14**, 737–742.
22 W. Francke, S. Schulz, V. Sinnwell, W. A. König and Y. Roisin, *Liebigs Ann. Chem.*, 1989, 1195–1201; H.-L. Wang, C.-H. Zhao, G. Szöcs, S. P. Chinta, S. Schulz and C. O. Brumata, *J. Chem. Ecol.*, 2013, **39**, 790–796.
23 J. Hartung, T. M. Kopf, R. Kneuer and P. Schmidt, *C. R. Acad. Sci., Paris, Chim./Chem.*, 2001, **4**, 649–666.
24 D. P. Curran, N. A. Porter and B. Giese, in *Stereochemistry of Radical Reactions: Concepts, Guidelines, and Synthetic Applications*, Wiley, Weinheim, 1995, vol. X, ch. X, pp. 27–115.
25 B. Giese, B. Koppling, T. Göbel, J. Dickhaut, G. Thoma, K. J. Kulicke and F. Trach, in *Organic Reactions*, ed.

L. A. Paquette, Wiley, Weinheim, 1996, vol. 48, ch. 2, pp. 301–856.
26 J. Hartung, C. Schur, I. Kempter and T. Gottwald, *Tetrahedron*, 2010, **66**, 1365–1374.
27 T. Gottwald, M. Greb and J. Hartung, *Synlett*, 2004, 65–68.
28 For 2-(prop-2-en-1-yl)cyclopentan-1-ol: S. Baskaran, I. Islam and S. Chandrasekaran, *J. Org. Chem.*, 1990, **55**, 891–895; D. P. Curran and H. J. Liu, *J. Chem. Soc., Perkin Trans. 1*, 1994, 1377–1393; L. S. Hegedus and J. M. McKearin, *J. Am. Chem. Soc.*, 1982, **104**, 2444–2451.
29 For 2-(3-methylbut-2-en-1-yl)-cyclopentan-1-ol: L. Streinz and M. Romaňuk, *Collect. Czech. Chem. Commun.*, 1978, **43**, 647–654.
30 For 2-(prop-2-en-1-yl)-cyclohexan-1-ol: S. Baskaran, I. Islam and S. Chandrasekaran, *J. Org. Chem.*, 1990, **55**, 891–895; J. M. Schomaker, B. R. Travis and B. Borhan, *Org. Lett.*, 2003, **5**, 3089–3092; V. Spezialé, M. Armat and A. Lattes, *J. Heterocycl. Chem.*, 1976, **13**, 349–356.
31 For 2-(1-methylenecyclohex-2-yl)-ethan-1-ol: A. Segre, R. Viterbo and G. Parisi, *J. Am. Chem. Soc.*, 1957, **79**, 3503–3505; G. E. Gream, A. K. Serelis and T. I. Stoneman, *Aust. J. Chem.*, 1974, **27**, 1711–1729.
32 J. Hartung, S. Hünig, R. Kneuer, M. Schwarz and H. Wenner, *Synthesis*, 1997, 1433–1438.
33 For *cis*-[2-(ethyen)-cyclohex-1-yl]-methanol and *cis*-[2-(methylprop-1-en-1-yl)-cyclohex-1-yl]-methanol: B. D. Kelly, J. M. Allen, R. E. Tundel and T. H. Lambert, *Org. Lett.*, 2009, **11**, 1381–1383.
34 For *trans*-[2-(ethylen)-cyclohex-1-yl]-methanol and *trans*-[2-(methylprop-1-en-1-yl)-cyclohex-1-yl]-methanol: R. Kuhn and I. Butula, *Liebigs Ann. Chem.*, 1968, **718**, 50–77; I. J. Jakovac, H. B. Goodbrand, K. P. Lok and J. B. Jones, *J. Am. Chem. Soc.*, 1982, **104**, 4659–4665; R. M. Borzilleri and S. M. Weinreb, *J. Am. Chem. Soc.*, 1994, **116**, 9789–9790; R. M. Borzilleri, S. M. Weinreb and M. Parvez, *J. Am. Chem. Soc.*, 1995, **117**, 10905–10913; B. D. Kelly, J. M. Allen, R. E. Tundel and T. H. Lambert, *Org. Lett.*, 2009, **11**, 1381–1383.
35 For 2-{(1*S*,4*S*,5*R*)-2,6,6-trimethylbicyclo[3.1.1]hept-2-en-4-yl} ethanol: R. K. Guy and R. A. DiPietro, *Synth. Commun.*, 1992, **22**, 687–692; X. Wei, J. C. Lorenz, S. Kapadia, A. Saha, N. Haddad, C. A. Busacca and C. H. Senanayake, *J. Org. Chem.*, 2007, **72**, 4250–4253; P. A. Grieco, J. D. Clark and C. T. Jagoe, *J. Am. Chem. Soc.*, 1991, **113**, 5488–5489; M. T. Reetz and A. Gansäuer, *Tetrahedron*, 1993, **49**, 6025–6030.
36 J. Hartung, I. Kempter, T. Gottwald, M. Schwarz and R. Kneuer, *Tetrahedron: Asymmetry*, 2009, **20**, 2097–2104.
37 For (1-methylcyclohex-1-en-4-yl)-methanol: T. Inukai and M. Kasai, *J. Org. Chem.*, 1965, **30**, 3567–3569.
38 S. A. Monti and G. L. White, *J. Org. Chem.*, 1975, **40**, 215–217.
39 M. Arnone, J. Hartung and B. Engels, *J. Phys. Chem. A*, 2005, **109**, 5943–5950.
40 J. Hartung, R. Kneuer, M. Schwarz and M. Heubes, *Eur. J. Org. Chem.*, 2001, 4733–4736.
41 J. Hartung, S. Altermann, U. Bergsträßer, T. Gottwald, I. Kempter, C. Schur and M. Heubes, *Tetrahedron*, 2009, **65**, 7527–7532.
42 J. Hartung, U. Bergsträsser, K. Daniel, N. Schneiders, I. Svoboda and H. Fuess, *Tetrahedron*, 2009, **65**, 2567–2573.
43 U. Bünzli-Trepp, *Handbuch für die systematische Nomenklatur der Organischen Chemie, Metallorganischen Chemie und Koordinationschemie*, Logos-Verlag, Berlin, 2001, pp. 15–56.
44 A. Hantzsch and J. H. Weber, *Ber. Dtsch. Chem. Ges.*, 1887, **20**, 3118–3132.
45 O. J. Widman, *Prakt. Chem.*, 1888, **38**, 185–201.
46 G. P. Moss, *Pure Appl. Chem.*, 1999, **71**, 513–529.
47 A. Baeyer, *Ber. Dtsch. Chem. Ges.*, 1900, **33**, 3771–3775.
48 J. Hartung, B. Hertel and F. Trach, *Chem. Ber.*, 1993, **126**, 1187–1191.
49 A. L. J. Beckwith and B. P. Hay, *J. Am. Chem. Soc.*, 1989, **111**, 230–234.
50 K. S. Pitzer and W. E. Donath, *J. Am. Chem. Soc.*, 1959, **81**, 3213–3218.
51 J. Hartung, T. Gottwald and R. Kneuer, *Synlett*, 2001, 749–752.
52 J. C. Tripp, C. H. Schiesser and D. P. Curran, *J. Am. Chem. Soc.*, 2005, **127**, 5518–5527.
53 W. Damm, B. Giese, J. Hartung, T. Hasskerl, K. N. Houk, O. Hueter and H. Zipse, *J. Am. Chem. Soc.*, 1992, **114**, 4067–4079.
54 R. J. Abraham, M. A. Warne and L. Griffiths, *J. Chem. Soc., Perkin Trans. 2*, 1997, 2151–2160.
55 M. J. Frisch, G. W. Trucks, H. B. Schlegel, G. E. Scuseria, M. A. Robb, J. R. Cheeseman, J. A. Montgomery Jr., T. Vreven, K. N. Kudin, J. C. Burant, J. M. Millam, S. S. Iyengar, J. Tomasi, V. Barone, B. Mennucci, M. Cossi, G. Scalmani, N. Rega, G. A. Petersson, H. Nakatsuji, M. Hada, M. Ehara, K. Toyota, R. Fukuda, J. Hasegawa, M. Ishida, T. Nakajima, Y. Honda, O. Kitao, H. Nakai, M. Klene, X. Li, J. E. Knox, H. P. Hratchian, J. B. Cross, V. Bakken, C. Adamo, J. Jaramillo, R. Gomperts, R. E. Stratmann, O. Yazyev, A. J. Austin, R. Cammi, C. Pomelli, J. W. Ochterski, P. Y. Ayala, K. Morokuma, G. A. Voth, P. Salvador, J. J. Dannenberg, V. G. Zakrzewski, S. Dapprich, A. D. Daniels, M. C. Strain, O. Farkas, D. K. Malick, A. D. Rabuck, K. Raghavachari, J. B. Foresman, J. V. Ortiz, Q. Cui, A. G. Baboul, S. Clifford, J. Cioslowski, B. B. Stefanov, G. Liu, A. Liashenko, P. Piskorz, I. Komaromi, R. L. Martin, D. J. Fox, T. Keith, M. A. Al-Laham, C. Y. Peng, A. Nanayakkara, M. Challacombe, P. M. W. Gill, B. Johnson, W. Chen, M. W. Wong, C. Gonzalez and J. A. Pople, *Gaussian 03 (Revision E.01)*, Gaussian, Inc., Wallingford, CT, 2004.
56 J. B. Foresman and Æ. Frisch, *Exploring Chemistry with Electronic Structure Methods*, Gaussian Inc., Pittsburgh, PA, 2nd edn, 1996.
57 A. D. Becke, *J. Chem. Phys.*, 1993, **98**, 5648–5652.
58 C. Lee, W. Yang and R. G. Parr, *Phys. Rev. B: Condens. Matter*, 1988, **37**, 785–789.
59 A. D. Becke, *Phys. Rev. A*, 1988, **38**, 3098–3100.

60 I. V. Alabugin and M. Manoharan, *J. Am. Chem. Soc.*, 2005, **127**, 12583–12594.
61 G. Schaftenaar and J. H. Noordik, *Comput.-Aided Mol. Des.*, 2000, **14**, 123–134.
62 B. Fuchs, in *Topics in Stereochemistry*, ed. E. L. Eliel and N. L. Allinger, Wiley, New York, 1978, vol. 10, pp. 1–94.
63 R. A. Marcus, *J. Phys. Chem.*, 1968, **72**, 891–899.
64 P. Gisdakis and N. Rösch, *J. Am. Chem. Soc.*, 2001, **123**, 697–701.
65 C. W. Wu and J.-J. Ho, *J. Org. Chem.*, 2006, **71**, 9595–9601.
66 G. S. Hammond, *J. Am. Chem. Soc.*, 1955, **77**, 334–338.
67 I. Kempter, B. Frensch, T. Kopf, R. Kluge, R. Csuk, I. Svoboda, H. Fuess and J. Hartung, *Tetrahedron*, 2014, **70**, 1918–1927.

4. Erzeugung und Reaktivität tertiärer *O*-Radikale

4.1 Zusammenfassung

O-tert-Alkylthiohydroxamate dienen als Quellen tertiärer Sauerstoff-Radikale und sind in Ausbeuten von bis zu 64 % aus tertiären *O*-Alkylisoharnstoffen und 3-Hydroxy-5-(4-methoxyphenyl)-4-methylthiazol-2(3*H*)-thion synthetisierbar. Geschwindigkeitskonstanten *k* aus Umsetzungen der *O*-Radikalvorläufer in Gegenwart von Bromtrichlormethan spiegeln die hohe Reaktivität der tertiären *O*-Radikale in typischen Elementarreaktionen wider. Das 5-Phenyl-2-methylpent-2-oxyl-Radikal abstrahiert intramolekular ein δ-H-Atom mit einer Geschwindigkeitskonstante von $k^{\text{Subst}} = 10^7–10^8\ \text{s}^{-1}$. Eine Größenordnung höher ist die Geschwindigkeitskonstante der 5-*exo*-Addition des 2-Phenyl-5-hexen-2-oxyl-Radikals ($k^{5\text{-}exo} = 10^8–10^9\ \text{s}^{-1}$), dessen Ringschluss 2,5-*cis*-selektiv erfolgt. Der *exo*-spezifische Angriff des *p*-Chlorcumyloxyl-Radikals an Norbornen erfolgt mit einer bimolekularen Geschwindigkeitskonstante von $k^{\text{Add}} = 1 \times 10^7\ \text{M}^{-1}\ \text{s}^{-1}$. Ursache der *exo*-spezifischen Addition an Norbornen sowie der 2,5-*cis*-Cyclisierung sind Torsionsspannungen in den *endo*- bzw. 2,5-*trans*-Übergangszuständen, was theoretische Analyseverfahren in diesem Zusammenhang verdeutlichen.

4.2 Wissenschaftlicher Hintergrund, Zielsetzung und Strategie

Um tertiäre *O*-Radikale in der organischen Synthesechemie routinemäßig einsetzen zu können, müssen deren Reaktivitäten und Selektivitäten bekannt sein. Fundamental sind hierbei Methoden zur Darstellung tertiärer *O*-Radikalvorläufer sowie zur Freisetzung entsprechender *O*-Radikale unter neutralen und nicht-oxidativen Bedingungen.[1–2] Versuche, etablierte Syntheseverfahren für primäre und sekundäre Thiohydroxamate[2–4] auf die Synthese tertiärer *O*-Ester zu übertragen, gelangen in frühren Arbeiten nur ansatzweise.[1,5] Erst durch Einsatz tertiärer *O*-Alkylisoharnstoffe[6–8] als Alkylierungsregenzien konnten tertiäre *O*-Alkylthiohydroxamate[9] in Ausbeuten von bis zu 25 % hergestellt werden (Schema 4.1).[5,10] Analysen weiterer Reaktionsprodukte, die erlaubt hätten den Reaktionsverlauf genauer zu verstehen und die Reaktionsparameter ausbeutesteigernd anzupassen, blieben bisher aus. Um die Chemie tertiärer Alkoxyl-Radikale aus Thiohydroxamsäure-*O*-ester weiterzuentwickeln, war das Ziel dieses Projektes, die Synthese tertiärer *O*-Alkylthio-

hydroxamate im präparativen Maßstab zu erschließen. Die dargestellten Zielmoleküle bilden dabei die Basis für konkurrenzkinetische Experimente im zweiten Teil der Studie, um mit Hilfe des Radikaluhr-Konzepts[11,12] Referenzreaktionen in der Sauerstoff-Radikalchemie kinetisch zu kalibrieren.

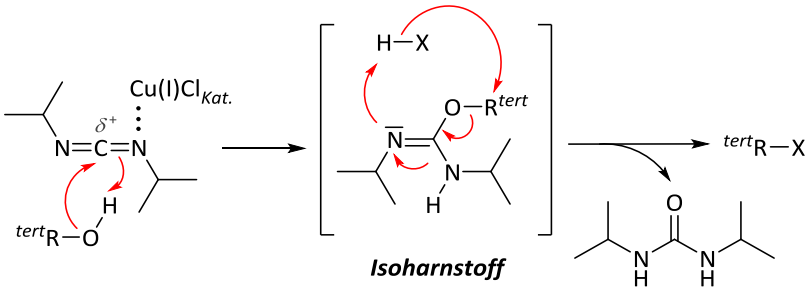

Schema 4.1. Veresterung tertiärer Alkohole durch *O*-Alkylisoharnstoffe. R^{tert} = CY_3 mit Y = Alkyl, Aryl; HX = Carbon- oder Thiohydroxamsäure.

Für die vorliegenden Studie ergaben sich folgende Aufgabenstellungen, um Grundlagen für eine Anwendung tertiärer *O*-Radikale in der organischen Synthese zu schaffen.

- Prüfung der Isoharnstoff-Methode unter Verwendung von Thiohydroxamsäuren und tertiären Alkoholen auf Ausbeutensteigerungen und weitere Reaktionsprodukte.
- Nutzung der tertiären Thiohydroxamsäure-*O*-ester als *O*-Radikalquellen für die δ-H-Abstraktion, 5-*exo*-*trig*-Cyclisierung und intermolekulare Addition.
- Formulierung von quantitativen Aussagen zur Reaktivität und Selektivität tertiärer *O*-Radikale mit Hilfe unimolekularer Vergleichsreaktionen und theoretischer Analyseverfahren.

4.3 Ergebnisse und Diskussion

4.3.1 Erzeugung und Eigenschaften tertiärer *O*-Alkylthiohydroxamate

O-Alkyl- und *O*-Cumylisoharnstoffe entstehen *in situ* aus den Alkoholen **1a**–**1f** und Diisopropylcarbodiimid (DIC) in Gegenwart katalytischer Megen Kupfer(I)-chlorid. Mit 3-Hydroxy-5-(4-methoxyphenyl)-4-methylthiazol-2(3*H*)-thion (MAnTTOH, **2**) reagieren die Isoharnstoffe zu den tertiären *O*-Alkylthiohydroxamaten **3a**–**3f**. Zusätzliche Reaktions-

produkte sind Eliminierungsprodukte der Alkohole **1c**–**1f** (12–24 % pro Millimol MAnTTOH, nicht abgebildet) sowie die *N*-Oxide **4a**–**4f** (Tabelle 4.1).

Tabelle 4.1. Produkte und Ausbeuten der Umsetzung von 3-Hydroxy-5-(4-methoxyphenyl)-4-methylthiazol-2(3*H*)-thion (**2**) mit *O*-Alkyl- und *O*-Cumylisoharnstoffen

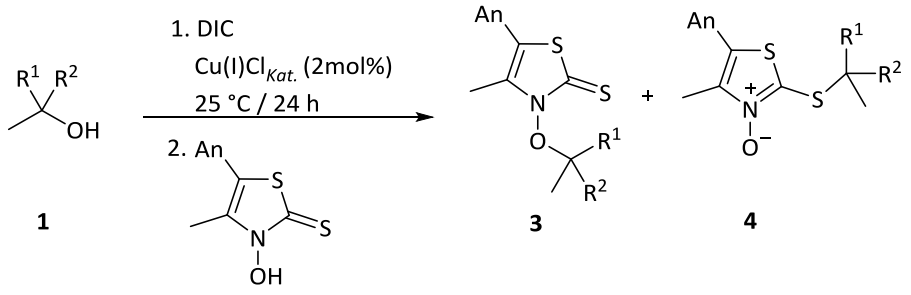

Eintrag	**1** / **3** / **4**	R^1	R^2	*T* / °C	**3** / %	Schmp. **3** / °C	**4** / %
1	**a**[a]	CH_3	CH_3	24	58–64[c]	112	25[e]
2	**b**[a]	CH_3	C_2H_5	0	45–47[d]	72	33[e]
3	**c**[a]	CH_3	$(CH_2)_3C_6H_5$	0	44	64	11[e]
4	**d**[b]	CH_3	C_6H_5	−30	15	108	38
5	**e**[b]	CH_3	*p*-ClC_6H_4	−30	13	95	33
6	**f**[b]	$(CH_2)_2CH=CH_2$	C_6H_5	−30	18	110	27[e]

[a] 5.5-facher Überschuss an tertiärem Alkohol und DIC, pro Millimol MAnTTOH (**2**), [b] 2-facher Überschuss an tertiärem Alkohol und DIC, pro Millimol MAnTTOH (**2**), [c] aus fünf Experimenten, [d] Wert aus drei Experimenten, [e] ^{1}H-NMR-Ausbeute.

Als blassgelbe oder farblose Feststoffe zeigen die Thiohydroxamsäuren **3a**–**3f** charakteristische UV/Vis-Absorptionsbanden bei 336–338 nm[13,14] und sind Ausgangsverbindungen für die Untersuchung der konkurrenzkinetischen Reaktionen. Mit Hilfe des entwickelten Verfahrens sind präparative Mengen an *O*-Alkylthiohydroxamaten (beispielsweise 1.5 g an **3f**) für die angestrebten Untersuchungen zugänglich.

4.3.2 Reaktivität und Selektivität tertiärer *O*-Radikale in Elementarreaktionen

(A) Homolytische Substitution

Thermische und photochemische Umsetzungen des *O*-(2-Methyl-5-phenylpentyl)-thiohydroxamats **3c** in Gegenwart von Bromtrichlormethan liefern als Hauptprodukt 2,2-Dimethyl-5-phenyltetrahydrofuran (**6**) (Tabelle 4.2). Als Nebenprodukte entstehen 2-Methyl-5-phenylpentan-2-ol (**1c**), Aceton (**7**) und das *in situ* gebildete δ-Bromhydrin **5**, das nach spontaner HBr-Eliminierung zu Produkt **6** kondensiert. Aus dem Thiazolthion-Fragment bilden sich das Disulfid **8** und das Abfangprodukt 5-(4-Methoxyphenyl)-4-methyl-2-(trichlormethylsulfanyl)thiazol (**9**).

Tabelle 4.2. Produkte und Ausbeuten der Umsetzungen des 3-(5-Phenyl-2-methylpent-2-oxy)thiazol-2(3*H*)-thions **3c** mit Bromtrichlormethan

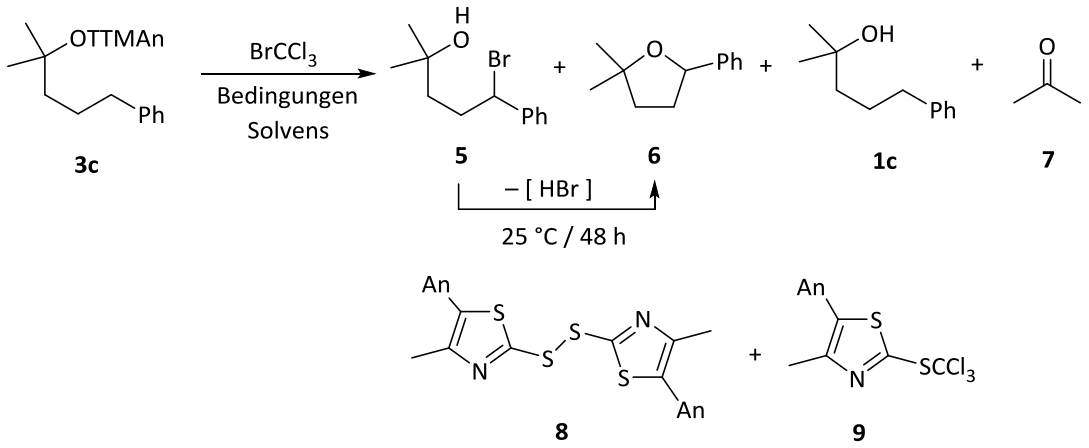

Eintrag	Bedingungen	Solvens	**1c**/%	**5**/%	**6**/%	**7**/%	**8**/%	**9**/%
1	$h\nu$ / 25 °C[a]	C_6D_6	36	41	22	3–5	40	10
2	$h\nu$ / 25 °C	$C_6D_5CF_3$	23	–[c]	58	–[b]	34	27
3	AIBN / 80 °C	C_6H_6	–[b]	–[c]	61	–[b]	–[b]	–[b]

[a] *In situ*-Messung (^{1}H-NMR) nach 2 h bei 21 °C, interner Standard: Pentachlorbenzol, [b] nicht bestimmt, [c] nicht beobachtet.

Das Produktverhältnis [**5**+**6**]/[**7**] spiegelt die relative Reaktivität zwischen Substitution und Fragmentierung wider (Schema 4.2). Mit der Geschwindigkeitskonstanten der Fragmentierung des *tert*-Butoxyl-Radikals (k^{Frag} = 2.0 × 10^4 s^{-1}, 25 °C in C_6H_6)[15] und einem Korrekturfaktor $\mathbf{F_c}$ (150–350)[16,17] für die bevorzugte Abspaltung eines Ethyl-Radikals anstelle eines

Methyl-Radikals, kann nach Gleichung 1 die Geschwindigkeitskonstante k^{Subst}**Ic** berechnet werden. Sie beträgt für das Radikal **Ic**: k^{Subst}**Ic** = 0.4–1.5 × 10^8 s^{-1} (25 °C, C_6D_6).

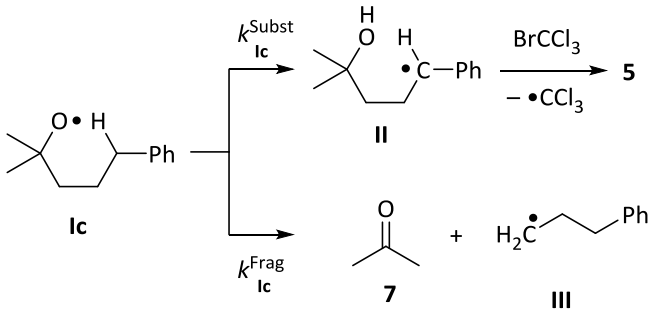

Schema 4.2. Konkurrenzkinetische Betrachtung der Substitution (k^{Subst}) und Fragmentierung (k^{Frag}) des Alkoxyl-Radikals **Ic** in Gegenwart von Bromtrichlormethan.

$$k^{Subst}_{Ic} = \frac{[\mathbf{5} + \mathbf{6}]}{[\mathbf{7}]}\ k^{Frag} \times \mathbf{F}_c \qquad \text{(Gleichung 1)}$$

(B) Intramolekulare Addition

Die Bestrahlung von (2-Phenyl-5-hexen-2-oxyl)-thiazol-2(3*H*)-thion **3f** in Gegenwart von Bromtrichlormethan liefert als Hauptprodukte die diastereomeren, β-bromierten Tetrahydrofurane *cis*-**10** und *trans*-**10** (Schema 4.3). Weitere Reaktionsprodukte sind der tertiäre Alkohol **1f** und das Fragmentierungsprodukt Acetophenon (**11**).

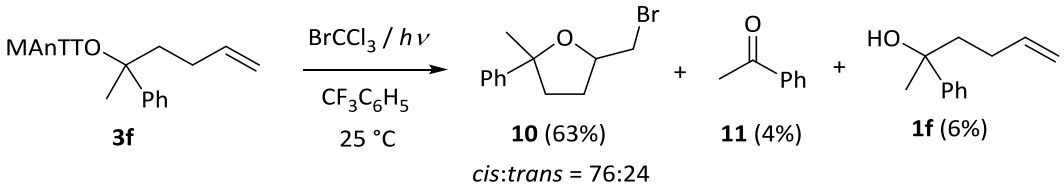

Schema 4.3. Umsetzung von 2-Phenyl-5-hexen-2-yl-esters **3f** in Gegenwart von Bromtrichlormethan. Weitere Produkte: Disulfid **8** (30%) und Abfangprodukt **9** (45%).

Die Geschwindigkeitskonstanten des *cis*- und *trans*-Ringschlusses des Radikals **If** ergeben sich nach Gleichung 2 aus den Ausbeutenverhältnissen der Produkte *cis*/*trans*-**10** und **11** sowie der Geschwindigkeitskonstanten der Fragmentierung des 2-(4-Methyphenyl)-but-2-oxyl-Radikals zum (4-Methylphenyl)methylketon (k^{Frag} = 2.5 × 10^8 s^{-1}, 22 °C in CH_3CN)[16] (Schema 4.4). Daraus ergibt sich: $k^{5\text{-}exo(cis)}$**If** = 3 × 10^9 s^{-1} und $k^{5\text{-}exo(trans)}$**If** = 1 × 10^9 s^{-1}.

$$k_{\mathbf{If}}^{5\text{-}exo(cis)} = \frac{[cis\text{-}\mathbf{10}]}{[\mathbf{11}]}\, k^{Frag} \quad \text{bzw.} \quad k_{\mathbf{If}}^{5\text{-}exo(trans)} = \frac{[trans\text{-}\mathbf{10}]}{[\mathbf{11}]}\, k^{Frag} \qquad \text{(Gleichung 2)}$$

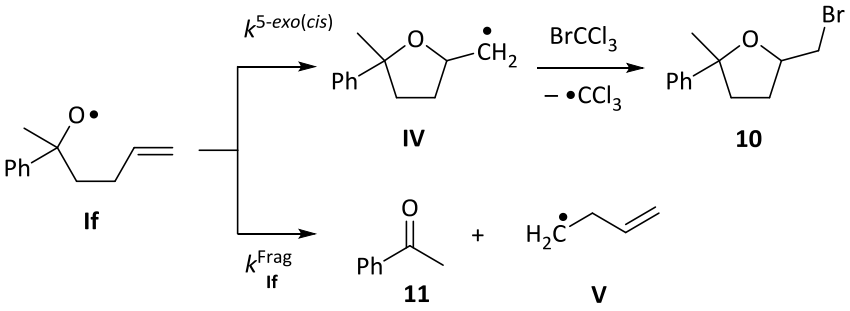

Schema 4.4. Konkurrenzkinetische Betrachtung der intramolekularen Addition ($k^{5\text{-}exo}$) und Fragmentierung (k^{Frag}) des Alkoxyl-Radikals **If** in Gegenwart von Bromtrichlormethan.

Das *O*-Radikal **If** cyclisiert 2,5-*cis*-selektiv, was anhand von Berechnungen[18] auf Basis des Twist-Modells in Kooperation mit Jens Hartung darauf zurückgeführt werden kann, dass für einen axial gebundenen Phenyl-Rest in paralleler Stellung zur Vinyl-Gruppe (*cis*-$_2$T^3) geringere sterische Wechselwirkungen entstehen, als es für die axiale Anordnung der Methyl-Gruppe (*trans*-^{2}T$_3$) der Fall ist (Abbildung 4.1). Übergangszustände, bei denen C3 und die Vinyl-Gruppe auf der gleichen Seite stehen (*cis*-^{2}T$_3$ und *trans*-$_2$T^3), sind aufgrund sterischer und ekliptischer Abstoßungen generell ungünstiger.

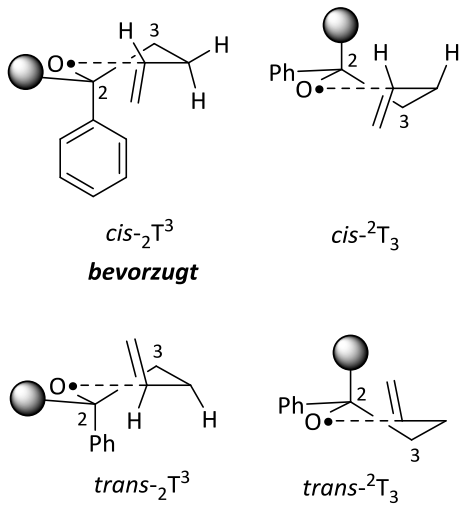

Abbildung 4.1 Twist-Modell-Übergangszustände zur Beschreibung der Stereoselektivität in 5-*exo*-Cyclisierungen des *O*-Radikals **If**. Graue Kugel = Methyl-Gruppe.

(C) Intermolekulare Addition

Bimolekulare Additionsreaktionen zwischen *tert*-Butyl- **3a**, Cumyl- **3d** oder *p*-Chlorcumyl-substituierten Thiohydroxamsäure-*O*-ester **3e** mit Norbornen (**12**) liefern nach photochemischer Aktivierung in Gegenwart von Bromtrichlormethan die 2-Brom-3-alkoxy-bicyclo[2.2.1]heptane (**14a**, **14d** und **14e**), die Ketone **7**, **11** und **13** sowie die Alkohole **1a**, **1d** und **1e** (Tabelle 4.3).[19,20] Norbornen (**12**) bietet dabei den Vorteil, dass dessen allylische H-Atome, aufgrund einer hohen Bindungsdissoziationsenergie (453.5 ± 4 kJ/mol)[21] des geometrisch gespannten Substrats, nicht abstrahiert werden können.

Tabelle 4.3. Produkte der intermolekularen Additionsreaktion der Thiohydroxamate **3a**, **3d** und **3e** mit Norbornen (**12**) in Gegenwart von Bromtrichlormethan

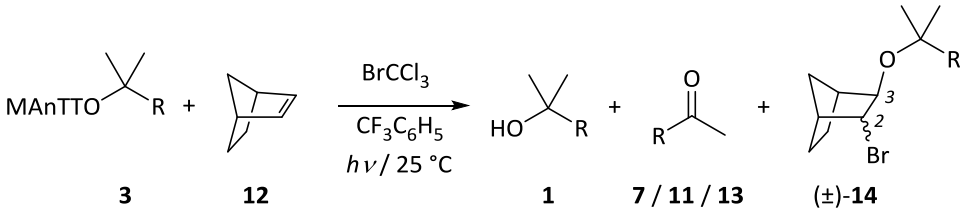

3 **12** **1** **7** / **11** / **13** (±)-**14**

Eintrag	**3**	R	c_0[12] / M	**1** / %	**7** / **11** / **13** / %	**14** (2-*exo*:2-*endo*)[b] / %
1	**3a**	CH_3	2.760	**1a**: –[a]	**7**: –[a]	**14a**: 20 (20:80)
2	**3d**	C_6H_5	2.760	**1d**: –[a]	**11**: –[a]	**14d**: 46 (28:72)
3	**3e**	*p*-ClC_6H_4	2.760	**1e**: –[a]	**13**: –[a]	**14e**: 44 (28:72)
4	**3e**[d]	*p*-ClC_6H_4	0.210	**1e**: 27	**13**: 19	**14e**: 36 (30:70)
5	**3e**[d]	*p*-ClC_6H_4	0.105	**1e**: 30	**13**: 30	**14e**: 29 (24:76)
6	**3e**[d]	*p*-ClC_6H_4	0.050	**1e**: 38	**13**: 27	**14e**: 12 (22:78)

[a] nicht bestimmt, [b] 3-*exo*-Konfiguration für beide Stereoisomere, [c] nicht beteiligt, [d] GC-Analyse und Ausbeuten der Reaktionsprodukte.

Zur Abschätzung der bimolekularen Geschwindigkeitskonstanten dienen die Ausbeuten an **14e** und **13** bei verschiedenen Norbornenkonzentrationen (Tabelle 4.3, Eintrag 4–6, Schema 4.5). Unter Zugrundelegung der Fragmentierung von **Ie** zu *p*-Chloracetophenon (**13**) (k^{Frag}**Ie** = 1×10^6 s^{-1}, 22 °C in CH_3CN)[22] ergibt sich nach Gleichung 3 die Geschwindigkeitskonstante k^{Add}**Ie** der intermolekularen Addition von **Ie** an Norbornen (**12**) in α,α,α-Trifluortoluol bei 25 °C. Sie beträgt k^{Add}**Ie** = 1×10^7 M^{-1} s^{-1}.

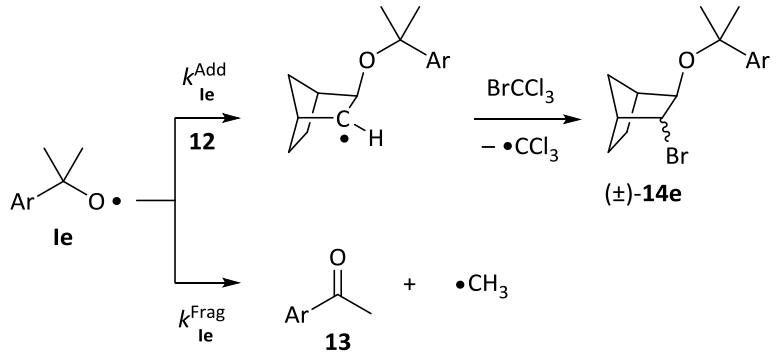

Schema 4.5. Konkurrenzkinetische Betrachtung der Addition (k^{Add}) und Fragmentierung (k^{Frag}) des Radikals **Ie** in Gegenwart von Norbornen (**12**) und Bromtrichlormethan.

$$\frac{[\mathbf{14e}]}{[\mathbf{13}]} = \frac{k^{Add}_{\mathbf{Ie}}}{k^{Frag}_{\mathbf{Ie}}}\,[\,\mathbf{12}\,] \quad \Leftrightarrow \quad k^{Add}_{\mathbf{Ie}} = \frac{[\mathbf{14e}]/[\mathbf{13}]}{[\mathbf{12}]}\,k^{Frag}_{\mathbf{Ie}} \qquad \text{(Gleichung 3)}$$

Die tertiären *O*-Radikale **Ia**, **Id**, **Ie** addieren *exo*-spezifisch an Norbornen (**12**), ähnlich wie das sterisch weniger gehinderte Methoxyl-Radikal.[9,10,19] Der anschließende Bromeinfang verläuft *trans*-selektiv (Abbildung 4.2).

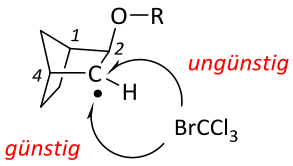

exo-**VI**

Abbildung 4.2. Angriffsmöglichkeiten von Bromtrichlormethan am 2-Alkoxybicyclo[2.2.1]-heptan-3-yl-Radikal *exo*-**VI**. R = $(CH_3)_3C$, C_6H_5, *p*-Cl-C_6H_4.

Reaktions- ($\Delta_R E$) und Aktivierungsenergien ($\Delta E^{\ddagger}$) des *exo*- und *endo*-selektiven Angriffs tertiärer Alkoxyl-Radikale an Norbornen (**12**) wurden in Kooperation mit Jens Hartung berechnet. Als Modell-Radikale dienten das *tert*-Butoxyl-Radikal **Ia** sowie zur Berücksichtigung sterischer Aspekte das Methoxyl-Radikal **Ig**. Beide Radikale zeigen unabhängig von verwendeten Dichtefunktionalverfahren (B3LYP/6-31+G**, BHandHLYP/6-31+G** und BHandHLYP/6-311G**)[23–27] einen stark exothermen Reaktionsverlauf mit vergleichbaren Barrieren für die *exo*- und *endo*-Addition an Norbornen (**12**) ($\Delta_R E$, Tabelle 4.4 exemplarisch für B3LYP/6-31+G**), was gemäß dem Hammond-Postulat[28] kinetische Reaktionskontrolle und frühe, Edukt-ähnliche Übergangszustände impliziert.

Tabelle 4.4. Energien (B3LYP/6-31+G**) der *exo*- und *endo*-Addition des Methoxyl- und des *tert*-Butoxyl-Radikals an Norbornen (**12**). **Ia**: R = $C(CH_3)_3$, **Ig**: R = CH_3.

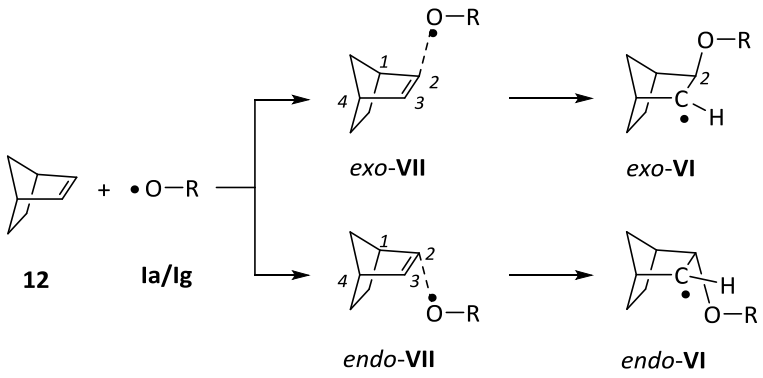

Eintrag	Radikal	$\Delta E^{\ddagger}$ /kJ mol^{-1}	$\Delta_R E$ /kJ mol^{-1}	$\Delta E_i^{\ddagger}$ /kJ mol^{-1}	$\Delta E^{\ddagger}_{TD}$ /kJ mol^{-1}
1	*exo*-**VIa**	14.8	−66.6	41.4	−26.6
2	*endo*-**VIa**	30.4	−67.0	59.2	−28.8
3	*exo*-**VIg**	7.7	−80.5	37.0	−29.3
4	*endo*-**VIg**	20.3	−78.8	52.3	−32.0

Die berechneten Reaktions- ($\Delta_R E$) und Aktivierungsenergien ($\Delta E^{\ddagger}$) erlauben unter Anwendung der Marcus-Theorie[28–30], Aussagen zu intrinsischen Barrieren ($\Delta E_i^{\ddagger}$, Spannung / Sterik) einer thermoneutralen Reaktion (Gleichung 4) sowie zu thermodynamischen Barrieren ($\Delta E^{\ddagger}_{TD}$: Energien des Bindungsbruch bzw. der Bindungsbildung, Gleichung 5) für die intermolekularen *exo*- und *endo*-Additionen der Radikale **Ia** und **Ig** an Norbornen (**12**) zu formulieren (Tabelle 4.4).

$$\Delta E^{\ddagger}_i = \frac{\Delta E^{\ddagger} - \frac{\Delta_R E}{2} + \sqrt{(\Delta E^{\ddagger})^2 - (\Delta_R E)(\Delta E^{\ddagger})}}{2} \qquad \text{(Gleichung 4)}$$

$$\Delta E^{\ddagger} = \Delta E^{\ddagger}_i + \Delta E^{\ddagger}_{TD} \qquad \text{(Gleichung 5)}$$

Den Berechnungen zufolge ist die *exo*-Addition (*exo*-**VI**) beider Radikale (**Ia**, **Ig**) mit geringeren Spannungseffekten verbunden als die *endo*-Addition (*endo*-**VI**) ($\Delta E_i^{\ddagger}$, Tabelle 4.4). Thermodynamische Beiträge ($\Delta E^{\ddagger}_{TD}$) und Angriffsmöglichkeiten beider Radikale sind vergleichbar, woraus folgt, dass intrinsische Effekte für die *exo*-Selektivität verantwortlich sind und mit zunehmender Sterik des Alkoxyl-Radikals steigen.

Der *exo*-Angriff des *O*-Radikals an die π-Bindung von **12** hat zur Folge, dass sich das Wasserstoffatom an C2 in die *endo*-Richtung bewegt, während sich das benachbarte olefinische Wasserstoffatom an C3 zum *O*-Radikal hin orientiert. Die daraus resultierende, synklinale Anordung des Wasserstoffatoms an C2 und dem Brückenkopf-Wasserstoffatom an C1 ist mit geringeren Tosrionsspannungen verbunden als es für einen *endo*-Angriff des *O*-Radikals der Fall wäre, der zu ekliptisch angeordneten Wasserstoffatomen an C1 und C2 führt (Abbildung 4.3).

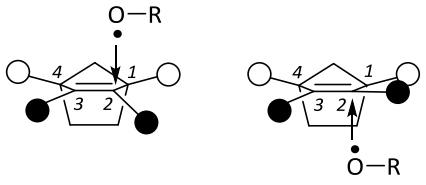

exo-Angriff (**bevorzugt**) *endo*-Angriff

Abbildung 4.3. *Exo*- und *endo*-Angriff eines tertiären *O*-Radikals an Norbornen (**12**). Weiße Kugeln: Brückenkopf H-Atome; schwarze Kugeln: olefinische H-Atome.

4.4 Fazit & Ausblick

Der synthetische Zugang zu tertiären *O*-Alkylthiohydroxamten mit Hilfe der Isoharnstoff-Methode eröffnet Möglichkeiten, Reaktivitäten tertiärer *O*-Radikale genauer zu untersuchen. Die ersten zur Verfügung stehenden Daten zeigen unerwarteterweise, dass tertiäre *O*-Radikale noch reaktiver sind als primäre und sekundäre Analoga.

Überraschend sind insbesondere die Reaktivität und 2,5-*cis*-Selektivität des 2-Phenyl-5-hexen-2-oxyl-Radikals **If**, das in dieser Arbeit als Modell-Radikal für 5-*exo*-Cyclisierungen fungiert. In weiterführenden Arbeiten ist demnach die Ursache der Reaktivitätssteigerung im Vergleich zu primären und sekundären Derivaten von Bedeutung, aber auch die Allgemeingültigkeit der *cis*-Selektivität für Substituenten in Position 1. Beide Effekte lassen sich durch eine Substituentenvariation (z. B. CF_3, CCl_3, 4-Cl-C_6H_4, OMe, CO_2Me, 4-MeO-C_6H_4) in direkter Nachbarschaft zum *O*-Radikal überprüfen.

4.5 Literaturverzeichnis

[1] B. P. Hay, A. L. J. Beckwith, *J. Org. Chem*. **1989**, *54*, 4330–4334.

[2] J. Hartung, T. Gottwald, K. Špehar, *Synthesis* **2002**, *11*, 1469–1498.

[3] J. Hartung, *Eur. J. Org. Chem.* **2001**, 619–632.

[4] J. Hartung, C. Schur, I. Kempter, T. Gottwald, *Tetrahedron* **2010**, *66*, 1365–1374.

[5] T. Gottwald, *Dissertation* **2004**, Julius-Maximilians-Universität Würzburg.

[6] L. J. Mathias, *Synthesis* **1979**, 561–576.

[7] M. Mikołajczyk, P.Kiełbasiński, *Tetrahedron* **1981**, *37*, 233–284.

[8] E. Cuny, R. Jäger, *Chem. Unserer Zeit* **2010**, *44*, 40–48.

[9] J. Hartung, N. Schneiders, T. Gottwald, *Tetrahedron Lett.* **2007**, *48*, 6027–6030.

[10] N. Schneiders, *Dissertation* **2008**, Technische Universität Kaiserslautern.

[11] M. Newcomb in *Radicals in Organic Synthesis*; P. Renaud, M. P. Sibi, Eds.; Wiley-VCH-Weinheim, 2001, Vol. 1, Kapitel 3.1, 317–324.

[12] D. Griller, K. U. Ingold, *Acc. Chem. Res.* **1980**, *13*, 317–323.

[13] J. Hartung, T. Gottwald, K. Špehar, *Synlett* **2003**, 227–229.

[14] J. Hartung, C. Schur, I. Kempter, T. Gottwald, *Tetrahedron* **2010**, *66*, 1365–1374.

[15] M. Weber, H. Fischer, *J. Am. Chem. Soc.* **1999**, *121*, 7381–7388.

[16] M. Bietti, O. Lanzalunga, M. Salamone, *J. Org. Chem*. **2005**, *70*, 1417–1422.

[17] R. Atkinson, *Int. J. Chem. Soc*. **1997**, *29*, 99–111.

[18] J. Hartung, K. Daniel, C. Rummey, G. Bringmann, *Org. Biomol. Chem*. **2006**, *4*, 4089–4100.

[19] J. Hartung, N. Schneiders, T.Gottwald, *Tetrahedron Lett.* **2007**, *48*, 6027–6030.

[20] P. C. Wong, D. Griller, J. C. Scaiano, *J. Am. Chem. Soc.* **1982**, *104*, 5106–5108.

[21] P. M. Nunes, S. G. Estácio, G. T. Lopes, F. Agapito, R. C. Santos, B. J. Costa Cabral, R. M. Borges dos Santos, J. A. Martinho Simoes, *J. Phys. Chem. A* **2009**, *113*, 6524–6530.

[22] E. Baciocchi, M. Bietti, M. Salamone, S. Steenken, *J. Org. Chem*. **2002**, *67*, 2266–2270.

[23] Gaussian 03, Revision E.01, M. J. Frisch, G. W. Trucks, H. B. Schlegel, G. E. Scuseria, M. A. Robb, J. R. Cheeseman, J. A. Montgomery, Jr., T. Vreven, K. N. Kudin, J. C. Burant, J. M. Millam, S. S. Iyengar, J. Tomasi, V. Barone, B. Mennucci, M. Cossi, G. Scalmani, N. Rega, G. A. Petersson, H. Nakatsuji, M. Hada, M. Ehara, K. Toyota, R. Fukuda, J. Hasegawa, M. Ishida, T. Nakajima, Y. Honda, O. Kitao, H. Nakai, M. Klene, X. Li, J. E. Knox, H. P. Hratchian, J. B. Cross, V. Bakken, C. Adamo, J. Jaramillo, R. Gomperts, R. E. Stratmann, O. Yazyev, A. J. Austin, R. Cammi, C. Pomelli, J. W. Ochterski, P. Y. Ayala, K. Morokuma, G. A. Voth, P. Salvador, J. J. Dannenberg, V. G. Zakrzewski, S. Dapprich, A. D. Daniels, M. C. Strain, O. Farkas, D. K. Malick, A. D. Rabuck, K. Raghavachari, J. B. Foresman, J. V. Ortiz, Q. Cui, A. G. Baboul, S. Clifford, J. Cioslowski, B. B. Stefanov, G. Liu, A. Liashenko, P. Piskorz, I. Komaromi, R. L. Martin, D. J. Fox, T. Keith, M. A. Al-Laham, C. Y. Peng, A. Nanayakkara, M. Challacombe, P. M. W. Gill, B. Johnson, W. Chen, M. W. Wong, C. Gonzalez, J. A. Pople, Gaussian, Inc., Wallingford CT, **2004**.

[24] J. B. Foresman, Æ. Frisch, *Exploring Chemistry with Electronic Structure Methods*, 2nd ed. **1996**, Gaussian Inc., Pittsburgh, PA.

[25] A. D. Becke, *J. Chem. Phys.* **1993**, *98*, 5648–5652.

[26] C. Lee, W. Yang, R. G. Parr, *Phys. Rev.* **1988**, *B37*, 785–789.

[27] A. D. Becke, *Phys. Rev*. **1988**, *A38*, 3098–3100.

[28] G. S. Hammond, *J. Am. Chem. Soc.* **1955**, *77*, 334–338.

[29] R. A. Marcus, *J. Phys. Chem*. **1968**, *72*, 891–899.

[30] W. J. Albery, *Ann. Rev. Phy. Chem.* **1980**, *31*, 227–263.

[31] L. H. Gade In *Koordinationschemie*, Wiley-VCH, Weinheim, **1998**, 1. Auflage, 443–479.

4.6 Forschungsartikel

Tertiary Alkoxyl Radicals from 3-Alkoxythiazole-2(3*H*)-thiones

Christine Schur, Nina Becker, Uwe Bergsträßer, Thomas Gottwald, and Jens Hartung*,

Tetrahedron **2011**, *67*, 2338–2347.

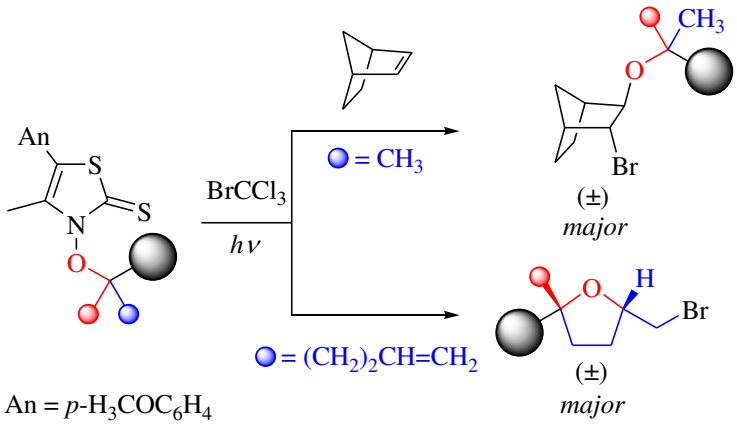

Tetrahedron 67 (2011) 2338–2347

Contents lists available at ScienceDirect

Tetrahedron

journal homepage: www.elsevier.com/locate/tet

Tertiary alkoxyl radicals from 3-alkoxythiazole-2(3*H*)-thiones

Christine Schur [a], Nina Becker [a], Uwe Bergsträßer [a], Thomas Gottwald [b], Jens Hartung [a,*]

[a] *Fachbereich Chemie, Organische Chemie, Technische Universität Kaiserslautern, Erwin-Schrödinger-Straße, D-67663 Kaiserslautern, Germany*
[b] *Institut für Organische Chemie, Universität Würzburg, Am Hubland, 97074 Würzburg, Germany*

ARTICLE INFO

Article history:
Received 16 September 2010
Received in revised form 21 December 2010
Accepted 29 December 2010
Available online 8 January 2011

Keywords:
Addition
Alkoxyl radical
O-Alkyl isourea
Bromocyclization
Bromohydrin ether
Fragmentation
Homolytic substitution
Radical clock
Stereoselective synthesis
Thiazolethione
Thiohydroxamic acid

ABSTRACT

This study deals with the synthesis of *tert*-*O*-alkyl thiohydroxamates and their use as *tert*-alkoxyl radical precursors. *tert*-Alkoxyl radicals were applied in mechanistic studies to determine rate constants of (i) *p*-chlorocumyloxyl radical addition to bicyclo[2.2.1]heptene ($k=1\times10^7$ M^{-1} s^{-1}), (ii) 2-phenylhex-5-en-2-oxyl radical 5-*exo*-*trig*-cyclization ($k^{cis}=3\times10^9$ s^{-1}, $k^{trans}=1\times10^9$ s^{-1}), and (iii) 2-methyl-5-phenylpent-2-oxyl to 2-hydroxy-2-methyl-5-phenylpent-5-yl radical isomerization (1,5-H-atom shift; $k=0.4–1.5\times10^8$ s^{-1}). The reactions pose key steps in synthesis of 2,2,5-substituted tetrahydrofurans and 2-bromo-3-alkoxybicyclo[2.2.1]heptanes. Stereoselectivity in 5-*exo*-*trig* cyclization (2,5-cis) and intermolecular addition (*exo*/*endo*>99:1), originates from torsional strain in transition structures of alkoxyl radical reactions.

1. Introduction

In a given chemical environment, *tert*-alkoxyl radicals undergo fast unimolecular and bimolecular reactions, to leave diagnostic product mixtures. Chemical changes thereby follow distinct patterns of homolytic substitution (S_R), β-C,C-homolysis (D_R), and π-bond addition (A_R), to mention the most important elementary reactions (Scheme 1).[1–4] It is this combination of reactivity and selectivity that explains the significance, *tert*-alkoxyl radicals have gained for elucidating reaction mechanisms in physical organic chemistry,[5–7] atmospheric science,[8] biochemistry,[9–11] and macromolecular chemistry.[12,13] With the advent of more selective progenitors, this interest, however, has partly shifted from mechanistic to more synthetically oriented studies. The desire to apply alkoxyl radicals in synthesis thereby comes from electrophilic properties of the radical oxygen, for example, in additions or homolytic substitutions. Alkoxyl radicals therefore add a component to organic synthesis that is not available from other intermediates.[14–16]

In an earlier study, we had shown that 3-alkoxy-5-(4-methoxyphenyl)-4-methylthiazole-2(3*H*)-thiones (e.g., **1**) almost quantitatively liberate alkoxyl radicals, if thermally or photochemically activated in the presence of a mediator.[17] Primary and secondary 3-alkoxy-5-(4-methoxyphenyl)-4-methylthiazole-2(3*H*)-thiones are synthetically available in yields between 70 and 90%.[17] Attempts to prepare tertiary derivatives thereof from

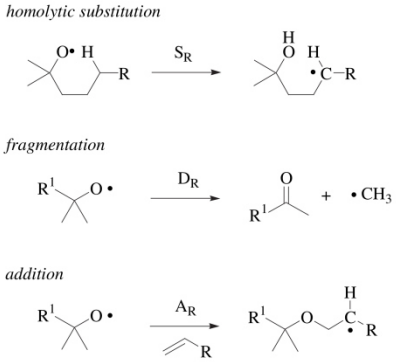

Scheme 1. Alkoxyl radical elementary reactions relevant for the present study [for R^1 see Fig. 1; R=alkyl or phenyl (vide infra); nomenclature: A=associative step, S=substitution, D=dissociative step, R=radical-based transformation].

* Corresponding author. Tel.: +49 631 205 2431; fax: +49 631 205 3921; e-mail address: hartung@chemie.uni-kl.de (J. Hartung).

0040-4020/$ – see front matter © 2011 Elsevier Ltd. All rights reserved.
doi:10.1016/j.tet.2010.12.071

alcohols or haloalkanes under solvolysis conditions, on the other hand, were not successful.[18,19,24] Strategies to apply Lewis-acids for more effective carbon electrophile-activation resulted in precipitation of thiohydroxamate complexes.[20–22] None of these complexes were receptive for O-alkylation.[23]

Since *tert*-alkoxyl radicals for synthetic applications remained difficult to generate,[24] we chose to develop a practical method for synthesis of 3-(*tert*-alkoxy)-thiazole-2(3*H*)-thiones **1a**–**f** (Fig. 1). To validate the performance of these compounds, we devised a project on synthesis of 2,2,5-substituted tetrahydrofurans and 2-bromo-3-alkoxybicyclo[2.2.1]heptanes from intra- and intermolecular alkoxyl radical reactions. The compounds (vide infra) are derivatives of mono- and bicyclic secondary metabolites, pharmaceuticals, and pesticides, which sometimes are difficult to prepare in ionic reactions.[25–27] The most important results from the study show that synthesis of tertiary *O*-alkyl thiohydroxamates **1a**–**f** using a newly developed procedure is feasible in up to 64% yield. If activated, the molecules liberate *tert*-alkoxyl radicals, suitable for application in mechanistic and synthetic studies.

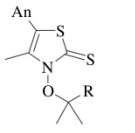

1

1	R
a	CH_3
b	C_2H_5
c	$(CH_2)_3C_6H_5$
d	C_6H_5
e	4-ClC_6H_4

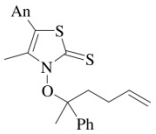

1f

An = 4-$(H_3CO)C_6H_4$

Fig. 1. Structure formulas and indexing of tertiary 3-alkoxythiazole-2(3*H*)-thiones **1a**–**f**.

2. Results and interpretation

2.1. Tertiary 3-alkoxy-4-methylthiazole-2(3*H*)-thiones

The general strategy for *O*-alkylthiohydroxamate synthesis from thiohydroxamic acids requires selective alkylation at oxygen. The thiohydroxamic acid we chose in this study, 3-hydroxy-5-(4-methoxyphenyl)-4-methylthiazole-2(3*H*)-thione (MAnTTOH; **2**), has a remarkable affinitity for substitution at oxygen instead of sulfur, if treated with an appropriate carbon electrophile.[17] To develop a synthetic method (**1a**, **1b**; Section 2.1), investigate thermal stability (**1d**; Section 2.2), perform intramolecular reactions (**1c**, **1f**; Section 2.3 And 2.4), and explore intermolecular alkoxyl radical additions (**1a**, **1d**–**e**; Section 2.5), we selected *tert*-alcohols **3a**–**f** as substrates to in situ generate carbon electrophiles.

In previous studies[28,29] we had discovered that *O*-*tert*-butyl-*N*,*N*-diisopropyl isourea[30,31] is a suitable reagent to use for developing a more efficient and general method for *tert*-O-alkylation of acid **2**. The isourea is available from *tert*-butanol **3a**, diisopropyl carbodiimide (DIC), and catalytic amounts of CuCl. We now report that slow addition of 5.5 equiv of the alkylation reagent to a CH_2Cl_2-solution of thiohydroxamic acid at 24 °C furnishes O-*tert*-butyl ester **1a** in 58–64% yield, besides *S*-*tert*-butyl derivative **4a** (25%).[17,19,32]

A change in solvent to DMF, fewer *O*-*tert*-butyl isourea equivalents, or lower reaction temperature (≤0 °C) reduces the yield of *tert*-butyl ester **1a**. Higher rates of *O*-*tert*-butyl isourea addition lead to formation of 1,2-bis-[5-(4-methoxyphenyl)-4-methylthiaz-3-yl]-disulfane (**5**)[33] as additional product in up to 13% yield, whereas the yield of product **1a** decreases. Substitution of dicyclohexyl carbodiimide (DCC) for DIC (cf. Table 1, entry 1) was not successful in our hands (22% of **1a** under conditions used in Table 1, entry 1).

Table 1
Products of 3-hydroxy-5-(4-methoxyphenyl)-4-methylthiazole-2(3*H*)-thione alkylation and selected characteristics of target products **1a**–**f**

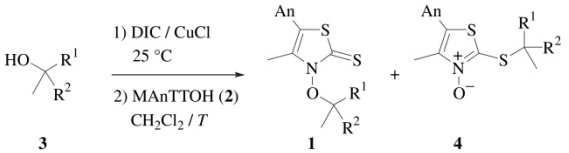

3 **1** **4**

Entry	**1**/**3**/**4**	R^1	R^2	*T*/°C	**1**/%	Mp **1**/°C	**4**/%
1	**a**	CH_3	CH_3	24	58–64[a]	112	25[c]
2	**b**	CH_3	C_2H_5	0	45–47[b]	72	33[c]
3	**c**	CH_3	$(CH_2)_3C_6H_5$	0	44	64	11[c]
4	**d**	CH_3	C_6H_5	−30	15	108	38
5	**e**	CH_3	*p*-ClC_6H_4	−30	13	95	33
6	**f**	$(CH_2)_2CH{=}CH_2$	C_6H_5	−30	18	110	27[b]

[a] Mean value from five experiments.
[b] Mean value from three experiments.
[c] Determined via ^1H and ^{13}C NMR.

We furthermore used the in situ method to convert *tert*-amyl alcohol **3b**, 2-methyl-5-phenylpentan-2-ol (**3c**) (44–47%; Table 1, entries 2 and 3), and 2-arylalcohols **3d**–**f** (13–18%; Table 1, entries 4–6) into *O*-esters **1b**–**f**. Alkylsulfanylthiazole *N*-oxides **4b**–**f**, but also alkenes, such as a 52/48-mixture of 2-methyl-5-phenylpent-1-ene and 2-methyl-5-phenylpent-2-ene (63–76% from **3c**), α-methylstyrene (**6**) (39% from **3d**), *p*-chloro-α-methylstyrene (48% from **3e**), and a 63/37-mixture of 2-phenylhexa-1,5-diene and 5-phenylhexa-1,4-diene (24–38% from **3f**), were found as by-products. Since we had no head space equipment available, elimination products formed from **3a** and **3b** escaped analysis.

3-Alkoxythiazolethiones were obtained as colorless (**1c**–**f**) to pale yellow (**1a**,**b**) crystalline compounds that melted between 64 °C (**1c**) and 112 °C (**1a**). Electronic spectra of the thiazolethiones in solutions of EtOH showed a band located at λ=336–338 nm (ε ~3.20–3.28 m^2 mol^{-1}). This absorption is relevant for photochemical alkoxyl radical generation from **1** (vide infra). The only NMR-spectroscopic aspect that deserves attention was a systematic absence of ^{13}C resonances from methyl groups attached to tertiary C-atoms, in the room temperature NMR spectra (except of **1a** and **1b**). Resonances of protons bound to such *unseen* carbons were broad. The reason behind this observation is a slow topomerization of substituents by N,O-rotation, as clarified via low temperature NMR-spectroscopy. For example, on cooling a solution of *p*-chlorocumyl ester **1e**, proton resonances of diastereotopic CH_3-groups coalesce at −3 °C (referenced versus the MeOH NMR thermometer).[34,35] At −62 °C two base line separated signals at δ_H 1.89 and 2.11 are found, which correlate with sharp resonances at δ_C 22.0 and 31.9 ppm (HMQC). The barrier to N,O-rotation ($\Delta G^{\ddagger}_{270}$=53 kJ mol^{-1}) that was calculated from the spectral information (Supplementary data) is, in view of an estimated precision of ±10%, close to the value of 44 kJ mol^{-1} reported for ester **1d** (coalescence temperature: 276 K).[18]

In the crystal structure of **1e**, the *p*-chlorocumyl substituent is almost orthogonally offset from the heterocyclic plane [C2–N3–O1–C14=96.8(2)°] (Fig. 2). The N3–O1–C14 angle [116.0 (1)°] is widened and correlates with the value of ~116° that was predicted for *tert*-*O*-esters of **2** on the basis of a Taft–Dubois-relationship.[18] Distances N3–O1 [1.383(2) Å] and C2–S2 [1.659(3) Å] fit into a N–O/C=S-correlation derived from crystallographic data of ten MAnTTORs (Supplementary data). N,O-bond lengthening in this

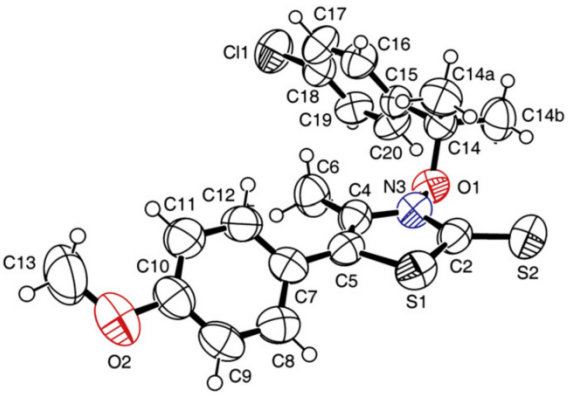

Fig. 2. Ellipsoid graphic (50% probability) of 3-[2-(*p*-chlorophenyl)-2-propoxy]-thiazolethione **1e** in the solid state [293 K; H-atoms were drawn as circles of an arbitrary radius; the (*M*)-enantiomer was selected from the racemate in the unit cell; C2/*c*, *Z*=8].

product class, by introducing a sterically demanding substituent at oxygen, causes a shortening of the associated C=S bond. This structural responsivity is stronger than for any other type of investigated thiohydroxamic acid, and explains why heterocycle **2** handles strain at oxygen so well.[18]

2.2. Thermal stability

N-Cumyloxythiazolethione **1d** (mp 108 °C) decomposes within 60 min, if heated in boiling toluene (Scheme 2). The reaction provides disulfide **5**, α-methylstyrene **6**, acetophenone **7**, and thiolactam **8**.[36] The product spectrum suggests a Tschugaeff-type fragmentation, which should have also afforded MAnTTOH (**2**). To detect the latter, a color test was performed using Fe(II)-stained TLC-sheets. A green color thereby denotes Fe(II)/(bis)thiohydroxamate formation, and thus a positive analytical response. During thermal decomposition of **1d**, while continuously being checked with the spotting test, a transient positive analytical response (green spot) is found, however, only within a quite narrow time frame. Intensity and time-line of the photometric response correlate with results from a control, starting from thiohydroxamic acid **2** in boiling toluene. We stopped the reaction as no further acid **2** was detectable. Analysis of this solution (^{1}H NMR, TLC) shows disulfide **5** as major product.

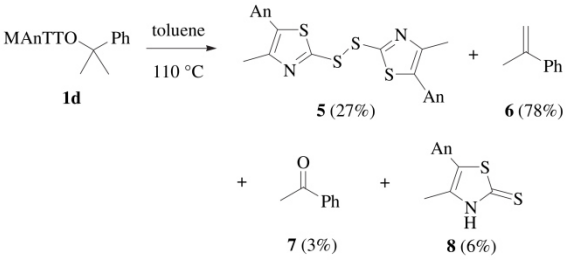

Scheme 2. Products of thermal 3-cumyloxythiazolethione decomposition.

2.3. Homolytic substitution

3-Alkoxy-5-(4-methoxyphenyl)-4-methylthiazole-2(3*H*)-thiones liberate alkoxyl radicals, if photochemically excited (λ=350 nm, 25 °C) or heated in the presence of initiator AIBN. For both modes of activation C_6H_6 or $C_6H_5CF_3$ are useful solvents, and $BrCCl_3$ the preferred mediator for conducting synthetic and mechanistic investigations.[17]

Photolysis of 3-(2-methyl-5-phenylpent-2-oxy)-thiazolethione **1c** and $BrCCl_3$ (c_0=1.70 M) in a solution of C_6D_6 furnishes alcohol **3c** (36%), δ-bromohydrin **9** (41%), tetrahydrofuran **10** (22%), disulfide **5** (20%), and 5-(4-methoxyphenyl)-4-methyl-2-trichloromethylsulfanyl thiazole (**11**) (10%). Acetone (**12**) is obtained in 3–5% yield. A triplet at δ=2.91 (*J*=6.5 Hz) points to 3-bromo-1-phenylpropane formation. Signal overlap (^{1}H NMR/GC) precluded quantitative analysis of this product. As the solution is allowed to rest for 48 h at 25 °C, bromoalcohol **9** is converted into additional 2,2-dimethyl-5-phenyltetrahydrofuran (**10**).[37] The latter compound was isolated from additional photochemical and thermally-induced experiments that used the same reactant concentrations, leading to similar yields of **10** (Table 2, entries 2 and 3).

From product analysis we conclude that the 2-methyl-5-phenylpent-2-oxyl radical (**Ic**) is formed in photochemical and thermally-induced reactions starting from *N*-alkoxythiazolethione **1c** and $BrCCl_3$ (Scheme 3). A 1,5-H-atom shift transforms alkoxyl radical **Ic** into stabilized benzylic radical **II**. The latter abstracts a Br-atom from $BrCCl_3$ to give δ-bromohydrin **9** and •CCl_3. Bromoalcohol **9** cyclizes upon standing to furnish tetrahydrofuran **10**. The total amount of 1,5-H-shifted intermediate **II** therefore relates to the combined yield of products **9** and **10** (63%). Since acetone (**12**) and 3-bromo-1-phenylpropane are formed as by-products, radical **Ic** not only undergoes 1,5-H-atom shift **Ic**→**II** but also β-C,C-homolysis **Ic**→**III**+**12**. On the assumption that both reactions follow kinetic control, and Br-atom trapping by **II** is quantitative,[17] the ratio (**9**+**10**)/**12**=12.6–21.0 reflects relative reactivity of 1,5-H-atom shift versus β-C,C homolysis, that is, $k^{S_{R_{1c}}}/k^{D_{R_{1c}}}$. The rate constant for the β-fragmentation thereby can be approximated with the value for acetone liberation from *tert*-butoxyl radical fragmentation ($k^{D_{R_{1a}}}$ =2.0×10^4 s^{-1}, for 25 °C in C_6H_6).[38] Since the ethyl radical forms by a factor of 150–350 faster from alkoxyl radical β-C,C-fragmentation than the methyl radical,[7,39] a value of 3.0×10^6 s^{-1} was used as lower and 7.0×10^6 s^{-1} as upper limit for unknown $k^{D_{R_{1c}}}$. The range obtained for $k^{S_{R_{1c}}}$ (0.4–1.5×10^8 s^{-1}) indicates that the 1,5-H-shift in *tert*-alkoxyl radical **Ic**, in spite of its steric encroachment near oxygen, is not slower than 1,5-H-shift in the 1-pentoxyl radical (k^{S_R} =2.7×10^7 s^{-1} at 20 °C).[40,41]

Yields of alcohol **3c** between 23 and 36% show that an effective H-atom donor exists in reaction mixtures used for mechanistic experiments starting from **1c** (Table 2). Since benzylic radicals, for example, **II**, abstract a Br-atom from $BrCCl_3$ much faster than an H-atom from any known reductant, the issue of radical reduction is restricted to alkoxyl radical **Ic**. Although this chemistry does not interfere with the kinetic analysis outlined above and in the following sections, clarifying the nature of the reductant could also mean finding ways to inhibit unwanted alkoxyl radical consumption. A control performed by photolyzing *tert*-butoxythiazolethione **1a** in solutions of C_6D_6 or CCl_4, provided *t*-BuOH, disulfide **5**, and at least one additional thiazole-derived product. Attempts, to separate the additional thiazole derivative failed. On the basis of signal integration it seems that a methyl group attached to thiazole probably is the unknown H-atom donor. Support for this interpretation comes from mass-balancing: the yield of alcohol **3c**, and of other alcohols obtained from 3-alkoxythiazolethiones, for example, **1c**–**f** (Sections 2.4 and 2.5), never exceeded the amount of thiazole-derived products that remained unidentified.

In previous work, we had explained formation of thiazole **11** via •CCl_3-addition to the thiocarbonyl group of a 3-alkoxy-5-(4-methoxyphenyl)-4-methylthiazole-2(3*H*)-thione. This step is crucial for the mechanistic model, because it explains how •CCl_3 is able to propagate the chain reaction.[17] The major thiazole-derived product from **1c**, however, was disulfide **5**. Controls performed by photolyzing CCl_3-adduct **11** and $BrCCl_3$ in a solution of C_6D_6 (for 45 min, λ=350 nm, 25 °C) provided 58% of unspent material **11** and

Table 2
Products formed from 3-(5-phenyl-2-methylpentoxy)-thiazolethione **1c** and $BrCCl_3$

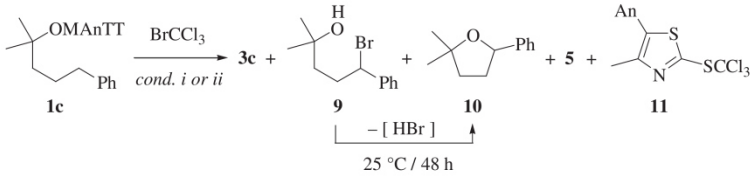

Entry	Conditions	Solvent	**3c**/%	**9**/%	**10**/%
1	(i) hv (350 nm)/25 °C[a]	C_6D_6	36	41	22
2	(i) hv (350 nm)/25 °C[b]	$C_6H_5CF_3$	23	—[c]	58
3	(ii) AIBN 80 °C	C_6H_6	—[c]	—[c]	(84) 61[d]

[a] In situ-analysis (^{1}H NMR) after 2 h; additional products: 20% of **5**, 10% of **11**, and 3–5% of acetone (**12**).
[b] Product composition after work up; additional products: 17% of **5**, 27% of **11**.
[c] Not determined.
[d] Number in parentheses refer to yield prior to work up (^{1}H NMR); yield of thiazole-derived products **5** and **11** not determined.

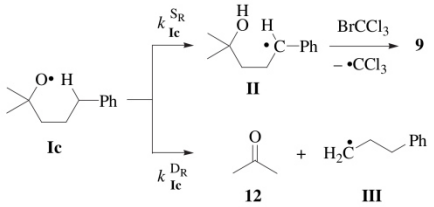

Scheme 3. Proposed scheme for mechanistic discussion of 2-methyl-5-phenylpent-2-oxyl radical reactivity in the presence of $BrCCl_3$ (roman numbers refer to transients).

21% of disulfide **5**. Subjecting disulfide **5** and $BrCCl_3$ to the same conditions did not give **11**. This information shows that **11** cannot be precursor of the entire amount of **5**. In view of the strain imposed by *tert*-*O*-alkyl substitution (cf. Section 2.1),[18] it moreover seems that fragmentation of excited **1c** occurs in competition to the chain process, leading directly to O-radical **Ic** and a thiyl radical, that is the monomer of disulfide **5**.

2.4. Intramolecular addition

Photolysis of a solution of *N*-(2-phenylhex-5-en-2-oxy)-thiazolethione **1f** and $BrCCl_3$ (c_0=0.83 M) provides 2-methyl-2-phenyl-5-bromomethyltetrahydrofuran (**13**),[42] acetophenone **7**, alkenol **3f**, disulfide **5**, and trichloromethylsulfanyl thiazole **11** (Scheme 4). 1-Phenylpent-4-en-1-one, a product of interest for the mechanistic discussion outlined below, was not detected using authentic reference (^{1}H and ^{13}C NMR, GC). A modification of the reaction conducted in boiling C_6H_6 using AIBN as initiator provided 63% of bromomethyltetrahydrofuran **13** (*cis*/*trans*=73:27), 8% of ketone **7**, and 21% of alkenol **3f**.

NOESY-spectra show a strong cross signal 5-H↔CH_3 for major bromocyclization product, which led to assignment of cis-configuration (i.e., *cis*-**13**). A 5-H↔C_6H_5 correlation and the absence of a 5-H↔CH_3 cross peak was taken as evidence for trans-configuration of the minor component (i.e., *trans*-**13**).

The chemical nature of products obtained leads us to the conclusion that radical **If** is liberated from *N*-alkenoxythiazolethione **1f** and $BrCCl_3$. Alkenoxyl radical **If** cyclizes stereoselectively (major: **If**→*cis*-**IV**), fragments (**If**→**7**+**V**), or abstracts a hydrogen atom (**If**→**3f**; vide supra). Since 5-*exo*-*trig* alkenoxyl radical addition to a terminal π-bond is irreversible and Br-atom abstraction by nucleophilic C-radicals from $BrCCl_3$ is virtually quantitative,[17] product ratios of 12 (for *cis*-**13**/**7**) and 3.8 (for *trans*-**13**/**7**; Scheme 4) reflect relative reactivity of cyclization versus β-C,C-homolysis for **If**, as expressed by $k^{A_{R^{cis}If}}/k^{D_{R_{If}}}$ and $k^{A_{R^{trans}If}}/k^{D_{R_{If}}}$ (Scheme 5). Approximation of the unknown value for $k^{D_{R_{If}}}$ with the rate constant of 2-(4-methylphenyl)-but-2-oxyl radical fragmentation into *p*-tolylacetophenone and $^{\bullet}C_2H_5$ (k^{D_R} =2.5×10^8 s^{-1} in CH_3CN at 22 °C),[7] provides $k^{A_{R^{cis}If}}$=3×10^9 s^{-1} and $k^{A_{R^{trans}If}}$=1×10^9 s^{-1}. Both values are slightly larger than references from 5-*exo*-*trig* cyclizations of structurally related secondary alkoxyl radicals to double bonds of the same substitution pattern.[43,44]

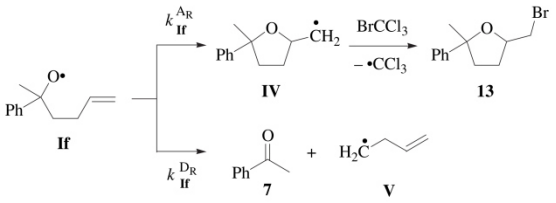

Scheme 5. Reaction scheme for kinetic analysis of 2-phenylhex-5-en-2-oxyl radical reactions.

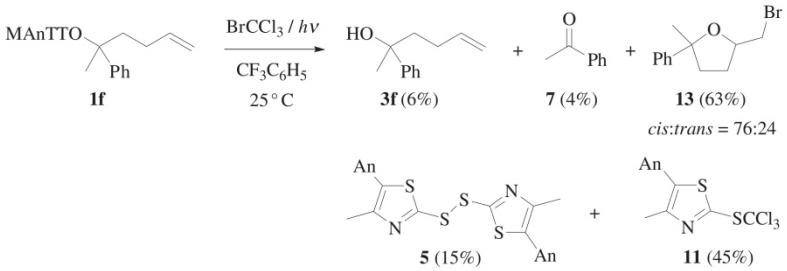

Scheme 4. Products formed from 3-(2-phenylhex-5-en-2-oxy)-thiazolethione **1f** and $BrCCl_3$.

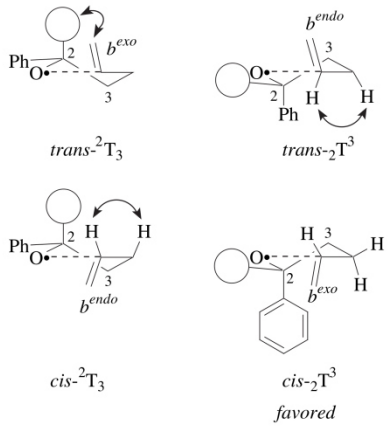

Fig. 3. Transition structure model on the origin of 2,5-cis-stereoselectivity in cyclization **If**→**IV** (CIP hierarchy for assignment of relative configurations: Ph>CH_3; the CH_3 substituent was drawn as a circle of an arbitrary radius for tutorial reasons; one enantiomer of the radical was arbitrarily chosen for presentation; arrows represent origin and effector of steric repulsion).

The observed 2,5-cis-stereoselectivity **If**→*cis*-**IV** for alkenoxyl radical cyclization is new: 1-alkyl-4-penten-1-oxyl radical cyclize 2,5-trans-selectivity, whereas 1-aryl-4-penten-1-oxyl radicals furnish a ~50/50-mixture of stereoisomers.[43,44] To explain stereoselectivity in this chemistry, a mnemonic device exists. It is applicable to kinetically controlled reactions and considers steric effects in transition structures.[45] Low in energy and thus significantly populated transition structures thereby derive from $_2T^3$- *and* $^2T_3$ conformers of tetrahydrofuran. One of the C,O-bonds is at equilibrium distance of 1.47 Å and the second, that is, the newly formed bond, stretched to ~2.05 Å (Fig. 3).[45] This geometry takes stereoelectronic prerequisites for the O-radical addition to the π-bond and minimization of torsional strain, that is, a twist rather than an envelope conformer, into account. Since the inner carbon of the vinyl group is part of the three atom unit defining the twist plane, two bisectional (*b*) arrangements for the $=CH_2$-segment exist. The conformer having the vinyl terminus and the second next neighbor, that is, C3 on opposite sides is referred to as *exo*-bisectional (b^{exo}). The opposite orientation is called *endo*-bisectional (b^{endo}). In the *exo*-bisectional form, which is the favored arrangement, H-atoms at positions 4 and 5 exhibit synclinal orientation. The *endo*-bisectional arrangement, on the other hand, leads to an eclipsing of hydrogens at the two carbons thus increasing torsional strain of the conformers (Fig. 3). Since the phenyl group in benzyloxyl radicals favors co-planar alignment of aromatic plane and radical oxygen,[46] axial phenyl, and *exo*-bisectional vinyl group orientation lead to no significant steric repulsion (Fig. 3, bottom right). In the *trans*-$^2T_3$-configured transition structure, 1,3-interactions between vinyl and methyl groups arise that increase free energy of this conformer.[45] For a rapidly equilibrating system, selectivity of a reaction, according to transition state theory and the Curtin-Hammett-principle is given by a Boltzmann-distribution covering all relevant intermediates. For our simplified model this means that the lowest in energy conformer out of the ensemble of four intermediates displayed in Fig. 3, that is, transition structure *cis*-$_2T^3$, is relevant for describing stereoselectivity of the 5-exo-ring closure of alkenoxyl radical **If**.

2.5. Intermolecular addition

2.5.1. Synthetic and kinetic aspects. Photochemical reactions of 3-alkoxythiazolethiones **1a**, **1d**, and **1e** in $C_6H_5CF_3$-solutions containing an excess of bicyclo[2.2.1]heptene (**14**) (c_0=2.76 M) and $BrCCl_3$ (c_0=278 mM) furnish 3-alkoxy-2-bromobicyclo[2.2.1]heptanes **16a**, **16d**, and **16e**. Yields of β-bromohydrin ethers grow along the series of transferred radicals *tert*-butoxyl (20%), *p*-chlorocumyloxyl (44%), and cumyloxyl (46%) (Table 4, entries 1–3). 1-Bromo-2-trichloromethylbicyclo[2.2.1]heptane **17**[47,48] and 2-chloro-1-thiazylsulfanylbicyclo[2.2.1]heptane **18** are formed as co-products. Trichloromethylsulfanyl thiazole **11** was surprisingly not found. Controls indicate that compound **11** is converted into adduct **18**, if photolyzed in an excess of olefin **14**. The mechanism of this reaction is under current investigations.

As the norbornene concentration is lowered from 0.21 M to 0.05 M, the fraction of addition product **16e** deminishes, whereas the amount of *p*-chloroacetophenone **15** grows (Table 5, entries 4–6). *p*-Chlorophenyl-2-propanol (**3e**) is obtained as additional product, presumably for reasons outlined in Section 2.3. Its yield supplemented the percentage of *p*-chlorocumyloxyl radical-derived products to 73–89%. A plot of ratios **16e**:**15** versus norbornene concentration was linear ([**16e**]/[**15**]=(9.33 M^{-1})[**14**]; R^2=0.9997). The slope, according to a kinetic model that takes irreversible *p*-chlorocumyloxyl radical fragmentation into ketone **15** and •CH_3, and a kinetically controlled addition of *p*-chlorocumyloxyl radical **Ie** to olefin **14** into account, corresponds to the ratio of $k^{A_{R_{Ie}}}/k^{D_{R_{Ie}}}$ (Scheme 6 and Supplementary data). Approximation of $k^{D_{R_{Ie}}}$ for the reaction **Ie**→**15** in $C_6H_5CF_3$ with the value determined in CH_3CN ($k^{D_{R_{Ie}}}=1\times10^6$ s^{-1} for 22 °C)[6,49] provides the rate constant $k^{A_{R_{Ie}}}=1\times10^7$ M^{-1} s^{-1}. This value is one order of magnitude higher than an EPR-spectroscopically determined reference for *tert*-butoxyl radical addition to olefin **14** ($k^{A_{R_{Ia}}}=1.1\times10^6$ s^{-1} for 27 °C).[50]

2.5.2. Stereochemical aspects. NOESY-cross signals 2-H↔7-H and 3-H↔6-H correlate with 3-*exo*-2-*endo*-configuration of major isomers of alkoxyl radical addition products **16a**, **16d**, and **16e** (Table 3, entries 1–3). For the minor isomers, 3-H↔2-H, 2-H↔6-H, and 3-H↔5-H NOESY-cross signals were found pointing to 3-*exo*-2-*exo*-configuration. Alkoxyl radical addition to norbornene **14** therefore had appeared almost exclusively from the *exo*-side. Products of Br-atom trapping, i.e., **16a**, **16d**, and **16e**, show typical 2-exo/2-endo-ratios imposed by steric shielding of the exo-face of adduct radical **VI** by a sterically demanding substituent.[47]

Since the origin of the *exo*-stereoselectivity of alkoxyl radical additions was not evident from the literature,[47,51] it was pursued using electronic structure methods.[52,53] To investigate the role of steric effects, the methoxyl radical (**Ig**) was included into the study. Experimental stereoselectivities for addition of **Ig** and the *tert*-butoxyl radical (**Ia**) to olefin **14** are identical.[15] Based on method assessment for reproducing relative energies of radicals and transition structures from our own studies,[45,54] and from work of other groups,[55,56] we chose Becke's three parameter hybrid functional (B3LYP)[57,58] and Becke's half and half functional (BHandHLYP)[59] in combination with the 6-31+G** basis set for conducting the computational analysis. The selected basis set includes diffuse and polarization wave functions, which are needed to adequately reproduce selectivities in radical additions. For exploring basis set dependence, the results were supplemented by BHandHLYP/6-311G**-calculations.[56]

Equilibrium structures of reactands **Ia**/**g** and **14**, conformationally flexible products **VIa**/**g**, and transition structures *exo*/*endo*-**VIIa**/**g** were located on respective potential energy surfaces according to an established procedure.[45] Calculation of second derivatives (Hessian matrix) that lacked in negative eigenvalues or imaginary frequency by diagonalization, characterized computed structures of alkoxyl radicals **Ia**/**g**, olefin **14**, and bicyclic carbon radicals *exo*/*endo*-**VIa**/**g** as minima. Exactly one imaginary frequency *i* associated with an O,C2-stretching vibration shows that computed structures *exo*-**VIIa**/**g** and *endo*-**VIIa**/**g** are transition

structures with respect to C,O-bond formation (Table 4). Geometrical parameters of transition structures **VIIa**/**g** relevant for explaining the origin of *exo*-selectivity are listed in Table 4, zero-point energy-corrected electronic energies (*E* for 0 K), Gibbs free energies (*G* for 298.15 K), and expectation values of the spin operator (for radicals) in the Supplementary data.

Table 3
Products of 3-alkoxythiazolethione photoreactions with norbornene **14** and $BrCCl_3$

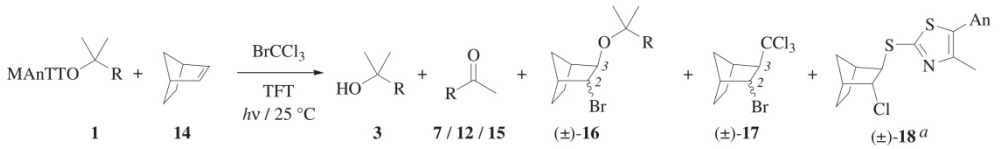

1 **14** **3** **7 / 12 / 15** (±)-**16** (±)-**17** (±)-**18** [a]

Entry	**1**	R	c_0^{14}/M	**3**/%	**7**/**12**/**15**/%	**16**/%(2-*exo*/2-*endo*)[b]	**17**/%(2-*exo*/2-*endo*)[b,c]
1	**1a**	CH_3	2.76	—[e]	**12**: —[d]	**16a**: 20 (20:80)	90 (7:93)
2	**1d**	C_6H_5	2.76	—[e]	**7**: —[d]	**16d**: 46 (28:72)	92 (5:95)
3	**1e**	*p*-ClC_6H_4	2.76	—[e]	**15**: —[d]	**16e**: 44 (28:72)	93 (7:93)
4	**1e**	*p*-ClC_6H_4	0.21	27	**15**: 19	**16e**: 36 (30:70)	82 —[e]
5	**1e**	*p*-ClC_6H_4	0.11	30	**15**: 30	**16e**: 29 (24:76)	89 —[e]
6	**1e**	*p*-ClC_6H_4	0.05	38	**15**: 26	**16e**: 12 (22:78)	73 —[e]

[a] Not quantified.
[b] 3-*exo*-configuration (GC, ^{1}H NMR).
[c] Yield referenced versus $BrCCl_3$.
[d] Not detected (GC).
[e] Not determined.

Table 4
Selected geometrical parameters of transition structures *exo*/*endo*-**VIIa**/**g**[a]

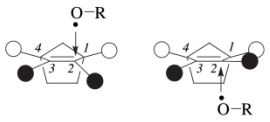

exo-**VII** *endo*-**VII**

VII/R	i[b]/cm^{-1}	O–C2/Å	O–C2–C3/°	H1–C1–C2–H2/°	H4–C4–C3–H3/°
exo-**VIIa**/*t*-Bu	−227	2.105	112.0	41.5	−28.8
	(−390)	(2.039)	(111.6)	(43.7)	(−29.5)
	[−407]	[2.024]	[109.3]	[−43.7]	[−29.7]
exo-**VIIg**/CH_3	−157	2.211	102.9	36.0	−26.4
	(−357)	(2.082)	(106.4)	(46.0)	(−28.4)
	[−389]	[2.056]	[105.8]	[40.8]	[−27.7]
endo-**VIIa**/*t*-Bu	−290	2.104	101.3	−0.3	−20.7
	(−443)	(2.054)	(103.1)	(−2.0)	(−20.3)
	[−453]	[2.043]	[102.5]	[−2.0]	[−20.0]
endo-**VIIg**/CH_3	−277	2.124	98.0	−3.6	−22.7
	(−430)	(2.062)	(101.0)	(0.9)	(−21.1)
	[−454]	[2.043]	[100.8]	[0.8]	[−20.7]

[a] Figures B3LYP/6-31+G** structures, numbers in parentheses to BHandHLYP/6-31+G** structures, and values in brackets to BHandHLYP/6-311G** structures (○ and ● symbolize key H-atoms relevant for explaining stereoselectivity).
[b] i=Imaginary mode of vibration.

Table 5
Zero-point vibrational energy-corrected activation energies ($\Delta E^{\ddagger}$), reaction energies ($\Delta_R E$), intrinsic energy barriers ($\Delta E_i^{\ddagger}$), thermodynamic contribution $\Delta E_{TD}^{\ddagger}$ to $\Delta E^{\ddagger}$, free energy differences ($\Delta G_{298.15}=G_{298.15}^{exo}-G_{298.15}^{endo}$), and estimated transition structure positioning $x^{\ddagger}$ for alkoxyl radical additions to norbornene **14** (Scheme 7, Eqs. 1–3)

Reaction	Method	$\Delta E^{\ddagger}$/kJ mol^{-1}	$\Delta_R E$/kJ mol^{-1}	ΔE_i/kJ mol^{-1}	$\Delta E_{TD}^{\ddagger}$/kJ mol^{-1}	$x^{\ddagger}$	$\Delta G_{298.15}$/kJ mol^{-1}
Ia+**14**→***exo*-VIa**	B3LYP/6-31+G**	14.8	−66.6	41.4	−26.6	0.0	≡0.0
(R=*t*-Bu)	BHandHLYP/6-31+G**	32.0	−74.9	64.0	−32.0	0.2	≡0.0
	BHandHLYP/6-311G**	28.2	−76.6	60.4	−32.2	0.2	≡0.0
Ia+**14**→***endo*-VIa**	B3LYP/6-31+G**	30.4	−67.0	59.2	−28.8	0.2	15.9
(R=*t*-Bu)	BHandHLYP/6-31+G**	50.3	−75.3	81.7	−33.4	0.3	18.4
	BHandHLYP/6-311G**	46.0	−77.6	80.1	−34.1	0.3	18.1
Ig+**14**→***exo*-VIg**	B3LYP/6-31+G**	7.7	−80.5	37.0	−29.3	(−0.8)	≡ 0.0
(R=CH_3)	BHandHLYP/6-31+G**	24.6	−87.9	60.6	−36.0	0.1	≡ 0.0
	BHandHLYP/6-311G**	21.8	−88.5	57.3	−35.7	0.0	≡ 0.0
Ig+**14**→***endo*-VIg**	B3LYP/6-31+G**	20.3	−78.8	52.3	−32.0	0.0	12.6
(R=CH_3)	BHandHLYP/6-31+G**	39.9	−86.6	77.0	−37.1	0.2	15.3
	BHandHLYP/6-311G**	37.3	−87.4	74.7	−37.4	0.2	15.6

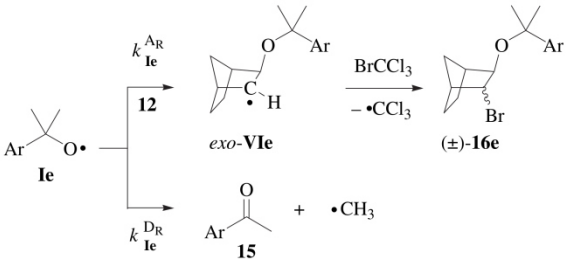

Scheme 6. Elementary reactions for kinetic analysis of intermolecular alkoxyl radical addition to norbornene **14** via the *p*-chlorocumyloxyl-'radical clock' (Ar=*p*-ClC_6H_4).

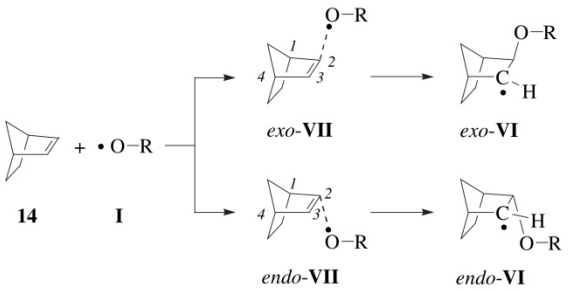

Scheme 7. Structure formulas and indexing of reactands for modeling alkoxyl radical addition to norbornene **14** [R=$C(CH_3)_3$ for **Ia**, **VIa**, and **VIIa**; R=CH_3 for **Ig**, **VIg**, and **VIIg**; see also Table 4 and the Supplementary data].

Computed zero-point vibrational energy-corrected electronic barriers ($\Delta E^{\ddagger}$) were split into an intrinsic term ($\Delta E_i^{\ddagger}$) and a thermodynamic component ($\Delta E_{TD}^{\ddagger}$), according to Marcus-theory (Eqs. 1–3).[60–62] The intrinsic part reflects steric contributions in a thermoneutral, i.e., degenerated reaction having a barrier of $\Delta E_i^{\ddagger}$ located at $x^{\ddagger}$=0.5 on the reaction coordinate (Fig. 4). The thermodynamic part refers to energy terms originating from bond formation and bond breaking.

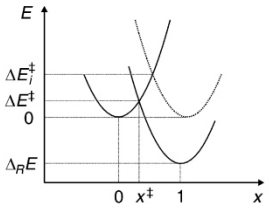

Fig. 4. Positioning of activation ($\Delta E^{\ddagger}$) and intrinsic barrier ($\Delta E_i^{\ddagger}$) according to Marcus-theory in $E(x)$ profiles using harmonic potentials of equal curvature for initial (x=0) and final state (x=1).[60,61]

$$\Delta E_i^{\ddagger} = \frac{\Delta E^{\ddagger} - \frac{\Delta_R E}{2} + \sqrt{\left(\Delta E^{\ddagger}\right)^2 - (\Delta_R E)\left(\Delta E^{\ddagger}\right)}}{2} \quad (1)$$

$$X^{\ddagger} = \frac{1}{2}\left(1 + \frac{\Delta_R E}{4\Delta E^{\ddagger}}\right) \quad (2)$$

$$\Delta E^{\ddagger} = \Delta E_i^{\ddagger} + \Delta E_{TD}^{\ddagger} \quad (3)$$

Calculated atomic distances, angles, and energy differences change gradually but not fundamentally, as the applied theoretical methods were varied (Tables 4 and 5). Independent from the method, theory predicts strongly exothermic reactions and thus a high barrier for the reverse reaction, which means kinetic reaction control. Reaction energies for *exo*- and *endo*-additions of the radicals **Ia** and **Ig** are surprisingly similar. If compared to methoxyl radical additions, the *tert*-butoxyl radical additions, however, are consistently less exothermic. Location of the B3LYP-calculated transition structure *exo*-**VIIg** at $x^{\ddagger}$=−0.8 shows that values obtained with this method should be treated with more care than the BHandHLYP data.[56] Calculated O···C2-distances of 2.0–2.2 Å and values for the $x^{\ddagger}$ parameter between 0 and 0.3 (for exception vide supra) correlate with early transition structures on the reaction coordinates. Computed Gibbs free energies at 298.15 K favor transition structures *exo*-**VIIa**/**g** by 15–18 kJ over structures *endo*-**VIIa**/**g**, which leads to theoretical *exo*/*endo*-ratios of >99:1. These numbers agree in an excellent manner with the experimental findings.

The origin of the *exo*-selectivity in alkoxyl radical additions to norbornene **14** in this model arises from subtle geometrical changes that occur in an early phase of the reaction. As the radical approaches the π-bond, the hydrogen at the attacked olefinic carbon moves backward. The vicinal olefinic hydrogen, on the other hand, shifts toward the incoming radical (cf. angles H1–C1–C2–H1 and H3–C3–C4–H4 in Table 4).[63] In transition structures *endo*-**VIIa**/**g** these changes lead to an eclipsing of hydrogens at the attacked carbon and the proximal bridgehead position. In the approach from the opposite side, that is, via intermediate *exo*-**VIIa**/**g**, the same hydrogens show synclinal orientation leading to less torsional strain (Table 4). These strain effects are furthermore evident from lower intrinsic barriers $\Delta E_i^{\ddagger}$ for *exo*-additions, while thermodynamic contribution $\Delta E_{TD}^{\ddagger}$ to the activation barrier remain for *exo*/*endo*-transition structures approximately similar.

In terms of steric effects, it becomes apparent from the computed numbers that *tert*-butoxyl radical additions were throughout the study associated with higher intrinsic barriers than methoxyl radical additions. These trends were attributed to a small but systematic size effect on alkoxyl radical reactivity.

3. Concluding remarks

The strong affinity of 3-hydroxy-5-(4-methoxyphenyl)-4-methylthiazole-2(3*H*)-thione (**2**) for alkylation at oxygen, in combination with the driving force of *O*-alkyl isoureas to transfer *tert*-alkyl groups to nucleophiles paved the road to synthesis of a new class of *tert*-alkoxyl radical progenitors.[18,64] Although the chosen compounds (i.e., **1a**–**f**) pose a selection from our laboratory, we think that the method offers a general solution for converting trialkyl-substituted alcohols into *tert*-alkoxyl radical precursors. Synthetic problems arose in esterifications of tert-2-arylalkan-2-ols (e.g. 3**d**), due to extensive elimination. Fortunately, an upscaling in such cases was feasible. This approach may be helpful in selected instances, to prepare sufficient material for conducting more specialized investigations using the thiohydroxamate method for *tert*-alkoxyl radical generation.

Using *O*-alkyl thiohydroxamates **1a** and **1c**–**f**, we were for the first time able to prepare 2,2,5-substituted tetrahydrofurans (i.e., **10**, **13**) and 2-bromo-3-alkoxynorbornans (i.e., **16a**, **16d**–**e**) via an alkoxyl radical pathway, which operates under mild and neutral conditions. The rate constants from the mechanistic part of the study show that *tert*-alkyl substitution near oxygen does not reduce alkoxyl radical reactivity, at least in the investigated cases. However, we believe that true value of these data lies in the possibility they offer for more precisely setting up the selectivity requirement for new syntheses based on *tert*-alkoxyl radical chemistry.

Bicyclo[2.2.1]heptene (**14**) was a rewarding alkene to explore intermolecular alkoxyl radical additions. Its strained double bond and comparatively strong C,H-bonds offer favorable characteristics for the addition. Still we conclude from the kinetic data that intermolecular

alkoxyl radical additions have the potential to become more and more important, as the knowledge about this reaction increases.

As a final remark, we wish to address the aspect of stereoselectivity in *tert*-alkoxyl radical additions. It is well understood that stereoselectivity in cyclization is attainable via substrate control.[45] However, it seems worth to emphasize that stereoelectronic effects and geometrical changes within the π-bond, as a system approaches its transition structure, add another important component to this picture. With the wisdom of hindsight, it could have been anticipated that similar means for stereocontrol in intermolecular additions must exist, because the underlying reaction is the same. As we continue to seek for new stereoselective radical additions, the seemingly insignificant geometrical change in the early phase of the alkoxyl radical addition may be the most valuable hint, where to look.

4. Experimental

4.1. General

For general laboratory practice and instrumentation see Ref. 17 and the Supplementary data.

4.2. 3-(Alkoxy)-5-(4-methoxyphenyl)-4-methylthiazole-2(3*H*)-thiones

*4.2.1. General method for esterification of alcohols **3a**–**c**.* CuCl (2 mol %) was added to a stirred solution of alcohol **3** (5.5 mmol) and DIC (5.5 mmol). Stirring was continued for 22–24 h at 20 °C. The resulting product was transferred into a syringe and was added over a period of 90 min in a dropwise manner at 24 °C (for **3a**) or at 0 °C (for **3b**,**c**) to a solution of 3-hydroxy-5-(4-methoxyphenyl)-4-methylthiazole-2(3*H*)-thione (MAnTTOH; **2**) (1 mmol) in CH_2Cl_2 (2 mL). After complete addition, solids were removed by filtration to afford a clear solution, which was concentrated under reduced pressure. The remaining oil was purified by column chromatography (SiO_2) using the eluent gradient (EG) specified below.

*4.2.2. General method for esterification of 2-arylalcohols **3d**–**f**.* CuCl (2 mol %), alcohol **3** (2 mmol), and DIC (2 mmol) were stirred for 24–26 h at 20 °C as described in general method 4.2.1. The solution was added at −30 °C to a solution of 3-hydroxy-5-(4-methoxyphenyl)-4-methylthiazole-2(3*H*)-thione (**2**) (1 mmol) and CH_2Cl_2 (2 mL). The resulting mixture was worked up as specified in Section 4.2.1.

*4.2.3. Esterification of 2-methylpropan-2-ol (**3a**).* *tert*-Butanol **3a** (408 mg, 5.5 mmol) was treated as described in general method 4.2.1. EG: *tert*-butyl methyl ether/pentane=1:1 (v/v)→acetone/pentane=1:1 (v/v). 3-(2-*Methylprop*-2-*oxy*)-5-(4-*methoxyphenyl*)-4-*methylthiazole*-2(3*H*)-*thione* (**1a**).[28] Yield: 198 mg (64%), pale yellow solid, mp 114–115 °C. R_f=0.45 for *tert*-butyl methyl ether/pentane=1:1 (v/v). UV (EtOH) λ_{max} (log ε/m^2 mol^{-1})=337 nm (3.25), 260 (2.89), 228 (3.13). Anal. Calcd for $C_{15}H_{19}NO_2S_2$ (309.44): C, 58.22; H, 6.19; N, 4.53. Found: C, 58.21; H, 6.02; N, 4.36. 2-(2-*Methylpropyl*-2-*sulfanyl*)-5-(4-*methoxyphenyl*)-4-*methylthiazole N-oxide* (**4a**). Yield: 78.3 mg (25%) yellow oil. R_f=0.30 for acetone/pentane=1:1 (v/v). ^{1}H NMR ($CDCl_3$, 400 MHz) δ 1.47 (s, 9H), 2.45 (s, 3H), 3.85 (s, 3H), 6.98 (d, 2H, *J*=8.6 Hz), 7.36 (d, 2H, *J*=8.3 Hz). ^{13}C NMR ($CDCl_3$, 101 MHz) δ 12.9, 31.4, 52.5, 55.4, 114.6, 122.9, 129.8, 131.9, 133.5, 141.6, 160.4.

*4.2.4. Esterification of 2-methylbutan-2-ol (**3b**).* *tert*-Amylalcohol **3b** (485 mg, 5.5 mmol) was treated as described in general method 4.2.1. EG: *tert*-butyl methyl ether/pentane=1:1 (v/v)→acetone/pentane=1:1 (v/v). 3-(2-*Methylbut*-2-*oxy*)-5-(4-*methoxyphenyl*)-4-*methylthiazole*-2(3*H*)-*thione* (**1b**). Yield: 152 mg (47%) pale yellow solid, mp 72–73 °C. R_f=0.52 for *tert*-butyl methyl ether:-pentane=1:1 (v/v). UV (EtOH) λ_{max} (log ε/m^2 mol^{-1})=338 nm (3.26), 227 (3.17). ^{1}H NMR ($CDCl_3$, 400 MHz) δ 1.06 (t, 3H, *J*=7.5 Hz), 1.56 (br s, 6H), 1.98–2.08 (m, 2H), 2.30 (s, 3H), 3.83 (s, 3H), 6.94 (d, 2H, *J*=8.8 Hz), 7.24 (d, 2H, *J*=8.9 Hz). ^{13}C NMR ($CDCl_3$, 151 MHz) δ 8.97, 14.1, 25.7, 35.0, 55.4, 94.6, 114.4, 119.3, 122.8, 129.8, 134.4, 159.7, 182.4. Anal. Calcd for $C_{16}H_{21}NO_2S_2$ (323.47): C, 59.41; H, 6.54; N, 4.33. Found: C, 59.37; H, 6.53; N, 4.26. 2-(2-*Methylbutyl*-2-*sulfanyl*)-5-(4-*methoxyphenyl*)-4-*methylthiazole N-oxide* (**4b**) Yield: 106 mg (33%), yellowish oil. R_f=0.33 for acetone/pentane=1:1 (v/v). ^{1}H NMR ($CDCl_3$, 600 MHz) δ 0.98 (t, 3H, *J*=7.4 Hz), 1.35 (s, 6H), 1.68 (q, 2H, *J*=7.4 Hz) 2.39 (s, 3H), 3.79 (s, 3H), 6.93 (d, 2H, *J*=8.7 Hz), 7.30 (d, 2H, *J*=8.5 Hz). ^{13}C NMR ($CDCl_3$, 151 MHz) δ 9.2, 12.8, 28.3, 35.6, 55.2, 56.5, 114.4, 122.5, 129.6, 131.9, 133.8, 141.2, 160.3.

*4.2.5. Esterification of 2-methyl-5-phenylpentan-2-ol (**3c**).* Alcohol **3c** (980 mg, 5.5 mmol) was treated as described in general method 4.2.1. EG: *tert*-butyl methyl ether/pentane=1:5 (v/v)→*tert*-butyl methyl ether/pentane=1:1 (v/v)→acetone:pentane=1:1 (v/v). 3-(2-*Methyl*-5-*phenylpent*-2-*oxy*)-5-(4-*methoxyphenyl*)-4-*methythiazole*-2(3*H*)-*thione* (**1c**). Yield: 182 mg (44%), colorless solid, mp 64 °C. R_f=0.59 for *tert*-butyl methyl ether/pentane=1:1 (v/v). UV (EtOH) λ_{max} (log ε/m^2 mol^{-1})=337 nm (3.21), 260 (2.87). ^{1}H NMR ($CDCl_3$, 400 MHz) δ 1.54 (s, 6H), 1.80–1.93 (m, 2H), 1.95–2.10 (m, 2H), 2.22 (s, 3H), 2.67 (t, 2H, *J*=7.3 Hz), 3.84 (s, 3H), 6.94 (d, 2H, *J*=8.8 Hz), 7.16–7.30 (m, 7H). ^{13}C NMR ($CDCl_3$, 101 MHz) δ 14.1, 26.2, 26.3, 26.9, 36.1, 42.0, 55.4, 94.0, 114.4, 119.3, 122.9, 125.8, 128.3, 128.5, 129.8, 134.4, 142.1, 159.8, 182.4. MS (EI) *m*/*z* 270 (5), 238 (15), 152 (100), 104 (68). Anal. Calcd for $C_{23}H_{27}NO_2S_2$ (413.59): C, 66.79; H; 6.58; N, 3.39. Found: C; 66.88; H; 6.58; N, 3.05. 2-(2-*Methyl*-5-*phenylpentyl*-2-*sulfanyl*)-5-(4-*methoxyphenyl*)-4-*methylthiazole N-oxide* (**4c**). Yield: 43.7 mg (11%), yellowish oil. R_f=0.38 for acetone/pentane=1:1 (v/v). ^{1}H NMR ($CDCl_3$, 400 MHz) δ 1.42 (s, 6H), 1.70–1.73 (m, 2H), 1.81–1.89 (m, 2H), 2.45 (s, 3H), 2.64 (t, 2H, *J*=7.2 Hz), 3.87 (s, 3H), 7.00 (d, 2H, *J*=8.6 Hz), 7.12–7.20 (m, 3H),7.24–7.27 (m, 2H), 7.35 (d, 2H, *J*=8.6 Hz). ^{13}C NMR ($CDCl_3$, 101 MHz) δ 12.9, 26.8, 27.0, 29.1, 36.0, 42.6, 55.4, 56.1, 114.6, 122.9, 125.6, 128.3, 128.5, 128.9, 131.9, 141.5, 142.1, 160.5, 160.6.

*4.2.6. Esterification of 2-phenylpropan-2-ol (**3d**).* Cumylalcohol **3d** (2.05 g, 15.0 mmol) and MAnTTOH (**2**) (1.91 g, 7.5 mmol) were treated as described in general method 4.2.2. 3-(2-*Phenylprop*-2-*oxy*)-5-(4-*methoxyphenyl*)-4-*methylthiazole*-2(3*H*)-*thione* (**1d**).[18] Eluent used for chromatographic purification: *tert*-butyl methyl ether/pentane=1:2 (v/v). Yield: 421 mg (15%), colorless crystals, mp 108 °C. R_f=0.36 for pentane/Et_2O=2:1 (v/v). 2-(2-*Phenylpropyl*-2-*sulfanyl*)-5-(4-*methoxyphenyl*)-4-*methylthiazole N-oxide* (**4d**). Cumylalcohol **3d** (1.36 g, 10.0 mmol) and MAnTTOH (**2**) (1.26 g, 5.0 mmol) were treated as described in general method in Section 2.2. Eluent for chromatographic purification: acetone/pentane=1:1 (v/v). Yield: 713 mg (38%), colorless solid, mp 72–73 °C. R_f=0.24 for acetone/pentane=1:1 (v/v). ^{1}H NMR ($CDCl_3$, 400 MHz) δ 1.90 (s, 6H), 2.39 (s, 3H), 3.82 (s, 3H), 6.93 (d, 2H, *J*=8.5 Hz), 7.19–7.24 (m, 3H), 7.30–7.34 (m, 2H), 7.56 (d, 2H, *J*=7.4 Hz). ^{13}C NMR ($CDCl_3$, 101 MHz) δ 12.6, 30.3, 55.4, 56.7, 114.5, 122.9, 126.7, 127.4, 128.3, 129.7, 131.6, 135.0, 140.7, 144.7, 160.3. Anal. Calcd. For $C_{20}H_{21}NO_2S_2$ (371.51): C, 64.66; H, 5.70; N, 3.77. Found: C, 64.46; H, 5.95; N, 3.85.

*4.2.7. Esterification of 2-(4-chlorophenyl)-propan-2-ol (**3e**).* *p*-Chlorocumyl alcohol **3e** (1.71 g, 10.0 mmol) and MAnTTOH (**3**) (1.27 g, 5.0 mmol) were treated as described in general method 4.2.2. EG: *tert*-butyl methyl ether/pentane=1:2 (v/v)→*tert*-butyl methyl ether/pentane=1:1 (v/v)→acetone/pentane=1:1 (v/v). 3-[2-(4-*Chlorophenyl*)-*prop*-2-*oxy*]-5-(4-*methoxyphenyl*)-4-*methylthiazole*-2(3*H*)-*thione* (**1e**). Yield: 264 mg (13%), colorless crystals, mp 110 °C. R_f=0.44 for pentane/Et_2O=1:1 (v/v). UV (MeOH) λ_{max} (log ε/m^2 mol^{-1}) 337 nm (3.01), 223 (3.19). ^{1}H NMR (400 MHz, $CDCl_3$) δ 1.66 (s, 3H), 1.99 (s, 6H), 3.81 (s, 3H), 6.89 (d, 2H, *J*=8.5 Hz), 7.13 (d, 2H, *J*=8.6 Hz), 7.36 (d, 2H, *J*=8.5 Hz), 7.53 (d, 2H, *J*=8.6 Hz).

^{13}C NMR ($CDCl_3$, 50 MHz, 20 °C) δ 13.8, 27.9, 55.4, 91.9, 114.5, 119.0, 122.8, 127.1, 128.5, 129.8, 134.2, 134.3, 143.5, 159.9, 182.5. MS (EI) *m*/*z* 253 (67), 236 (35), 205 (25), 177 (27), 155 (86), 152 (100), 137 (68), 117 (85), 102 (56). Anal. Calcd. For $C_{20}H_{20}ClNO_2S_2$ (405.96): C, 59.17; H, 4.97; N, 3.45. Found: C, 59.22; H, 4.99; N, 3.29. Crystals suitable for X-ray diffraction were grown from a saturated solution in pentane/Et_2O=1:1 (v/v). *T*=293(2) K, λ=0.71073 Å, monoclinic, C2/*c*, *a*=17.561(4) Å, *b*=8.8759(18) Å, *c*=26.777(5) Å, β=106.73(3)°, *Z*=8, μ=0.414 mm^{-1}, completeness to 2θ=95.1%, goodness-of-fit on F^2=0.747, final *R* indices [$I>2\sigma(I)$]: *R*1=0.0312, *wR*2=0.0612. 2-[2-(4-*Chlorophenyl*)-*propyl*-2-*sulfanyl*]-5-(4-*methoxyphenyl*)-4-*methyl*-*thiazole N-oxide* (**4e**). Yield: 658 mg (33%), colorless solid, mp 102 °C. R_f=0.29 for acetone/pentane=1:1 (v/v). ^{1}H NMR ($CDCl_3$, 400 MHz) δ 1.89 (s, 6H), 2.42 (s, 3H), 3.85 (s, 3H), 6.97 (d, 2H, *J*=8.9 Hz), 7.25–7.31 (m, 4H), 7.50–7.52 (d, 2H, *J*=8.5 Hz). ^{13}C NMR ($CDCl_3$, 101 MHz) δ 12.7, 30.3, 55.4, 56.3, 114.5, 122.8, 128.2, 128.4, 129.8, 132.0, 133.2, 134.1, 141.0, 143.4, 160.4. Anal. Calcd. For $C_{20}H_{20}ClNO_2S_2$ (405.97): C, 59.17; H, 4.97; N, 3.45. Found: C, 58.83; H, 4.71; N, 3.44.

*4.2.8. Esterification of 2-phenylhex-5-en-2-ol (**3f**).* Alkenol **3f** (7.05 g, 40 mmol) and MAnTTOH (**2**) (5.06 g, 20 mmol) were treated as described in general method 4.2.2. EG: pentane/Et_2O/CH_2Cl_2=5:1:1 (v/v/v)→acetone/pentane=1:2 (v/v). 3-(1-*Methyl*-1-*phenylpent*-4-*en*-1-*oxy*)-5-(4-*methoxyphenyl*)-4-*methylthiazole*-2(3*H*)-*thione* (**1f**). Yield 1.48 g (18%), colorless solid, mp 94–95 °C. R_f=0.30 for pentane/Et_2O/CH_2Cl_2=5:1:1 (v/v/v). UV (EtOH) λ_{max} (log ε/m^2 mol^{-1}) 338 nm (3.28). ^{1}H NMR ($CDCl_3$, 400 MHz) δ 1.55 (s, 3H), 1.72–1.80 (m, 1H), 1.88 (s, 3H), 1.91–2.00 (m, 1H), 2.62 (dt, 1H, J_d=12.8 Hz, J_t=4.6 Hz), 2.89 (dt, 1H, J_d=12.6 Hz, J_t=5.0 Hz), 3.79 (s, 3H), 4.91 (dd, 1H, *J*=10.2, 1.5 Hz), 4.95 (dd, 1H, *J*=17.2, 1.6 Hz), 5.75 (ddt, 1H, J_d=16.8, 10.2 Hz, J_t=6.4 Hz), 6.87 (d, 2H, *J*=8.5 Hz), 7.10 (d, 2H, *J*=8.2 Hz), 7.34–7.41 (m, 3H), 7.53 (d, 2H, *J*=7.5 Hz). ^{13}C NMR ($CDCl_3$, 151 MHz) δ 13.6, 20.2, 29.4, 42.4, 55.3, 95.1, 114.3, 114.7, 118.7, 122.7, 126.2, 128.3, 128.6, 129.1, 129.7, 134.6, 137.7, 159.7, 182.1. Anal. Calcd. For $C_{23}H_{25}NO_2S_2$ (411.58): C, 67.12; H, 6.12; N, 3.40. Found: C, 67.22; H, 6.05; N, 3.68. 2-(1-*Methyl*-1-*phenylpent*-4-*enyl*-2-*sulfanyl*)-5-(4-*methoxyphenyl*)-4-*methylthiazole N-oxide* (**4f**). Yield 2.19 g (27%), yellowish oil. R_f=0.35 for acetone/pentane=1:1 (v/v). ^{1}H NMR ($CDCl_3$, 400 MHz) δ 1.82–1.92 (m, 1H),1.92 (s, 3H), 2.07–2.23 (m, 2H), 2.34–2.41 (m, 1H), 2.39 (s, 3H), 3.83 (s, 3H), 4.93 (dd, 1H, *J*=10.2, 1.5 Hz), 4.98 (dd, 1H, *J*=16.2, 1.2 Hz), 5.75 (ddt, 1H, *J*=16.9, 10.4 , 6.3 Hz), 6.93 (d, 2H, *J*=8.6 Hz), 7.22–7.24 (m, 3H), 7.31–7.34 (m, 2H), 7.53 (d, 2H, *J*=7.4 Hz). ^{13}C NMR ($CDCl_3$, 151 MHz) δ 12.6, 26.2, 29.1, 42.1, 55.4, 60.2, 114.5, 114.9, 123.0, 127.3, 127.4, 128.4, 129.8, 131.6, 134.7, 137.7, 140.7, 142.9, 160.3.

4.3. Alkoxyl radical reactions

*4.3.1. Reaction of 3-(tert-butoxy)-thiazolethione **1a** with norbornene **14**.* An oxygen-free solution of norbornene (**14**) (4.80 g, 51.0 mmol), *tert*-butoxythiazolethione **1a** (158 mg, 510 µmol), and $BrCCl_3$ (1.01 g, 5.10 mmol) in dry $C_6H_5CF_3$ (18.5 mL, c_0^{14}=2.76 M) was photolyzed for 40 min at 25 °C in a Rayonet® chamber reactor equipped with 12 light bulbs (λ=350 nm). The resulting mixture was concentrated under reduced pressure (100→20 mbar, 40 °C) to furnish a residue, which was purified by column chromatography (SiO_2) using pentane/Et_2O=20:1 (v/v) as eluent. 2-*endo*-3-*exo*-2-*Bromo*-3-*trichloromethylbicyclo*[2.2.1]*heptane* 2-*endo*-3-*exo*-(**17**).[47] Yield: 1.24 g (84%), colorless oil. R_f=0.68 for pentane/Et_2O=20:1 (v/v). 2-*exo*-3-*exo*-2-*Bromo*-3-*trichloromethylbicyclo*[2.2.1]*heptane* 2-*exo*-3-*exo*-(**17**).[47] Yield: 93.1 mg (6%), colorless oil, R_f=0.60 for pentane/Et_2O=20:1 (v/v). 2-*Bromo*-3-(2-*methylprop*-2-*oxy*)-*bicyclo*[2.2.1]*heptane* (**16a**). Yield: 25.3 mg (20%), colorless oil, 20/80-mixture of 2-*exo*-3-*exo*/2-*endo*-3-*exo*-isomers. R_f=0.40 for pentane/Et_2O=20:1 (v/v). Anal. Calcd. For $C_{11}H_{19}OBr$ (247.17): C, 53.45; H, 7.75. Found: C, 53.22; H, 7.69. 2-*endo*-3-*exo*-2-*Bromo*-3-(2-*methylprop*-2-*oxy*)-*bicyclo*[2.2.1]*heptane* 2-*endo*-3-*exo*-(**16a**). ^{1}H NMR ($CDCl_3$, 600 MHz) δ 1.16–1.22 (m, 1H), 1.20 (s, 9H), 1.31 (dq, 1H, J_d=10.4 Hz, J_q=1.8 Hz), 1.41–1.46 (m, 1H), 1.50–1.58 (m, 1H), 1.71–1.76 (m, 1H), 1.85 (ddt, 1H, J_d=12.4, 9.3 Hz, J_t=2.9 Hz) 2.01 (d, 1H, *J*=5.0 Hz), 2.35–2.40 (m, 1H), 3.43 (t, 1H, *J*=2.3 Hz), 3.90–3.91 (m, 1H). ^{13}C NMR ($CDCl_3$, 151 MHz) δ 23.8, 25.0, 28.8, 34.5, 42.8, 44.6, 63.6, 73.6, 83.4. MS (EI) *m*/*z* 248 (2), 246 (2), 233 (3), 191 (16), 175 (5), 110 (11), 93 (15), 57 (100). 2-*exo*-3-*exo*-3-*Bromo*-3-(2-*methylprop*-2-*yl*)-*bicyclo*[2.2.1]-*heptane* 2-*exo*-3-*exo*-(**16a**). ^{1}H NMR ($CDCl_3$, 600 MHz) δ 1.10–1.19 (m, 3H), 1.21 (s, 9H), 1.43–1.51 (m, 1H), 1.51–1.57 (m, 1H), 1.97 (dquint, 1H, J_d=10.3 Hz, J_{quint}=1.9 Hz), 2.05–2.06 (m, 1H), 2.48–2.49 (m, 1H), 3.37–3.39 (m, 1H), 4.00 (dd, 1H, *J*=6.1, 2.0 Hz). ^{13}C NMR (151 MHz, $CDCl_3$) δ 25.4, 27.5, 28.1, 33.4, 44.8, 46.6, 62.0, 74.2, 74.9. MS (EI) *m*/*z* 248 (1) 246, 233 (3), 191 (17), 175 (3), 110 (11), 93 (14), 57 (100).

*4.3.2. Conversion of 3-(2-methyl-5-phenylpent-2-oxy)-thiazolethione **1c**.* $BrCCl_3$ 310 mg (750 µmol) and 1.50 g (7.50 mmol, 0.75 mL) in C_6H_6 (9.0 mL) according to procedure in Section 4.3.1. Eluent used for chromatographic purification: pentane/*tert*-butyl methyl ether=10:1 (v/v)→pentane/*tert*-butyl methyl ether=2:1 (v/v). 2,2-*Dimethyl*-5-*phenyltetrahydrofuran* (**10**):[37] Yield: 76.6 mg (58%), yellow liquid, R_f=0.65 for *tert*-butyl methyl ether/pentane=1:2 (v/v). 5-(4-*Methoxyphenyl*)-4-*methyl*-2-(*trichlormethylsufanyl*)-*thiazole* **11**.[17] Yield: 71.9 mg (27%), yellowish crystals. R_f=0.43 for *tert*-butyl methyl ether/pentane=1:2 (v/v). 1,2-*Bis*-[5-(4-*methoxyphenyl*)-4-*methylthiaz*-2-*yl*]-*disulfane* (**5**).[33] Yield: 59.0 mg (33%), yellowish oil. R_f=0.19 for *tert*-butyl methyl ether/pentane=1:2 (v/v). 2-Methyl-5-phenylpentan-2-ol (**3c**). Yield: 30.5 mg (23%), yellowish oil. R_f=0.18 for *tert*-butyl methyl ether/pentane=1:2 (v/v).

*4.3.3. Conversion of 3-(1-methyl-1-phenylpent-4-enyloxy)-thiazolethione **1f**.* Alkenoxythiazolethione **1f** (308 mg, 748 µmol) and $BrCCl_3$ (1.49 g, 7.50 mmol) in C_6H_6 (9 mL) are treated according to procedure 4.3.1 (35 min reaction time). GC/MS analysis of the reaction mixture using *n*-decane as internal standard: *phenyl methyl ketone* (**7**) (3.3 mg, 4%). The reaction mixture was worked up as described in procedure 4.3.1. 5-*Bromomethyl*-2-*methyl*-2-*phenyltetrahydrofuran* (**13**).[42] Yield: 120 mg (63%), yellowish oil, 74/26-mixture of cis/trans-isomers. R_f=0.42 (*trans*) and 0.36 (*cis*) for pentane/Et_2O=10:1 (v/v). Anal. Calcd. For $C_{12}H_{15}OBr$ (255.15): C, 56.49; H, 5.93. Found: C, 56.14; H, 6.03. *trans*-5-*Bromomethyl*-2-*methyl*-2-*phenyltetrahydrofuran trans*-(**13**). ^{1}H NMR ($CDCl_3$, 600 MHz) δ 1.56 (s, 3H), 1.87–1.97 (m, 2H), 2.09–2.16 (m, 1H), 2.22–2.29 (m, 1H), 3.45 (dd, 1H, *J*=10.0, 6.6 Hz), 3.54 (dd, 1H, *J*=10.0, 4.5 Hz), 4.26–4.30 (m, 1H), 7.21–7.24 (m, 1H), 7.31–7.34 (m, 2H), 7.37–7.38 (m, 2H). ^{13}C NMR ($CDCl_3$, 151 MHz) δ 30.1, 30.4, 36.2, 38.8, 77.8, 86.0, 124.5, 126.5, 128.2, 147.5. MS (EI) *m*/*z* 241 (56), 239 (56), 179 (1), 177 (1), 161 (6), 143 (7), 128 (7), 117 (13), 115 (13), 105 (100). *cis*-5-*Bromomethyl*-2-*methyl*-2-*phenyltetrahydrofuran cis*-(**13**). ^{1}H NMR ($CDCl_3$, 600 MHz) δ 1.52 (s, 3H), 1.72–1.76 (m, 1H), 2.09–2.16 (m, 1H), 2.21–2.29 (m, 2H), 3.29 (dd, 1H, *J*=10.0, 7.5 Hz), 3.54 (dd, 1H, *J*=10.0, 5.4 Hz), 4.41–4.45 (m, 1H), 7.21–7.24 (m, 1H), 7.31–7.34 (m, 2H), 7.43–7.45 (m, 2H). ^{13}C NMR ($CDCl_3$, 151 MHz) δ 29.8, 30.7, 35.7, 39.2, 78.6, 85.7, 124.6, 126.5, 128.1, 148.1. MS (EI) *m*/*z* 241 (50), 239 (50), 161 (4), 143 (7), 128 (9), 117 (16), 115 (16), 105 (100). 5-(4-*Methoxyphenyl*)-4-*methyl*-2-(*trichlormethylsufanyl*)-*thiazole* **10**.[17] Yield: 119 mg (45%), yellowish crystals. R_f=0.14 for pentane/Et_2O=10:1 (v/v). 2-*Phenyl*-5-*hexen*-2-*ol*.[17] Yield: 119 mg (45%), yellowish crystals. R_f=0.14 for pentane/Et_2O=10:1 (v/v). 2-*Phenyl*-5-*hexene*-2-*ol*[65] (**3f**). Yield: 7.9 mg (6%), yellowish oil. R_f=0.07 for pentane/Et_2O=10:1 (v/v). 1,2-*Bis*-[5-(4-*methoxyphenyl*)-4-*methylthiaz*-2-*yl*]-*disulfane* (**5**).[33] Yield: 55.0 mg (15%), yellow oil.

Crystallographic data (excluding structure factors) for the structure of 3-(4-chlorocumyloxy)-alkoxythiazolethione **1e** in this paper have been deposited with the Cambridge Crystallographic

Data Centre as supplementary publication (CCDC 791992). Copies of the data can be obtained, free of charge, on application to CCDC, 12 Union Road, Cambridge CB2 1EZ, UK [fax: +44 (0)1223 336033 or e-mail: deposit@ccdc.cam.ac.uk].

Acknowledgements

We thank Dipl.-Chem. Steffen Danner for helpful discussions on computational chemistry. This work is part of Ph.D. theses of C.S., Dr. Nina Becker (born Schneiders), and T.G.

Supplementary data

Instrumentation, reagent specification, 3-alkoxythiazole-2(3*H*)-thione transformations, kinetic analyses, variable temperature NMR, N–O/C=S-bond length correlation, computational details and data. Supplementary data associated with this article can be found in the online version at doi:10.1016/j.tet.2010.12.071.

References and notes

1. Gray, P.; Williams, A. *Chem. Rev.* **1959**, *59*, 239–328.
2. Walling, C.; Jacknow, B. B. *J. Am. Chem. Soc.* **1960**, *82*, 6108–6112.
3. Griller, D.; Ingold, K. U. *Acc. Chem. Res.* **1980**, *13*, 317–323.
4. Elson, I. H.; Mao, S. W.; Kochi, J. K. *J. Am. Chem. Soc.* **1975**, *97*, 335–341.
5. Howard, J. A.; Scaiano, J. C. In *Radical Reaction Rates in Liquids—Oxyl-, Peroxyl-, and Related Radicals*; Fischer, H., Ed.; Landolt-Börnstein, Springer: Berlin, 1984; Vol. 13d, pp 5–127.
6. Baciocchi, E.; Bietti, M.; Salamone, M.; Steenken, S. *J. Org. Chem.* **2002**, *67*, 2266–2270.
7. Bietti, M.; Lanzalunga, O.; Salamone, M. *J. Org. Chem.* **2005**, *70*, 1417–1422.
8. Atkinson, R. *Atmos. Environ.* **2007**, *41*, 8468–8485.
9. Batteridge, D. J. *Metabolism* **2000**, *49*, 3–8.
10. Möller, M.; Adam, W.; Marquardt, S.; Saha-Möller, C. R. *Free Radical Biol. Med.* **2005**, *39*, 473–482.
11. Halliwell, B.; Gutteridge, J. M. C. *Free Radicals in Biology and Medicine*, 3rd ed.; Oxford Universtiy: Oxford, 1999, Chapter 2, pp 36–104.
12. Griffiths, P. G.; Rizzardo, E.; Solomon, D. H. *J. Macromol. Sci.* **1982**, *A17*, 45–50.
13. Rizzardo, E.; Serelis, A. K.; Solomon, D. H. *Aust. J. Chem.* **1982**, *35*, 2013–2024.
14. Suárez, E. In *Radicals in Organic Synthesis*; Renaud, P., Sibi, M. P., Eds.; Wiley-VCH: Weinheim, 2001; Vol. 2, pp 440–454.
15. Hartung, J.; Schneiders, N.; Gottwald, T. *Tetrahedron Lett.* **2007**, *48*, 6027–6030.
16. Hartung, J.; Gottwald, T.; Špehar, K. *Synthesis* **2002**, 1469–1498.
17. Hartung, J.; Schur, C.; Kempter, I.; Gottwald, T. *Tetrahedron* **2010**, *66*, 1365–1374.
18. Hartung, J.; Bergsträßer, U.; Daniel, K.; Schneiders, N.; Svoboda, I.; Fuess, H. *Tetrahedron* **2009**, *65*, 2567–2573.
19. Hartung, J.; Daniel, K.; Bergsträßer, U.; Kempter, I.; Schneiders, N.; Danner, S.; Schmidt, P.; Svoboda, I.; Fuess, H. *Eur. J. Org. Chem.* **2009**, 4135–4142.
20. Walter, W.; Schaumann, E. *Synthesis* **1971**, 111–130.
21. Chmiak, A.; Przychodzen, R. *J. Heteroatom Chem.* **2002**, *13*, 169–194.
22. Bond, A. D.; Jones, W. *J. Chem. Soc., Dalton Trans.* **2001**, 3045–3051.
23. Hartung, J.; Kneuer, R.; Schwarz, M.; Svoboda, I.; Fuess, H. *Eur. J. Org. Chem.* **1999**, 97–106.
24. Hay, B. P.; Beckwith, A. L. J. *J. Am. Chem. Soc.* **1988**, *110*, 4415–4416.
25. Volz, F.; Krause, N. *Org. Biomol. Chem.* **2007**, *5*, 1519–1521.
26. Buchbauer, G.; Weck, A. M. *Chem. Ztg.* **1985**, *109*, 255–265.
27. Krieger, H. *Arzneim. Forsch.* **1968**, *18*, 129–134.
28. Hartung, J.; Daniel, K.; Gottwald, T.; Groß, A.; Schneiders, N. *Org. Biomol. Chem.* **2006**, *4*, 2313–2322.
29. Hartung, J.; Schneiders, N.; Bergsträßer, U. *Acta Crystallogr.* **2006**, *E62*, o4713–o4714.
30. Mathias, L. J. *Synthesis* **1979**, 561–576.
31. Schmidt, E.; Moosmüller, F. *Justus Liebigs Ann. Chem.* **1955**, *597*, 235–240.
32. Hartung, J.; Kneuer, R.; Laug, S.; Schmidt, P.; Špehar, K.; Svoboda, I.; Fuess, H. *Eur. J. Org. Chem.* **2003**, 4033–4052.
33. Hartung, J.; Daniel, K.; Schmidt, P.; Laug, S.; Svoboda, I.; Fuess, H. *Acta Crystallogr.* **2005**, *E61*, o3971–o3973.
34. Van Geet, A. L. *Anal. Chem.* **1970**, *42*, 679–680.
35. Hansen, E. W. *Anal. Chem.* **1985**, *57*, 2993–2994.
36. Hartung, J.; Daniel, K.; Svoboda, I.; Fuess, H. *Acta Crystallogr.* **2005**, *E61*, o1744–o1746 By mistake wrong chemical shifts were provided for compound **8** in the original report. The correct values are given in the Supplementary data.
37. Kundu, R.; Ball, Z. T. *Org. Lett.* **2010**, *12*, 2460–2463.
38. Weber, M.; Fischer, H. *J. Am. Chem. Soc.* **1999**, *121*, 7381–7388.
39. Atkinson, R. *Int. J. Chem. Kinet.* **1997**, *29*, 99–111.
40. Čeković, Ž *Tetrahedron* **2003**, *59*, 8073–8090.
41. Horner, J. H.; Choi, S. Y.; Newcomb, M. *Org. Lett.* **2000**, *2*, 3369–3372.
42. Zhao, P.; Incarvito, C. D.; Hartwig, J. F. *J. Am. Chem. Soc.* **2006**, *128*, 9642–9643.
43. Hartung, J.; Gallou, F. *J. Org. Chem.* **1995**, *60*, 6706–6716.
44. Hartung, J.; Hiller, M.; Schmidt, P. *Chem.—Eur. J.* **1996**, *2*, 1014–1023.
45. Hartung, J.; Daniel, K.; Rummey, C.; Bringmann, G. *Org. Biomol. Chem.* **2006**, *4*, 4089–4100.
46. Avila, D. V.; Ingold, K. U.; Di Nardo, A. A.; Zerbetto, F.; Zgierski, M. Z.; Lusztyk, J. *J. Am. Chem. Soc.* **1995**, *117*, 2711–2718.
47. Giese, B.; Jay, K. *Angew. Chem., Int. Ed.* **1977**, *16*, 466–467.
48. Giese, B.; Jay, K. *Chem. Ber.* **1979**, *112*, 298–303.
49. Avila, D. V.; Brown, C. E.; Ingold, K. U.; Lusztyk, J. *J. Am. Chem. Soc.* **1993**, *115*, 466–470.
50. Wong, P. C.; Griller, D.; Scaiano, J. C. *J. Am. Chem. Soc.* **1982**, *104*, 5106–5108.
51. For exo-selectivity in electrophile addition to norbornene-derived enolates see: von Rague Schleyer, P. *J. Am. Chem. Soc.* **1967**, *89*, 701–703.
52. Frisch, M. J.; Trucks, G. W.; Schlegel, H. B.; Scuseria, G. E.; Robb, M. A.; Cheeseman, J. R.; Montgomery, J. A., Jr.; Vreven, T.; Kudin, K. N.; Burant, J. C.; Millam, J. M.; Iyengar, S. S.; Tomasi, J.; Barone, V.; Mennucci, B.; Cossi, M.; Scalmani, G.; Rega, N.; Petersson, G. A.; Nakatsuji, H.; Hada, M.; Ehara, M.; Toyota, K.; Fukuda, R.; Hasegawa, J.; Ishida, M.; Nakajima, T.; Honda, Y.; Kitao, O.; Nakai, H.; Klene, M.; Li, X.; Knox, J. E.; Hratchian, H. P.; Cross, J. B.; Adamo, C.; Jaramillo, J.; Gomperts, R.; Stratmann, R. E.; Yazyev, O.; Austin, A. J.; Cammi, R.; Pomelli, C.; Ochterski, J. W.; Ayala, P. Y.; Morokuma, K.; Voth, G. A.; Salvador, P.; Dannenberg, J. J.; Zakrzewski, V. G.; Dapprich, S.; Daniels, A. D.; Strain, M. C.; Farkas, O.; Malick, D. K.; Rabuck, A. D.; Raghavachari, K.; Foresman, J. B.; Ortiz, J. V.; Cui, Q.; Baboul, A. G.; Clifford, S.; Cioslowski, J.; Stefanov, B. B.; Liu, G.; Liashenko, A.; Piskorz, P.; Komaromi, I.; Martin, R. L.; Fox, D. J.; Keith, T.; Al-Laham, M. A.; Peng, C. Y.; Nanayakkara, A.; Challacombe, M.; Gill, P. M. W.; Johnson, B.; Chen, W.; Wong, M. W.; Gonzalez, C.; Pople, J. A. *Gaussian 03, Revision C.01*; Gaussian: Wallingford CT, 2004.
53. Jensen, F. *Introduction to Computational Chemistry*; Wiley: Chichester, UK, 1999.
54. Hartung, J.; Kneuer, R.; Rummey, C.; Bringmann, G. *J. Am. Chem. Soc.* **2004**, *126*, 12121–12129.
55. Alabugin, I. V.; Manoharan, M. *J. Am. Chem. Soc.* **2005**, *127*, 12583–12594.
56. Tripp, J. C.; Schiesser, C. H.; Curran, D. P. *J. Am. Chem. Soc.* **2005**, *127*, 5518–5527.
57. Becke, A. D. *J. Chem. Phys.* **1993**, *98*, 5648–5652.
58. Lee, C.; Yang, W.; Parr, R. G. *Physiol. Rev.* **1988**, *B37*, 785–789.
59. Becke, A. D. *Physiol. Rev.* **1988**, *A38*, 3098–3100.
60. Marcus, R. A. *J. Phys. Chem.* **1968**, *72*, 891–899.
61. Gisdakis, P.; Rösch, N. *J. Am. Chem. Soc.* **2001**, *123*, 697–701.
62. Wu, C. W.; Ho, J.-J. *J. Org. Chem.* **2006**, *71*, 9595–9601.
63. For similar structural changes in carbon radical addition to olefins see: Damm, W.; Giese, B.; Hartung, J.; Hasskerl, T.; Houk, K. N.; Hüter, O.; Zipse, H. *J. Am. Chem. Soc.* **1992**, *114*, 4067–4079.
64. Beckwith, A. L. J.; Hay, B. P. *J. Am. Chem. Soc.* **1989**, *111*, 230–234.
65. Menéndez Pérez, B.; Schuch, D.; Hartung, J. *Org. Biomol. Chem.* **2008**, *6*, 3532–3541.

5. Heterocyclische *O*-(*tert*-Butyl)thiohydroxamate

5.1 Zusammenfassung

3-(*tert*-Butoxy)-4-methylthiazol-2(3*H*)-thione aus *O*-(*tert*-Butyl)isoharnstoff und 3-Hydroxy-4-methylthiazol-2(3*H*)-thionen sind stabile, kristalline Sauerstoff-Radikalvorläufer. Im Vergleich dazu, lagert das in Analogie hergestellte, 1-(*tert*-Butoxy)pyridin-2(1*H*)-thion spontan zum O-(*tert*-Butyl)pyridin-2-sulfenat um. Stabilitätsunterschiede beider Thiohydroxamat-Klassen lassen sich auf unterschiedlich starke N,O-Bindungen zurückführen, was N,O-Bindungsordungen zwischen 1.3–1.4 in diesem Zusammenhang verdeutlichen. Drei überlagernde, partielle π-Bindungsanteile verschiedener Stärke, sind der MO-Theorie (Molekülorbital-Theorie) zufolge, dafür verantwortlich, dass die N,O-Bindungsordnung steigt. In 3-(*tert*-Butoxy)thiazol-2(3*H*)-thionen führt die Summe der π-Wechselwirkungen zu einer stärkeren Stabilisierung der N,O-Bindung und damit zu einer höheren Bindungsordnung als für das 1-(*tert*-Butoxy)pyridin-2(1*H*)-thion. Die photochemische Aktivierung der 3-(*tert*-Butoxy)-4-methylthiazol-2(3*H*)-thione liefert *tert*-Butoxyl-Radikale, die mit Hilfe der Elektronen-Spin-Resonanz-Spektroskopie und der intermolekularen Addition an Styrol, in Gegenwart von Bromtrichlormethan, nachgewiesen wurden.

5.2 Wissenschaftlicher Hintergrund, Zielsetzung und Strategie

Tertiäre Sauerstoff-Radikalvorläufer können aus 3-Hydroxy-5-(4-methoxyphenyl)-4-methylthiazol-2(3*H*)-thion und einem tertiären *O*-Alkylisoharnstoff (Isoharnstoff-Methode) in bis zu 64 % Ausbeute hergestellt werden. In typischen Elementarreaktionen, wie inter- und intramolekularen Additionen oder Substitutionen, zeigen die aus den Thiohydroxamaten erzeugten tertiären *O*-Radikale, trotz größerer sterischer Belastung, eine vergleichbare oder sogar höhere Reaktivität als primäre und sekundäre Analoga (Kapitel 4).[1] Warum tertiäre 3-Alkoxythiazol-2(3*H*)-thione bis dato die einzige stabile Thiohydroxamat-Klasse zur Erzeugung tertiärer Sauerstoff-Radikale in der organischen Synthesechemie darstellen, soll in dieser Studie durch eine Kombination aus Theorie und Experiment untersucht werden.

Konkrete Ziele dieses Projektes lagen daher darin,

- *O*-(*tert*-Butyl)thiohydroxamate aus *O*-(*tert*-Butyl)-*N*,*N*-diisopropylisoharnstoff und weiteren cyclischen Thiohydroxamsäuren, wie 3-Hydroxy-4-methylthiazol-2(3*H*)-thion, 3-Hydroxy-4-methyl-5-(4-nitrophenyl)thiazol-2(3*H*)-thion und 1-Hydroxypyridin-2(1*H*)-thion herzustellen,
- anhand theoretischer Berechnungen (Dichtefunktional-Theorie und Møller-Plesset-Störungsrechnung 2. Ordnung) Aussagen zur Stabilität der tertiären Thiohydroxamate zu treffen und
- nachzuweisen, dass 3-(*tert*-Butoxy)thiazolthione durch photochemische Anregung *tert*-Butoxyl-Radikale erzeugen.

5.3 Ergebnisse und Diskussion

5.3.1 Erzeugung und Eigenschaften von (*O*-*tert*-Butyl)thiohydroxamaten

Thiohydroxamsäuren: Die für diese Studie ausgewählten 3-Hydroxy-4-methylthiazol-2(3*H*)-thione **1a**[2] und **2a**[3] wurden nach literaturbekannten Verfahren hergestellt und repräsentieren die cyclischen Thiohydroxamsäuren mit der derzeit vielfältigsten Anwendungsbreite.[1,4,5] 3-Hydroxy-4-methyl-5-(4-nitrophenyl)thiazol-2(3*H*)-thion (**3a**) ist neu und aus 4-Nitrophenylaceton[6] in Anlehnung zur Synthese von MAnTTOH (**1a**)[2] darstellbar. Das 1-Hydroxypyridin-2(1*H*)-thion (**4a**) wurde von Mitarbeitern der Arbeitsgruppe für frühere Studien synthetisiert und der Allgemeinheit zur Verfügung gestellt (Abb. 5.1).

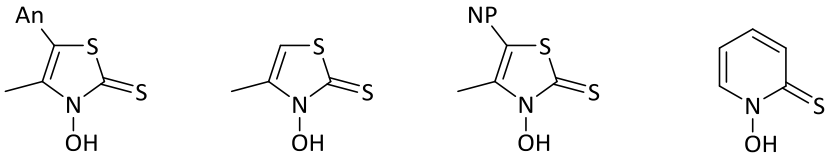

1a MAnTTOH **2a** MTTOH **3a** MNPTTOH **4a** PTOH

Abbildung 5.1. Thiohydroxamsäuren für die Herstellung der *O*-*tert*-Butylthiohydroxamate. MAnTTOH = 3-Hydroxy-5-(4-methoxyphenyl)-4-methylthiazol-2(3*H*)-thion, An = Anisyl = 4-$CH_3OC_6H_4$, MTTOH = 3-Hydroxy-4-methylthiazol-2(3*H*)-thion, MNPTTOH = 3-Hydroxy-4-methyl-5-(4-nitrophenyl)thiazol-2(3*H*)-thion, PTOH = 1-Hydroxypyridin-2(1*H*)-thion.

3-(tert-Butoxy)-4-methylthiazol-2(3H)-thione: In Analogie zur vorherigen Studie (Kapitel 4)[1], in der die Thiohydroxamsäure **1a** über die Isoharnstoff-Methode zu den *O*-alkylierten- **1b** und *S*-alkylierten Produkten **6b** führte (Tabelle 5.1, Eintrag 1), reagieren die 3-Hydroxy-4-methylthiazol-2(3*H*)-thione **2a**–**3a** in Gegenwart von *O*-(*tert*-Butyl)-*N*,*N*-diisopropylisoharnstoff[7,8] zu den Thiohydroxamsäure-*O*-estern **2b**–**3b**. Die *N*-Oxide **7b**–**8b** entstehen als Nebenprodukte der Alkylierung (Tabelle 5.1).

Tabelle 5.1 Alkylierung der 3-Hydroxy-4-methylthiazol-2(3*H*)-thione **1a**–**3a** über die Isoharnstoff-Methode und physikalische Parameter der *O*-Alkylierungsprodukte **1b**–**3b**

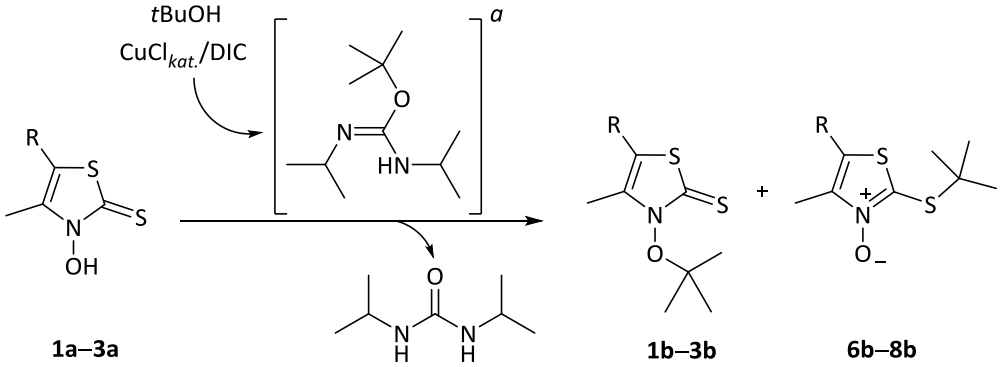

1a–3a **1b–3b** **6b–8b**

Eintrag	R	**1b–3b** / %	λ_{max} **1b–3b** / nm	Schmp. **1b–3b** / °C	**6b–8b** / %[e]
1	4-CH_3O-C_6H_4[b]	**1b**: 58–64 %[c]	**1b**: 337	**1b**: 114–115	**6b**: 25 %
2	H	**2b**: 42–55 %[c]	**2b**: 319	**2b**: 56–57	**7b**: 24 %
3	4-NO_2-C_6H_4	**3b**: 39–43 %[d]	**3b**: 324, 377	**3b**: 153	**8b**: 17 %

[a] *in situ* aus 5.5 Äquivalente an *t*BuOH und Diisopropylcarbodiimid (DIC), [b] Ergebnis der vorherigen Studie (Kapitel 4), [c] aus 3 Experimenten, [d] aus 2 Experimenten, [e] repräsentativ aus einem Experiment iosliert.

Als farblose (**2b**) oder gelbe Feststoffe (**1b**, **3b**) zeigen die tertiären Ester die in der Tabelle 5.1 aufgeführten Schmelzpunkte. 3-(*tert*-Butoxy)-4-methyl-5-(4-nitrophenyl)thiazol-2(3*H*)-thion (MNPTTO*t*Bu, **3b**) kristallisiert aus einer Diethylether/*n*-Pentan-Mischung (*v*:*v* = 1:1) in der monoklinen Raumgruppe $P2_1/n$ (Abbildung 5.2). Jede Elementarzelle verfügt dabei über vier Moleküle MNPTTO*t*Bu (**3b**) entlang der zwei stereogenen Achsen [N3–O8] und [C5–*para*-Nitrophenyl-Gruppe]. Der *tert*-Butyl-Rest ist um 94°, die 4-Nitrophenyl-Gruppe um 26° aus der nahezu planaren Ebene des Heterocyclus herausgedreht. Der große

N3,O8,C9-Bindungswinkel von 116.8(1)° in **3b** zeigt, dass tertiäre 3-Alkoxythiazolthione sterischer Belastung bei *O*-Alkylierung entgegenwirken können. Für primäre und sekundäre *O*-Alkylthiohydroxamate ist der gleiche Winkel [N3, O8, C9] 4–5° kleiner.[9] Bindungslängen in **3b** (siehe Seite 107) entsprechen literaturbekannten Werten des 3-(Cumyloxyl)-5-(4-methoxyphenyl)-4-methyl-thiazol-2(3*H*)-thion.[9]

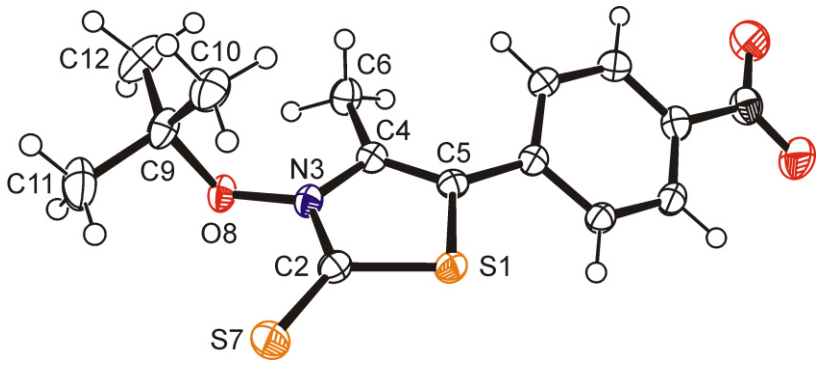

Abbildung 5.2 Ellipsoidgrafik der Kristallstruktur von 3-(*tert*-Butoxy)-4-methyl-5-(4-nitrophenyl)thiazol-2(3*H*)-thion (**3b**) bei 150 K (50 % Wahrscheinlichkeit). Wasserstoffatome: willkürlicher Radius, Sauerstoff: rot, Stickstoff: blau, Schwefel: orange.

Die Kristallstruktur von 3-(*tert*-Butoxy)-4-methyl-5-(4-nitrophenyl)thiazol-2(3*H*)-thion (**3b**) zeigt unterschiedlich große *tert*-Butoxyl-Bindungswinkel zwischen den Atomen O8, C9 und den Kohlenstoff-Atomen C10–C12 [O8, C9, C10 = 111.6° / O8, C9, C11 = 103.1° / O8, C9, C12 = 105.8°]. Studien strukturell verwandter Peroxide folgend, sind Winkel kleiner 109° das Resultat π-symmetrischer Wechselwirkungen zwischen dem σ(O,O)-Orbital und dem σ*(C,C)-Orbital antiperiplanar oder antiklinal angeordneter C-C-Bindungen, die den O,C,C-Bindungswinkel reduzieren (Abbildung 5.3).[10,11]

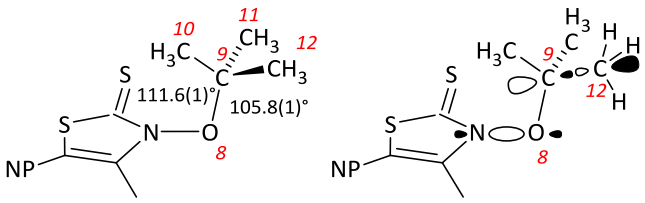

Abbildung 5.3 Molekülorbital-Modell zur Veranschaulichung der unterschiedlich großen *tert*-Butoxyl-Bindungswinkel O8, C9, C10–C12 in **3b** durch π-symmetrische Wechselwirkungen. NP = 4-Nitrophenyl.

Die *tert*-Butoxyl-Radikalvorläufer **1b**–**3b** lassen sich über diagnostische kernmagnetische Resonanzen der Thiocarbonyl-Gruppe (182 ± 2 ppm) sowie dem Singulett der *tert*-Butyl-Protonen (1.60 ± 0.04 ppm) charakterisieren. In Ethanol zeigen die Verbindungen **1b**–**3b** maximale UV/Vis-Absorptionsbanden, die auf spektroskopischen Überlagerungen von $\pi\rightarrow\pi^*$ und $n\rightarrow\pi^*$-Anregungen des Alkenylsulfanylthiocarbonyl-Chromophors[12] beruhen. Das 4-Nitrophenyl-Derivat **3b** verfügt über eine zusätzliche Absorptionsbande bei 377 nm, die auf die Nitrophenyl-Gruppe[13] in Nachbarschaft zum Heterocyclus zurückzuführen ist (Tabelle 5.1). Infrarotabsorptionsspektren der Thiohydroxamate **1b**–**3b** in Acetonitril, die in Kooperation mit Manuel Zimmer aufgenommen wurden, besitzen die stärkste Bande bei 1300 ± 50 cm^{-1}, die zweifelsfrei der C,N-Streckschwingung zugeordnet wurde. Vier bis sechs weitere intenssitätsschwache Banden im Fingerprintbereich (1200 – 850 cm^{-1}) kombinieren zu *exo*- und *endo*-cyclischen Gerüstschwingungen (C=S-/C,N-Streckschwingung; N,O-Biegeschwingung, C,H-Schwingungen). Diese Zuordnung gelang J. Hartung und M. Zimmer durch Dichtefunktional-Rechnungen (DFT-D3 / B3LYP / TZVP), theoretische Isotopensubstitutionen und durch Animation der berechneten und experimentell gemessenen Schwingungsspektren (siehe Kapitel 5.6 sowie Anhang C).

1-(tert-Butoxy)pyridin-2(1H)-thion: Die Umsetzung des 1-Hydroxypyridin-2(1*H*)-thions **4a** mit *O*-(*tert*-Butyl)-*N*,*N*-diisopropylisoharnstoff[7,8] zeigt im ^{1}H-NMR der Reaktionsmischung den (*tert*-Butyl)thiohydroxamsäure-*O*-ester **4b**[14] sowie das 2-(*tert*-Butyl)sulfanylpyridin *N*-Oxid (**9b**) (Schema 5.1).

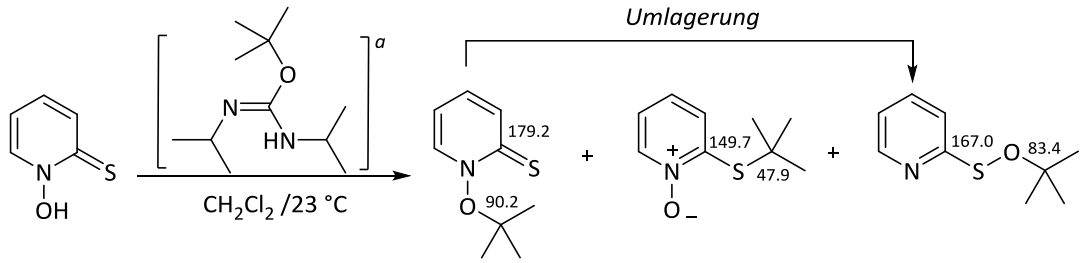

Schema 5.1. Alkylierung des 1-Hydroxypyridin-2(1*H*)-thions (**4a**) (Isoharnstoff-Methode) und charakteristische kernmagnetische Resonanzen (^{13}C) der Produkte **4b**, **9b** und **10b**. [a] *In situ* aus *t*BuOH (5.5 Äquivalente), DIC (5.5 Äquivalente), Cu(I)Cl (2 mol%).

Die Untersuchung (^{1}H-, ^{13}C-NMR-Spektroskopie) der durch Säulenchromatographie erhaltenen Fraktion, in der das *O*-(*tert*-Butyl)thiohydroxamat **4b** erwartet wurde, zeigte Resonanzen, die dem Sulfenat **10b** zugeordnet wurden (Schema 5.1). Weder bei der Synthese der 5-Ring-Heterocyclen **1b**–**3b**, noch für das 1-(*tert*-Butoxy)pyridinthion **4b** fiel in früheren Arbeiten[1,14–16] eine derartige Umlagerung auf. Eine schnelle Zersetzung von **10b** verhindert bis dato die Isolierung und zweifelsfreie Charakterisierung der Verbindung. J. Hartung beobachtete in einem anderen Zusammenhang eine ähnliche Umlagerung des 1-Pentoxypyridin-2(1*H*)-thions (**4c**)[17]→ **10c** (Schema 5.2). Ein präparativer Ansatz liefert das Sufenat **10c** in analysenreiner Form und stützt durch Vergleich der ^{13}C-NMR-Daten von **4b**, **9b**, **10b** mit **4c**, **9c**, **10c** die Umlagerung von **4b** → **10b**.

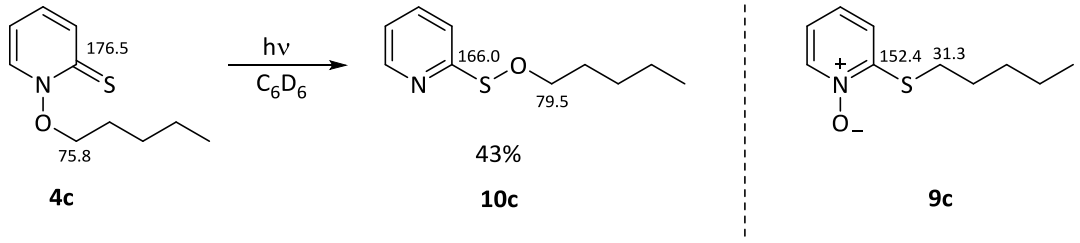

Schema 5.2. Photoreaktion des 1-Pentoxypyridin-2(1*H*)thions (**4c**) zum *O*-Pentyl-2-pyridylsulfenat (**10c**) sowie *N*-Oxid **9c**, das bei der Herstellung von **4c**[17] entsteht mit signifikanten kernmagnetischen Resonanzen (^{13}C).

5.3.2 Theoretische Berechnungen

Hintergrund und Substrate: Um Aussagen darüber treffen zu können, ob Regioselektivitäten bei der Veresterung der Thiohydroxamsäuren **1a**–**4a** mit Produktstabilitäten korrelieren und ob elektronische Wechselwirkungen zwischen dem Heterocyclus und dem *O*-Alkylrest auf konstitutionellen Unterschieden der *O*-Alkylpyridinthione und *O*-Alkylthiazolthione beruhen, wurden strukturelle Parameter und Bildungswärmen der *O*-(*tert*-Butyl)-Derivate **2b**/**4b**, der *S*-(*tert*-Butyl)-Verbindungen **7b**/**9b** sowie der *O*-(*tert*-Butyl)sulfenate **10b**/**11b** in Kooperation mit Jens Hartung berechnet. Zur Berücksichtigung sterischer Aspekte wurden die Rechnungen um die Methyl-Analoga der Thiazolthione **2d**/**7d**/**11d** sowie der Pyridinthione **4d**/**9d**/**10d** ergänzt.

Methoden: Die Berechnungen[18] erfolgten auf Grundlage der Dichtefunktional-Theorie (DFT: B3LYP[19,20] und BHandHLYP[21]) und Møller-Plesset-Störungsrechnung 2. Ord-

nung (MP2)[22–24] mit 6-31+G**[25–27] als Basissatz.[28–31] Zur Methodenevaluierung wurden die Bindungslängen und –winkel der *O*-(*tert*-Butyl)thiohydroxamate **2b**/**2d**, **3b** und **4b**/**4d** mit den drei Methoden berechnet und mit den Kristallstrukturdaten von **3b**, dem 3-Cumyloxyl-4-methylthiazol-2(3*H*)-thion[32] und dem *trans*-(1-*tert*-Butyl)-cyclohex-4-yl-pyridin-2(1*H*)-thion[33] verglichen (siehe Seite 107). Der Vergleich zeigt, dass die B3LYP-Methode experimentelle N,O- und C,S-Bindungslängen am genausten reproduziert, weshalb sie für alle folgenden Rechnungen verwendet wurde.

Minimunstrukturen und Rotationsbarrieren der N,O-Bindung: Zur Abwägung thermochemischer Trends wurden die energieärmsten Konformere der *O*-alkylierten- **2b/d**, **4b/d** und *S*-alkylierten-Verbindungen **7b/d**, **9b/d** sowie der Sulfenate **10b/d**, **11b/d** identifiziert. Dazu wurden die relativen Energien der genannten Verbindungen bei verschiedenen Torsionswinkeln ω (in 15° Schritten) berechnet und korreliert (siehe Seite 110).

In globalen Minimumstrukturen ($G_{(298)}^{min}$ = 0 kJ/mol) **2b/d** und **4b/d** ist der *O*-(*tert*-Butyl)-Rest annähernd orthogonal ($\omega_{C2,N,O,C9}$ = 90° ± 9°, Tabelle 5.3) zum Heterocyclus angeordnet. Davon abweichende Diederwinkel $\omega_{C2,N,O,C9}$ führen zu energiereichen Konformeren, mit synperiplanarer (syn, $\omega_{C2,N,O,C9}$ = 0°) oder antiperiplanarer (anit, $\omega_{C2,N,O,C9}$ = 180°) Konformation in lokalen Maxima. Die Differenz der freien Gibbs-Energien zwischen energetischem Minimum und Maximum beschreibt die Rotationsbarriere[34] des *tert*-Butyl-Rests um die rotationsgehinderte N,O-Bindung (Tabelle 5.3).

Tabelle 5.3. Berechnete (B3LYP/6-31+G**// B3LYP/6-31+G**) Torsionswinkel und Rotationsbarrieren der Thiazolthione **2b/d** und Pyridinthione **4b/d**. R = CH_3, $C(CH_3)_3$.

ω = 0 ° (syn) ω = 180 ° (anti) **2** ω = 0 ° (syn) ω = 180 ° (anti) **4**

Eintrag	Verbindung	$\omega_{C2,N,O,C9}^{min}$ / Grad [a]	$\Delta G_{(298)}^{syn}$ / kJ mol^{-1} [b]	$\Delta G_{(298)}^{anti}$ / kJ mol^{-1} [c]
1	MTTO*t*Bu (**2b**)	91.3	49.7	89.7
2	MTTOCH_3 (**2d**)	83.4	38.5	65.3
3	PTO*t*Bu (**4b**)	99.9	63.5	44.4
4	PTOCH_3 (**4d**)	83.9	44.4	35.1

[a] $G_{(298)}^{min}$ = 0 kJ mol^{-1}, [b] $\Delta G_{(298)}^{syn} = G_{(298)}^{syn} - G_{(298)}^{min}$; [c] $\Delta G_{(298)}^{anti} = G_{(298)}^{anti} - G_{(298)}^{min}$

Minimumstrukturen der *S*-alkylierten Verbindungen **7d/b** und **9b** zeigen nahezu gauche Konformationen ($\omega_{N,C2,S7,C9}$ = 63 ± 5°). Nur das *S*-methylierte-Pyridinthion **9d** ist antiperiplanar ($\omega_{N,C2,S7,C9}$ = 180°) angeordnet.[35,36] Gleichgewichtsstrukturen der Sulfenate besitzen Dach-Konformationen mit größeren Winkeln für die sterisch anspruchsvolleren *tert*-Butyl-Derivate **10b**, **11b** ($\omega_{C2,S7,O8,C9}$ = 108°) im Vergleich zu den Methyl-Analoga **10d** und **11d** ($\omega_{C2,S7,O8;C9}$ = 89° ± 2°).

Relative Stabilitäten der Minimumstrukturen: Für beide Thiohydroxamat-Klassen stellen die Sulfenate **10b/d** und **11b/d** die thermodynamisch stabilsten Produkte dar, gefolgt von den *S*-alkylierten Verbindungen **7b/d**, **9b/d** und den *O*-Alkyl-Derivaten **2b/d**, **4b/d**. Mit Ausnahme von **7b** sind dabei tertiäre Thiohydroxamate stabiler als primären *O*-Methylthiohydroxamate (Abbildung 5.4).

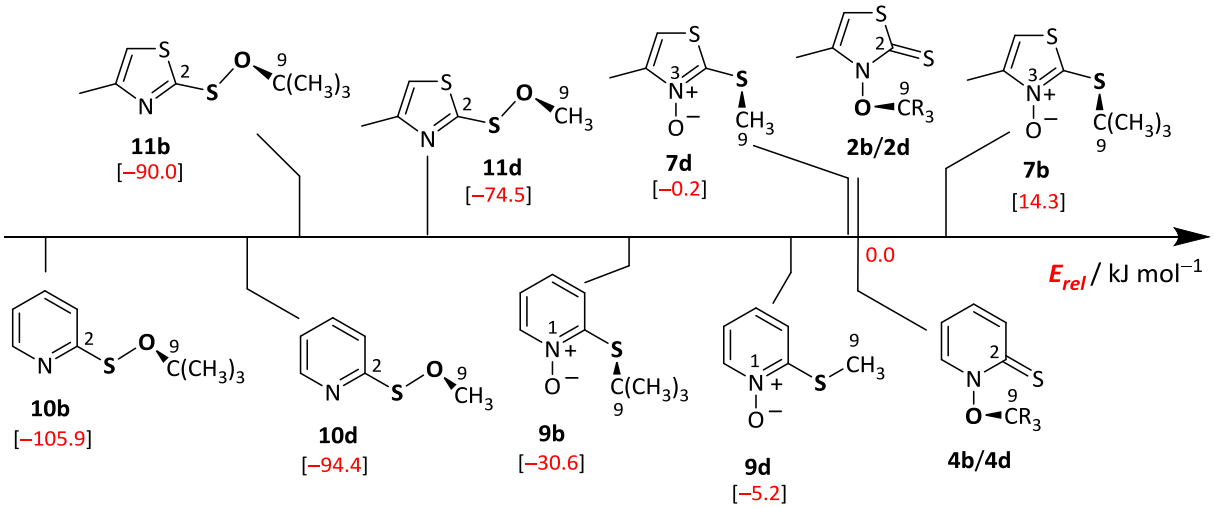

Abbildung 5.4. Berechnete (B3LYP/6-31+G**//B3LYP/6-31+G**) relative Energien der *O*-Alkylthiohydroxamate **2b/d**, **4b/d**, der *S*-Alkyl-Derivate **7b/d**, **9b/d** sowie der *O*-Alkyl-Sulfenate **10b/d**, **11b/d**. CR_3 = CH_3 oder $C(CH_3)_3$. Relative Energien (E_{rel}) der Thiazolthione (oben) beziehen sich auf andere Hyperflächen als die relative Energien (E_{rel}) der Pyridinthione (unten).

Für das Pyridinthion stimmt die berechnete Stabilitätsreihe mit den experimentellen Beobachtungen überein. Thiazolthione liefern bei der Bildung primärer und sekundärer Radikalvorläufer nur selten *S*-alkylierte Produkte[37], tertiäre Substrate stellen dabei eine Ausnahme dar und noch nie wurde die Bildung von Sulfenaten beobachtet. Demnach

beruhen Regioselektivitäten bei der Alkylierung von 3-Hydroxy-4-methylthiazol-2(3*H*)-thionen nicht auf thermodynamischen Effekten, sondern folgen kinetischen Faktoren. Die selektive *O*-Alkylierung des 3-Hydroxy-4-methyl-5-anisylthiazol-2(3*H*)-thions mit Methyltosylat sowie die selektive *S*-Alkylierung der gleichen Thiohydroxamsäure mit Methyliodid stützen die Interpretation zu den berechneten relativen Stabilitäten der Thiazolthion-abgeleiteten-Derivate **2**, **7** und **11**.[37]

N,O-Bindungsordnung: Die Bindungsstärke zwischen zwei Atomen lässt sich der Molekülorbital-Theorie folgend über Bindungsordnungen (BO)[38–39] beschreiben. Dazu werden experimentelle und theoretische N,O-Bindungslängen[40–42] gegen bekannte N,O-Bindungsordnungen aufgetragen und aus der resultierenden Geradensteigung die gesuchte Bindungsordnung bestimmt (siehe Anhang C, Seite 420). Für die *O*-(*tert*-Butyl)- und *O*-Methylthiohydroxamate **2b/d**, **3b**, **4b/d** ergeben sich daraus N,O-Bindungsordnungen von 1.3−1.4 und zeigen damit partielle π–Anteile der N,O-Bindung. Im direkten Vergleich haben *tert*-Butoxy-Derivate (z. B. **2b**: BO = 1.35) eine höhere Bindungsordnung als Methoxy-Derivate (z.B. **2d**: BO = 1.33) und Thiazolthione eine höhere Bindungsordung als Pyridinthione (**4b**: BO = 1.33, **4d**: BO = 1.29).

Ursache der partiellen π(N,O)-Bindung: Gemäß der Natural Orbital Bond-Theorie (NOB-Theorie)[43–46] beruht die partielle π(N,O)-Bindung in den Thiohydroxamaten **2**, **3** und **4** auf unterschiedlich starken und überlagernden Wechselwirkungen mit π-Symmetrie, die die Bindungsordnung erhöhen ($\pi^1_{N,O}$ und $\pi^2_{N,O}$) oder senken ($\pi^3_{N,O}$) (Abbildung 5.5).

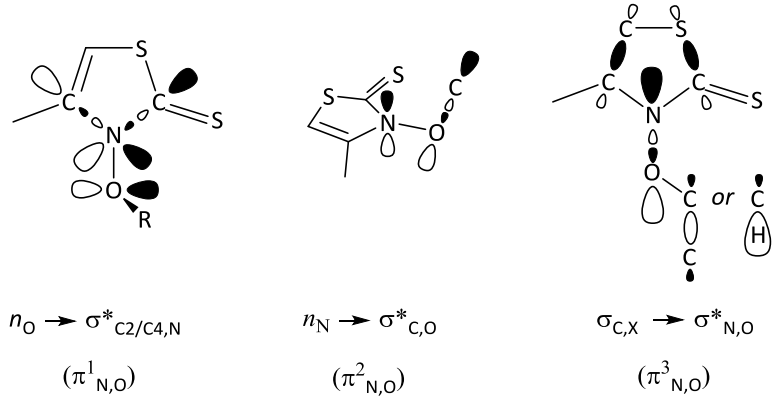

Abbildung 5.5. Beschreibung der π(N,O)-Bindung in *O*-Alkylthiazolthionen basierend auf der NOB-Theorie[43–46] (X = C ,H). π(N,O)-Bindung = $\Sigma\ \pi^{1-3}_{N,O}$.

Bindungsordnung erhöhend ist die Überlappung des nicht-bindenden p-Orbitals am Sauerstoff mit den $\sigma^*_{N,C}$-Orbitalen des Heterocycluses ($\pi^1_{N,O}$) sowie die Überlappung des nicht-bindenden p-Orbitals am Stickstoff mit dem $\sigma^*_{C,O}$-Orbital ($\pi^2_{N,O}$). Destabilisierend für die π(N,O)-Bindung und damit Bindungsordnung senkend sind Elektronen im $\sigma^*_{N,O}$-Orbital, die aus Überlappungen von σ-Elektronen des Heterocyclus und der Alkylgruppe ($\pi^3_{N,O}$) stammen (Abbildung 5.5). In Summa überwiegen stabilisierende Effekte, wodurch die Bindungsordnung steigt. Für tertiäre Thiazolthione ist die partielle π(N,O)-Bindung stärker als für Methyl-Analoga oder für Pyridinthion-Derivate.

Überlappungen der $\pi^1_{N,O}$- und $\pi^2_{N,O}$-Wechselwirkungen sind für einen Diederwinkel $\omega_{C2,N,O,C9}$ = 90° maximal. Signifikante Abweichungen davon führen zur Schwächung der π(N,O)-Bindung und erhöhen die Rotationsbarriere. Demnach beeinflussen sterische (Thiocarbonyl-Gruppe, 4-CH_3-Gruppe) und stereoelektronische Faktoren die Höhe der Rotationsbarriere in cyclischen Thiohydroxamaten. Da sich die Diederwinkeländerungen kaum auf die Energie der nicht-bindenden Orbitale am Stickstoff und Sauerstoff auswirken (NBO-Theorie), haben Coulomb-Abstoßungen zwischen den genannten Atomen keinen bedeutenden Beitrag zur Rotationsbarriere.[34] Strukturell äußern sich ungünstige Diederwinkel ($\omega > 90° < \omega$) in langen N,O-Abständen. Die Thiocarbonyl-Bindung reagiert darauf mit Verlängerung ($\omega < 90°$) oder Verkürzung ($\omega > 90°$) des C,S-Abstandes (Abbildung 5.6).

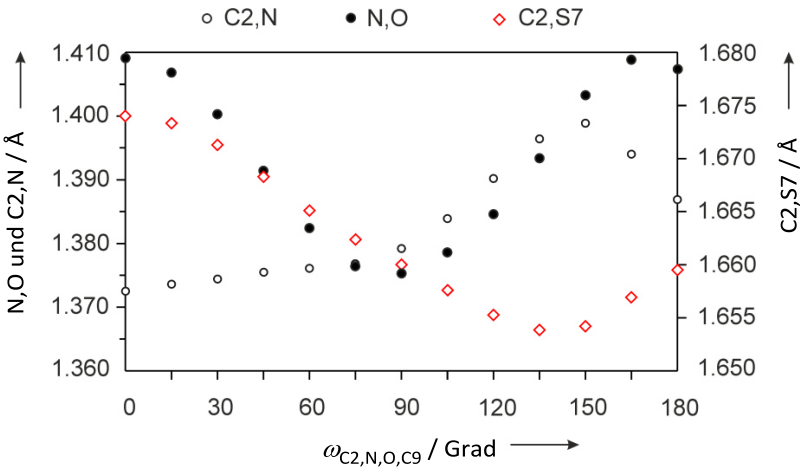

Abbildung 5.6. Diederwinkelabhängigkeit $\omega_{C2,N,O,C9}$ von den N,O- und C2,N-Bindungslängen am Beispiel von 3-(*tert*-Butoxy)thiazolthion **2b**. (Atom-Nummerierung gemäß Abbildung 5.2).

Einfluss des Bindungswinkels $\alpha_{N,O,C9}$ auf die π(N,O)-Bindung: Durch Zunahme des Thiohydroxamat-Bindungswinkels $\alpha_{N,O,C9}$ (90°→130°, Abbildung 5.7) steigt der p-Anteil des nicht-bindenden Sauerstoff-Hybridorbitals (z.B. **2b**, 32 % → 55 %) und dessen Energie sowie die Fähigkeit Elektronen an die σ*-Orbitale der Thiohydroxamat-Kerne abzugeben. Dadurch werden die beschriebenen π–symmetrischen-Wechselwirkungen der N,O-Bindung begünstigt. *O*-(*tert*-Butyl)thiohydroxamate besitzen aufgrund eines größeren sterischen Ausmaßes einen größeren Bindungswinkel $\alpha_{N,O,C9}$ und damit einen stärkeren π-Bindungsanteil sowie eine kürzere N,O-Bindung als *O*-Methylthiohydroxamate (Abbildung 5.8). Da sich die π-Wechselwirkungen $\pi^1_{N,O}$ und $\pi^2_{N,O}$ stabilisierend auf das π*-Orbital der Thiocarbonyl-Gruppe auswirken, reagiert sie auf große Bindungswinkel $\alpha_{N,O,C9}$ und kurze N,O-Bindungen durch Verlängerung des C,S-Abstandes. Die Thiocarbonyl-Gruppe verhält sich demnach invers zu Änderungen der N,O-Bindung (siehe Seite 120) .[9]

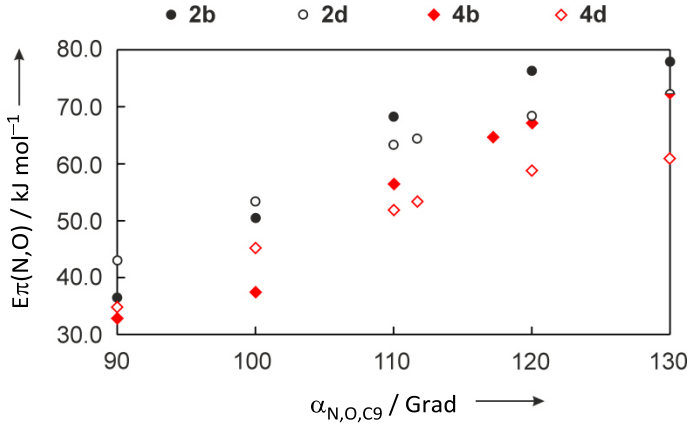

Abbildung 5.7. Bindungswinkelabhängigkeit von der Energie der π(N,O)-Bindung in heterocyclischen *O*-Alkylthiohydroxamaten. $E\pi(N,O) = \Sigma\, E\pi^{1-3}(N,O)$ (siehe Abbildung 5.5).

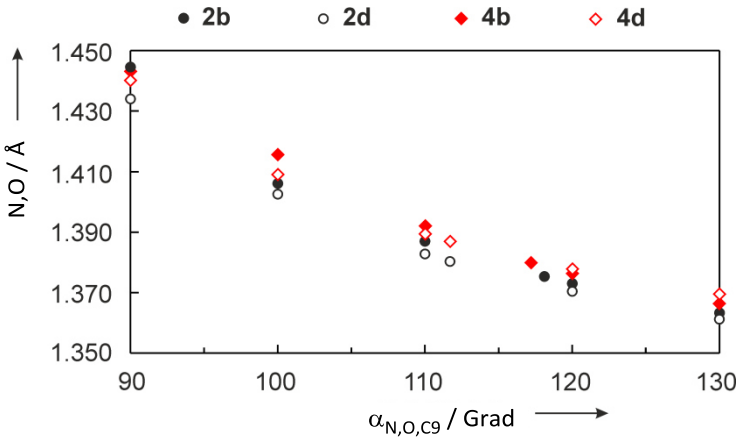

Abbildung 5.8. Korrelation zwischen Thiohydroxamat-Bindungswinkel N, O, C9 und der N,O-Bindungslänge in heterocyclischen *O*-Alkylthiohydroxamaten.

Der beschriebene Stabilisierungsmechanismus ist für 3-Alkoxythiazol-2(3*H*)-thione effektiver als für 3-Alkoxypyridin-2(1*H*)-thione und verdeutlicht damit die höhere Stabilität der 5-Ring-Heterocyclen im Allgemeinen und bei der Herstellung tertiärer Derivate im Besonderen.

5.3.3 *tert*-Butoxyl-Radikaleinfang mit 5,5-Dimethylpyrrolidin-1-oxid und Styrol

5,5-Dimethylpyrrolidin-1-oxid (DMPO): Kurzlebige Alkoxyl-Radikale lassen sich mit DMPO[47] in persistente Radikale überführen und nachweisen (Elektronen-Spin-Resonanz-Spektroskopie).[48,49] Das Nitroxid-Radikal **12**[2,50–52] entsteht nach kurzer Bestrahlung (350 nm, 2 min) einer anaeroben, benzolischen Lösung der *O*-(*tert*-Butyl)thiohydroxamate **1b**–**3b** in Gegenwart von DMPO. Das Spektrum der gut untersuchten Verbindung **12** zeigt die bekannte Hyperfeinaufspaltung zum Stickstoffatom (a_N), den Wasserstoffatomen in β- und γ-Position (a_H^{β} & a_H^{γ}) sowie die chemische Verschiebung *g* (Tabelle 5.5).

Tabelle 5.5 *tert*-Butoxyl-Radikaleinfang mit 5,5-Dimethyl-1-pyrrolidin *N*-oxid zum Nitroxid-Radikal **12** und dessen chemische Verschiebung (*g*) sowie die Kopplungskonstanten (*a*).

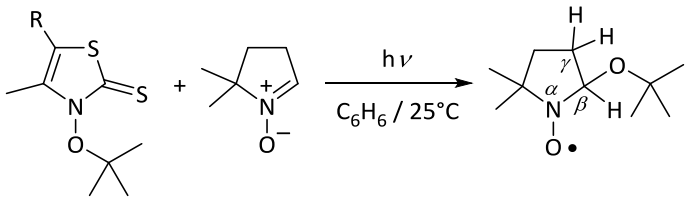

1b–3b *DMPO* **12**

Eintrag	**1b**–**3b**	R	g [a]	a_N/G [a]	a_H^{β}/G [a]	a_H^{γ}/G [a]
1	**1b**	4-CH_3O-C_6H_4	2.009	13.17	7.96	1.93
2	**2b**	H	2.009	13.15	7.94	–[b]
3	**3b**	4-NO_2-C_6H_4	2.009	13.17	7.94	1.90

[a] H = 3478 G, ν = 9.779 × 10^9 Hz, Modulation Amplitude = 0.0001 T, [b] nicht beobachtet.

Styrol: Die photochemische Umsetzung von 3-(*tert*-Butoxy)-4-methylthiazol-2(3*H*)-thion **2b** mit Styrol liefert in Gegenwart von Bromtrichlormethan regioselektiv 2-Brom-2-phenyl-1-(*tert*-butoxy)ethan (Schema 5.3).

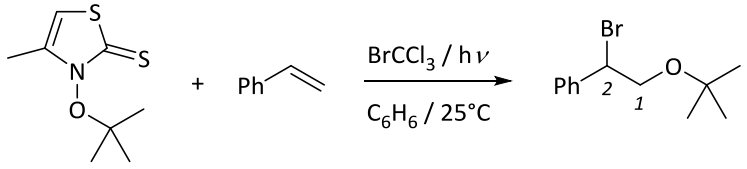

2b *Styrol* **13** (26%)

Schema 5.3. Photochemische Umsetzung des *O*-(*tert*-Butyl)thiohydroxamats **2b** mit Styrol und Bromtrichlormethan.

5.4 Fazit & Ausblick

Die Existenz von *O*-(*tert*-Butyl)thiazol-2(3*H*)-thionen basiert auf Stabilitäten im Grundzustand. Günstige π-symmetrische Wechselwirkungen des Stickstoff- und Sauerstoffatoms mit dem Heterocyclus oder dem Alkyl-Rest führen, insbesondere für sterisch anspruchsvolle Reste, zu einer Erhöhung der N,O-Bindungsordnung auf 1.4 und damit zu einer sterischen Stabilisierung der tertiären Thiazolthione (MO- und NBO-Theorie). Für Pyridinthion-Derivate sind die stabilisierenden Effekte weniger effektiv und verdeutlichen damit die Schwierigkeiten, die mit der Synthese entsprechender Radikalvorläufer verbunden sind. Die beschriebene Stabilisierung von σ-Heteroatom-Heteroatom-Bindungen durch zusätzliche π-Wechselwirkungen benachbarter nicht-bindernder p- oder sp-Hybridorbitale mit Orbitalen angrenzender Atome kann in zukünftigen Studien Stabilitätsunterschiede zwischen beliebig kombinierten Heteroatomen, wie zum Beispiel Sauerstoff, Stickstoff, Chlor, Brom, Iod, Fluor, erklären. Für tertiäre 3-Alkoxythiazol-2(3*H*)-thione können die Grundzustandsstabilitäten dazu genutzt werden die Vielfalt tertiärer *O*-Alkylthiohydroxamate weiterzuentwickeln und nach Verlassen des Grundzustandes, durch photochemische oder thermische Aktivierung, den Einfluss polarer Effekte auf Stereoselektivitäten in Additionsreaktionen tertiärer *O*-Radikale zu untersuchen.

5.5 Literaturverzeichnis

[1] C. Schur, N. Becker, U. Bergsträßer, T. Gottwald, J. Hartung, *Tetrahedron* **2011**, *67*, 2338–2347.

[2] A. Groß, N. Schneiders, K. Daniel, T. Gottwald, J. Hartung, *Tetrahedron* **2008**, *64*, 10882–10889.

[3] D. H. R. Barton, D. Crich, G. Kretschmar, *J. Am. Chem. Soc.* **1986**, 39–54.

[4] C. Schur, H. Kelm., T. Gottwald, A. Ludwig, R. Kneuer, J. Hartung, *Org. Biomol. Chem.* **2014**, *12*, 8288–8307.

[5] I. Kempter, B. Frensch, T. Kopf, R. Kluge, R. Csuk, I. Svoboda, H. Fuess, J. Hartung, *Tetrahedron* **2014**, *70*, 1918–1927.

[6] P. J. Stang, T. E. Dueber, *J. Am. Chem. Soc.* **1977**, 2602–2610.

[7] L. F. Tietze, G. Brasche, A. Grube, N. Böhnke, C. Stadler, *Chem. Eur. J.* **2007**, *13*, 8543–8563.

[8] L. J. Mathias, *Synthesis* **1979**, 561–576.

[9] J. Hartung, U. Bergsträßer, K. Daniel, N. Schneiders, I. Svoboda, *Tetrahedron* **2009**, *65*, 2567–2573.

[10] J. Hartung, I. Svoboda, in *The Chemistry of Peroxides,* Z. Rappoport (Ed.), Wiley, **2006**, Chichester, 93–144.

[11] S. L. Khursan, V. L. Antonovsky, *Russ. Chem. Bull.* **2003**, *52*, 1312–1325.

[12] J. Hartung, K. Špehar, I. Svoboda, H. Fuess, M. Arnone, B. Engels, *Eur. J. Org. Chem*. **2005**, 869–881.

[13] S. Nagakura, M. Jojima, Y. Maruyama, *J. Mol. Spectrosc.* **1964**, *13*, 174–192.

[14] B. P. Hay, A. L. J. Beckwith, *J. Org. Chem.* **1989**, *54*, 4330–4334.

[15] T. Gottwald, *Dissertation* **2004**, Julius-Maximilians-Universität Würzburg.

[16] N. Schneiders, *Dissertation* **2008**, Technische Universität Kaiserslautern.

[17] J. Hartung, R. Kneuer, M. Schwarz, I. Svoboda, H. Fuess, *Eur. J. Org. Chem.* **1999**, 97–106.

[18] J. B. Foresman, Æ. Frisch, *Exploring Chemistry with Electronic Structure Methods*, 2nd ed. **1996**, Gaussian Inc., Pittsburgh, PA.

[19] A. D. Becke, *J. Chem. Phys.* **1993**, *98*, 5648–5652.

[20] C. Lee, W. Yang, R. G. Parr, *Phys. Rev.* **1988**, *B37*, 785–789.

[21] A. D. Becke, *Phys. Rev*. **1988**, *A38*, 3098–3100.

[22] C. Møller, M. S. Plesset, *Phys. Rev.* **1934**, *46*, 618–622.

[23] M. J. Frisch, M. Head-Gordon, J. A. Pople, *Chem. Phys. Lett.* **1990**, *166*, 281–289.

[24] M. Head-Gordon, T. Head-Gordon, *Chem. Phys. Lett.* **1994**, *220*, 122–128.

[25] R. Ditchfield, W. J. Hehre, J. A. Pople, *J. Chem. Phys.* **1971**, *54*, 724–728.

[26] W. J. Hehre, R. Ditchfield, J. A. Pople, *J. Chem. Phys.* **1972**, *56*, 2257–2261.

[27] Gaussian 03, Revision E.01, M. J. Frisch, G. W. Trucks, H. B. Schlegel, G. E. Scuseria, M. A. Robb, J. R. Cheeseman, J. A. Montgomery, Jr., T. Vreven, K. N. Kudin, J. C. Burant, J. M. Millam, S. S. Iyengar, J. Tomasi, V. Barone, B. Mennucci, M. Cossi, G. Scalmani, N. Rega, G. A. Petersson, H. Nakatsuji, M. Hada, M. Ehara, K. Toyota, R. Fukuda, J. Hasegawa, M. Ishida, T. Nakajima, Y. Honda, O. Kitao, H. Nakai, M. Klene, X. Li, J. E. Knox, H. P. Hratchian, J. B. Cross, V. Bakken, C. Adamo, J. Jaramillo, R. Gomperts, R. E. Stratmann, O. Yazyev, A. J. Austin, R. Cammi, C. Pomelli, J. W. Ochterski, P. Y. Ayala, K. Morokuma, G. A. Voth, P. Salvador, J. J. Dannenberg, V. G. Zakrzewski, S. Dapprich, A. D. Daniels, M. C. Strain, O. Farkas, D. K. Malick, A. D. Rabuck, K. Raghavachari, J. B. Foresman, J. V. Ortiz, Q. Cui, A. G. Baboul, S. Clifford, J. Cioslowski, B. B. Stefanov, G. Liu, A. Liashenko, P. Piskorz, I. Komaromi, R. L. Martin, D. J. Fox, T. Keith, M. A. Al-Laham, C. Y. Peng, A. Nanayakkara, M. Challacombe, P. M. W. Gill, B. Johnson, W. Chen, M. W. Wong, C. Gonzalez, J. A. Pople, Gaussian, Inc., Wallingford CT, **2004**.

[28] V. A. Rassolov, J. A. Pople, M. A. Ratner, T. L. Windus, *J. Chem. Phys.* **1998**, *109*, 1223–1229.

[29] V. A. Rassolov, M. A. Ratner, J. A. Pople, P. C. Redfern, L. A. Curtiss, *J. Comp. Chem.* **2001**, *22*, 976–984.

[30] M. M. Francl, W. J. Pietro, W. J. Hehre, J. S. Binkley, D. J. DeFrees, J. A. Pople, and M. S. Gordon, *J. Chem. Phys.* **1982**, *77*, 3654–3665.

[31] R. D. Bach, G. J. Wolwer, B. A. Coddens, *J. Am. Chem. Soc.* **1984**, *106*, 6098–6099.

[32] J. Hartung, N. Schneiders, U. Bergsträßer, *Acta Cryst.* **2006**, *E62*, o4713–o4714.

[33] J. Hartung, M. Hiller, Margit; M. Schwarz, I. Svoboda, Ingrid; H. Fuess, *Liebigs Ann.* **1996**, 2091–2097.

[34] J. Hartung, R. Kneuer, M. Schwarz, M. Heubes, *Eur. J. Org. Chem*. **2001**, 4733–4736.

[35] J. Hartung, K. Daniel, U. Bergsträßer, I. Kempter, N. Schneiders, S. Danner, P. Schmidt, I. Svoboda, H. Fuess, *Eur. J. Org. Chem*. **2009**, 4135–4142.

[36] J. Hartung, R. Kneuer, S. Laug, P. Schmidt, K. Špehar, I. Svoboda, H. Fuess, *Eur. J. Org. Chem*. **2003**, *20*, 4033–4052.

[37] J. Hartung, C. Schur, I. Kempter, T. Gottwald, *Tetrahedron* **2010**, *66*, 1365–1374.

[38] N. B. H. Jonathan, *J. Mol. Spectrosc.* **1960**, *4*, 75–83.

[39] R. A. W. Johnstone, R. M. S. Loureiro, M. L. S. Cristiano, G. Labat, *ARKIVOC* **2010**, 142–169.

[40] K. L. Shi, R.Q-Wang, T. C. W. Mak, *J. Mol. Struc.* **1987**, *160*, 109–116.

[41] K. P. Huber, G. Herzberg, in *Molecular Spectra and Molecular Structure IV*. Constants of Diatomic Molecules, Van Nostrand, New York, N.Y. **1979**, pp. 466–484.

[42] R. Polák, J. Fišer, *Chem. Phys*. **2004**, *303*, 73–83.

[43] J. P. Foster, F. Weinhold, *J. Am. Chem. Soc.* **1980**, *102*, 7211–7218.

[44] A. E. Reed, L. A. Curtiss, F. Weinhold, *Chem Rev.* **1988**, *88*, 899–926.

[45] NBO 5.9. E.D. Glendening, J.K. Badenhoop, A.E. Reed, J.E. Carpenter, J.A. Bohmann, C.M. Morales, F. Weinhold, Theoretical Chemistry Institute, University of Wisconsin, Madison, WI, **2009**, http://www.chem.wisc.edu/~nbo5.

[46] E. D. Glendening, D. Eric, C. R. Landis, F. Weinhold, *Computational Molecular Science*, 2012, **2**, 1–43.

[47] D. L. Haire, J. W. Hilborn, E. G. Janzen, *J. Am. Chem. Soc*. **1986**, *51*, 4298–4300.

[48] F. Bär, A. Berndt, K. Dimroth *Chemie in unserer Zeit* **1975**, 18–24.

[49] F. Bär, A. Berndt, K. Dimroth *Chemie in unserer Zeit* **1975**, 43–49.

[50] E. G. Janzen, J. I-Ping Liu *J. Magn. Reson.* **1973**, *9*, 510–512.

[51] M. J. Davies, T. F. Slater, Biochem. *J.* **1986**, *240*, 789–795.

[52] J. Hartung, K. Daniel, T. Gottwald, A. Groß, N. Schneiders, *Org. Biomol. Chem*. **2006**, *4*, 2313–2322.

5.6 Forschungsartikel

Heterocyclic *O*-(*tert*-Butyl) Thiohydroxamates

Christine Schur, Manuel Zimmer, Harald Kelm, Markus Gerhards, and Jens Hartung

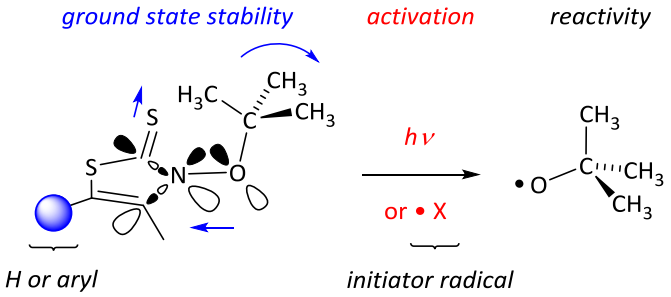

Summary: 3-Hydroxy-1,3-thiazole-2(3*H*)thiones react with *O*-(*tert*-butyl)-*N*,*N*-diisopropyl isourea to furnish heterocyclic *O*-(*tert*-butyl) thiohydroxamates in up to 64% yield. The compounds are stable crystalline solids, showing carbon-13 resonances for the thiocarbonyl group at 183±1 ppm, and vibrational combinations from the *O*-alkyl thiohydroxamate functional group, situated in the range between 950 and 1300 cm^{-1}. 1-(*tert*-Butoxy)pyridine-2(1*H*)thione, prepared similarly, is a labile compound, quantitatively rearranging into *O*-(*tert*-butyl) pyridine-2-sulfenate. Differences in chemical behavior relate to N,O-bond strengths, as expressed for 3-(*tert*-butoxy)-1,3-thiazole-2(3*H*)thiones by a N,O-bond order of 1.4. Molecular orbital theory describes partial multiple bonding between nitrogen and oxygen as σ(N,O)-bond in combination with three superimposed π(N,O)-bonds of different strengths. Photoexciting 3-(*tert*-butoxy)thiazole-2(3*H*)thiones or adding an initiator radical to thiocarbonyl sulfur disconnects ground state stabilizing mechanisms, inducing homolytic breaking of N,O-bond. *tert*-Butoxyl radicals liberated from heterocyclic *O*-(*tert*-butyl) thiohydroxamates in photochemical experiments furnish spin-adducts, which were detected by electron spin resonance spectroscopy, or a 1-(*tert*-butoxy)-2-bromoalkane formed by intermolecularly adding to an alkene in the presence of bromotrichloromethane.

Introduction

Oxygen radicals are reactive intermediates, transforming hydrocarbons with unique chemical reactivity and selectivity.[1–3] Hydrocarbon pollutants are broken down by oxygen radicals into lower alcohols and aldehydes, for being washed out from the atmosphere by rainfall.[4] Burning fossil fuels with dioxygen in combustion chambers oxidizes hydrocarbons via alkoxyl radical mechanisms, liberating chemical energy for propelling vehicles.[5] In biochemistry, immune systems of mammals rely on hydroxyl radicals for destroying pathogenic germs.[6] Other oxygen radicals in combination with singlet dioxygen and oxygen radical anions transform nucleic acids, proteins, and secondary metabolites into xenobiotics, which contribute to develop symptoms of oxidative stress.[7] In biosynthesis, enzymes generate alkoxyl radicals for constructing carbon-oxygen bonds in intramolecular additions with otherwise unattainable rate and selectivity.[3,8]

Mechanistically, most alkoxyl radical reactions are additions, substitutions, and fragmentations.[3] Fragmentations are unimolecular processes, with rate constants

depending on solvent polarity, neighboring groups at reaction centers, and temperature. In a competition system, fragmentation serves as internal clock, for comparing rates of an unimolecular to a bimolecular process. In molar solutions of alkenes, rates of alkoxyl radical fragmentation, addition, and substitution converge, yielding fingerprint mixtures of oxy-functionalized products.[9–10] Analyzing such mixtures allows to trace rates and concentration of involved reactants (Scheme 1).[11–13]

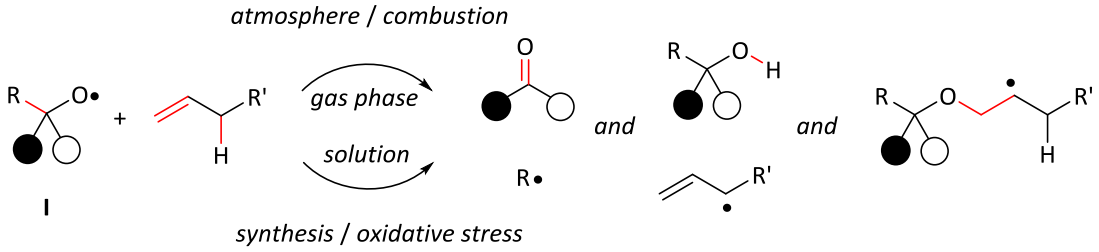

Scheme 1 Products formed from alkoxyl radical/alkene compositions (colorless circles denote carbon substituents, black circles a hydrogen, heteroatom group, or a carbon substituent).[11]

Synthesis with alkoxyl radicals takes profit from complementary selectivity in additions to non-activated alkenes, when compared, for example, to ionic alkenol bromo-cyclization.[11,14,15] Trapping alkoxyl radical addition products with a bromine atom donor affords β-bromohydrin ethers with unique radical selectivity, which is of interest for preparing bioactive compounds from the marine environment or for technical and synthetic use (Figure 1).[11, 16–18]

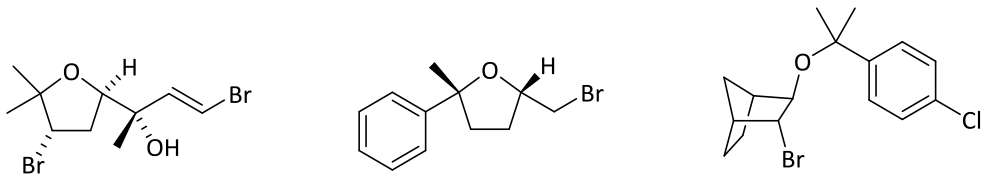

Figure 1 Structure formulas of a naturally occurring tertiary β-bromohydrin ether (left: pantofuranoid E), and two bromohydrin ethers prepared from tertiary alkoxyl radical reactions (center and right). [11,16,17]

Standard reagents for generating tertiary alkoxyl radicals are alkanols,[19,20] *O*-alkyl nitrites,[21] alkyl hypohalites,[22] alkyl hydroperoxides,[23,24] dialkyl peroxides,[25–28] *O*-alkyl peresters,[29] *O*-alkyl benzene sulfenates,[30] *N*-alkoxyphthalimides,[31] and *O*-alkyl

thiohydroxamates (Scheme 2).[23,32] State-of-the-art synthesis with radicals occurs in pH-neutral non-oxidative environment and proceeds via linear chain reactions in the absence of tin hydride mediators.[33,34] Meeting these demands restricts the type of available precursors to the *O*-alkyl thiohydroxamates, which however are difficult to prepare from tertiary alcohols.[23] Synthesis of tertiary *O*-alkyl thiohydroxamates in attractive yields, at the moment, is developed only for a single thiohydroxamic acid (i.e. **1a**), using *O*-(*tert*-alkyl) isoureas as carbon electrophiles.[11,35–37] To broaden the scope for preparing *O*-(*tert*-butyl) esters, starting from heterocyclic thiohydroxamic acids having quite different chemical properties, we conducted the present experimental and theoretical investigation.

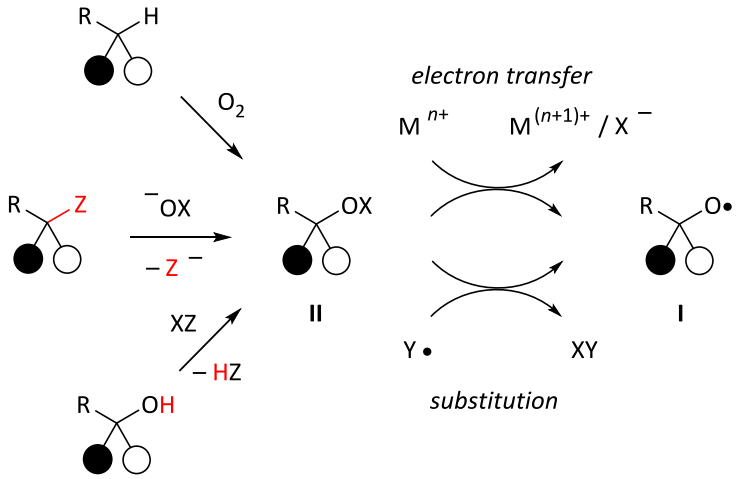

Scheme 2 Approaches to synthesis of alkoxyl radical progenitors **II** starting from a hydrocarbon (top left, X = OH), a carbon electrophile (center left; Z = e.g. halogen, arylsulfonyloxy or *N*,*N*-dialkyl-*O*-isoureyl; $^{-}$OX = e.g. thiohydroxamate), or an alcohol [bottom left; **X**Z = e.g. **NO**Cl, *t*BuO**Cl**, PhI(OAc)$_2$/**I**$_2$/HgO], and conditions for liberating oxygen radical **I** (right).[23].

The major results from the study show that 3-(*tert*-butoxy)thiazole-2(3*H*)thiones prepared from underlying 3-hydroxythiazole-2(3*H*)thiones are stable compounds, while a derived pyridine-2(1*H*)thione quantitatively rearranges into a *O*-(*tert*-butyl) pyridine-sulfenate. Differences in chemical properties relate to N,O-bond strengths, as expressed for 3-(*tert*-butoxy)-1,3-thiazole-2(3*H*)thiones by a bond order of 1.4. Molecular orbital theory describes partial multiple bonding between nitrogen and oxygen as σ(N,O)-bond in combination with three superimposed π(N,O)-bonds of different strengths. Photoexciting a

3-(*tert*-butoxy)-1,3-thiazole-2(3*H*)thione, or adding an initiator radical to thiocarbonyl sulfur, disconnects ground state stabilizing effects and releases *tert*-butoxyl radicals, as exemplified by spin trapping experiments and intermolecular addition.

Results and Interpretation

1 Thiohydroxamic acids

(i) *Significance of selected thiohydroxamic acids*. *O*-Alkyl derivatives of 3-hydroxy-5-(4-methoxyphenyl)-4-methylthiazole-2(3*H*)thione (MAnTTOH) (**1a**), 3-hydroxy-4-methyl-thiazole-2(3*H*)thione (MTTOH) (**2a**), and 1-hydroxypyridine-2(1*H*)thione (PTOH) (**4a**) cover a spectrum of chemical properties, meeting most of the demands in synthetic and mechanistic alkoxyl radical chemistry.[23,38,39] Colorless *O*-esters of 3-hydroxythiazolethione **2a** and pale-yellow *O*-alkyl derivatives of *p*-methoxyphenyl-substituted acid **1a** withstand acidic and basic conditions, allowing final chemical modifications of the ester side chain, for finalizing syntheses of more complex alkoxyl radical progenitors. Compounds of this kind are stable when stored, and quantitatively liberate alkoxyl radicals within thirty minutes when heated or being photolyzed. Alkoxyl radical reactions involving 1-(alkoxy)pyridine-2(1*H*)thiones (i.e. esters of **1a**) are complete with a minute or less. Depending on the chemical nature of the *O*-alkyl group, the compounds may be stored or decompose with hour.[38,40] For generating alkoxyl radicals from a compound with storage stability, by illuminating with blue light emitting diode,[41] we developed 3-hydroxy-4-methyl-5-(4-nitrophenyl)thiazole-2(3*H*)thione (MNPTTOH) (**3a**), and introduce this compound here for the first time (Figure 2).

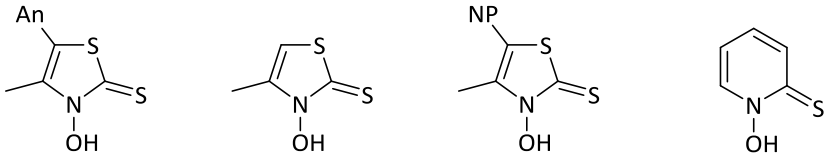

Figure 2 Structure formulas of cyclic thiohydroxamic acids **1a–4a** used for preparing *O*-(*tert*-butyl) esters {An = *para*-**an**isyl [*p*-$C_6H_4(OCH_3)$]; NP = *para*-**n**itro**p**henyl [*p*-$C_6H_4(NO_2)$]}.

(ii) *Synthesis of heterocyclic thiohydroxamic acids*. Synthesis 3-hydroxy-5-(4-methoxyphenyl)-4-methylthiazole-2(3*H*)thione (MAnTTOH) (**1a**) and *p*-nitrophenyl-derivative MNPTTOH (**3a**) (Scheme 3) followed an adapted procedure, developed for preparing 3-

hydroxy-4-methylthiazolethione **2a** (MTTOH) by Kretzschmar and Barton.[42–44] 1-Hydroxy-pyridinethione **4a** (PTOH) precipitates by adding one equivalent of hydrochloric acid to an aqueous solution sodium omadine^{TM}.[45]

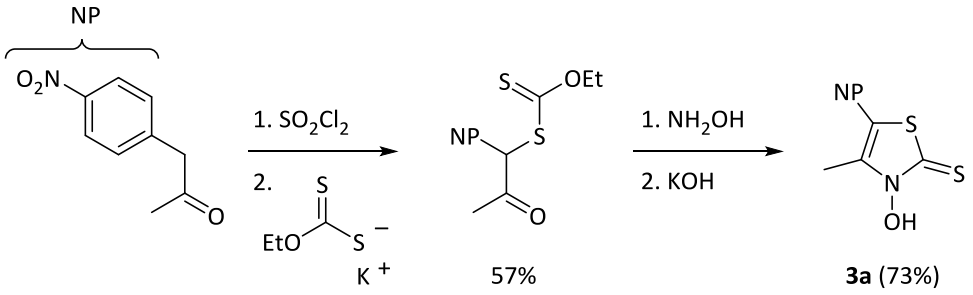

Scheme 3 Synthesis of 3-hydroxy-4-methyl-5-(4-nitrophenyl)thiazole-2(3*H*)thione (**3a**).

Thiohydroxamic acids are colorless (**2a**, **4a**) to yellow (**1a**, **3a**) solids, dissolving in lower alkanols, dimethyl sulfoxide, or aqueous alkali hydroxide. Hydroxyl groups give rise to broad proton-NMR resonances between 9.0 and 12.5 ppm in solutions of deuterochloroform or dimethyl sulfoxide. Thiocarbonyl carbons show characteristic resonances at 173±4 ppm.

2. Preparation, spectroscopic properties, and structural aspects of 3-alkoxy-4-methylthiazole-2(3*H*)thiones

(i) *General remarks on atom numbering for structural discussions*. Numbering of atoms within heterocycles follows the Hantzsch-Widman notation (for examples, see Figures 4 and 6).[46,47] Atoms relevant for structural and spectroscopic discussions, attached to heterocycles, such as the thione sulfur (S7), thiohydroxamate oxygen (O8), ester carbon (C9), and carbons bound to C9 (C10–12), are for tutorial reasons numbered chronologically.

(ii) *The alkylation reagent*. *O*-(*tert*-Butyl)-*N*,*N*-diisopropyl isourea (**5**) is an unstable liquid prepared from *tert*-butanol and *N*,*N*-diisopropylcarbodiimide (DIC) in a copper (I)-chloride-catalyzed reaction at room temperature (20±2 °C) (Scheme 4).[48] The yield of isourea **5** under such conditions goes through a maximum of 61 % after ~ 24 hours. Beyond this point of time, the fraction of decomposition product diisopropyl urea (DIU) increases.

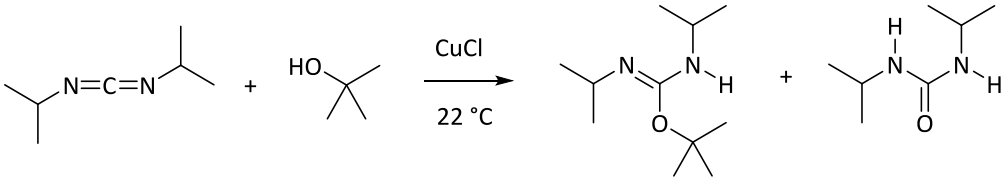

DIC **5** (~61%) *DIU* (~39%)

Scheme 4. Synthesis of *O*-(*tert*-butyl)-*N*,*N*-diisopropyl isourea.[48]

The proton-NMR spectrum of *O*-(*tert*-butyl)-*N*,*N*-diisopropyl isourea (**5**) recorded in solution of deuterochloroform displays a singlet at 1.47 ppm for *tert*-butyl protons, two sets of septets at 3.13 ppm and 3.66 ppm, and two doublets at 1.04 and 1.08 ppm for the two isopropyl groups.[49] Resonances of DIU in deuterochloroform show chemical shifts of 5.49 ppm (d) for the amine proton, and at 1.00 (d), 3.62 (sept), and 3.64 (sept) for isopropyl protons.

(iii) *Thiazole-derived O-(tert-butyl) thiohydroxamates*. *O*-(*tert*-Butyl) thiohydroxamate **1b** forms in average yields of 61±3% (*n* = 3), by adding a 5.5-molar excess of *O*-(*tert*-butyl) isourea **5** at room temperature to a solution of MAnTTOH (**1a**) in dichloromethane (Table 1, entry 1).[11] All parameter variations we undertook for raising efficiency of the synthesis, by decreasing reaction temperature, changing solvent to dimethylformamide, modifying isourea concentration and aliquots, increased the fraction of DIU and lowed yields of ester **1b**.[50] Treating MTTOH (**2a**) and MNPTTOH (**3a**) with isourea **5**, as specified for MAnTTOH (**1a**), provides *tert*-butyl thiohydroxamates **2b** and **3b** in 39–55% yields (Table 1, entries 2–3).

Thiazole-derived *tert*-butyl thiohydroxamates are colorless (**2b**) to yellow solids (**1b**, **3b**), melting at 57 °C (**2b**), 115 °C (**1b**), and 153 °C (**3b**). The compounds are stable when stored at room temperature in standard glassware. When heated to 130 °C at a pressure of 8 × 10^{-3} millibars, 3-(*tert*-butoxy)-4-methylthiazolethione (MTTO*t*Bu) (**2b**), gradually darkens and finally turns black without showing any signs of boiling. From this information we concluded that distilling is no alternative to chromatography for purifying *tert*-butyl esters **1b–3b**. A proton NMR-spectrum recorded from the black material showed almost exclusively resonances of ester **2b**.

Table 1 Products formed from 4-methylthiazole-derived thiohydroxamates **1a–3a** and *O*-(*tert*-butyl)-*N*,*N*-diisopropyl isourea (**5**).

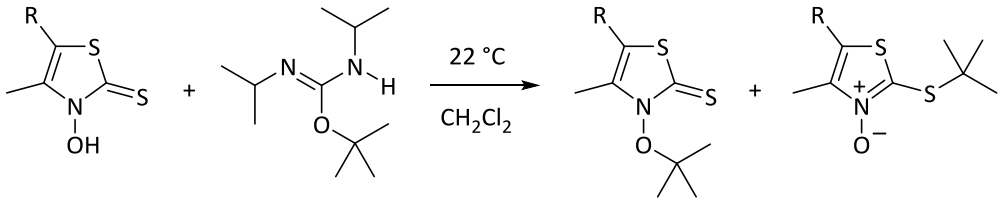

1a–3a **5** **1b–3b** **6b–8b**

entry	R	**1b–3b** / %	**6b–8b** / % [a]
1	*p*-$C_6H_4(OCH_3)$	**1b**: 58–64 [b]	**6b**: 25
2	H	**2b**: 42–55 [b]	**7b**: 24
3	*p*-$C_6H_4(NO_2)$	**3b**: 39–43 [c]	**8b**: 17

[a] Isolated from one representative experiment. [b] 3 Experiments. [c] 2 Experiments.

(iv) *S-Alkylation*. *S*-(*tert*-Butyl) thiohydroximates **6b–8b** form as side products in 17–25% yields from reactions between acids **1a–3a** and *O*-(*tert*-butyl) isourea **5**. The products are colorless crystalline solids, quantitatively separating from *O*-esters **1b–3b** during chromatography, given ratio-of-fronts close to zero for the combination of ether/alkane-mixtures as eluents, and silica gel as stationary phase.

(v) *Electronic spectra of 3-(tert-butoxy)thiazolethiones*. *O*-(*tert*-Butyl) esters **1b–3b** absorb near UV/light, with maxima gradually shifting in solutions of methanol from 319 nanometers for **2b** via 337 for **1b** to 377 nanometers for **3b**.

According to theory, the lowest in energy electronic absorption band of 3-(alkoxy)thiazole-2(3*H*)thiones arises from $\pi \rightarrow \pi^*$- and $n \rightarrow \pi^*$-transitions between orbitals involving predominantly the heterocyclic alkenylsulfanylthiocarbonyl chromophore.[38] The singlet excited state rapidly converts into a triplet, which is antibonding for the nitrogen-oxygen bond.[51]

The absorption band at 377 nanometers in ester **3b**, we assigned to $\pi \rightarrow \pi^*$-transitions between orbitals of the *p*-nitrophenyl group. The band is shifted 37 nanometers from the nitrobenzene band (λ_{max} = 340 nm), due to electron conjugation within in ester **3b**.[52] The band located at 324 nanometers, in this interpretation, is the thioazole-2(3*H*)thione band, relevant for homolytically breaking the N,O bond.[38,53]

(vi) *Proton-NMR and carbon-13 chemical shifts of O-tert-butyl esters*. Carbon-13 NMR-resonances suitable for identifying products of thiohydroxamate *O*-alkylation originate from thiocarbonyl carbon C2 (183±1 ppm) and heterocyclic enamine carbon C5 (117±3 ppm for **1a** and **3a**; 102.5 for **2a**). The half-width of the carbon-13 resonance from the three magnetically equivalent methyl groups of the *tert*-butyl substituent of ester **1b** measures 2.3 Hz, which compares to line widths of the remaining signals (2.2±0.8Hz). *O*-Cumyl esters of **1a** exert broad resonances for methyl carbons bound to C9 (for atom numbering, refer to Figures 4 and 6), due to hindered rotation of the tertiary alkyl group about the N,O-bond.[11,35] For pro-diastereotopic methyl protons in **1b**, the phenomenon of hindered rotation is not similarly observable. From comparable steric size of a *tert*-butyl and a cumyl group,[54,55] we expect similar rate retarding effects on N,O-rotation.

For characterizing *tert*-butyl esters **1b–3b** via proton NMR-spectroscopy, we used chemical shifts from the singlet of the 4-methyl substituent of the heterocycle (2.4±0.1 ppm), the quartet of C5-H in **2b** (6.15 ppm), and the singlet for the nine magnetically equivalent protons of the *tert*-butyl group (1.56±0.09 ppm) (all values for $CDCl_3$ and 20 °C).

(vii) *Assigning thiocarbonyl stretchings and nitrogen-oxygen vibrations in heterocyclic O-(tert-butyl) thiohydroxamates*. For identifying infrared absorptions from the thiohydroxamate entity, we calculated vibrational spectra for minimum conformations of heterocyclic *O*-(*tert*-butyl) thiohydroxamates **1b–3b** (sections 4.1–4.2 for **2b–3b** and ESI for **1b**) at the DFT-D3/B3LYP/TZVP-level of theory, which includes disperion energies for predicting vibrational modes more reliable than methods used hereafter for other purposes.

The strongest infrared absorption of 3-(*tert*-butoxy)-4-methylthiazole-2(3*H*)thione (**2b**) in a solution of acetonitrile is positioned at 1300 cm^{-1} and originates from largely uncoupled C,N-stretching vibration toward C2.

The thiocarbonyl stretching vibration in ester **2b** couples to vibrations from the heterocyclic core, and bonds formed with substituents, particularly the alkoxy and the 4-methyl group, but also the C5-H bond. Vibrational coupling gives rise to three weak in intensity bands located at 982, 1012 and 1153 cm^{-1}, showing moderate to small contribution from thiocarbonyl stretching. These bands are located with similar relative intensity at 964, 1022 and 1152 cm^{-1} in the computed, scaled (0.99) vibrational spectrum (Figure 3).

Elongation of the N,O-bond couples with thiocarbonyl stretching, C,H-bending and

ring deformation vibrations from the heterocyclic core, leading to weak infrared absorptions at 883, 1138, 1155, and 1191 cm^{-1} in the experimental spectrum and at 887, 1152, 1170 and 1206 cm^{-1} in the computed spectrum.

Carbon-nitrogen stretching vibrations of 5-aryl-substituted thiazolethiones **1b** and **3b** couple to bending, torsional, skeletal, and deformation modes, but remain located in the spectral region of 1300±50 cm^{-1}. Thiocarbonyl stretchings couple in both compounds more extensively, providing up to six diagnostic but low-in-intensity vibrations between 950 and 1350 cm^{-1} (ESI).

To sum up, thiocarbonyl stretching [56–61] and N,O-elongation combine in 3-(alkoxy)-4-methylthiazole-2(3*H*)thiones to a set of weak in intensity skeletal vibrations, spectroscopically located in the fingerprint-region.

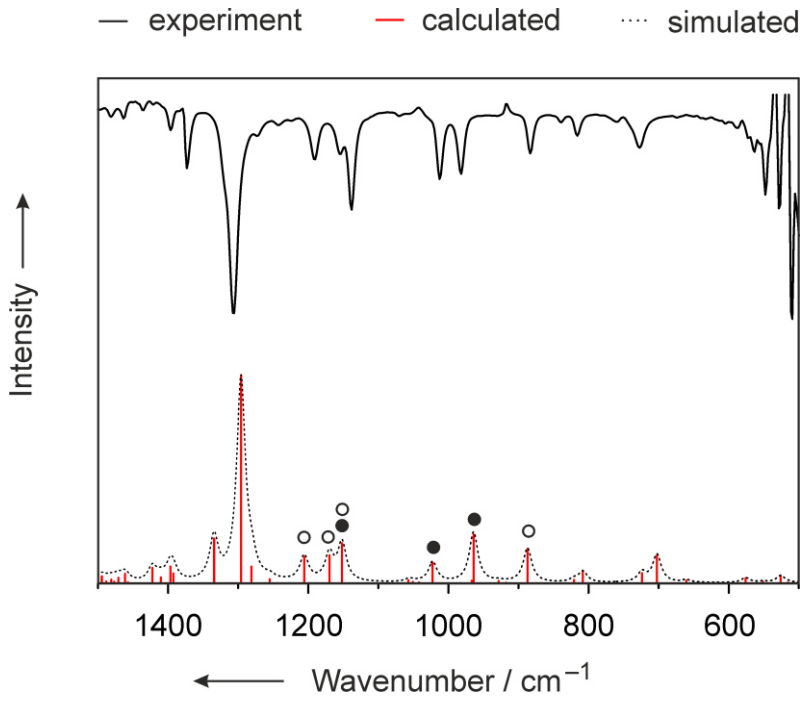

Figure 3 Experimental infrared spectrum of 3-(*tert*-butoxy)-4-methylthiazolethione **2b** (top; 20 °C in CH_3CN) and computed harmonic frequencies for the equilibrium structure of **2b** (bottom; ● = contribution from C=S-stretching vibration; ○ contribution from N,O-stretching vibration; experimental = FTIR in acetonitrile, 75µm pathlength, 28 mM solution of **2b**; calculated = DFT-D3/B3LYP/TZVP, scaling factor 0.99; simulated = Lorentzian functions with a full width at half maximum of 15 cm^{-1}; for minimum structure of compound **2b** used in vibrational analysis, see Figure 6).

(viii) *Crystallography*. *p*-Nitrophenyl-substituted *tert*-butyl ester **3b** (MNPTTO*t*Bu) crystalizes from a solution of diethyl ether and pentane in monoclinic space group $P2_1/n$. The unit cell comprises four molecules of MNPTTO*t*Bu (**3b**), forming sulfur-sulfur [S1···S1' = 3.506(4) Å] and sulfur-hydrogen bonded (*P*/*P*)···(*M*/*M*)-atropisomers [S7···H',C' = 2.975(4) Å]. Stereogenic elements in ester **3b** are the N,O-bond,[62] and the C,C-bond connecting the thiazolethione nucleus to the twisted *p*-nitrophenyl group [±26.10(7)]° (Figure 4).

Bond angle N3,O8,C9 = 116.8(1) ° is larger than the standard bond angle at oxygen.[63] For primary, secondary, and tertiary *O*-alkyl derivatives of MAnTTOH (**1a**), the size of the N3,O8,C9-angle linearly correlates with the Taft-Dubois-steric substituent parameter, pointing to strain as major inductor for angle widening at O8.

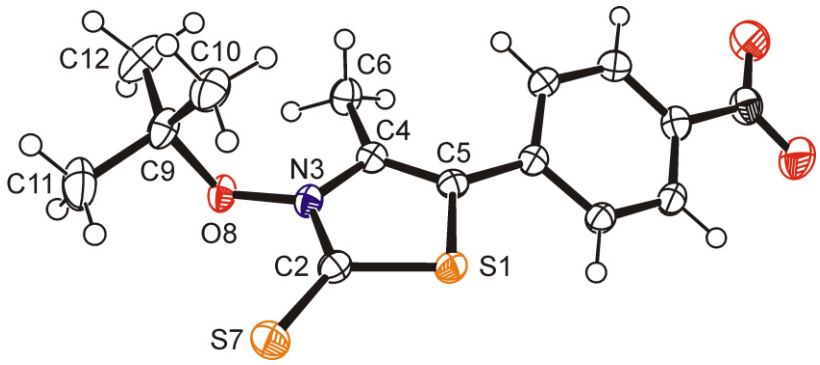

Figure 4 Ellipsoid graphic of 3-(*tert*-butoxy)-4-methyl-5-(4-nitrophenyl)thiazole-2(3*H*)thione (**3b**) in the solid state (50% probability level; 160 K; hydrogen atoms are drawn as circles of an arbitrary radius; oxygen is depicted in red, nitrogen in blue, and sulfur in orange).

Probably an electronic and not a steric effect is responsible for dispersion of bond angles at *tert*-butyl carbon C9, which gradually decrease from synperiplanar arranged methyl carbon C10 [111.6(1) °] via anticline carbon C12 [105.8(1)°] to the second anticline carbon C11 [103.1(1)°]. Similar bond angle dispersion is known from structural peroxide chemistry, and explained by π-bonding between the σ(O,O)-bond and the σ^*(C,C)-orbital in antiperiplanar or anticline orientation. π-Bonding reduces the size of involved bond angles (Figure 5).[64,65]

Lengths of single and double bonds of the thiazole-2(3*H*)thione core converge, pointing to electron delocalization similar to bonding in heteroaromatics (Table 2, entry 12).[11,35]

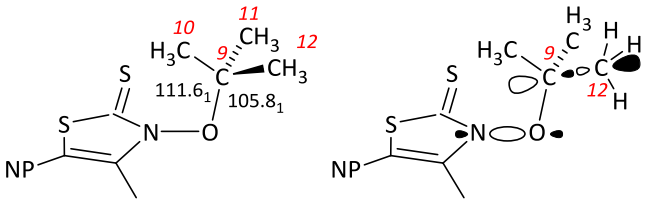

Figure 5 Molecular orbital model on angle dispersion in *tert*-butyl thiohydroxamate **3b** (for similar interaction with σ^*(C9,C11), refer to the text; O,C9,C11 = 103.1_1°; NP = 4-nitrophenyl; subscripts describe the confidence range of the final digit).

3 Formation and rearrangement of 1-(*tert*-butoxy)pyridine-2(1*H*)thione

(i) *Products of 1-hydroxypyridine-2(1H)thione-alkylation*. 1-Hydroxypyridine-2(1*H*)-thione (**4a**) provides 1-(*tert*-butoxy)pyridinethione **4b** in up 27% yield besides 15% *S*-(*tert*-butyl) thiohydroximate **9b**,[32,66] when treated with *O*-(*tert*-butyl)-*N*,*N*-diisopropyl isourea as specified in section 2 (Scheme 5).

In earlier studies, we had prepared *tert*-butyl ester **4b** from 2,2-dimethyl-2-bromopropane and 1-hydroxypyridine-2(1*H*)thione tetraethylammonium salt in a solution of dimethylformamide. Yields under such conditions never exceeded 1–4%.[32,66] When stored in a refrigerator the compound decomposed into yet unidentified pyridine derivatives.

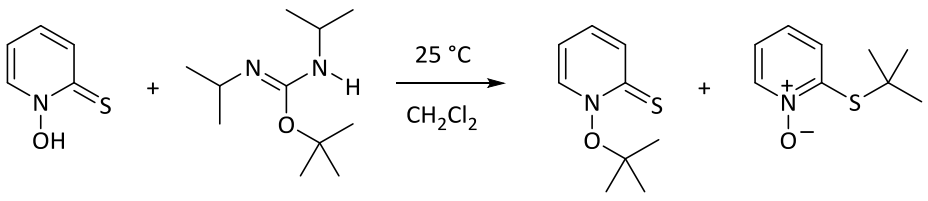

4a **5** **4b** (24-27%) [a] **9b** (15%) [b]

Scheme 5 Products of 1-hydroxypyridine-2(1*H*)thione-alkylation ([a] 2 experiments; [b] isolated from one representative experiment).

(ii) *The O-alkyl thiohydroxamate-O-alkyl sulfenate rearrangement*. A sample of 1-(*tert*-butoxy)pyridine-2(1*H*)thione (**4b**) purified by chromatography on silica gel furnished a yellow oil, displaying proton and carbon-13 NMR-chemical shifts a new compound. By comparing the data to references from our spectra library, we assigned molecular formula **10b** to the new product (Scheme 6).[67] On standing in a solution of deuterochloroform, *O*-(*tert*-butyl) sulfenate **10b** decomposes into yet unidentified pyridine derivatives.

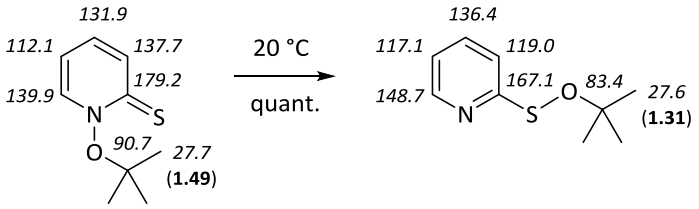

4b **10b**

Scheme 6 Rearrangement of 1-(*tert*-butoxy)pyridine-2(1*H*)thione (**4b**) [numbers in italics refer to carbon-13 NMR-shifts, figures in parenthesis to proton NMR-shifts ($CDCl_3$, 20 °C)].

(iii) *Synthesis of an O-alkyl pyridine-2-sulfenate as chemical reference*. The compound used as structural reference for characterizing rearranged product **10b** is *O*-pentyl pyridine-2-sulfenate **10c**, prepared in 51% yield from 1-(pentoxy)pyridine-2(1*H*)thione (**4c**) in photochemical reaction (Scheme 7 and the ESI). Sulfenate **10c** is a colorless oil, decomposing with moderate rate when contacted to silica gel during chromatography. Once pure, the compound is stable on storing in a refrigerator.

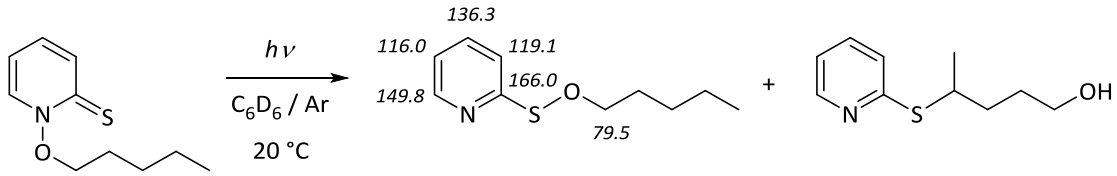

4c **10c** (51%) **11** (32%)

Scheme 7 Products from anaerobic photodecomposition of 1-(pentoxy)pyridine-2(1*H*)thione (**4c**) [numbers in italics refer to carbon-13 NMR-shifts ($CDCl_3$, 20 °C)].

4 Structure, bonding, and stability of heterocyclic *O*-alkyl thiohydroxamates

4.1 Objective, models and validation of the approach

(i) *Outline*. To understand electronic interplay between *N*-heterocyclic thiolactames and alkoxy substitution at nitrogen, we investigated structure and bonding of heterocyclic *O*-alkyl thiohydroxamates using electronic structure methods.[68] For separating steric from electronic effects, we complemented structure/energy-data from *tert*-butyl esters by data for methyl substitution.

Before computationally investigating compounds, we assessed methods for

reproducing solid state structural properties of 3-(alkoxy)thiazole-2(3*H*)thiones and 1-(alkoxy)pyridine-2(1*H*)thiones (section 4.1). The finest method served as default for investigating conformational characteristics of heterocyclic *O*-alkyl thiohydroxamates (section 4.2), stability of isomers occurring in synthesis (section 4.3), N,O-bonding (section 4.4), and the phenomenon of steric stabilization (section 4.5).

(ii) *Theory*. For theoretically analyzing points of interest, we selected a double ζ-basis set, abbreviated in the Gaussian03-systematic as 6-31+G**.[69–71] The 6-31G**-basis is parameterized for computing energy functions involving first, second, and third row atoms.[72,73] Polarization and diffuse functions[74] allow to treat with reasonable precision bonding between heteroatoms interacting by non-bonding electron pair effects, and bonding in cross-conjugated π-electron systems.[75]

All methods preselected for being combined with the 6-31+G**-basis cover electron correlation: Becke's 3 parameter Lee-Yang-Parr hybrid functional (B3LYP),[76,77] Becke's half and half Lee-Yang-Parr hybrid functional (BHandHLYP),[78] and second order Møller-Plesset-perturbation theory (MP2)[79–81]. For translating results from density functional theory to a more tutorial bonding model, we used natural bond orbital (NBO)-theory.[82,83]

(iii) *Quality of the approach*. B3LYP-theory in combination with the 6-31+G**-basis set reproduces structure of the thiohydroxamate group in 3-(*tert*-butoxy)-4-methylthiazole-2(3*H*)thione (**2b**) with deviation of 0.4% for the thiocarbonyl group, 0.4% for the nitrogen-oxygen bond, 1.3% for the nitrogen-carbon C2-bond, and 0.1% for the carbon-oxygen bond, when referenced toward the crystal structure of *O*-cumyl ester **2e** (Table 2, entries 1 and 11).[84] Bond angles at endocyclic nitrogen N3 and thiohydroxamate oxygen O8, and the dihedral angle along the N,O-bond, deviate no more than 1.4% from the experimental reference. Computed angles at *tert*-butyl carbon C9 gradually increase from 104.7 degrees for O8,C9,C11 via 105.2 degrees for O8,C9,C12 to 112.1 degrees for O8,C9,C10, reproducing the angle dispersion noted from the crystal structure of *tert*-butyl ester **3b** (Figures 4 and 5).

Table 2 Computed and experimental parameters of *O*-alkyl thiohydroxamates

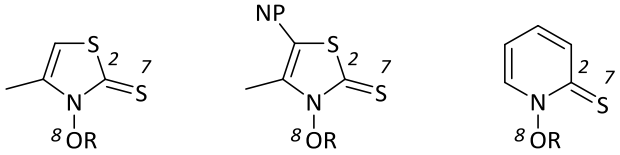

2 **3** **4**

entry	compd. / R	C2,S7 / Å	C2,N / Å	N,O8 / Å	O8,C / Å	C2,N,C / deg	N,O8,C / deg	C2,N,O,C / deg
1 [a]	**2b** / *t*Bu	1.660	1.380	1.375	1.512	117.6	118.1	91.3
2 [b]	**2b** / *t*Bu	1.651	1.360	1.355	1.483	117.3	118.5	91.3
3 [c]	**2b** / *t*Bu	1.648	1.379	1.378	1.501	118.0	115.4	93.2
4 [a]	**2d** / CH_3	1.659	1.375	1.380	1.447	118.8	111.7	83.4
5 [a]	**3b** / *t*Bu	1.656	1.381	1.373	1.515	118.0	118.0	92.2
6 [b]	**3b** / *t*Bu	1.647	1.361	1.354	1.485	117.8	118.4	92.2
7 [a]	**4b** / *t*Bu	1.678	1.401	1.380	1.502	124.7	117.2	99.9
8 [b]	**4b** / *t*Bu	1.667	1.378	1.359	1.475	124.8	117.5	99.7
9 [c]	**4b** / *t*Bu	1.661	1.397	1.381	1.493	125.9	114.3	98.9
10 [a]	**4d** / CH_3	1.678	1.398	1.387	1.446	125.6	111.7	83.9
11 [d,e]	**2e** / Cumyl	1.654_2	1.363_3	1.370_2	1.511_3	116.9_2	116.4_2	95.6_2
12 [e,f]	**3b** / *t*Bu	1.656_2	1.363_2	1.378_2	1.521_2	117.9_1	116.8_1	93.7_2
13 [e,g]	**4f** / Cx*	1.666_4	1.377_5	1.384_4	1.482_7	125.3_3	112.4_2	99.9_3

[a] B3LYP/6-31+G**. [b] BHandHLYP/6-31+G**. [c] MP2/6-31+G**. [d] X-ray diffraction at 293 K. [e] Subscripts refer to the confidence range of the final digit. X-ray diffraction at 160 K. [f] X-ray diffraction at 297 K; Cx* = *trans*-(1-*tert*-butyl)cyclohex-4-yl.

BHandHLYP-theory underestimates the length of the thiocarbonyl group, the N,O-distance, and the length between *tert*-butyl carbon C9 and thiohydroxamate oxygen O8. The method, however treats the thiohydroxamate C,N-bond more precisely than the B3LYP-density functional and MP2-theory (Table 2, entries 2, 6, and 8). Møller-Plesset-theory predicts a shorter distance between thiocarbonyl carbon and sulfur, a shorter bond between thiohydroxamate oxygen O8 and ester carbon C9, and a smaller bond angle at O8 (Table 2, entries 3 and 9).

From the quality of computed data, we chose B3LYP-theory as standard for

computing structure and bonding of *O*-alkyl thiohydroxamates. Our decision was guided by the ability of B3LYP-theory to reproduce the combination of N,O- and C=S-bond lengths. The lengths of the two bonds are interrelated by a mechanism explaining most questions raised with the study. For cross-checking thermochemical data we applied MP2-theory.

4.2 Heterocyclic *O*-alkyl thiohydroxamates

(i) *Conformation along the N,O-bond – the thiohydroxamate dihedral angle* ω. In the computed minimum conformer of MTTO*t*Bu (**2b**), the *tert*-butyl substituent is offset by 91.3 degrees from the thiazolethione plane (Figure 6, Table 2, entry 1). Substituting methyl for *tert*-butyl reduces thiohydroxamate dihedral angle ω = C2,N,O,C by 8 degrees. Replacing 4-methyl-2-thiooxo-(3*H*)thiaz-3-yl by 2-thiooxo-(1*H*)pyrid-1-yl increases ω by 9 degrees for *O*-methyl- and for *O*-(*tert*-butyl) substitution. From this information we concluded that the preferred value of ω is 90 degrees, allowing ±10 degrees variation for responding to steric demand of the *O*-alkyl substituent and structural peculiarities of the heterocyclic core.

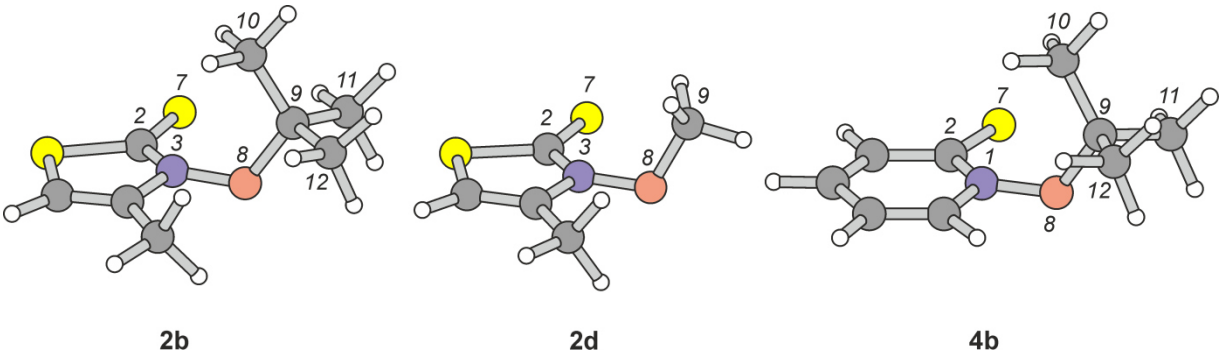

2b **2d** **4b**

Figure 6 Representative minimum conformers of heterocyclic *O*-alkyl thiohydroxamates (sulfur is depicted in yellow, oxygen in red, nitrogen in blue, carbon in gray, and hydrogen in white; B3LYP/6-31+G**).

(ii) *Barrier to N,O-rotation*. Rotations about N,O-bonds in thiazole- and pyridine-derived thiohydroxamates occur in secondary and tertiary alkyl esters sufficiently slow, for being investigated by dynamic NMR-spectroscopy.[11,35,85,86] Simulating the process is feasible by a sequence of conformers differing in dihedral angle ω, for covering a conformational space of 360 degrees. Given a plane of symmetry, rotating by180 degrees provides a complete conformational analysis for rotation about the N,O-bond in thiazole- and pyridine-derived *O*-alkyl thiohydroxamates (Figure 7).

Displacing the *tert*-butyl substituent in ester **2b** from the equilibrium dihedral angle of 91.3 degrees by enlarging or reducing ω, raises conformational energy until maxima are reached, showing synperiplanar orientation of carbons C9 and C2 (ω = 0 °) or antiperiplanar (ω = 180 °) (Figure 7). Assuming that likewise modelled high in energy conformers are maxima on the potential energy surface, Gibbs free energies differences between an equilibrium structure and planar a conformation translate into barriers to N,O-rotation (Table 3).

The modelled potential energy curve for N,O-rotation in *tert*-butyl ester **2b** is dissymmetric, showing a barrier of 49.7 kJ mol^{-1} for torsional movement past the thione sulfur and 89.7 for the movement past the 4-methyl substituent (Figure 7). The dihedral angle/energy-profile for methyl ester **2d** is similar. Lower barriers correlate with smaller steric congestion at oxygen in *O*-methyl ester **2d** (Table 3, entries 1–2).

The experimental barrier to N,O-rotation in *O*-isopropyl thiohydroxamate **2f**, measured in a solution of dimethyl ether at a temperature of 200 Kelvin, is 42±7 kJ mol^{-1}.[85] Extrapolating this value by the Gibbs-Helmholtz-equation furnishes a $\Delta\Delta G^{\ddagger}$ of 46±9 kJ mol^{-1} for a temperature of 298.15 Kelvin. By comparing experimental to modelled activation parameters, we concluded that the experimental barrier refers to the torsional movement of the *O*-isopropyl group past thione sulfur.

Modelling potential energy curves for rotating the *O*-(*tert*-butyl) group or the *O*-methyl group past hydrogen or past thione sulfur in pyridine-2(1*H*)thiones **4b** and **4d**, furnishes again dissymmetric dihedral angle/energy-curves (Figure 7). This time the barrier for shifting the alkyl substituent past thione sulfur is higher (63.5 kJ mol^{-1}), than topomerizing a carbon substituent past hydrogen from the C6,H-bond (44.4 kJ mol^{-1}).

The extrapolated barrier $\Delta\Delta G^{\ddagger}$ to N,O-rotation in 1-(isopropoxy)pyridine-2(1*H*)thione (**4f**) is 36±2 kJ mol^{-1}, which is in between the barrier modelled for torsional movements of a *tert*-butyl (**4b**) and a methyl group (**4d**) past the C6,H-bond.[85]

The steric effect exerted by thione sulfur in the pyridinethiones is more pronounced than in thiazolethiones, due to smaller exocyclic bond angle N,C2,S7, for example, of 123.7 in **4b** (128.9 ° in **2b**). Downsizing the substituent at thiohydroxamate oxygen from *tert*-butyl to methyl lowers barriers, supporting the hypothesis that steric effects contribute to conformational energy of N,O-rotamers (Table 3, entries 4–5).

To sum up, lowest in energy conformers of thiazole- and pyridine-derived *O*-alkyl thiohydroxamates show orthogonal alignment between heterocyclic plane and substituent at oxygen.

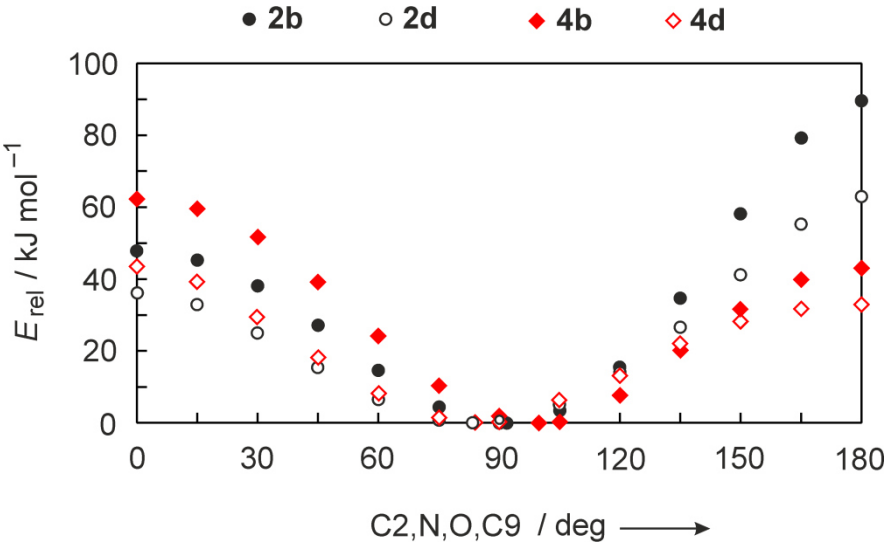

Figure 7 Energy changes for rotating *tert*-butyl and methyl groups about N,O bonds in heterocyclic *O*-alkyl thiohydroxamates (B3LYP/6-31+G**).

Table 3 Barriers to rotation about N,O-bonds in heterocyclic *O*-alkyl thiohydroxamates

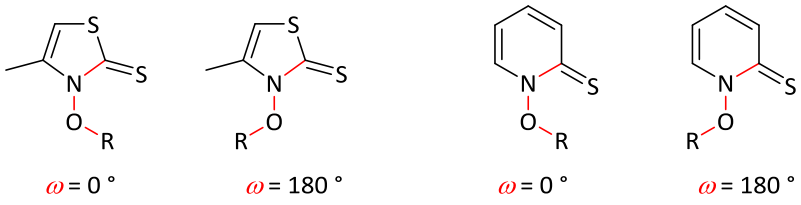

2 **4**

entry	compd. / R	$\Delta G(298.15)^{0\,\circ}$ / kJ mol^{-1} [a,b]	$\Delta G(298.15)^{180\,\circ}$ / kJ mol^{-1} [b,c]	$\Delta G(298.15)^{exp}$ / kJ mol^{-1} [d]
1	**2b** / *t*Bu	49.7	89.7	– [e]
2	**2d** / CH_3	38.5	65.3	– [e]
3	**2f** / *i*Pr	– [e]	– [e]	46±9
4	**4b** / *t*Bu	63.5	44.4	– [e]
5	**4d** / CH_3	44.4	35.1	– [e]
6	**4f** / *i*Pr	– [e]	– [e]	36±2 [d]

[a] $\Delta G(298.15)^{0\,\circ} = G(298.15)^{0\,\circ} - G(298.15)^{min}$; *min* is short for global minimum; $G(298.15)^{0\,\circ}$ refers to ω = 0 °. [b] B3LYP/6-31+G**// B3LYP/6-31+G**. [c] $\Delta G(298.15)^{180\,\circ} = G(298.15)^{180\,\circ} -$

G(298.15)^{min}; *G*(298.15)$^{180\ °}$ refers to ω = 180 °. [d] Extrapolated from DNMR studies in $(CD_3)_2O$.[85]

4.3 *O*-Alkyl thiohydroxamate isomers

(i) *Significance and design of the study*. To understand how heterocyclic groups effect stability of *O*-alkyl thiohydroxamates, we modelled heats of formation of isomers, coexisting in solution or in neat compounds, when being stored.[87–89] Product classes considered in this part of the project are *O*-alkyl thiohydroxamates, *S*-alkyl thiohydroximates and *O*-alkyl sulfenates. Minimum structures for the latter two product classes were obtained from potential energy scans of dihedral angles on the B3LYP-level of theory. For validating computed thermochemical data, we additionally minimized all energy functions in MP2-theory.

(ii) *S-alkyl thiohydroximates*. Minimum structures of thiazole-derived *S*-alkyl thiohydroximates **7b**/**7d** show a vertical displacement of the carbon substituent from the heterocyclic plane, declining from 67.2 degrees for the N3,C2,S7,C9-angle in case of *tert*-butyl-substitution (for **7b**) to 58.2 degrees for methyl derivative **7d**. Energy-minimized structures of 2-(alkylsulfanyl)pyridine 1-oxides show gauche conformation for atoms N1,C2,S7,C9 in case of *tert*-butyl substitution at sulfur (63.3 ° in **9b**), and antiperiplanar for methyl substitution (Figure 8).

The antiperiplanar conformation is the only structural motif encountered so far in crystal structures of 2-alkylsulfanyl-1,3-thiazole 3-oxides and -pyridine 1-oxides.[15,87,90,91]

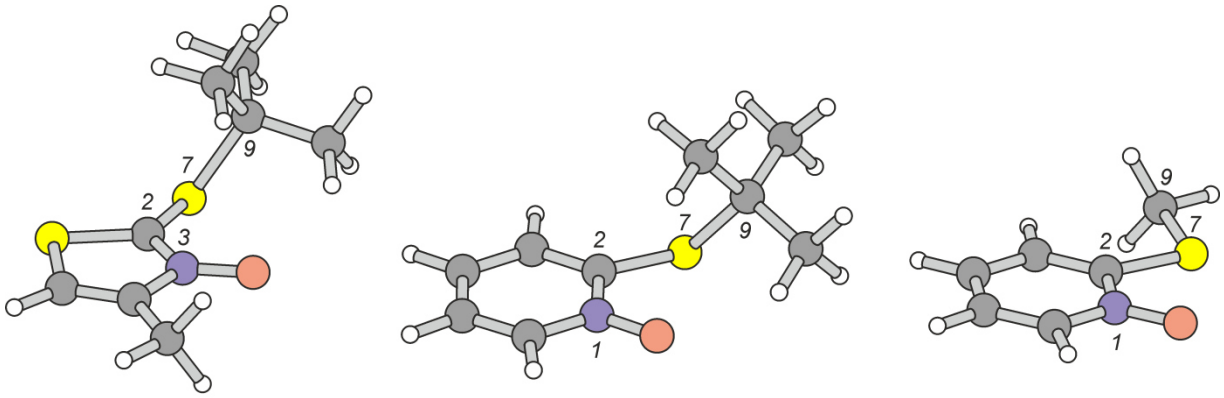

7b **9b** **9d**

Figure 8 Minimum structures of selected *S*-alkyl thiohydroximates (sulfur is depicted in yellow, oxygen in red, nitrogen in blue, carbon in gray, and hydrogen in white; B3LYP/6-31+G**).

(iii) *O-Alkyl sulfenates*. Minimum structures of *O*-alkyl sulfenates **10** and **12** show rooftop-conformations, as evident from dihedral angles along the sulfur-oxygen bond of 108±1 degrees for *tert*-butyl derivatives **10b** and **12b**, and 89±2 degrees for *O*-methyl derivatives **10d** and **12d** (Figure 9).[64] Sulfur-oxygen bond lengths predicted by theory are 1.688 Ångstrøms for pyridines **10b** and **10d**, and 1.684 Ångstrøms for thiazole-derived *O*-esters **12b** and **12d**.

A reference from crystallography, *O*-[*trans*-(4-*tert*-butyl)cyclohexyl]-2,4-dinitrophenylsulfenate, shows 2.7% shorter sulfur-oxygen bond [1.642(1) Å], but a similar value for the C,O,S,C-dihedral angle [92.0(1) °], agreeing, in summary, reasonably with the computed data, for example, for thiazole-derived sulfenates **12b/d**.[92]

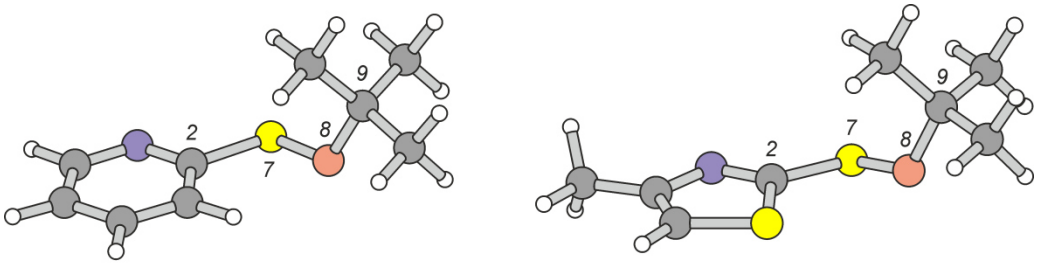

10b **12b**

Figure 9 Minimum conformers of heterocyclic *O*-(*tert*-butyl) sulfenates (sulfur is depicted in yellow, oxygen in red, nitrogen in blue, carbon in gray, and hydrogen in white; B3LYP/6-31+G**).

(iv) *Stability of isomers*. According to theory, *O*-alkyl sulfenates **10** and **12** are the

most stable of the *O*-alkyl thiohydroxamate isomers, regardless of the underlying heterocycle and the steric size of the carbon substituent. In Møller-Plesset-theory, predicted driving forces are slightly but systematically more pronounced than in density functional theory. Second in stability are *S*-alkyl thiohydroximates **7** and **9**, except of *S*-(*tert*-butyl) thiohydroximate **7b**, which is in both theories thermochemically less stable than *O*-(*tert*-butyl) thiohydroxamate **2b** (Tables 4 and 5).

The only isomerization described experimentally for 3-(alkoxy)thiazole-2(3*H*)thiones is a methyl shift from oxygen to sulfur. The reaction seems to be restricted to the solid state and requires about four years for attaining a 84/16-ratio of rearranged/non-rearranged isomers.[87]

Primary and secondary 1-(benzyloxy)pyridine-2(1*H*)thiones quantitatively isomerize within hours into 2-(*S*-benzylsulfanyl)pyridine 1-oxides.[88,90] Tertiary 1-alkoxypyridine-2(1*H*)thione **4b** quantitatively isomerizes into sulfenate **10b**. The origin of the specificity for selecting one or the other pathway is not evident from our data. By looking at the chemistry of 1-(alkoxy)-2(1*H*)pyridones and 1-(acyloxy)pyridine-2(1*H*)-thiones we suggest that rearrangement **4** → **9** occurs via substitution,[93] and rearrangement **4** → **10** by a frontier molecular orbital-controlled sigmatropic shift.[94]

1-(Methoxy)pyridine-2(1*H*)thione **4d** escaped for years synthesis and characterization.[45] We finally separated trace-amounts of a yellow oil, showing UV/Vis-absorptions of the pyridine-2(1*H*)thione-chromophore, and proton- and carbon-13 NMR-resonances proving the existence of *O*-methyl thiohydroxamate **4d**.[66] Within hours of standing in an amber-colored flask, in the dark, and in a refrigerator, the material decomposed into a complex mixture of yet unidentified pyridines. On the basis of information from the present study we believe that the compound rearranges into *O*-methyl sulfenate **10d** for undergoing secondary transformations.

Modelled thermochemical data, in summary, pose a useful guideline for organizing experimentally observed chemical differences between pyridine- and 1,3-thiazole-derived heterocyclic *O*-alkyl thiohydroxamates.

Table 4 Computed energies of thiazole-derived *O*-alkyl thiohydroxamates and isomers

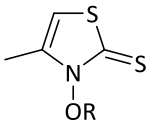

2

$E \equiv 0.0$ kJ mol^{-1}

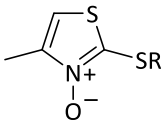

7

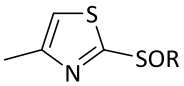

12

entry	theory [a]	**2** / R	E_{rel} / kJ mol^{-1} [b]	
			7	**12**
1	B3LYP	**2b** / *t*Bu	**7b**: 14.3	**12b**: –90.0
2	MP2	**2b** / *t*Bu	**7b**: 5.0	**12b**: –105.3
3	B3LYP	**2d** / CH_3	**7d**: –0.2	**12d**: –74.5
4	MP2	**2d** / CH_3	**7d**: –20.0	**12d**: –100.0

[a] In combination with the 6-31+G**-basis set. [b] E_{rel} = relative energy (zero-point vibrational energy-corrected) at a temperature of 0 Kelvin, referenced versus *O*-alkyl thiohydroxamates **2b** (entries 1 and 2) or **2d** (entries 3 and 4).

Table 5 Computed energies of pyridine-derived *O*-alkyl thiohydroxamates and isomers

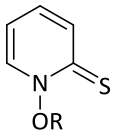

4

$E \equiv 0.0$ kJ mol^{-1}

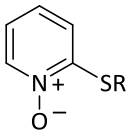

9

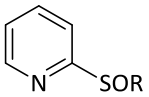

10

entry	theory [a]	**4** / R	E_{rel} / kJ mol^{-1} [b]	
			9	**10**
1	B3LYP	**4b** / *t*Bu	**9b**: –5.2	**10b**: –105.9
2	MP2	**4b** / *t*Bu	**9b**: –21.2	**10b**: –117.2
3	B3LYP	**4d** / CH_3	**9d**: –30.6	**10d**: –94.4
4	MP2	**4d** / CH_3	**9d**: –40.4	**10d**: –112.0

[a] In combination with the 6-31+G**-basis set. [b] E_{rel} = relative energy (zero-point vibrational energy-corrected) at a temperature of 0 Kelvin, referenced versus *O*-alkyl thiohydroxamates **4b** (entries 1 and 2) or **4d** (entries 3 and 4).

4.4 π-Bonding between nitrogen and oxygen

(i) *Bond order (BO)-analysis*. Bond orders are guidelines for rating bond strengths between a set of atoms.[95,96] Correlating experimental N,O-distances to bond orders from hydroxylamine ($BO_{N,O}$ = 1),[97] the triplet-nitrosyl anion (2), nitrogen monoxide (2.5), and the nitrosyl cation (3)[98,99] provides a linear relationship [$d_{N,O}^{exp}$ = 1.6490 – 0.1966 × $BO_{N,O}$ (correlation coefficient *R*2 = 0.9996). A distance/bond order correlation for the same molecules, supplemented by N,O-distances from *O*-(*tert*-butyl) hydroxylamine ($BO_{N,O}$ = 1) and 2-nitroso-2-methylpropane (2) furnishes nearly identical gradient and intercept for a linear correlation [$d_{N,O}^{calc}$ = 1.6316 – 0.1897 × $BO_{N,O}$ (*R*2 = 0.9900); B3LYP/6-31+G**; ESI]. A third approach using harmonic force constants from vibrational spectroscopy for characterizing N,O-bond strengths[95,100,101] was not further pursued, once the degree of vibrational coupling in heterocyclic *O*-(*tert*-butyl) thiohydroxamates became apparent (cf. section 2).

The N,O-distance of 1.378 Ångstrøms, determined by X-ray diffraction for *O*-(*tert*-butyl) thiohydroxamate **3b**, translates by the experimental correlation into a bond order of 1.38 (Table 6, entry 3). Theoretical bond order analysis provides value of 1.36. Computed N,O-distances of *O*-alkyl thiohydroxamates **2** and **4** correlates to bond orders of 1.35 for 3-(*tert*-butoxy)thiazolethione **2b**, 1.33 for methyl ester **2d** and *tert*-butyl ester **4b**, and 1.29 for (methoxy)pyridinethione **4d** (Table 6, entries 1–2 and 4–5).

Table 6 N,O-Bond orders in heterocyclic *O*-alkyl thiohydroxamates

entry	compd / R	$d_{N,O}$ / Å [a]	$BO_{N,O}$ [b]
1	**2b** / *t*Bu	1.3754	1.35
2	**2d** / CH_3	1.3803	1.32
3	**3b** / *t*Bu	1.3734 (1.378) [c]	1.36 (1.38) [d]
4	**4b** / *t*Bu	1.3800	1.33
5	**4d** / CH_3	1.3871	1.29

[a] Calculated (B3LYP/6-31+G**). [b] Form $d_{N,O}^{calc}$ = 1.6316 – 0.1897 × $BO_{N,O}$ (refer to the text). [c] Figure in parentheses refers to the experimental value (X-ray diffraction, 160 K). [d] From $d_{N,O}^{exp}$ = 1.6490 – 0.1966 × $BO_{N,O}$ (refer to the text).

Bond order analysis for heterocyclic *O*-alkyl thiohydroxamates, in summary, points to partial double bonding between nitrogen and oxygen, becoming more significant as the steric size of the ester substituent increases, and being stronger in thiazole-derived thiohydroxamates than in pyridine derivatives.

(ii) *Molecular orbital model*. According to natural bond orbital (NBO)-theory,[82] bonding between nitrogen and oxygen in heterocyclic *O*-alkyl thiohydroxamates occurs by superimposing three π(N,O)-bonds of different strength, to a σ(N,O)-bond formed from the two heteroatoms with similar molecular orbital coefficients (Figure 10; ESI).

The first π-bond [π^1(N,O)] results from overlapping non-bonding electron pairs at oxygen and σ^*(N,C)-orbitals from the heterocyclic core (Figure 10). In NBO-theory, the two non-bonding electron pairs at thiohydroxamate oxygen differ in hybridization, similar to ether oxygens.[102] One non-bonding electron pair shows 99.9% *p*-character, the second is *sp*-hybridized. In the minimum conformation, overlapping between the *p*-type orbital and the σ^*(N,C)-orbitals is for stereoelectronic reason at maximum, contributing stronger to the π^1(N,O)-bond, than the second interaction using the *sp*-hybridized non-bonding electron pair as donor.

The second π-bond, π^2(N,O), forms between the non-bonding electron pair at nitrogen and the σ^*(O,C9)-orbital. NBO-theory predicts 99.9% *p*-character for the non-bonding electron pair at nitrogen, being incorporated into a planar heterocyclic core, and interacting with adjacent π-systems, particularly the thiocarbonyl group.

σ-Electrons from the heterocyclic core and the *O*-alkyl group overlap with the σ^*(N,O)-orbital, to form a third π-bond, π^3(N,O). Populating the σ^*(N,O)-orbital counterbalances to some extend bond order-increasing contributions from π^1(N,O)- and π^2(N,O)-bonding.

By relative bond energy, the π^1(N,O)-bond in thiazolethiones **2b** and **2d** (55±2 kJ mol^{-1}) is stronger than in pyridinethiones **4b** and **4d** (45±3 kJ mol^{-1}). The strength of the π^2(N,O)-bond depends on alkyl substitution at ester oxygen, gradually rising from methyl esters **2d** and **4d** (11 kJ mol^{-1}) via *tert*-butyl ester **4d** (17 kJ mol^{-1}) to 3-(*tert*-butoxy)thiazolethione **2d** (76 kJ mol^{-1}). Strength of π^3(N,O)-bonding, again, depends on the nature of the heterocyclic core and is higher for thiazolethiones **2b** and **2d** (70±1 kJ mol^{-1}) than for pyridinethiones **4b** and **4d** (54±1 kJ mol^{-1}) (ESI).

Molecular orbital theory, in summary, relates higher N,O-bond orders in thiazole-derived *O*-alkyl thiohydroxamates to stronger π(N,O)-bonds.

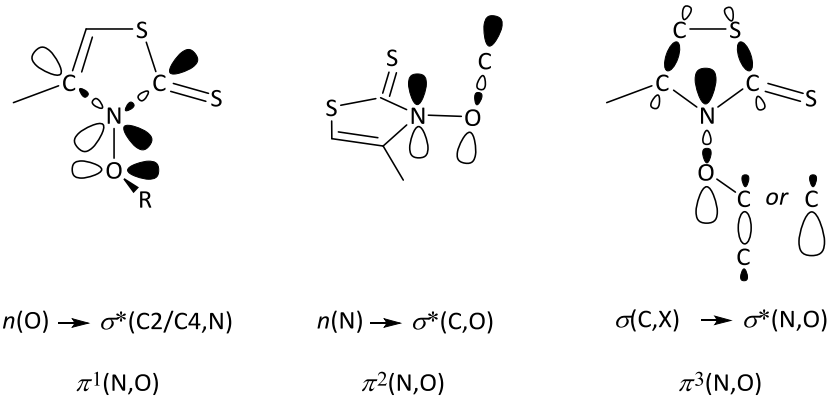

Figure 10 Molecular orbital model for π-bonding between nitrogen and oxygen in thiazole-derived *O*-alkyl thiohydroxamates (NBO-analysis; X = C or H; ESI).

(iii) *Dihedral angle dependency of π(N,O)-bond strength*. Bond strengths of π^1(N,O)- and π^2(N,O)-bonds depend on the size of dihedral angle ω. Strength of the bond π^3(N,O) is nearly independent from ω. Energies of bonds π^1(N,O) and π^2(N,O) reach maxima at ω = 90 degrees, and minima for 0 and 180 degrees. Increasing or decreasing ω, starting from 90-degrees, reduces π(N,O)-bond strengths and causes the distance between nitrogen and oxygen to increase. The distance between carbon C2 and sulfur S7 from the thiocarbonyl group shortens upon rotating the alkyl group toward methyl in **2** and hydrogen in **4**, and lengthens for alkyl group rotation toward thione sulfur. Bond distances between nitrogen and carbon C2 follow this trend, however, with opposite sign (Figure 11).

In crystal structures, the *O*-alkyl substituent is offset by 90±10 degrees from the thiohydroxamate plane.[35,87] Orthogonal arrangement takes profit from maximum π(N,O)-bond energy. From this information we concluded that a fraction of the barrier to N,O-rotation is stereoelectronic in orgin. The remaining fraction should be steric of origin, since energies of non-bonding electron pairs at nitrogen and oxygen vary insignificantly upon N,O-rotation, and not with the systematic expected for a conformational effect of Coulomb repulsion.[103–105] We therefore concluded that non-bonding electron pair repulsion plays a secondary role, if any, for explaining barriers to N,O-rotation in heterocyclic *O*-alkyl thiohydroxamates (ESI).[85]

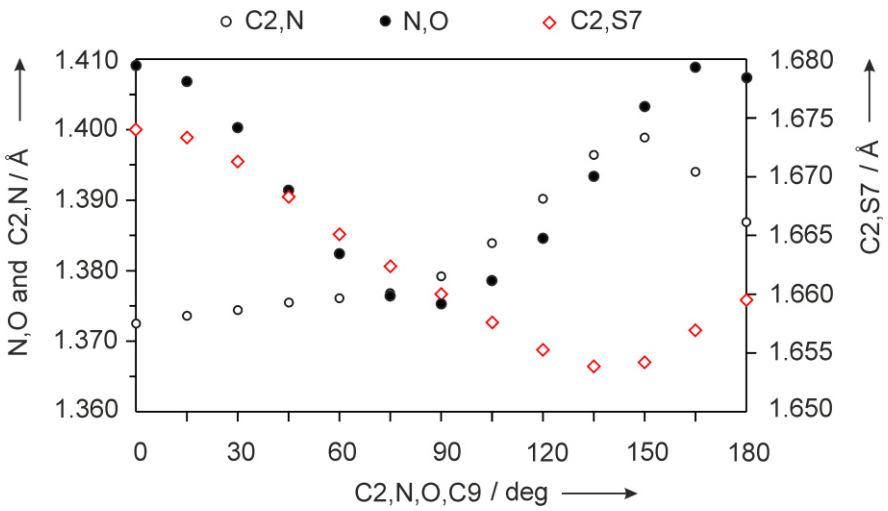

Figure 11 Dihedral angle dependency of thiohydroxamate bond lengths, exemplified by torsional movement of the *tert*-butyl group in 3-(*tert*-butoxy)thiazolethione **2b** (for indexing of atom positions, see Figure 6).

4.5 Responses to thiohydroxamate bond angle variation

(i) *Response from steric encroachment*. The size of bond angle N,O,C9 experimentally correlates with steric encroachment exerted by alkyl substitution at thiohydroxamate oxygen.[35] Density functional theory reproduces this trend, predicting 6.4 degrees larger N,O,C9-angle by substituting *tert*-butyl for methyl in 3-(alkoxy)-4-methylthiazole-2(3*H*)thiones (Table 2, entries 1 and 4) and 5.5 degrees for the same substitution in 1-(alkoxy)pyridine-2(1*H*)thiones (Table 2, entries 7 and 10).

(ii) *Response from hybridization at oxygen*. Increasing the N,O,C9-angle size from 90 to 130 degrees changes hybridization at oxygen. NBO-theory predicts the *p*-character of the more stabilized non-bonding electron pair to increase by this variation, beginning at 32% for a N,O,C9-bond angle of 90 degrees, via 48% for the equilibrium structure (118.1 °) to 55% for 130 degrees (values for **2b**; for data of **2c**, **4b**, and **2d**, refer to the ESI). The second non-bonding electron pair at oxygen retains full *p*-character. The percentage of *p*-character of non-bonding electron pairs at oxygen correlates with orbital energy, and the ability to donate electrons in π(N,O)-interactions. Stronger π(N,O)-bonds show up in shorter N,O-bonds (Figures 12 and 13). Steric congestion at thiohydroxamate oxygen, in summary, strengthens the N,O-bond.

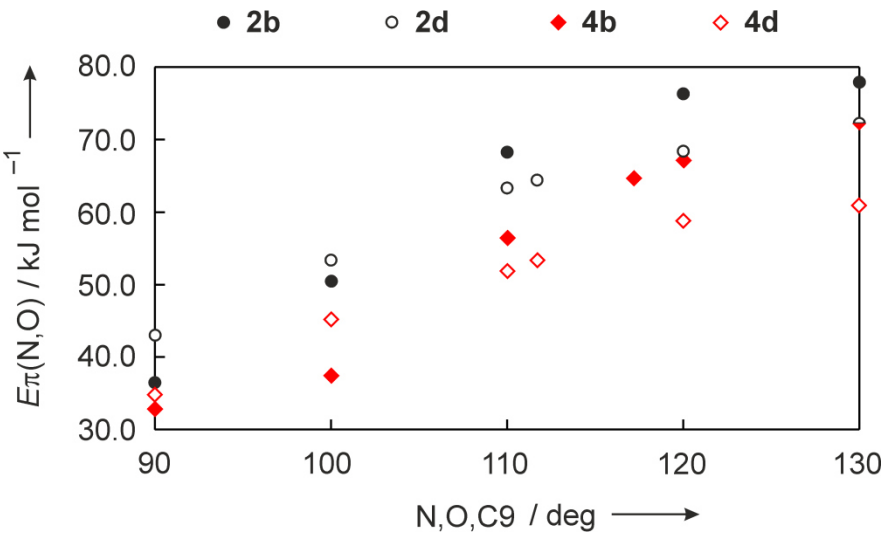

Figure 12 Bond angle dependency of π(N,O)-bond energy in heterocyclic *O*-alkyl thiohydroxamates [$E\pi$(N,O) = $E\pi^1$(N,O) + $E\pi^2$(N,O) + $E\pi^3$(N,O); cf. Figure 10]

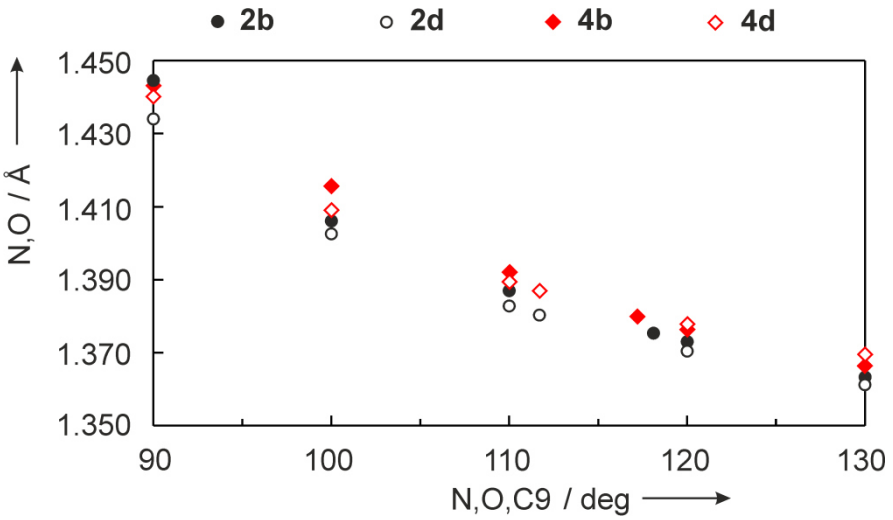

Figure 13 Correlation between thiohydroxamate bond angle N,O,C9 and N,O-bond lengths in heterocyclic *O*-alkyl thiohydroxamates.

(iii) *Response from the carbon-sulfur double bond*. π^1(N,O)-bonding transfers electron density from oxygen to nitrogen. Nitrogen is the donor for the π^2(N,O)-bond, but also for a stabilizing interaction with the π^*(C2,S7)-orbital from the thiocarbonyl group. The response to widening the N,O,C9-angle from the thiocarbonyl group is lengthening of the C2,S7-distance in combination with shortening of the N,O-bond (Figure 14).

(iv) *Response from crystallography*. Inverse N,O/C=S-correlations were discovered by crystallographers, stating that thiazole-derived *O*-alkyl thiohydroxamates respond to steric encroachment at oxygen by shortening and thus strengthening the N,O-bond. Lengthening

of C=S bonds was proposed to energetically counterbalance N,O-bond strengthening. From a smaller gradient of the N,O/C=S-correlation in the pyridine-2(1*H*)thione series, crystallographers concluded that this type of heterocycle is not similarly able to cope with steric congestion at thiohydroxamte oxygen.[35]

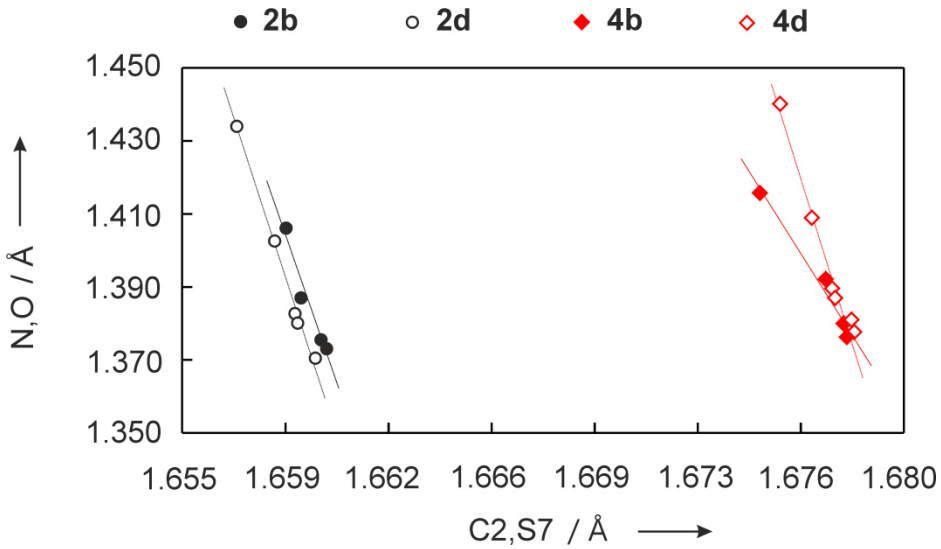

Figure 14 Correlation between nitrogen-oxygen and thiocarbonyl bond lengths in heterocyclic *O*-alkyl thiohydroxamates

5. *tert*-Butoxyl radicals from heterocyclic O-(*tert*-butyl) thiohydroxamates

5.1 Disconnecting ground state stabilizing effects

For liberating alkoxyl radicals from 3-(alkoxy)thiazole-2(3*H*)thiones, the ground state stabilizing mechanism has to be disconnected, for example, by changing the electronic state or chemically modifying the thiohydroxamate group. In this study, we used photoexcitation for liberating *tert*-butoxyl radicals, which were spin-trapped (section 5.2), or added to styrene (section 5.3).

5.2 Spin trapping of *tert*-butoxyl radicals

When photoexcited with 350 nm-light in solutions of benzene, *O*-*tert*-butyl thiohydroxamates **1b**–**3b** react with 5,5-dimethylpyrroline 1-oxide (DMPO) to provide nitroxyl radical **13**, as shown by a diagnostic electron spin resonance (ESR) at a *g*-factor of 2.009. The hyperfine structure of the resonance shows α-coupling from nitrogen-14, β- and γ-couplings from protons.[39,106,107] (Table 7 and Figure 15).

Table 7 ESR-spectroscopic data of pyrrolidine 1-oxyl radical **13** obtained from photoreactions between *O*-(*tert*-butyl) thiohydroxamates and DMPO

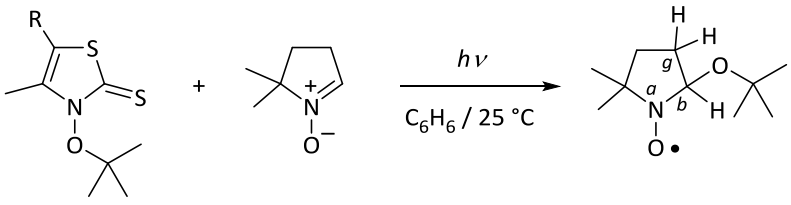

1b–3b *DMPO* **13**

entry	**1b–3b** / R		**13**		
		g	a_N / G	$a_{H(\beta)}$ / G	$a_{H(\gamma)}$ / G
1	**1b** / *p*-$C_6H_4(OCH_3)$	2.009	13.15	7.94	–[b]
2	**2b** / H	2.009	13.17	7.96	1.93
3	**3b** / *p*-$C_6H_4(NO_2)$	2.009	13.17	7.94	1.90

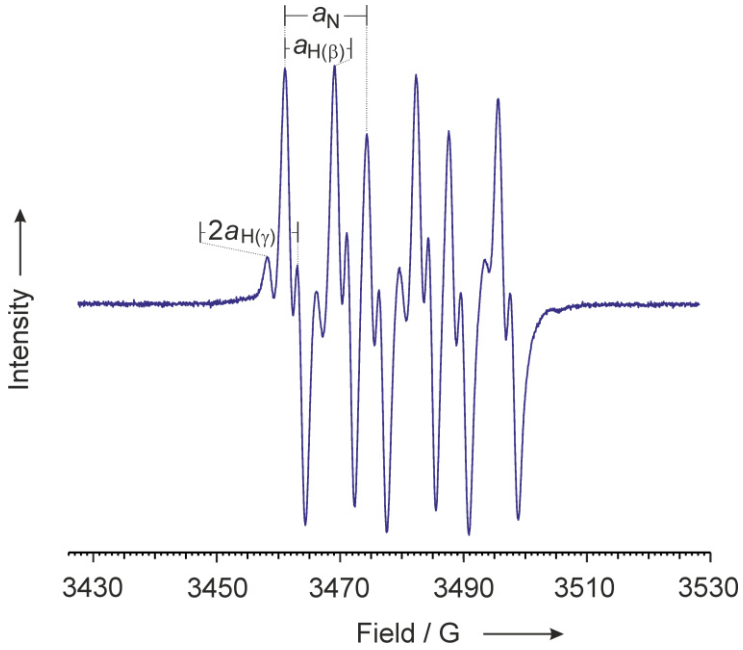

Figure 15 ESR-spectrum of nitroxyl radical **13**, obtained from photoreaction of MNPTTO*t*Bu (**3b**) and DMPO in a solution of benzene at room temperature.

5.3 Trapping of *tert*-butoxyl radicals by intermolecular addition

Photolyzing a solution of 3-(*tert*-butoxy)thiazolethione **2b** in benzene, being 2.76 molar in styrene and 0.13 molar in bromotrichloromethane, furnishes 2-bromo-2-phenyl-1-(*tert*-butoxy)ethane (**14**) in 26% yield (Scheme 8).

A proton NMR-spectrum of bromohydrin ether **14** recorded in deuterochloroform displays a diagnostic singlet at 1.17 ppm for the three magnetically equivalent methyl groups of the *tert*-butyl group. Diastereotopic protons at carbon C1 furnish baseline separated signals at 3.81 and 3.91 ppm, being split by hyperfine couplings into doublet of doublets.

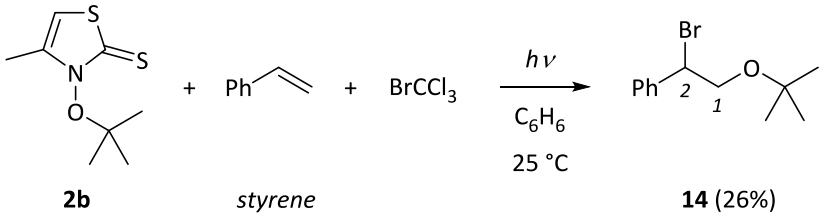

2b *styrene* **14** (26%)

Scheme 8 Multicomponent reaction for synthesis of 2-bromohydrin ether **14**.

Bromohydrin ether **14** forms by adding *tert*-butoxyl radical **Ib** to the terminal alkene carbon of styrene, which is the position bearing in the highest occupied molecular orbital and the lowest unoccupied molecular orbital the largest molecular orbital coefficient (Scheme 9).[12,108,109] Trapping of adduct **III** by bromotrichloromethane furnishes bromohydrin ether **14** in yields comparing to the *tert*-butoxyl radical addition product to norbornene.[110] The trichloromethyl radical, which is left from homolytic displacement at bromotrichloromethane, has three major options for stabilizing secondary reactions. The first option is to add to the thiocarbonyl sulfur of 3-(*tert*-butoxy)thiazole-2(3*H*)thione **2b**, yielding 2-(trichloromethylsulfanyl)thiazole **15**. The second option is to add to the alkenyl group of styrene, giving rise to 3,3,3-trichloro-1-bromo-1-phenylpropane (**16**).[111] The third option is to combine with a second of its kind to give hexachloroethane (**17**). Hexachloroethane (**17**) and products of bromotrichloromethane addition across an alkene π-bond are common contaminants in bromohydrin ether syntheses by the alkoxyl radical method. For unknown reasons, we did not isolate expected trapping product **15** (Figure 16).

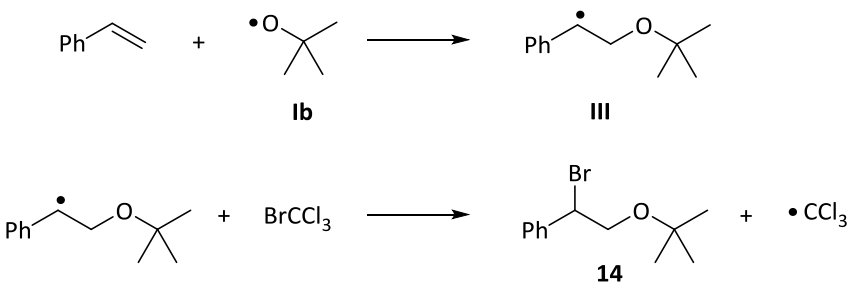

Scheme 9 Addition-substitution sequence for explaining formation of bromohydrin ether **14**.

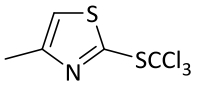

15

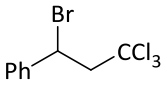

16

17

Figure 16 Expected (**15**) and detected (**16** and **17**) products formed from trichloromethyl radical reactions.

Concluding Remarks

Thiazole-derived *O*-(*tert*-butyl) thiohydroxamates are stable compounds, liberating *tert*-butoxyl radicals by homolytically breaking the N,O-bond when activated with light or attacked by radicals at thione sulfur. The esters are accessible in up 64% yield from thiohydroxamic acids and an *O*-(*tert*-butyl) isourea. Characterizing products of thiohydroxamate *O*-alkylation is feasible from diagnostic thiocarbonyl carbon-13 resonances and stretching vibrations associated with the 3-alkoxy-4-methylthiazole-2(3*H*)thione core.

Ground state stability of heterocyclic *O*-(*tert*-butyl) thiohydroxamates arises from partial multiple bonding between nitrogen and oxygen, being explained in molecular orbital by a σ(N,O)-bond and three superimposed π(N,O)-bonds of different strengths. Steric congestion at thiohydroxamate oxygen strengthens π(N,O)-bonding, explaining the unusual stability of 3-(*tert*-butoxy)thiazole-2(3*H*)thiones. 1-(Alkoxy)pyridine-2(1*H*) thiones exert a similar stabilizing mechanism, however, being less effective.

The underlying principle, to use non-bonding electron pairs from proximate heteroatoms for strengthening a weak σ-bond by supplementary π-interactions, according to our interpretation, is not restricted to the N,O-bond of thiohydroxamates. Nitrogen, phosphorous, oxygen, sulfur, fluorine, chlorine, bromine, and iodine in all possible combinations are in principle able to form σ- and π-bonds according to the suggested model.

The attractive feature of the N,O-bonding model developed in this article is the fact that the heteroatom-heteroatom bond stabilizing mechanism applies to the ground state. On the leave of the ground state, stabilizing interactions disappear, making the heteroatom-heteroatom bond a predetermined breaking point for liberating reactive intermediates. Insights of this kind provide a guideline for designing new radical precursors and adapting their properties. For us, the approach provides perspectives for examining standing

questions on polar selectivity effects in tertiary alkoxyl radical additions, which we pursue at the moment in our laboratory.

Experimental

1. General

For general laboratory practice and instrumentation see the ESI.

2. 3-Hydroxy-4-methyl-5-(4-nitrophenyl)-thiazole-2(3*H*)thione (3a)

2.1 1-Chloro-1-(4-nitrophenyl)propan-2-one

A solution of sulfuryl chloride (5.51 g, 3.3 mL, 40.8 mmol) in dichloromethane (15 mL) is added in a dropwise manner to an ice-cooled (0 °C) to a solution of 1-(4-nitrophenyl)-propan-2-one (**5**)[112] (6.00 g, 33.5 mmol) in dichloromethane (20 mL), causing a change in color from red to pale yellow. The reaction mixture was continued for two hours at 21 °C, and washed afterwards with an aqueous saturated solution of $NaHCO_3$ (50 mL) and water (50 mL). The organic phase was separated, dried ($MgSO_4$), and concentrated under reduced pressure to leave an orange oil, which was purified by column chromatography using diethyl ether/pentane = 1:1 (*v*/*v*) as eluent. Yield: 5.47 g (25.6 mmol, 76 %), pale yellow oil, which crystallizes on standing at –32 °C. R_f = 0.50 [diethyl ether/pentane = 1:1 (*v*/*v*)]. M.p. 38 °C. ^{1}H NMR ($CDCl_3$, 400 MHz) δ 2.31 (s, 3 H), 5.40 (s, 1 H), 7.60–7.64 (m, 2 H), 8.24–8.27 (m, 2 H). ^{13}C NMR ($CDCl_3$, 100.6 MHz) δ 26.1, 64.6, 124.1, 129.0, 141.7, 148.2, 199.1. MS (EI) *m/z* (%) 213 (M^+, <1), 172 (35), 171 (100), 163 (5), 151 (13), 141 (22), 133 (7), 124 (20), 112 (12), 103 (8), 89 (70), 77 (18), 63 (42), 51 (14). Anal. Calcd. for $C_9H_8NO_3Cl$ (213.62): C, 50.60; H, 3.77; N, 6.56; Found: C, 50.24; H, 3.90; N, 6.52.

2.2 1-(Ethoxythiocarbonylsulfanyl)-1-(4-nitrophenyl)propan-2-one

A solution of 1-chloro-1-(4-nitrophenyl)-propan-2-one (339 mg, 1.59 mmol) in acetone (2 mL) was added at 0 °C to a suspension of potassium *O*-ethyldithiocarbonate (256 mg, 1.60 mmol) in acetone (2 mL). The resulting slurry was stirred for two hours at 21 °C. Solids were filtred off, and the filtrate concentrated under reduced pressure. The remaining red oil was purified by chromatography using diethyl ether/pentane = 1:1 (*v*/*v*) as eluent. Yield: 359 mg (1.20 mmol, 75 %), pale yellow solid. R_f = 0.57 [diethyl ether/pentane =

1:1 (*v*/*v*)]. m.p. 61 °C. ^{1}H NMR ($CDCl_3$, 600 MHz) δ 1.40 (t, *J* = 7.0 Hz, 3 H), 2.32 (s, 3 H), 4.61 (q, J = 7.1 Hz, 2 H), 5.76 (s, 1 H), 7.50–7.59 (m, 2 H), 8.18–8.25 (m, 2 H). ^{13}C NMR ($CDCl_3$, 100.6 MHz) δ 13.7, 28.9, 63.7, 71.1, 124.1, 130.1, 140.9, 147.9, 200.2, 211.2. MS (EI) *m/z* (%) 299 (M^+, 3), 266 (100), 257 (24), 239 (57), 211 (68), 194 (23), 180 (32), 168 (64), 152 (60), 137 (27), 131 (35), 121 (76), 103 (41), 103 (8), 89 (80), 77 (77), 63 (61), 51 (34). Anal. Calcd. for $C_{12}H_{13}NO_4S_2$ (299.36): C, 48.15; H, 4.38; N, 4.68; S, 21.42, Found: C, 48.36; H, 4.50; N, 4.74. S, 21.48.

2.2 1-(Ethoxythiocarbonylsulfanyl)-1-(4-nitrophenyl)propan-2-one oxime

Hydroxyl ammonium hydrochloride (94.3 mg, 1.36 mmol) and pyridine (104 mg, 1.31 mmol) were sequentially added in one portion at added 0 °C to a suspension of 1-(ethoxythiocarbonylsulfanyl)-1-(4-nitrophenyl)propan-2-one (315 mg, 1.05 mmol) in methanol (5 mL). The resulting mixture was stirred for fourteen hours at 22 °C and afterwards concentrated under reduced pressure. The remaining oil residue was taken up in dichloromethane (20 mL) and washed successively with 0.5 M aqueous hydrochloric acid (20 mL) and brine (20 mL). The organic phase was dried ($MgSO_4$) and concentrated under reduced pressure. The remaining oil oil was purified by chromatography, using diethyl ether/pentane = 1:2 (*v*/*v*) as eluent. Yield: 260 mg (828 mmol, 79 %), pale yellow oil, 86/14-mixture of (*E*)/(*Z*)-stereoisomers (isomers A and B). Anal. Calcd. for $C_{12}H_{14}N_2O_4S_2$ (314.37) (mixture of stereoisomers A and B): C, 45.85; H, 4.49; N, 8.91; S, 20.40, Found: C, 45.74; H, 4.55; N, 8.83, S, 20.37. *Isomer A*. R_f = 0.38 [diethyl ether/pentane = 1:2 (*v*/*v*)] ^{1}H NMR ($CDCl_3$, 200 MHz) δ 1.38 (t, *J* = 7.1 Hz, 3 H), 1.93 (s, 3 H), 4.60 (q, J = 7.1 Hz, 2 H), 5.65 (s, 1 H), 7.53–7.66 (m, 2 H), 8.05 (br. s, 1 H), 8.15–8.26 (m, 2 H). ^{13}C NMR ($CDCl_3$, 100.6 MHz) δ 13.66, 13.70, 57.7, 70.7, 123.7, 129.8, 144.4, 147.5, 155.2, 211.1. *Isomer B*. R_f = 0.26 [diethyl ether/pentane = 1:2 (*v*/*v*)]. ^{1}H NMR ($CDCl_3$, 200 MHz) δ 1.38 (t, *J* = 7.1 Hz, 3 H), 1.99 (s, 3 H), 4.63 (q, *J* = 7.1 Hz, 2 H), 6.51 (s, 1 H), 7.55–7.62 (m, 2 H), 8.16–8.23 (m, 2 H), 8.60 (br. s, 1 H, OH). ^{13}C NMR ($CDCl_3$, 100.6 MHz) δ 13.6, 18.4, 49.8, 70.8, 123.9, 129.1, 143.2, 147.5, 153.2, 210.5.

2.4 3-Hydroxy-4-methyl-5-(4-nitrophenyl)thiazole-2(3*H*)thione (3a)

A solution of (ethoxythiocarbonylsulfanyl)-1-(4-nitrophenyl)propan-2-one oxime (5.58 g, 17.7 mmol) in dichloromethane (104 mL) was added at 0 °C to a solution of

potassium hydroxide [4.00 g, 86% (*w*/*w*), 61.3 mmol] in water (104 mL). The resulting suspension was stirred for two hours at 23 °C and hereafter diluted with water (~700 mL), all solids were dissolved. The aqueous layer was separated, washed with dichloromethane (200 mL) and acidified to pH 1 by adding concentrated hydrochloric acid. The precipitate was collected and dried. Yield: 4.42g (16.5 mmol, 93 %), yellow solid. The crude precipitate was used for preparing *O*-esters. An analytically pure sample was obtained by crystallizing from dimethyl formamide. Yellow needles. M.p. 162 °C. ^{1}H NMR (DMSO[d_6], 400 MHz) δ 2.38 (s, 3 H), 7.72 (d, *J* = 8.8 Hz, 2 H), 8.29 (d, *J* = 8.8 Hz, 2 H), 12.51 (br.s, 1 H). ^{13}C NMR (DMSO[d_6], 100.6 MHz) δ 12.8, 114.5, 124.3, 129.0, 136.8, 137.4, 146.6, 177.3. UV (methanol): λ_{max} (lg ε/m^{2}mol^{-1}) 377 nm (3.15), 313 (2.94), 263 (2.90), 205 (3.28). Anal. Calcd. for $C_{10}H_8N_2O_3S_2$ (268.31): C, 44.77; H, 3.01; N, 10.44; S, 23.90, Found: C, 44.61; H, 3.08; N, 10.46, S, 23.98.

3 Alkylation of 3-hydroxy-4-methylthiazole-2(3*H*)thiones with in situ-generated *O*-(*tert*-butyl)-*N*,*N*-diisopropyl isourea

3.1 General method

Copper(I)-chloride (2 mol%) was added at 22 °C to solution of *tert*-butanol (5.5 mmol) and diisopropyl carbodiimide (5.5 mmol). The reaction mixture was stirred for twenty-four hours at 22 °C and hereafter transferred into a syringe, for being added (20µL/min) to a solution of a 3-hydroxythiazole-2(3*H*)thione (**1a**–**3a**) or 1-hydroxypyridine-2(1*H*)thione (**4a**) in dichloromethane (2 mL/mmol) at 23 °C. After complete addition, solids were immediately filtered off and washed with dichloromethane (3 × 10 mL). Filtrate and washings were combined to furnish a clear solution, which was concentrated under reduced pressure. The remaining oil was purified by column chromatography (SiO_2) using an eluent gradient specified individually below.

3.2 Alkylation of 3-hydroxy-4-methylthiazole-2(3*H*)thione (2a)

Reagents: 3-hydroxy-4-methylthiazol-2(3*H*)thione (**2a**) (1.48 g, 10 mmol), *tert*-butanol (3.72 g, 50.0 mmol), DIC (6.30 g, 50.0 mmol) and copper(I)-chloride (98 mg, 1.00 mmol). Eluent gradient used for chromatographic purification: ether/pentane = 1:1 (*v*/*v*) → acetone. *3-(2-Methylprop-2-oxy)-4-methylthiazole-2(3H)thione* (**2b**). Yield: 988 mg (4.86 mmol, 49 %) off-white solid. M.p. 56–57 °C, R_f = 0.36 [diethyl ether/pentane = 1:1 (*v*/*v*)]. ^{1}H NMR ($CDCl_3$,

400 MHz) δ 1.57 (s, 9 H), 2.26 (d, *J* = 1.2 Hz, 3 H), 6.15 (q, *J* = 1.2 Hz, 1 H). ^{13}C NMR ($CDCl_3$, 100 MHz) δ 15.2, 28.8, 91.8, 102.9, 139.8, 184.1. UV (methanol): λ_{max} (lg ε/m^2mol^{-1}) 319 nm (3.05), 211 (2.99). IR (CCl_4) ν_{max} / cm^{-1} 2981, 2933, 1306, 1191, 1155, 1138, 1012, 982, 883, 839, 816, 854, 816, 727. Anal. Calcd. for $C_8H_{13}NOS_2$ (203.32): C, 47.26; H, 6.44; N, 6.89; S, 31.54, Found: C, 47.09; H, 6.30; N, 6.87, S, 31.45. *2-(2-Methylpropyl-2-sulfanyl)-4-methylthiazole N-oxide* (**7b**). Yield: 491 mg (2.42 mmol, 24 %) off-white solid. M.p. 105 °C. R_f = 0.41 (acetone). ^{1}H NMR ($CDCl_3$, 600 MHz) δ 1.43 (s, 9 H), 2.36 (d, *J* = 0.9 Hz, 3 H), 7.12 (d, *J* = 0.9 Hz, 1 H). ^{13}C NMR ($CDCl_3$, 150.9 MHz) δ 13.9, 31.3, 52.5, 114.6, 135.5, 146.4. MS (EI) *m/z* (%) 203 (M^+, <1), 187 (4), 147 (61), 131 (100), 86 (20), 71 (16), 57 (44). Anal. Calcd. for $C_8H_{13}NOS_2$ (203.32): C, 47.26; H, 6.44; N, 6.89; S, 31.54, Found: C, 47.37; H, 6.23; N, 6.94, S, 31.37.

3.3 Alkylation of 3-hydroxy-4-methyl-5-(4-nitrophenyl)thiazole-2(3*H*)thione (3a)

Reagents: 3-hydroxy-4-methyl-5-(4-nitrophenyl)thiazole-2(3*H*)thione (**3a**) (1.34 g, 4.99 mmol), *tert*-butanol (2.04 g, 27.5 mmol), DIC (3.47 g, 27.5 mmol) and copper(I)-chloride (51 mg, 515 μmol). Eluent gradient used for chromatographic purification: ether/pentane = 1:1 (*v*/*v*) → ethyl acetate. *3-(2-Methylprop-2-oxy)-4-methyl-5-(4-nitrophenyl)-thiazole-2(3H)thione* (**3b**). Yield: 624 mg (1.92 mmol, 39 %), fluffy yellow crystals. M.p. 153 °C. R_f = 0.33 [diethyl ether/pentane = 1:1 (*v*/*v*)]. ^{1}H NMR ($CDCl_3$, 400 MHz) δ 1.64 (s, 9 H), 2.42 (s, 3 H), 7.49−7.52 (m, 2 H), 8.28−8.31 (m, 2 H). ^{13}C NMR ($CDCl_3$, 100 MHz) δ 14.7, 28.9, 92.6, 116.4, 124.4, 128.9, 137.1, 137.3, 147.2, 183.3. UV (methanol): λ_{max} (lg ε/m^2mol^{-1}) 377 nm (3.18), 324 (2.96), 265 (2.99), 205 (3.33). IR (CCl_4) ν_{max} / cm^{-1} 2981, 2933, 1523, 1350, 1327, 1271, 1171, 1132, 1110, 1030, 990, 943, 910, 854, 816, 754, 695, 613, 566. Anal. Calcd. for $C_{14}H_{16}N_2O_3S_2$ (324.42): C, 51.83; H, 4.97; N, 8.64; S, 19.76, Found: C, 51.70; H, 4.94; N, 8.64, S, 19.84. *2-(2-Methylpropyl-2-sulfanyl)-4-methyl-5-(4-nitrophenyl)-thiazole N-oxide* (**8b**). Yield: 271 mg (837 μmol, 17 %), orange oil. R_f = 0.26 (ethyl acetate). ^{1}H NMR ($CDCl_3$, 400 MHz) δ 1.51 (s, 9 H), 2.52 (s, 3 H), 7.63−7.65 (m, 2 H), 8.33−8.35 (m, 2 H). ^{13}C NMR ($CDCl_3$, 100.6 MHz) δ 13.2, 31.4, 53.0, 124.5, 129.0, 129.3, 136.6, 137.0, 143.8, 148.0. MS (EI) *m/z* (%) 220 (100), 190 (21), 174 (5), 163 (3), 147 (29), 135 (7), 121 (6), 115 (6), 103 (22), 91 (7), 77 (15), 69 (14), 63 (9), 51 (6). Anal. Calcd. for $C_{14}H_{16}N_2O_3S_2$ (324.42): C, 51.83; H, 4.97; N, 8.64; S, 19.76, Found: C, 51.48; H, 5.26; N, 8.68, S, 19.85.

4 Alkylation of 1-hydroxypyridine-2(1*H*)thione (4a)

4.1 Alkylation with *tert*-butyl bromide

Reagents: 1-hydroxypyridine-2(1*H*)thione tetraethylammonium salt (2.72 g, 10.6 mmol), *tert*-butyl bromide (1.45 g, 10.6 mmol) and dimethyl formamide (35 mL). Eluent used for chromatographic purification: *tert*-butyl methyl ether. *1-(2-Methylprop-2-oxy)-pyridine-2(1H)thione* (**4b**). Yield: 70 mg (382 μmol, 4 %), pale yellow solid, m.p. 54 °C, R_f = 0.61 (*tert*-butyl methyl ether). ^{1}H NMR ($CDCl_3$, 600 MHz) δ 1.49 (s, 9 H), 6.52 (td, J_t = 6.9 Hz, J_d = 1.7 Hz, 1 H), 7.05 (ddd, *J* = 8.6, 6.9, 1.5 Hz, 1 H), 7.63 (dd *J* = 8.0, 1.5 Hz, 1 H), 7.66 (dd, *J* = 6.5, 1.7 Hz, 1 H). ^{13}C NMR ($CDCl_3$, 150 MHz) δ 27.7, 90.7, 112.2, 132.0, 137.7, 139.9, 179.2. UV (ethanol): λ_{max} (lg ε/m^2mol^{-1}) 364 nm (2.68), 291 (3.03). Anal. Calcd. for $C_9H_{13}NOS$ (183.27): C, 58.98; H, 7.15; N, 7.64; S, 17.49, Found: C, 58.68; H, 6.97; N, 7.65, S, 17.09.

4.2 Alkylation with in situ-generated *O-tert*-butyl-*N,N*-diisopropyl isourea

Reagents: 1-hydroxypyridine-2(1*H*)thione (643 mg, 5.06 mmol), *tert*-butanol (2.04 g, 27.5 mmol), DIC (3.47 g, 27.5 mmol) and copper(I)-chloride (50.0 mg, 505 μmol). Eluent gradient used for chromatographic purification: diethyl ether → acetone. Yield: 221 mg (1.21 mmol, 24 %), yellow oil, 82/18-mixture of 1-(2-methylprop-2-oxy)pyridine-2(1*H*)thione (**4b**) and *O*-(2-methylprop-2-yl) pyridine-2-sulfenate (**10b**). R_f = 0.80 (diethyl ether). *O-(2-methylprop-2-yl) pyridine-2-sulfenate* (**10b**). ^{1}H NMR ($CDCl_3$, 400 MHz) δ 1.35 (s, 9 H), 6.92 (ddd, *J* = 7.5, 4.8, 1.1 Hz, 1 H), 7.34 (dt, J_d = 8.1 Hz, J_t = 1.1 Hz, 1 H), 7.60 (td, J_t = 7.8 Hz, J_d = 1.9 Hz, 1 H), 8.32 (d, *J* = 4.8 Hz, 1 H). ^{13}C NMR ($CDCl_3$, 100.6 MHz) δ 27.6, 83.4, 117.1, 119.0, 136.4, 148.7, 167.1. ^{1}H NMR (C_6D_6, 400 MHz) δ 1.13 (s, 9 H), 6.42 (ddd, *J* = 7.5, 4.8, 1.1 Hz, 1 H), 7.08 (td, J_t = 7.8 Hz, J_d = 1.9 Hz, 1 H), 7.25 (dt, J_d = 8.1 Hz, J_t = 1.1 Hz, 1 H), 8.21−8.27 (m, 1 H). ^{13}C NMR (C_6D_6, 100.6 MHz) δ 27.5, 82.8, 116.9, 118.9, 136.2, 149.0, 167.8. *2-(2-methylpropyl-2-sulfanyl)pyridine 1-oxide* (**9b**). Yield: 109 (594, μmol, 12 %), colorless oil. R_f = 0.31 (acetone). ^{1}H NMR ($CDCl_3$, 400 MHz) δ 1.52 (s, 9 H), 7.08 (ddd, J = 1.9, 6.5, 6.6 Hz, 1 H), 7.6 (td, J_d = 1.4 Hz, J_t = 7.5 Hz, 1 H), 7.52 (dd, *J* = 8,0, 2.0 Hz, 1 H), 8.27 (dd, *J* = 1.1, 6.4 Hz, 1 H). ^{13}C NMR ($CDCl_3$, 150.9 MHz) δ 30.9, 47.9, 122.4, 124.4, 129.0, 139.8, 149.7. GC/MS (EI) *m/z*. (%): 17.95 min/ 183 (M^+, <1), 167 (5), 127 (30), 111 (100), 78 (16), 67 (33), 57 (19). HRMS (EI^+) *m/z* 183.0718 (M^+); calculated mass for $C_9H_{13}NOS$:183.0718.

5 Spin trapping with 5,5-dimethyl-1-pyrroline 1-oxide (DMPO)

A solution of an *O*-alkyl thiohydroxamate [9.59 mg (31.0 μmol) for **1b**, 5.97 mg (29.4 μmol) for **2b**, 10.0 mg (30.8 μmol) for **3b**] in benzene (300 μL, 0.10 M) was transferred into an ESR-tube, charged with a solution of 5,5-dimethyl-1-pyrroline 1-oxide (3.59 mg, 31.7 μmol) in benzene (300 μL, 0.11 M). The solution was flushed for five minutes with a gentle stream of argon, photolyzed for two minutes at ~25 °C in a Rayonet® chamber reactor equipped with twelve 350 nm light bulbs, and placed into the cavity of an ESR-spectrometer. The spectral data from trapping experiments using O-(*tert*-butyl) esters **1b**–**3b** are summarized in Table 7.

6 Intermolecular trapping with styrene and bromotrichloromethane

A solution of 3-(*tert*-butoxy)thiazole-2(3*H*)thione **2b** (208 mg, 1.02 mmol), styrene (2.22 g, 21.3 mmol, c_0 = 2.76 M), and bromotrichloromethane (1.00 mL, 10.0 mmol) in benzene (7.7 mL) was photolyzed at ~25 °C in a Rayonet® chamber reactor equipped with twelve 350 nm light bulbs, until the starting material was completely consumed (~30 min, tlc). The solution was concentrated under reduced pressure to leave an oil, which was purified by chromatography (SiO_2). Eluent used for chromatographic purification: ether/pentane = 1:50 (*v*/*v*) → ether/pentane = 1:20 (*v*/*v*). *2-Brom-2-phenyl-1-(2-methyl-2-propoxy)ethane* (**14**). Yield: 69.3 mg (270 μmol, 26 %), colorless oil. R_f = 0.65 [diethyl ether/pentane = 1:20 (*v*/*v*)].^{1}H NMR ($CDCl_3$, 400 MHz) δ 1.20 (s, 9 H), 3.80 (dd, *J* = 6.4, 10.4 Hz, 1 H), 3.90 (dd, *J* = 7.3, 10.4 Hz, 1 H), 4.99 (t, *J* = 6.8 Hz, 1 H), 7.29−7.39 (m, 3 H), 7.41−7.46 (m, 2 H). ^{13}C NMR ($CDCl_3$, 100.6 MHz) δ 27.5, 53.5, 67.0, 73.8, 127.9, 128.4, 128.5, 139.6. GC/MS (EI) *m/z* (%): 16.22 min/ 258 (M^+, <1), 185 (16), 183 (17), 147 (46), 120 (19), 104 (64), 103 (30), 91 (56), 78 (19), 77 (17), 65 (13), 57 (100). Anal. Calcd. for $C_{12}H_{17}OBr$ (257.17): C, 56.05; H, 6.66; Found: C, 56.18; H, 6.60.

Acknowledgements. We thank Dr. Reinhard Philipp for recording EPR-spectra of compounds 13 and helpful technical suggestions. This work is part of the Ph.D. thesis of C.S.

Notes and References

† Electronic supplementary information (ESI) available: Instrumentation, Reagents and Chromatography, Supplementary O-alkyl thiohydroxamate reactions, archive of NMR-

spectra, description of computational details, compilation of computed data, and details for vibrational analysis.ESI associated with this article can be found in the online version at doi: .....

Crystallographic data (excluding structure factors) for compound **3b** reported in this paper have been deposited with the Cambridge Crystallographic Data Centre as supplementary publication (CCDC 1057369). Copies of the data can be obtained, free of charge, on application to CCDC, 12 Union Road, Cambridge CB2 1EZ, UK, (fax: +44-(0)1223-336033 or e-mail: deposit@ccdc.cam.ac.uk).

‡ To the memory of Alan Roy Katritzky, for introducing us to the wealth of heterocyclic chemistry.

[1] P. Gray, A. Williams, *Chem. Rev*. **1959**, *59*, 239–328.

[2] P. Brun, B. Waegell, in *Reactive Intermediates*, R. A. Abramovitch Ed., Vol. 3, Kluwer Academic Press, Plenum Publishers, New York, N.Y. **1983**, 367–426.

[3] J. Hartung, T. Gottwald, K. Špehar, *Synthesis* **2002**, *11*, 1469−1498.

[4] R. P. Wayne, in *Chemistry of Atmospheres*, 2nd Ed., Oxford University Press, Oxford, **1991**, 208–275.

[5] S. W. Benson, P. S. Nangia, *Acc. Chem. Res.* **1979**, *12*, 223–228.

[6] J. Fukutu, J. L. Ignarro, *Acc. Chem. Res.*, **1997**, *30*, 149–162.

[7] B. Halliwell, J. M. C. Gutteridge, in *Free Radicals in Biology and Medicine*, 3rd. Ed. Oxford University Press, Oxford, **1999**, 617–851.

[8] V. Ullrich, R. Brugger, *Angew. Chem. Int. Ed. Engl*. **1994**, *33*, 1911–1919.

[9] P. C. Wong, D. Griller, J. C. Scaiano, *J. Am. Chem. Soc*. **1982**, *104*, 5106–5108.

[10] M. Salamone, L. Mangiacapra, M. Bietti, *J. Org. Chem*. **2015**, *80*, 1149−1154.

[11] C. Schur, N. Becker, U. Bergsträßer, T. Gottwald, J. Hartung, *Tetrahedron* **2011**, *67*, 2338−2347.

[12] M. J. Jones, G. Moad, E. Rizzardo, D. H. Solomon, *J. Org. Chem.* **1989**, *54*, 1607−1611.

[13] W. Adam, J. Hartung, H. Okamoto, C. R. Saha-Moller, K. Špehar, *J. Photochem. Photobiol.* **2000**, *72*, 619–624.

[14] T. Gottwald, M. Greb, J. Hartung, *Synlett* **2004**, 65–68.

[15] J. Hartung, R. Kneuer, S. Laug, P. Schmidt, K. Špehar, I. Svoboda, H. Fuess, Eur. *J. Org. Chem.*, **2003**, 4033–4052.

[16] M. Cueto, J. Darias, *Tetrahedron* **1996**, *52*, 5899–5906.

[17] G. Buchbauer, A. M. Weck, *Chem. Ztg*. **1985**, *109*, 255–265.

[18] H. Krieger, *Arzneimittel Forsch*. **1968**, *18*, 129–134.

[19] M. Lj. Mihailović, Ž. Čeković, D. Jeremić, *Tetrahedron* **1965**, *21*, 2813–2821.

[20] H. Togo, M. Katohgi, *Synlett* **2001**, 565–581.

[21] D. H. R. Barton, J. M. Beaton, L. E. Geller, M. M. Pechet, *J. Am. Chem. Soc.* **1961**, *83*, 246–278.

[22] C. Walling, A. Padwa, *J. Am. Chem. Soc.* **1963**, *85*, 1593–1597.

[23] J. Hartung, *Eur. J. Org. Chem*. **2001**, 619–632.

[24] D. Kao, A. Chaintreau, J.-P. Lepoittevin, E. Giménez-Arnau, *J. Org. Chem*. **2011**, *76*, 6188–6200.

[25] J. E. Leffler, in *An Introduction to Free Radicals*, J. Wiley & Sons, Inc., New York, N.Y., **1993**, 126–147.

[26] H. J. H. Fenton, *J. Chem. Soc*., *Transaction* **1894**, *65*, 899–910.

[27] C. Walling, *Acc. Chem. Res*., **1975**, *8*, 125–131.

[28] D. T. Sawyer, in *Oxygen Chemistry*, Oxford, University Press, Oxford, 1991, 19–51.

[29] K. U. Ingold, *Acc. Chem. Res*., **1969**, *2*, 1–9.

[30] A. L. J. Beckwith, B. P. Hay, G. M. Williams, *Chem. Commun*. **1989**, 1202–1203.

[31] S. Kim, T. A. Lee, Y. Song, *Synlett* **1998**, 471–472.

[32] B. P. Hay, A. L. J. Beckwith, *J. Am. Chem. Soc*. **1988**, *110*, 4415–4416.

[33] B. Giese, *in Radials in Organic Synthesis – The Formation of Carbon-Carbon Bonds,* Oxford University Press, **1986**.

[34] M. Bodenstein, *Z. Phys. Chem.* **1913**, *85*, 329–397.

[35] J. Hartung, U. Bergsträsser, K. Daniel, N. Schneiders, I. Svoboda, H. Fuess, *Tetrahedron* **2009**, *65*, 2567–2573.

[36] W. Walter, E. Schaumann, *Synthesis* **1971**, *3*, 111−130.

[37] A. Chimiak, R. Przychodzen, *J. Heteroatom Chem*. **2002**, *13*, 169–194.

[38] J. Hartung, K. Špehar, I. Svoboda, H. Fuess, M. Arnone, B. Engels, *Eur. J. Org. Chem*., **2005**, 869−881.

[39] J. Hartung, K. Daniel, T. Gottwald, A. Groß, N. Schneiders, *Org. Biomol. Chem*. **2006**, *4*, 2313−2322.

[40] J. Hartung, F. Gallou, *J. Org. Chem*. **1995**, *60*, 6706−6716.

[41] H. Ritter, G. Maatz, J. Hartung, C. Schur **2009**, PCT/EP2009/006617.

[42] J. Hartung, T. Gottwald, K. Špehar, *Synlett* **2003**, *2*, 227−229.

[43] C. Schur, I. Kempter, J. Hartung, *Org. Synth*. **2012**, *89*, 409−419.

[44] D. H. R. Barton, D. Crich, G. Kretschmar, *J. Am. Chem. Soc.* **1986**, 39−54.

[45] E. Shaw, J. Bernstein, K. Losee, W. A. Lott, *J. Am. Chem. Soc.* **1950**, *72*, 4362−4364.

[46] A. Hantzsch, J. H. Weber, *Ber. Dtsch. Chem. Ges*. **1887**, *20*, 3118–3132.

[47] O. J. Widman, *Prakt. Chem*. **1888**, *38*, 185–201.

[48] L. J. Mathias, *Synthesis* **1979**, 561−576.

[49] L. F. Tietze, G. Brasche, A. Grube, N. Böhnke, C. Stadler, *Chem. Eur. J.* **2007**, *13*, 8543−8563.

[50] R. Jaeger, *J. Phys. Org. Chem.* **1998**, *11*, 47–53.

[51] M. Arnone, J. Hartung, B. Engels, *J. Phys. Chem. A*. **2005**, *109*, 5943–5950.

[52] S. Nagakura, M. Jojima, Y. Maruyama, *J. Mol. Spectrosc.* **1964**, *13*, 174–192.

[53] A. Groß, N. Schneiders, K. Daniel, T. Gottwald, J. Hartung, *Tetrahedron* **2008**, *64*, 10882–10889.

[54] D. P. White, J. C. Anthony, A. Oyefeso, *J. Org. Chem*. **1999**, *64*, 7707–7716.

[55] R. W. Taft, in *Steric Effects in Organic Chemistry*; M. S. Newman (Ed.), Wiley: New York, ch. 13, **1956**, p. 556.

[56] R. K. Ritchie, H. Spedding, D. Steele*, Spectrochim. Acta* **1971**, *27A*, 1597–1608.

[57] For an early investigation of IR-absorptions in 1-hydroxypyridine-2(1*H*)thione leading to a different assignment of bands, see: A. R. Katritzky, R. A. Jones, *J. Chem. Soc*., **1960**, 2947−2953.

[58] For vibrational analysis of thiolactones, see: J. Hodge Markgraf, *Heterocycles* **1984**, *22*, 2601−2655.

[59] For landmark contribution on vibrational analysis of thioamides, see: K.A. Jensen, P.H. Nielsen, *Acta Chem. Scand* **1966**, *20*, 597–629.

[60] For vibrational analysis of thiosemicarbazones, see: D. M. Wiles, B. A. Gingras, T. Suprunchuk, *Can. J. Chem.* **1967**, *45*, 469−473.

[61] For vibrational analysis of thioureas, see: R. K. Gosavi, U. Agarwala, C. N. R. Rao, *J. Am. Chem. Soc.* **1967**, *89*, 235–239.

[62] J. Hartung, M. Schwarz, I. Svoboda, H. Fuess, *Acta Cryst. C* **2003**, *59*, o682–o684.

[63] F. H. Allen, O. Kenwood, D. G. Watson, L. Brammer, A. G. Orpen, R. Taylor, *J. Chem. Soc., Perkin Trans. 2*, **1987**, 1−19.

[64] J. Hartung, I. Svoboda, in *The Chemistry of Peroxides,* Z. Rappoport (Ed.), Wiley, **2006**, Chichester, 93−144.

[65] S. L. Khursan, V. L. Antonovsky, *Russ. Chem. Bull.* **2003**, *52*, 1312–1325.

[66] J. Hartung, M. Hiller, M. Schwarz, I. Svoboda, H. Fuess, *Liebigs Ann.* **1996**, 2091−2097.

[67] For a study, provisionally assigning a structure as tertiary *O*-alkyl pyridine-2-sulfenate, see: R. C. Cambie, P. K. Davy, L.H. Mitchell, C.E.F. Rickard, P.S. Rutledge, *Aust. J. Chem.*, **1998**, *51*, 653–660. Since carbon-13 NMR-data provided for the compound deviate significantly from data documented in this article, we think that the provisionally assigned structure needs reinterpretation.

[68] J.B. Forseman, Æ Frisch, in *Exploring Chemistry With Electronic Structure Methods*, 2nd ed; Gaussian, Inc: Pittsburg, PA, **1996**.

[69] R. Ditchfield, W. J. Hehre, and J. A. Pople, *J. Chem. Phys.* **1971**, *54*, 724−728.

[70] W. J. Hehre, R. Ditchfield, and J. A. Pople, *J. Chem. Phys.* **1972**, *56*, 2257−2261.

[71] Gaussian 03, Revision E.01, M. J. Frisch, G.W. Trucks, H.B. Schlegel, G.E. Scuseria, M.A. Robb, J.R. Cheeseman, J.A. Montgomery, Jr., T. Vreven, K.N. Kudin, J.C. Burant, J.M. Millam, S.S. Iyengar, J. Tomasi, V. Barone, B. Mennucci, M. Cossi, G. Scalmani, N. Rega, G.A. Petersson, H. Nakatsuji, M. Hada, M. Ehara, K. Toyota, R. Fukuda, J. Hasegawa, M. Ishida, T. Nakajima, Y. Honda, O. Kitao, H. Nakai, M. Klene, X. Li, J.E. Knox, H.P. Hratchian, J.B. Cross, V. Bakken, C. Adamo, J. Jaramillo, R. Gomperts, R. E. Stratmann, O. Yazyev, A. J. Austin, R. Cammi, C. Pomelli, J.W. Ochterski, P.Y. Ayala, K. Morokuma, G.A. Voth, P. Salvador, J.J. Dannenberg, V. G. Zakrzewski, S. Dapprich, A.D. Daniels, M.C. Strain, O. Farkas, D.K. Malick, A.D. Rabuck, K. Raghavachari, J.B. Foresman, J.V. Ortiz, Q. Cui, A.G. Baboul, S. Clifford, J. Cioslowski, B.B. Stefanov, G. Liu, A. Liashenko, P. Piskorz, I. Komaromi, R.L. Martin, D.J. Fox, T. Keith, M.A. Al-Laham, C.Y. Peng, A. Nanayakkara, M. Challacombe, P.M.W. Gill, B. Johnson, W. Chen, M.W. Wong, C. Gonzalez, J.A. Pople, Gaussian, Inc., Wallingford CT, 2004.

[72] V. A. Rassolov, J. A. Pople, M. A. Ratner, and T. L. Windus, *J. Chem. Phys.* **1998**, *109*, 1223−1229.

[73] V. A. Rassolov, M. A. Ratner, J. A. Pople, P. C. Redfern, L. A. Curtiss, *J. Comp. Chem.* **2001**, *22*, 976−984.

[74] M. M. Francl, W. J. Pietro, W. J. Hehre, J. S. Binkley, D. J. DeFrees, J. A. Pople, and M. S. Gordon, *J. Chem. Phys.* **1982**, *77*, 3654−3665.

[75] R. D. Bach, G. J. Wolwer, B. A. Coddens, *J. Am. Chem. Soc.*, **1984**, *106*, 6098–6099.

[76] A. D. Becke, *J. Chem. Phys.* **1993**, *98*, 5648–5652.

[77] C. Lee, W. Yang, R.G. Parr, *Phys. Rev.* **1988**, *B37*, 785–789.

[78] A. D. Becke, *Phys. Rev*. **1988**, *A38*, 3098–3100.

[79] C. Møller, M. S. Plesset, *Phys. Rev.* **1934**, *46*, 618–622.

[80] M. J. Frisch, M. Head-Gordon, J. A. Pople, *Chem. Phys. Lett.* **1990**, *166*, 281–289.

[81] M. Head-Gordon, T. Head-Gordon, *Chem. Phys. Lett.* **1994**, *220*, 122–128.

[82] NBO 5.9. E.D. Glendening, J.K. Badenhoop, A.E. Reed, J.E. Carpenter, J.A. Bohmann, C.M. Morales, F. Weinhold, Theoretical Chemistry Institute, University of Wisconsin, Madison, WI, **2009**, http://www.chem.wisc.edu/~nbo5.

[83] E. D. Glendening, D. Eric, C. R. Landis, F. Weinhold, *Computational Molecular Science* **2012**, *2*, 1−43

[84] J. Hartung, N. Schneiders, U. Bergsträßer, *Acta Cryst.* **2006**, *E62*, o4713−o4714.

[85] J. Hartung, R. Kneuer, M. Schwarz, M. Heubes, *Eur. J. Org. Chem*. **2001**, 4733−4736.

[86] M. Raban, D. Kost, *Tetrehedron* **1984**, *40*, 3345–3381.

[87] J. Hartung, K. Daniel, U. Bergsträsser, N. Schneiders, S. Danner, P. Schmidt, I. Svoboda, H. Fuess, *Eur. J. Org. Chem.* **2009**, 4135–4142.

[88] J. Hartung, M. Hiller, P. Schmidt, *Chem. Eur. J.* **1996**, *2*, 1014−1023.

[89] A. L. J. Beckwith, B. P. Hay, *J. Org. Chem.* **1989**, *54*, 4330–4334.

[90] J. Hartung, I. Svoboda, H. Fuess, *Acta Cryst. C* **1996**, *C52*, 2841−2844.

[91] J. Hartung, I. Svoboda, H. Fuess, *Z. Kristallogr*. **1998**, *213*, 319–320.

[92] J. M. White, J. Giordano, A. J. Green, *Acta Cryst.* **1996**, *C52*, 2783–2785.

[93] U. Schöllkopf, I. Hoppe, *Liebigs Ann. Chem.* **1972**, *765*, 153–170.

[94] V. K. Yadav, A. Yadav, P. Pande, K. K. Kapoor, *Ind. J. Chem*. **1994**, *33B*, 1129−1133.

[95] N. B. H. Jonathan, *J. Mol. Spectrosc.* **1960**, *4*, 75−83.

[96] R. A. W. Johnstone, R. M. S. Loureiro, M. L. S. Cristiano, G. Labat, *ARKIVOC* **2010**, 142–169.

[97] K. L. Shi, R.Q-Wang, T. C. W. Mak, *J. Mol. Struc.* **1987**, *160*, 109−116.

[98] K. P. Huber, G. Herzberg, in Molecular Spectra and Molecular Structure IV. Constants of Diatomic Molecules, Van Nostrand, New York, N.Y. **1979**, pp. 466–484.

[99] R. Polák, J. Fišer, *Chem. Phys*. **2004**, *303*, 73–83.

[100] P. A. Giguère, J. D. Liu, *Can. J. Chem.* **1952**, *30*, 948–962.

[101] C. J. Marsden, B. J. Smith, *J. Mol. Struct. (Theochem)* **1989**, *187*, 337–357.

[102] A. D. Bain, J.C. Bunzli, D.C. Frost, L Weiler, *J. Am. Chem. Soc.* **1973**, *95*, 291–292.

[103] A. Chung-Phillips, K. A. Jebber, *J. Chem. Phys.* **1995**, *102*, 7080–7087.

[104] J. P. Snyder, L. Carlsen, *J. Am. Chem. Soc.* **1977**, *99*, 2931–2942

[105] S. Wolfe, *Acc. Chem. Res*. **1972**, *5*, 102–111.

[106] J.-L. Clément, N. Ferré, D. Siri, H. Karoui, A. Rockenbauer, P. Tordo, *J. Org. Chem*. **2005**, *70*, 1198−1203.

[107] E. G. Janzen, J. I-Ping Liu *J. Magn. Reson.* **1973**, *9*, 510−512.

[108] B. Giese, J. He, W. Mehl, *Chem. Ber.* **1988**, *121*, 2063−2066.

[109] I. Flemming in *Grenzorbitale und Reaktionen organsicher Verbindungen,* Wiley-VCH-Weinheim, **1979**.

[110] J. Hartung, N. Schneiders, T. Gottwald, *Tetrahedron Lett.* **2007**, *48*, 6027-6030.

[111] M. S. Kharash, O. Reinmuth, W. H. Urry, *J. Am. Chem. Soc.* **1947**, *69*, 1105–1110.

[112] P. J. Stang, T. E. Dueber, *J. Am. Chem. Soc.* **1977**, 2602−2610.

Anhang A

Supporting Information for:

Annulated and Bridged Tetrahydrofurans from Alkenoxyl Radical Cyclization

Christine Schur,[a] Harald Kelm,[a] Thomas Gottwald,[b] Arne Ludwig,[b] Rainer Kneuer,[b] and Jens Hartung*

[a] *Fachbereich Chemie, Organische Chemie, Technische Universität Kaiserslautern, Erwin-Schrödinger-Straße, D-67663 Kaiserslautern, Germany.* [b] *Institut für Organische Chemie, Universität Würzburg, Am Hubland, 97074 Würzburg, Germany*

Contents

A1 General Remarks: (*i*) Numbering of compounds in the *Electronic Supporting Information* and the accompanying publication are consistent. (*ii*) References refer exclusively to the *Electronic Supporting Information*.

A2 Instrumentation

A2.1 NMR-spectroscopy: Proton- and carbon-13-NMR spectra were measured with FT-NMR DPX 200, DPX 400 and DMX 600 instruments (*Bruker*). Chemical shifts refer to the *δ*-scale. Proton resonances of residual non-deuterated solvent molecules (δ_H 7.26 for $CDCl_3$; δ_H 7.16 for benzene; δ_H 2.50 for DMSO), and carbon-13 chemical shifts of $CDCl_3$ (δ_C 77.0), C_6D_6 (δ_C 128.06), and DMSO-d_6 (δ_C 39.52) served as internal standards.

A2.2 Electron impact mass spectrometry: Mass spectra (EI, 70 eV) were recorded with a Mass Selective Detector HP 6890 (*Hewlett Packard*).

A2.3 High resolution mass spectrometry were measured with a GCT Premier Micromass instrument (*Waters*).

A2.4 Optical rotations of chiral compounds at λ = 589 nm were recorded with a Krüss P3001/RS-polarimeter and a Perkin-Elmer polarimeter type 241 (λ_1 = 546 nm und λ_2 = 579 nm), and extrapolated using the Drude equation.[1]

A2.5 UV/Vis-spectra were recorded in 1-cm quartz cuvettes with a Cary 100 Conc UV/Vis spectrophotometer (Varian).

A2.6 Combustion analyses were performed with a Carlo Erba 1106 instrument (analytical laboratory, Universität Würzburg) and a vario Micro cube (analytical laboratory, Technische Universität Kaiserslautern).

A2.7 Melting points [°C] were determined on a Koffler hot-plate melting point microscope (*Reichert*) and are not corrected.

A3 Reagents and Chromatography

A3.1 Reagents: Benzene, dimethyl formamide, dichloromethane, tetrahydrofuran and diethyl ether were purified and dried according to standard procedures.[2] All other reagents were used as received from commercial suppliers (Sigma Aldrich, Acros Organics, Fisher Scientific, Merck), unless otherwise indicated. 3-Hydroxy-4-methylthiazole-2(3*H*)-thione,[3] 3-hydroxy-4-methylthiazole-2(3*H*)-thione tetraethylammonium salt,[4] isopropyltriphenyl-phosphonium bromide,[5] diethyl azodicarboxylate (DEAD),[6] *trans*-hexahydrophthalic acid anhydride[7–9] were prepared according to published procedures.

A3.2 Thin layer chromatography: Reaction progress was monitored via thin layer chromatography (tlc) on aluminum sheets coated with silica gel (60 F_{254}, *Merck*). Compounds on developed tlc-sheets were detected with the aid of the UV-VIS indicator commercially disposed on the sheets, showing colored or darker spots by illuminating devloped sheets with a hand lamp emitting 254 nm light. Alternatively, developed tlc-sheets were stained by Ekkert´s reagent and subsequently heated, leading to blue-green spots for organobromines, blue spots for alcohols and yellow spots for 3-alkenoxy-4-methylthiazole-2(3*H*)-thiones (e.g. **1**).

A3.3 Column chromatography: Geduran Si60-silica gel (40–63 μm) served as stationary phase for column chromatography (flash chromatography).

A3.4 Gas chromatography coupled to mass spectrometry: Mass spectra (EI, 70 eV) were recorded with a Mass Selective Detector HP 6890 (*Hewlett Packard*) connected to an Agilent-gaschromatograph.

A4 Alkenols

A4.1 ***trans*-2-(Prop-2-en-1-yl)-cyclopentan-1-ol** was prepared from cyclopentene oxide and 2-propen-1-yl magnesium bromide.[10–12] ^{1}H-NMR ($CDCl_3$, 400 MHz) δ 1.15–1.29 (m, 1 H), 1.49–1.64 (m, 2 H), 1.66–1.84 (m, 2 H), 1.85–1.97 (m, 2 H), 2.03 (dt, J_d = 13.9 Hz, J_t =7.1 Hz, 1 H), 2.18 (dt, J_d = 14.0 Hz, J_t = 6.9 Hz, 1 H), 3.86 (q, J = 5.5 Hz, 1 H), 4.95–5.13 (m, 2 H), 5.77–5.93 (m, 1 H). The spectrum showed no resonance for the hydroxyl proton. ^{13}C-NMR ($CDCl_3$, 100 MHz) δ 21.6, 29.7, 34.3, 38.1, 47.6, 78.7, 115.6, 137.6.

A4.2 ***cis*-2-(Prop-2-en-1-yl)-cyclopentan-1-ol**. A solution of *p*-nitrobenzoic acid (7.35 g, 44.0 mmol), *trans*-2-(prop-2-en-1-yl)-cyclopentan-1-ol (2.06 g, 16.3 mmol), and triphenylphosphine (12.9 g, 49.0 mmol) in benzene (80 mL) was treated in a dropwise manner with diethyl azodicarboxylate (DEAD, 8.83 g, 49.0 mmol). The reaction mixture was stirred for four hours at 21 °C. The solvent was removed under reduced pressure to leave an oil, which was purified by column chromatography [diethyl ether/pentane = 1:20 (*v*/*v*)]. *cis-2-(Prop-2-en-1-yl)cyclopent-1-yl 4-nitrobenzoate* (3.58 g, 13.0 mmol, 80 %), yellowish liquid. R_f = 0.22 for diethyl ether/pentane = 1:20 (*v*/*v*). ^{1}H-NMR ($CDCl_3$, 600 MHz) δ 1.53–1.61 (m, 1 H), 1.64–1.73 (m, 1 H), 1.83–1.90 (m, 2 H), 1.91–1.98 (m, 1 H), 2.02–2.12 (m, 2 H), 2.16 (dt, J_d = 14.2, J_t = 7.3 Hz, 1 H), 2.31 (dt, J_d = 13.9, J_t = 7.0 Hz, 1 H), 4.92–5.01 (m, 2 H), 5.45 (t, J = 4.8 Hz, 1 H), 5.80 (ddt, J_d = 17.0, 10.1, J_t = 7.0 Hz, 1 H), 8.17–8.20 (m, 2 H), 8.27–8.31 (m, 2 H). ^{13}C-NMR ($CDCl_3$, 150 MHz) δ 22.0, 29.6, 32.5, 33.9, 44.3, 79.5, 115.6, 123.5, 130.5, 136.2, 137.1, 150.4, 164.2. Anal. Calcd. for $C_{15}H_{17}NO_4$ (275.31): C, 65.44; H, 6.22; N, 5.09; Found: C, 65.21; H, 6.30; N, 5.01. *cis*-2-(Prop-2-en-1-yl)cyclopent-1-yl 4-nitrobenzoate (3.44 g, 12.5 mmol) was dissolved in a solution of tetrahydrofuran/methanol [1:1 (*v*/*v*) (10 mL)] and cooled to 0 °C (ice bath). A solution of potassium hydroxide in methanol/water [1:1 (*v*/*v*) (1 M, 14 mL)] was added in one portion to the solution of the benzoate, while beeing cooled with an ice bath to 0 °C. The resulting mixture was stirred for ninety minutes at 22 °C. Dichloromethane (50 mL) was added and the resulting mixture was washed with a saturated aqueous solution sodium hydrogen carbonate (25 mL) and subsequently with brine (25 mL). The organic solvent was removed under reduced pressure (600 mbar/40 °C) to leave an oil, which was purified by chromatography [diethyl ether/pentane = 1:2 (*v*/*v*)]. Yield 1.19 g (9.43 mmol, 75%), colorless liquid. R_f = 0.32 for diethyl ether/pentane = 1:2 (*v*/*v*). ^{1}H-NMR ($CDCl_3$, 400 MHz) δ 1.30–1.46 (m, 2 H), 1.51–1.69 (m, 2 H), 1.69–1.90 (m, 4 H), 2.10–2.20 (m, 1 H), 2.21–

2.32 (m, 1 H), 4.12–4.21 (m, 1 H), 4.95–5.11 (m, 2 H), 5.87 (ddt, J_d = 17.1, 10.2, J_t = 6.9Hz, 1 H). ^{13}C-NMR ($CDCl_3$, 100 MHz) δ 21.9, 28.7, 33.7, 34.6, 45.2, 74.5, 115.0, 138.2. Anal. Calcd. for $C_8H_{14}O_4$ (126.20): C, 76.14; H, 11.28; Found: C, 75.72; H, 11.23.

A4.3 ***trans*-2-(3-Methylbut-2-en-1-yl)-cyclopentan-1-ol** was prepared from cyclopentanone, following the procedure of Streinz and Romaňuk.[13] Separation of *cis*- and *trans*-cyclopentanols was achieved by column chromatography, using diethyl ether/pentane = 1:3 (*v*/*v*) as eluent. *cis-2-(3-methylbut-2-en-1-yl)-cyclopentan-1-ol*. R_f = 0.31. *trans-2-(3-methylbut-2-en-1-yl)-cyclopentan-1-ol*. R_f = 0.19. ^{1}H-NMR ($CDCl_3$, 400 MHz) δ 1.20 (dq, J_d = 12.6, J_q = 7.9 Hz, 1 H), 1.48–1.64 (m, 5 H), 1.65–1.78 (m, 5 H), 1.82–1.99 (m, 3 H), 2.04–2.16 (m, 1 H), 3.83 (q, *J* = 5.8 Hz, 1 H), 5.18 (t, *J* = 7.2 Hz, 1 H). The spectrum showed no resonance for the hydroxyl proton. ^{13}C-NMR ($CDCl_3$, 100 MHz) δ 17.8, 21.6, 25.8, 29.7, 31.9, 34.2, 48.6, 78.8, 123.0, 132.5.

A4.4 ***trans*-2-(Prop-2-en-1-yl)-cyclohexan-1-ol** was prepared from cyclohexene oxide and 2-propen-1-yl magnesium bromide, according to the method described by Chandrasekaran and co-workers.[10,14,15] ^{1}H-NMR ($CDCl_3$, 400 MHz) δ 0.85–1.02 (m, 1 H), 1.09–1.40 (m, 4 H), 1.57–1.82 (m, 4 H), 1.88–2.04 (m, 2 H), 2.37–2.52 (m, 1 H), 3.26 (td, J_t = 9.8, J_d = 4.5 Hz, 1 H), 4.97–5.11 (m, 2 H), 5.85 (ddt, J_d = 17.2, 10.0, J_t = 7.3 Hz, 1 H). ^{13}C-NMR ($CDCl_3$, 100 MHz) δ 24.9, 25.5, 30.4, 35.5, 37.5, 44.9, 74.6, 116.0, 137.5.

A4.5 ***cis*-2-(Prop-2-en-1-yl)-cyclohexan-1-ol** was prepared from *trans*-2-(prop-2-en-1-yl)-cyclohexan-1-ol[15] (317 mg, 2.26 mmol) by inverting the configuration at the hydroxyl carbon, according to the procedure described in section 4.2. Reaction time: one hour. Eluent for column chromatography [diethyl ether/pentane = 1:10 (*v*/*v*), R_f = 0.47]. *cis-2-(Prop-2-en-1-yl)-cyclohexan-1-yl 4-nitrobenzoate*: 410 mg (1.42 mmol, 63 %), colorless crystals. M.p. 62–64 °C. ^{1}H-NMR ($CDCl_3$, 600 MHz) δ 1.32–1.41 (m, 1 H), 1.49–1.61 (m, 4 H), 1.66–1.76 (m, 2 H), 1.77–1.83 (m, 1 H), 1.99–2.09 (m, 2 H), 2.09–2.16 (m, 1 H), 4.94 (d, *J* = 17.1 Hz, 1 H), 4.98 (d, *J* = 10.1 Hz, 1 H), 5.28–5.33 (m, 1 H), 5.76 (ddt, J_d = 17.1, 10.1, J_t = 7.0, Hz, 1 H), 8.22 (d, *J* = 9.2 Hz, 2 H), 8.31 (d, *J* = 9.2 Hz, 2 H). ^{13}C-NMR ($CDCl_3$, 63 MHz) δ 21.0, 25.0, 27.4, 30.1, 36.9, 40.2, 74.0, 116.4, 123.6, 130.6, 136.2, 136.3, 150.4, 164.0. Anal. Calcd. for $C_{16}H_{19}NO_4$ (289.33): C, 66.42; H, 6.62; N, 4.84; Found: C, 66.55; H, 6.73; N, 4.86. *cis-2-(Prop-2-en-1-yl)-*

cyclohexan-1-ol ^{1}H-NMR ($CDCl_3$, 400 MHz) δ 1.15–1.27 (m, 1 H), 1.28–1.69 (m, 8 H), 1.70–1.79 (m, 1 H), 1.98 (dt, *J* = 14.1, 7.2 Hz, 1 H), 2.14 (dt, *J* = 14.0, 7.0 Hz, 1 H), 3.80–3.90 (m, 1 H), 4.92–5.06 (m, 2 H), 5.78 (ddt, *J* = 17.1, 10.0, 7.2, 7.2 Hz, 1 H). ^{13}C-NMR ($CDCl_3$, 100 MHz) δ 20.4, 25.0, 26.3, 32.9, 36.5, 41.2, 69.0, 115.6, 137.4. Anal. Calcd. for $C_9H_{16}O_4$ (140.22): C, 77.09; H, 11.50; Found: C, 76.90; H, 11.59.

A4.6 *cis*-[2-(Ethenyl)-cyclohex-1-yl]-methanol[16] was prepared from *cis*-8-oxabicyclo-[4.3.0]nonan-7-ol, obtained by the method of Lambert and co-workers as single diastereomer, and subsequent Wittig-alkenylation. ^{1}H-NMR ($CDCl_3$, 400 MHz) δ 1.27–1.81 (m, 10 H), 2.48 (dq, J_d = 8.6, J_q = 4.1 Hz, 1 H), 3.36–3.58 (m, 2 H), 4.97–5.15 (m, 2 H), 6.05 (ddd, *J* = 17.1, 10.2, 8.9 Hz, 1 H). ^{13}C-NMR ($CDCl_3$, 100 MHz) δ 22.3, 25.0, 25.2, 30.9, 41.0, 42.5, 65.5, 115.1, 139.3.

A4.7 *trans*-[2-(Ethenyl)-cyclohex-1-yl]-methanol. A solution of *trans*-1,2-cyclohexane-dicarboxylic acid anhydride (5.00 g, 32.4 mmol) in tetrahydrofuran (15 mL) was added in a dropwise manner to a suspension of sodium borohydride (2.49 g, 65.8 mmol) in tetrahydrofuran (75 mL) at 0 °C. The reaction mixture was stirred for three hours in an ice bath, which was allowed to thaw (temperature of the ice bath after 3 hours: 15 °C). This mixture was cooled to 0 °C and *slowly* treated with methanol (10 mL). The rate of methanol addition thereby is crucial to prevent extensive gas evolution. The likewise obtained mixture was concentrated under reduced pressure (300 mbar/ 40 °C) to leave a residue, which was taken up in a mixture of brine (100 mL) and ethyl acetate (65 mL), and cooled to 0 °C. An aqueous 2 M solution of hydrochloric acid (32 mL, 64 mmol) was added to this mixture at 0 °C. The phases were separated. The cold aqueous layer was extracted rapidly with ethyl acetate (3 × 50 mL). Combined organic layers were washed with brine (70 mL) and concentrated under reduced pressure (200 mbar/ 40 °C) to leave a colorless solid (4.31 g, 27.2 mmol, 84 %), which was recrystallized from ethyl acetate (20 mL). *trans-2-(Hydroxymethyl)-cyclohexanecarboxylic acid.*[17,18] Yield 3.33 g (21.0 mmol, 65 %), colorless crystals. M.p. 99–100 °C. ^{1}H-NMR (DMSO-d_6, 600 MHz) δ 0.94–1.04 (m, 1 H), 1.11–1.23 (m, 2 H), 1.28–1.37 (m, 1 H), 1.56 (tdt, J_t = 11.0, 3.8, J_d = 7.2 Hz, 1 H), 1.66 (d, *J* = 9.2 Hz, 2 H), 1.81 (d, *J* = 12.1 Hz, 2 H), 1.97 (td, J_t = 11.4, J_d = 3.7 Hz, 1 H), 3.16 (dd, *J* = 10.3, 7.0 Hz, 1 H), 3.34 (dd, *J* = 10.3, 4.0 Hz, 1 H), 4.34 (br. s., 1 H), 11.95 (br. s., 1 H). ^{13}C-NMR (DMSO-d_6, 150 MHz)

δ 25.0, 25.1, 28.1, 29.5, 41.0, 45.3, 64.1, 176.8. Anal. Calcd. for $C_8H_{14}O_3$ (158.20): C, 60.74; H, 8.92; Found: C, 60.44; H, 9.22. *trans*-2-(Hydroxymethyl)-cyclohexanecarboxylic acid was treated with a catalytic amount of *p*-toluenesulfonic acid monohydrate to afford *trans*-8-oxabicyclo[4.3.0]nonan-7-one,[8,19] which was reduced with DIBAL-H to furnish *trans*-8-oxabicyclo[4.3.0]nonan-7-ol[16] as mixture of the hydroxyaldehyde and stereoisomeric lactols. *Lactol – major stereoisomer*. ^{1}H-NMR ($CDCl_3$, 400 MHz) δ 0.95–2.04 (m, 9 H), 3.31 (dd, *J* = 10.8, 7.8 Hz, 1 H), 3.43–3.45 (m, 1 H), 4.09 (t, *J* = 7.3 Hz, 1 H), 5.30 (t, *J* = 4.0 Hz, 1 H). The spectrum displayed no resonance for the hydroxyl proton. ^{13}C-NMR ($CDCl_3$, 100 MHz) δ 24.8, 25.5, 25.6, 28.1, 40.4, 49.5, 72.5, 98.3. *Lactol – minor stereoisomer*. ^{1}H-NMR ($CDCl_3$, 400 MHz) δ 0.95–2.04 (m, 9 H), 3.58 (dd, *J* = 11.0, 7.6 Hz, 1 H), 3.90 (t, *J* = 7.0 Hz, 1 H), 4.04–4.07 (m, 1 H), 5.07 (dd, *J* = 7.1, 5.9 Hz, 1 H). The spectrum displayed no resonance for the hydroxyl proton.^{13}C-NMR ($CDCl_3$, 100 MHz) δ 25.5, 25.6, 26.5, 27.4, 44.4, 52.3, 71.4, 102.5. *Hydroxyaldehyde*. ^{1}H-NMR ($CDCl_3$, 400 MHz) δ 0.95–2.04 (m, 10 H), 3.42–3.49 (m, 1 H), 3.55–3.60 (m, 1 H), 9.58 (d, *J* = 7.1, 5.9 Hz, 1 H). The spectrum displayed no resonance for the hydroxyl proton. ^{13}C-NMR ($CDCl_3$, 100 MHz) δ 24.8, 24.9, 25.8, 27.7, 39.9, 53.6, 66.6, 205.4. Wittig-alkenylation of *trans*-8-oxabicyclo[4.3.0]nonan-7-ol[16] in extension to the method described for the cis-isomer[16] in section 4.6 furnished *trans-[2-(ethenyl)-cyclohex-1-yl]-methanol.* ^{1}H-NMR ($CDCl_3$, 400 MHz) δ 0.98–1.37 (m, 5 H), 1.52–1.87 (m, 6 H), 3.43 (dd, *J* = 11.0, 5.8 Hz, 1 H), 3.60 (dd, *J* = 10.9, 4.7 Hz, 1 H), 4.95 (dd, *J* = 10.1, 2.0 Hz, 1 H), 5.03 (dd, *J* = 17.2, 2.0 Hz, 1 H), 5.70 (dt, J_d = 17.2, J_t = 9.6 Hz, 1 H). ^{13}C-NMR ($CDCl_3$, 100 MHz) δ 25.7, 25.8, 29.1, 33.4, 44.3, 45.9, 67.1, 114.0, 143.8. Anal. Calcd. for $C_9H_{16}O$ (140.22): C, 77.09; H, 11.50; Found: C, 76.54; H, 11.56.

A4.8 *cis*-[2-(Methylprop-1-en-1-yl)-cyclohex-1-yl]-methanol was prepared in extension to the method described by Lambert[16] for *cis*-[2-(ethenyl)-cyclohex-1-yl]-methanol. In an atmosphere of nitrogen, isopropyltriphenylphosphonium bromide (2.90 g, 7.53 mmol) was suspended in dry tetrahydrofuran (30 mL) and cooled to 0 °C. *n*-Butyl lithium (4.7 mL, 7.52 mmol, 1.6 M in hexane) was added to this mixture in one portion at 0 °C. The resulting deep red-colored suspension was stirred for two and a half hours at 21 °C. Meanwhile *cis*-8-oxabicyclo[4.3.0]nonan-7-ol, was dissolved in dry tetrahydrofuran (20 mL) and treated at –78 °C with a solution of *n*-butyl lithium (3.0 mL, 4.8 mmol) in hexane (1.6 M). The reaction mixture was afterwards allowed to warm for three minutes to 0 °C, and was then cooled to

–78 °C again. To this mixture was added in a dropwise manner the solution of 2-propylidene triphenylphosphine in tetrahydrofuran within twenty-five minutes. The cooling bath was removed after complete addition of the phosphorous reagent, and the reaction mixture is allowed to warm to 21 °C. The reaction mixture was stirred for additional 5 hours at room temperature and then treated with a saturated aqueous ammonium chloride solution (40 mL) and water (40 mL). Phases were separated. The aqueous layer was extracted with diethyl ether (2 × 20 mL). Combined organic layers were washed with brine (60 mL) and concentrated under reduced pressure (800 mbar/ 40 °C) to afford an oily residue, which was purified by chromatography [diethyl ether/pentane = 1:1 (*v*/*v*)]. Yield: 679 mg (4.03 mmol, 80 %) colorless oil. R_f = 0.39 for diethyl ether/pentane = 1:1 (*v*/*v*). ^{1}H-NMR ($CDCl_3$, 400 MHz) δ 1.26–1.38 (m, 2 H), 1.40–1.57 (m, 6 H), 1.64 (d, *J* = 1.2 Hz, 3 H), 1.67–1.75 (m, 2 H), 1.71 (d, *J* = 0.9 Hz, 3 H), 2.65–2.73 (m, 1 H), 3.38–3.48 (m, 2 H), 5.35 (dt, J_d = 10.1, J_t = 1.2 Hz, 1 H). ^{13}C-NMR ($CDCl_3$, 100 MHz) δ 17.8, 22.1, 24.7, 25.3, 26.2, 31.7, 34.4, 43.0, 66.1, 124.1, 132.2. Anal. Calcd. for $C_{11}H_{20}O$ (168.28): C, 78.51; H, 11.98; Found: C, 78.26; H, 11.88.

A4.9 ***trans*-[2-(Methylprop-1-en-1-yl)-cyclohex-1-yl]-methanol** was prepared according to the procedure outlined in section 4.7 for the cis-isomer. ^{1}H-NMR ($CDCl_3$, 400 MHz) δ 1.00–1.12 (m, 2 H), 1.19–1.32 (m, 3 H), 1.49–1.60 (m, 2 H), 1.63 (d, *J* = 1.6 Hz, 3 H), 1.67–1.83 (m, 3 H), 1.63 (d, *J* = 1.6 Hz, 3 H), 1.98 (qd, J_q = 10.5, J_d = 3.8 Hz, 1 H), 3.32–3.41 (m, 1 H), 3.56 (dd, *J* = 10.8, 5.0 Hz, 1 H), 4.96–5.02 (m, 1 H). ^{13}C-NMR ($CDCl_3$, 100 MHz) δ 18.1, 25.8 (2C/HMQC), 25.9, 29.3, 33.4, 40.1, 45.2, 67.8, 130.0, 131.2. Anal. Calcd. for $C_{11}H_{20}O$ (168.28): C, 78.51; H, 11.98; Found: C, 78.15; H, 12.07.

A4.10 2-(1-Methylenecyclohex-2-yl)-ethan-1-ol was prepared from cyclohexanone according to the method reported by Segre[20] and Gream[21], and respective co-workers. ^{1}H-NMR ($CDCl_3$, 400 MHz) δ 1.24–1.35 (m, 1 H), 1.40–1.58 (m, 4 H), 1.60–1.78 (m, 3 H), 1.85–1.97 (m, 1 H), 1.98–2.09 (m, 1 H), 2.17–2.29 (m, 2 H), 3.66 (t, *J* = 6.6 Hz, 2 H), 4.60 (s, 1 H), 4.66 (s, 1 H). ^{13}C-NMR ($CDCl_3$, 100 MHz) δ 23.9, 28.7, 33.9, 34.4, 35.0, 39.8, 61.4, 105.9, 152.6.

A4.11 (1-Methylcyclohex-1-en-4-yl)-methanol was prepared from 2-methylbuta-1,3-diene (isoprene) and methyl acrylate in a Diels-Alder-reaction as described by Inukai and Kasai[22], and reduction of *O*-methyl-(1-methylcyclohex-1-en-4-yl)-carboxylate by $LiAlH_4$ according to Monti and co-workers.[23] ^{1}H-NMR ($CDCl_3$, 400 MHz) δ 1.15–1.35 (m, 1 H), 1.39 (s, 1 H), 1.61–1.90 (m, 3 H), 1.65 (s, 3 H), 1.91–2.20 (m, 3 H), 3.41–3.63 (m, 2 H), 5.38 (br. s., 1 H). ^{13}C-NMR ($CDCl_3$, 100 MHz) δ 23.6, 25.6, 28.2, 29.5, 36.2, 67.9, 119.8, 134.1.

A4.12 2-{(1*S*,4*S*,5*R*)-2,6,6-Trimethylbicyclo[3.1.1]hept-2-en-4-yl}-ethanol (verbenylethanol) was prepared by converting (*S*)-*cis*-verbenol into 2-{(1*S*,4*S*,5*R*)-2,6,6-trimethylbicyclo[3.1.1]hept-2-en-4-yl}-ethenyl ether[24,25] {$[\alpha]_D^{25}$ = 98.0 (*c* = 1.02/ethanol)}, followed by [1.3] sigmatropic rearrangement of the vinyl ether into 2-{(1*S*,4*S*,5*R*)-2,6,6-trimethylbicyclo[3.1.1]hept-2-en-4-yl}-ethanal[26,27] {$[\alpha]_D^{25}$ = –74.6 (*c* = 1.03/ethanol)}, and reduction of this aldehyde as follows. A suspension of 2-{(1*S*,4*S*,5*R*)-2,6,6-trimethylbicyclo[3.1.1]hept-2-en-4-yl}-ethanal (650 mg, 3.63 mmol), lithium aluminium hydride (207 mg, 5.50 mmol) and diethyl ether (20 mL) was stirred for one hour at 20 °C, and carefully hydrolyzed by an aqueous solution of 2 M hydrochloric acid (10 mL). After phase separation, the aqueous layer was extracted with diethyl ether (3 × 20 mL). The organic phases from the reaction

mixture and combined organic washings were combined and concentrated under reduced pressure to leave a residue, which was purified by chromatography [diethyl ether/pentane = 1:1 (*v*/*v*), (R_f = 0.40)]. Yield: 480 mg (2.66 mmol, 73 %) colorless oil. $[\alpha]_D^{25}$ = –85.8 (*c* = 1.03/ethanol). ^{1}H-NMR ($CDCl_3$, 400 MHz) δ 0.85 (s, 3 H), 1.13 (d, *J* = 8.9 Hz, 1 H), 1.28 (s, 3 H), 1.33–1.45 (m, 1 H), 1.49–1.61 (m, 1 H), 1.63–1.69 (m, 4 H), 1.89–1.99 (m, 2 H), 2.18 (dt, J_d = 8.7, J_t = 5.7 Hz, 1 H), 2.31–2.42 (m, 1 H), 3.71 (t, *J* = 6.8 Hz, 2 H), 5.14 (br. s., 1 H). ^{13}C-NMR ($CDCl_3$, 100 MHz) δ 20.4, 22.9, 26.5, 27.9, 36.3, 36.6, 40.6, 45.1, 47.6, 61.3, 112.0, 144.8. Anal. Calcd. for $C_{12}H_{20}O$ (180.29): C, 79.94; H, 11.18; Found: C, 79.95; H, 11.08.

A5 4-Toluenesulfonic Acid *O*-Esters from Alkenols

A5.1 General method. A solution of an alkenol (1 mmol), 1.4-diazabicyclo[2.2.2]octane (DABCO, 2 mmol) in dichloromethane (2 mL) was cooled in an ice-bath to 0 °C and treated with 4-toluenesulfonyl chloride (1.5 mmol) in portions over a period of 5 min. The slurry was stirred for 2 hours at 20 °C and diluted with dichloromethane (8 mL) to afford a suspension which was washed with aqueous 2 M aqueous hydrochloric acid (10 mL) and a saturated aqueous solution of $NaHCO_3$ (10 mL). The organic layer was separated, dried ($MgSO_4$), and concentrated under reduced pressure. The remaining oil was purified by chromatography (SiO_2).

A5.2 *trans*-[2-(Prop-2-en-1-yl)-cyclopent-1-yl] 4-toluenesulfonate[28] was prepared from *trans*-2-(prop-2-en-1-yl)cyclopentan-1-ol (545 mg, 4.32 mmol) according to procedure 5.1. Eluent used for chromatographic purification: diethyl ether/pentane = 1:3 (*v*/*v*). Yield: 1.16 g (4.14 mmol, 96 %), colorless liquid. R_f = 0.53 for diethyl ether/pentane = 1:3 (*v*/*v*). ^{1}H-NMR ($CDCl_3$, 400 MHz) δ 1.13–1.23 (m, 1 H), 1.52–1.64 (m, 1 H), 1.64–1.73 (m, 1 H), 1.74–1.81 (m, 2 H), 1.81–1.92 (m, 2 H), 1.99–2.14 (m, 2 H), 2.44 (s, 3 H), 4.48–4.57 (m, 1 H), 4.84–4.94 (m, 2 H), 5.48–5.67 (m, 1 H), 7.33 (d, *J* = 8.3 Hz, 2 H), 7.78 (d, *J* = 8.3 Hz, 2 H). ^{13}C-NMR ($CDCl_3$, 150 MHz) δ 21.6, 22.2, 28.9, 31.9, 36.8, 45.1, 88.4, 116.3, 127.8, 129.7, 134.3, 135.9, 144.4. Anal. Calcd. for $C_{15}H_{20}O_3S$ (280.38): C, 64.26; H, 7.19; S, 11.43; Found: C, 64.42; H, 7.02; S, 11.36.

A5.3 *cis*-[2-(Prop-2-en-1-yl)-cyclopent-1-yl] 4-toluenesulfonate was prepared from *cis*-2-(prop-2-en-1-yl)cyclopentan-1-ol (1.05 g, 8.32 mmol) according to procedure 5.1. Eluent used for chromatographic purification: diethyl ether/pentane = 1:3 (*v*/*v*). Yield: 1.87 g (6.69 mmol, 80 %), colorless liquid. R_f = 0.49 for diethyl ether/pentane = 1:3 (*v*/*v*). ^{1}H-NMR ($CDCl_3$, 400 MHz) δ 1.34–1.47 (m, 1 H), 1.51–1.61 (m, 1 H), 1.69–1.91 (m, 5 H), 1.98–2.09 (m, 1 H), 2.11–2.20 (m, 1 H), 2.44 (s, 3 H), 4.86–4.97 (m, 3 H), 5.59–5.72 (m, 1 H), 7.33 (d, *J* = 8.0 Hz, 2 H), 7.78 (d, *J* = 8.4 Hz, 2 H). ^{13}C-NMR ($CDCl_3$, 100 MHz) δ 21.4, 21.6, 28.6, 32.5, 33.3, 45.0, 86.8, 115.6, 127.7, 129.7, 134.5, 136.8, 144.4. Anal. Calcd. for $C_{15}H_{20}O_3S$ (280.38): C, 64.26; H, 7.19; S, 11.43; Found: C, 64.37; H, 7.03; S, 11.49.

A5.4 *trans*-[2-(3-Methylbut-2-en-1-yl)-cyclopent-1-yl] 4-toluenesulfonate was prepared from 2-(3-methylbut-2-en-1-yl)-cyclopentan-1-ol (2.00 g, 13.0 mmol) according to procedure 5.1. Eluent used for chromatographic purification: diethyl ether/pentane = 1:5 (*v*/*v*). Yield: 2.76 g (8.95 mmol, 69 %), colorless liquid. R_f = 0.36 for diethyl ether/pentane = 1:5 (*v*/*v*). ^{1}H-NMR ($CDCl_3$, 600 MHz) δ 1.13–1.20 (m, 1 H), 1.50 (s, 3 H), 1.55–1.64 (m, 1 H), 1.63 (s, 3 H), 1.65–1.72 (m, 1 H), 1.72–1.77 (m, 1 H), 1.77–1.81 (m, 2 H), 1.82–1.89 (m, 1 H), 1.93 (dt, J_d = 14.3, J_t = 7.1 Hz, 1 H), 1.98–2.05 (m, 1 H), 2.44 (s, 3 H), 4.49–4.53 (m, 1 H), 4.89 (s, 1 H), 7.33 (d, *J* = 8.5 Hz, 2 H), 7.78 (d, *J* = 8.5 Hz, 2 H). ^{13}C-NMR ($CDCl_3$, 100 MHz) δ 17.7, 21.6, 22.2, 25.7, 29.0, 30.9, 32.0, 46.0, 88.8, 121.7, 127.8, 129.7, 133.0, 134.4, 144.3. Anal. Calcd. for $C_{17}H_{24}O_3S$ (308.43): C, 66.20; H, 7.48; S, 10.39; Found: C, 66.35; H, 7.96; S, 10.03.

A5.5 *trans*-[2-(Prop-2-en-1-yl)-cyclohex-1-yl 4-toluenesulfonate[28] was prepared from *trans*-2-(prop-2-en-1-yl)-cyclohexan-1-ol (3.82 g, 27.2 mmol) according to procedure 5.1. Eluent used for chromatographic purification: diethyl ether/pentane = 1:3 (*v*/*v*). Yield: 6.72 g (22.8 mmol, 84 %), colorless liquid. R_f = 0.52 for diethyl ether/pentane = 1:3 (*v*/*v*). ^{1}H-NMR ($CDCl_3$, 400 MHz) δ 0.91–1.00 (m, 1 H), 1.14 (qt, J_q = 12.4, J_t = 3.5 Hz, 1 H), 1.24 (qt, J_q = 12.6, J_t = 3.4 Hz, 1 H), 1.40–1.48 (m, 1 H), 1.51–1.61 (m, 2 H), 1.66–1.75 (m, 2 H), 1.81–1.87 (m, 1 H), 1.95–2.01 (m, 1 H), 2.26–2.32 (m, 1 H), 2.44 (s, 3 H), 4.26 (td, J_t = 10.0, J_d = 4.4 Hz, 1 H), 4.90–4.99 (m, 2 H), 5.61 (dddd, *J* = 17.0, 10.3, 7.9, 6.5 Hz, 1 H), 7.33 (d, *J* = 7.9 Hz, 2 H), 7.80 (d, *J* = 8.2 Hz, 2 H). ^{13}C-NMR ($CDCl_3$, 100 MHz) δ 21.6, 24.3, 24.4, 29.7, 32.5, 36.1, 41.8, 85.6, 116.7, 127.6, 129.7, 134.7, 135.7, 144.4. Anal. Calcd. for $C_{16}H_{22}O_3S$ (294.41): C, 65.27; H, 7.53; S, 10.89; Found: C, 65.23; H, 7.52; S, 10.95.

A5.6 *cis*-[2-(Prop-2-en-1-yl)-cyclohexyl-1-yl 4-toluenesulfonate was prepared from *cis*-2-(prop-2-en-1-yl)-cyclohexan-1-ol (990 mg, 7.06 mmol) according to procedure 5.1. Eluent used for chromatographic purification: diethyl ether/pentane = 1:3 (*v*/*v*). Yield: 1.81 g (6.15 mmol, 87 %), colorless liquid. R_f = 0.46 for diethyl ether/pentane = 1:3 (*v*/*v*). Eluent used for chromatographic purification: diethyl ether/pentane = 1:3 (*v*/*v*), R_f = 0.46. ^{1}H-NMR ($CDCl_3$, 400 MHz) δ 1.16–1.27 (m, 1 H), 1.30–1.44 (m, 3 H), 1.46–1.55 (m, 3 H), 1.61–1.68 (m, 1 H), 1.84–2.02 (m, 3 H), 2.44 (s, 3 H), 4.77 (br. s., 1 H), 4.89–4.96 (m, 2 H), 5.62 (ddt, J_d = 17.2, 10.1, J_t = 7.1 Hz, 1 H), 7.32 (d, *J* = 8.2 Hz, 2 H), 7.80 (d, *J* = 8.2 Hz, 2 H). ^{13}C-NMR ($CDCl_3$, 100 MHz) δ 20.3, 21.6, 24.4, 26.3, 30.6, 30.0, 40.9, 82.5, 116.4, 127.6, 129.6, 134.8, 136.2,

144.3. Anal. Calcd. for $C_{16}H_{22}O_3S$ (294.41): C, 65.27; H, 7.53; S, 10.89; Found: C, 65.48; H, 7.38; S, 10.95.

A5.7 ***trans*-[2-(Ethenyl)-cyclohex-1-yl]-methyl 4-toluenesulfonate**[29] was prepared from *trans*-[2-(ethenyl)-cyclohex-1-yl]-methanol (365 mg, 2.60 mmol) according to procedure 5.1. Eluent used for chromatographic purification: diethyl ether/pentane = 1:3 (*v*/*v*). Yield: 682 mg (2.32 mmol, 89 %), colorless liquid. R_f = 0.52 for diethyl ether/pentane = 1:3 (*v*/*v*). ^{1}H-NMR ($CDCl_3$, 600 MHz) δ 1.04–1.25 (m, 4 H), 1.42 (tdt, J_t = 11.1, 3.4, J_d = 7.1, 1 H), 1.64–1.75 (m, 3 H), 1.77–1.85 (m, 2 H), 2.46 (s, 3 H), 3.82 (dd, *J* = 9.4, 6.7 Hz, 1 H), 4.05 (dd, *J* = 9.4, 3.2 Hz, 1 H), 4.86–4.93 (m, 2 H), 5.49 (ddd, *J* = 17.0, 10.3, 9.1 Hz, 1 H), 7.35 (d, *J* = 8.2 Hz, 2 H), 7.78 (d, *J* = 8.2 Hz, 2 H). ^{13}C-NMR ($CDCl_3$, 100 MHz) δ 21.6, 25.4 (2C/ HMQC), 28.8, 33.2, 41.0, 44.1, 73.6, 115.1, 127.9, 129.7, 133.1, 141.5, 144.5. Anal. Calcd. for $C_{16}H_{22}O_3S$ (294.41): C, 65.27; H, 7.53; S, 10.89; Found: C, 65.38; H, 7.47; S, 10.82.

A5.8 ***cis*-[2-(Ethenyl)-cyclohex-1-yl]-methyl 4-toluenesulfonate** was prepared from *cis*-[2-(ethenyl)-cyclohexan-1-yl]-methanol (365 mg, 2.60 mmol) according to procedure 5.1. Eluent used for chromatographic purification: diethyl ether/pentane = 1:3 (*v*/*v*). Yield: 682 mg (2.32 mmol, 89 %), colorless liquid. R_f = 0.52 for diethyl ether/pentane = 1:3 (*v*/*v*). ^{1}H-NMR ($CDCl_3$, 400 MHz) δ 1.15–1.34 (m, 2 H), 1.36–1.55 (m, 5 H), 1.57–1.66 (m, 1 H), 1.90 (dtt, J_d = 10.5, J_t = 7.2, 3.8 Hz, 1 H), 2.37–2.46 (m, 4 H), 3.75–3.88 (m, 2 H), 4.89–4.99 (m, 2 H), 5.75–5.90 (m, 1 H), 7.32 (d, *J* = 7.8 Hz, 2 H), 7.76 (d, *J* = 8.3 Hz, 2 H). ^{13}C-NMR ($CDCl_3$, 100 MHz) δ 21.6, 21.8, 24.4, 24.6, 30.4, 39.0, 40.2, 72.5, 116.3, 127.8, 129.7, 133.1, 137.1, 144.5. Anal. Calcd. for $C_{16}H_{22}O_3S$ (294.41): C, 65.27; H, 7.53; S, 10.89; Found: C, 65.24; H, 7.52; S, 10.92.

A5.9 ***trans*-[2-(Methylprop-1-en-1-yl)-cyclohex-1-yl]-methyl 4-toluenesulfonate** was prepared from *trans*-[2-(methylprop-1-en-1-yl)-cyclohex-1-yl]-methanol (1.54 g, 9.15 mmol) according to procedure 5.1. Eluent used for chromatographic purification: diethyl ether/pentane = 1:5 (*v*/*v*). Yield: 2.73 g (8.46 mmol, 92 %), colorless liquid. R_f = 0.41 for Eluent used for chromatographic purification: diethyl ether/pentane = 1:5 (*v*/*v*), R_f = 0.41 diethyl ether/pentane = 1:5 (*v*/*v*) . ^{1}H-NMR ($CDCl_3$, 400 MHz) δ 0.97–1.12 (m, 2 H), 1.13–1.23 (m, 2 H), 1.26–1.37 (m, 1 H), 1.51 (d, *J* = 1.5 Hz, 3 H), 1.54–1.62 (m, 1 H), 1.60 (d, *J* = 1.5 Hz, 3

H), 1.63–1.73 (m, 2 H), 1.74–1.80 (m, 1 H), 1.90–2.00 (m, 1 H), 2.44 (s, 3 H), 3.75 (dd, *J* = 9.3, 6.8 Hz, 1 H), 3.97 (dd, *J* = 9.2, 3.1 Hz, 1 H), 4.71–4.76 (m, 1 H), 7.33 (d, *J* = 8.1 Hz, 2 H), 7.75 (d, *J* = 8.3 Hz, 2 H). ^{13}C-NMR ($CDCl_3$, 100 MHz) δ 18.0, 21.6, 25.5, 25.6, 25.7, 29.0, 33.2, 38.2, 42.1, 73.9, 127.9, 128.2, 129.6, 132.0, 133.1, 144.4. Anal. Calcd. for $C_{18}H_{26}O_3S$ (322.46): C, 67.05; H, 8.13; S, 9.94; Found: C, 66.79; H, 8.10; S, 9.96.

A5.10 *cis*-[2-(Methylprop-1-en-1-yl)-cyclohex-1-yl]-methyl 4-toluenesulfonate was prepared from *cis*-[2-(methylprop-1-en-1-yl)-cyclohex-1-yl]-methanol (631 mg, 3.75 mmol) according to procedure 5.1. Eluent used for chromatographic purification: diethyl ether/pentane = 1:1 (*v*/*v*). Yield: 1.10 g (3.40 mmol, 91 %), colorless liquid. R_f = 0.59 for diethyl ether/pentane = 1:1 (*v*/*v*). ^{1}H-NMR ($CDCl_3$, 400 MHz) δ 1.17–1.31 (m, 2 H), 1.35–1.48 (m, 5 H), 1.55 (s, 3 H), 1.59–1.69 (m, 1 H), 1.63 (s, 3 H), 1.87 (ddt, J_d = 10.8, 7.2, J_t = 3.5 Hz, 1 H), 2.44 (s, 3 H), 2.56–2.69 (m, 1 H), 3.79 (d, *J* = 7.3 Hz, 2 H), 5.16 (d, *J* = 10.0 Hz, 1 H), 7.33 (d, *J* = 8.1 Hz, 2 H), 7.75 (d, *J* = 8.1 Hz, 2 H). ^{13}C-NMR ($CDCl_3$, 100 MHz) δ 17.9, 21.59, 21.62, 24.1, 24.8, 26.1, 31.4, 33.8, 39.7, 73.2, 122.4, 127.8, 129.7, 133.22, 133.23, 144.4. Anal. Calcd. for $C_{18}H_{26}O_3S$ (322.46): C, 67.05; H, 8.13; S, 9.94; Found: C, 67.10; H, 8.00; S, 9.87.

A5.11 2-(1-Methylenecyclohex-2-yl)-eth-1-yl 4-toluenesulfonate[30] was prepared from 2-(1-methylenecyclohex-2-yl)-ethan-1-ol (1.89 g, 13.5 mmol) according to procedure 5.1. Eluent used for chromatographic purification: diethyl ether/pentane = 1:3 (*v*/*v*). Yield: 3.80 g (12.9 mmol, 95 %), colorless liquid. R_f = 0.48 for diethyl ether/pentane = 1:3 (*v*/*v*). ^{1}H-NMR ($CDCl_3$, 600 MHz) δ 1.16–1.24 (m, 1 H), 1.37–1.50 (m, 2 H), 1.52–1.67 (m, 4 H), 1.92–2.00 (m, 2 H), 2.10–2.17 (m, 2 H), 2.45 (s, 3 H), 4.00–4.10 (m, 2 H), 4.42 (s, 1 H), 4.61 (s, 1 H), 7.34 (d, *J* = 8.2 Hz, 2 H), 7.78 (d, *J* = 8.2 Hz, 2 H). ^{13}C-NMR ($CDCl_3$, 150.9 MHz) δ 21.6, 23.8, 28.5, 31.1, 33.4, 34.3, 38.9, 69.0, 106.4, 127.9, 129.8, 133.1, 144.7, 150. Anal. Calcd. for $C_{16}H_{22}O_3S$ (294.41): C, 65.27; H, 7.53; S, 10.89; Found: C, 65.52; H, 7.43; S, 10.76.

A5.12 (1-Methylcyclohex-1-en-4-yl)-methyl 4-toluenesulfonate was prepared from 1-(methylcyclohex-1-en-4-yl)-methanol (257 mg, 2.03 mmol) according to procedure 5.1. Eluent used for chromatographic purification: diethyl ether/pentane = 1:7 (*v*/*v*). Yield: 493 mg (1.76 mmol, 86 %), colorless liquid. R_f = 0.25 for diethyl ether/pentane = 1:7 (*v*/*v*). ^{1}H-NMR ($CDCl_3$, 400 MHz) δ 1.21–1.33 (m, 1 H), 1.54–1.77 (m, 2 H), 1.60 (s, 3 H), 1.81–2.09

(m, 4 H), 2.45 (s, 3 H), 3.89 (d, *J* = 6.7 Hz, 2 H), 5.22–5.33 (m, 1 H), 7.34 (d, *J* = 8.2 Hz, 2 H), 7.79 (d, *J* = 8.2 Hz, 2 H). ^{13}C-NMR ($CDCl_3$, 150 MHz) δ 21.6, 23.4, 25.0, 27.7, 28.8, 32.9, 74.4, 118.9, 127.8, 129.8, 133.0, 134.0, 144.6. Anal. Calcd. for $C_{15}H_{20}O_3S$ (280.38): C, 64.26; H, 7.19; S, 11.43; Found: C, 64.33; H, 6.85; S, 11.13.

A5.13 2-{(1*S*,4*S*,5*R*)-2,6,6-Trimethylbicyclo[3.1.1]hept-2-en-4-yl}-ethyl 4-toluenesulfonate was prepared from 2-[{(1*S*,4*S*,5*R*)-2,6,6-trimethylbicyclo[3.1.1]hept-2-en-4-yl]}-ethan-1-ol (440 mg, 2.44 mmol) according to procedure 5.1. Eluent used for chromatographic purification: diethyl ether/pentane = 1:1 (*v*/*v*). Yield: 690 mg (2.06 mmol, 85 %), yellowish liquid. R_f = 0.71 for diethyl ether/pentane = 1:1 (*v*/*v*). $[\alpha]_D^{25}$ = –38.9 (*c* = 1.01/ethanol). ^{1}H-NMR ($CDCl_3$, 400 MHz) δ 0.78 (s, 3 H), 0.99–1.06 (m, 1 H), 1.23 (s, 3 H), 1.53–1.64 (m, 1 H), 1.61 (s, 3 H), 1.64–1.79 (m, 2 H), 1.92 (t, *J* = 5.1 Hz, 1 H), 2.12 (dt, J_d = 8.9, J_t = 5.6 Hz, 1 H), 2.23–2.31 (m, 1 H), 2.45 (s, 3 H), 4.03–4.14 (m, 2 H), 4.94 (br. s., 1 H), 7.35 (d, *J* = 8.2 Hz, 2 H), 7.80 (d, *J* = 8.2 Hz, 2 H). ^{13}C-NMR ($CDCl_3$, 150.9 MHz) δ 20.4, 21.6, 22.9, 26.4, 27.7, 32.4, 35.9, 40.7, 44.6, 47.5, 69.1, 118.8, 127.9, 129.8, 133.2, 144.6, 145.6.

A6 Bromocyclization with *N*-Bromosuccinimide

A6.1 Bromocyclization of *trans*-2-(prop-2-en-1-yl)-cyclopentan-1-ol. A solution of *trans*-2-(prop-2-en-1-yl)-cyclopentan-1-ol (126 mg, 1.00 mmol) in dichloromethane (5 ml) was treated at room temperature in small portions with *N*-bromosuccinimide (267 mg, 1.50 mmol). The resulting suspension was stirred for 14 days at room temperature (~20 °C). Solids were filtrated off and the filtrate washed with an aqueous saturated solution of sodium thiosulfate (10 mL). The aqueous washing was extracted with petroleum ether (4 × 20 mL). Combined organic layers were dried ($MgSO_4$) and concentrated under reduced pressure to furnish a residue, which was purified by column chromatography on SiO_2 as stationary phase and a 9/1-mixture (*v*/*v*) of petroleum ether/diethyl ether as eluent. *1,4-trans-4,6-cis-4-Brom-2-oxabicyclo[4.3.0]nonane*. Yield 40 mg (20 %), yellow oil, R_f = 0.59 [petroleum ether /diethyl ether = 9/1 (*v*/*v*)]. ^{1}H-NMR ($CDCl_3$, 250 MHz): δ = 1.07–1.31 (m, 1 H), 1.36–1.81 (m, 6 H), 1.83–2.00 (m, 1 H), 2.49– 2.68 (m, 1 H), 3.14–3.29 (m, 1 H), 3.55 (t, ^3J = 10.5 Hz, 1 H,), 3.99–4.20 (m, 2 H). ^{13}C-NMR ($CDCl_3$, 63 MHz) δ 19.6, 26.3, 28.0, 41.0, 45.5, 46.1, 73.6, 83.9. MS (70 eV, EI) *m*/*z* (%) 205.1 (1) [M^+], 124.1 (3), 111.1 (56), 67.0 (100). Anal. Calcd. for $C_8H_{13}BrO$ (205.09): C, 46.85; H, 6.39; Found: C, 46.78; H, 6.25. *1,3-cis-1,5-trans-3-Bromomethyl-2-oxabicyclo[3.3.0]-octane*. *trans*-**3b**. Yield 17.9 mg (9 %), yellow oil, R_f = 0.49 [petroleum ether/diethyl ether = 9/1 (*v*/*v*)]. ^{1}H-NMR ($CDCl_3$, 250 MHz) δ 1.12–1.27 (m, 1 H), 1.42–1.54 (m, 1 H), 1.61–1.86 (m, 4 H), 1.90–2.24 (m, 3 H), 3.38–3.53 (m, 2 H), 3.68 (dt, ^3J_d = 10.8 Hz, ^3J_t = 6.3 Hz, 1 H), 4.65–4.81 (m, 1 H). ^{13}C-NMR ($CDCl_3$, 63 MHz) δ 21.2, 25.0, 27.3, 31.8, 36.0, 49.8, 86.7, 90.9. MS (70 eV, EI) *m*/*z* (%)205.1 (1) [M^+], 124.1 (3), 111.1 (62), 67.0 (100), 41.1 (19). Anal. Calcd. for $C_8H_{13}BrO$ (205.09): C, 46.85; H, 6.39; Found: C, 46.71; H, 6.29. *1,3-trans-1,5-trans-3-Brommethyl-2-oxabicyclo[3.3.0]-octane trans*-**3b**. Yield 42.1 mg (21 %), yellow oil, R_f = 0.43 [petroleum ether/diethyl ether = 9/1 (*v*/*v*)]. ^{1}H-NMR ($CDCl_3$, 250 MHz) δ 1.11–1.31 (m, 1 H), 1.33–1.55 (m, 2 H), 1.60–1.75 (m, 1 H), 1.74–1.84 (m, 1 H), 1.97–2.25 (m, 4 H), 3.41–3.61 (m, 2 H), 3.81 (dt, ^3J_d = 17.2 Hz, ^3J_t = 6.4 Hz, 1 H,), 4.72-4.83 (m, 1 H). ^{13}C-NMR ($CDCl_3$, 63 MHz) δ 21.1, 25.3, 27.1, 33.7, 36.4, 51.8, 87.5, 89.9.

A7 NMR-Spectra of Alkenols, Tosylates and Bromocyclization Products

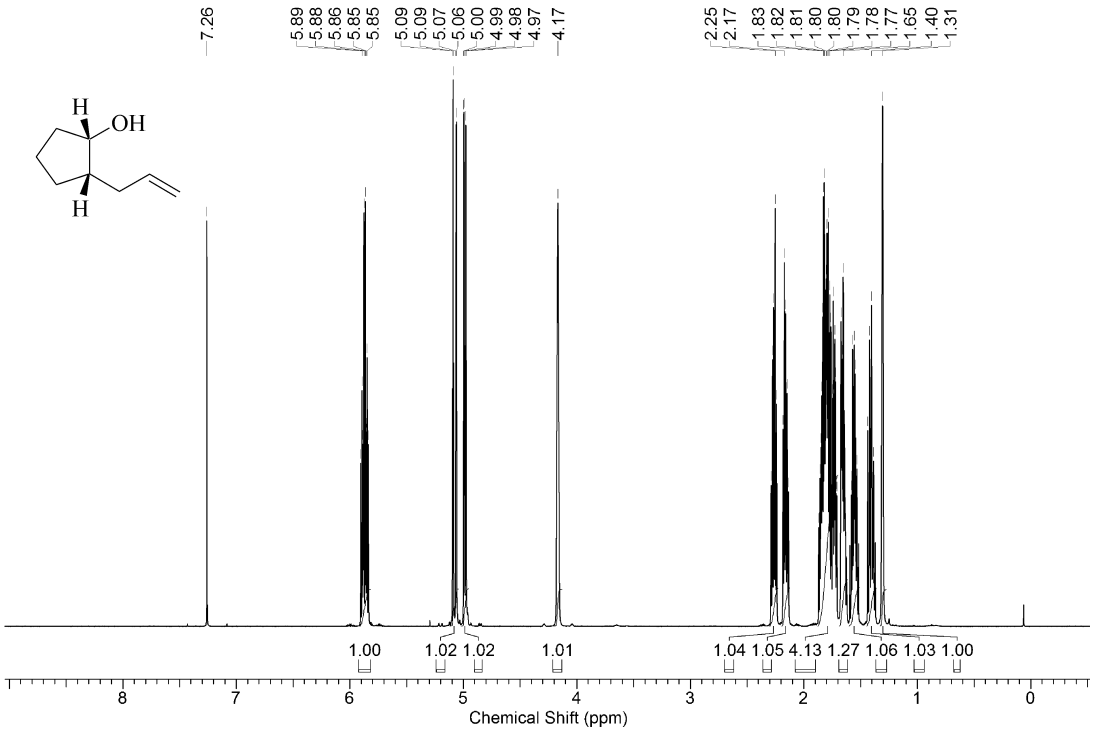

Figure A1. Proton-1 NMR-spectrum of *trans*-2-(prop-2-en-1-yl)-cyclopentan-1-ol (600MHz, $CDCl_3$, 23 °C).

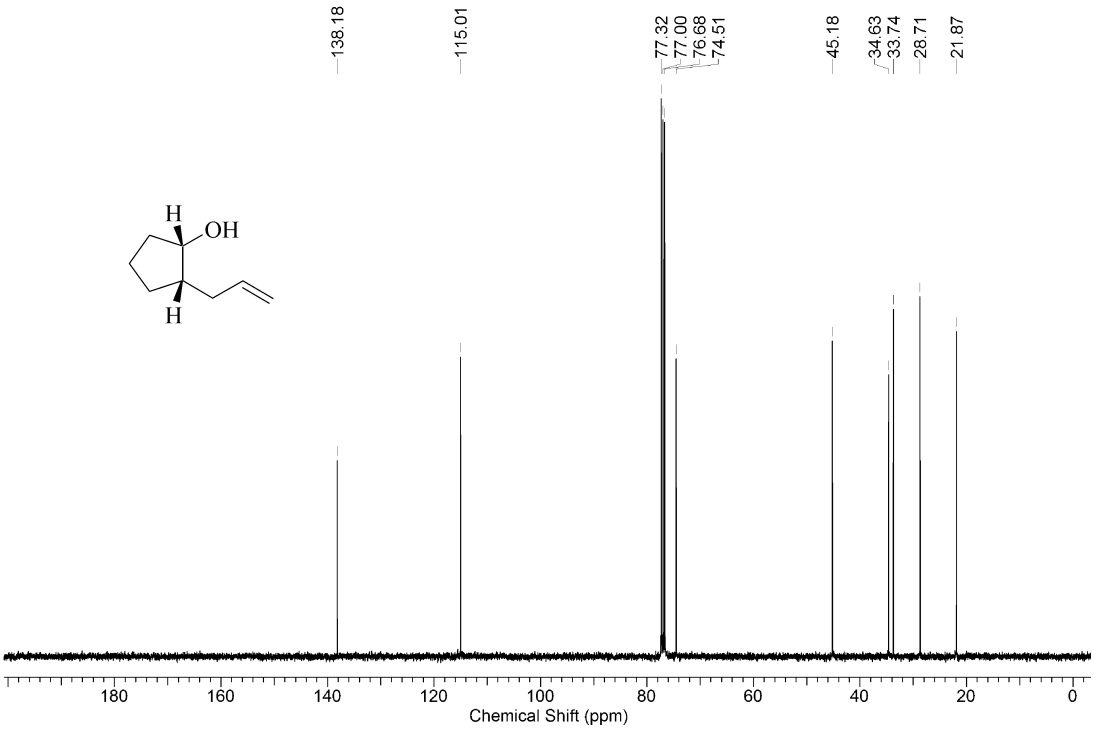

Figure A2. Carbon-13 NMR-spectrum of *trans*-2-(prop-2-en-1-yl)-cyclopentan-1-ol (100MHz, $CDCl_3$, 23 °C).

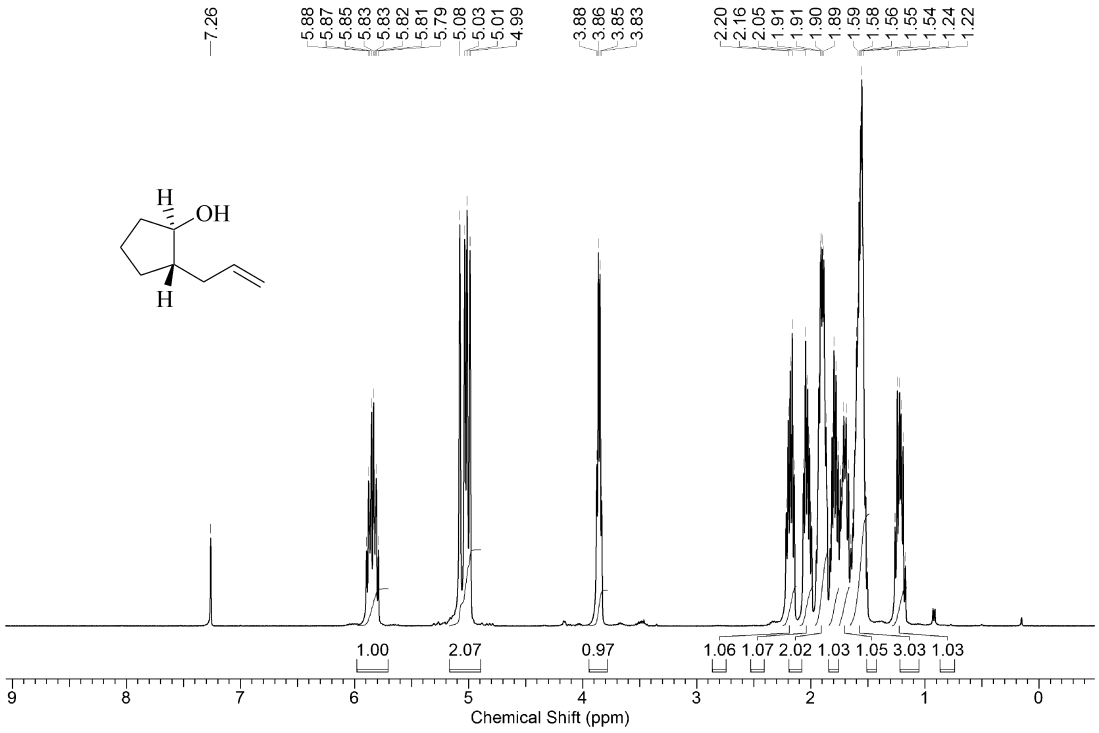

Figure A3. Proton-1 NMR-spectrum of *cis*-2-(prop-2-en-1-yl)-cyclopentan-1-ol (400MHz, $CDCl_3$, 23 °C).

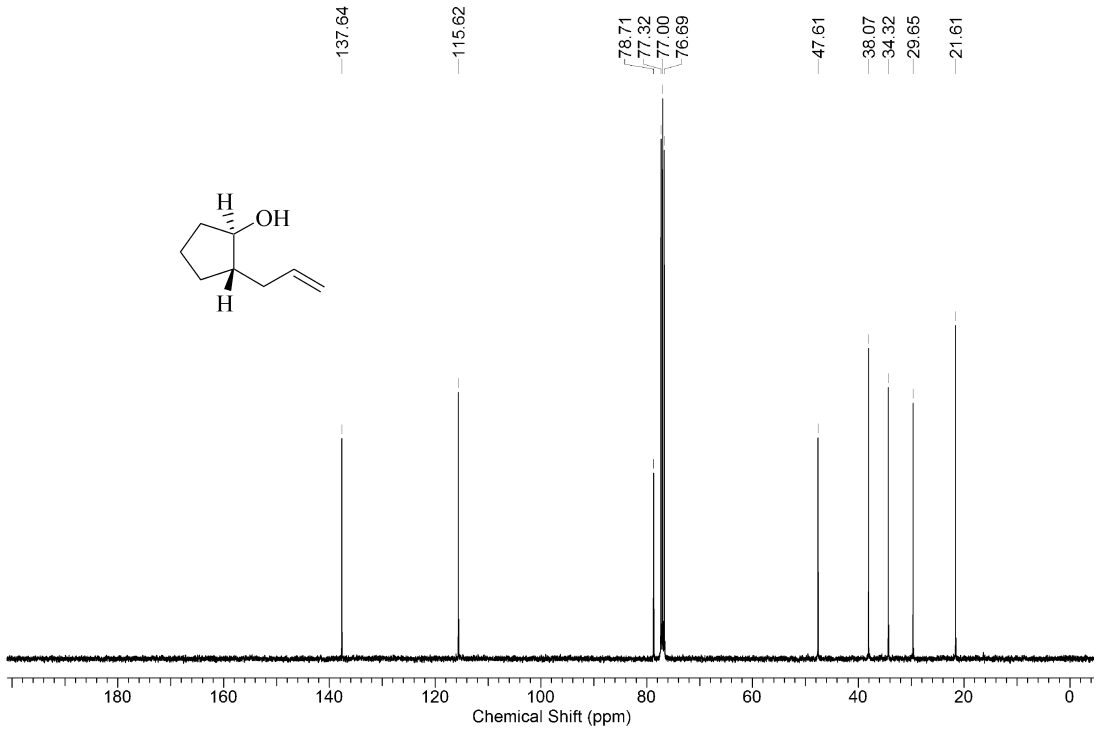

Figure A4. Carbon-13 NMR-spectrum of *cis*-2-(prop-2-en-1-yl)-cyclopentan-1-ol (100MHz, $CDCl_3$, 23 °C).

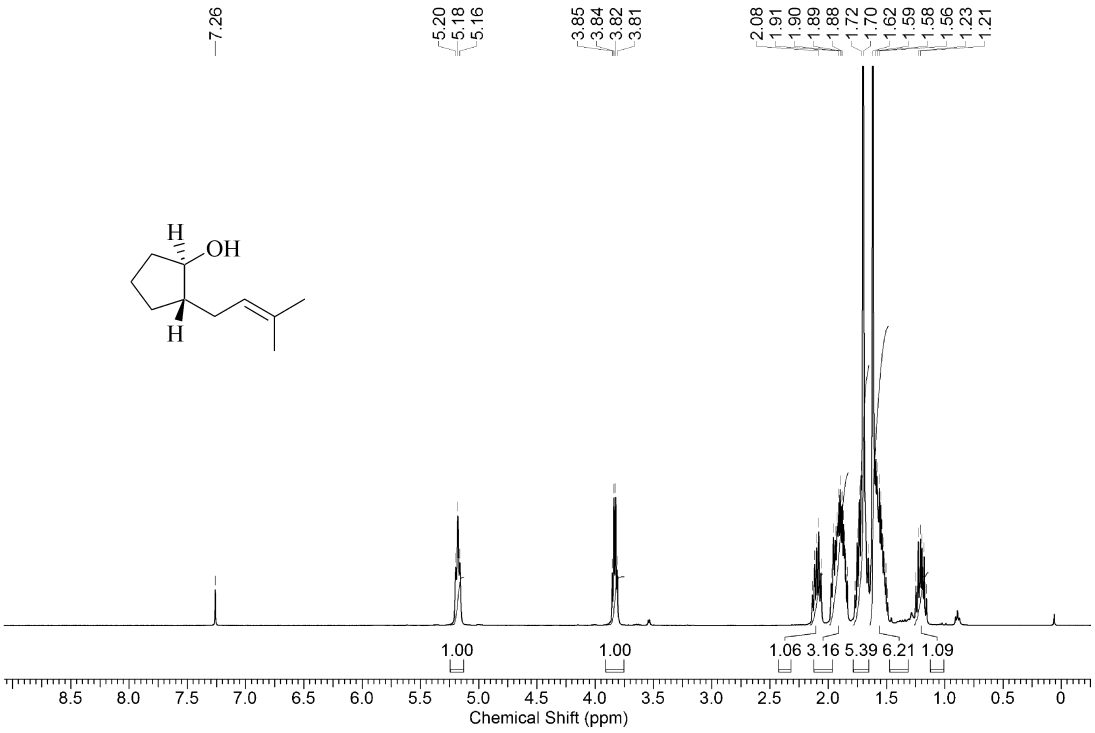

Figure A5. Proton-1 NMR-spectrum of *trans*-2-(3-methylbut-2-en-1-yl)-cyclopentan-1-ol (400MHz, $CDCl_3$, 23 °C).

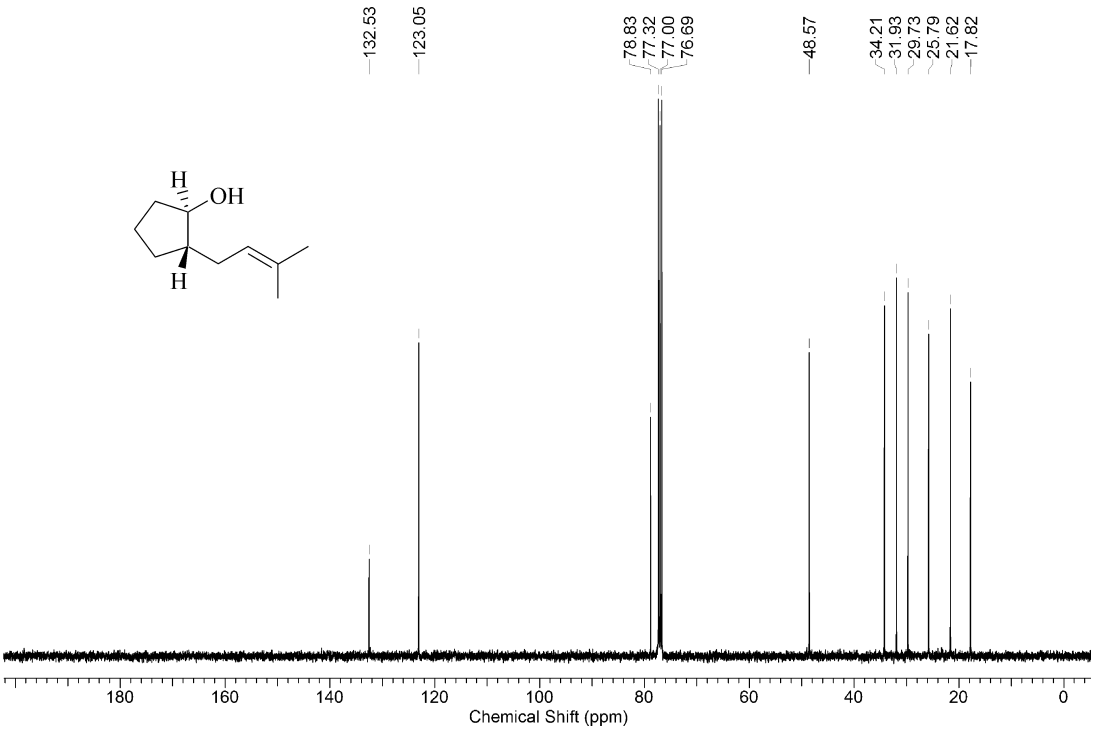

Figure A6. Carbon-13 NMR-spectrum of *trans*-2-(3-methylbut-2-en-1-yl)-cyclopentan-1-ol (100MHz, $CDCl_3$, 23 °C).

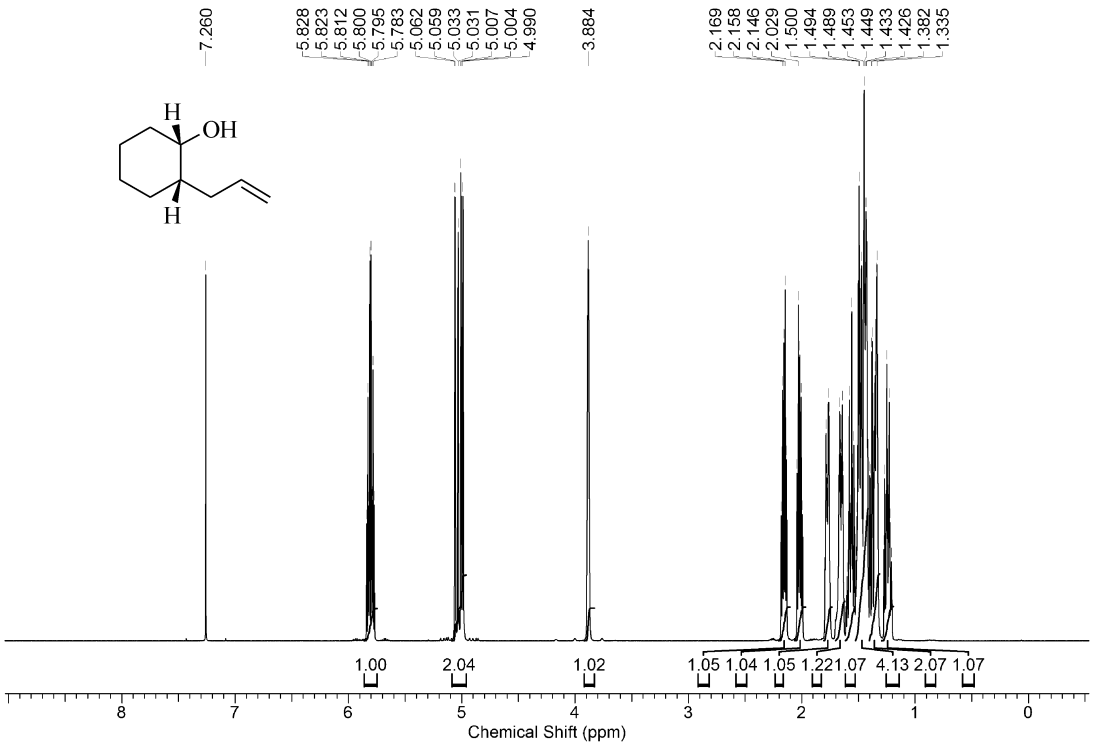

Figure A7. Proton-1 NMR-spectrum of *cis*-2-(prop-2-en-1-yl)-cyclohexan-1-ol (600MHz, $CDCl_3$, 23 °C).

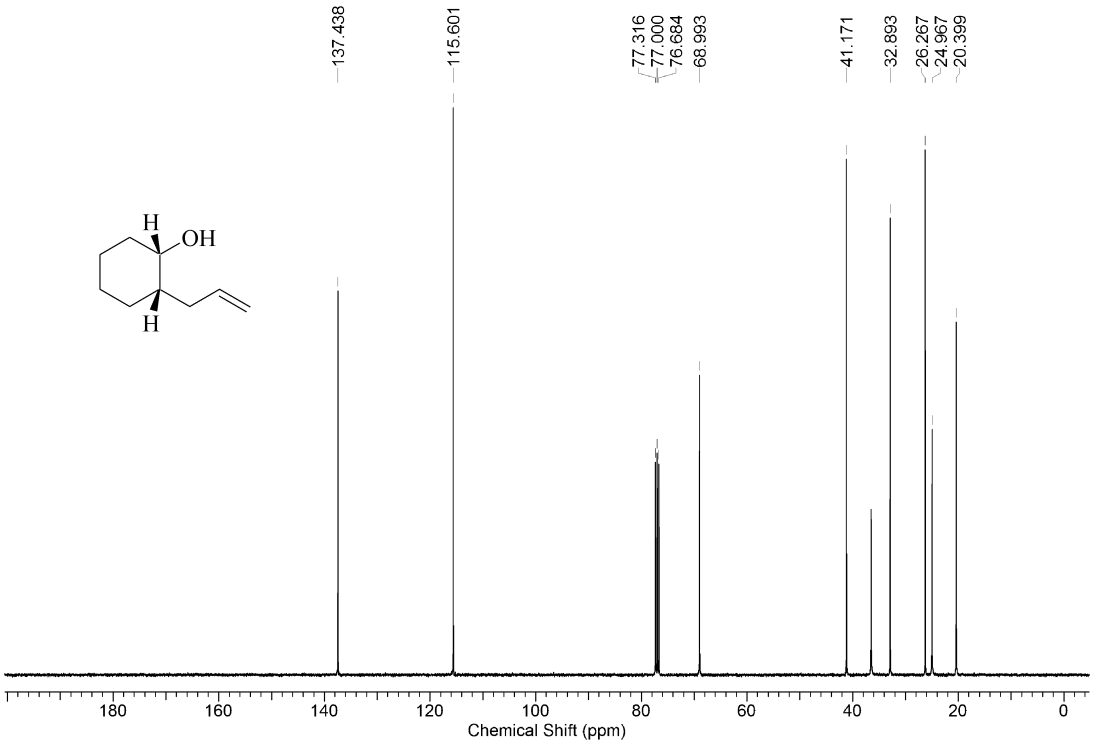

Figure A8. Carbon-13 NMR-spectrum of *cis*-2-(prop-2-en-1-yl)-cyclohexan-1-ol (100MHz, $CDCl_3$, 23 °C).

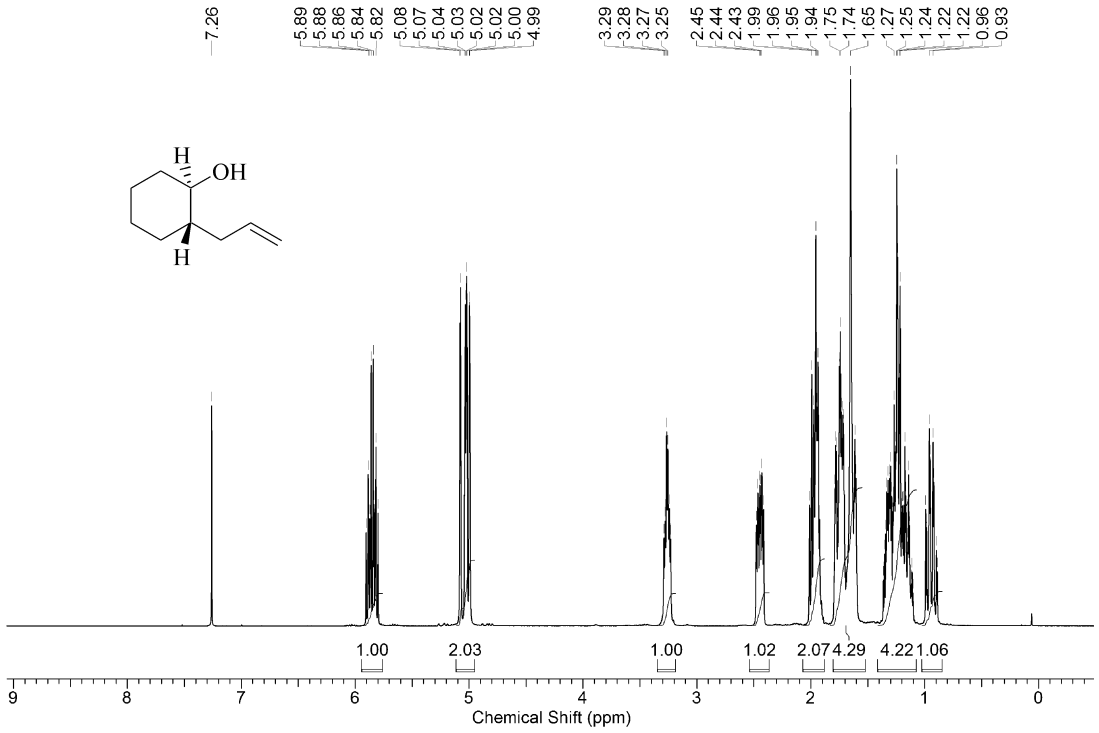

Figure A9. Proton-1 NMR-spectrum of *trans*-2-(prop-2-en-1-yl)-cyclopentan-1-ol (400MHz, $CDCl_3$, 23 °C).

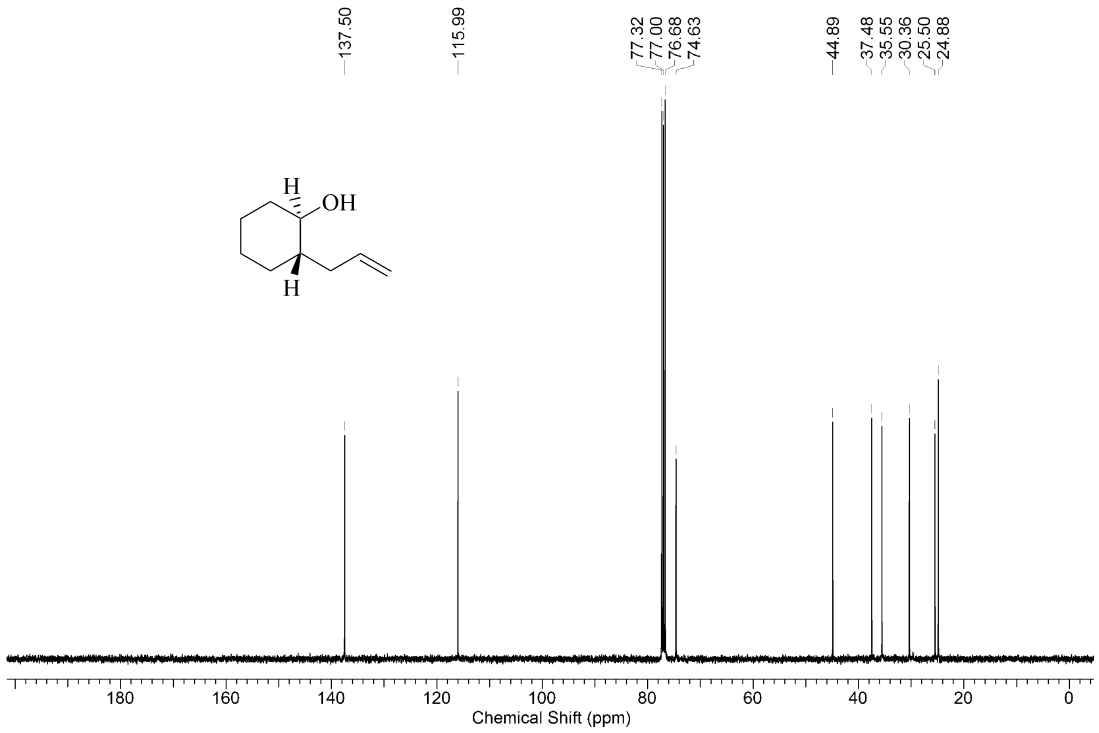

Figure A10. Carbon-13 NMR-spectrum of *trans*-2-(prop-2-en-1-yl)-cyclopentan-1-ol (100MHz, $CDCl_3$, 23 °C).

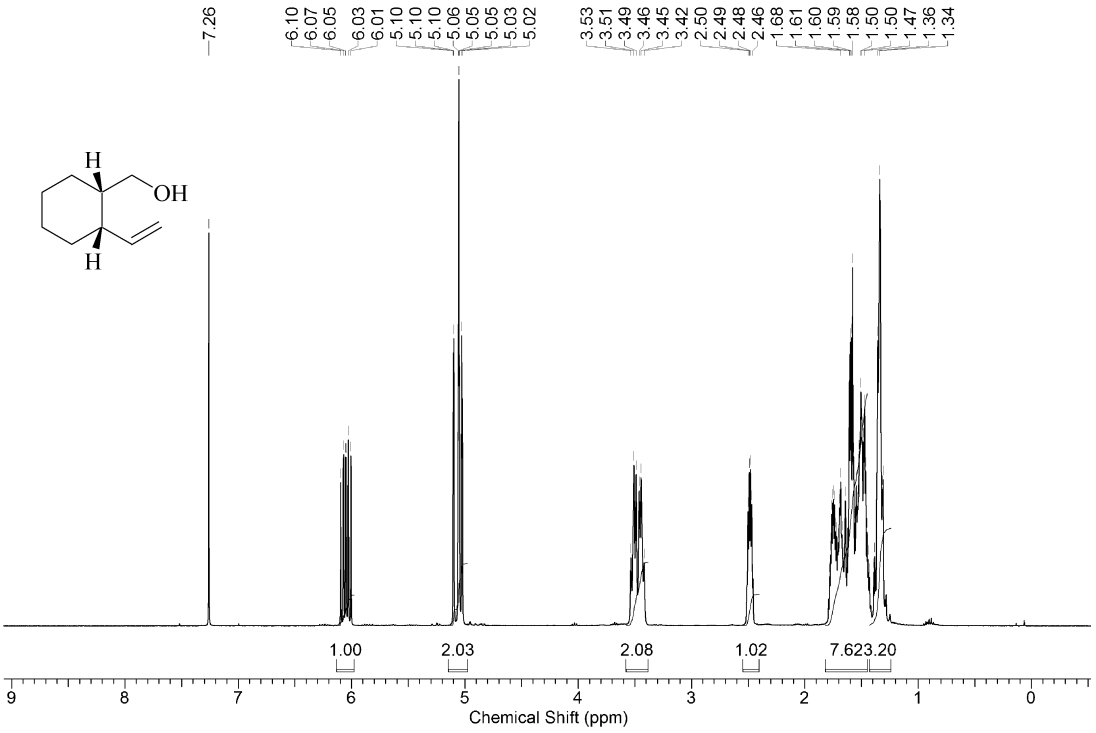

Figure A11. Proton-1 NMR-spectrum of *cis*-[2-(ethenyl)-cyclohex-1-yl]-methanol (400MHz, $CDCl_3$, 23 °C).

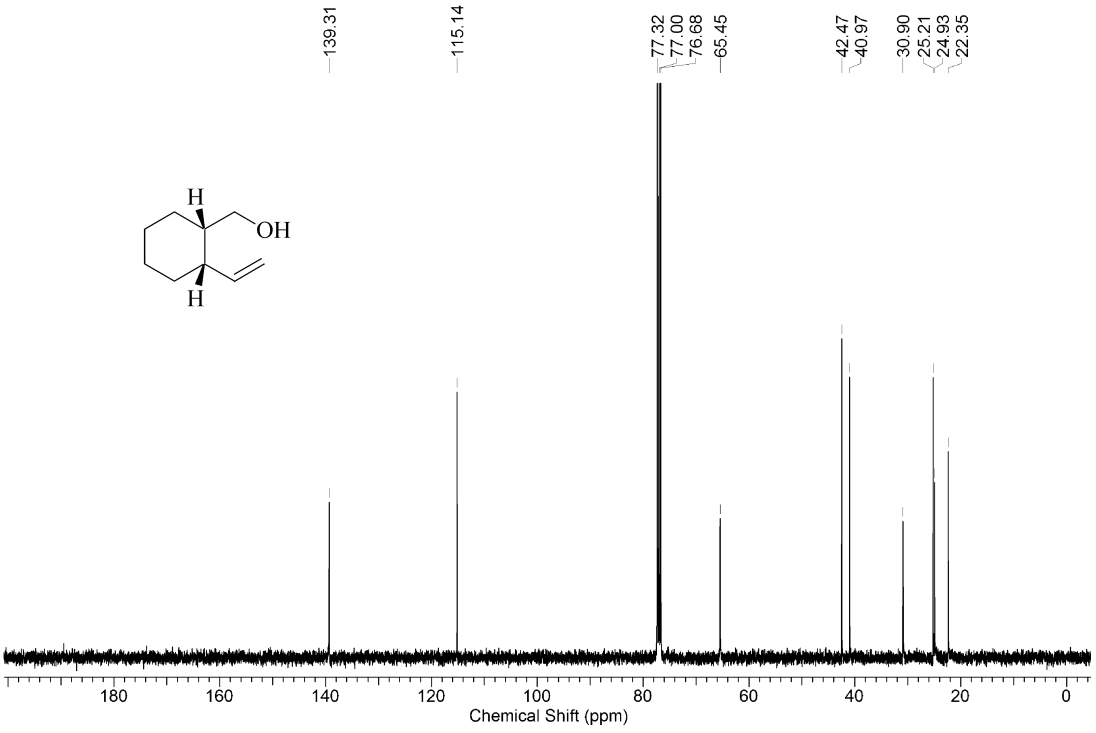

Figure A12. Carbon-13 NMR-spectrum of *cis*-[2-(ethenyl)-cyclohex-1-yl]-methanol (100MHz, $CDCl_3$, 23 °C).

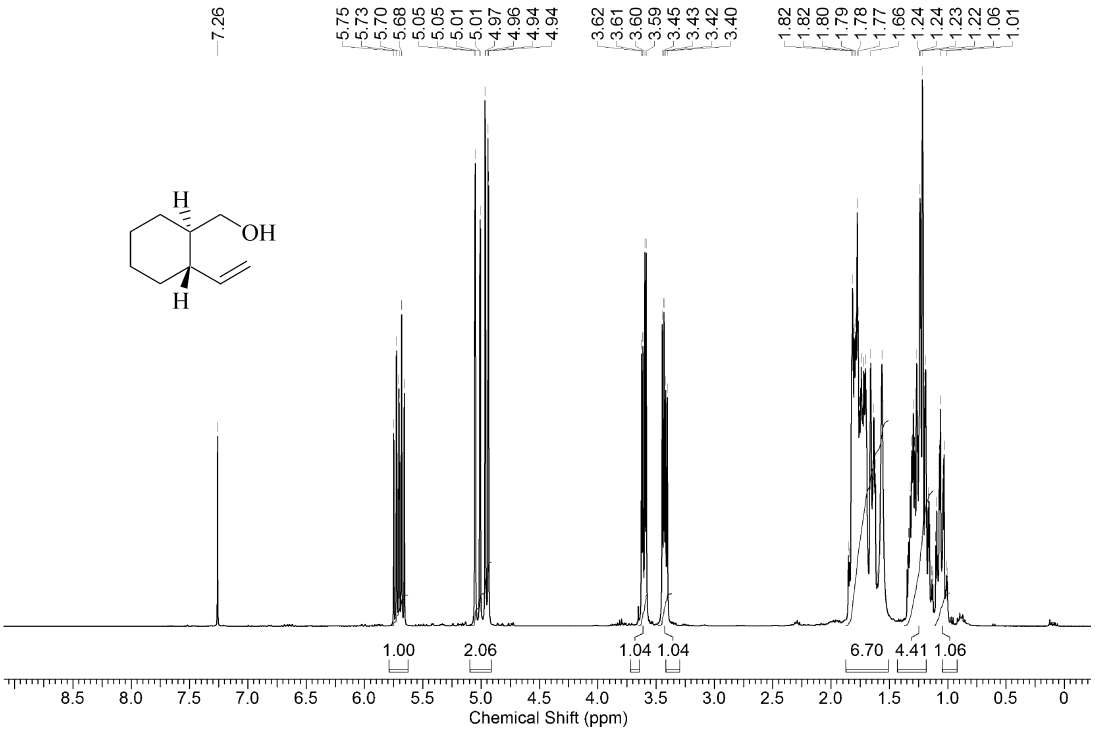

Figure A13. Proton-1 NMR-spectrum of *trans*-[2-(ethenyl)-cyclohex-1-yl]-methanol (400MHz, $CDCl_3$, 23 °C).

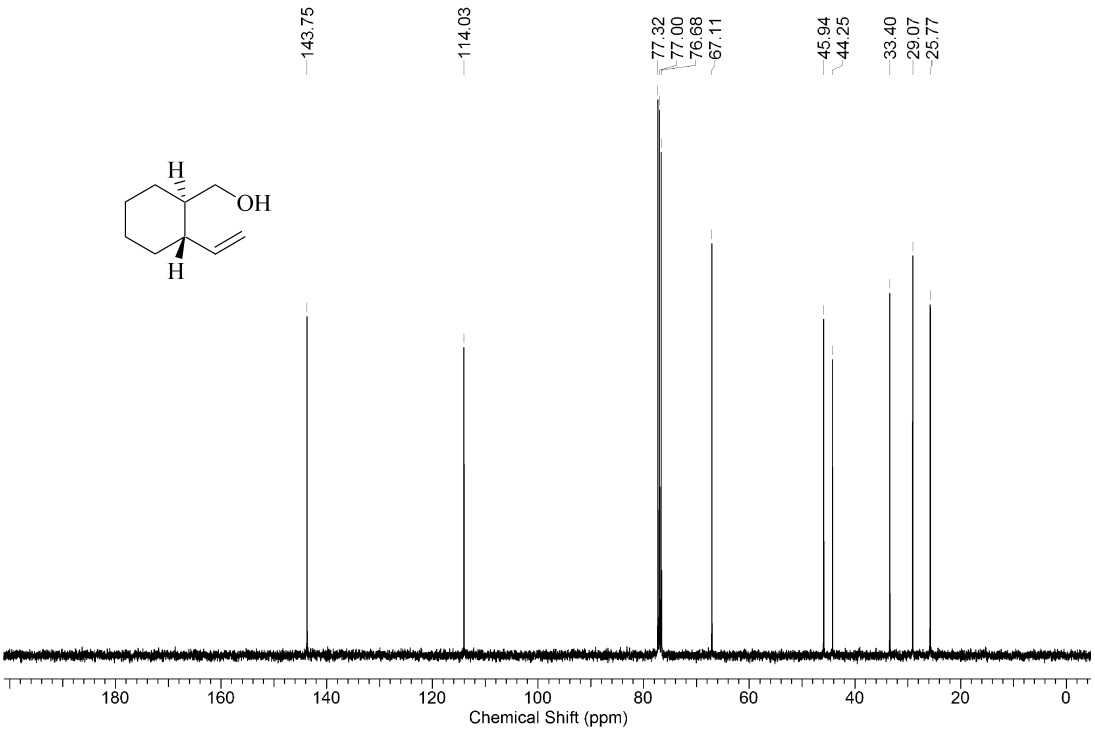

Figure A14. Carbon-13 NMR-spectrum of *trans*-[2-(ethenyl)-cyclohex-1-yl]-methanol (100MHz, $CDCl_3$, 23 °C).

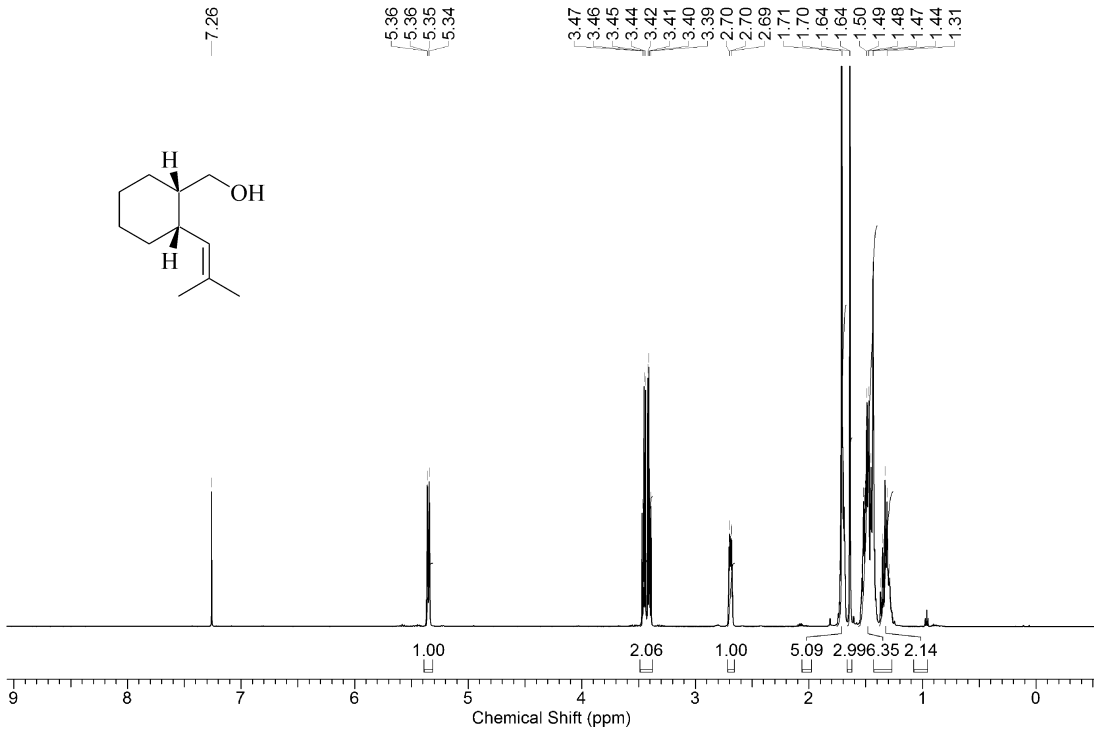

Figure A15. Proton-1 NMR-spectrum of *cis*-[2-(methylprop-1-en-1-yl)-cyclohex-1-yl]-methanol (600MHz, $CDCl_3$, 23 °C).

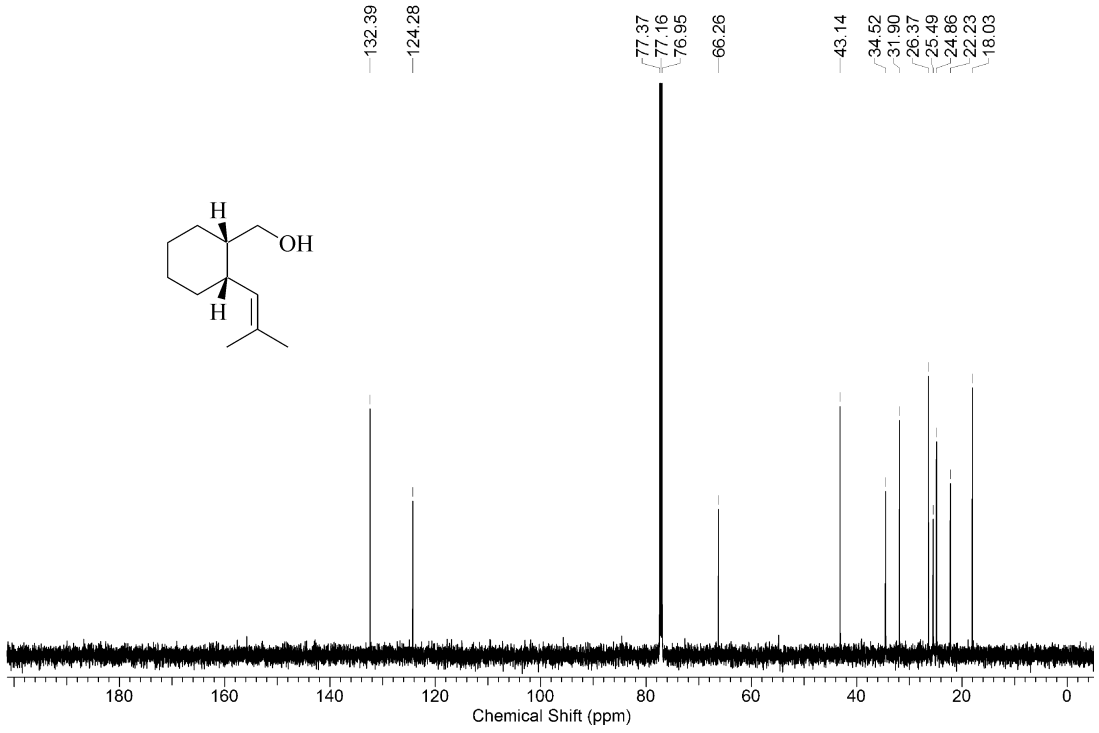

Figure A16. Carbon-13 NMR-spectrum of *cis*-[2-(methylprop-1-en-1-yl)-cyclohex-1-yl]-methanol (150MHz, $CDCl_3$, 23 °C).

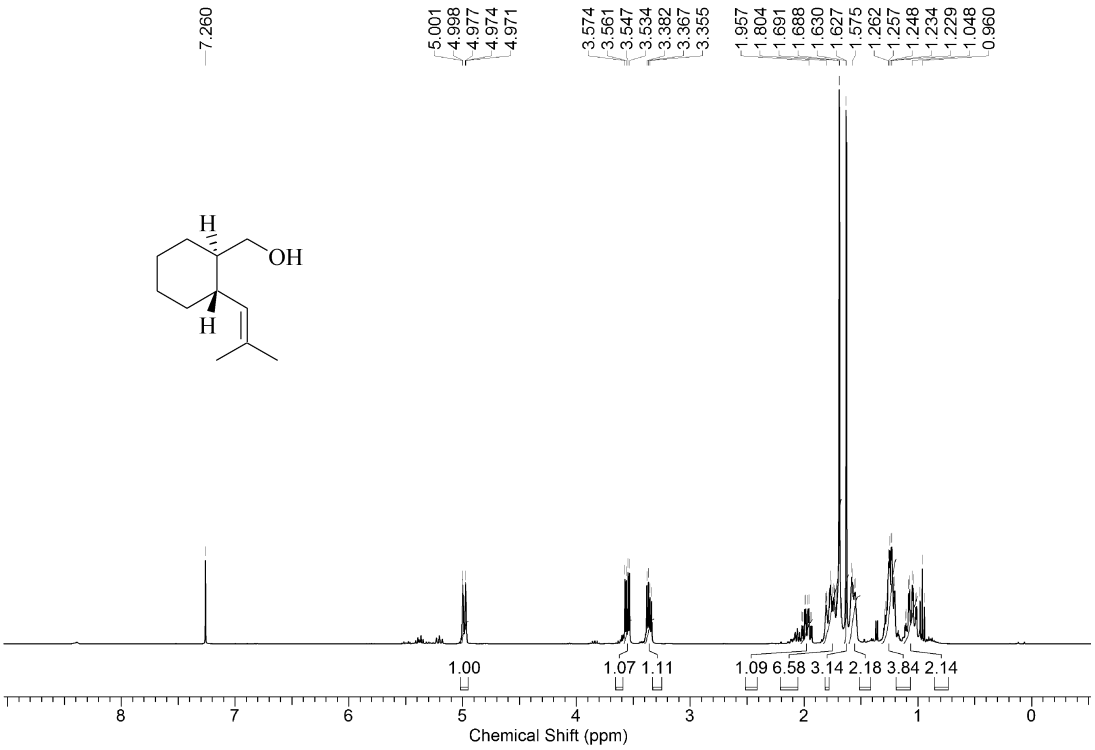

Figure A17. Proton-1 NMR-spectrum of *trans*-[2-(methylprop-1-en-1-yl)-cyclohex-1-yl]-methanol (400MHz, $CDCl_3$, 23 °C).

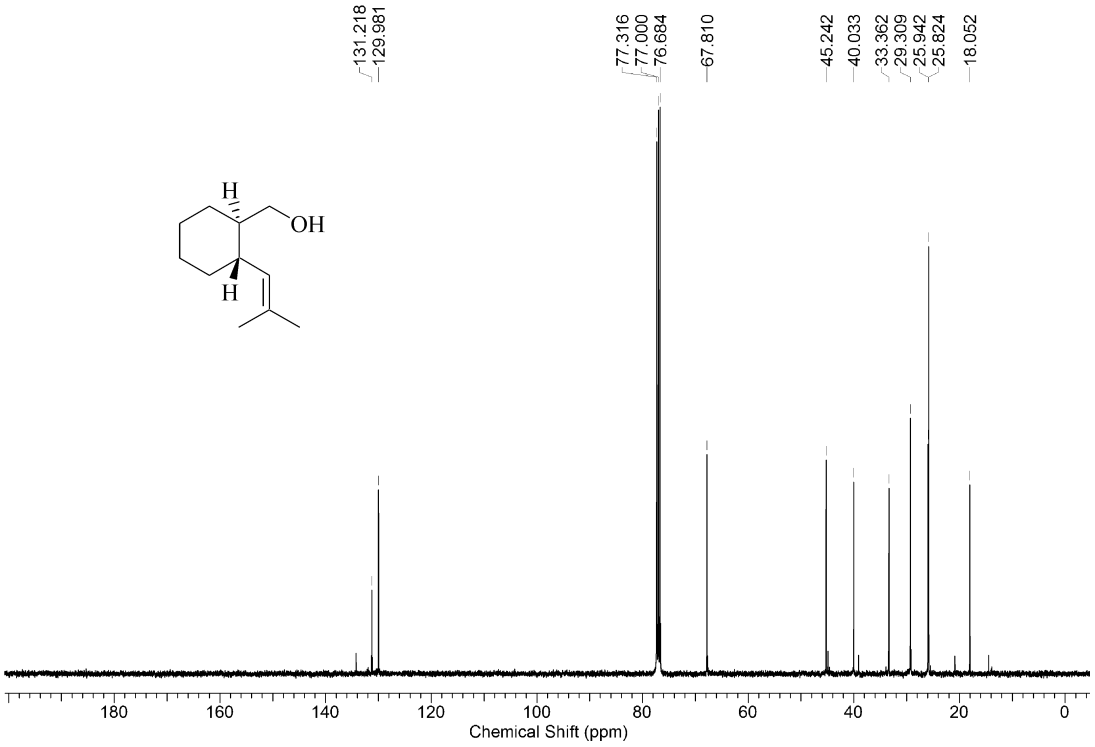

Figure A18. Carbon-13 NMR-spectrum of *trans*-[2-(methylprop-1-en-1-yl)-cyclohex-1-yl]-methanol (100MHz, $CDCl_3$, 23 °C).

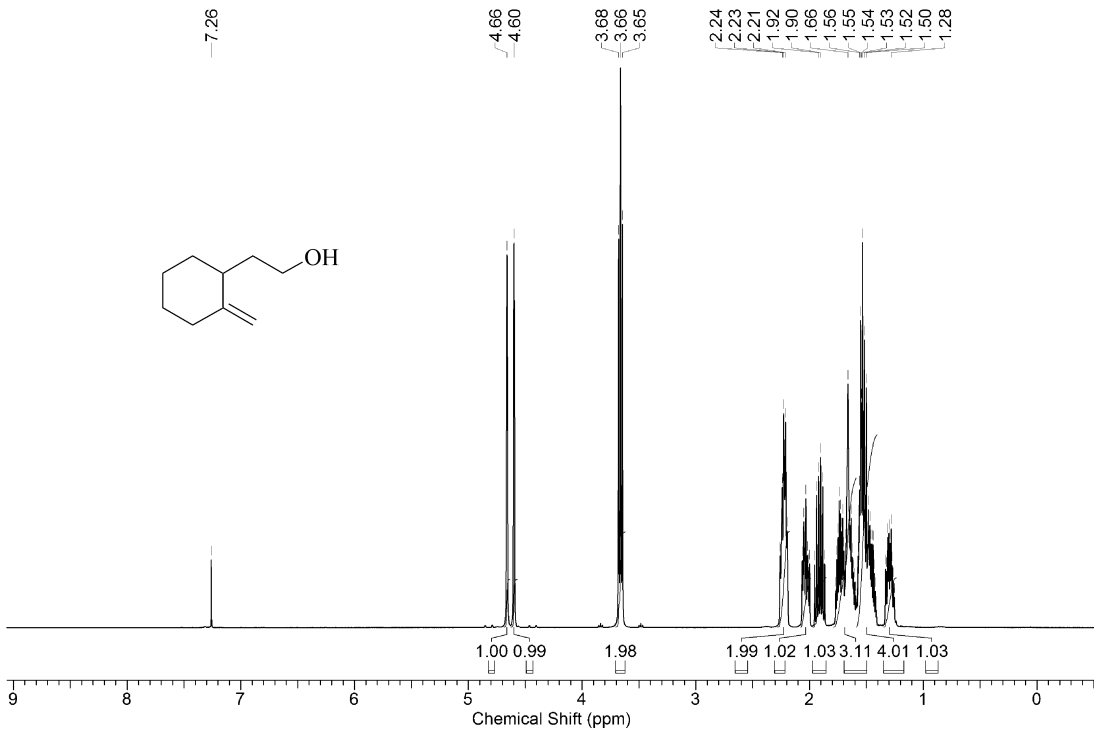

Figure A19. Proton-1 NMR-spectrum of 2-(1-methylenecyclohex-2-yl)-ethan-1-ol (400MHz, $CDCl_3$, 23 °C).

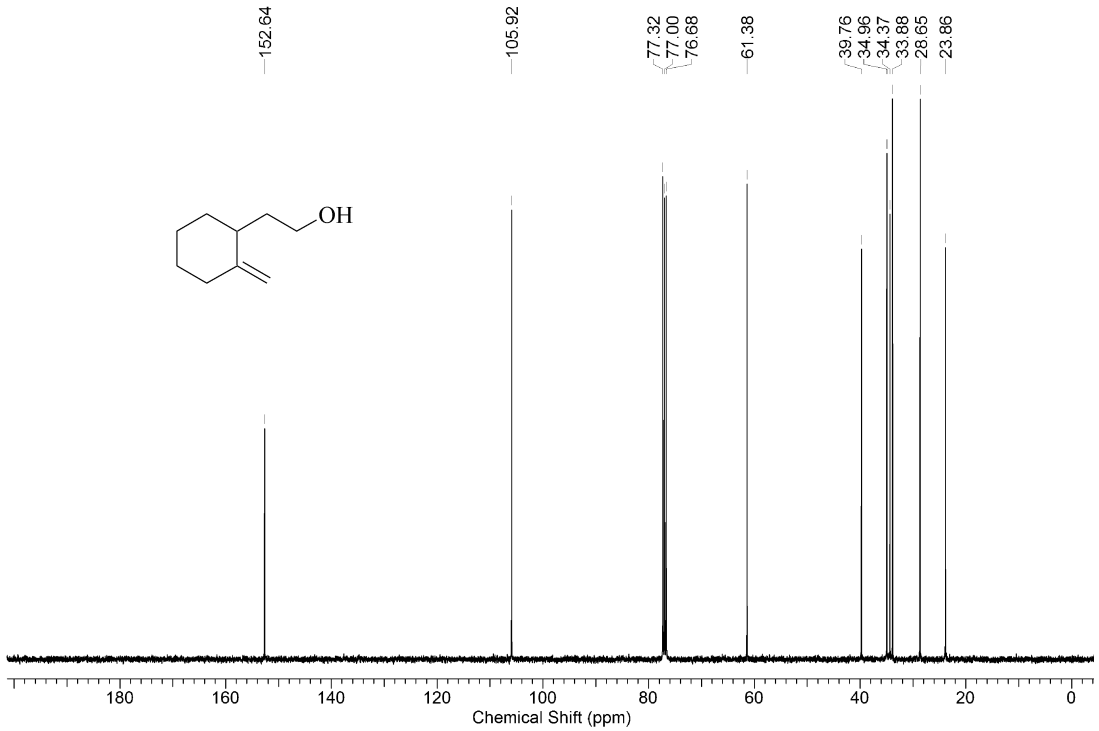

Figure A20. Carbon-13 NMR-spectrum of 2-(1-methylenecyclohex-2-yl)-ethan-1-ol (100MHz, $CDCl_3$, 23 °C).

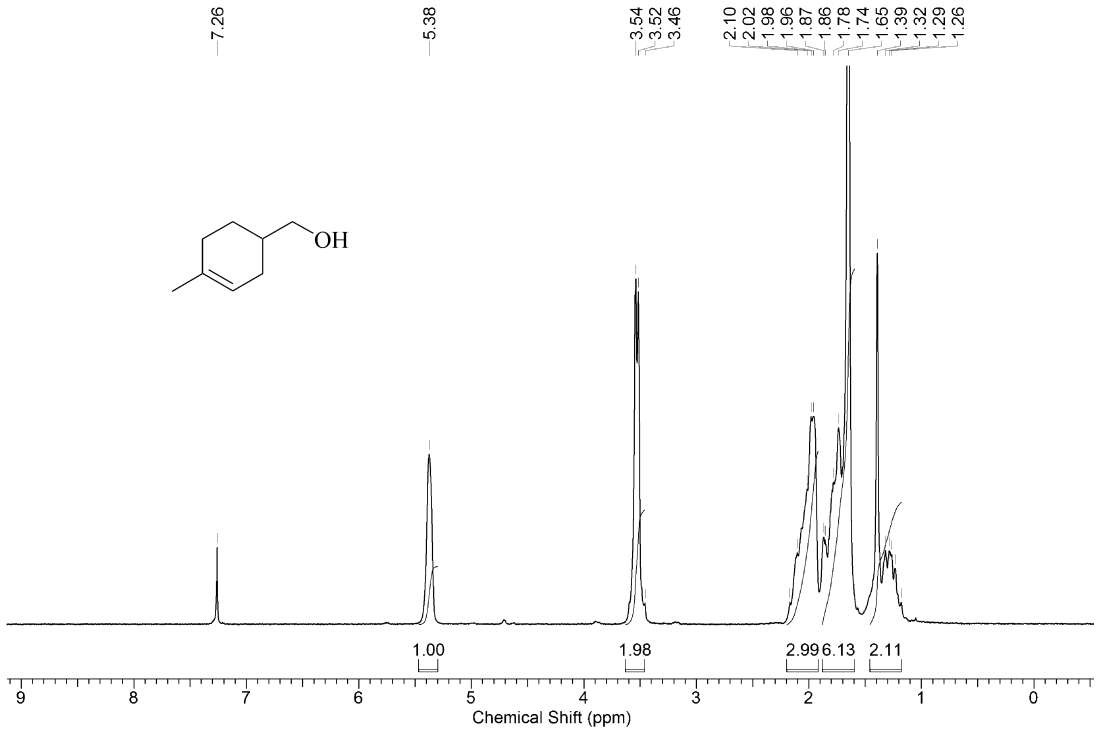

Figure A21. Proton-1 NMR-spectrum of (1-methylcyclohex-1-en-4-yl)-methanol (200MHz, $CDCl_3$, 23 °C).

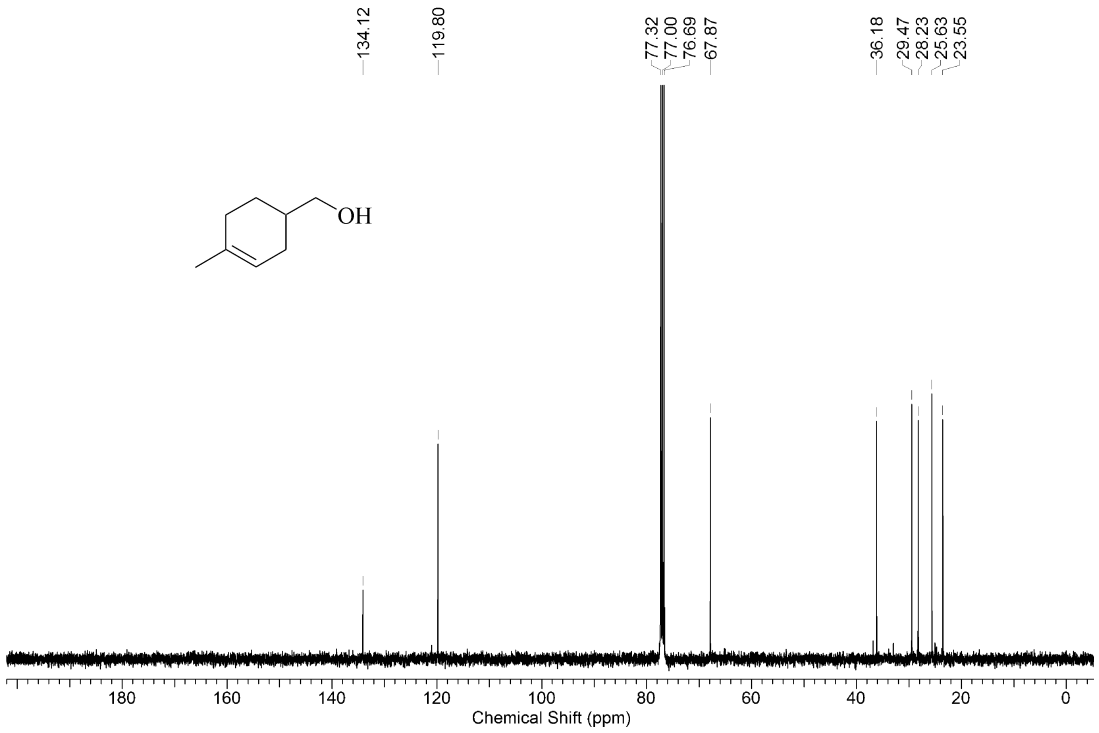

Figure A22. Carbon-13 NMR-spectrum of (1-methylcyclohex-1-en-4-yl)-methanol (100MHz, $CDCl_3$, 23 °C).

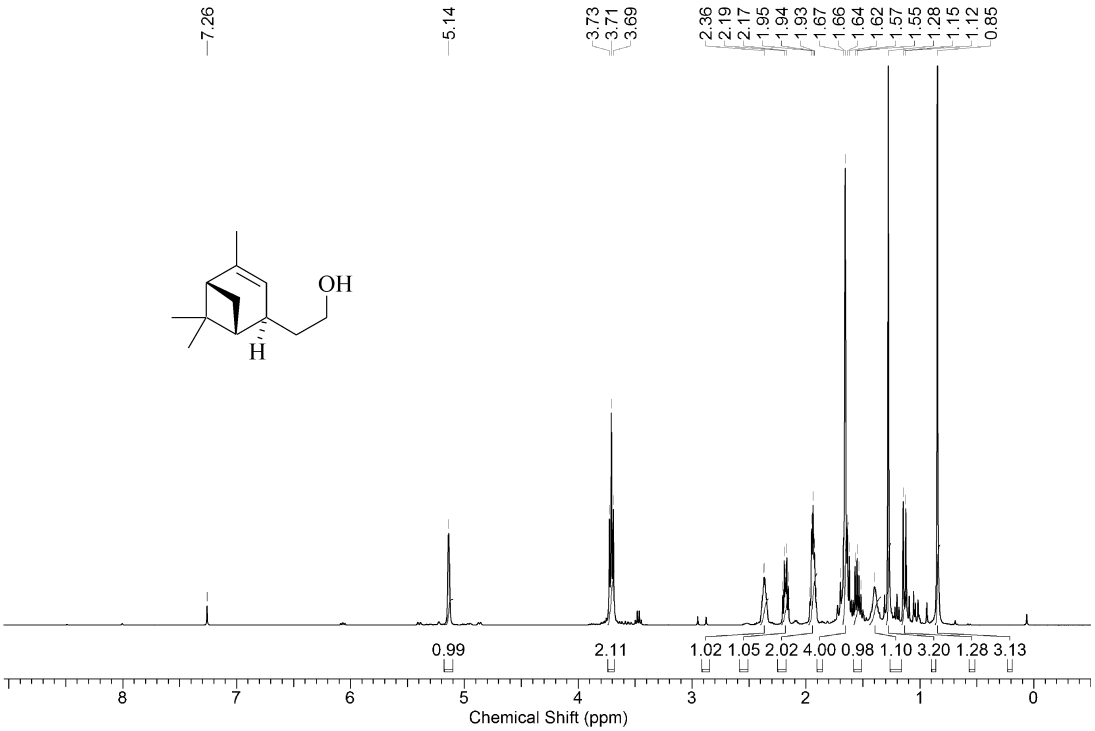

Figure A23. Proton-1 NMR-spectrum of 2-{(1*S*,4*S*,5*R*)-2,6,6-trimethylbicyclo[3.1.1]hept-2-en-4-yl}-ethanol (400MHz, $CDCl_3$, 23 °C).

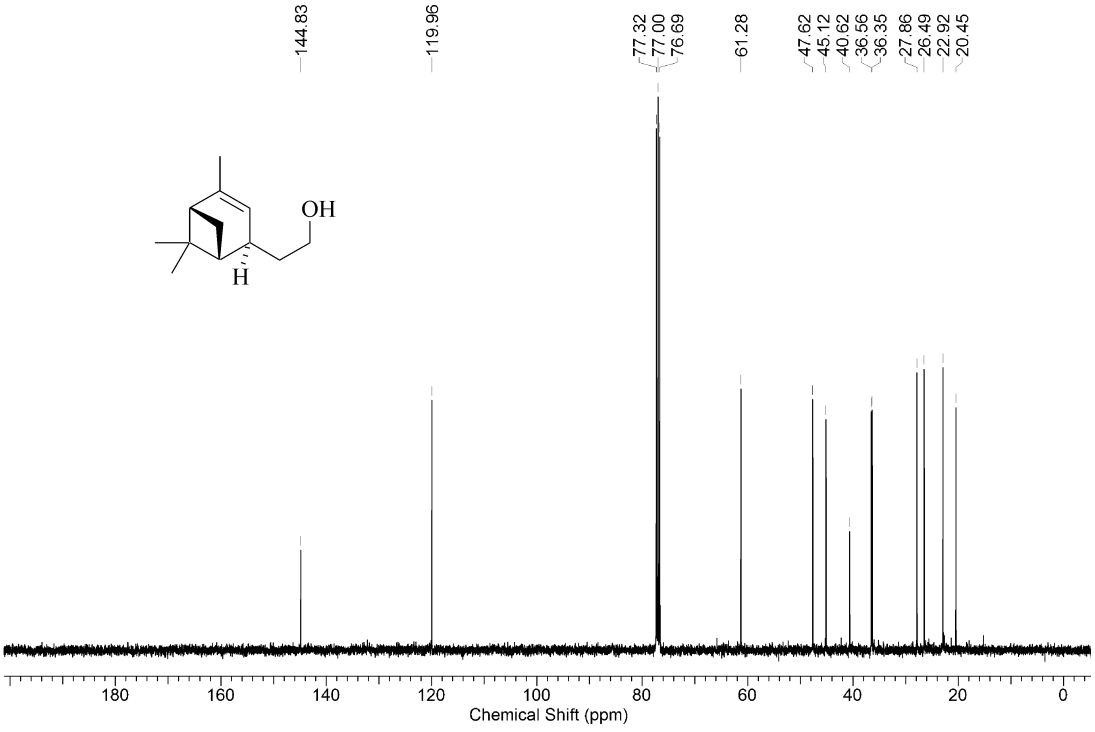

Figure A24. Carbon-13 NMR-spectrum of 2-{(1*S*,4*S*,5*R*)-2,6,6-trimethylbicyclo[3.1.1]hept-2-en-4-yl}-ethanol (100MHz, $CDCl_3$, 23 °C).

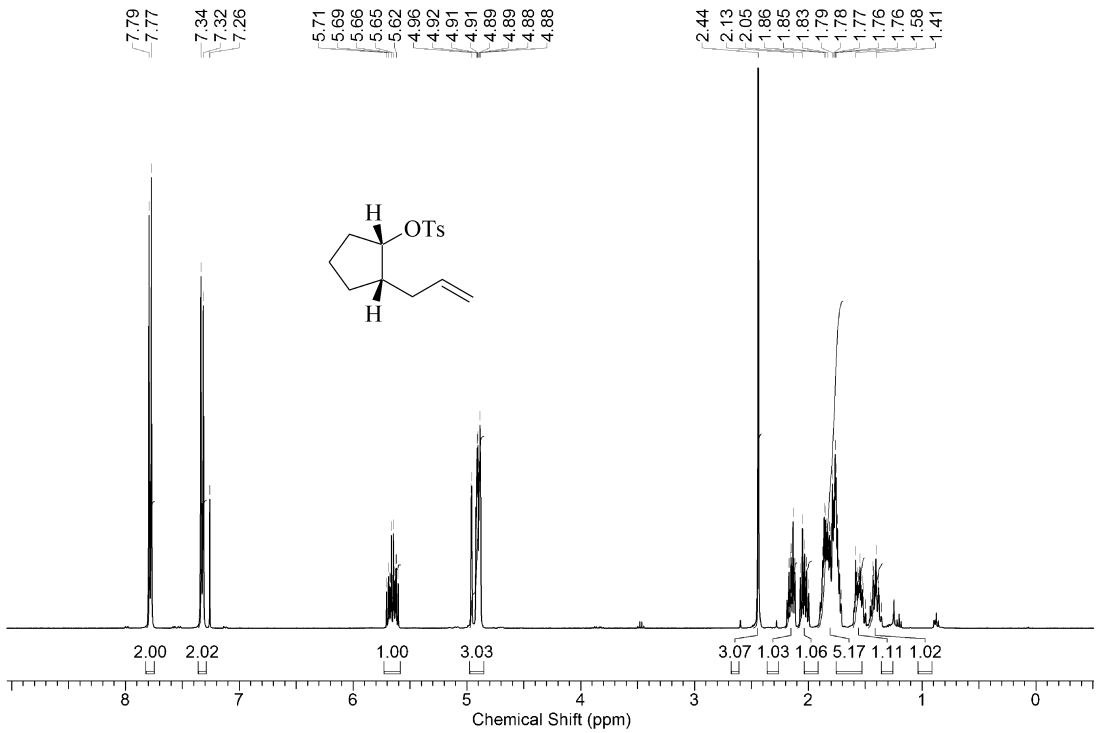

Figure A25. Proton-1 NMR-spectrum of *cis*-[2-(Prop-2-en-1-yl)-cyclopent-1-yl] 4-toluenesulfonate (400MHz, $CDCl_3$, 23 °C).

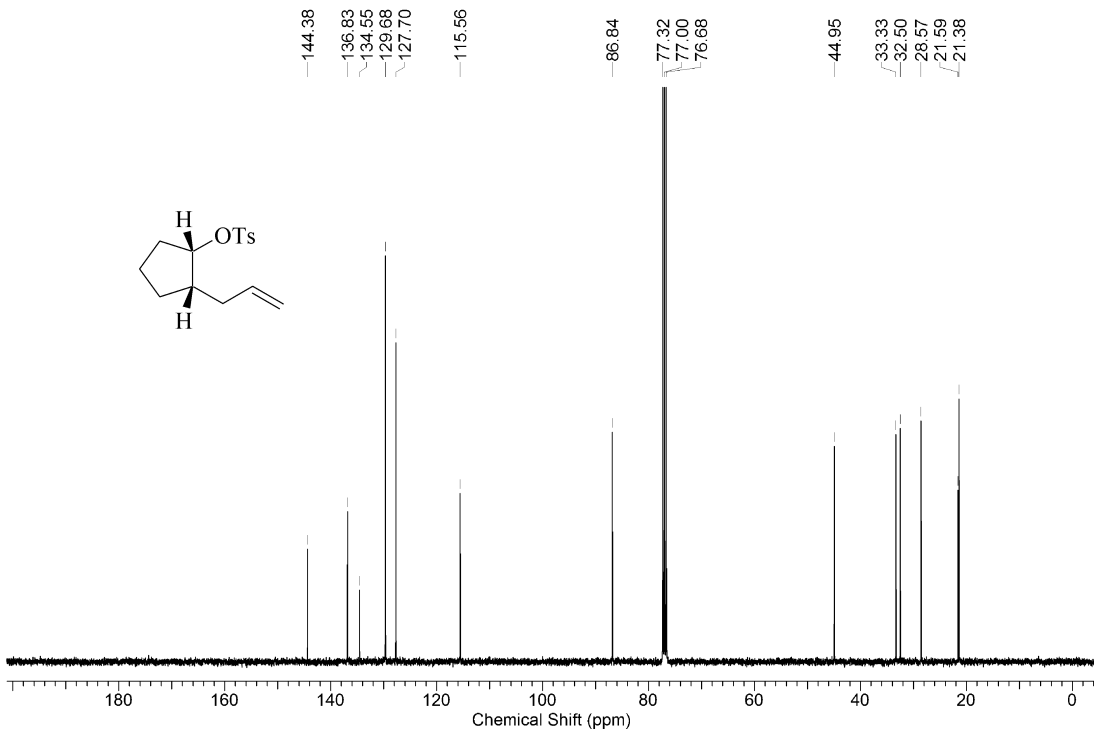

Figure A26. Carbon-13 NMR-spectrum of *cis*-[2-(Prop-2-en-1-yl)-cyclopent-1-yl] 4-toluenesulfonate (100MHz, $CDCl_3$, 23 °C).

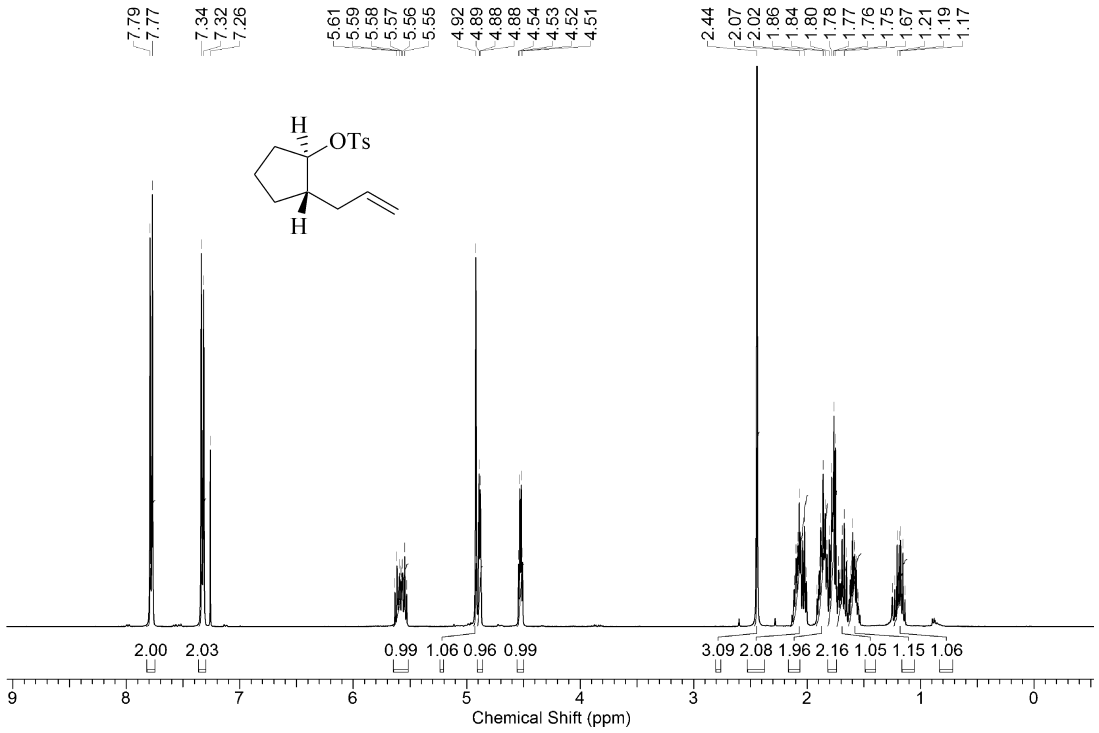

Figure A27. Proton-1 NMR-spectrum of *trans*-[2-(Prop-2-en-1-yl)-cyclopent-1-yl] 4-toluenesulfonate (400MHz, $CDCl_3$, 23 °C).

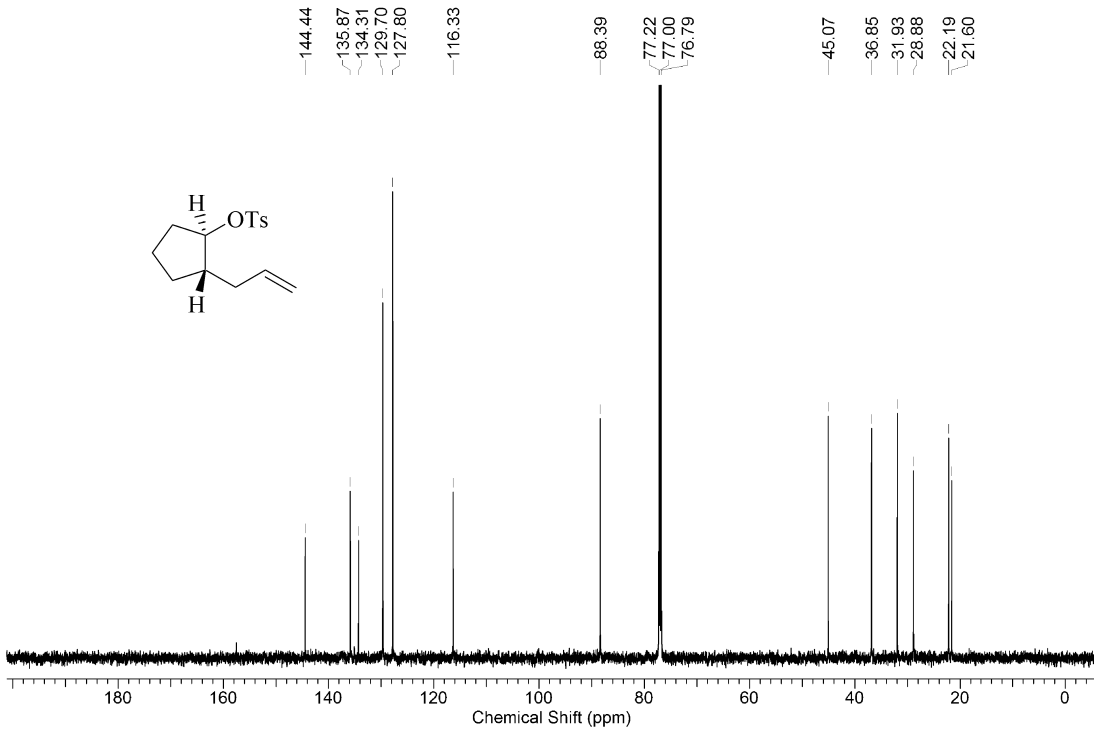

Figure A28. Carbon-13 NMR-spectrum of *trans*-[2-(Prop-2-en-1-yl)-cyclopent-1-yl] 4-toluenesulfonate (150MHz, $CDCl_3$, 23 °C).

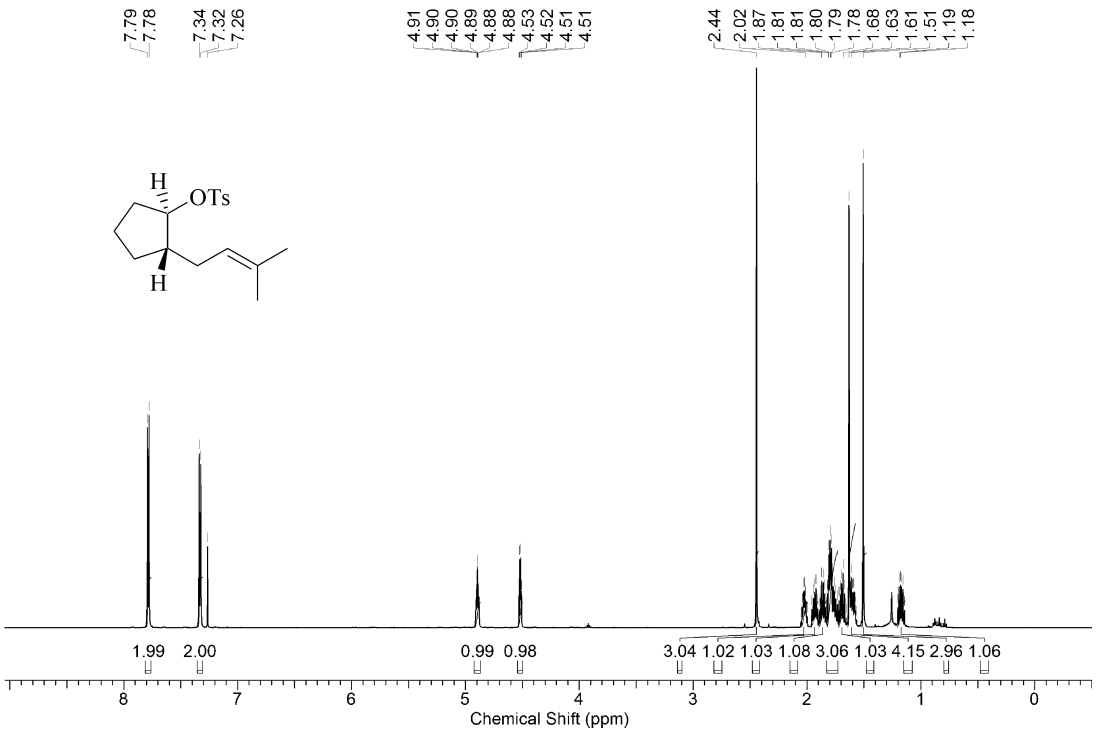

Figure A29. Proton-1 NMR-spectrum of *trans*-[2-(3-methylbut-2-en-1-yl)-cyclopent-1-yl] 4-toluenesulfonate (600MHz, $CDCl_3$, 23 °C).

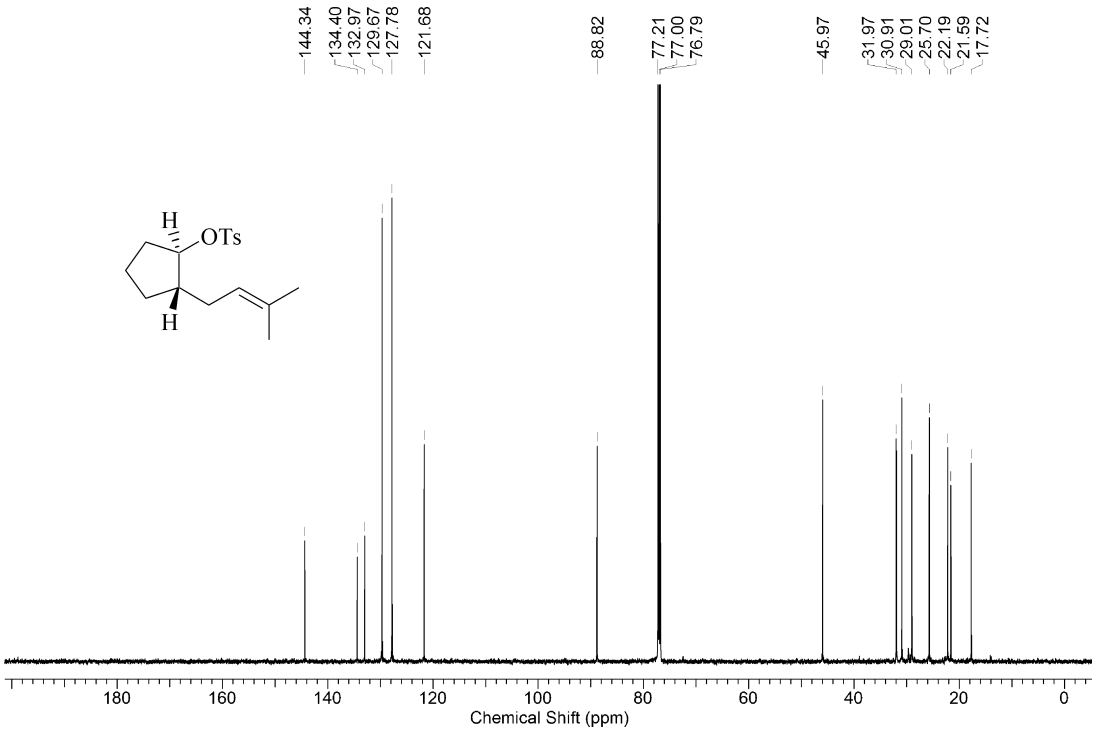

Figure A30. Proton-1 NMR-spectrum of *trans*-[2-(3-methylbut-2-en-1-yl)-cyclopent-1-yl] 4-toluenesulfonate (150MHz, $CDCl_3$, 23 °C).

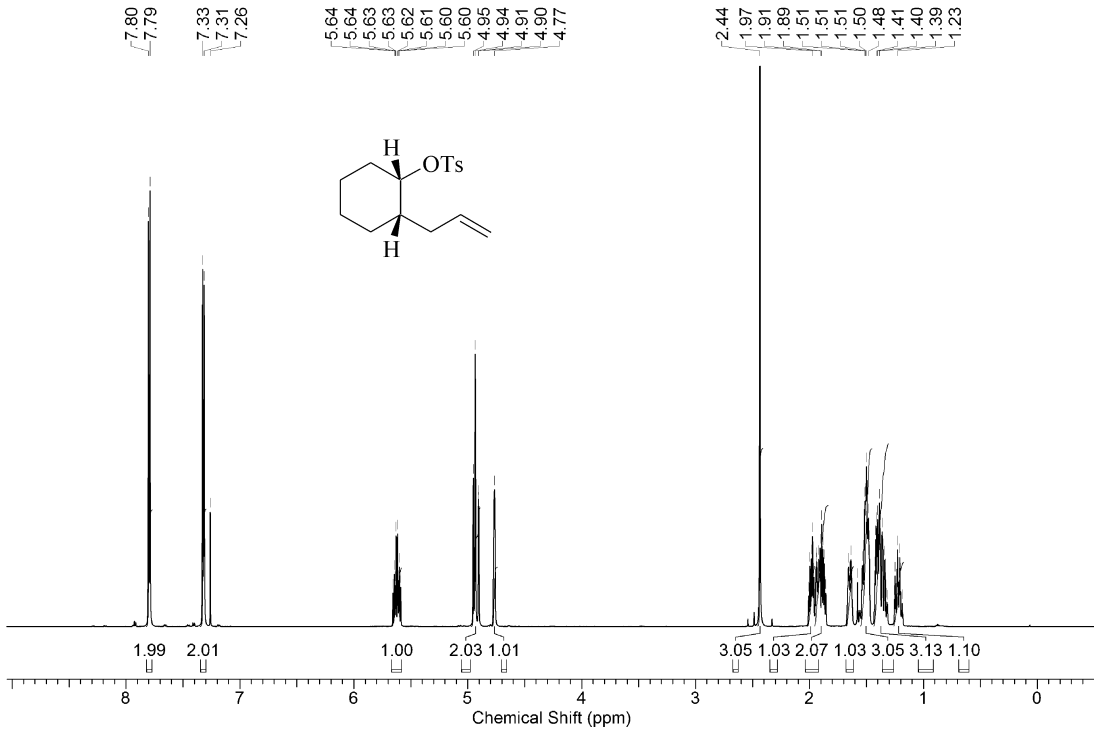

Figure A31. Proton-1 NMR-spectrum of *cis*-[2-(prop-2-en-1-yl)-cyclohexyl-1-yl 4-toluenesulfonate (600MHz, $CDCl_3$, 23 °C).

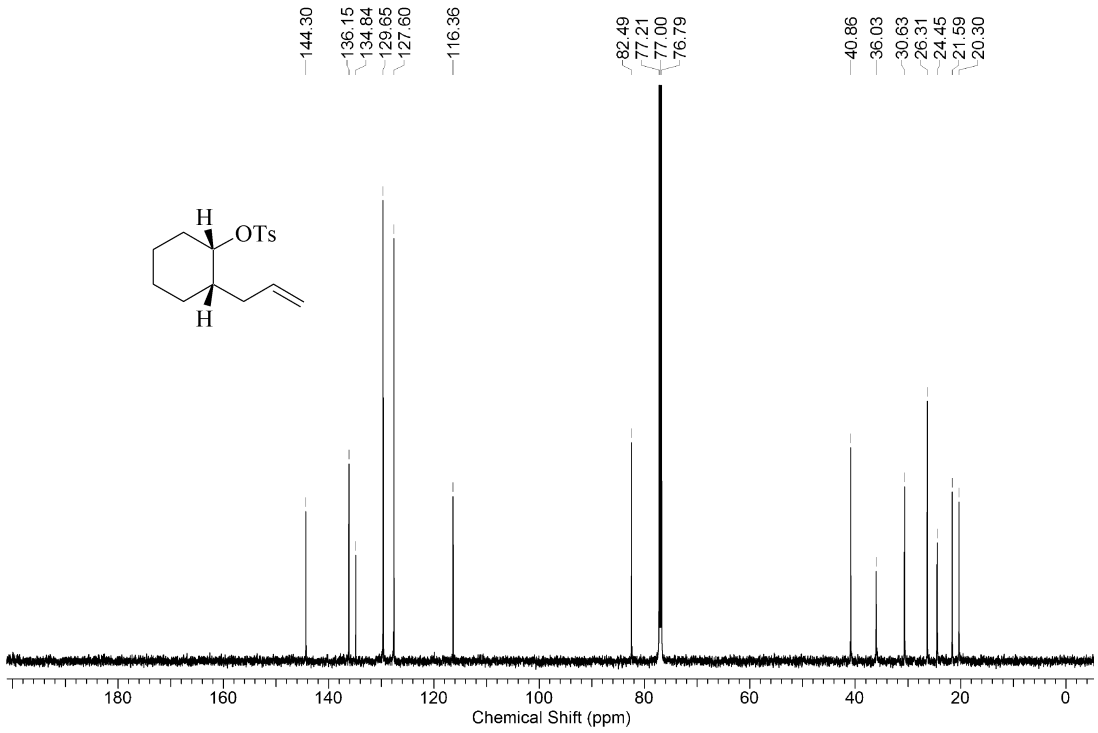

Figure A32. Carbon-13 NMR-spectrum of *cis*-[2-(prop-2-en-1-yl)-cyclohexyl-1-yl 4-toluenesulfonate (150MHz, $CDCl_3$, 23 °C).

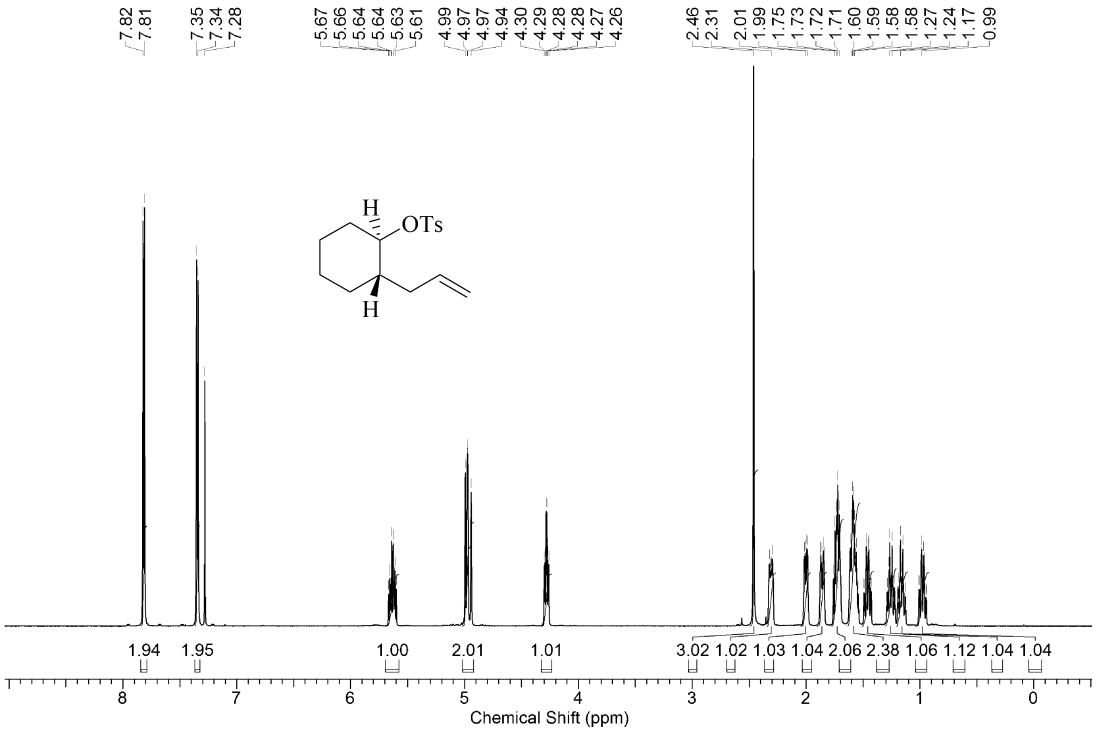

Figure A33. Proton-1 NMR-spectrum of *trans*-[2-(prop-2-en-1-yl)-cyclohexyl-1-yl 4-toluenesulfonate (600MHz, $CDCl_3$, 23 °C).

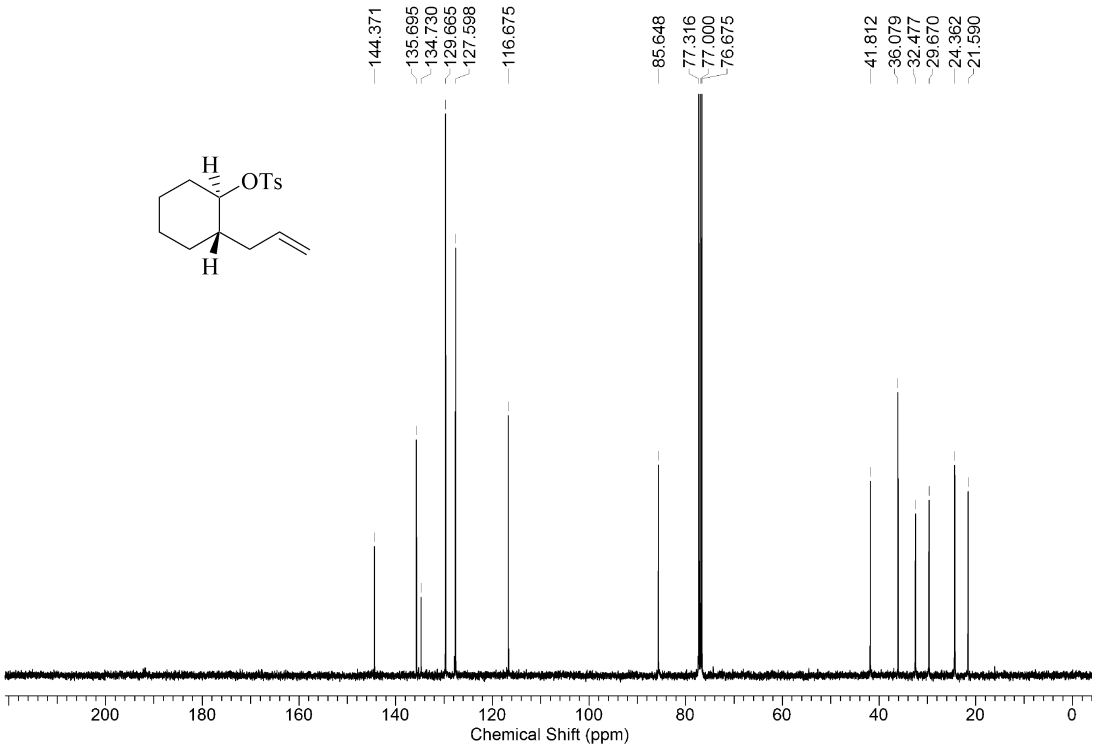

Figure A34. Carbon-13 NMR-spectrum of *trans*-[2-(prop-2-en-1-yl)-cyclohexyl-1-yl 4-toluenesulfonate (100MHz, $CDCl_3$, 23 °C).

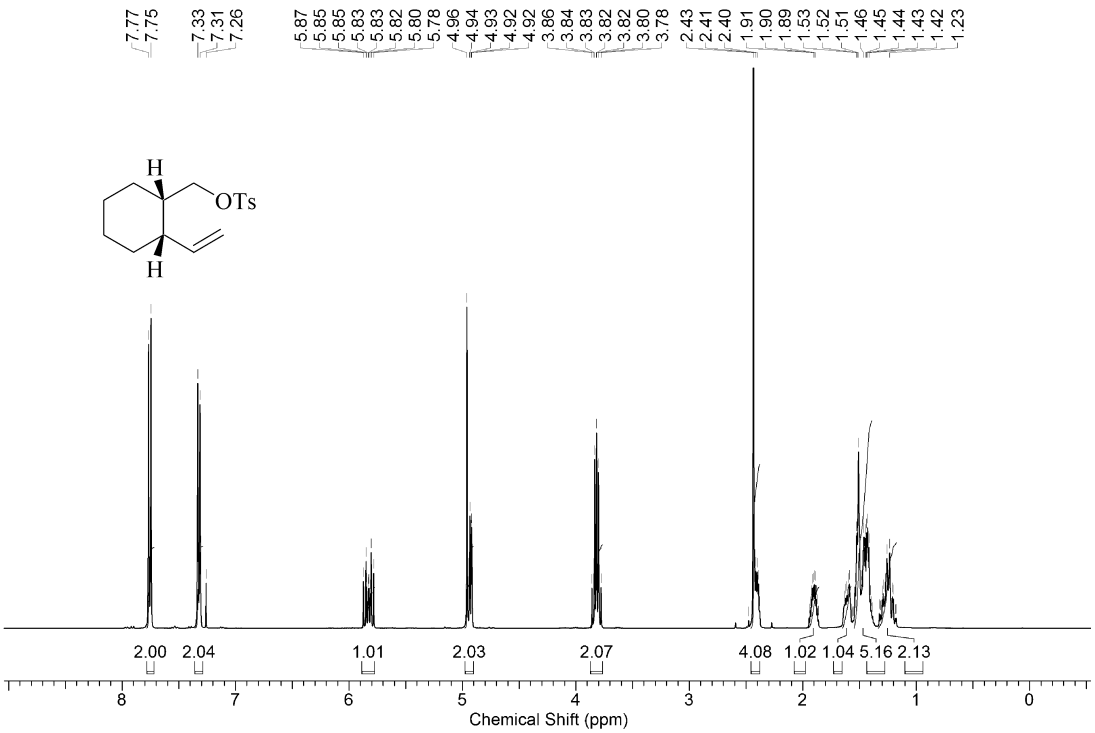

Figure A35. Proton-1 NMR-spectrum of *cis*-[2-(ethenyl)-cyclohex-1-yl]-methyl 4-toluene-sulfonate (400MHz, $CDCl_3$, 23 °C).

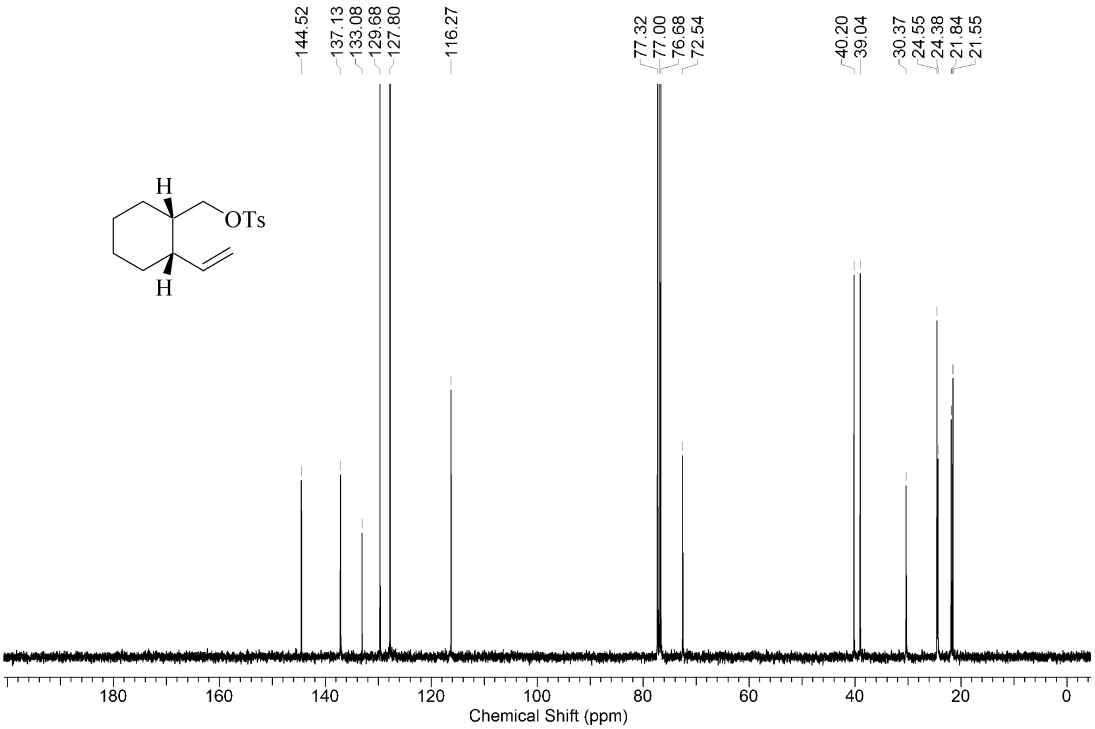

Figure A36. Carbon-13 NMR-spectrum of *cis*-[2-(ethenyl)-cyclohex-1-yl]-methyl 4-toluenesulfonate (100MHz, $CDCl_3$, 23 °C).

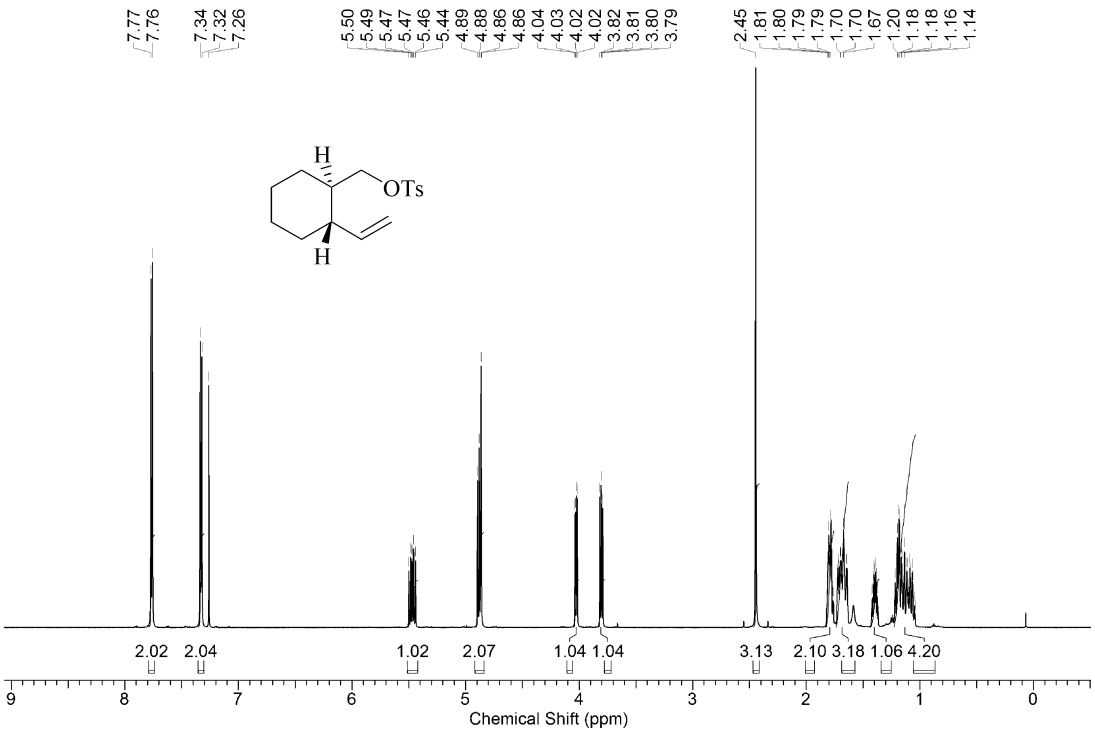

Figure A37. Proton-1 NMR-spectrum of *trans*-[2-(ethenyl)-cyclohex-1-yl]-methyl 4-toluene-sulfonate (600MHz, $CDCl_3$, 23 °C).

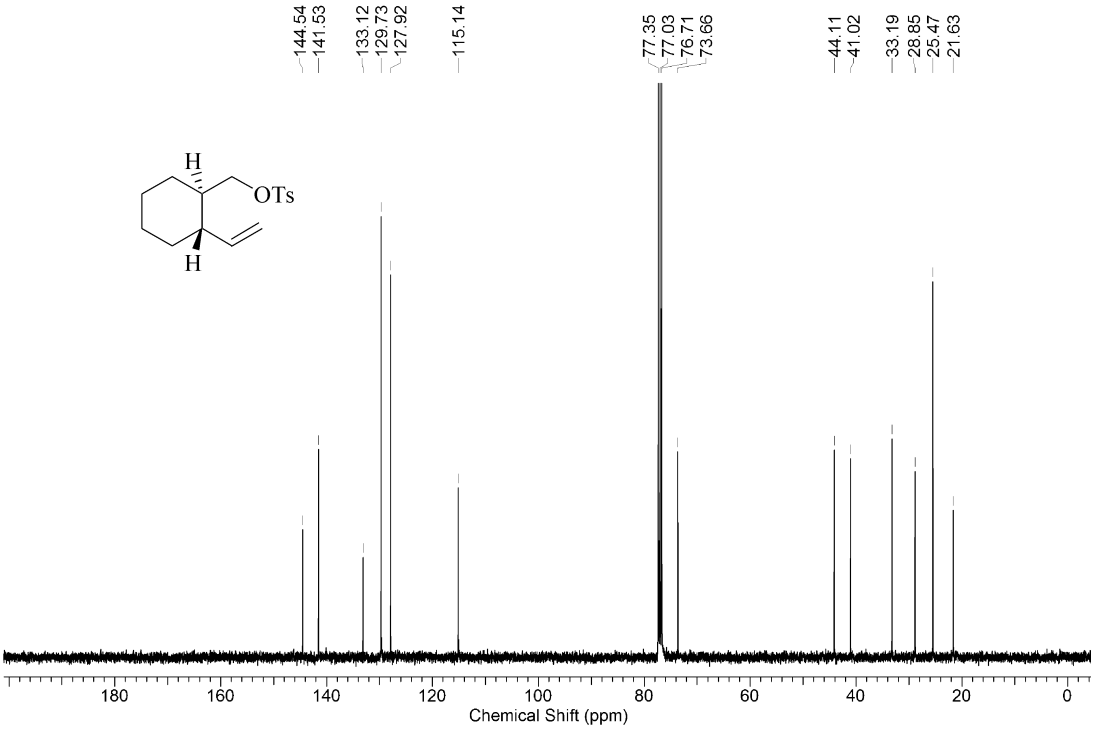

Figure A38. Carbon-13 NMR-spectrum of *trans*-[2-(ethenyl)-cyclohex-1-yl]-methyl 4-toluene-sulfonate (100MHz, $CDCl_3$, 23 °C).

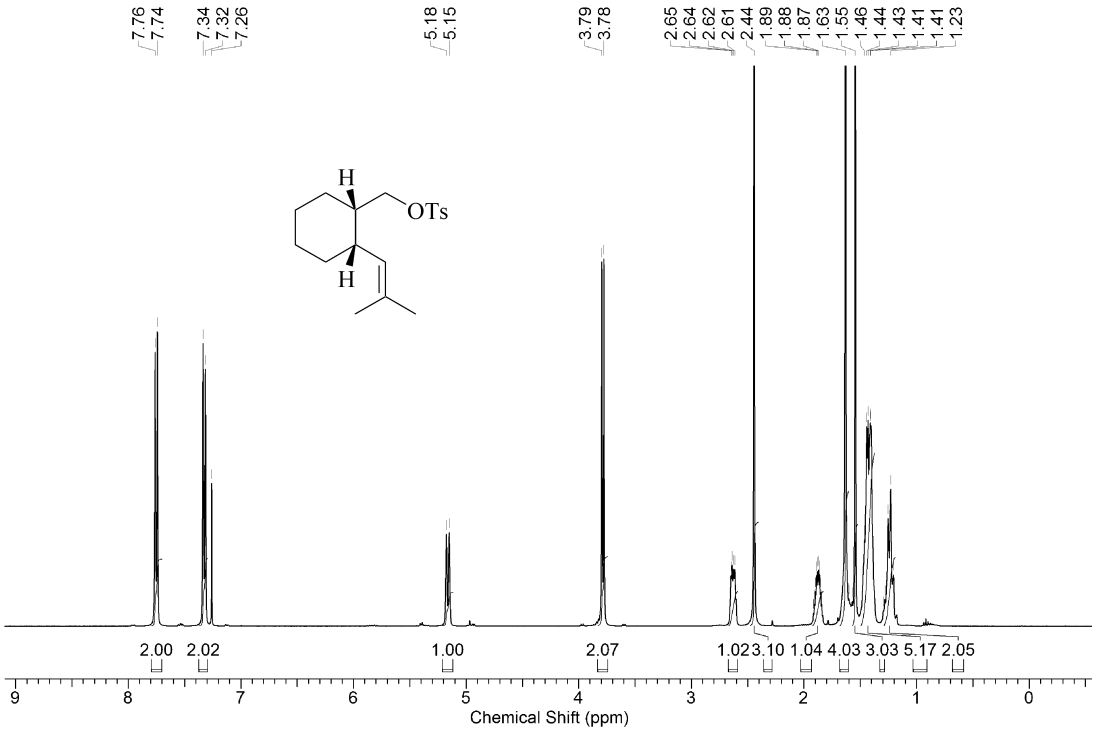

Figure A39. Proton-1 NMR-spectrum of *cis*-[2-(methylprop-1-en-1-yl)-cyclohex-1-yl]-methyl 4-toluenesulfonate (400MHz, $CDCl_3$, 23 °C).

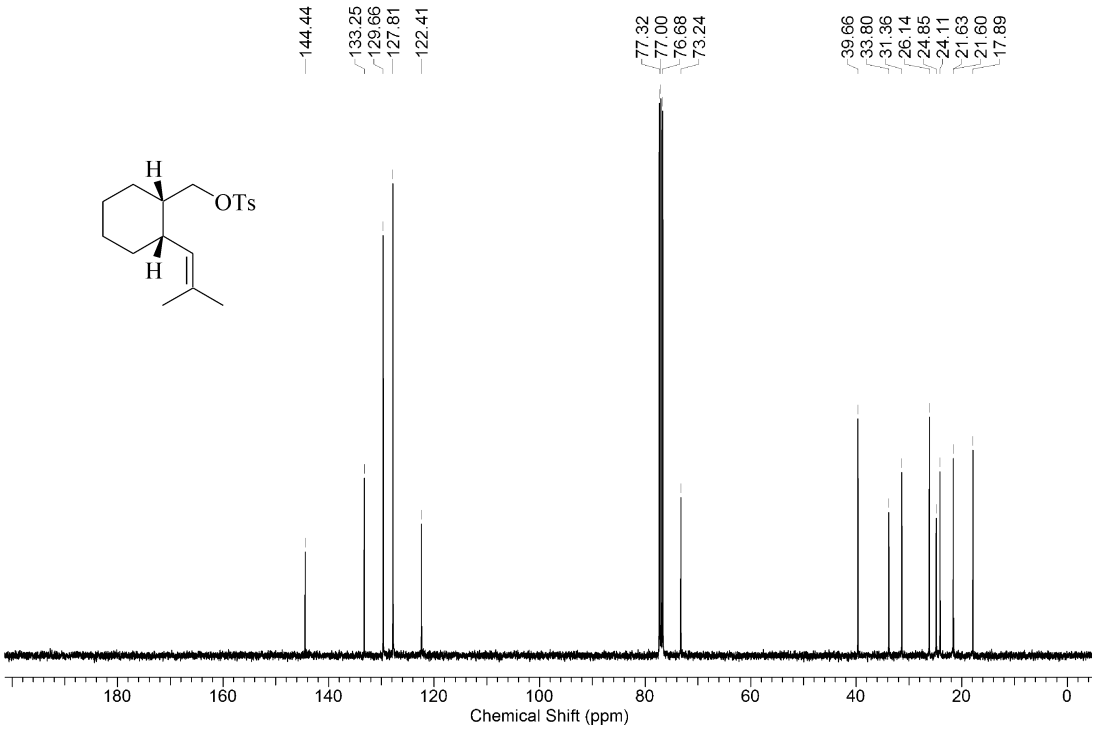

Figure A40. Carbon-13 NMR-spectrum of *cis*-[2-(methylprop-1-en-1-yl)-cyclohex-1-yl]-methyl 4-toluenesulfonate (100MHz, $CDCl_3$, 23 °C).

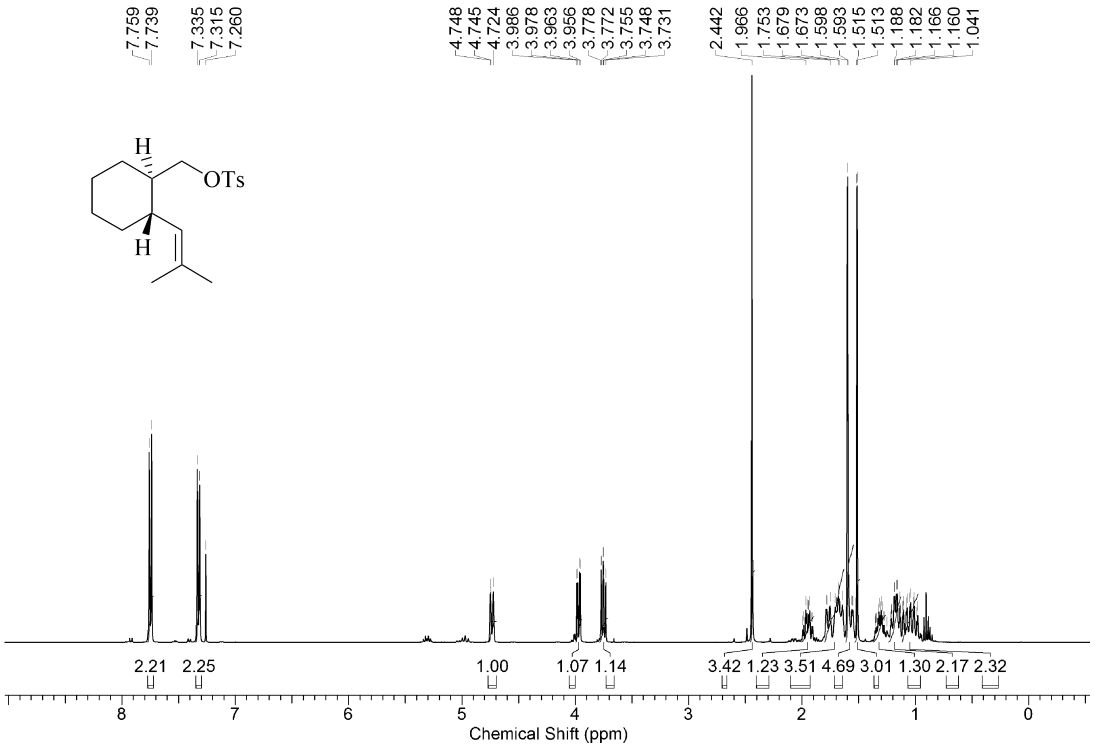

Figure A41. Proton-1 NMR-spectrum of *trans*-[2-(methylprop-1-en-1-yl)-cyclohex-1-yl]-methyl 4-toluenesulfonate (400MHz, $CDCl_3$, 23 °C).

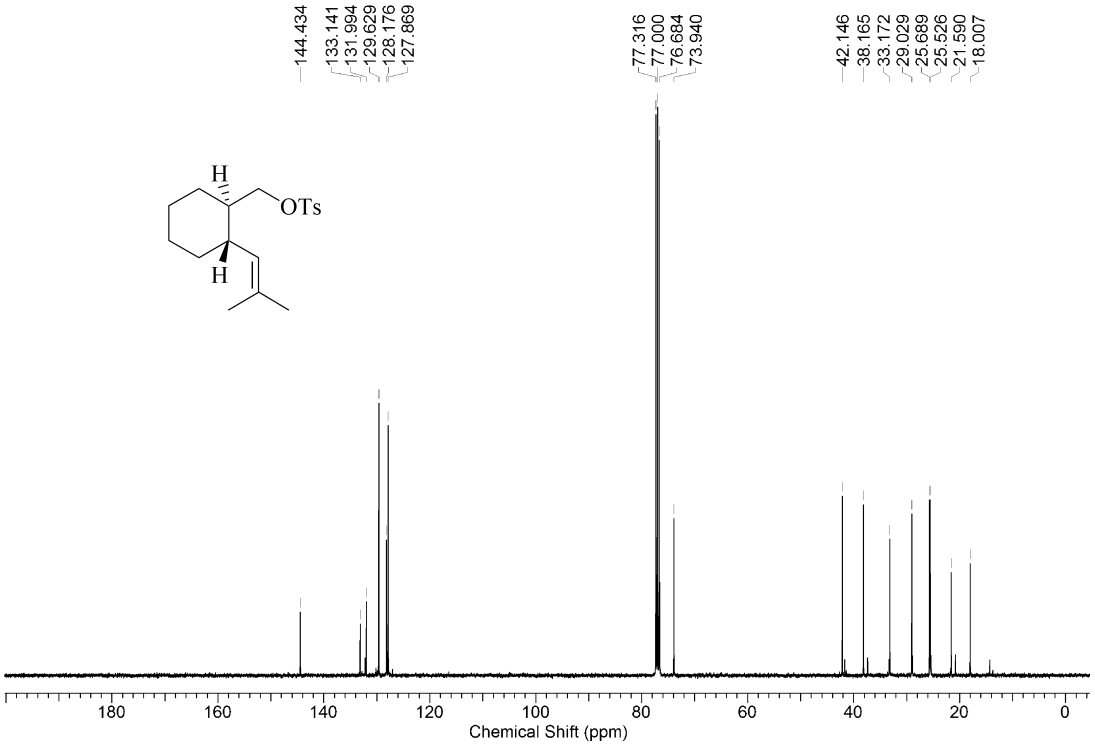

Figure A42. Carbon-13 NMR-spectrum of *trans*-[2-(methylprop-1-en-1-yl)-cyclohex-1-yl]-methyl 4-toluenesulfonate (100MHz, $CDCl_3$, 23 °C).

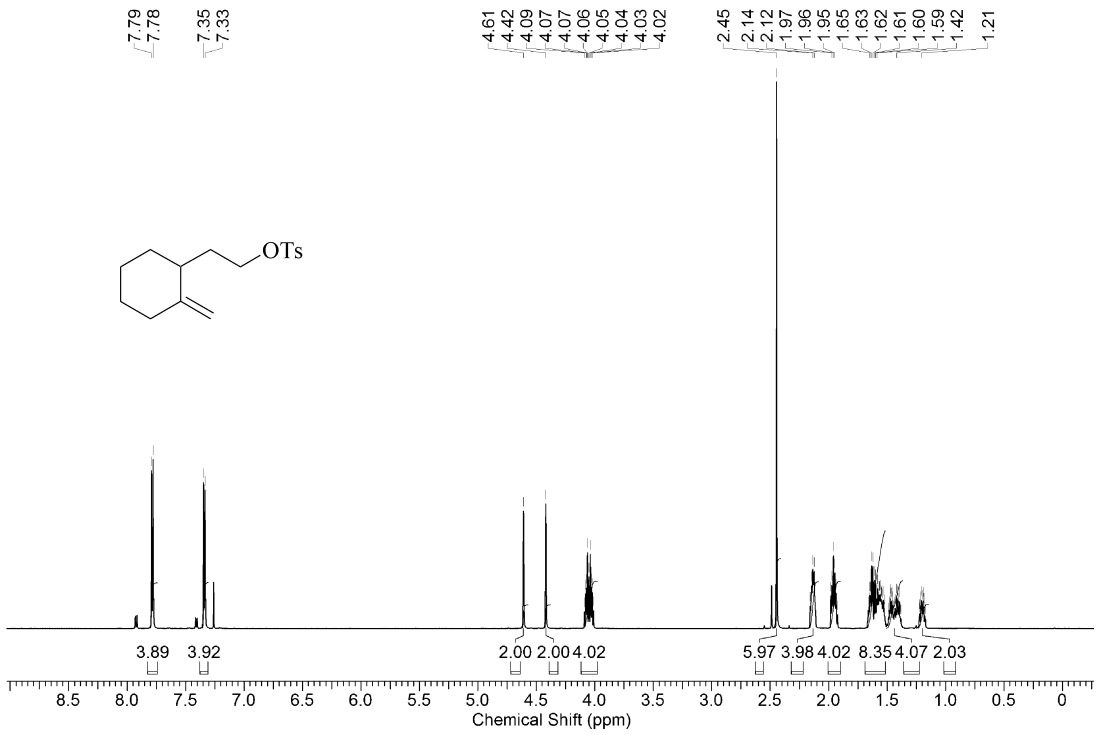

Figure A43. Proton-1 NMR-spectrum of 2-(1-methylenecyclohex-2-yl)-eth-1-yl 4-toluenesulfonate (600MHz, $CDCl_3$, 23 °C).

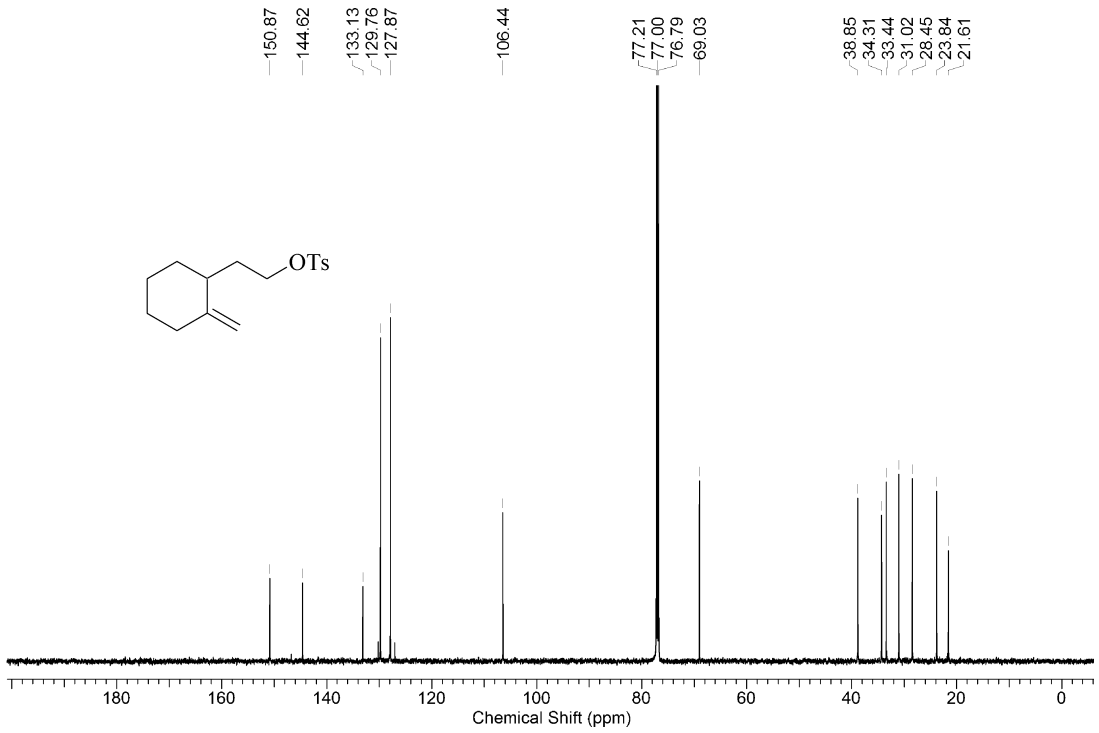

Figure A44. Carbon-13 NMR-spectrum of 2-(1-methylenecyclohex-2-yl)-eth-1-yl 4-toluenesulfonate (150MHz, $CDCl_3$, 23 °C).

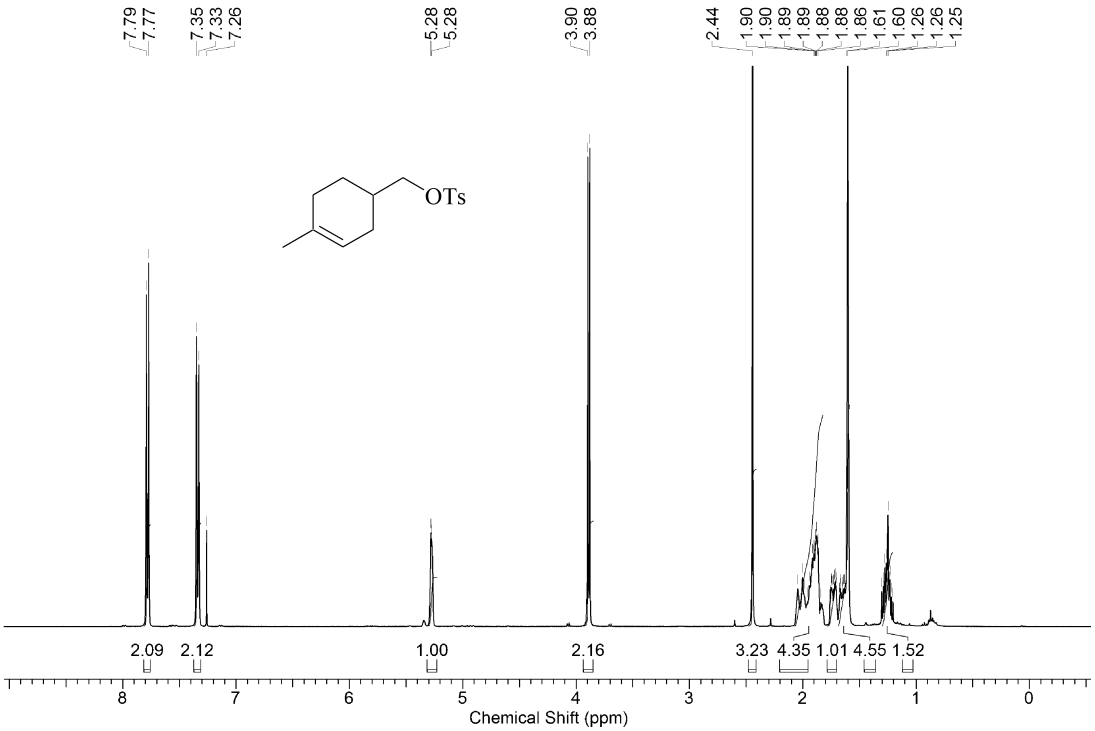

Figure A45. Proton-1 NMR-spectrum of (1-methylcyclohex-1-en-4-yl)-methyl 4-toluene-sulfonate (400MHz, $CDCl_3$, 23 °C).

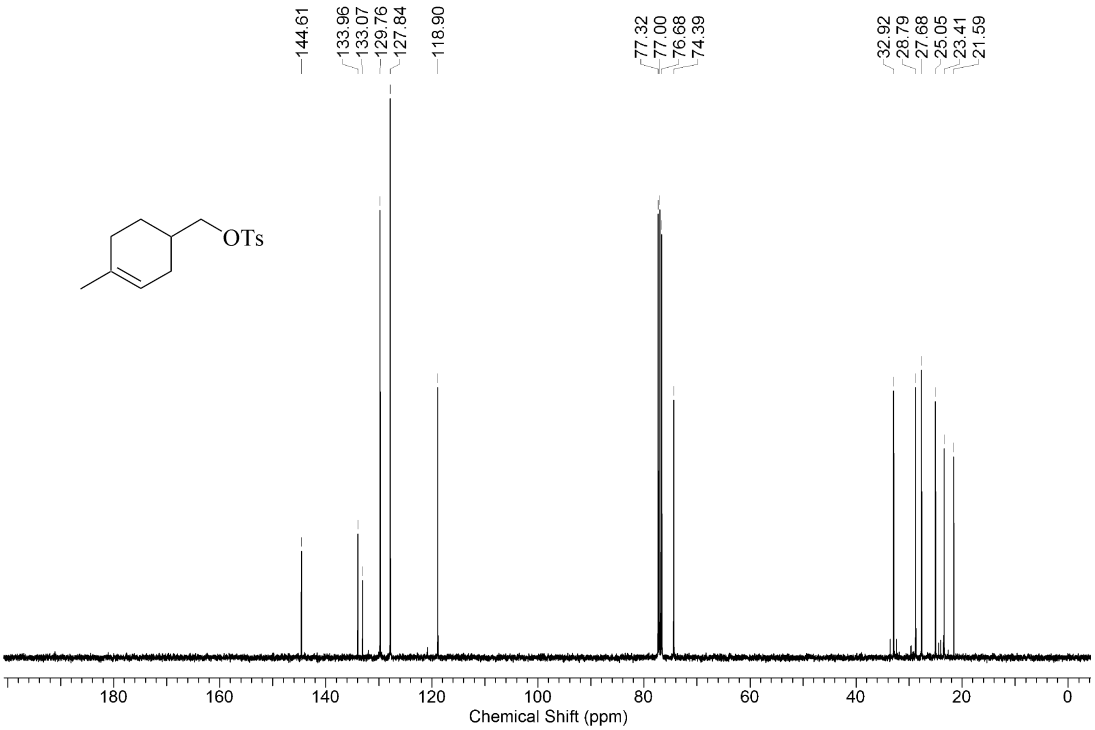

Figure A46. Carbon-13 NMR-spectrum of (1-methylcyclohex-1-en-4-yl)-methyl 4-toluene-sulfonate (100MHz, $CDCl_3$, 23 °C).

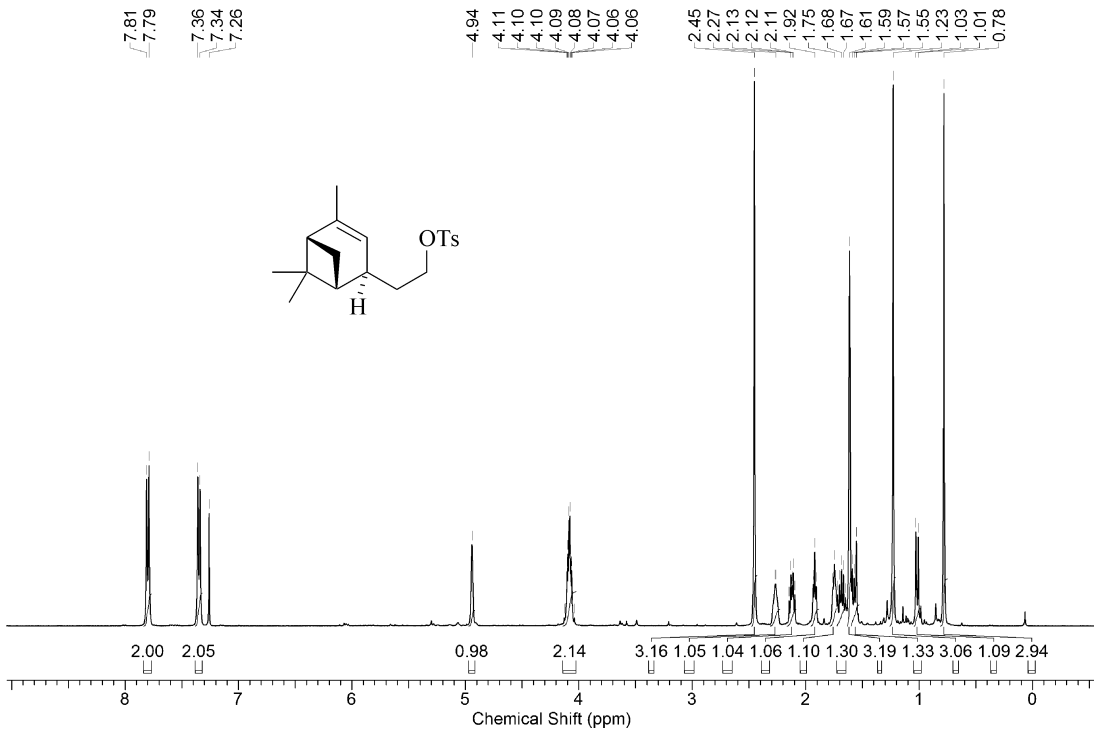

Figure A47. Proton-1 NMR-spectrum of 2-{(1*S*,4*S*,5*R*)-2,6,6-trimethylbicyclo[3.1.1]hept-2-en-4-yl}-ethyl 4-toluenesulfonate (400MHz, $CDCl_3$, 23 °C).

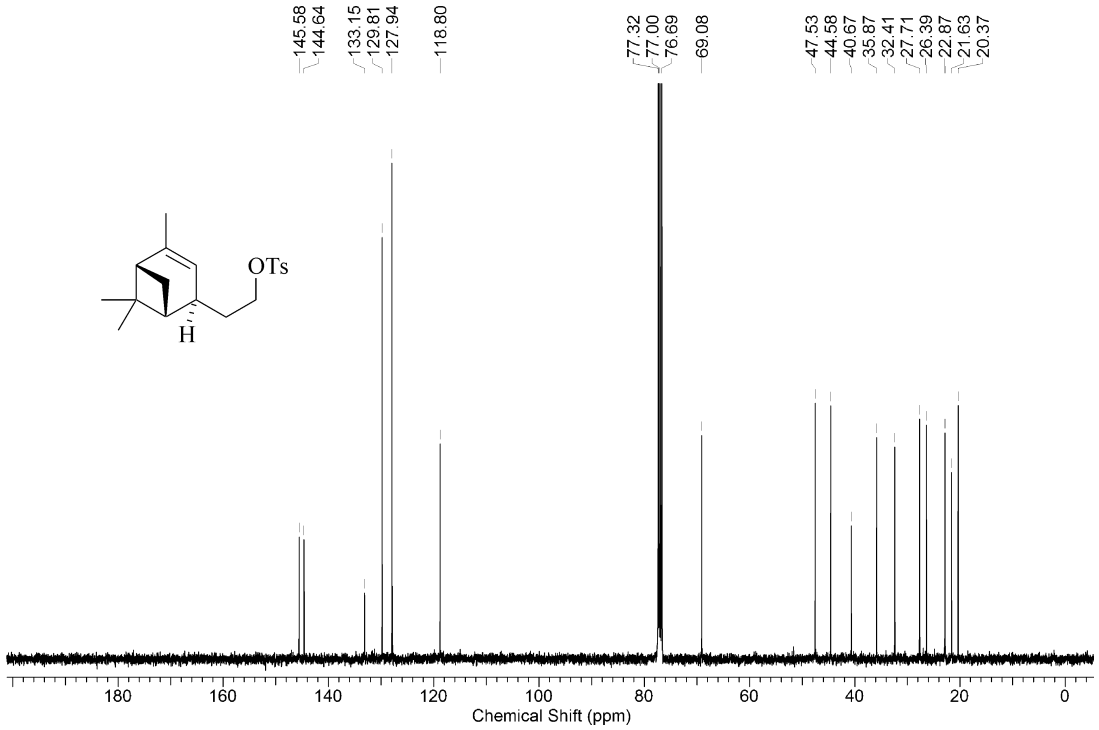

Figure A48. Carbon-1 NMR-spectrum of 2-{(1*S*,4*S*,5*R*)-2,6,6-trimethylbicyclo[3.1.1]hept-2-en-4-yl}-ethyl 4-toluenesulfonate (100MHz, $CDCl_3$, 23 °C).

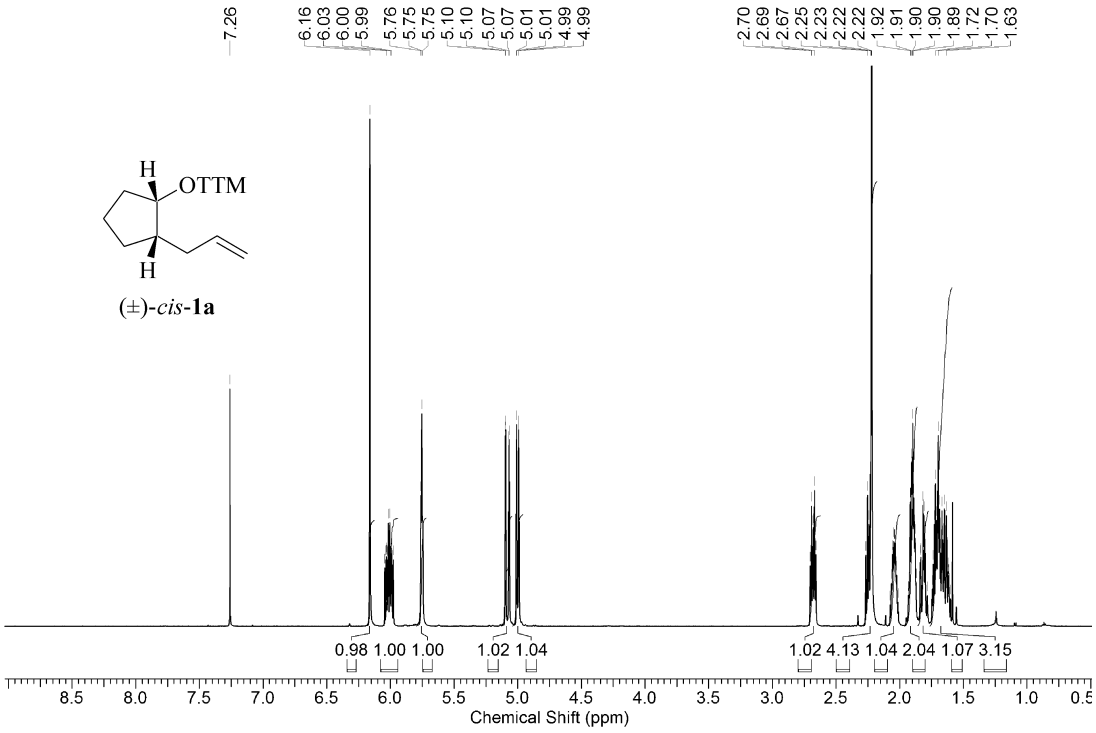

Figure A49. Proton-1 NMR-spectrum of 3-[*cis*-2-(prop-2-en-1-yl)-cyclopent-1-yloxy]-4-methylthiazole-2(3*H*)-thione *cis*-(**1a**) (600MHz, $CDCl_3$, 23 °C).

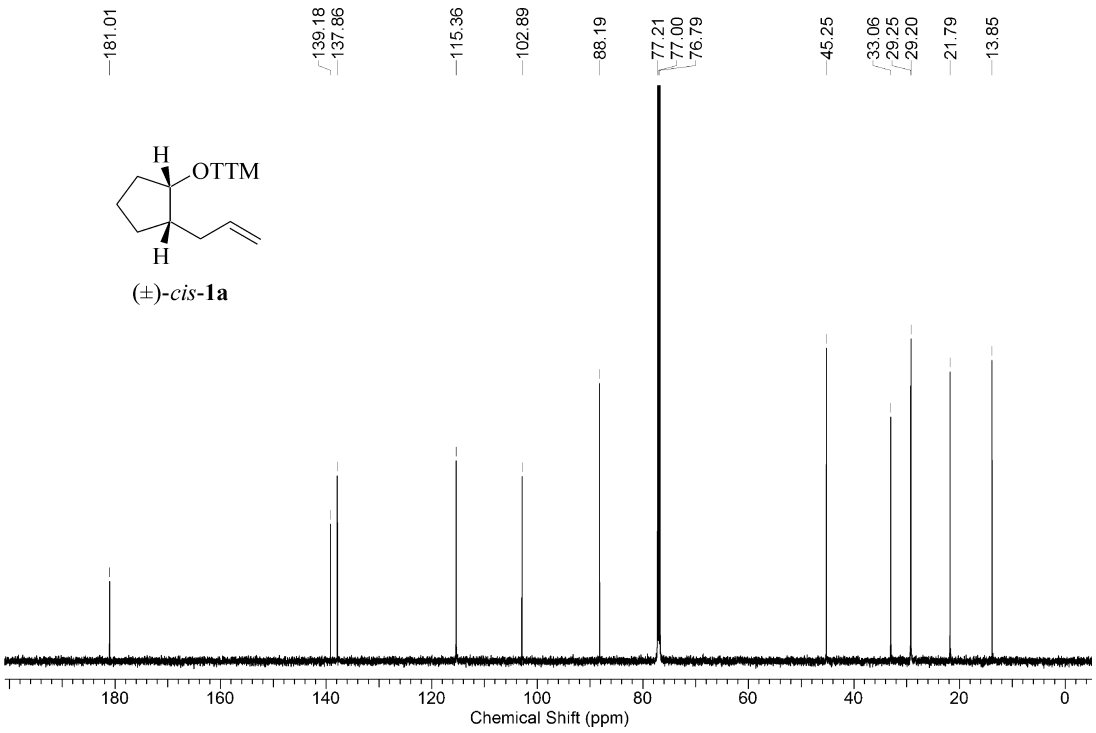

Figure A50. Carbon-1 NMR-spectrum of 3-[*cis*-2-(prop-2-en-1-yl)-cyclopent-1-yloxy]-4-methylthiazole-2(3*H*)-thione *cis*-(**1a**) (150MHz, $CDCl_3$, 23 °C).

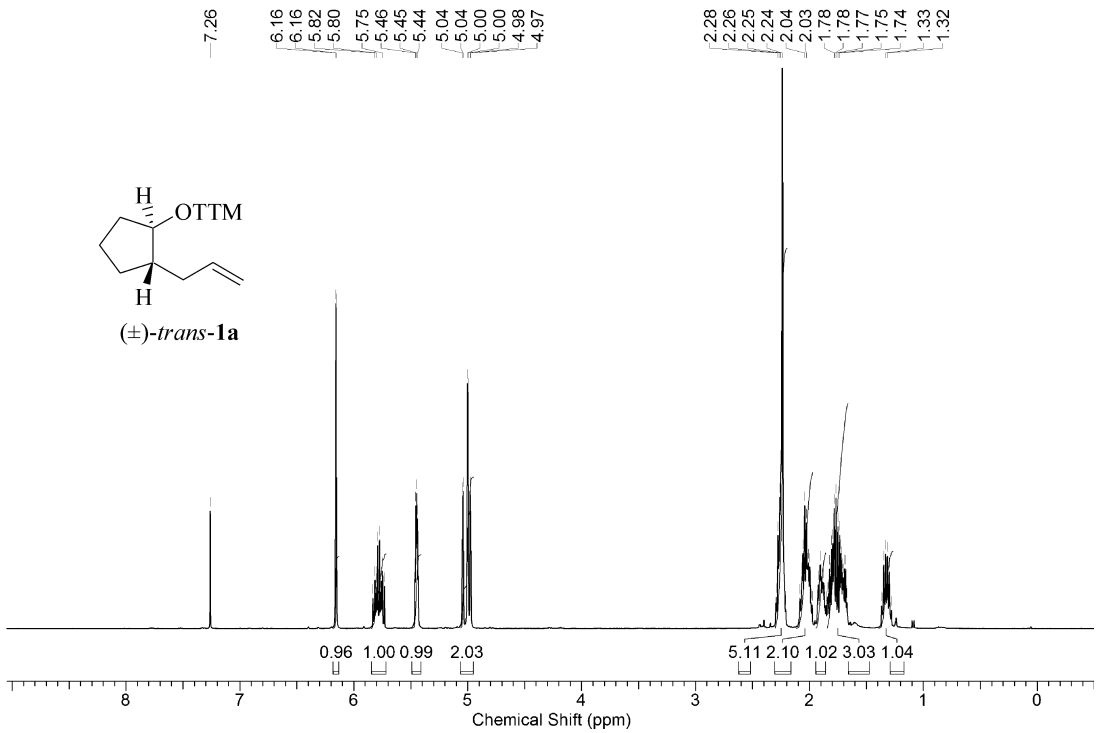

Figure A51. Proton-1 NMR-spectrum of 3-[*trans*-2-(prop-2-en-1-yl)-cyclopent-1-yloxy]-4-methylthiazole-2(3*H*)-thione *trans*-(**1a**) (400MHz, $CDCl_3$, 23 °C).

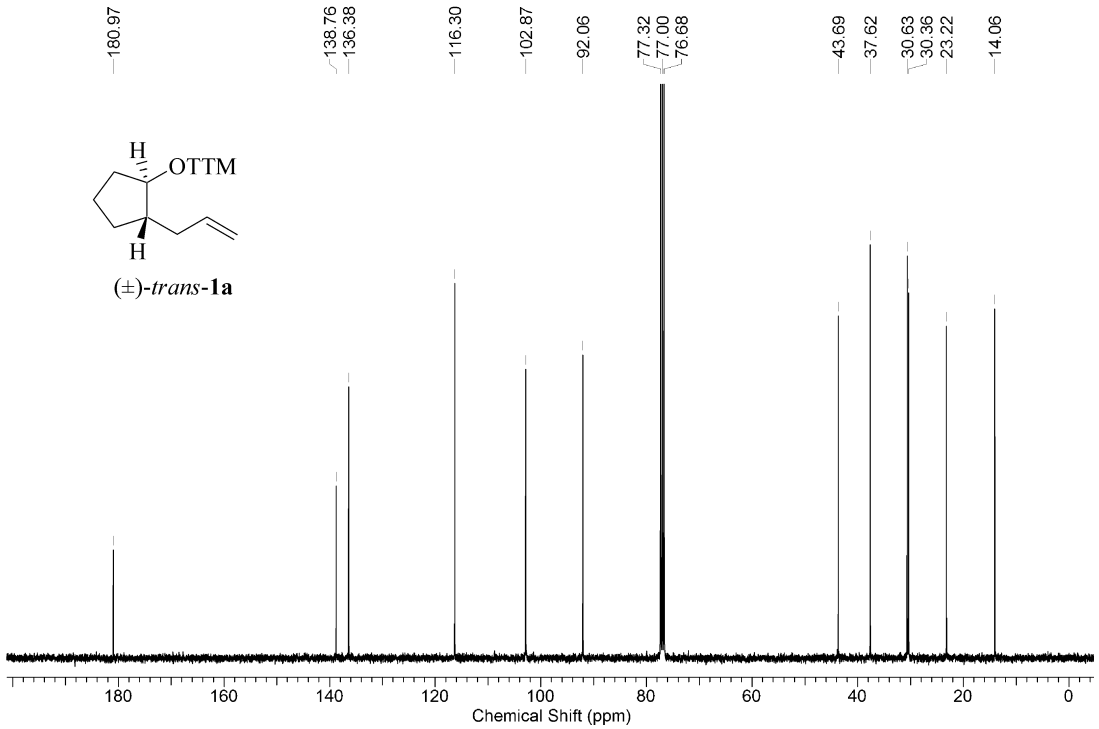

Figure A52. Carbon-13 NMR-spectrum of 3-[*trans*-2-(prop-2-en-1-yl)-cyclopent-1-yloxy]-4-methylthiazole-2(3*H*)-thione *trans*-(**1a**) (100MHz, $CDCl_3$, 23 °C).

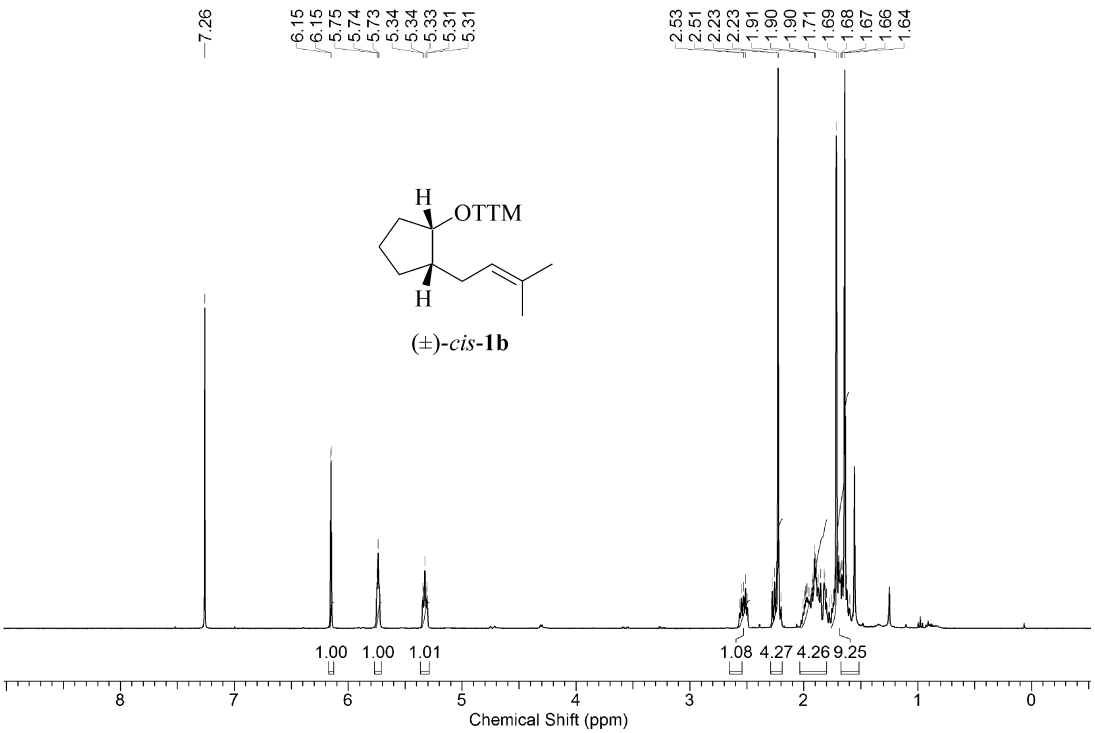

Figure A53. Proton-1 NMR-spectrum of 3-[*cis*-2-(3-methylbut-2-en-1-yl)-cyclopent-1-yloxy]-4-methylthiazole-2(3*H*)-thione *cis*-(**1b**) (400MHz, $CDCl_3$, 23 °C).

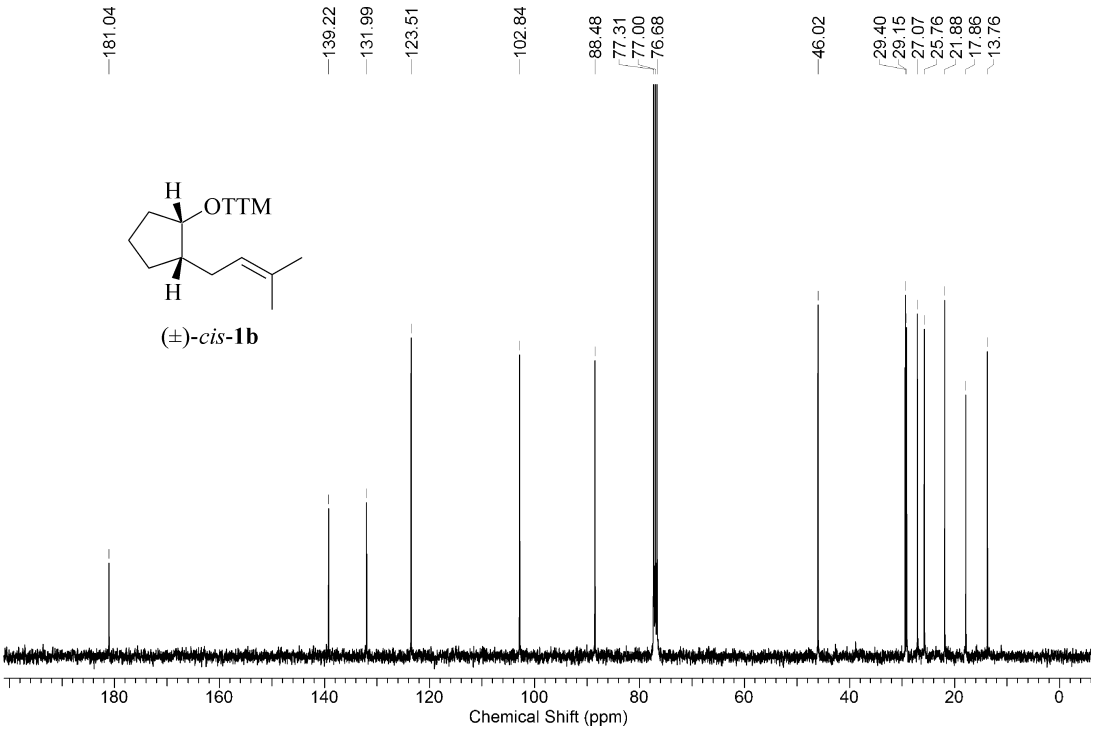

Figure A54. Carbon-13 NMR-spectrum of 3-[*cis*-2-(3-methylbut-2-en-1-yl)-cyclopent-1-yloxy]-4-methylthiazole-2(3*H*)-thione *cis*-(**1b**) (100MHz, $CDCl_3$, 23 °C).

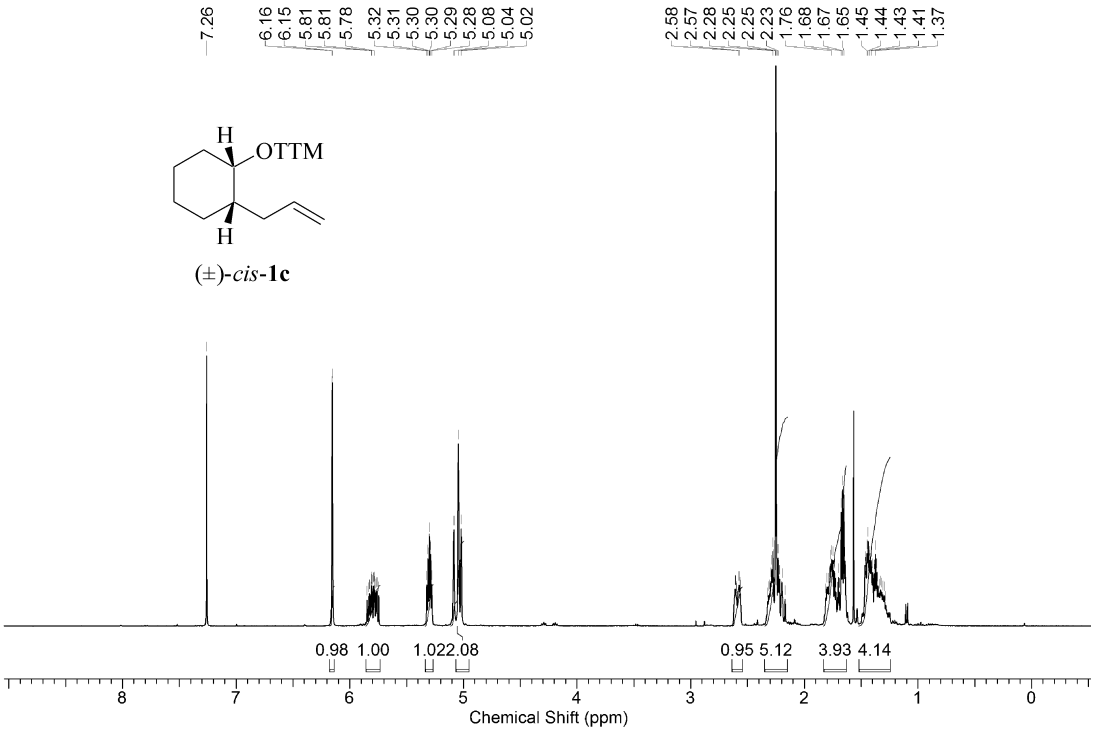

Figure A55. Proton-1 NMR-spectrum of 3-[*cis*-2-(prop-2-en-1-yl)-cyclohex-1-yloxy]-4-methylthiazole-2(3*H*)-thione *cis*-(**1c**) (400MHz, $CDCl_3$, 23 °C).

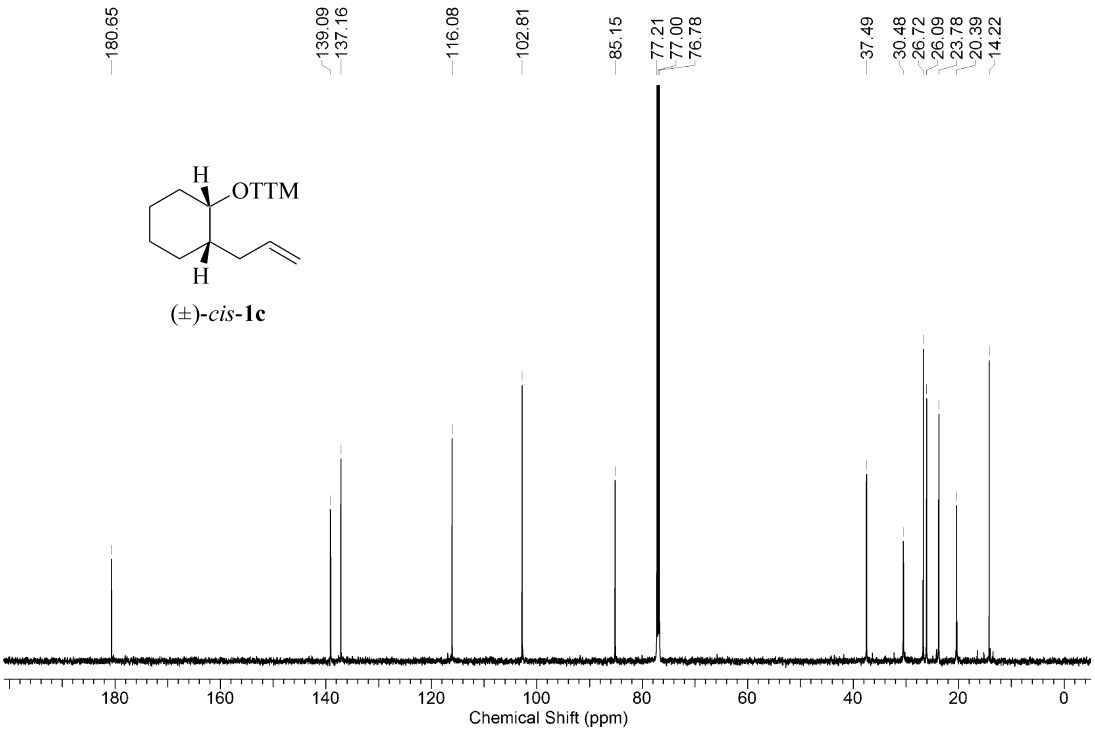

Figure A56. Carbon-13 NMR-spectrum of 3-[*cis*-2-(prop-2-en-1-yl)-cyclohex-1-yloxy]-4-methylthiazole-2(3*H*)-thione *cis*-(**1c**) (150MHz, $CDCl_3$, 23 °C).

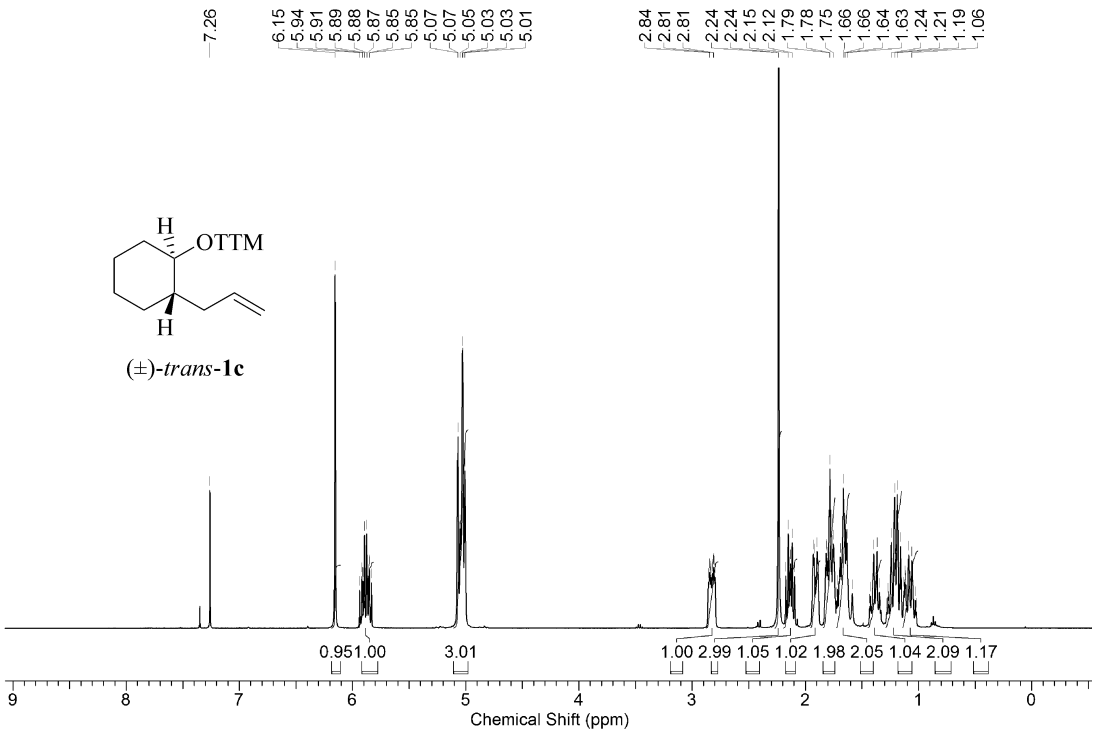

Figure A57. Proton-1 NMR-spectrum of 3-[*trans*-2-(prop-2-en-1-yl)-cyclohex-1-yloxy]-4-methylthiazole-2(3*H*)-thione *trans*-(**1c**) (400MHz, $CDCl_3$, 23 °C).

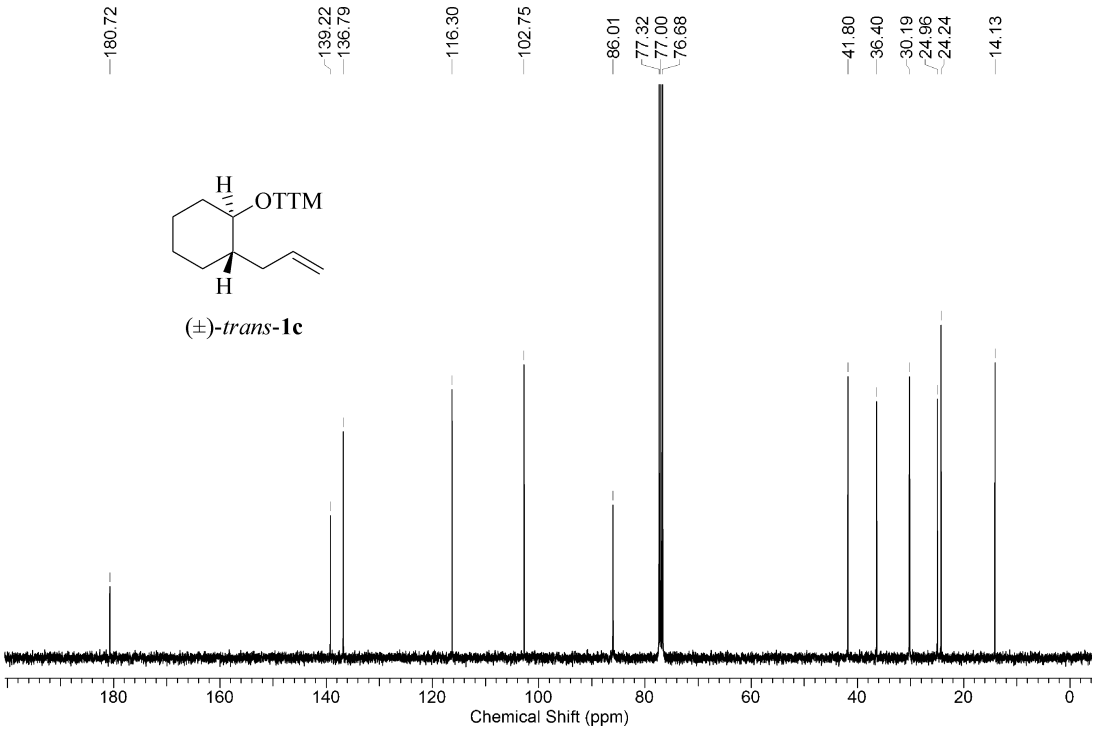

Figure A58. Carbon-13 NMR-spectrum of 3-[*trans*-2-(prop-2-en-1-yl)-cyclohex-1-yloxy]-4-methylthiazole-2(3*H*)-thione *trans*-(**1c**) (100MHz, $CDCl_3$, 23 °C).

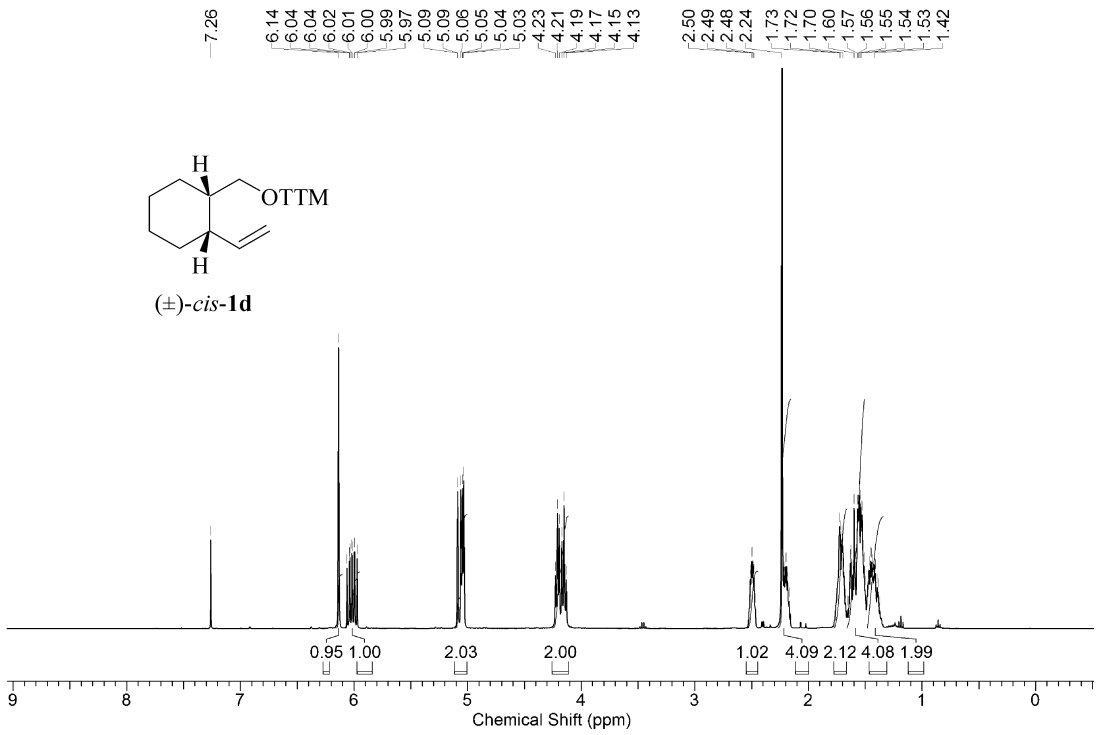

Figure A59. Proton-1 NMR-spectrum of 3-[*cis*-2-(eth-1-en-1-yl)-cyclohex-1-ylmethyloxy]-4-methylthiazole-2(3*H*)-thione *cis*-(**1d**) (400MHz, $CDCl_3$, 23 °C).

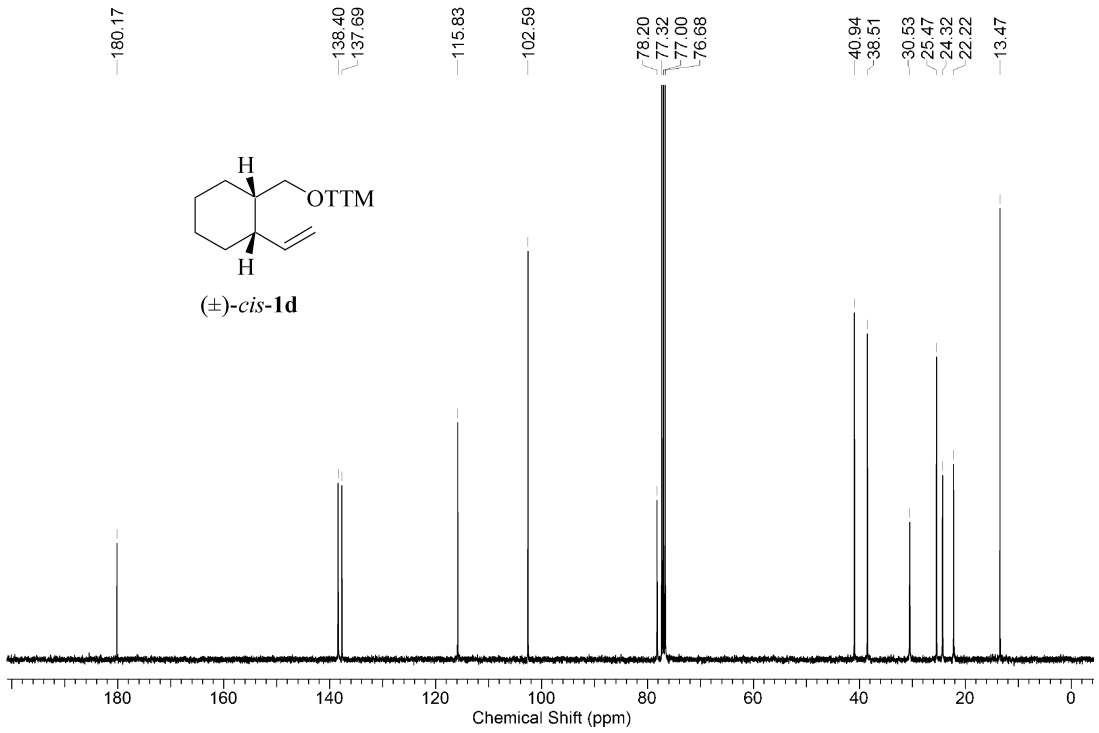

Figure A60. Carbon-13 NMR-spectrum of 3-[*cis*-2-(eth-1-en-1-yl)-cyclohex-1-ylmethyloxy]-4-methylthiazole-2(3*H*)-thione *cis*-(**1d**) (100MHz, $CDCl_3$, 23 °C).

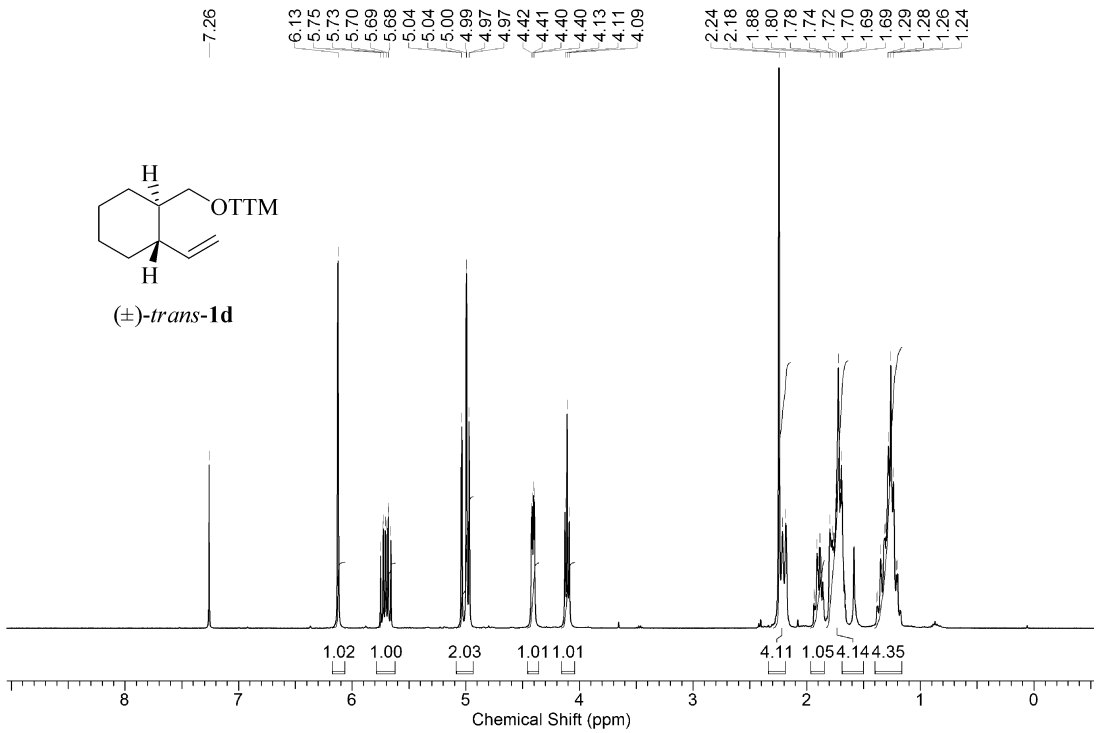

Figure A61. Proton-1 NMR-spectrum of 3-[*trans*-2-(eth-1-en-1-yl)-cyclohex-1-ylmethyloxy]-4-methylthiazole-2(3*H*)-thione *trans*-(**1d**) (400MHz, $CDCl_3$, 23 °C).

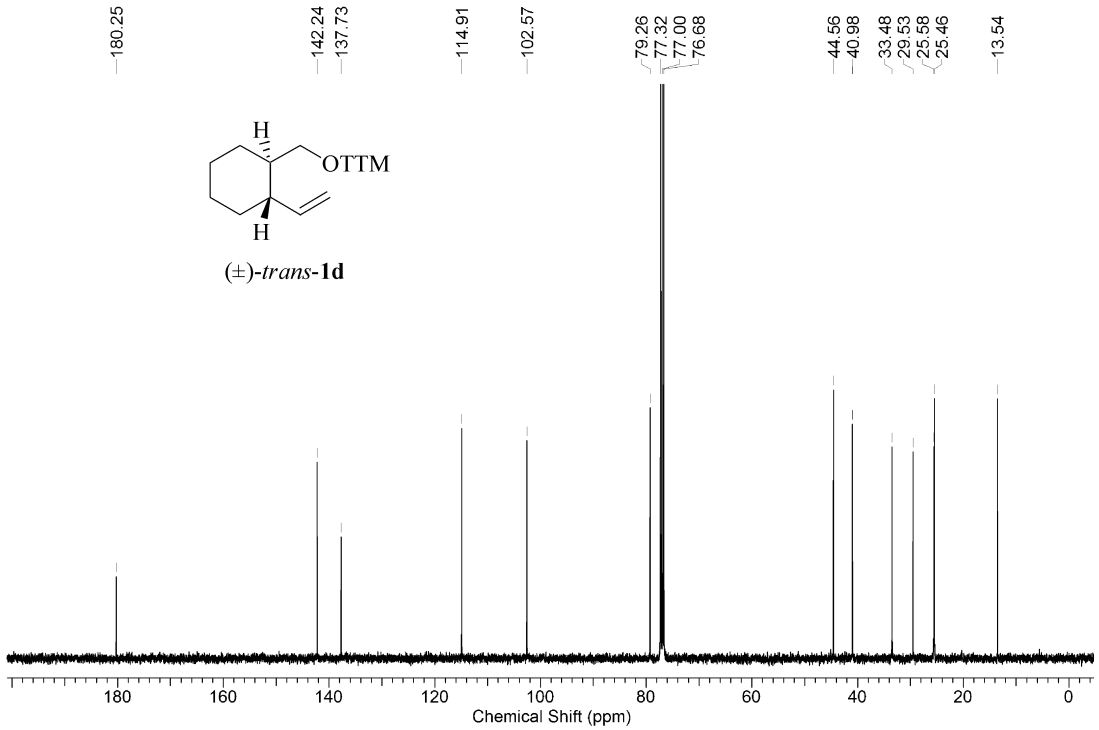

Figure A62. Carbon-13 NMR-spectrum of 3-[*trans*-2-(eth-1-en-1-yl)-cyclohex-1-ylmethyloxy]-4-methylthiazole-2(3*H*)-thione *trans*-(**1d**) (100MHz, $CDCl_3$, 23 °C).

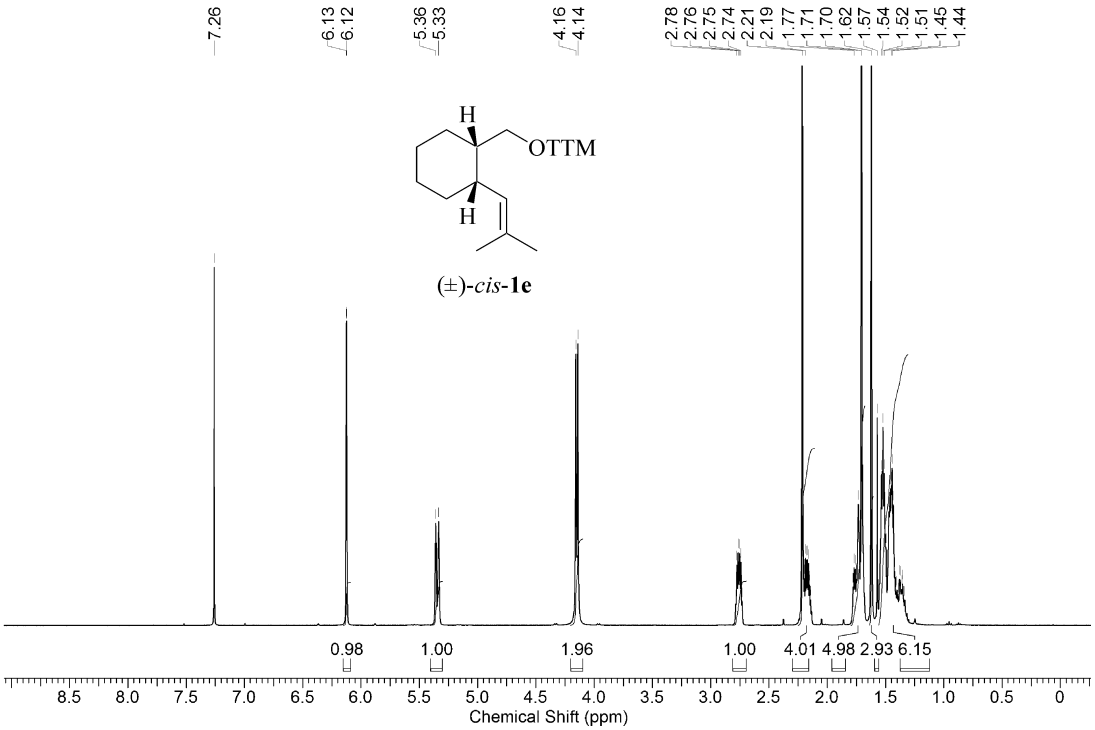

Figure A63. Proton-1 NMR-spectrum of 3-[*cis*-2-(2-methylprop-1-en-1-yl)-cyclohex-1-ylmethyloxy]-4-methylthiazole-2(3*H*)-thione *cis*-(**1e**) (400MHz, $CDCl_3$, 23 °C).

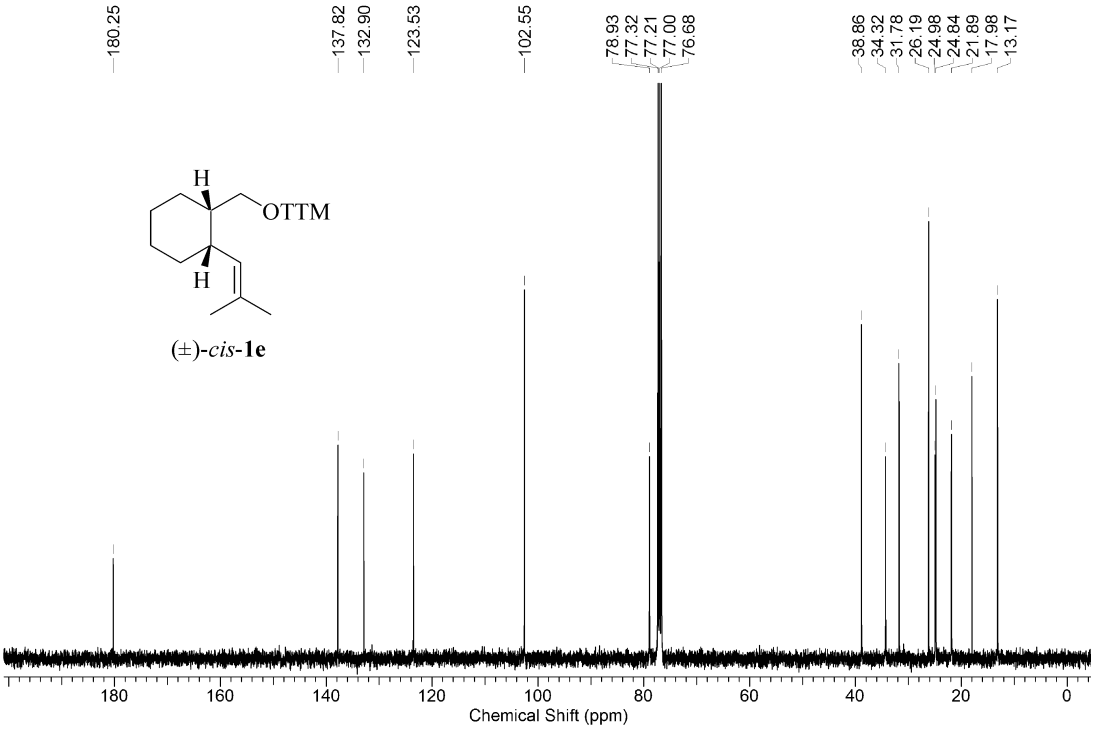

Figure A64. Carbon-13 NMR-spectrum of 3-[*cis*-2-(2-methylprop-1-en-1-yl)-cyclohex-1-ylmethyloxy]-4-methylthiazole-2(3*H*)-thione *cis*-(**1e**) (100MHz, $CDCl_3$, 23 °C).

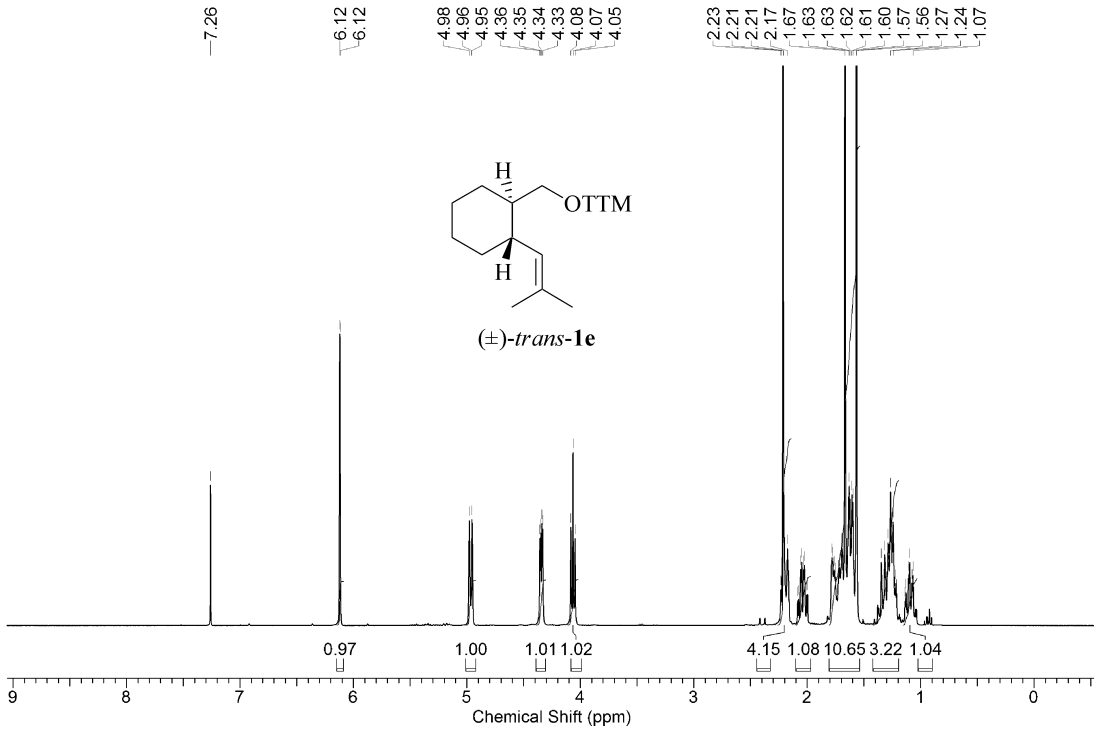

Figure A65. Proton-1 NMR-spectrum of 3-[*trans*-2-(2-methylprop-1-en-1-yl)-cyclohex-1-ylmethyloxy]-4-methylthiazole-2(3*H*)-thione *trans*-(**1e**) (400MHz, $CDCl_3$, 23 °C).

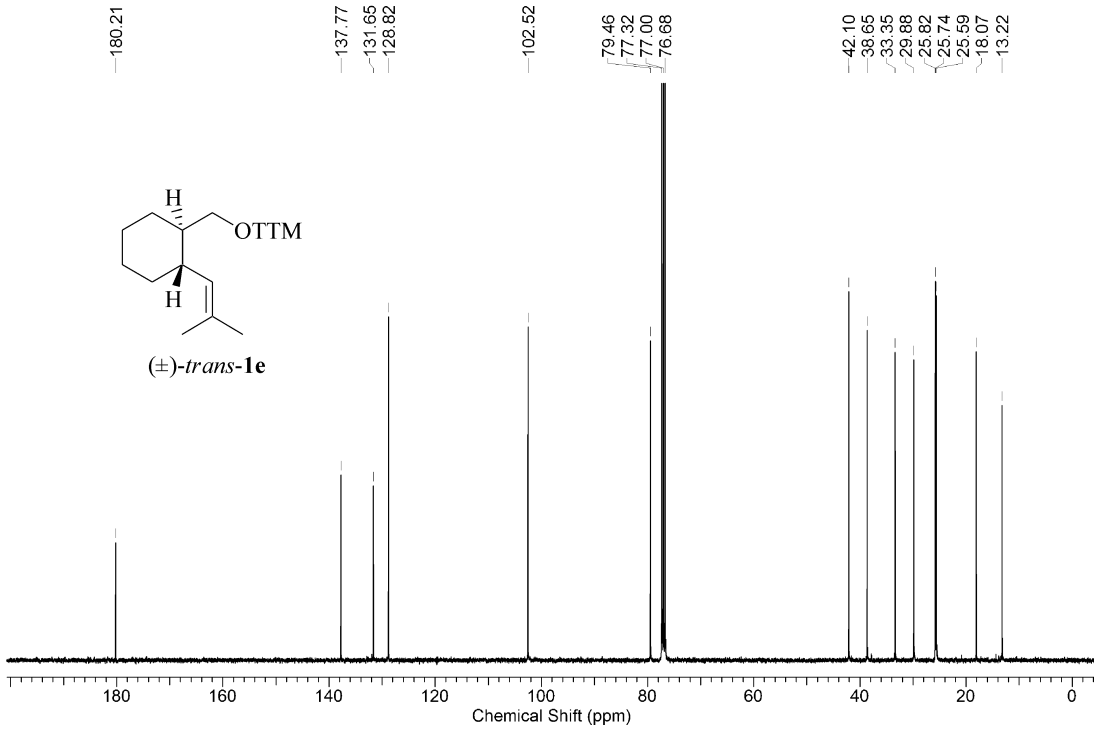

Figure A66. Carbon-13 NMR-spectrum of 3-[*trans*-2-(2-methylprop-1-en-1-yl)-cyclohex-1-ylmethyloxy]-4-methylthiazole-2(3*H*)-thione *trans*-(**1e**) (100MHz, $CDCl_3$, 23 °C).

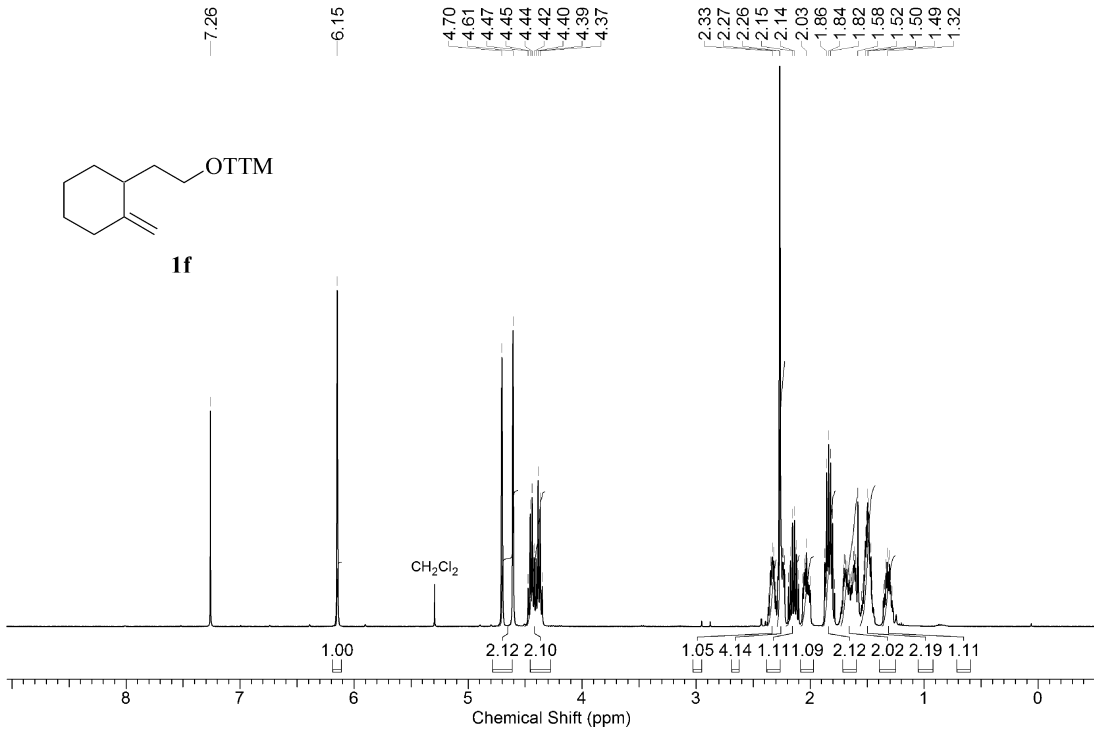

Figure A67. Proton-1 NMR-spectrum of 3-[2-(1-methylenecyclohex-2-yl)-eth-1-yl-2-oxy]-4-methylthiazole-2(3*H*)-thione (**1f**) (400MHz, $CDCl_3$, 23 °C).

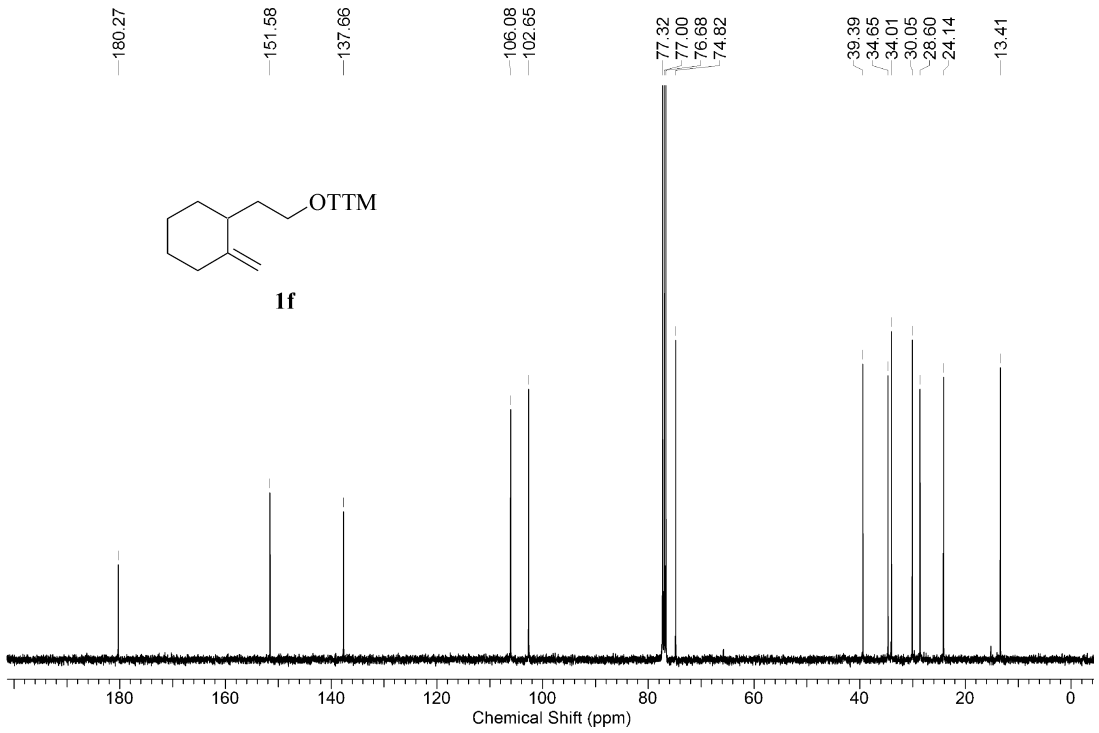

Figure A68. Carbon-13 NMR-spectrum of 3-[2-(1-methylenecyclohex-2-yl)-eth-1-yl-2-oxy]-4-methylthiazole-2(3*H*)-thione (**1f**) (100MHz, $CDCl_3$, 23 °C).

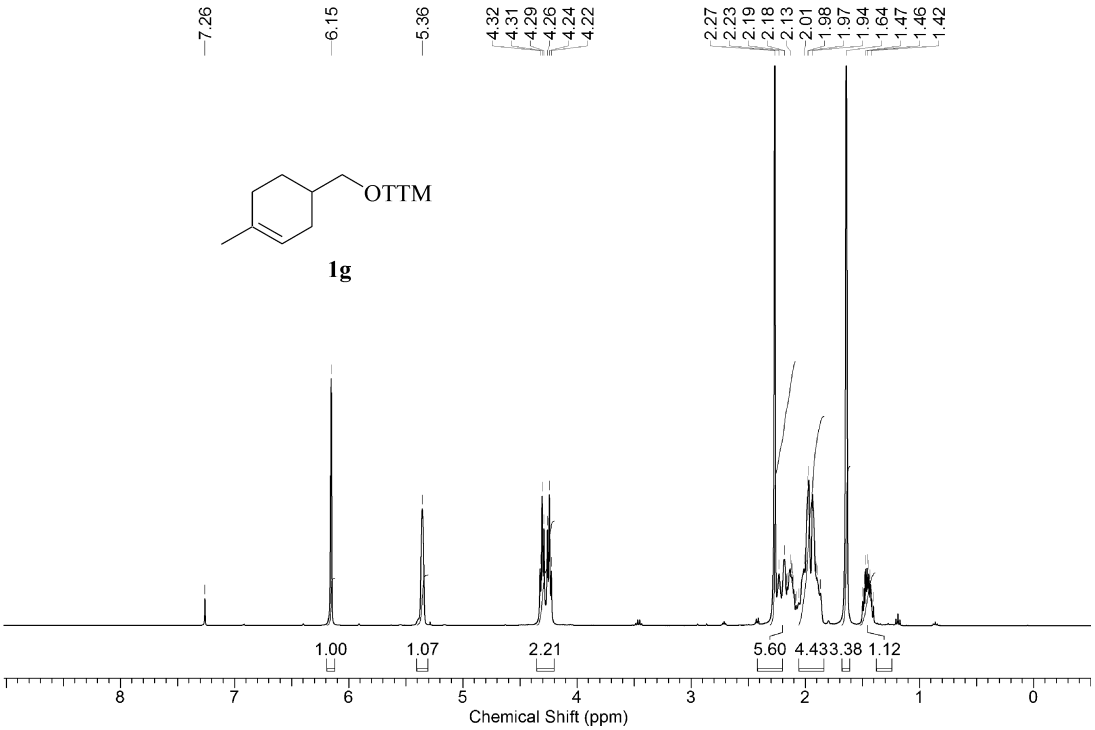

Figure A69. Proton-1 NMR-spectrum of 3-[(1-methylcyclohex-1-en-4-yl)-methyloxy]-4-methylthiazole-2(3*H*)-thione (**1g**) (400MHz, $CDCl_3$, 23 °C).

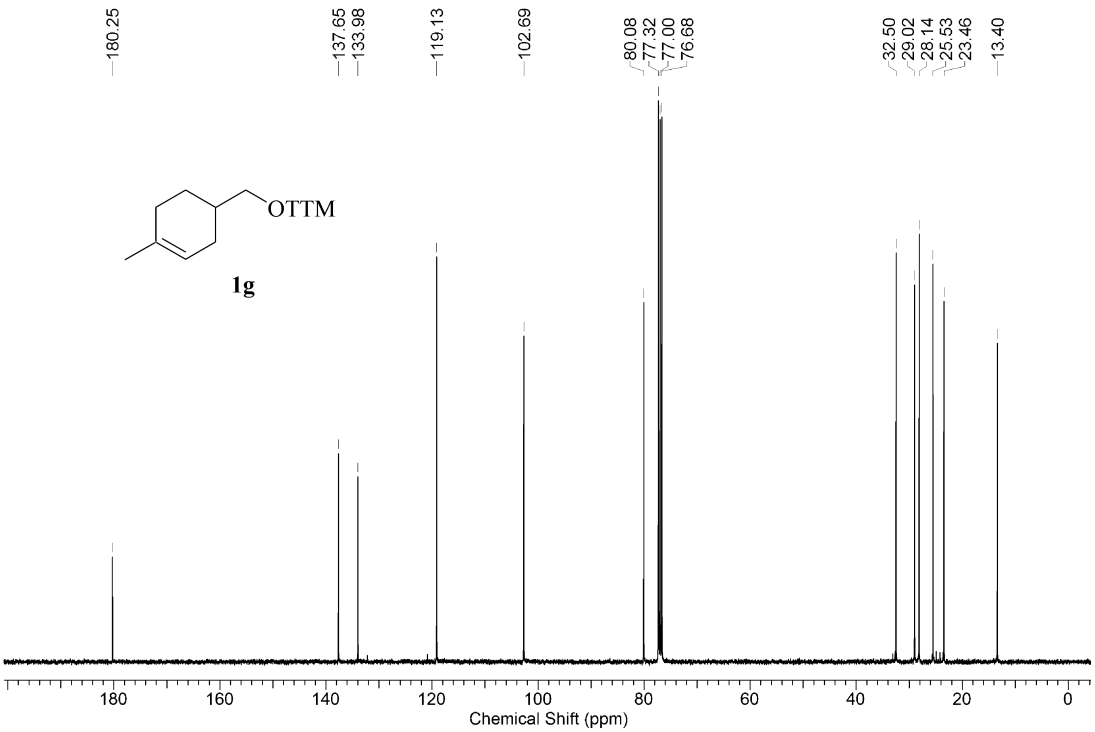

Figure A70. Carbon-13 NMR-spectrum of 3-[(1-methylcyclohex-1-en-4-yl)-methyloxy]-4-methylthiazole-2(3*H*)-thione (**1g**) (100MHz, $CDCl_3$, 23 °C).

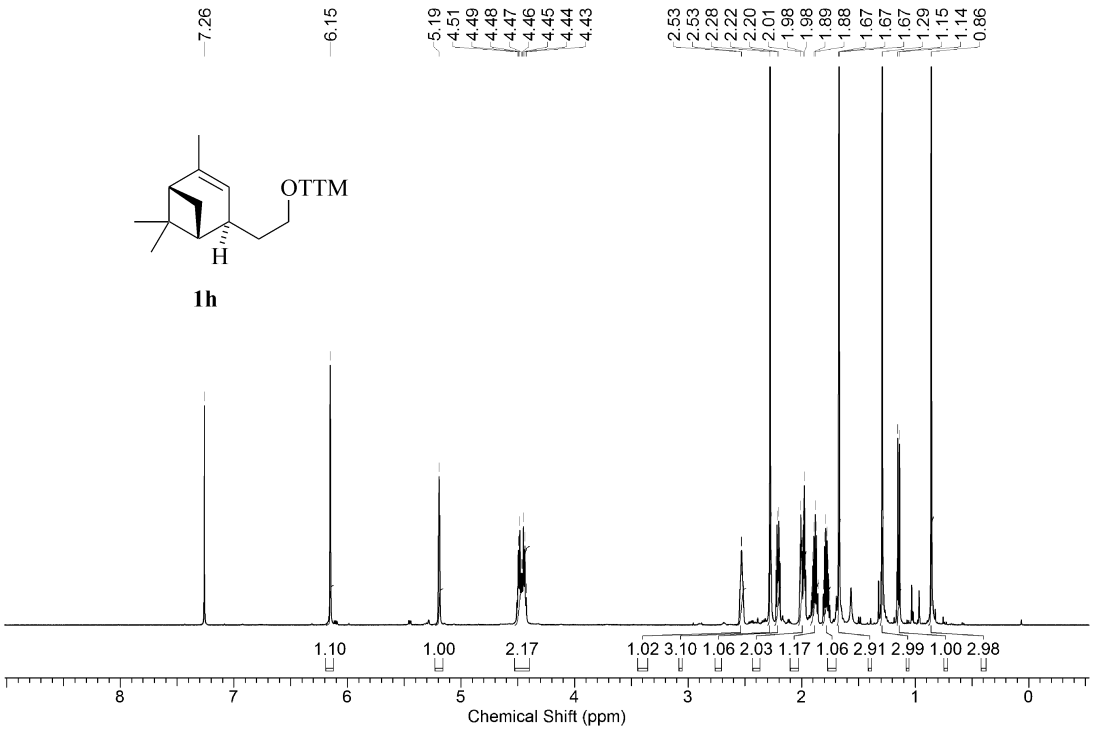

Figure A71. Proton-1 NMR-spectrum of 3-[{(1*S*,4*S*,5*R*)-2,6,6-trimethyl-bicyclo[3.1.1]-hept-2-en-4-yl}eth-1-yl-2-oxy]-4-methylthiazole-2(3*H*)-thione (**1h**) (600MHz, $CDCl_3$, 23 °C).

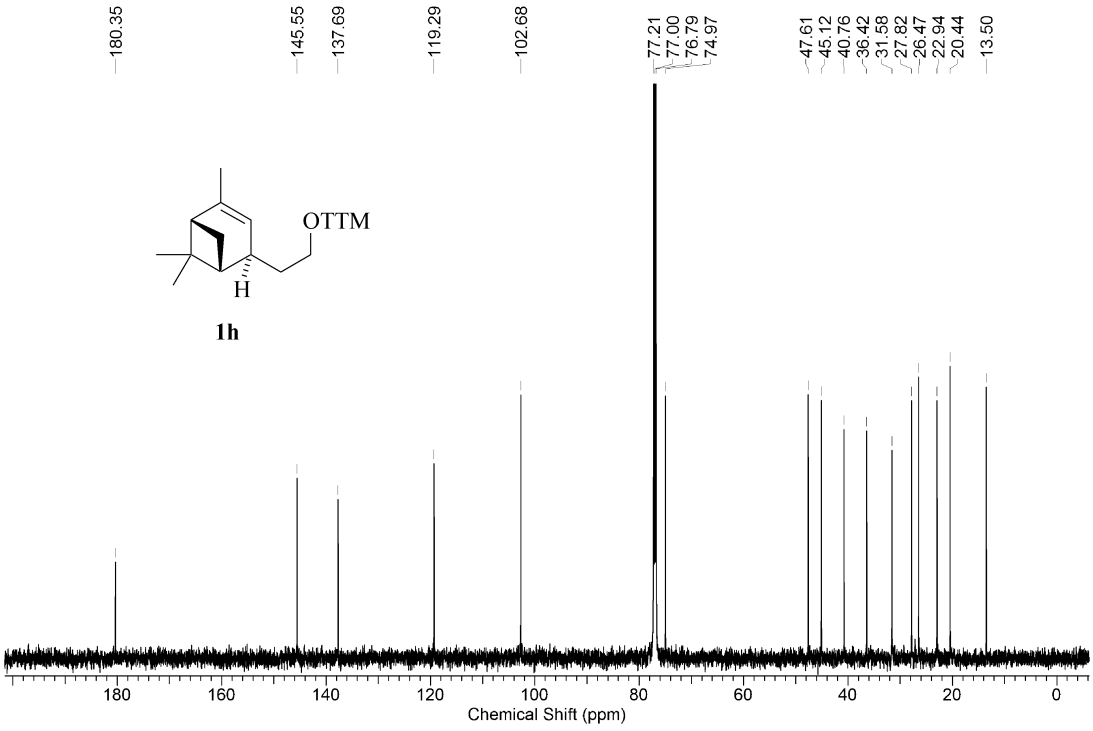

Figure A72. Carbon-13 NMR-spectrum of 3-[{(1*S*,4*S*,5*R*)-2,6,6-trimethyl-bicyclo[3.1.1]-hept-2-en-4-yl}eth-1-yl-2-oxy]-4-methylthiazole-2(3*H*)-thione (**1h**) (150MHz, $CDCl_3$, 23 °C).

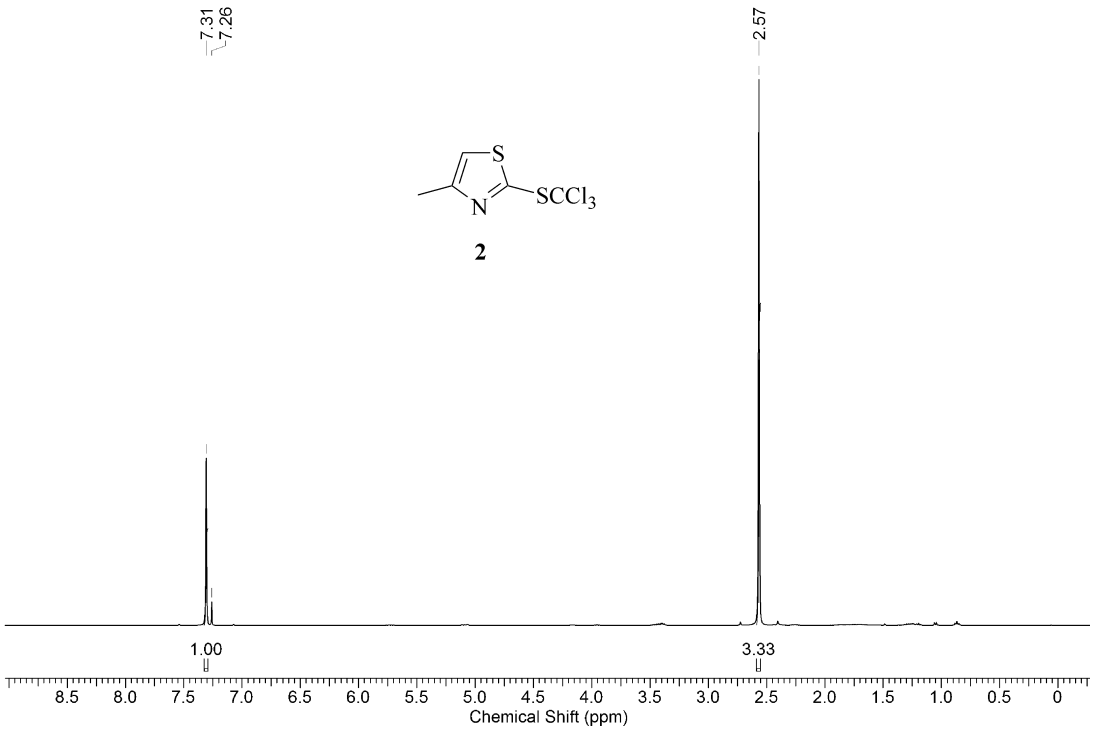

Figure A73. Proton-1 NMR-spectrum of 4-methyl-2-(trichloromethylsulfanyl)-thiazole (**2**) (400MHz, $CDCl_3$, 23 °C).

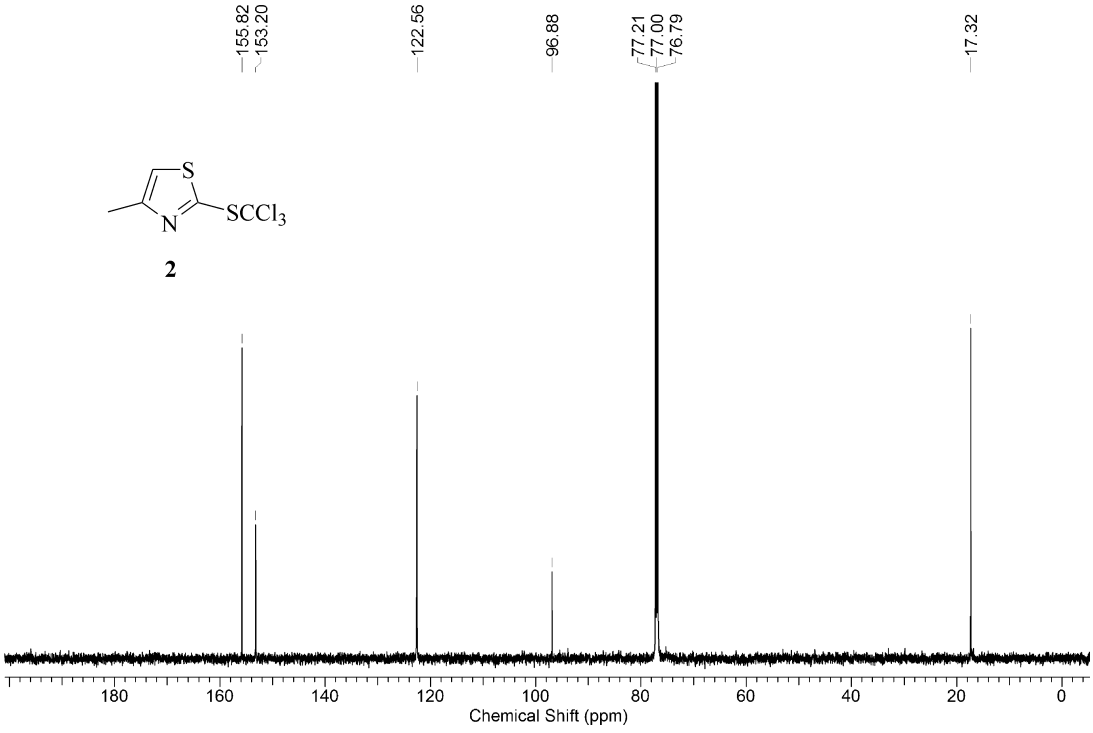

Figure A74. Carbon-13 NMR-spectrum of 4-methyl-2-(trichloromethylsulfanyl)-thiazole (**2**) (150MHz, $CDCl_3$, 23 °C).

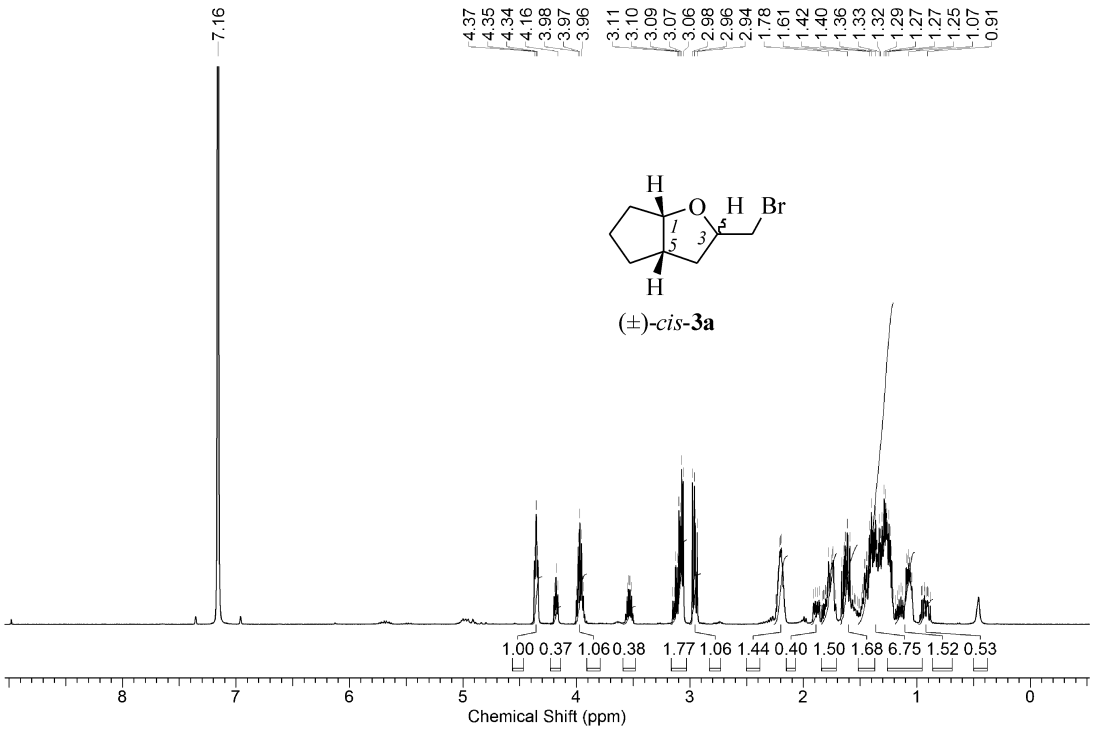

Figure A75. Proton-1 NMR-spectrum of 1,3-cis/trans-isomers, i.e *rel*-(1*S*,3*S*,5*S*)-**3a**/ *rel*-(1*S*,3*R*,5*S*)-**3a**, of 3-bromomethyl-2-oxabicyclo[3.3.0]octane *cis*-(**3a**) (400MHz, C_6D_6, 23 °C).

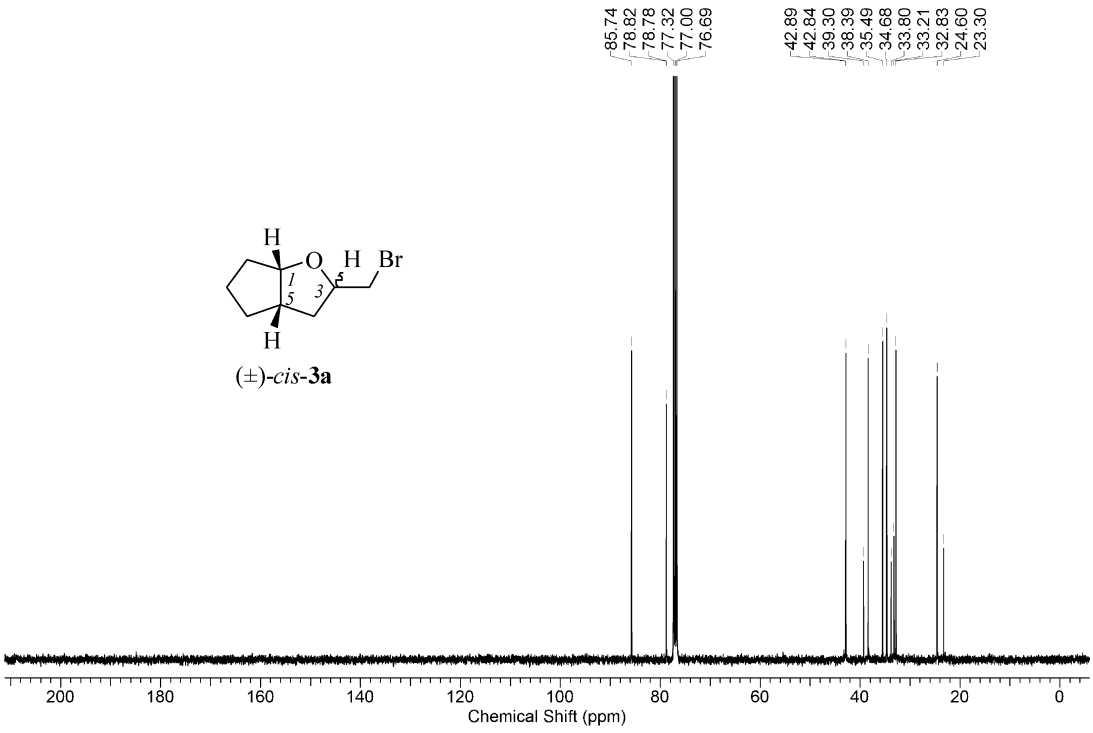

Figure A76. Carbon-13 NMR-spectrum of 1,3-cis/trans-isomers, i.e *rel*-(1*S*,3*S*,5*S*)-**3a**/ *rel*-(1*S*,3*R*,5*S*)-**3**, of 3-bromomethyl-2-oxabicyclo[3.3.0]octane *cis*-(**3a**) (100MHz, $CDCl_3$, 23 °C).

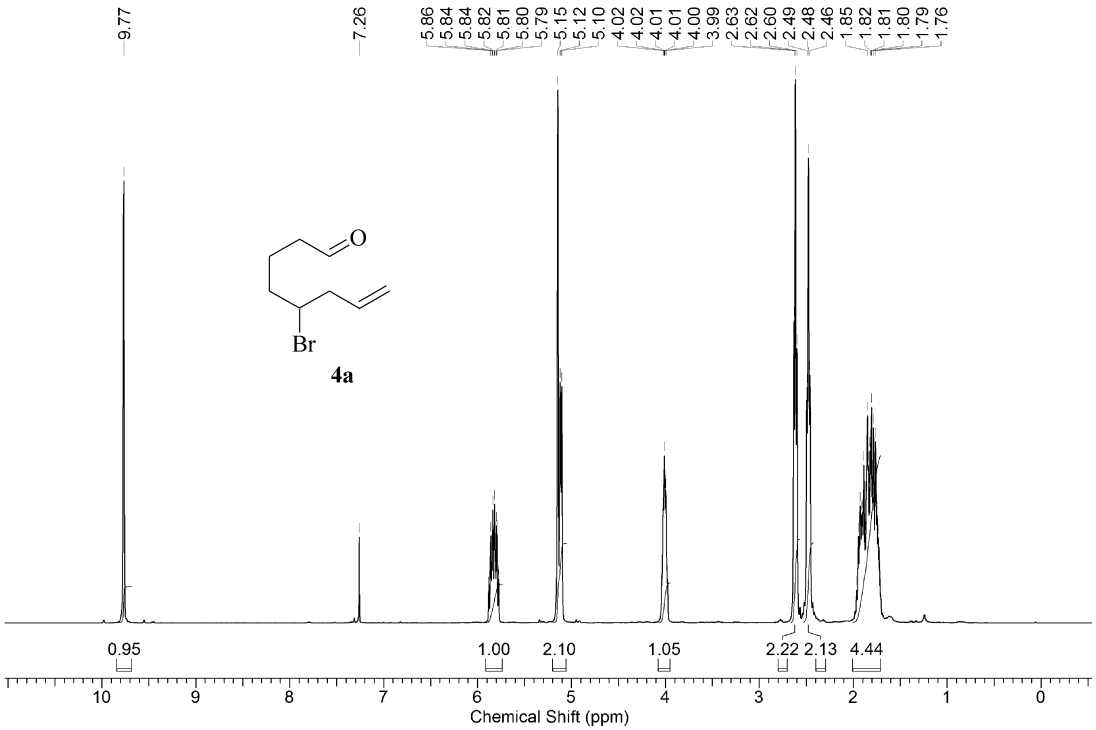

Figure A77. Proton-1 NMR-spectrum of 5-bromoct-7-enal (**4a**) (400MHz, $CDCl_3$, 23 °C).

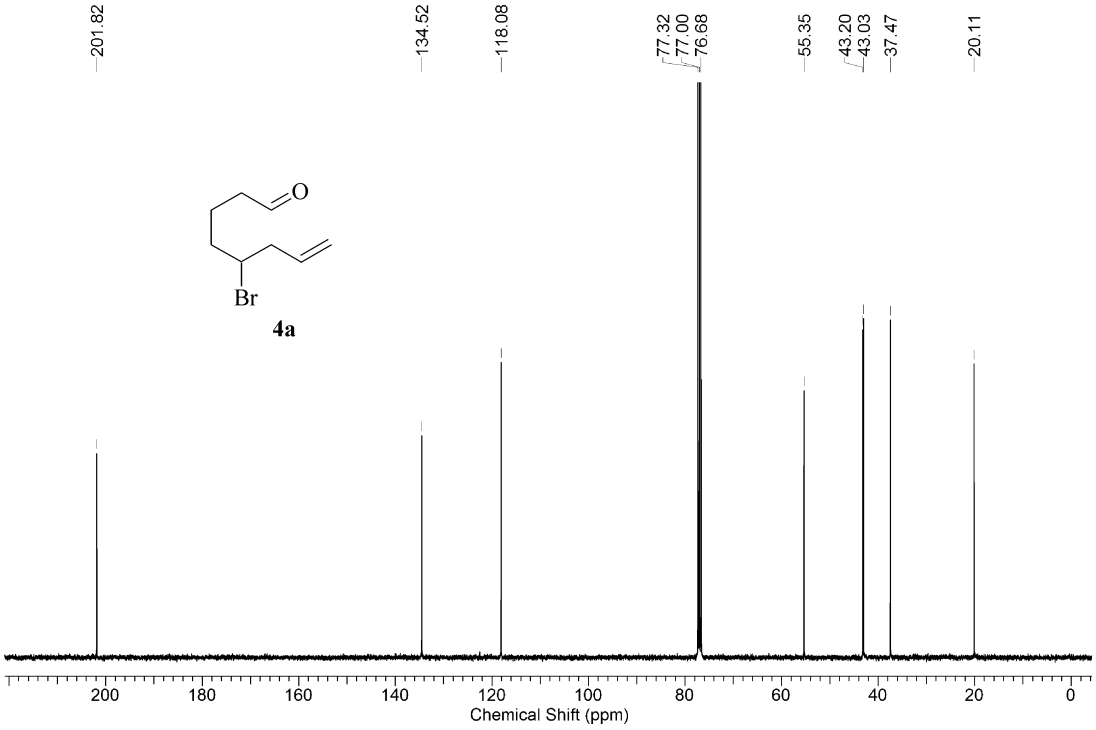

Figure A78. Carbon-13 NMR-spectrum of 5-bromoct-7-enal (**4a**) (100MHz, $CDCl_3$, 23 °C).

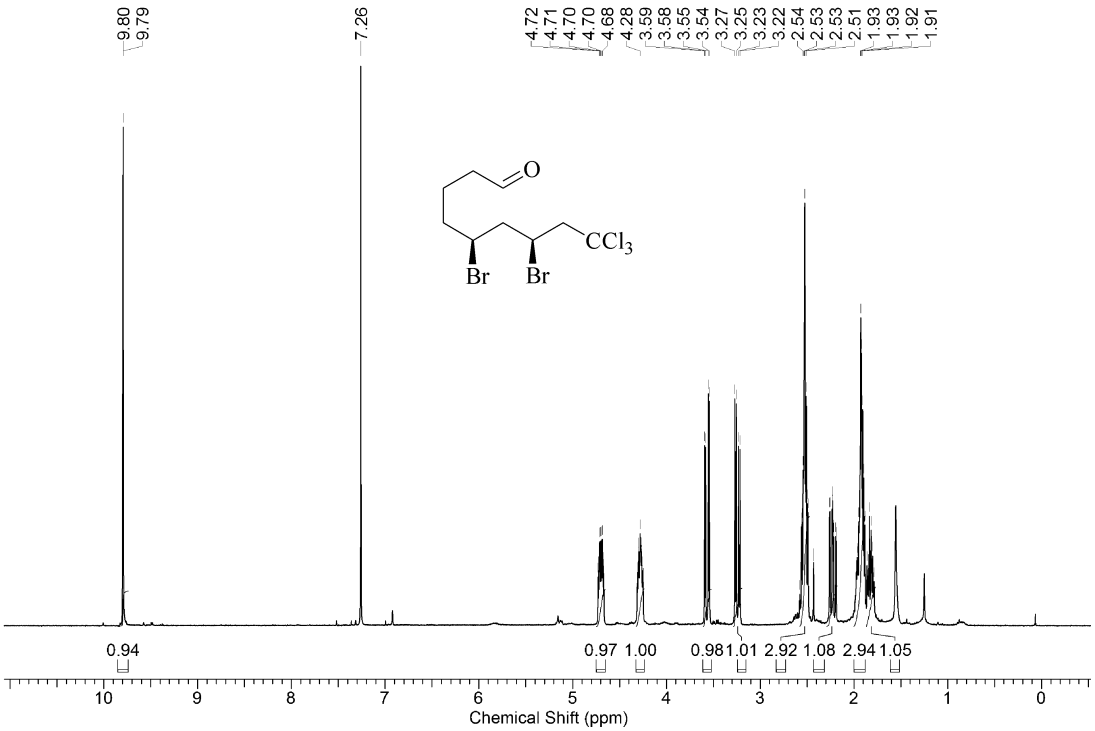

Figure A79. Proton-1 NMR-spectrum of *like*-5,7-dibromo-9,9,9-trichlorononanal (400MHz, $CDCl_3$, 23 °C).

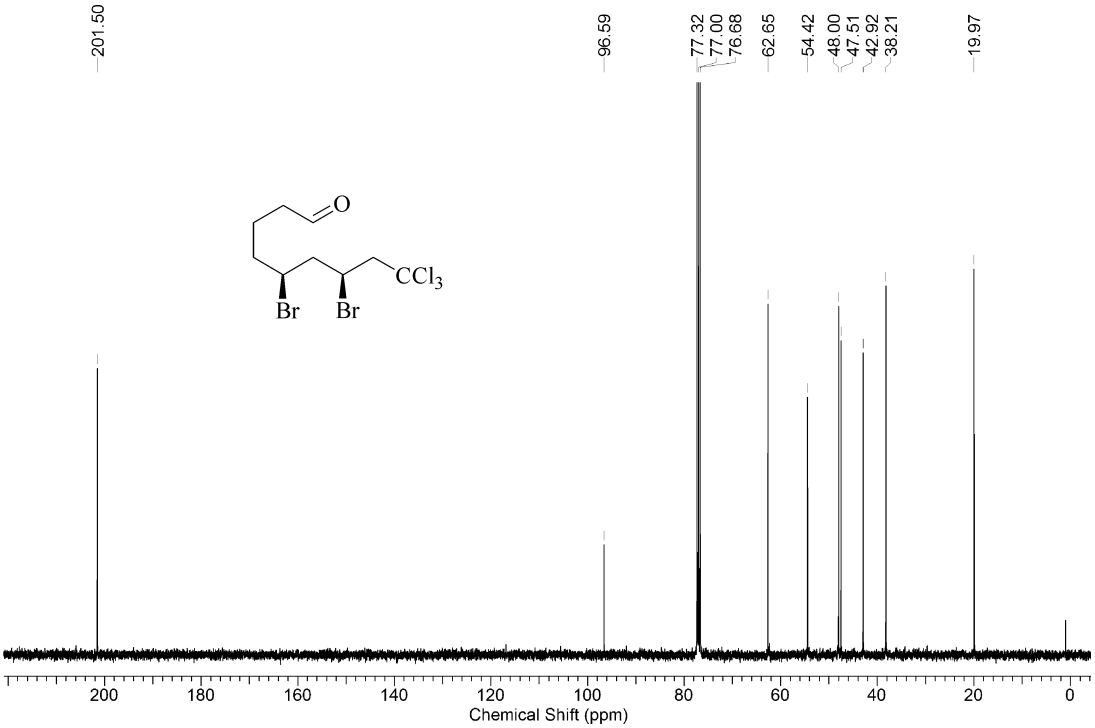

Figure A80. Carbon-13 NMR-spectrum of *like*-5,7-dibromo-9,9,9-trichlorononanal (100MHz, $CDCl_3$, 23 °C).

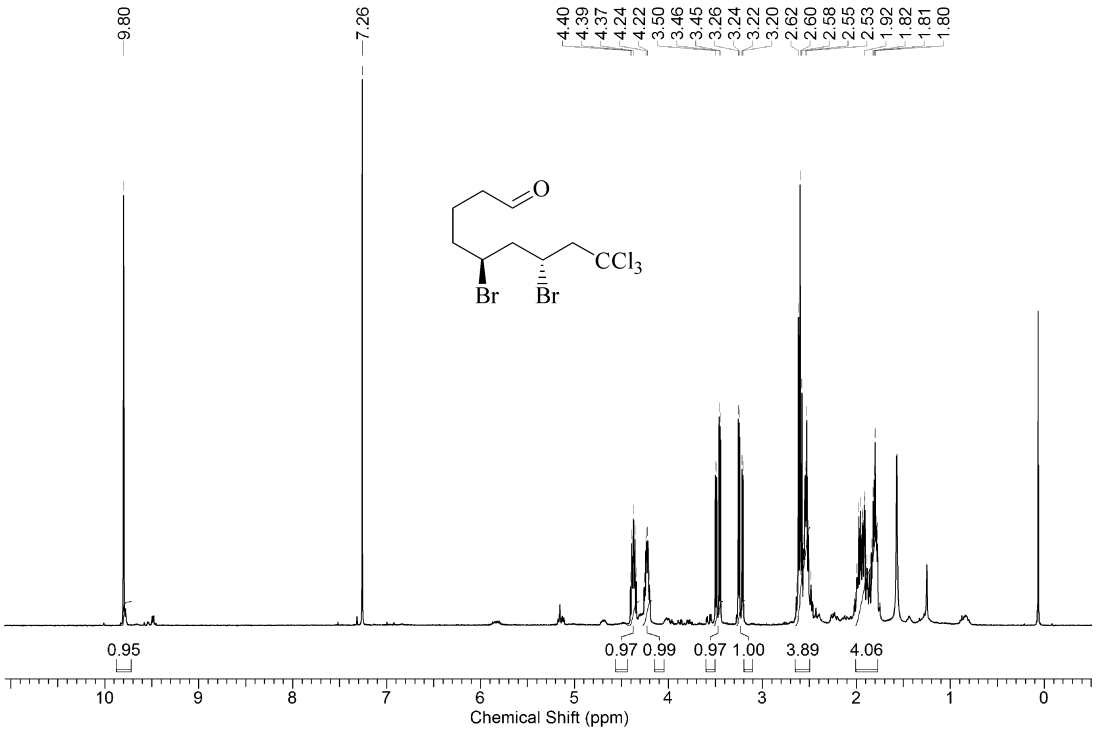

Figure A81. Proton-1 NMR-spectrum of *unlike*-5,7-dibromo-9,9,9-trichlorononanal (400MHz, $CDCl_3$, 23 °C).

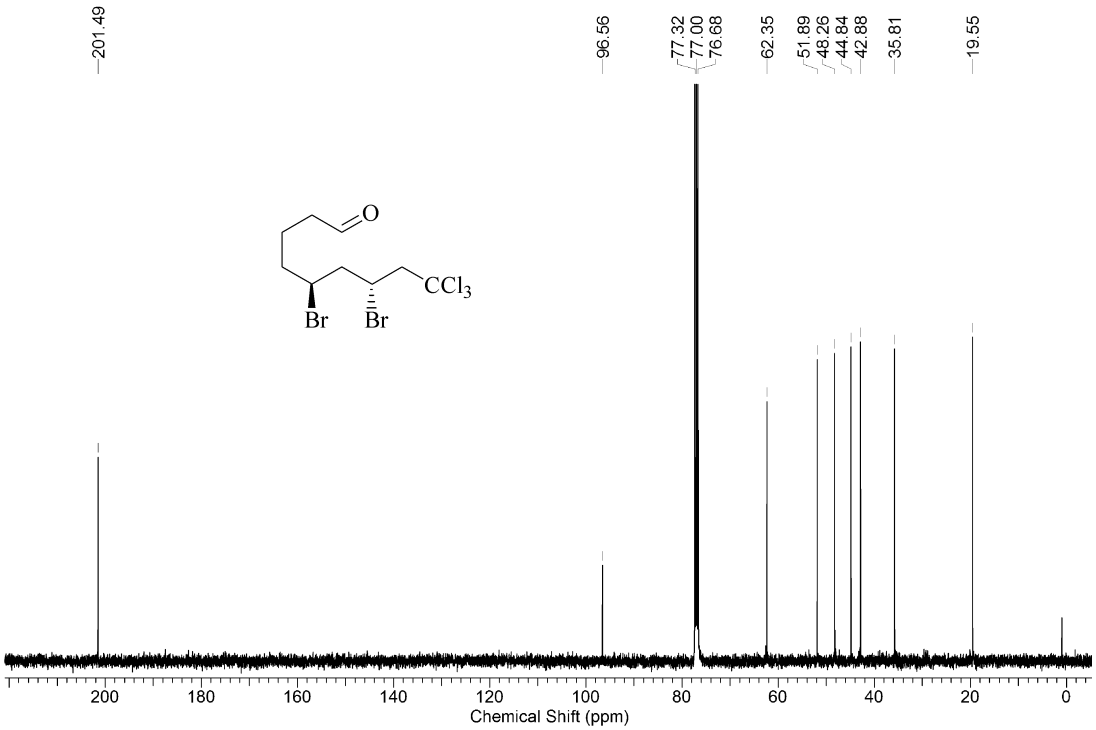

Figure A82. Carbon-13 NMR-spectrum of *unlike*-5,7-dibromo-9,9,9-trichlorononanal (100MHz, $CDCl_3$, 23 °C).

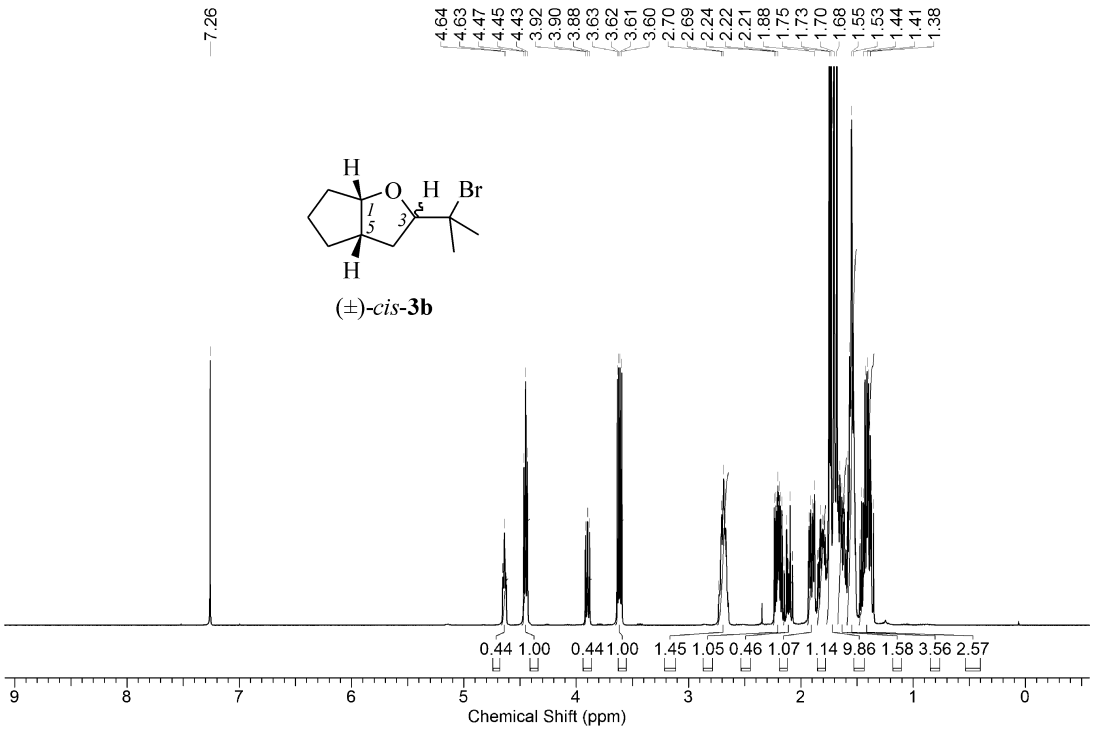

Figure A83. Proton-1 NMR-spectrum of 1,3-cis/trans-isomers, i.e. *rel*-(1*S*,3*S*,5*S*)-**3b**/ *rel*-(1*S*,3*R*,5*S*)-**3b**, of 3-(2-Bromoprop-2-yl)-2-oxabicyclo[3.3.0]octane *cis*-(**3b**) (400MHz, $CDCl_3$, 23 °C).

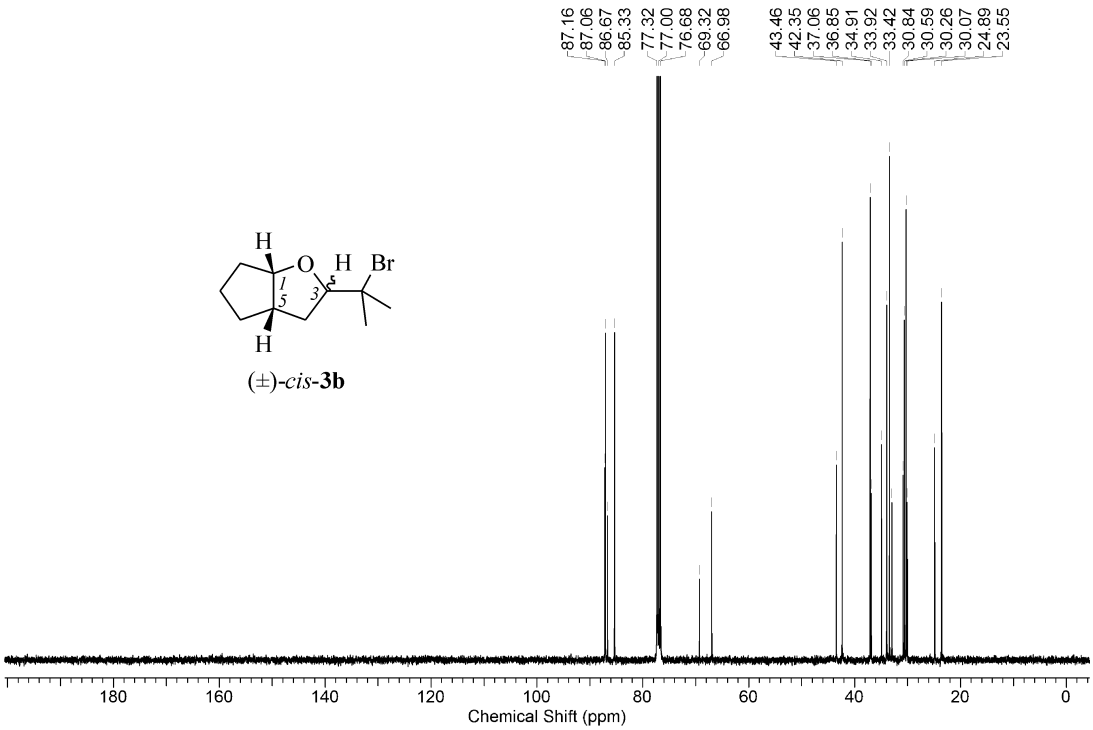

Figure A84. Carbon-13 NMR-spectrum of 1,3-cis/trans-isomers, i.e *rel*-(1*S*,3*S*,5*S*)-**3b**/ *rel*-(1*S*,3*R*,5*S*)-**3b**, of 3-(2-Bromoprop-2-yl)-2-oxabicyclo[3.3.0]octane *cis*-(**3b**) (100MHz, $CDCl_3$, 23 °C).

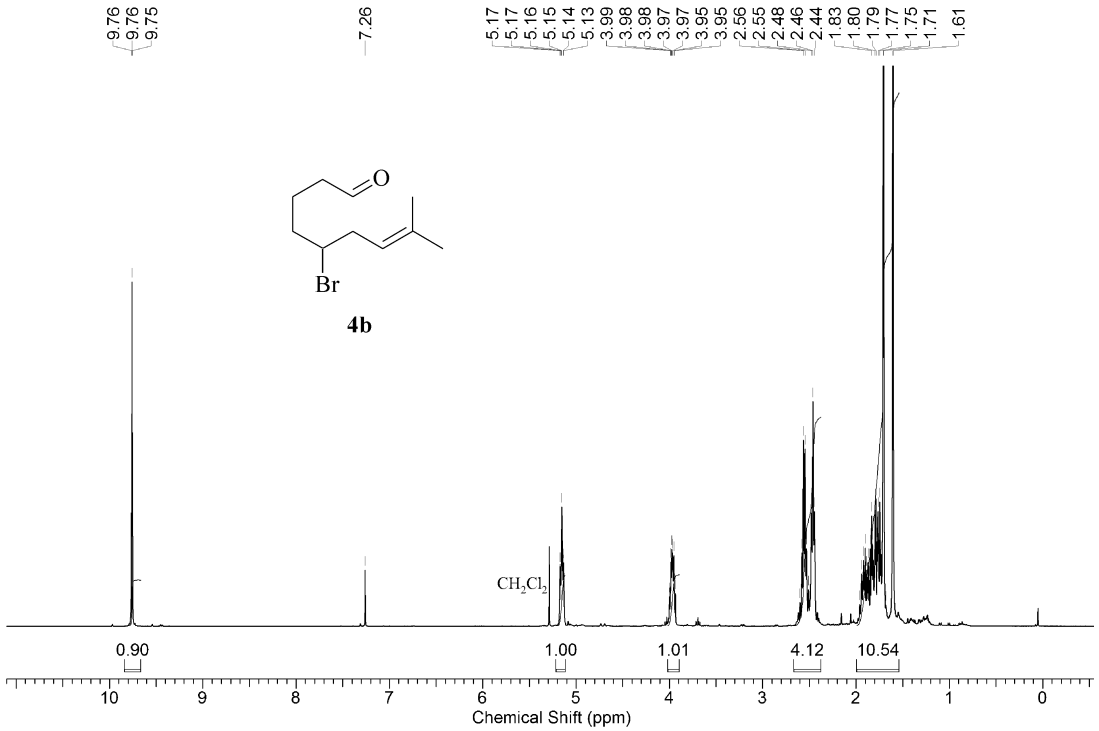

Figure A85. Proton-1 NMR-spectrum of 5-brom-8-methylnon-7-enal (**4b**) (400MHz, $CDCl_3$, 23 °C).

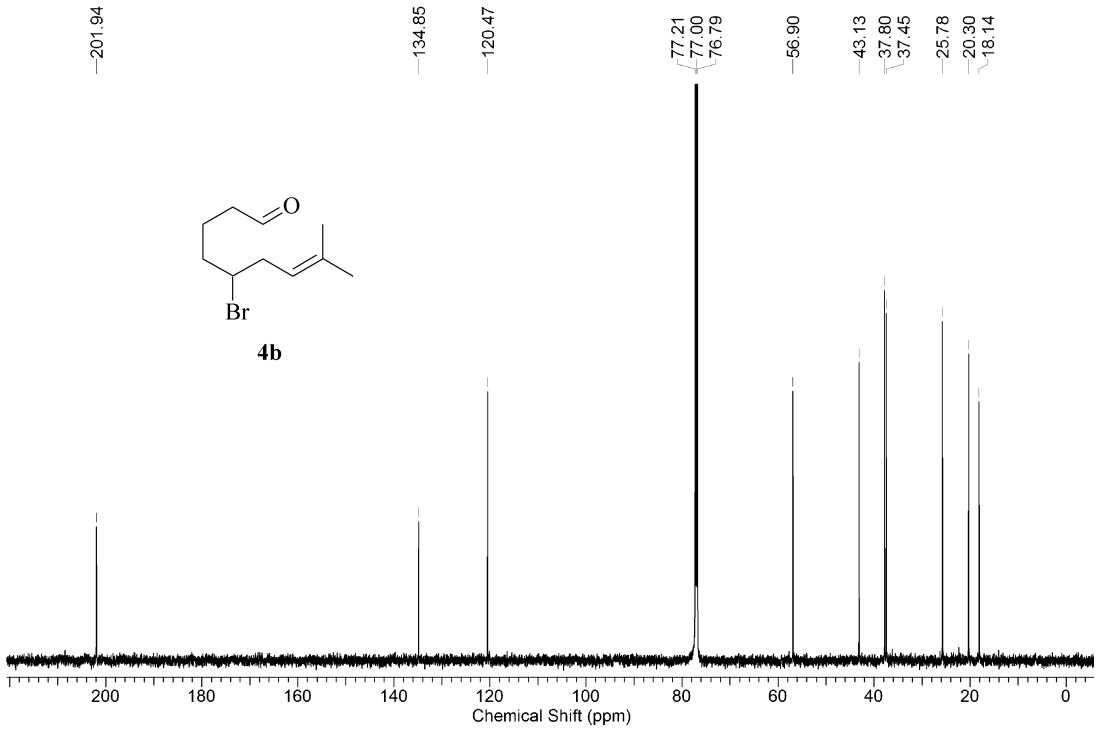

Figure A86. Carbon-13 NMR-spectrum of 5-brom-8-methylnon-7-enal (**4b**) (150MHz, $CDCl_3$, 23 °C).

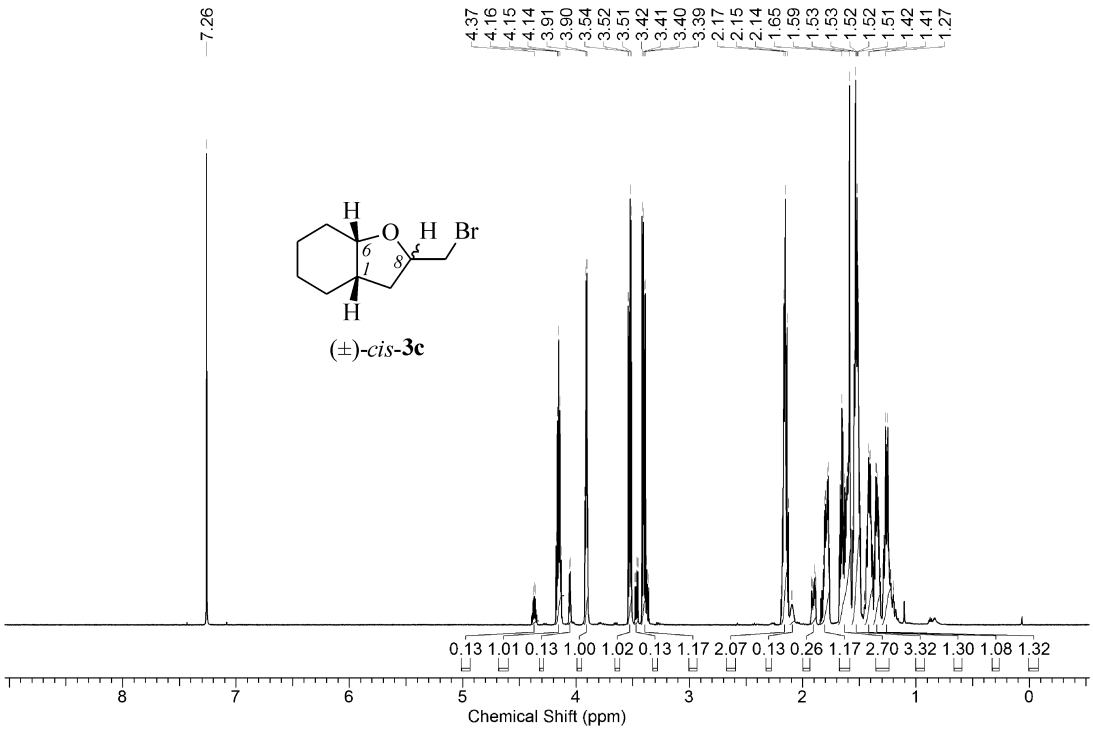

Figure A87. Proton-1 NMR-spectrum of 6,8-cis/trans-isomers, i.e *rel*-(1*S*,6*S*,8*S*)-**3c**/ *rel*-(1*S*,6*S*,8*R*)-**3c**, of 8-(bromomethyl)-7-oxabicyclo[4.3.0]nonane *cis*-(**3c**) (600MHz, $CDCl_3$, 23 °C).

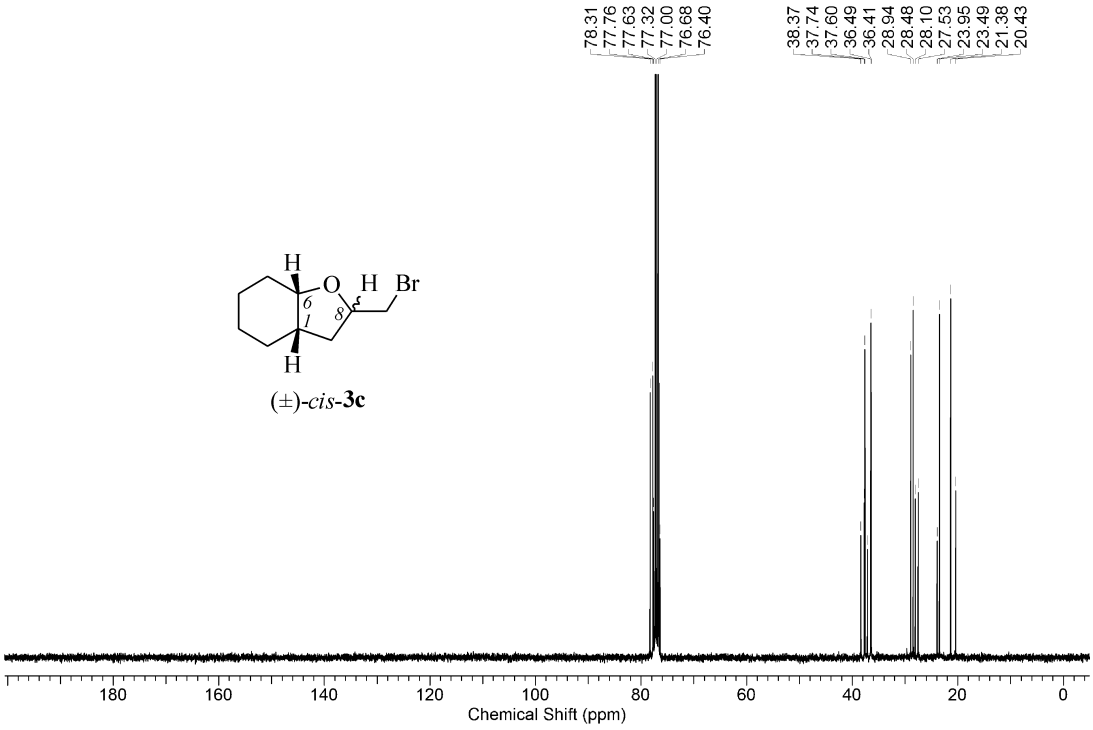

Figure A88. Carbon-13 NMR-spectrum of 6,8-cis/trans-isomers, i.e *rel*-(1*S*,6*S*,8*S*)-**3c**/ *rel*-(1*S*,6*S*,8*R*)-**3c**, of 8-(bromomethyl)-7-oxabicyclo[4.3.0]nonane *cis*-(**3c**) (100MHz, $CDCl_3$, 23 °C).

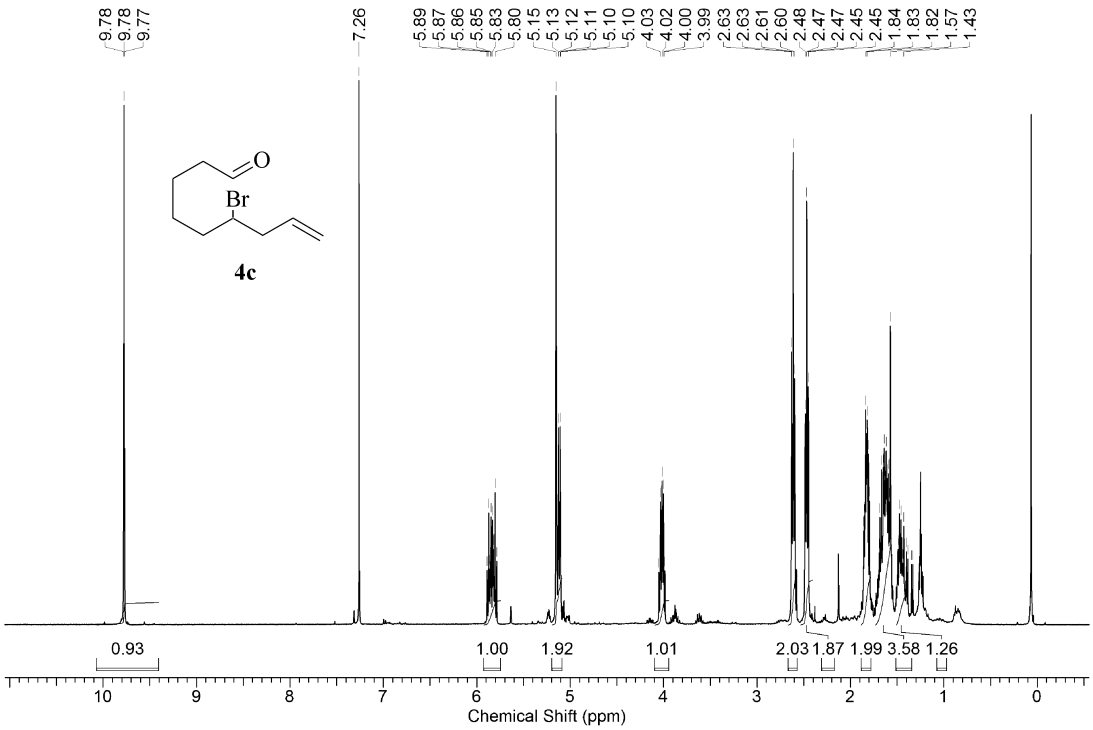

Figure A89. Proton-1 NMR-spectrum of 6-bromo-8-nonenal (**4c**) (400MHz, $CDCl_3$, 23 °C).

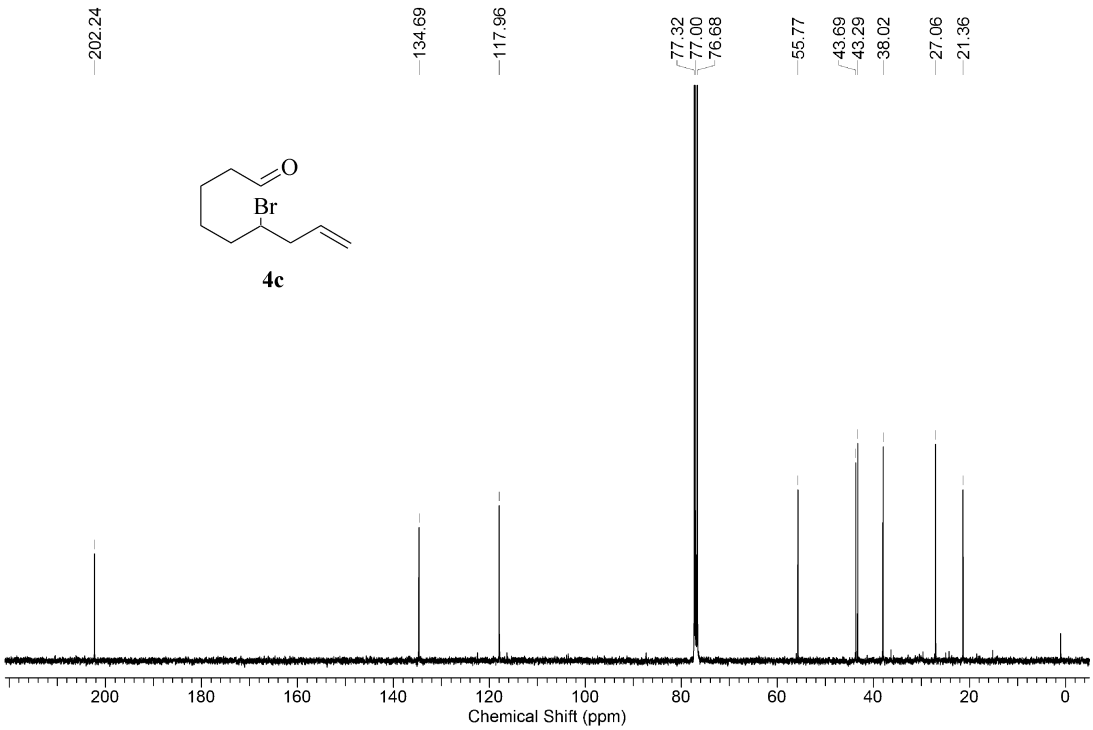

Figure A90. Carbon-13 NMR-spectrum of 6-bromo-8-nonenal (**4c**) (100MHz, $CDCl_3$, 23 °C).

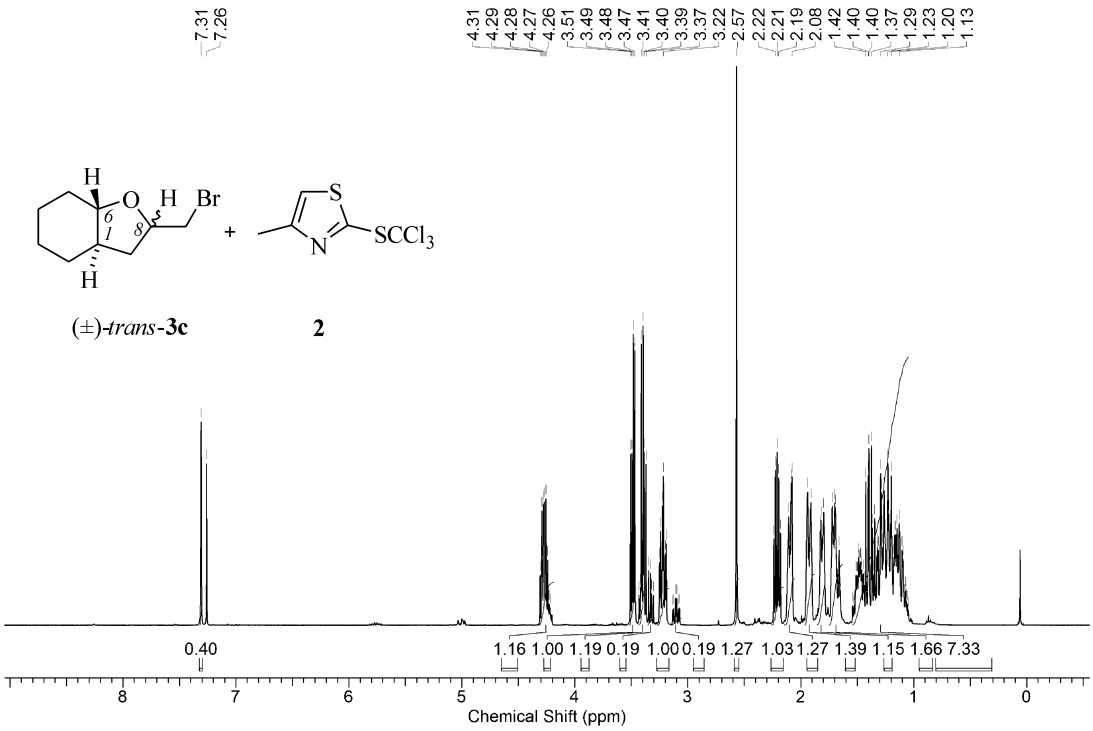

Figure A91. Proton-1 NMR-spectrum of 6,8-cis/trans-isomers, i.e *rel*-(1*R*,6*S*,8*S*)-**3c**/ *rel*-(1*R*,6*S*,8*R*)-**3c**, of 8-(bromomethyl)-7-oxabicyclo[4.3.0]nonane *trans*-(**3c**) and 4-methyl-2-(trichloromethylsulfanyl)-thiazole (**2**) (400MHz, $CDCl_3$, 23 °C).

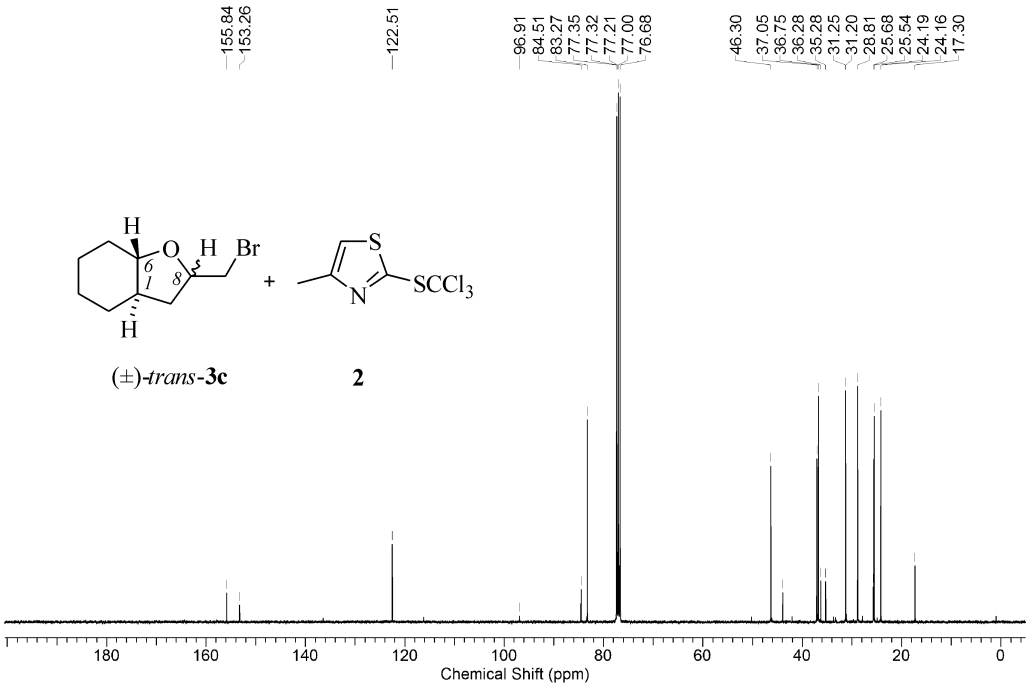

Figure A92. Carbon-13 NMR-spectrum of 6,8-cis/trans-isomers, i.e *rel*-(1*R*,6*S*,8*S*)-**3c**/ *rel*-(1*R*,6*S*,8*R*)-**3c**,of 8-(bromomethyl)-7-oxabicyclo[4.3.0]nonane *trans*-(**3c**) and 4-methyl-2-(trichloromethylsulfanyl)-thiazole (**2**) (100MHz, $CDCl_3$, 23 °C).

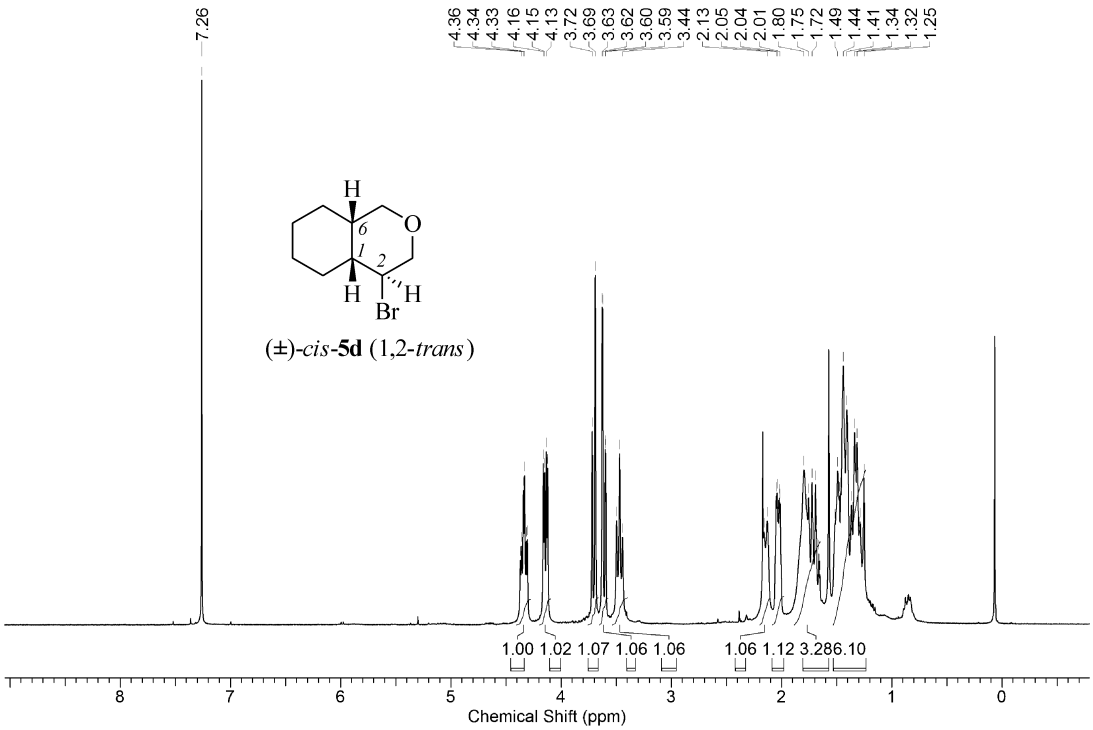

Figure A93. Proton-1 NMR-spectrum of, i.e *rel*-(1*S*,2*S*,6*S*)-**5d**, 2-bromo-4-oxabicyclo-[4.4.0]decane *cis*-(**5d**) (400MHz, $CDCl_3$, 23 °C).

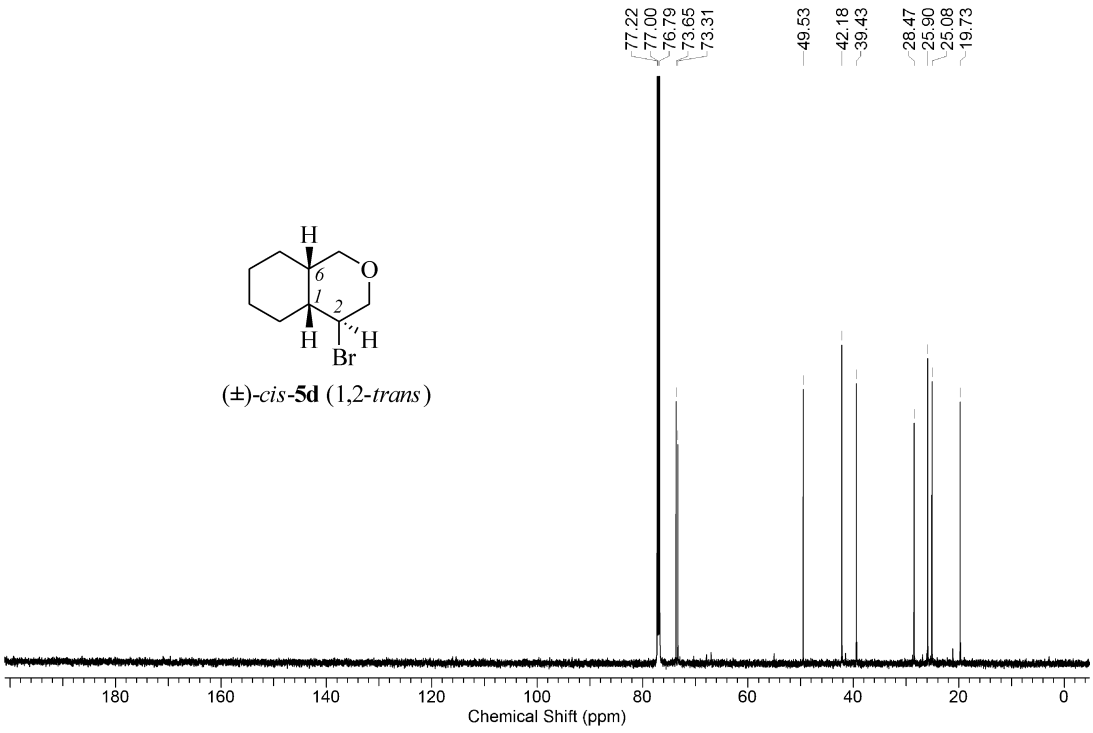

Figure A94. Carbon-13 NMR-spectrum of, i.e *rel*-(1*S*,2*S*,6*S*)-**5d**, 2-bromo-4-oxabicyclo-[4.4.0]decane *cis*-(**5d**) (150MHz, $CDCl_3$, −37 °C).

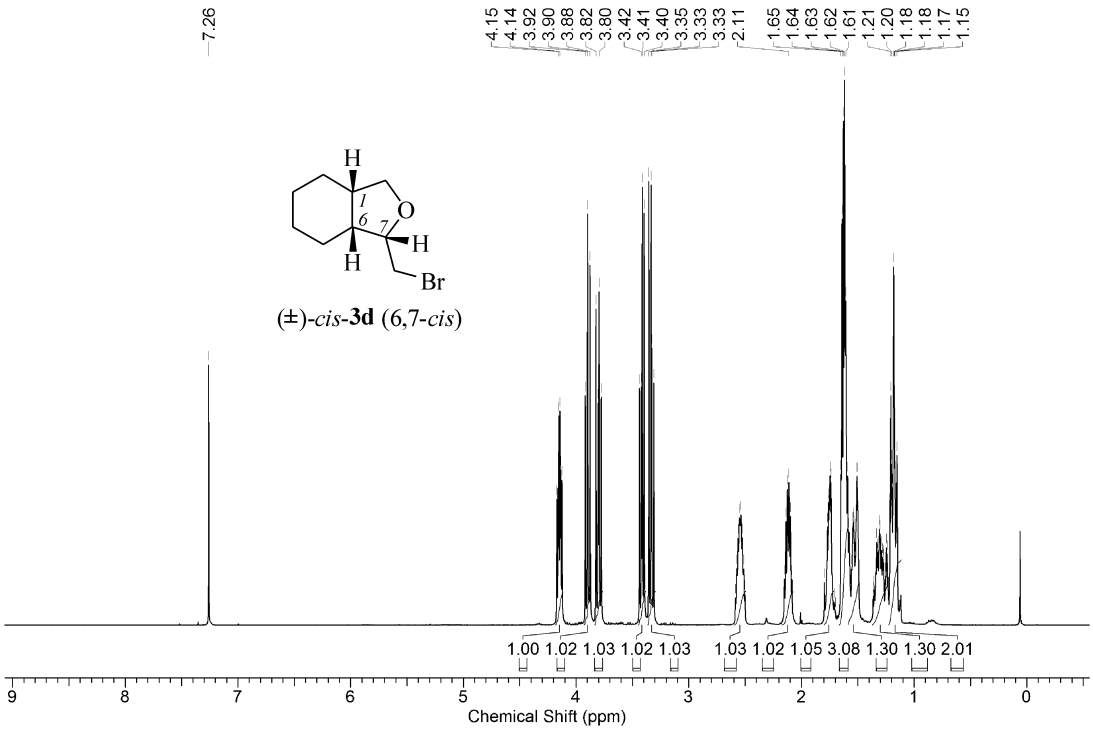

Figure A95. Proton-1 NMR-spectrum of, i.e *rel*-(1*S*,6*R*,7*S*)-**3d**, 7-bromomethyl-8-oxabicyclo[4.3.0]nonane *cis*-(**3d**) (400MHz, $CDCl_3$, 23 °C).

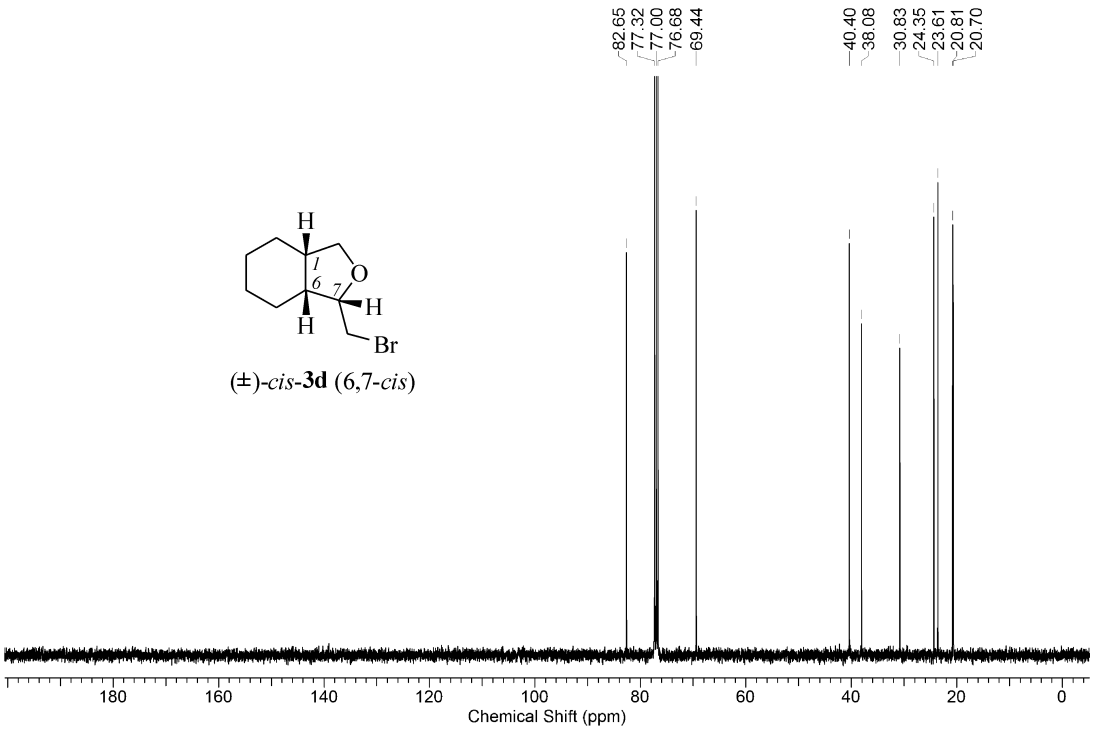

Figure A96. Carbon-13 NMR-spectrum of, i.e *rel*-(1*S*,6*R*,7*S*)-**3d**, 7-bromomethyl-8-oxabicyclo[4.3.0]nonane *cis*-(**3d**) (100MHz, $CDCl_3$, 23°C).

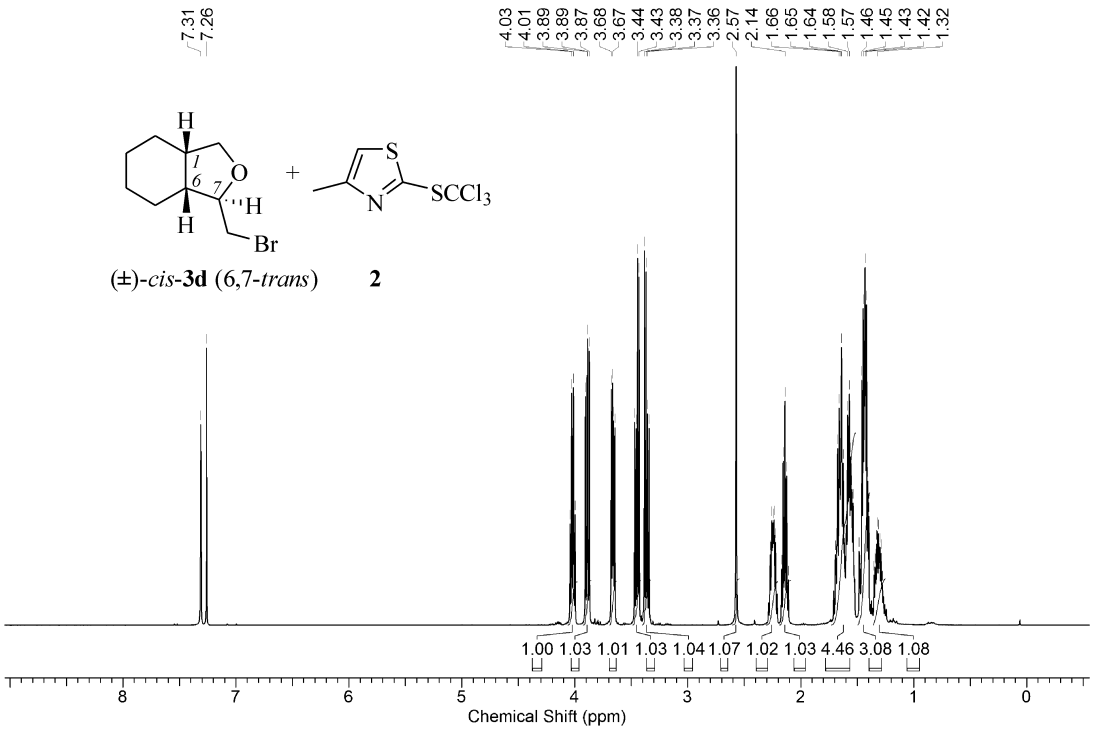

Figure A97. Proton-1 NMR-spectrum of, i.e *rel*-(1*S*,6*R*,7*R*)-**3d**, 7-bromomethyl-8-oxa-bicyclo[4.3.0]nonane *cis*-(**3d**) and 4-methyl-2-(trichloromethylsulfanyl)-thiazole (**2**) (400MHz, $CDCl_3$, 23 °C).

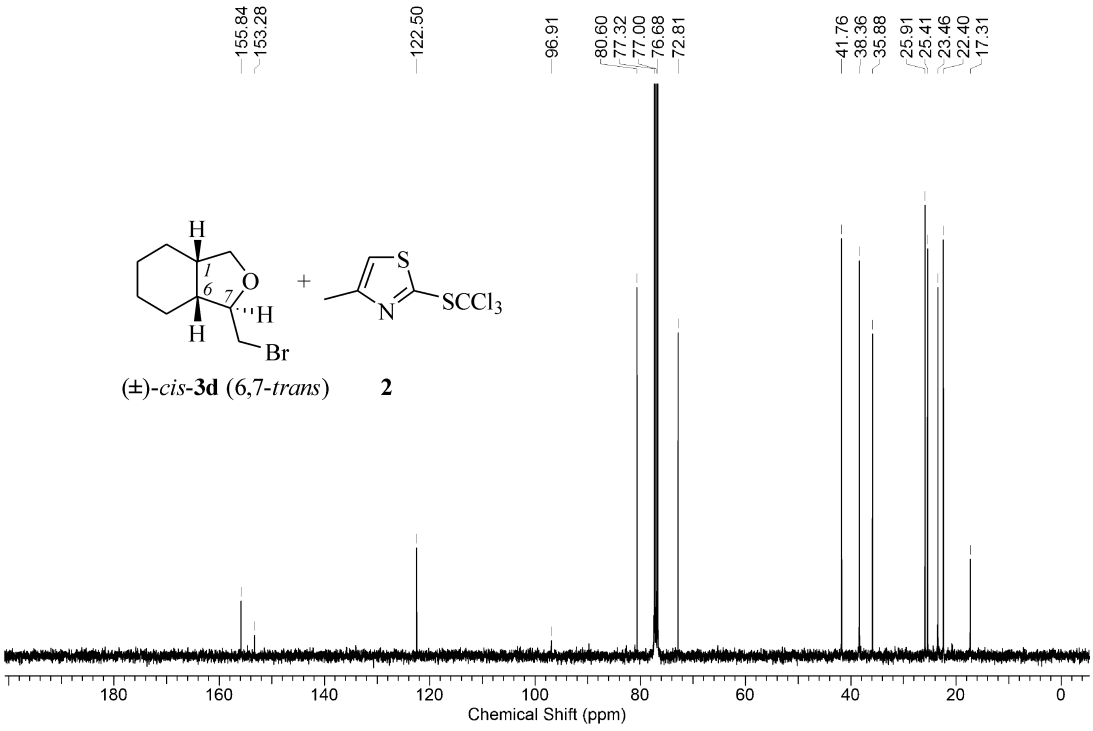

Figure A98. Carbon-13 NMR-spectrum of, i.e *rel*-(1*S*,6*R*,7*R*)-**3d**, 7-bromomethyl-8-oxa-bicyclo[4.3.0]nonane *cis*-(**3d**) and 4-methyl-2-(trichloromethylsulfanyl)-thiazole (**2**) (100MHz, $CDCl_3$, 23 °C).

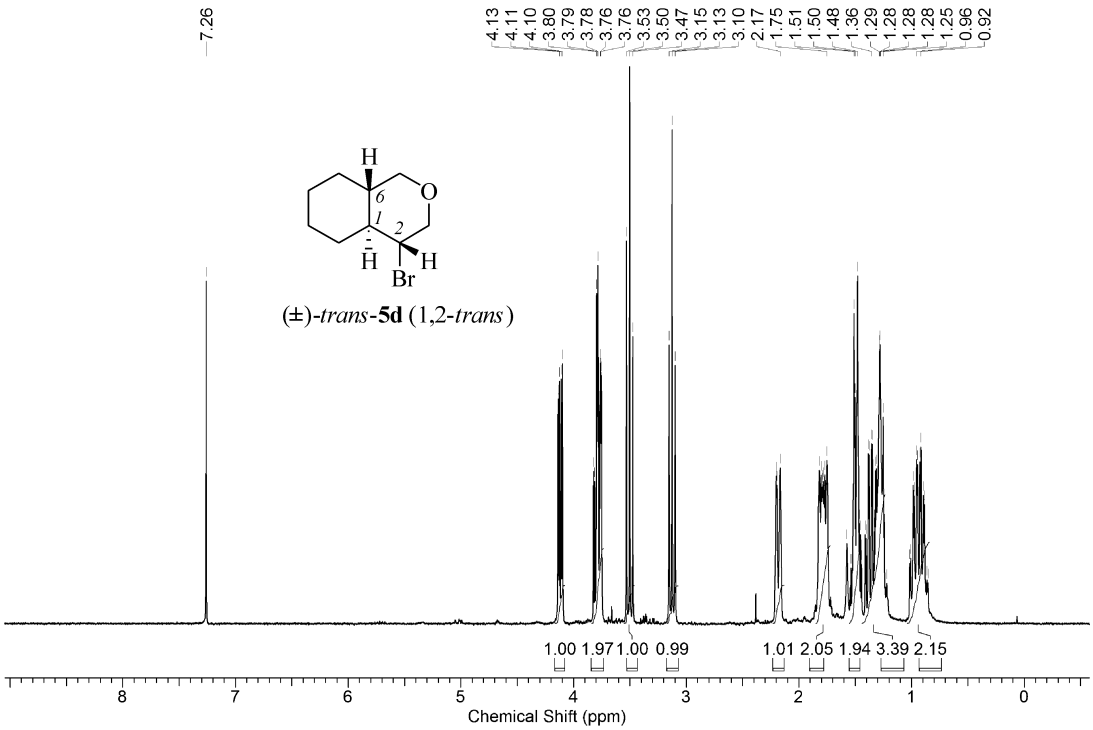

Figure A99. Proton-1 NMR-spectrum of, i.e *rel*-(1*R*,2*R*,6*S*)-**5d**, 2-bromo-4-oxa-bicyclo[4.4.0]decane *trans*-(**5d**) (400MHz, $CDCl_3$, 23 °C).

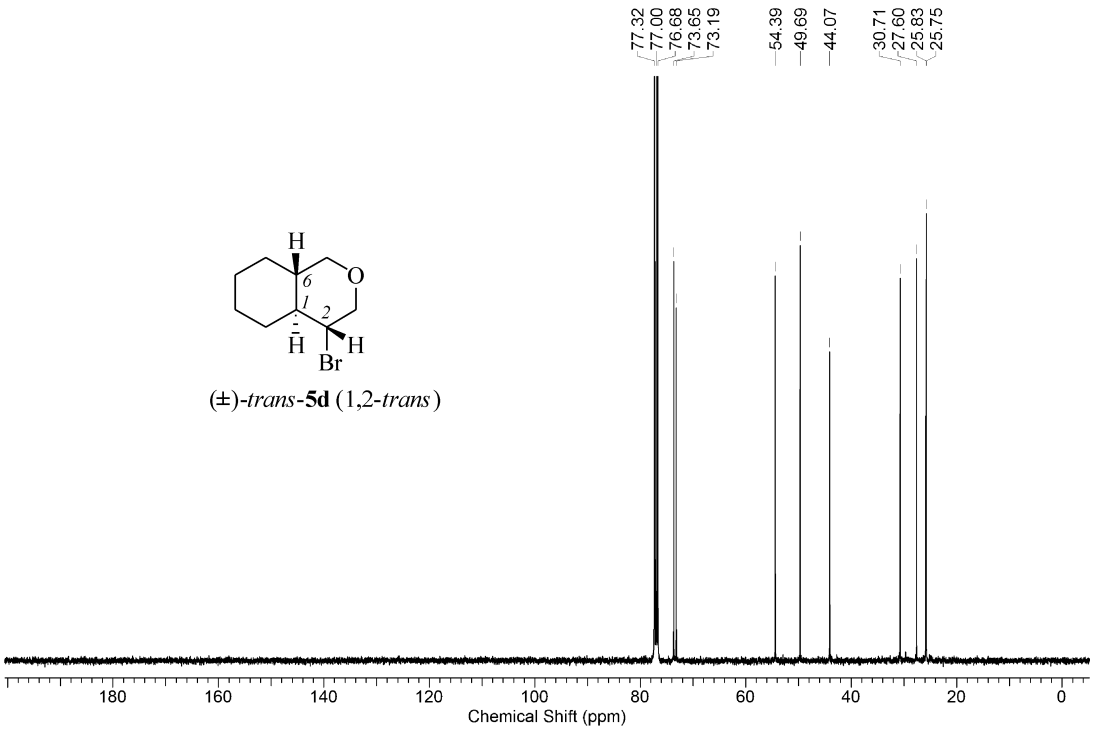

Figure A100. Carbon-13 NMR-spectrum of, i.e *rel*-(1*R*,2*R*,6*S*)-**5d**, 2-bromo-4-oxa-bicyclo[4.4.0]decane *trans*-(**5d**) (100MHz, $CDCl_3$, 23 °C).

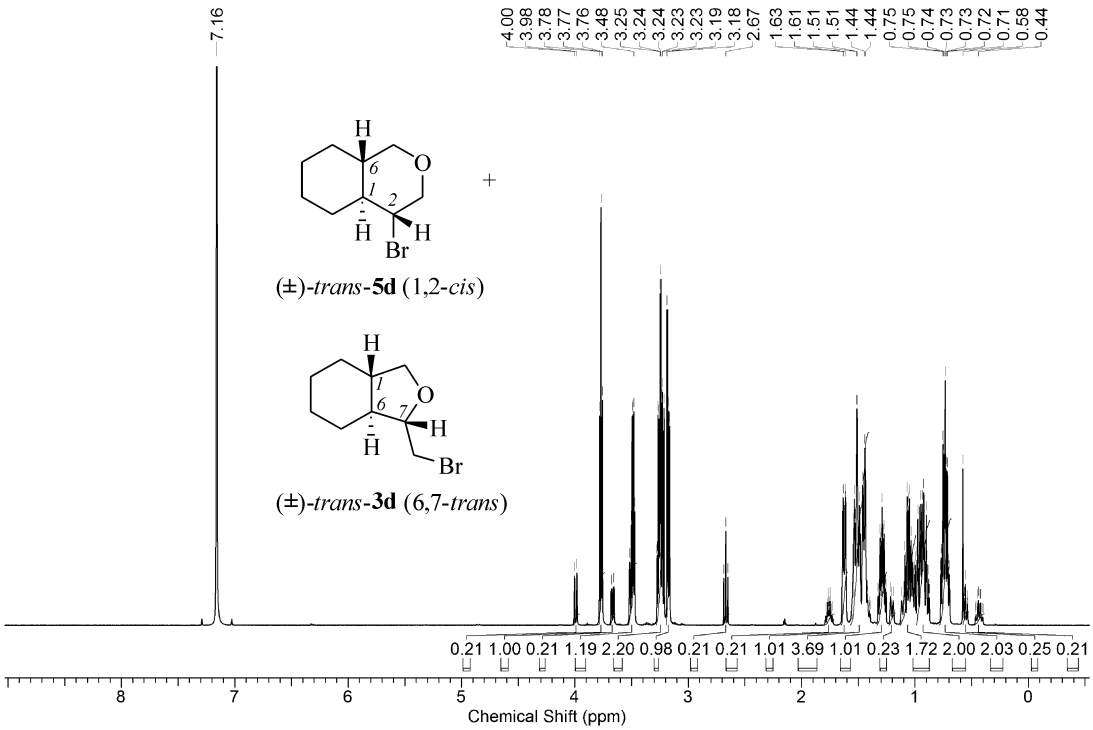

Figure A101. Proton-1 NMR-spectrum of, i.e *rel*-(1*R*,2*R*,6*S*)-**5d**, 2-bromo-4-oxabicycle-[4.4.0]decane *trans*-(**5d**) and of, i.e *rel*-(1*S*,6*S*,7*S*)-**3d**, 7-bromomethyl-8-oxabicyclo[4.3.0]-nonane *trans*-(**3d**) (600MHz, C_6D_6, 23 °C).

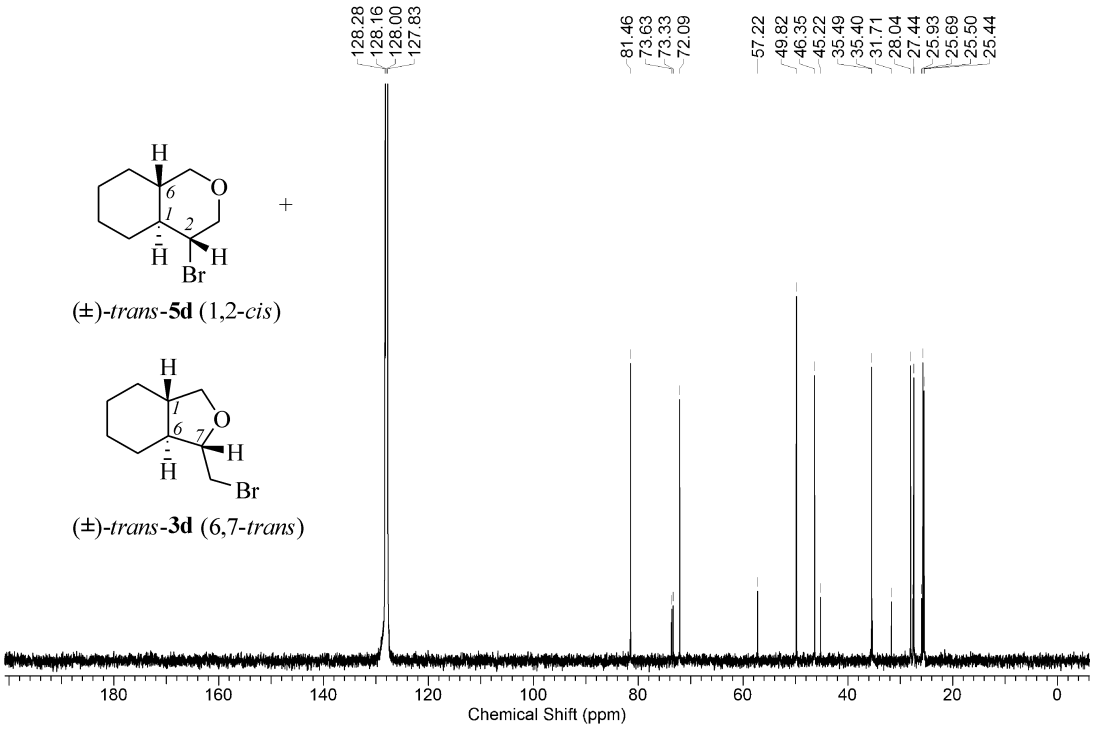

Figure A102. Carbon-13 NMR-spectrum of, i.e *rel*-(1*R*,2*R*,6*S*)-**5d**, 2-bromo-4-oxabicycle-[4.4.0]decane *trans*-(**5d**) and of, i.e *rel*-(1*S*,6*S*,7*S*)-**3d**, 7-bromomethyl-8-oxabicyclo[4.3.0]-nonane *trans*-(**3d**) (150MHz, C_6D_6, 23 °C).

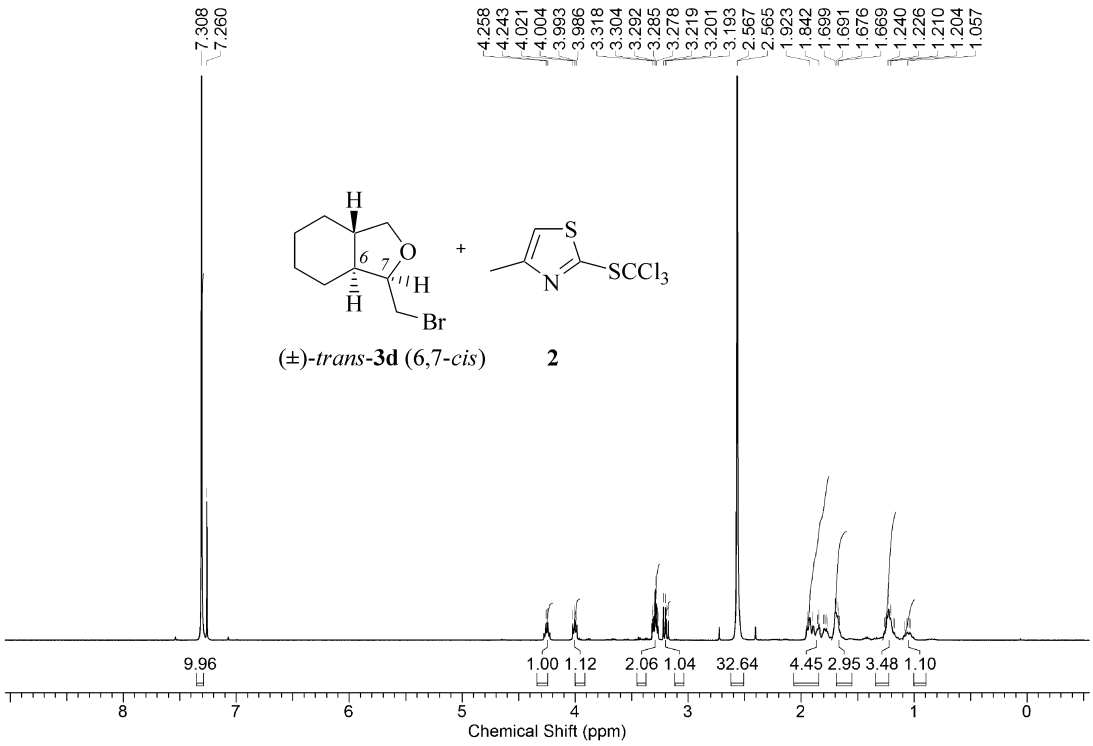

Figure A103. Proton-1 NMR-spectrum of, i.e *rel*-(1*S*,6*S*,7*R*)-**3d**, 7-bromomethyl-8-oxabicyclo[4.3.0]nonane *trans*-(**3d**) and 4-methyl-2-(trichloromethylsulfanyl)-thiazole (**2**) (400MHz, $CDCl_3$, 23 °C).

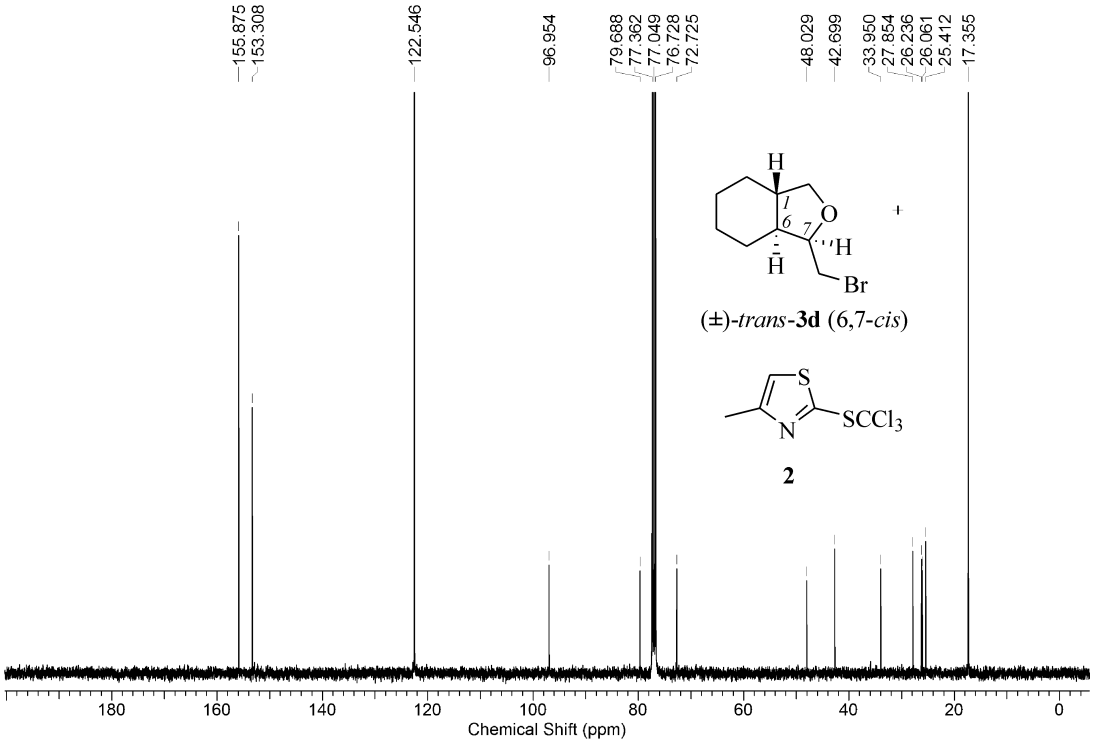

Figure A104. Carbon-13 NMR-spectrum of, i.e *rel*-(1*S*,6*S*,7*R*)-**3d**, 7-bromomethyl-8-oxabicyclo[4.3.0]nonane *trans*-(**3d**) and 4-methyl-2-(trichloromethylsulfanyl)-thiazole (**2**) (100MHz, $CDCl_3$, 23 °C).

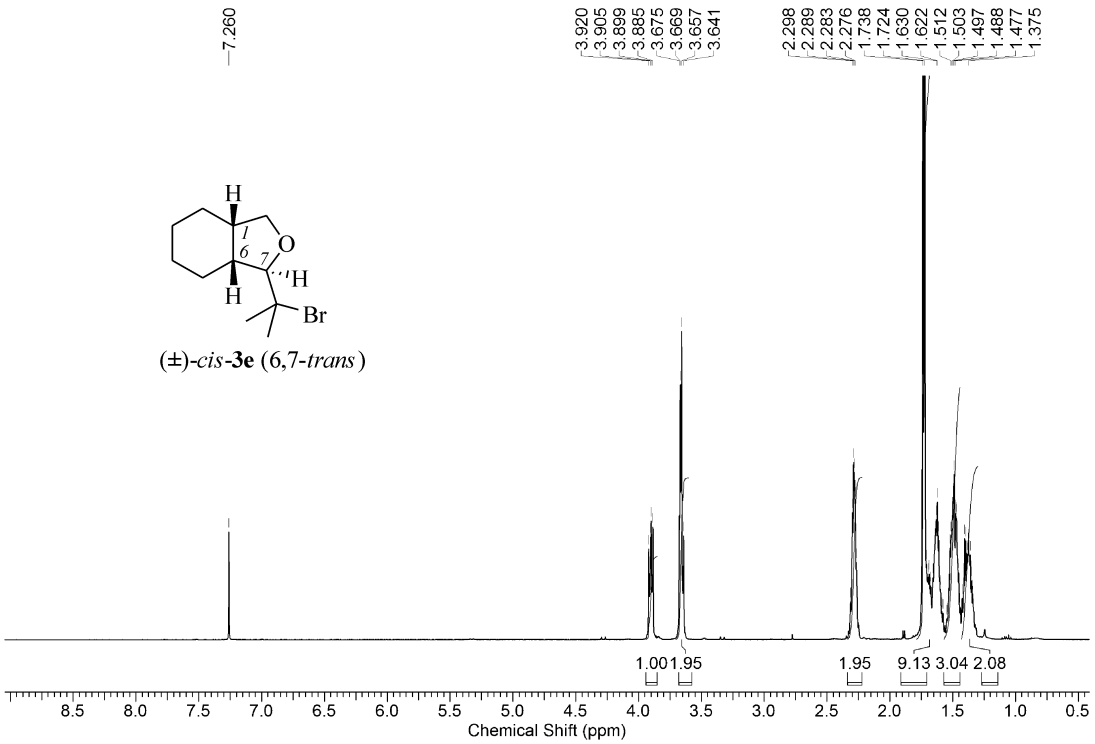

Figure A105. Proton-1 NMR-spectrum of, i.e *rel*-(1*R*,6*S*,7*R*)-**3e**, 7-(2-bromoprop-2-yl)-8-oxabicyclo[4.3.0]nonane *cis*-(**3e**) (400MHz, $CDCl_3$, 23 °C).

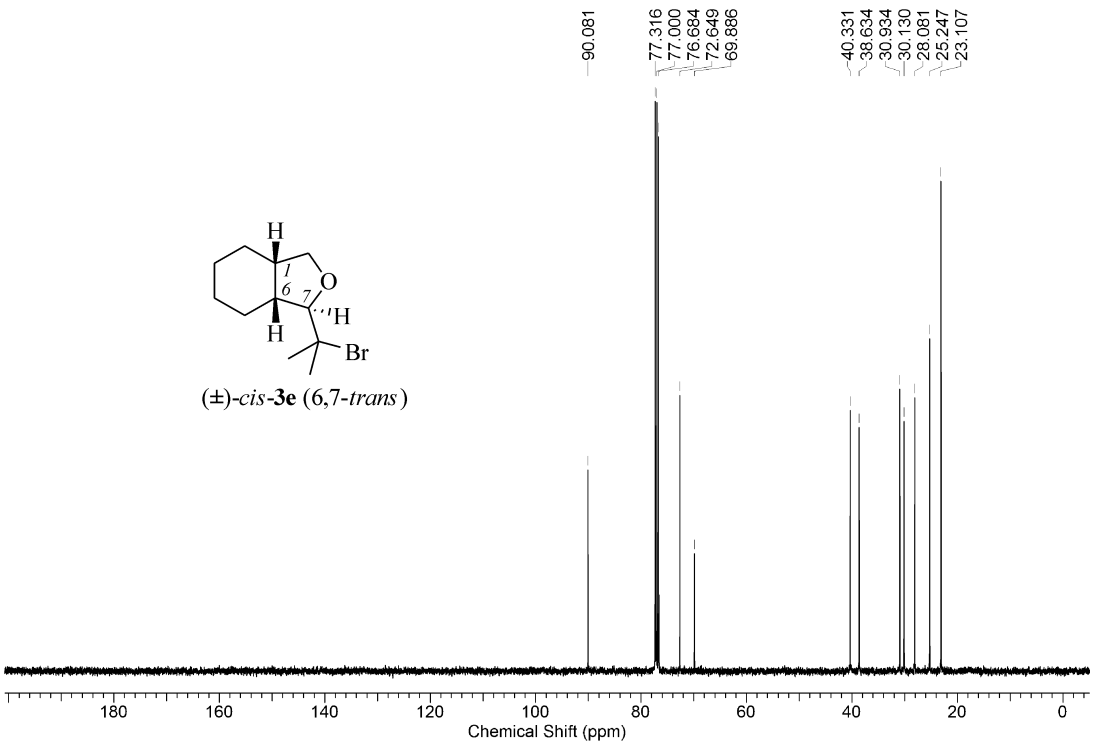

Figure A106. Carbon-13 NMR-spectrum of, i.e *rel*-(1*R*,6*S*,7*R*)-**3e**, 7-(2-bromoprop-2-yl)-8-oxabicyclo[4.3.0]nonane *cis*-(**3e**) (100MHz, $CDCl_3$, 23 °C).

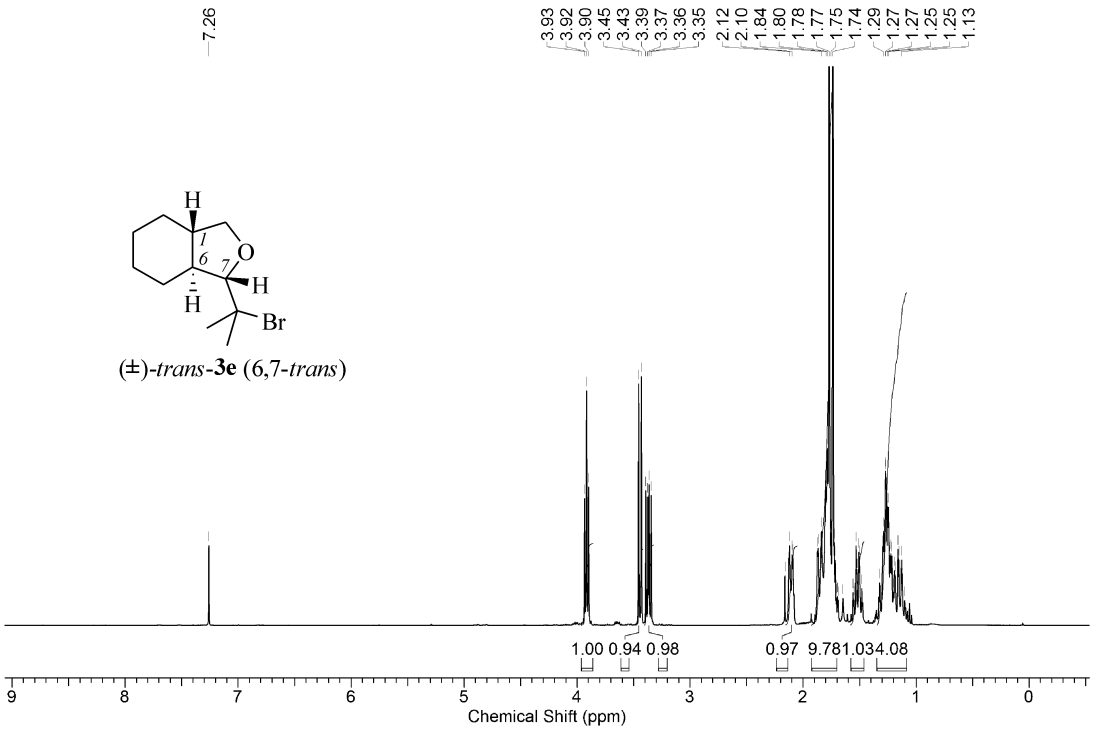

Figure A107. Proton-1 NMR-spectrum of, i.e *rel*-(1*S*,6*S*,7*S*)-**3e**, 7-(2-bromoprop-2-yl)-8-oxabicyclo[4.3.0]nonane *trans*-(**3e**) (400MHz, $CDCl_3$, 23 °C).

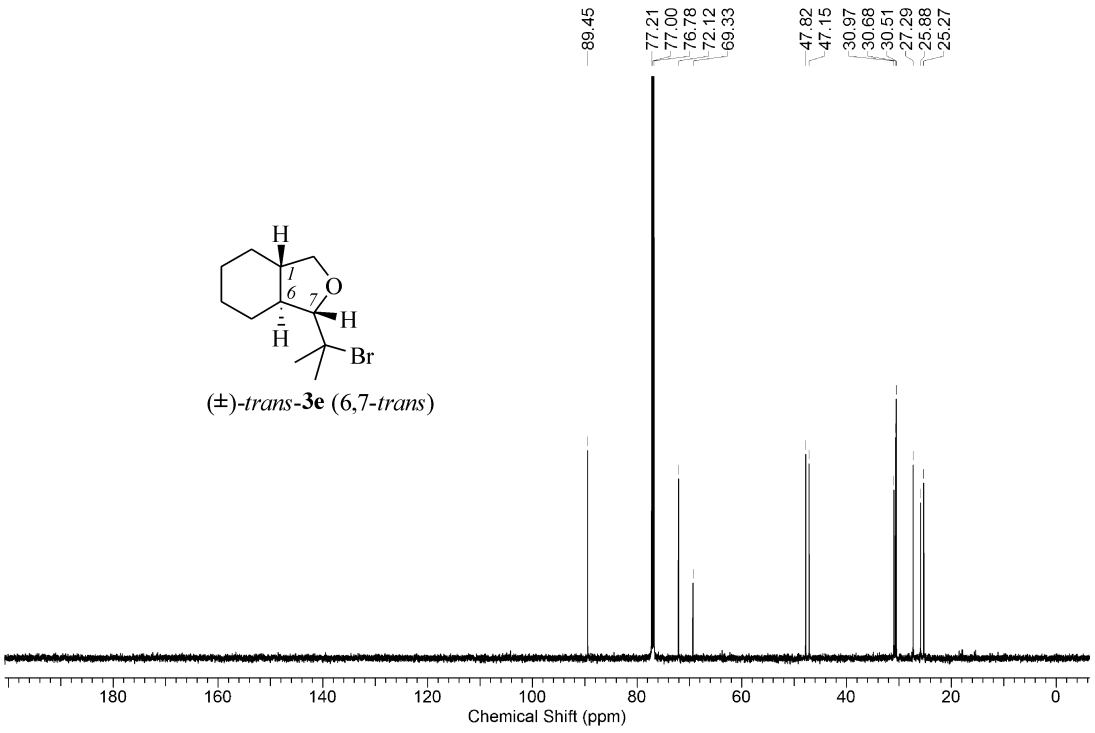

Figure A108. Carbon-13 NMR-spectrum of, i.e *rel*-(1*S*,6*S*,7*S*)-**3e**, 7-(2-bromoprop-2-yl)-8-oxabicyclo[4.3.0]nonane *trans*-(**3e**) (150MHz, $CDCl_3$, 23 °C).

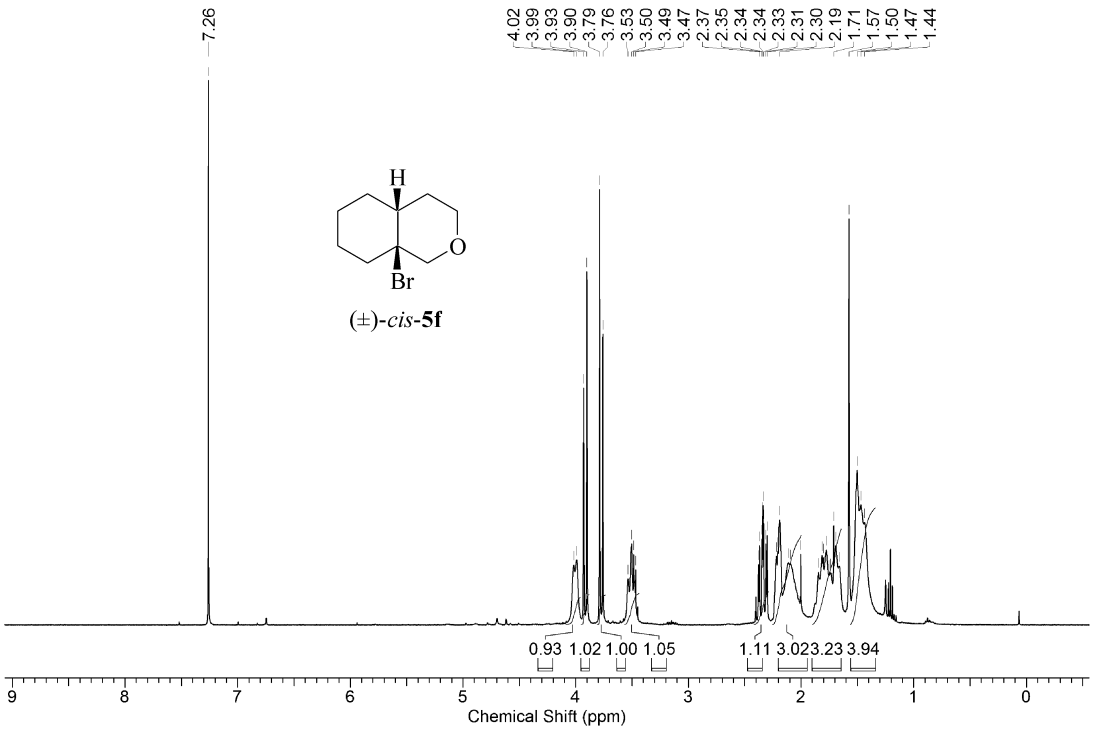

Figure A109. Proton-1 NMR-spectrum of *cis*-(1-bromo)-3-oxabicyclo[4.4.0]decane *cis*-(**5f**) (400MHz, $CDCl_3$, 23 °C).

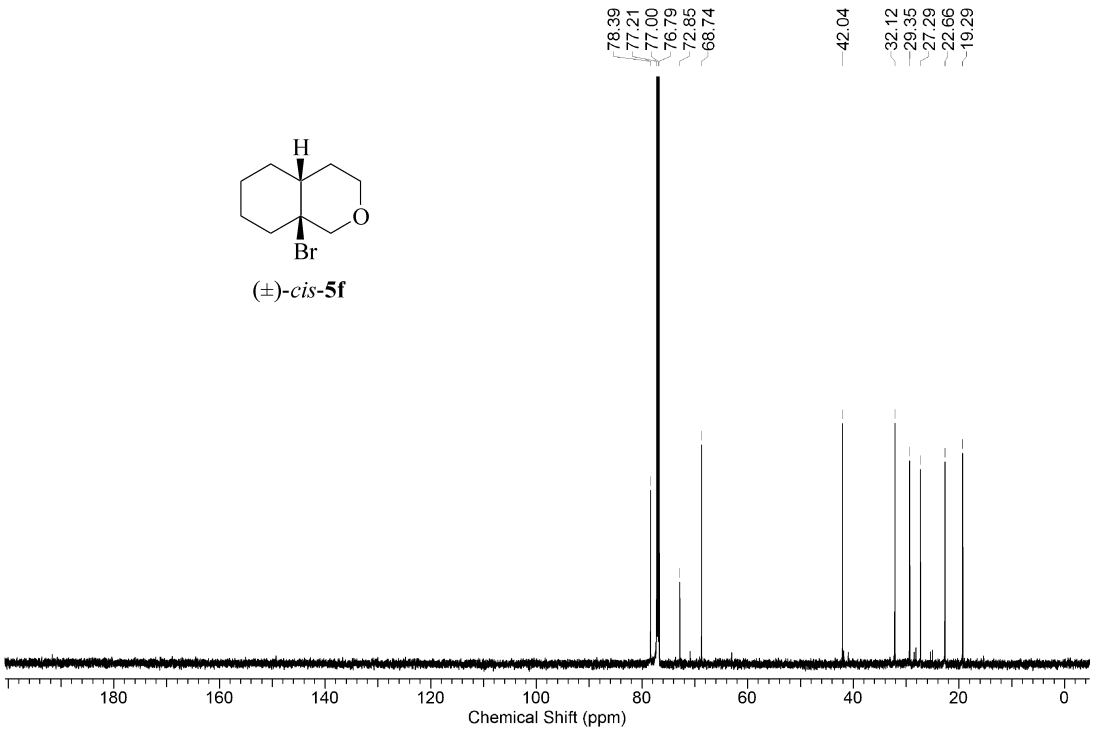

Figure A110. Carbon-13 NMR-spectrum of *cis*-(1-bromo)-3-oxabicyclo[4.4.0]decane *cis*-(**5f**) (150MHz, $CDCl_3$, 23 °C).

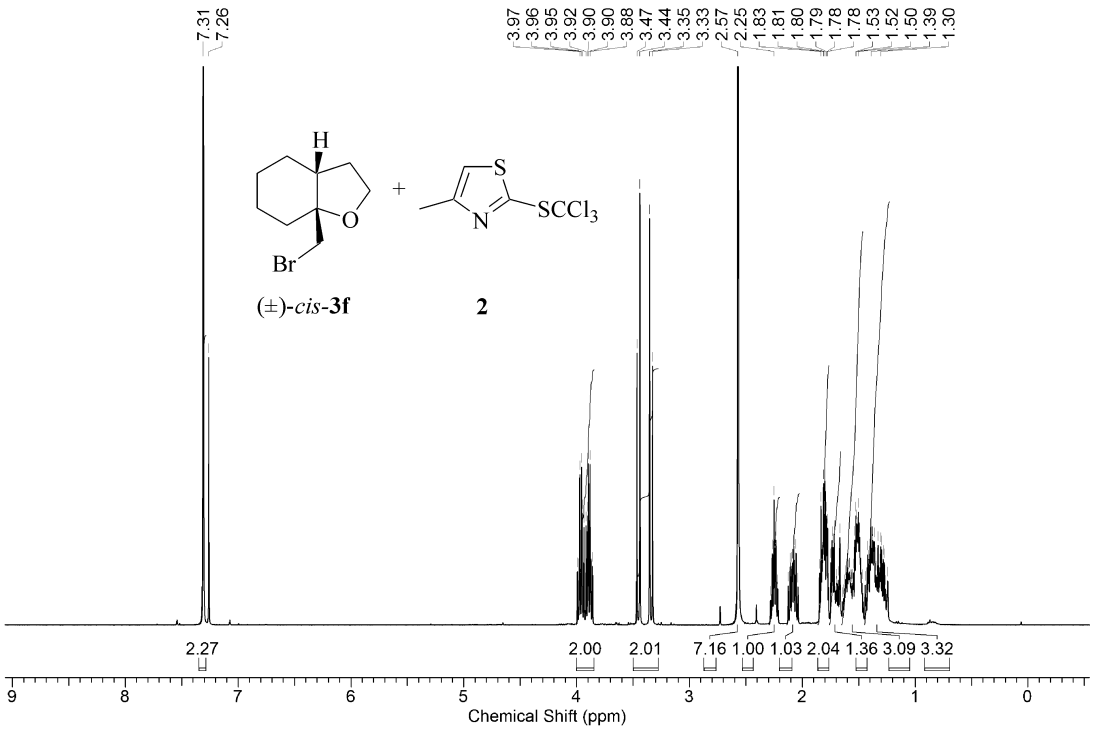

Figure A111. Proton-1 NMR-spectrum of *cis*-(1-bromomethyl)-9-oxabicyclo[4.3.0]nonane *cis*-(**3f**) and 4-methyl-2-(trichloromethylsulfanyl)-thiazole (**2**) (400MHz, $CDCl_3$, 23 °C).

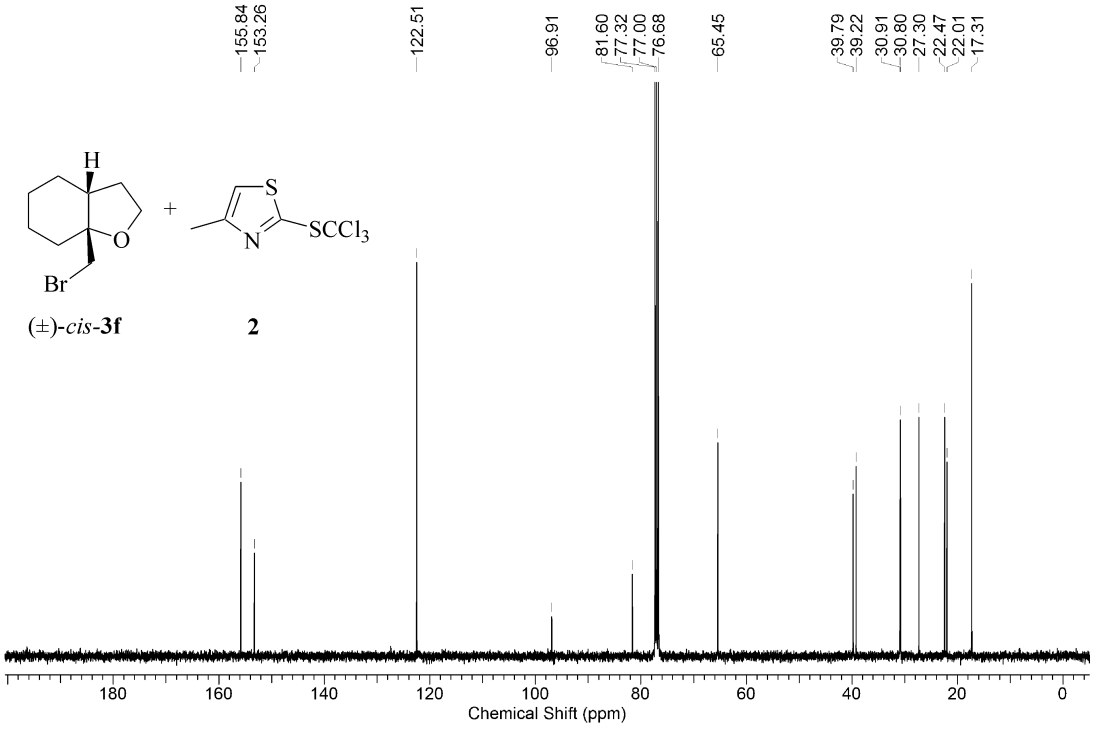

Figure A112. Carbon-13 NMR-spectrum of cis-(1-bromomethyl)-9-oxabicyclo[4.3.0]nonane *cis*-(**3f**) and 4-methyl-2-(trichloromethylsulfanyl)-thiazole (**2**) (100MHz, $CDCl_3$, 23 °C).

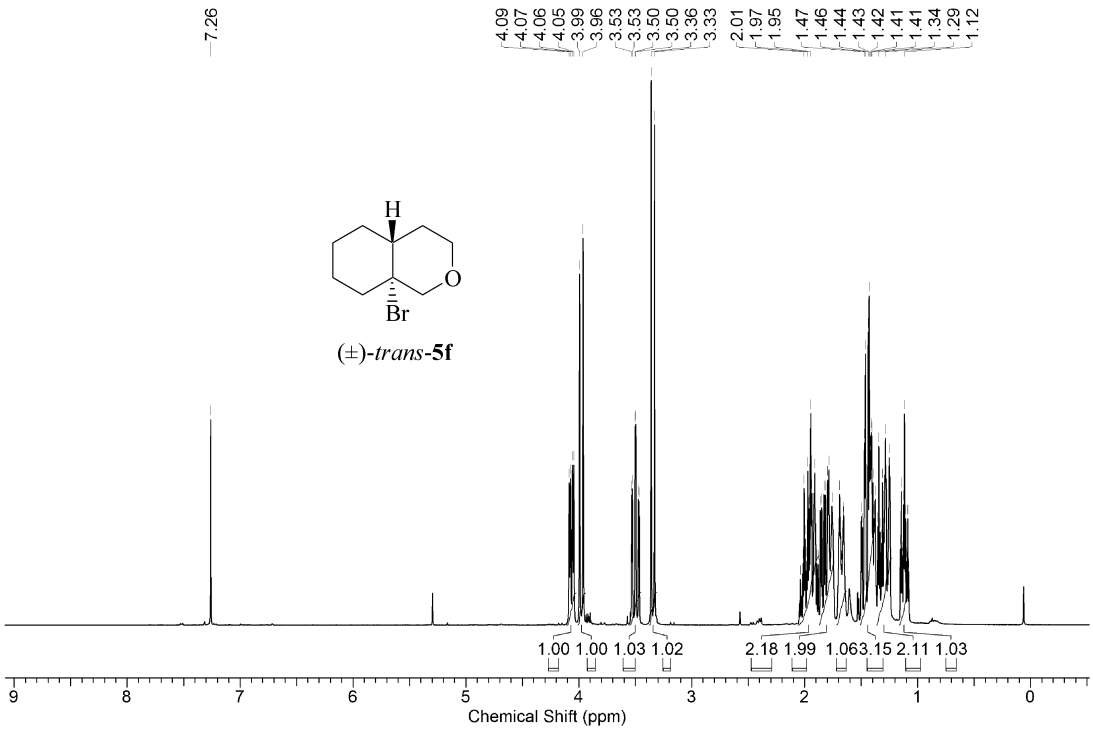

Figure A113. Proton-1 NMR-spectrum of *trans*-(1-bromo)-3-oxabicyclo[4.4.0]decane *trans*-(**5f**) (400MHz, $CDCl_3$, 23 °C).

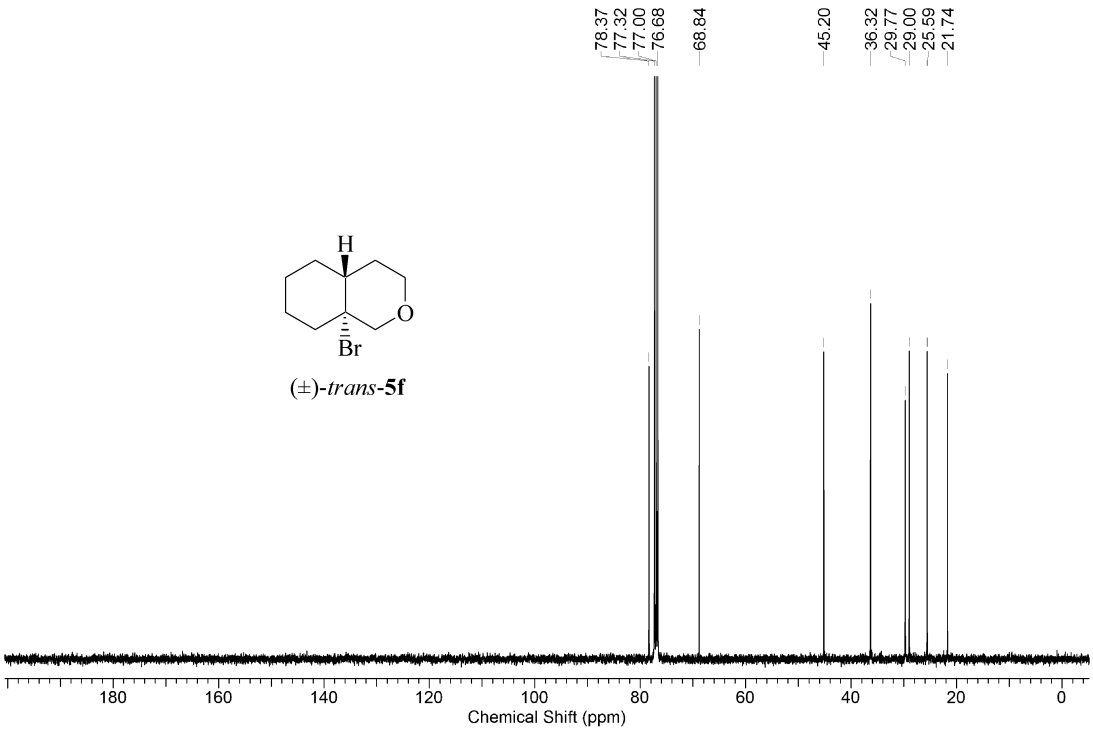

Figure A114. Carbon-13 NMR-spectrum of *trans*-(1-bromo)-3-oxabicyclo[4.4.0]decane *trans*-(**5f**) (100MHz, $CDCl_3$, 23 °C).

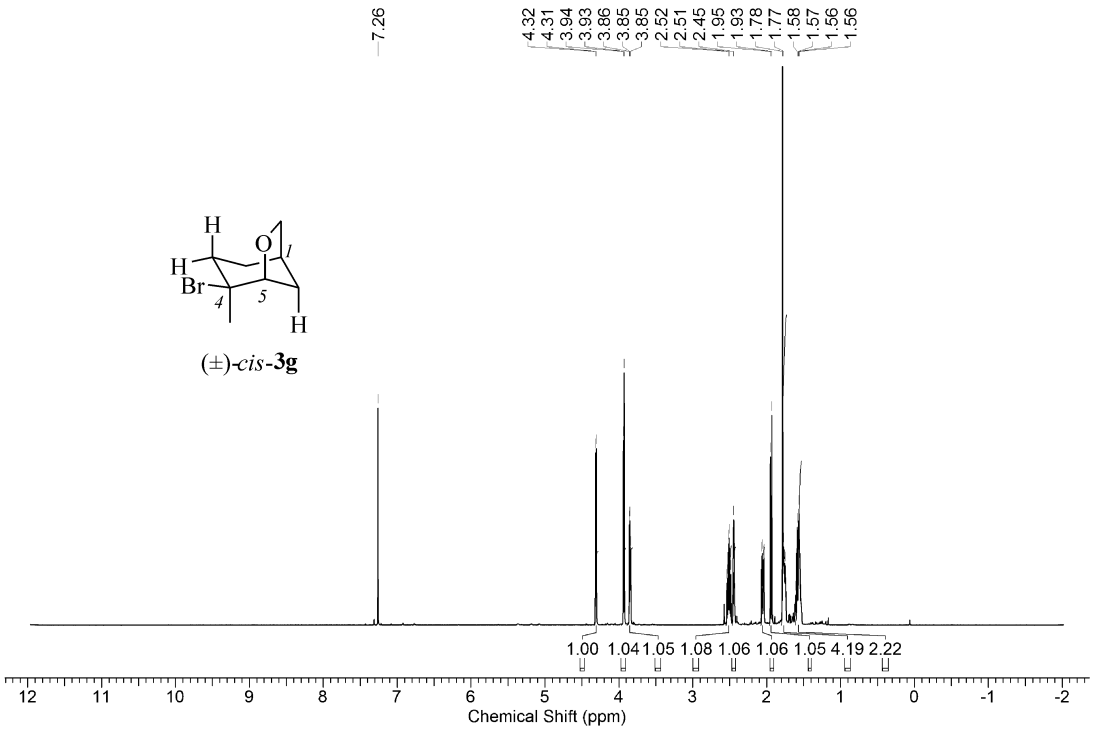

Figure A115. Proton-1 NMR-spectrum of, i.e *rel-(1R,4S,5R)*-**3g**, 4-bromo-4-methyl-6-oxa-bicyclo[3.2.1]octane *cis*-(**3g**) (400MHz, $CDCl_3$, 23 °C).

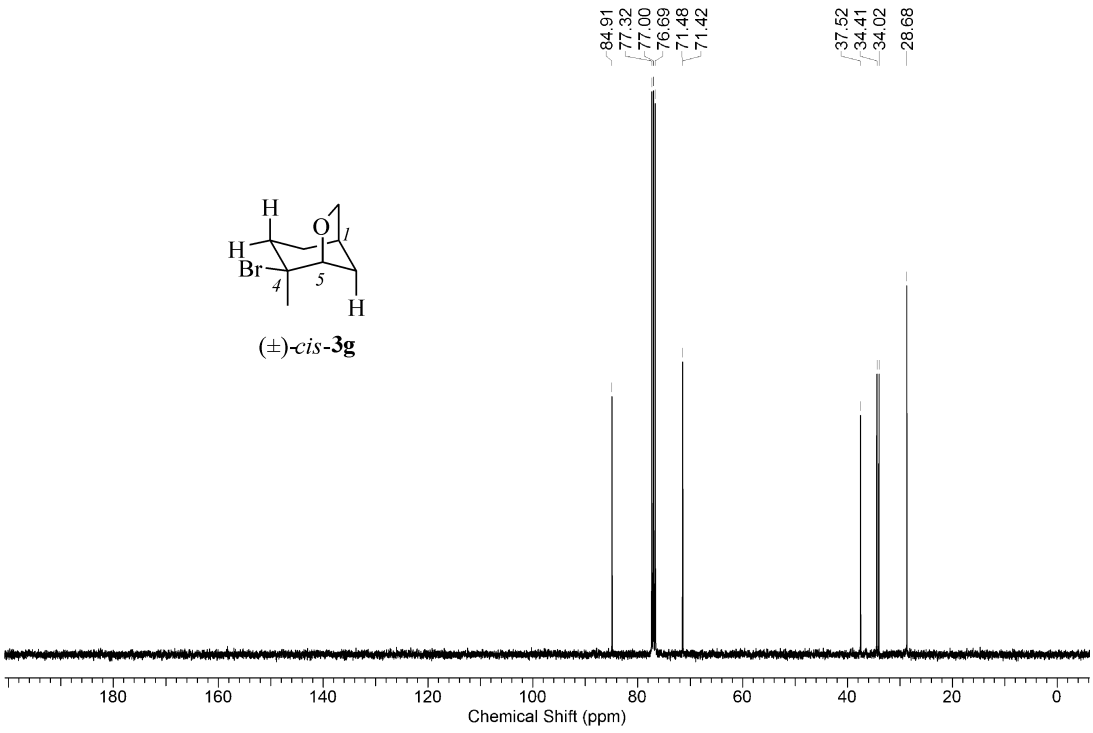

Figure A116. Carbon-13 NMR-spectrum of, i.e *rel-(1R,4S,5R)*-**3g**, 4-bromo-4-methyl-6-oxa-bicyclo[3.2.1]octane *cis*-(**3g**) (100MHz, $CDCl_3$, 23 °C).

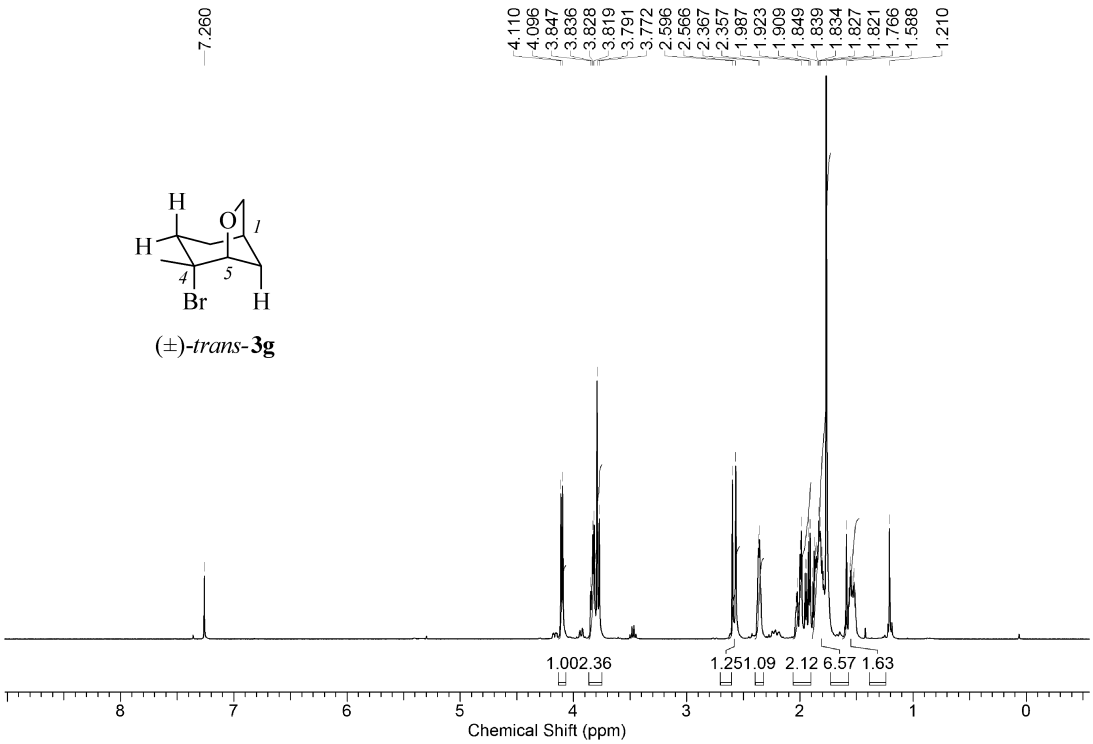

Figure A117. Proton-1 NMR-spectrum of, i.e. *rel-(1R,4R,5R)*-**3g**, 4-Bromo-4-methyl-6-oxa-bicyclo[3.2.1]octane *trans*-(**3g**) (400MHz, $CDCl_3$, 23 °C).

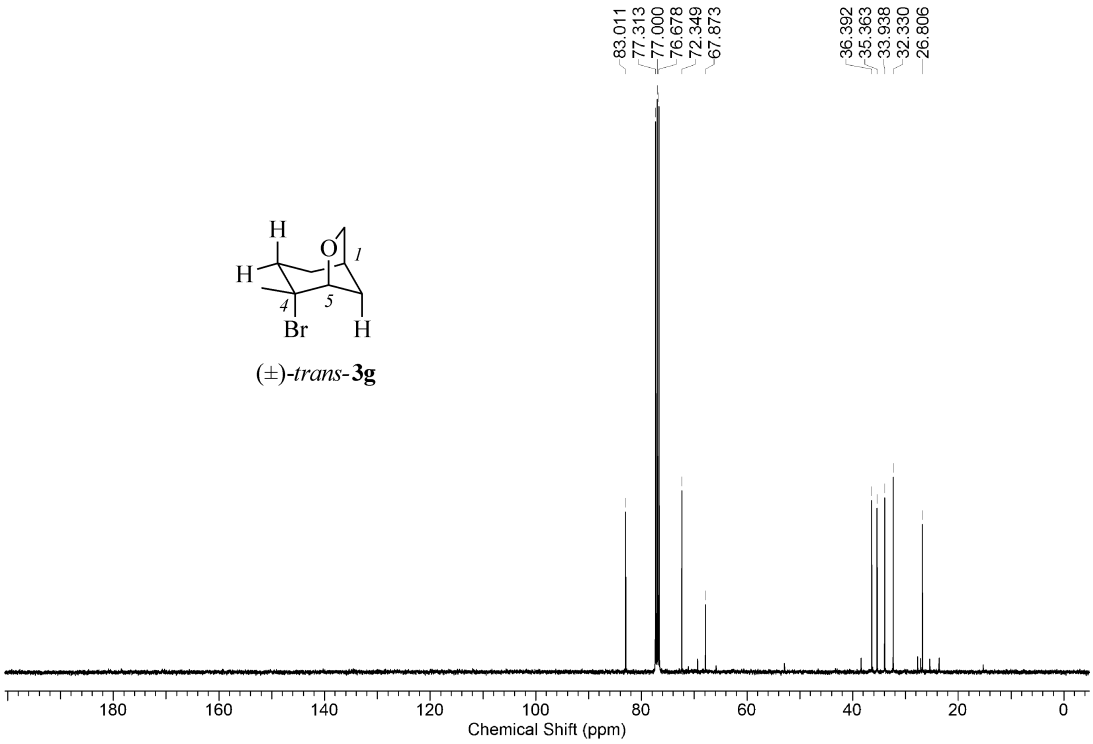

Figure A118. Carbon-13 NMR-spectrum of, i.e *rel-(1R,4R,5R)*-**3g**, 4-bromo-4-methyl-6-oxa-bicyclo[3.2.1]octane *trans*-(**3g**) (100MHz, $CDCl_3$, 23 °C).

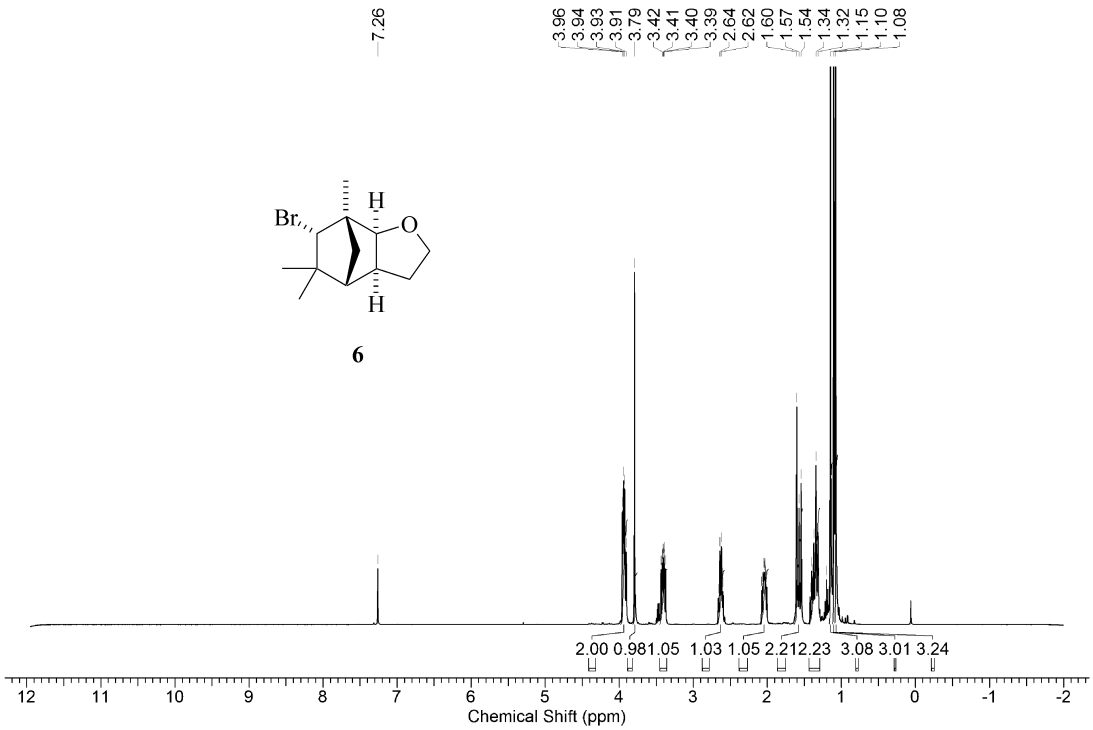

Figure A119. Proton-1 NMR-spectrum of i.e. *rel-(1R,2S,6S,7S,9S)*-9-bromo-1,8,8-trimethyl-3-oxatricyclo[5.2.1.0^{2,6}]-decane (**6**) (400MHz, $CDCl_3$, 23 °C).

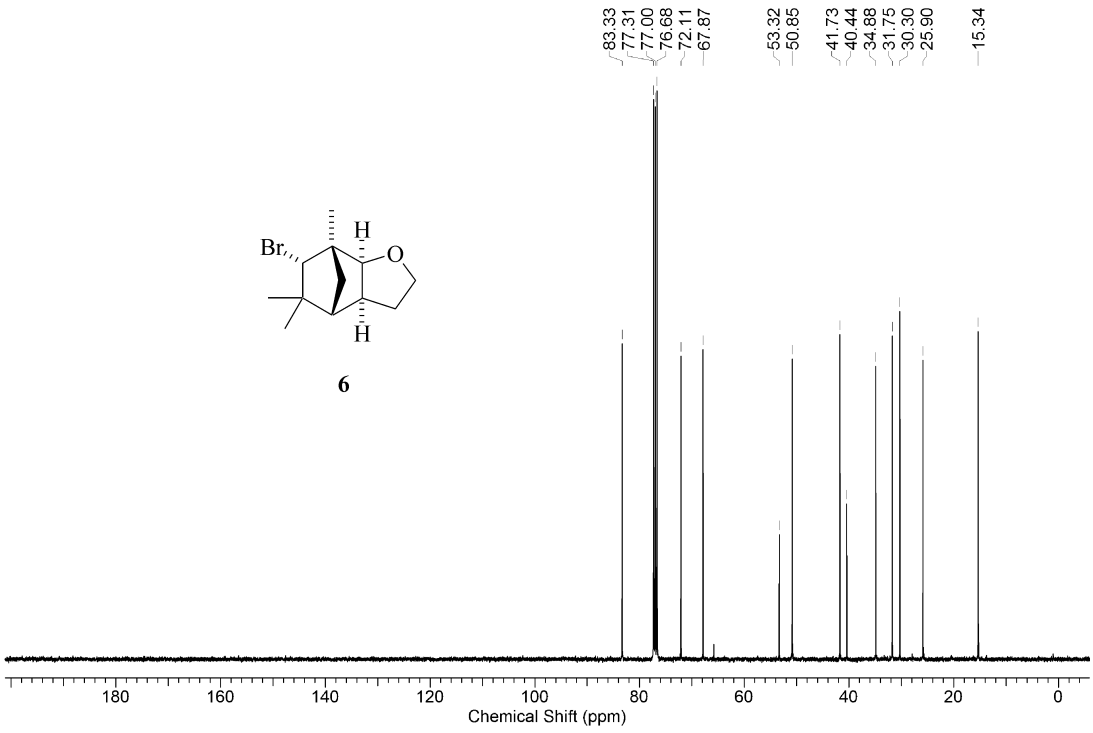

Figure A120. Proton-13 NMR-spectrum of i.e *rel-(1R,2S,6S,7S,9S)*-9-bromo-1,8,8-trimethyl-3-oxatricyclo[5.2.1.0^{2,6}]-decane (**6**) (100MHz, $CDCl_3$, 23 °C).

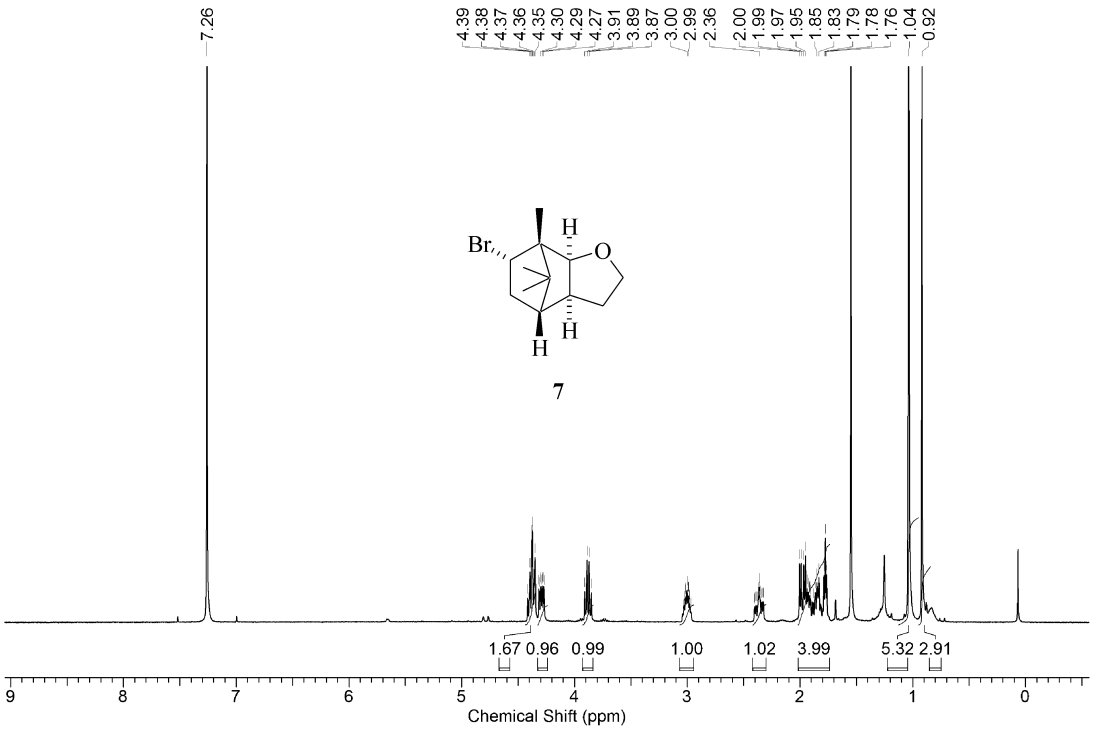

Figure A121. Proton-1 NMR-spectrum of i.e *rel-(1S,2S,6S,7S,9S)*-9-bromo-1,10,10-trimethyl-3-oxatricyclo[5.2.1.$0^{2,6}$]-decane (**7**) (400MHz, $CDCl_3$, 23 °C).

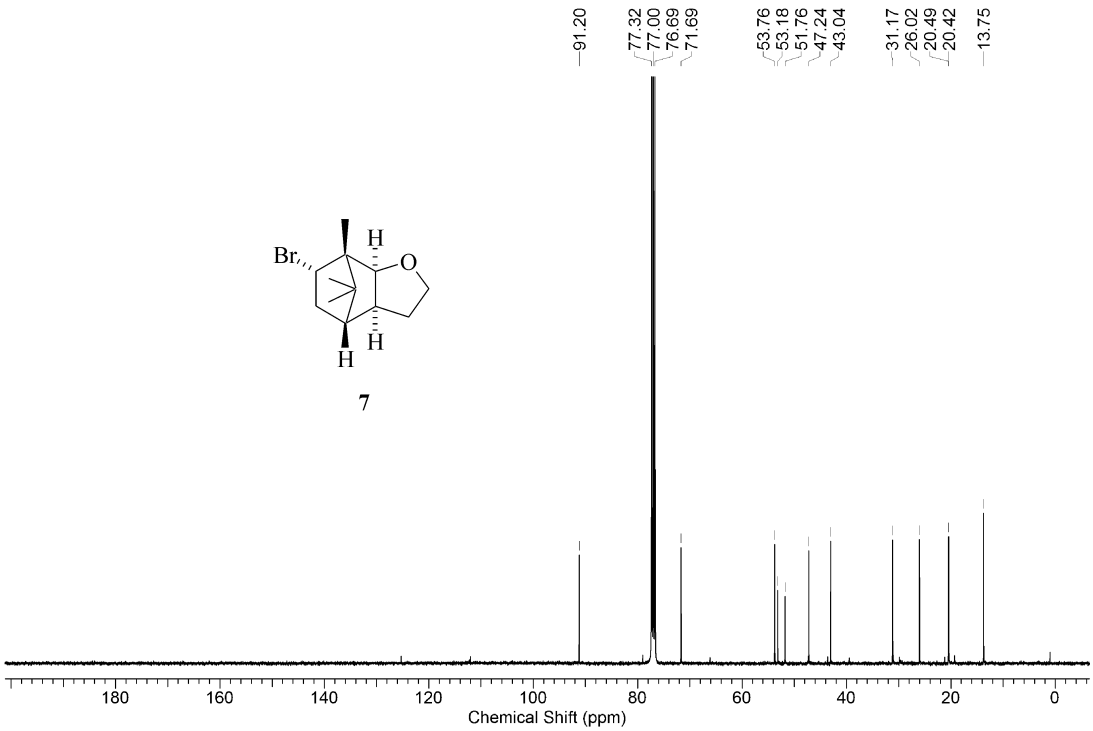

Figure A122. Carbon-13 NMR-spectrum of i.e *rel-(1S,2S,6S,7S,9S)*-9-bromo-1,10,10-trimethyl-3-oxatricyclo[5.2.1.$0^{2,6}$]-decane (**7**) (100MHz, $CDCl_3$, 23 °C).

A8 Computational Chemistry

A8.1 Computational Details

All calculations were carried out with Gaussian03[31], using the density functional/Hartree-Fock hybrid models B3LYP and BHandHLYP and split valance double-ζ basis set 6-31+G(d,p) and split valence triple-ζ basis set 6-311G(d,p). No symmetry or internal coordinate constraints were applied during energy function minimization. The ultrafine grid in combination with the tight option for energy function minimization was used. The absence of imaginary modes of vibration characterized computed structures as minima (for radicals **I, II,** and **VII** and for propene). Transition structures **TS-I** and **TS-VII** were located with the Berny algorithm. Hessian matrices of transition structures had exactly one negative stretching mode (Table 9 of the associated manuscript). Animations of eigenvector coordinates using Molden[32] were performed to verify that the imaginary mode correlates with the trajectory of C,O bond formation. Approximate Gibbs free energies ($G^{298.15}$) were obtained through thermochemical analysis for 298.15 K by unscaled frequency calculation from the thermal correction reported by Gaussian03. Likewise obtained Gibbs free energies take into account zero-point correction, thermal correction, and entropy. All transition structures were maxima on electronic potential energy hypersurface, which may not correspond to maxima on the free energy surface.

8.2 Ball-and-Stick Graphics from Modelled Structures

Graphics displaying computed equilibrium structures of oxygen radicals, addition products, and transition structures associated with oxygen radical additions were generated from B3LYP-calculated atomic coordinates. The results obtained from BHandHLYP-calculations provided almost identical conformations for the investigated structures. Oxygen is depicted in the ball-and-stick models in red, carbon in gray and hydrogen in white.

Table A1. Calculated zero point vibrational energy (ZPVE)-corrected electronic energies (*E*, 0 K) expectation values of spin the operator $\langle S^2 \rangle$ and free energies (*G*, 298.15K) for the 2-(cyclohexen-3-yl)-ethoxyl radical cyclization **Ii** → **Iii**.

method	**Ii**	parameter	**Ii**	TS-*cis*-**Ii**	TS-*trans*-**Ii**	*cis*-**IIi**	*trans*-**IIi**
B3LYP	*pe*-**Ii**	*E* + ZPVE / a.u. [a]	–387.657312	–387.650940	–387.629477	–387.674108	–387.670439
/6-31+G**		$\langle S^2 \rangle$	0.753802	0.778264	0.784693	0.753815	0.753984
		$G^{298.15}$ / a.u. [a]	–387.692413	–387.683999	–387.663009	–387.708058	–387.703786
BHandHLYP	*pe*-**Ii**	*E* + ZPVE / a.u. [a]	–387.413367	–387.398398	–387.375607	–387.431051	–387.426977
/6-31+G**		$\langle S^2 \rangle$	0.755213	0.826176	0.842594	0.755346	0.755562
		$G^{298.15}$ / a.u. [a]	–387.448360	–387.431259	–387.409043	–387.464567	–387.460005
BHandHLYP	*pe*-**Ii**	*E* + ZPVE / a.u. [a]	–387.481233	–387.465775	–387.442897	–387.498255	–387.494066
/6-311G**		$\langle S^2 \rangle$	0.754665	0.826681	0.842829	0.7554	0.755584
		$G^{298.15}$ / a.u. [a]	–387.516054	–387.498638	–387.476661	–387.531833	–387.527097
B3LYP	*pa*-**Ii**	*E* + ZPVE / a.u. [a]	–387.655174	–387.648548	– [b]	-387.672979	– [b]
/6-31+G**		$\langle S^2 \rangle$	0.753686	0.776177	– [b]	0.753956	– [b]
		$G^{298.15}$ / a.u. [a]	–387.690292	–387.681779	– [b]	–387.706516	– [b]
BHandHLYP	*pa*-**Ii**	*E* + ZPVE / a.u. [a]	–387.410795	–387.395737	– [b]	–387.430001	– [b]
/6-31+G**		$\langle S^2 \rangle$	0.755156	0.820896	– [b]	0.755609	– [b]
		$G^{298.15}$ / a.u. [a]	–387.445688	–387.428809	– [b]	–387.463260	– [b]
BHandHLYP	*pa*-**Ii**	*E* + ZPVE / a.u. [a]	–387.478854	–387.463263	– [b]	–387.497527	– [b]
/6-311G**		$\langle S^2 \rangle$	0.754575	0.821789	– [b]	0.755641	– [b]
		$G^{298.15}$ / a.u. [a]	–387.513728	–387.496441	– [b]	–387.530694	– [b]

[a] 1 a.u. = 1 Hartree = 2625.5 kJ mol^{-1}. [b] Identical with *trans*-**Ii** from *pe*-**Ii**.

Table A2. Calculated zero point vibrational energy (ZPVE)-corrected electronic energies (*E*, 0 K) expectation values of spin the operator $\langle S^2 \rangle$ and free energies (*G*, 298.15K) for the 4-pentenoxyl radical 5-exo-cyclization.

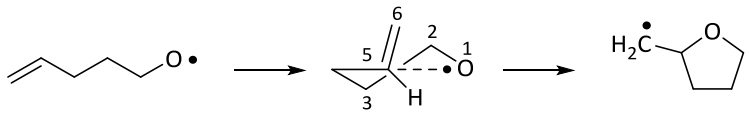

Ij TS-**Ij** ($_2T^3$) **IIj**

method	parameter	**Ij**	TS-**Ij**	**IIj**
B3LYP/6-31+G**	*E* + ZPVE / a.u. [a]	–270.975247	–270.967723	–270.990673
	$\langle S^2 \rangle$	0.753684	0.778657	0.753834
	$G^{298.15}$ / a.u. [a]	–271.007703	–270.997697	–271.021685
BHandHLYP/6-31+G**	*E* + ZPVE / a.u. [a]	–270.804872	–270.789272	–270.821432
	$\langle S^2 \rangle$	0.755148	0.826588	0.755247
	$G^{298.15}$ / a.u. [a]	–270.837439	–270.819113	–270.852280
BHandHLYP/6-311G**	*E* + ZPVE / a.u. [a]	–270.853885	–270.838018	–270.869791
	$\langle S^2 \rangle$	0.754563	0.826641	0.755332
	$G^{298.15}$ / a.u. [a]	–270.886313	–270.867816	–270.900557

[a] 1 a.u. = 1 Hartree = 2625.5 kJ mol^{-1}

Table A3. Calculated zero point vibrational energy (ZPVE)-corrected electronic energies (*E*, 0 K) expectation values of spin the operator $\langle S^2 \rangle$ and free energies (*G*, 298.15K) for the methoxyl radical transition structure TS^1-**VII**, and addition product *iso*-**VIII**.

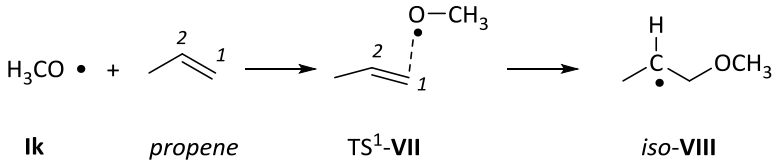

Ik *propene* TS^1-**VII** *iso*-**VIII**

method	parameter	**Ik**	*propene*	TS^1-**VII**	*iso*-**VIII**
B3LYP/6-31+G**	*E* + ZPVE / a.u. [a]	–115.026987	–117.843255	–232.863588	–232.892586
	$\langle S^2 \rangle$	0.753499	0	0.774311	0.753954
	$G_{298.15}$ / a.u. [a]	–115.049934	–117.868282	–232.895907	–232.924574
BHandHLYP/6-31+G**	*E* + ZPVE / a.u. [a]	–114.961999	-117.755443	–232.703774	–232.741734
	$\langle S^2 \rangle$	0.754977	0	0.821343	0.755624
	$G_{298.15}$ / a.u. [a]	–114.984919	–117.780411	–232.735641	–232.773478
BHandHLYP/6-311G**	*E* + ZPVE / a.u. [a]	–114.985163	–117.775341	–232.746863	–232.784295
	$\langle S^2 \rangle$	0.754332	0	0.822071	0.755667
	$G_{298.15}$ / a.u. [a]	–115.008074	–117.800297	–232.778726	–232.815991

[a] 1 a.u. = 1 Hartree = 2625.5 kJ mol^{-1} .

Table A4. Calculated zero point vibrational energy (ZPVE)-corrected electronic energies (*E*, 0 K) expectation values of spin the operator $\langle S^2 \rangle$ and free energies (*G*, 298.15K) for the methoxyl radical, transition structure TS^2-**VII**, and addition product **VIII**.

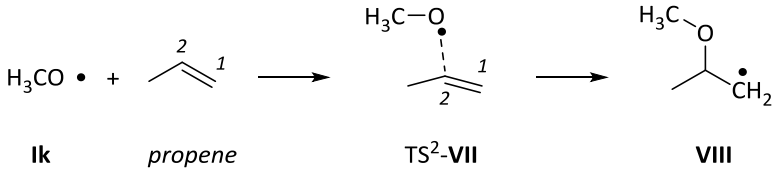

Ik *propene* TS^2-**VII** **VIII**

method	parameter	**Ik**	*propene*	TS^2-**VII**	**VIII**
B3LYP/6-31+G**	*E* + ZPVE / a.u. [a]	–115.026987	–117.843255	–232.862433	–232.890748
	$\langle S^2 \rangle$	0.753499	0	0.775952	0.753661
	$G_{298.15}$ / a.u. [a]	–115.049934	–117.868282	–232.893984	–232.921330
BHandHLYP/6-31+G**	*E* + ZPVE / a.u. [a]	–114.961999	–117.755443	–232.703249	–232.740760
	$\langle S^2 \rangle$	0.754977	0	0.823151	0.754984
	$G_{298.15}$ / a.u. [a]	–114.984919	–117.780411	–232.734388	–232.771144
BHandHLYP/6-311G**	*E* + ZPVE / a.u. [a]	–114.985163	–117.775341	–232.746689	–232.783726
	$\langle S^2 \rangle$	0.754332	0	0.823321	0.755082
	$G_{298.15}$ / a.u. [a]	–115.008074	–117.800297	–232.777810	–232.814067

[a] 1 a.u. = 1 Hartree = 2625.5 kJ mol^{-1} .

A8.3 The 2-(Cyclohexen-3-yl)-ethane-1-oxyl Radical Cyclization

A8.3.1 2-(Cyclohexen-3-yl)-ethane-1-oxyl radical *pe*-(Ij)

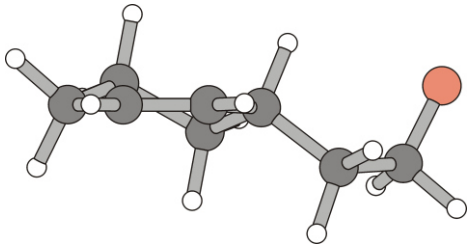

Figure A123. Ball-and-stick model showing the computed equilibrium structure of alkenoxyl radical *pe*-**Ij**.

(*i*) B3LYP/6-31+G**//B3LYP/6-31+G**

Standard orientation:

Center Number	Atomic Number	Atomic Type	Coordinates (Angstroms) X	Y	Z
1	6	0	2.747885	-0.256934	0.110777
2	6	0	2.158245	1.116702	-0.094916
3	6	0	0.847895	1.341920	-0.261108
4	6	0	-0.216312	0.266110	-0.224944
5	6	0	0.352276	-1.045928	0.352082
6	6	0	1.738080	-1.364248	-0.227487
7	6	0	-1.462312	0.767702	0.538204
8	6	0	-2.671934	-0.165532	0.431133
9	8	0	-3.170931	-0.345463	-0.833906
10	1	0	2.848808	1.958661	-0.114481
11	1	0	0.502111	2.361250	-0.432759
12	1	0	-0.545001	0.077763	-1.260665
13	1	0	0.433228	-0.950178	1.445226
14	1	0	-0.333917	-1.878119	0.156565
15	1	0	2.095098	-2.331183	0.146004
16	1	0	1.656729	-1.457776	-1.318844
17	1	0	3.086542	-0.357198	1.153900
18	1	0	3.652014	-0.365918	-0.502843
19	1	0	-1.755754	1.748535	0.143257
20	1	0	-1.213692	0.910216	1.599514
21	1	0	-3.525360	0.242943	1.016325
22	1	0	-2.496300	-1.154047	0.897615

Version=AM64L-G03RevE.01\State=2-A\HF=-387.8498053\S2=0.753802\S2-1=0.\
S2A=0.750011\RMSD=5.438e-09\RMSF=2.601e-06\ZeroPoint=0.1924931 \Thermal=
0.2016454\Dipole=-0.3969692,0.7057764,-0.2554294\PG=C01 [X(C8H13O1)]\
NImag=0\\@

(*ii*) BHandHLYP/6-31+G**//BHandHLYP/6-31+G**

Standard orientation:

Center Number	Atomic Number	Atomic Type	Coordinates (Angstroms) X	Y	Z
1	6	0	2.143476	1.102893	-0.095854
2	6	0	0.847299	1.332028	-0.272079
3	6	0	-0.218311	0.268357	-0.235776
4	6	0	0.336826	-1.032597	0.349112
5	6	0	1.713739	-1.358290	-0.218583
6	6	0	2.720331	-0.265067	0.124240
7	1	0	2.833091	1.934535	-0.116146
8	1	0	0.512043	2.344548	-0.451177
9	6	0	-1.448257	0.779202	0.520443
10	1	0	-0.538470	0.076372	-1.263027
11	1	0	0.412499	-0.931932	1.433957
12	1	0	-0.346300	-1.856771	0.154848
13	1	0	2.060008	-2.319767	0.154797
14	1	0	1.638479	-1.450085	-1.302127
15	1	0	3.040880	-0.360712	1.164090
16	1	0	3.622809	-0.381714	-0.474671
17	6	0	-2.656727	-0.139458	0.445229
18	8	0	-3.124165	-0.373058	-0.825310
19	1	0	-1.737853	1.749982	0.119749
20	1	0	-1.194690	0.937427	1.569682
21	1	0	-3.490389	0.248235	1.040650
22	1	0	-2.449038	-1.128063	0.871466

```
Version=AM64L-G03RevE.01\State=2-A\HF=-387.6131896\S2=0.755213\S2-1=0.\
S2A=0.750021\RMSD=9.026e-10\RMSF=6.453e-07\ZeroPoint=0.1998229\
Thermal=0.20881\Dipole=0.0279442,0.6627,-0.4279888\PG=C01 [X(C8H13O1)]\
NImag=0\\@
```

(*iii*) BHandHLYP/6-311G**//BHandHLYP/6-31+G**

Standard orientation:

Center Number	Atomic Number	Atomic Type	Coordinates (Angstroms) X	Y	Z
1	6	0	2.137025	1.098996	-0.102435
2	6	0	0.846774	1.329489	-0.278911
3	6	0	-0.221831	0.271312	-0.232680
4	6	0	0.328173	-1.028213	0.356730
5	6	0	1.702615	-1.359917	-0.209775
6	6	0	2.710486	-0.267589	0.126158
7	1	0	2.829134	1.926689	-0.129476
8	1	0	0.513530	2.340076	-0.464721
9	6	0	-1.446977	0.788368	0.523570
10	1	0	-0.548874	0.074869	-1.254914
11	1	0	0.404406	-0.923316	1.439807
12	1	0	-0.357294	-1.849256	0.165487
13	1	0	2.046821	-2.319321	0.166613
14	1	0	1.625793	-1.455160	-1.291537
15	1	0	3.031352	-0.357306	1.165169
16	1	0	3.611449	-0.389494	-0.471623
17	6	0	-2.659522	-0.125092	0.440611
18	8	0	-3.082536	-0.394752	-0.832755
19	1	0	-1.729920	1.759907	0.122962
20	1	0	-1.196096	0.945326	1.572204
21	1	0	-3.498302	0.268576	1.021370
22	1	0	-2.452164	-1.107699	0.881094

Version=AM64L-G03RevE.01\State=2-A\HF=-387.6810797\S2=0.754665\S2-1=0.\
S2A=0.750016\RMSD=4.947e-09\RMSF=7.86 2e-07\ZeroPoint=0.199847\ Thermal=
0.2085931\Dipole=0.0131019,0.61879,-0.3665296\PG=C01 [X(C8H13O1)]
\NImag=0\\@

A8.3.2 2-(Cyclohexen-3-yl)-ethoxyl radical – *pa*-(Ij)

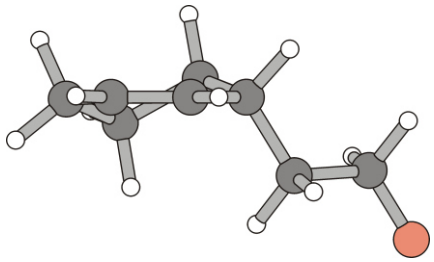

Figure A124. Ball-and-stick model showing the computed equilibrium structure of alkenoxyl radical *pa*-**Ij**

(*i*) B3LYP/6-31+G**//B3LYP/6-31+G**

Standard orientation:

Center Number	Atomic Number	Atomic Type	Coordinates (Angstroms) X	Y	Z
1	6	0	2.209017	1.057979	-0.221320
2	6	0	0.993282	1.401643	0.224121
3	6	0	-0.077326	0.414134	0.637752
4	6	0	0.514396	-1.007497	0.780930
5	6	0	1.480183	-1.350696	-0.363330
6	6	0	2.662218	-0.370487	-0.394065
7	1	0	2.921703	1.841233	-0.475500
8	1	0	0.732635	2.456773	0.302115
9	1	0	-0.442730	0.729903	1.628192
10	6	0	-1.285725	0.488594	-0.327886
11	1	0	1.057874	-1.068014	1.733261
12	1	0	-0.286172	-1.755427	0.838140
13	1	0	1.842089	-2.379964	-0.257734
14	1	0	0.947893	-1.303179	-1.322261
15	1	0	3.382736	-0.622032	0.400004
16	1	0	3.216459	-0.471438	-1.336384
17	6	0	-2.566470	-0.139092	0.242236
18	8	0	-3.644606	-0.125809	-0.602018
19	1	0	-2.833442	0.287135	1.228952
20	1	0	-2.410230	-1.222461	0.445603
21	1	0	-1.504498	1.539132	-0.556198
22	1	0	-1.044921	0.007348	-1.282674

Version=AM64L-G03RevE.01\State=2-A\HF=-387.8480682\S2=0.753686\S2-1=0.\
S2A=0.75001\RMSD=8.300e-09\RMSF=3.039e- 07\ZeroPoint=0.1928939\Thermal=
0.2019726\Dipole=0.0131466,0.7644402,-0.6522786\PG=C01 [X(C8H13O1)]\\@

(*ii*) BHandHLYP/6-31+G**//BHandHLYP/6-31+G**

Standard orientation:

Center Number	Atomic Number	Atomic Type	Coordinates (Angstroms) X	Y	Z
1	6	0	2.188672	1.052738	-0.221943
2	6	0	0.985808	1.392105	0.226870
3	6	0	-0.076822	0.409242	0.640846
4	6	0	0.515575	-1.000088	0.780260
5	6	0	1.463743	-1.338438	-0.365629
6	6	0	2.639000	-0.367510	-0.399552
7	1	0	2.893626	1.830925	-0.476854
8	1	0	0.728455	2.439111	0.307744
9	1	0	-0.436297	0.721549	1.624827
10	6	0	-1.276345	0.481292	-0.316218
11	1	0	1.066611	-1.056005	1.718880
12	1	0	-0.275749	-1.744209	0.846660
13	1	0	1.822403	-2.360739	-0.267282
14	1	0	0.928381	-1.286222	-1.312953
15	1	0	3.356071	-0.618861	0.385261
16	1	0	3.182603	-0.464332	-1.338410
17	6	0	-2.538392	-0.159304	0.241931
18	8	0	-3.616455	-0.106653	-0.605411
19	1	0	-2.813761	0.264208	1.213716
20	1	0	-2.396693	-1.232643	0.424087
21	1	0	-1.499915	1.524684	-0.533295
22	1	0	-1.031527	0.015533	-1.268494

Version=AM64L-G03RevE.01\State=2-A\HF=-387.6113827\S2=0.755156\S2-1=0.\
S2A=0.75002\RMSD=6.315e-09\RMSF=1.905e-07\ZeroPoint=0.2005873\Thermal=
0.2093876\Dipole=0.0258897,0.7306969, -0.5912948\PG=C01 [X(C8H13O1)]\\@

(*iii*) BHandHLYP/6-311G**//BHandHLYP/6-311G**

Standard orientation:

Center Number	Atomic Number	Atomic Type	Coordinates (Angstroms) X	Y	Z
1	6	0	2.184269	1.049823	-0.224674
2	6	0	0.988594	1.390714	0.225808
3	6	0	-0.075157	0.411643	0.641124
4	6	0	0.514110	-0.996818	0.785496
5	6	0	1.456952	-1.339595	-0.361807
6	6	0	2.631324	-0.369904	-0.403442
7	1	0	2.890517	1.824488	-0.481319
8	1	0	0.733439	2.436807	0.308274
9	1	0	-0.434758	0.726912	1.622484
10	6	0	-1.272700	0.480159	-0.315496
11	1	0	1.067792	-1.049107	1.721146
12	1	0	-0.277139	-1.738387	0.857397
13	1	0	1.814878	-2.360500	-0.262347
14	1	0	0.918448	-1.289328	-1.305846
15	1	0	3.352666	-0.620357	0.376020
16	1	0	3.168642	-0.467887	-1.344319
17	6	0	-2.537563	-0.152025	0.243426
18	8	0	-3.605164	-0.112051	-0.610117
19	1	0	-2.814976	0.283322	1.208578
20	1	0	-2.393346	-1.221379	0.442312
21	1	0	-1.493064	1.521211	-0.540798
22	1	0	-1.030761	0.006635	-1.263256

Version=AM64L-G03RevE.01\State=2-A\HF=-387678858\S2=0.754575\S2-1=0.\
S2A=0.750015\RMSD=3.414e-09\RMSF=2.073e-07 \ZeroPoint=0.2000038\ Thermal=
0.2087976\Dipole=0.0100209,0.6723876,-0.5265333\PG=C01 [X(C8H13O1)]\\@

A8.3.3 Transition structure TS[1]-*cis*-**Ij** ($_3T^4$)

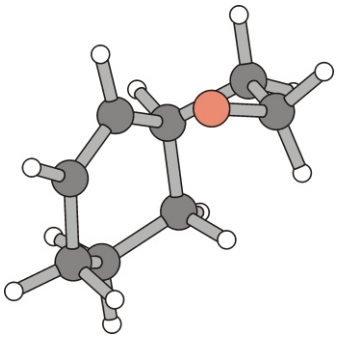

Figure A125. Ball-and-stick model of computed transition structure TS[1]-*cis*-**Ij** showing $_3T^4$-conformation of the cyclohexyl-annulated tetrahydrofuran subunit.

(*i*) B3LYP/6-31+G**//B3LYP/6-31+G**

Standard orientation:

Center Number	Atomic Number	Atomic Type	Coordinates (Angstroms) X	Y	Z
1	6	0	1.059457	-1.381949	0.389305
2	6	0	-0.059410	-0.749735	0.888483
3	6	0	-0.291296	0.738319	0.743204
4	6	0	0.663015	1.390573	-0.280550
5	6	0	2.088323	0.831154	-0.198852
6	6	0	2.086312	-0.684995	-0.453386
7	1	0	1.182989	-2.446122	0.576510
8	1	0	-0.637017	-1.258428	1.653284
9	6	0	-1.777159	0.933350	0.369608
10	1	0	-0.119314	1.199112	1.728230
11	1	0	0.281119	1.222211	-1.295445
12	1	0	0.664701	2.476258	-0.125373
13	1	0	2.737655	1.336144	-0.923335
14	1	0	2.508977	1.028772	0.796627
15	1	0	1.881251	-0.884945	-1.518422
16	1	0	3.076324	-1.116719	-0.258527
17	6	0	-2.076806	-0.059048	-0.768083
18	8	0	-1.560449	-1.308446	-0.433927
19	1	0	-3.169308	-0.168235	-0.885374
20	1	0	-1.680654	0.315352	-1.729045
21	1	0	-1.990598	1.970672	0.081246
22	1	0	-2.407151	0.687475	1.232669

Version=AM64L-G03RevE.01\State=2-A\HF=-387.8450213\S2=0.778264\S2-1=0.\
S2A=0.750142\RMSD=9.977e-09\RMSF=6.390e-07\ZeroPoint=0.1940813\Thermal=
0.2019898\Dipole=0.7681404,-0.6697273,-0.0444561\PG=C01 [X(C8H13O1)]\
NImag=1\\@

(*ii*) BHandHLYP/6-31+G**//BHandHLYP/6-31+G**

Standard orientation:

Center Number	Atomic Number	Atomic Type	Coordinates (Angstroms) X	Y	Z
1	6	0	1.052368	-1.372691	0.386576
2	6	0	-0.071383	-0.751074	0.870171
3	6	0	-0.296030	0.732552	0.737912
4	6	0	0.651916	1.381342	-0.276625
5	6	0	2.068434	0.830013	-0.187411
6	6	0	2.071331	-0.672870	-0.452412
7	1	0	1.179121	-2.427803	0.573049
8	1	0	-0.635362	-1.254138	1.637237
9	6	0	-1.768179	0.925181	0.362250
10	1	0	-0.121161	1.184116	1.716603
11	1	0	0.279252	1.211120	-1.285674
12	1	0	0.649067	2.459016	-0.123614
13	1	0	2.716714	1.338675	-0.897686
14	1	0	2.476372	1.020375	0.805640
15	1	0	1.866094	-0.863420	-1.509628
16	1	0	3.055113	-1.097524	-0.259576
17	6	0	-2.056111	-0.061673	-0.763949
18	8	0	-1.526059	-1.297735	-0.425085
19	1	0	-3.134428	-0.191553	-0.887879
20	1	0	-1.657362	0.303340	-1.714431
21	1	0	-1.981852	1.952589	0.071121
22	1	0	-2.397176	0.682406	1.216447

Version=AM64L-G03RevE.01\State=2-A\HF=-387.5997436\S2=0.826176\S2-1=0.\
S2A=0.750732\RMSD=2.934e-09\RMSF=5.526e-07\ZeroPoint=0.2013453\Thermal=
0.2089898\Dipole=0.7515801,-0.5706613,0.0225783\PG=C01 [X(C8H13O1)]\\@

(*iii*) BHandHLYP/6-311G**//BHandHLYP/6-311G**

Standard orientation:

Center Number	Atomic Number	Atomic Type	Coordinates (Angstroms) X	Y	Z
1	6	0	1.041007	-1.371515	0.388588
2	6	0	-0.079465	-0.748816	0.871069
3	6	0	-0.298588	0.735712	0.739092
4	6	0	0.656601	1.386226	-0.266311
5	6	0	2.066894	0.821979	-0.184345
6	6	0	2.053785	-0.677589	-0.459788
7	1	0	1.168274	-2.424136	0.579936
8	1	0	-0.634488	-1.243515	1.648026
9	6	0	-1.765263	0.930479	0.347488
10	1	0	-0.131885	1.183535	1.718911
11	1	0	0.283349	1.231541	-1.276222
12	1	0	0.663360	2.460590	-0.101186
13	1	0	2.717618	1.329619	-0.890906
14	1	0	2.477602	0.999650	0.808423
15	1	0	1.831491	-0.858135	-1.514086
16	1	0	3.035234	-1.111440	-0.284349
17	6	0	-2.036074	-0.066733	-0.772014
18	8	0	-1.516473	-1.296334	-0.410531
19	1	0	-3.111828	-0.193862	-0.911067
20	1	0	-1.623873	0.290299	-1.718917
21	1	0	-1.973320	1.955176	0.048179
22	1	0	-2.403130	0.692884	1.194831

Version=AM64L-G03RevE.01\State=2-A\HF=-387.6664803\S2=0.826681\S2-1=0.\
S2A=0.750703\RMSD=8.488e-09\RMSF=4.588e-07\ZeroPoint=0.2007052\Thermal=
0.2083489\Dipole=0.6728622,-0.5200177,0.0203533\PG=C01 [X(C8H13O1)]\\@

A8.3.4 Transition structure TS[1]-*trans*-**Ij** ($^3T_4$)

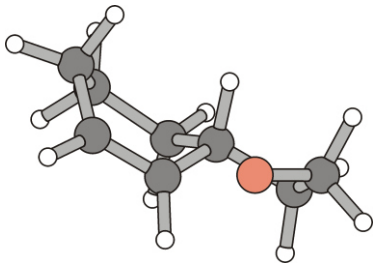

Figure A126. Ball-and-stick model of computed transition structure TS[1]-*trans*-**Ij** showing, $^3T_4$-conformation of the cyclohexyl-annulated tetrahydrofuran subunit.

(*i*) B3LYP/6-31+G//B3LYP/6-31+G****

Standard orientation:

Center Number	Atomic Number	Atomic Type	Coordinates (Angstroms) X	Y	Z
1	6	0	1.013337	-1.457806	-0.364381
2	6	0	-0.119558	-0.706264	-0.612946
3	6	0	-0.193967	0.620802	0.090699
4	6	0	1.061699	1.442554	-0.253748
5	6	0	2.342507	0.630237	0.126082
6	6	0	2.053725	-0.854381	0.535083
7	1	0	1.201871	-2.391558	-0.887435
8	1	0	-0.640649	-0.843071	-1.555738
9	6	0	-1.594327	1.170541	-0.146509
10	1	0	-0.128325	0.407750	1.168353
11	1	0	1.065487	1.681729	-1.324191
12	1	0	1.042990	2.398002	0.283248
13	1	0	3.035730	0.623238	-0.721639
14	1	0	2.869497	1.118098	0.953560
15	1	0	2.981787	-1.433332	0.514810
16	1	0	1.700975	-0.873494	1.577746
17	6	0	-2.518494	0.040960	0.390614
18	8	0	-1.962530	-1.218120	0.103456
19	1	0	-2.627323	0.171279	1.481637
20	1	0	-3.516741	0.115703	-0.069139
21	1	0	-1.784596	2.113087	0.378741
22	1	0	-1.769992	1.337675	-1.216961

Version=AM64L-G03RevE.01\State=2-A\HF=-387.8231135\S2=0.784693\S2-1=0.\
S2A=0.750181\RMSD=2.449e-09\RMSF=8.718e-07\ZeroPoint=0.1936369\Thermal=
0.2017788\Dipole=0.8133663,0.8276342,-0.2953951\PG=C01 [X(C8H13O1)]\\@

(*ii*) BHandHLYP/6-31+G**//BHandHLYP/6-31+G**

Standard orientation:

Center Number	Atomic Number	Atomic Type	Coordinates (Angstroms) X	Y	Z
1	6	0	0.997846	-1.445068	-0.373903
2	6	0	-0.128073	-0.695291	-0.617705
3	6	0	-0.193344	0.620949	0.091811
4	6	0	1.052385	1.436003	-0.245984
5	6	0	2.320507	0.622096	0.128087
6	6	0	2.028307	-0.848940	0.532403
7	1	0	1.188576	-2.366099	-0.900850
8	1	0	-0.639006	-0.817511	-1.558426
9	6	0	-1.585464	1.163525	-0.143442
10	1	0	-0.130825	0.400846	1.159172
11	1	0	1.057303	1.677731	-1.307422
12	1	0	1.037913	2.382075	0.291114
13	1	0	3.006718	0.613687	-0.714777
14	1	0	2.847700	1.104426	0.947820
15	1	0	2.948970	-1.424405	0.512496
16	1	0	1.673957	-0.873574	1.564645
17	6	0	-2.495893	0.036109	0.377054
18	8	0	-1.915832	-1.213422	0.122557
19	1	0	-2.629183	0.162482	1.454555
20	1	0	-3.476935	0.078406	-0.098541
21	1	0	-1.781139	2.093610	0.384763
22	1	0	-1.755021	1.339401	-1.204925

Version=AM64L-G03RevE.01\State=2-A\HF=-387.576392\S2=0.842594\S2-1=0.\
S2A=0.750957\RMSD=8.244e-09\RMSF=5.707e-07\ZeroPoint=0.2007846\Thermal=
0.2087024\Dipole=0.7542893,0.7530258,-0.1558416\PG=C01 [X(C8H13O1)]\\@

(*iii*) BHandHLYP/6-311G**//BHandHLYP/6-311G**

Standard orientation:

Center Number	Atomic Number	Atomic Type	Coordinates (Angstroms) X	Y	Z
1	6	0	-0.992232	-1.439601	0.382750
2	6	0	0.133156	-0.692111	0.616163
3	6	0	0.193570	0.622003	-0.096572
4	6	0	-1.050559	1.436481	0.240158
5	6	0	-2.317213	0.620743	-0.129498
6	6	0	-2.022975	-0.850803	-0.525698
7	1	0	-1.182212	-2.355623	0.915448
8	1	0	0.643099	-0.805711	1.557107
9	6	0	1.583746	1.164977	0.137992
10	1	0	0.130808	0.395360	-1.160996
11	1	0	-1.054390	1.680006	1.299746
12	1	0	-1.038765	2.379917	-0.298467
13	1	0	-3.002425	0.616121	0.712359
14	1	0	-2.843772	1.098200	-0.950582
15	1	0	-2.941620	-1.426659	-0.503476
16	1	0	-1.668067	-0.880041	-1.556173
17	6	0	2.498583	0.028257	-0.356369
18	8	0	1.892408	-1.213476	-0.144499
19	1	0	2.676152	0.164368	-1.425211
20	1	0	3.459620	0.059502	0.157273
21	1	0	1.781985	2.086170	-0.401470
22	1	0	1.743867	1.356527	1.196866

Version=AM64L-G03RevE.01\State=2-A\HF=-387.6429368\S2=0.842829\S2-1=0.\
S2A=0.750915\RMSD=7.917e-09\RMSF=6.073e-07\ZeroPoint=0.2000403\Thermal=
0.2080349\Dipole=0.6627798,0.6975946,-0.1386777\PG=C01 [X(C8H13O1)]\\@

A8.3.5 Transition structure TS^2-*cis*-**Ij** ($^2T_3$)

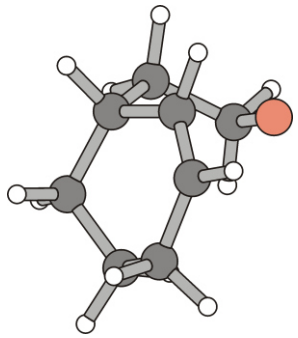

Figure A127 Ball-and-stick model showing the computed transition structure TS^2-*cis*-**Ij**, displaying $^2T_3$-conformation of the cyclohexyl-annulated tetrahydrofuran subunit.

(*i*) B3LYP/6-31+G**//B3LYP/6-31+G**

Standard orientation:

Center Number	Atomic Number	Atomic Type	Coordinates (Angstroms) X	Y	Z
1	6	0	1.154390	-1.286075	-0.537144
2	6	0	-0.039284	-0.766116	-0.995052
3	6	0	-0.377657	0.708702	-0.907531
4	6	0	0.738650	1.530538	-0.212959
5	6	0	1.487621	0.764664	0.888918
6	6	0	2.106922	-0.527121	0.336765
7	1	0	1.392603	-2.322233	-0.766946
8	1	0	-0.608555	-1.351523	-1.709456
9	1	0	-0.466686	1.080253	-1.938078
10	6	0	-1.782589	0.830287	-0.265231
11	1	0	1.470072	1.834601	-0.974247
12	1	0	0.312690	2.457204	0.189957
13	1	0	2.270028	1.401376	1.318029
14	1	0	0.804477	0.512002	1.706231
15	1	0	3.013460	-0.293239	-0.247234
16	1	0	2.450106	-1.173017	1.156147
17	6	0	-1.840490	-0.156499	0.908463
18	8	0	-1.322340	-1.381605	0.492240
19	1	0	-2.000346	1.862148	0.038299
20	1	0	-2.535900	0.534848	-1.005442
21	1	0	-2.890443	-0.328041	1.204415
22	1	0	-1.318163	0.248178	1.793041

Version=AM64L-G03RevE.01\State=2-A\HF=-387.8427554\S2=0.776177\S2-1=0.\
S2A=0.750128\RMSD=2.966e-09\RMSF=7.733e-07\ZeroPoint=0.1942075\Thermal=
0.2021442\Dipole=0.7596247,0.6361151,-0.0474504\PG=C01 [X(C8H13O1)]\\@

(*ii*) BHandHLYP/6-31+G**//BHandHLYP/6-31+G**

Standard orientation:

Center Number	Atomic Number	Atomic Type	Coordinates (Angstroms) X	Y	Z
1	6	0	1.150698	-1.277605	-0.529571
2	6	0	-0.047632	-0.772680	-0.970574
3	6	0	-0.383566	0.696970	-0.903310
4	6	0	0.723623	1.518852	-0.219682
5	6	0	1.470875	0.766365	0.877809
6	6	0	2.099535	-0.509597	0.329920
7	1	0	1.389852	-2.306249	-0.751322
8	1	0	-0.606429	-1.357437	-1.681273
9	1	0	-0.468918	1.054338	-1.929632
10	6	0	-1.774477	0.818933	-0.263122
11	1	0	1.449168	1.816242	-0.977078
12	1	0	0.299702	2.440365	0.174762
13	1	0	2.240651	1.406479	1.303625
14	1	0	0.794625	0.509741	1.688446
15	1	0	2.989983	-0.265919	-0.257147
16	1	0	2.450048	-1.142946	1.144169
17	6	0	-1.822436	-0.154413	0.904528
18	8	0	-1.295841	-1.368069	0.488110
19	1	0	-1.993777	1.842385	0.036369
20	1	0	-2.524598	0.519878	-0.992838
21	1	0	-2.856717	-0.340208	1.206490
22	1	0	-1.296581	0.246927	1.774573

Version=AM64L-G03RevE.01\State=2-A\HF=-387.5972355\S2=0.820896\S2-1=0.\
S2A=0.750663\RMSD=8.091e-09\RMSF=6.372e-07\ZeroPoint=0.2014988\Thermal=
0.2091774\Dipole=0.7493036,0.5447043,0.0068533\PG=C01 [X(C8H13O1)]\\@

(*iii*) BHandHLYP/6-311G**//BHandHLYP/6-311G**

Standard orientation:

Center Number	Atomic Number	Atomic Type	Coordinates (Angstroms) X	Y	Z
1	6	0	1.158882	-1.268696	-0.530906
2	6	0	-0.046745	-0.779361	-0.961755
3	6	0	-0.392359	0.688123	-0.905430
4	6	0	0.703615	1.520862	-0.219302
5	6	0	1.458019	0.774121	0.875738
6	6	0	2.101319	-0.490652	0.323416
7	1	0	1.408889	-2.293000	-0.753640
8	1	0	-0.599642	-1.368556	-1.671320
9	1	0	-0.474695	1.038067	-1.932769
10	6	0	-1.784486	0.800738	-0.270764
11	1	0	1.425500	1.827668	-0.974428
12	1	0	0.269372	2.435212	0.176397
13	1	0	2.217897	1.421156	1.305132
14	1	0	0.784471	0.504103	1.682301
15	1	0	2.984952	-0.234226	-0.266529
16	1	0	2.463822	-1.119518	1.134136
17	6	0	-1.812783	-0.161403	0.905379
18	8	0	-1.263266	-1.364716	0.500740
19	1	0	-2.018850	1.823127	0.015324
20	1	0	-2.527607	0.480696	-0.996868
21	1	0	-2.842745	-0.362713	1.208063
22	1	0	-1.298005	0.263314	1.770027

```
Version=AM64L-G03RevE.01\State=2-A\HF=-387.6640791\S2=0.821789\S2-1=0.\
S2A=0.75064\RMSD=4.929e-09\RMSF=7.479e-07\ZeroPoint=0.200816\Thermal=
0.2085137\Dipole=0.6657645,0.5032555,0.0077008\PG=C01 [X(C8H13O1)]\\@
```

A8.3.6 *cis*-7-Oxabicyclo[4.3.0]bicyclonon-5-yl radical *cis*-IIj (axial)

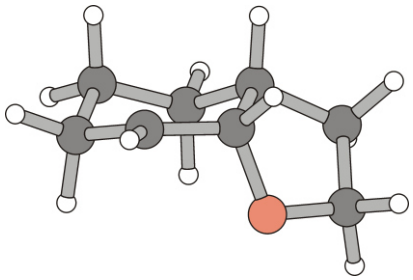

Figure A128. Ball-and-stick model showing the computed equilibrium structure of carbon radical *cis*-**IIj** (axial).

(*i*) B3LYP/6-31+G**//B3LYP/6-31+G**

Standard orientation:

Center Number	Atomic Number	Atomic Type	Coordinates (Angstroms) X	Y	Z
1	6	0	-0.358950	0.739792	0.637461
2	6	0	0.650278	1.392399	-0.324287
3	6	0	-0.278320	-0.803388	0.586268
4	6	0	2.077644	0.881200	-0.092319
5	6	0	1.086661	-1.377979	0.421322
6	6	0	2.154609	-0.640730	-0.320167
7	1	0	-0.155714	1.089564	1.657328
8	6	0	-1.830827	1.004879	0.234948
9	1	0	0.354248	1.175368	-1.359832
10	1	0	0.606739	2.482681	-0.206598
11	1	0	-0.752054	-1.227448	1.488895
12	8	0	-1.114900	-1.141548	-0.553124
13	1	0	2.780669	1.394502	-0.759002
14	1	0	2.388937	1.112120	0.936133
15	1	0	1.232194	-2.426428	0.668457
16	1	0	2.047225	-0.835360	-1.404168
17	1	0	3.144185	-1.027442	-0.046376
18	6	0	-2.276795	-0.312087	-0.457667
19	1	0	-2.658525	-0.168003	-1.472294
20	1	0	-3.051366	-0.823870	0.133739
21	1	0	-1.908622	1.867994	-0.434411
22	1	0	-2.454517	1.214197	1.109763

Version=AM64L-G03RevE.01\State=2-A\HF=-387.8699845\S2=0.753815\S2-1=0.\
S2A=0.75001\RMSD=2.850e-09\RMSF=6.468e-07\ZeroPoint=0.195877\Thermal=
0.2040855\Dipole=-0.5584699,-0.2602332,0.0623216\PG=C01 [X(C8H13O1)]\\@

(*ii*) BHandHLYP/6-31+G**//BHandHLYP/6-31+G**

Standard orientation:

Center Number	Atomic Number	Atomic Type	Coordinates (Angstroms) X	Y	Z
1	6	0	-0.379119	0.705385	0.689093
2	6	0	0.561385	1.389266	-0.303079
3	6	0	-0.259347	-0.819554	0.626743
4	6	0	2.002642	0.924761	-0.132622
5	6	0	1.121411	-1.340586	0.453521
6	6	0	2.116643	-0.583861	-0.355478
7	1	0	-0.157774	1.059141	1.694645
8	6	0	-1.854479	0.895848	0.337294
9	1	0	0.236059	1.172055	-1.321038
10	1	0	0.490373	2.468526	-0.176096
11	1	0	-0.707537	-1.258335	1.522046
12	8	0	-1.065074	-1.179270	-0.502872
13	1	0	2.654122	1.452929	-0.825930
14	1	0	2.347278	1.169399	0.872818
15	1	0	1.311622	-2.372313	0.703469
16	1	0	1.951682	-0.792651	-1.419387
17	1	0	3.124155	-0.930815	-0.134077
18	6	0	-2.135524	-0.257902	-0.637141
19	1	0	-2.162928	0.071569	-1.673122
20	1	0	-3.078440	-0.755535	-0.416608
21	1	0	-2.059077	1.868712	-0.101786
22	1	0	-2.470608	0.801340	1.228047

Version=AM64L-G03RevE.01\State=2-A\HF=-387.634349\S2=0.755346\S2-1=0.\
S2A=0.75002\RMSD=3.020e-09\RMSF=8.680e-07\ZeroPoint=0.2032979\Thermal=
0.2112579\Dipole=-0.6223805,-0.2238857,0.0965257\PG=C01 [X(C8H13O1)]\\@

(*iii*) BHandHLYP/6-311G**//BHandHLYP/6-311G**

Standard orientation:

Center Number	Atomic Number	Atomic Type	Coordinates (Angstroms) X	Y	Z
1	6	0	-0.383583	0.705319	0.692949
2	6	0	0.553403	1.389715	-0.300645
3	6	0	-0.258430	-0.818420	0.624622
4	6	0	1.994760	0.926563	-0.138424
5	6	0	1.125414	-1.331940	0.470320
6	6	0	2.108879	-0.582067	-0.355714
7	1	0	-0.165357	1.058891	1.697312
8	6	0	-1.857362	0.889644	0.335445
9	1	0	0.224276	1.172639	-1.315808
10	1	0	0.482887	2.467561	-0.173742
11	1	0	-0.720108	-1.261956	1.509298
12	8	0	-1.037685	-1.166784	-0.522069
13	1	0	2.640068	1.452308	-0.837076
14	1	0	2.345748	1.174179	0.862652
15	1	0	1.324598	-2.354867	0.741130
16	1	0	1.927478	-0.796232	-1.414565
17	1	0	3.118770	-0.925363	-0.147336
18	6	0	-2.131435	-0.274427	-0.630106
19	1	0	-2.194442	0.051542	-1.663820
20	1	0	-3.057340	-0.790017	-0.383848
21	1	0	-2.060092	1.857057	-0.112369
22	1	0	-2.474880	0.802200	1.224036

Version=AM64L-G03RevE.01\State=2-A\HF=-387.7009074\S2=0.7554\S2-1=0.\
S2A=0.75002\RMSD=5.613e-09\RMSF=9.426e-07\ ZeroPoint=0.2026525\Thermal=
0.2106306\Dipole=-0.5607397,-0.2060243,0.052826\PG=C01 [X(C8H13O1)]\\@

A8.3.7 *trans*-7-Oxabicyclo[4.3.0]bicyclonon-5-yl radical *trans*-**IIj**

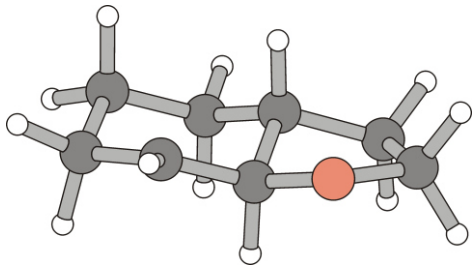

Figure A129. Ball-and-stick model showing the computed equilibrium structure of carbon radical *trans*-**IIj**.

(*i*) B3LYP/6-31+G**//B3LYP/6-31+G**

Standard orientation:

Center Number	Atomic Number	Atomic Type	Coordinates (Angstroms) X	Y	Z
1	6	0	2.231815	0.680023	-0.256150
2	6	0	0.976529	1.463162	0.190810
3	6	0	-0.269104	0.719407	-0.288911
4	6	0	-0.294324	-0.704969	0.288879
5	6	0	0.894102	-1.483152	-0.131399
6	6	0	2.205527	-0.814558	0.167848
7	1	0	2.303823	0.732283	-1.350516
8	1	0	3.136181	1.154704	0.142854
9	1	0	0.956815	1.554067	1.286909
10	1	0	1.011228	2.483457	-0.210859
11	6	0	-1.683156	1.186852	0.077696
12	1	0	-0.210499	0.612485	-1.381728
13	1	0	-0.280142	-0.608213	1.400363
14	8	0	-1.559263	-1.223635	-0.106828
15	1	0	0.820209	-2.528130	-0.413682
16	1	0	2.404276	-0.861944	1.255987
17	1	0	3.032970	-1.350577	-0.309838
18	6	0	-2.503498	-0.129925	-0.040953
19	1	0	-2.065165	1.972435	-0.581278
20	1	0	-1.707282	1.569832	1.105124
21	1	0	-3.169897	-0.274899	0.818868
22	1	0	-3.105756	-0.167461	-0.954490

Version=AM64L-G03RevE.01\State=2-A\HF=-387.8657538\S2=0.753984\S2-1=0.\
S2A=0.750012\RMSD=4.066e-09\RMSF=6.863e-07\ZeroPoint=0.195315\Thermal=
0.2035768\Dipole=-0.7266069,-0.2555679,0.1878537\PG=C01 [X(C8H13O1)]\\@

(*ii*) BHandHLYP/6-31+G**//BHandHLYP/6-31+G**

Standard orientation:

Center Number	Atomic Number	Atomic Type	Coordinates (Angstroms) X	Y	Z
1	6	0	-0.887495	-1.475088	-0.135065
2	6	0	0.294270	-0.698098	0.289060
3	6	0	0.268309	0.712883	-0.282484
4	6	0	-0.967993	1.452467	0.194049
5	6	0	-2.212376	0.677140	-0.258908
6	6	0	-2.192490	-0.805018	0.160566
7	1	0	-0.818056	-2.528623	-0.347840
8	1	0	0.274968	-0.608844	1.390536
9	8	0	1.545557	-1.208400	-0.099985
10	6	0	1.671863	1.174909	0.084239
11	1	0	0.212360	0.609380	-1.367539
12	1	0	-0.951953	1.536852	1.282318
13	1	0	-0.999876	2.466645	-0.200286
14	1	0	-3.111964	1.149510	0.130575
15	1	0	-2.275784	0.731234	-1.345403
16	1	0	-2.390160	-0.858201	1.239075
17	1	0	-3.012995	-1.333553	-0.318447
18	6	0	2.482137	-0.132243	-0.054787
19	1	0	1.697275	1.539453	1.109648
20	1	0	2.051679	1.963458	-0.558571
21	1	0	3.163872	-0.279134	0.780642
22	1	0	3.058829	-0.162695	-0.974841

Version=AM64L-G03RevE.01\State=2-A\HF=-387.6298725\S2=0.755562\S2-1=0.\
S2A=0.750023\RMSD=6.976e-09\RMSF=6.046e-07\ZeroPoint=0.2028954\Thermal=
0.2108076\.\Dipole=0.5778732,0.503979,0.2104386\PG=C01 [X(C8H13O1)]\\@

(*iii*) BHandHLYP/6-311G**//BHandHLYP/6-311G**

Standard orientation:

Center Number	Atomic Number	Atomic Type	Coordinates (Angstroms) X	Y	Z
1	6	0	-0.884448	-1.472635	-0.135359
2	6	0	0.295155	-0.697127	0.291601
3	6	0	0.267600	0.712991	-0.279854
4	6	0	-0.968022	1.451423	0.194902
5	6	0	-2.210356	0.675834	-0.259423
6	6	0	-2.189516	-0.805782	0.158190
7	1	0	-0.811972	-2.524979	-0.344736
8	1	0	0.272756	-0.606497	1.391911
9	8	0	1.543321	-1.207060	-0.097649
10	6	0	1.670398	1.174411	0.083797
11	1	0	0.211790	0.605884	-1.363326
12	1	0	-0.953310	1.534753	1.281907
13	1	0	-1.000674	2.464416	-0.198283
14	1	0	-3.109702	1.146474	0.128561
15	1	0	-2.271921	0.730468	-1.344643
16	1	0	-2.388393	-0.860651	1.235203
17	1	0	-3.007932	-1.333645	-0.321929
18	6	0	2.477953	-0.132792	-0.057981
19	1	0	1.697243	1.537440	1.108164
20	1	0	2.047891	1.961311	-0.559695
21	1	0	3.165060	-0.275815	0.772422
22	1	0	3.050005	-0.160619	-0.979601

Version=AM64L-G03RevE.01\State=2-A\HF=-387.6963209\S2=0.755584\S2-1=0.\
S2A=0.750023\RMSD=6.358e-09\RMSF=6.444e-07\ZeroPoint=0.2022549\Thermal=
0.2101704\\Dipole=0.521324,0.442767,0.189645\PG=C01 [X(C8H13O1)]\\@

A8.3.8 *cis*-7-Oxabicyclo[4.3.0]bicyclonon-5-yl Radical *cis*-**IIj** (equatorial)

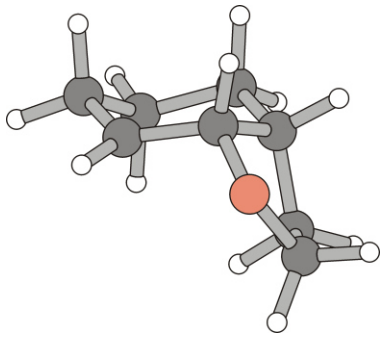

Figure A130. Equilibrium structure of carbon radical *cis*-**IIj** (equatorial).

(*i*) B3LYP/6-31+G**//B3LYP/6-31+G**

Standard orientation:

Center Number	Atomic Number	Atomic Type	Coordinates (Angstroms) X	Y	Z
1	6	0	2.303237	-0.129909	-0.448907
2	8	0	1.764768	1.006439	0.253420
3	6	0	0.414156	0.733942	0.674843
4	6	0	0.261601	-0.805511	0.605461
5	6	0	1.155800	-1.136488	-0.603969
6	6	0	-1.197688	-1.290972	0.546778
7	6	0	-2.056584	-0.543479	-0.483997
8	6	0	-1.992433	0.982022	-0.255782
9	6	0	-0.576787	1.459012	-0.181630
10	1	0	0.340088	1.080723	1.721390
11	1	0	0.734683	-1.230956	1.500486
12	1	0	-1.214807	-2.370095	0.346839
13	1	0	-1.648690	-1.158110	1.540642
14	1	0	-1.712734	-0.769530	-1.500977
15	1	0	-3.095347	-0.889719	-0.419567
16	1	0	-2.538396	1.515317	-1.042348
17	1	0	-2.526740	1.208663	0.687917
18	1	0	-0.285745	2.428173	-0.577160
19	1	0	1.505999	-2.173709	-0.598210
20	1	0	2.711468	0.209605	-1.407315
21	1	0	3.126510	-0.548293	0.146720
22	1	0	0.617758	-0.965285	-1.542559

Version=AM64L-G03RevE.01\State=2-A\HF=-387.8685609\S2=0.753956\S2-1=0.\
S2A=0.750011\RMSD=3.826e-09\RMSF=1.966e-06\ZeroPoint=0.195582\Thermal=
0.2038027\Dipole=0.7501928,0.0036996,-0.383314\PG=C01[X(C8H13O1)]\
NImag=0\\@

(*ii*) BHandHLYP/6-31+G**//BHandHLYP/6-31+G**

Standard orientation:

Center Number	Atomic Number	Atomic Type	Coordinates (Angstroms) X	Y	Z
1	6	0	0.416935	0.724675	0.673612
2	6	0	0.259251	-0.800766	0.601035
3	6	0	-1.190906	-1.278374	0.546556
4	6	0	-2.041322	-0.535336	-0.479187
5	6	0	-1.974346	0.977934	-0.254580
6	6	0	-0.561974	1.447244	-0.188718
7	1	0	0.331047	1.072290	1.708324
8	8	0	1.752394	0.983694	0.265827
9	6	0	1.139832	-1.125988	-0.605413
10	1	0	0.732341	-1.227331	1.485279
11	1	0	-1.211928	-2.349586	0.350707
12	1	0	-1.637436	-1.141127	1.532564
13	1	0	-1.699907	-0.762925	-1.487659
14	1	0	-3.072707	-0.877146	-0.415370
15	1	0	-2.515597	1.506538	-1.035775
16	1	0	-2.496259	1.209738	0.683481
17	1	0	-0.276000	2.416600	-0.564267
18	6	0	2.279554	-0.124147	-0.452961
19	1	0	1.489022	-2.154764	-0.606310
20	1	0	2.669604	0.225028	-1.405403
21	1	0	3.105622	-0.545170	0.119217
22	1	0	0.600900	-0.953137	-1.533465

Version=AM64L-G03RevE.01\State=2-A\HF=-387.6330996\S2=0.755609\S2-1=0.\
S2A=0.750023\RMSD=3.382e-09\RMSF=6.199e-07\ZeroPoint=0.2030983\Thermal=
0.2110232\Dipole=0.4324314,0.0510036,0.7106391\PG=C01 [X(C8H13O1)]\\@

(*iii*) BHandHLYP/6-311G**//BHandHLYP/6-311G**

Standard orientation:

Center Number	Atomic Number	Atomic Type	Coordinates (Angstroms) X	Y	Z
1	6	0	0.419322	0.721667	0.674249
2	6	0	0.257576	-0.802284	0.598880
3	6	0	-1.192364	-1.275824	0.547531
4	6	0	-2.041401	-0.531511	-0.476745
5	6	0	-1.968402	0.980904	-0.254702
6	6	0	-0.555898	1.443777	-0.189826
7	1	0	0.330282	1.067124	1.707868
8	8	0	1.752597	0.980327	0.267866
9	6	0	1.133486	-1.122568	-0.610685
10	1	0	0.733347	-1.231509	1.478577
11	1	0	-1.217648	-2.345719	0.353187
12	1	0	-1.636155	-1.135967	1.532993
13	1	0	-1.702794	-0.761201	-1.484220
14	1	0	-3.072492	-0.869151	-0.411068
15	1	0	-2.508033	1.509421	-1.035085
16	1	0	-2.487695	1.216283	0.682598
17	1	0	-0.265352	2.409573	-0.566242
18	6	0	2.275421	-0.126539	-0.450121
19	1	0	1.478389	-2.151086	-0.620313
20	1	0	2.671329	0.219333	-1.399884
21	1	0	3.095446	-0.556959	0.121869
22	1	0	0.594149	-0.938495	-1.534703

Version=AM64L-G03RevE.01\State=2-A\HF=-387.700045\S2=0.755641\S2-1=0.\
S2A=0.750023\RMSD=7.457e-09\RMSF=6.944e-07\ZeroPoint=0.2025178\Thermal=
0.2104199\Dipole=0.3879725,0.0527678,0.6471395\PG=C01 [X(C8H13O1)]\\@

A8.4 The 4-Pentenoxyl Radical Cyclization

A8.4.1 4-Pentenoxyl radical (Ij)

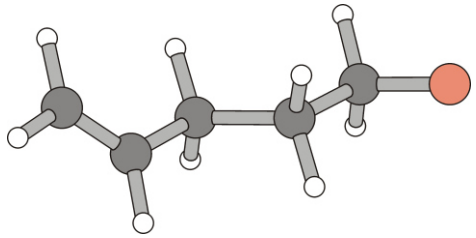

Figure A131. Equilibrium structure of alkenoxyl radical **Ij**.

(*i*) B3LYP/6-31+G**//B3LYP/6-31+G**

Standard orientation:

Center Number	Atomic Number	Atomic Type	Coordinates (Angstroms) X	Y	Z
1	6	0	3.002765	-0.021861	-0.431860
2	6	0	1.946396	-0.261177	0.350656
3	6	0	0.650646	0.503218	0.319475
4	6	0	-0.562098	-0.389227	-0.005333
5	6	0	-1.880583	0.390047	0.004449
6	8	0	-3.010696	-0.346030	-0.236400
7	1	0	3.909612	-0.615313	-0.361311
8	1	0	2.996920	0.778212	-1.169227
9	1	0	1.999456	-1.076305	1.074278
10	1	0	0.488779	0.975710	1.300830
11	1	0	0.723455	1.318303	-0.412511
12	1	0	-0.430866	-0.849474	-0.991813
13	1	0	-0.635749	-1.209109	0.719775
14	1	0	-2.050452	0.865517	0.996576
15	1	0	-1.858344	1.254696	-0.689718

Version=AM64L-G03RevE.01\State=2-A\HF=-271.1019187\S2=0.753684\S2-1=0.\
S2A=0.750011\RMSD=4.353e-09\RMSF=1.326e-07\ZeroPoint =0.1266719\ Thermal=
0.1342282\Dipole=-0.0665706,-0.6850188,-0.4549922\PG=C01 [X(C5H9O1)]\
NImag=0\\@

(*ii*) BHandHLYP/6-31+G**//BHandHLYP/6-31+G**

Standard orientation:

Center Number	Atomic Number	Atomic Type	Coordinates (Angstroms) X	Y	Z
1	6	0	2.978525	-0.036079	-0.429519
2	6	0	1.931156	-0.252697	0.352672
3	6	0	0.645193	0.511464	0.303372
4	6	0	-0.559876	-0.381238	0.008758
5	6	0	-1.864502	0.396005	0.008679
6	8	0	-2.984578	-0.358243	-0.235357
7	1	0	3.876649	-0.625907	-0.345847
8	1	0	2.973148	0.740439	-1.179655
9	1	0	1.982556	-1.044126	1.089690
10	1	0	0.490317	1.008685	1.263482
11	1	0	0.719039	1.297948	-0.446987
12	1	0	-0.434660	-0.863905	-0.958391
13	1	0	-0.627995	-1.175658	0.750462
14	1	0	-2.033971	0.893662	0.972273
15	1	0	-1.851434	1.210068	-0.725940

Version=AM64L-G03RevE.01\State=2-A\HF=-270.9362596\S2=0.755148\S2-1=0.\
S2A=0.750021\RMSD=0.000e+00\RMSF=6.860e-07\ZeroPoint=0.1313875\Thermal=
0.1389779\Dipole=-0.0479158,-0.648385,-0.4352557\PG=C01[X(C5H9O1)]\
NImag=0\\@

(*iii*) BHandHLYP/6-311G**//BHandHLYP/6-311G**

Standard orientation:

Center Number	Atomic Number	Atomic Type	Coordinates (Angstroms) X	Y	Z
1	6	0	2.968360	-0.042085	-0.433376
2	6	0	1.931316	-0.247714	0.355690
3	6	0	0.645861	0.514318	0.304608
4	6	0	-0.558331	-0.378105	0.013745
5	6	0	-1.863911	0.396104	0.000541
6	8	0	-2.977226	-0.363102	-0.232034
7	1	0	3.866277	-0.630099	-0.349975
8	1	0	2.957459	0.724705	-1.191746
9	1	0	1.986002	-1.029347	1.101069
10	1	0	0.490806	1.014443	1.261834
11	1	0	0.718502	1.297280	-0.447571
12	1	0	-0.429117	-0.868436	-0.947696
13	1	0	-0.631106	-1.165648	0.760468
14	1	0	-2.034443	0.900825	0.959745
15	1	0	-1.846342	1.205987	-0.737099

Version=AM64L-G03RevE.01\State=2-A\HF=-270.9849177\S2=0.754563\S2-1=0.\
S2A=0.750016\RMSD=6.138e-09\RMSF=1.988e-07\ZeroPoint=0.1310322\Thermal=
0.1385375\Dipole=-0.0482987,-0.600967,-0.3910608\PG=C01 [X(C5H9O1)]\
NImag=0\\@

A8.4.2 Transition structure TS-Ij

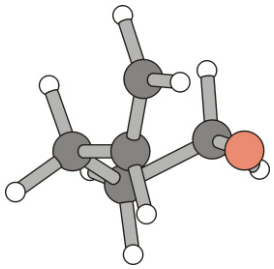

Figure A132. Ball-and-stick model of computed transition structure TS-**Ij**, showing $_2T^3$-conformation of the distorted tetrahydrofuran nucleus

(*i*) B3LYP/6-31+G**//B3LYP/6-31+G**

Standard orientation:

Center Number	Atomic Number	Atomic Type	Coordinates (Angstroms) X	Y	Z
1	8	0	-0.218440	-1.341831	-0.316148
2	6	0	-1.299215	-0.754709	0.343768
3	6	0	-1.398322	0.710961	-0.089756
4	6	0	0.025782	1.274149	0.084125
5	6	0	1.027929	0.276129	-0.443264
6	6	0	2.075669	-0.196800	0.313602
7	1	0	-1.213795	-0.834621	1.442497
8	1	0	-2.198724	-1.319062	0.043429
9	1	0	-2.134109	1.278339	0.492803
10	1	0	-1.692754	0.755213	-1.144904
11	1	0	0.225307	1.466235	1.145447
12	1	0	0.134371	2.228259	-0.446663
13	1	0	1.081715	0.161974	-1.522137
14	1	0	2.116102	-0.023639	1.385452
15	1	0	2.838349	-0.836432	-0.117594

Version=AM64L-G03RevE.01\State=2-A\HF=-271.0963414\S2=0.778657\S2-1=0.\
S2A=0.750143\RMSD=6.659e-09\RMSF=8.393e-07\ZeroPoint=0.1286182\Thermal=
0.1345837\Dipole=0.6178429,-0.337967,0.4867433\PG=C01 [X(C5H9O1)\NImag=1\\@

(*ii*) BHandHLYP/6-31+G**//BHandHLYP/6-31+G**

Standard orientation:

Center Number	Atomic Number	Atomic Type	Coordinates (Angstroms) X	Y	Z
1	8	0	-0.202708	-1.321345	-0.317738
2	6	0	-1.280902	-0.754350	0.348631
3	6	0	-1.396796	0.695908	-0.086321
4	6	0	0.013331	1.263575	0.074590
5	6	0	1.007429	0.260778	-0.440648
6	6	0	2.064785	-0.177627	0.313792
7	1	0	-1.173080	-0.827020	1.435209
8	1	0	-2.163194	-1.332226	0.063123
9	1	0	-2.128389	1.252671	0.495490
10	1	0	-1.697429	0.732419	-1.131399
11	1	0	0.214998	1.463794	1.125354
12	1	0	0.121954	2.204553	-0.461560
13	1	0	1.067249	0.145726	-1.510535
14	1	0	2.108110	0.014325	1.373846
15	1	0	2.824372	-0.813187	-0.107885

```
Version=AM64L-G03RevE.01\State=2-A\HF=-270.9226156\S2=0.826588\S2-1=0.\
S2A=0.750709\RMSD=3.664e-09\RMSF=4.925e-07\ZeroPoint=0.1333433\Thermal=
0.1391357\Dipole=0.5691574,-0.3174852,0.5117178\PG=C01[X(C5H9O1)]\
NImag=1\\@
```

(*iii*) BHandHLYP/6-311G**//BHandHLYP/6-311G**

Standard orientation:

Center Number	Atomic Number	Atomic Type	Coordinates (Angstroms) X	Y	Z
1	8	0	-0.190664	-1.312299	-0.325013
2	6	0	-1.266752	-0.761342	0.350179
3	6	0	-1.401377	0.687016	-0.081706
4	6	0	0.005272	1.262952	0.070605
5	6	0	1.001573	0.260628	-0.440750
6	6	0	2.055296	-0.170013	0.318179
7	1	0	-1.153658	-0.832639	1.435468
8	1	0	-2.145081	-1.346035	0.070823
9	1	0	-2.133466	1.237910	0.502389
10	1	0	-1.705948	0.719385	-1.124421
11	1	0	0.208969	1.469508	1.118288
12	1	0	0.108657	2.199674	-0.470915
13	1	0	1.071850	0.154182	-1.509346
14	1	0	2.088544	0.019551	1.377633
15	1	0	2.821379	-0.798584	-0.098847

```
Version=AM64L-G03RevE.01\State=2-A\HF=-270.9708623\S2=0.826641\S2-1=0.\
S2A=0.750674\RMSD=8.909e-09\RMSF=5.677e-07\ZeroPoint=0.1328445\Thermal=
0.1386177\Dipole=0.5187926,- 0.2920208,0.456006\PG=C01[X(C5H9O1)]\
NImag=1\\@
```

A8.4.3 Tetrahydrofur-2-yl methyl radical IIj

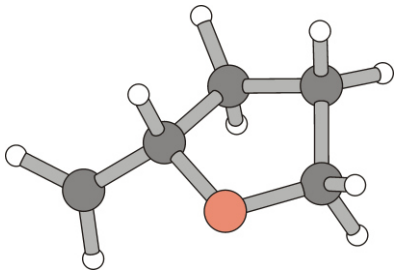

Figure A133. Ball-and-stick model for computed equilibrium structure of cyclized radical **IIj**.

(*i*) B3LYP/6-31+G**//B3LYP/6-31+G**

Standard orientation:

Center Number	Atomic Number	Atomic Type	Coordinates (Angstroms) X	Y	Z
1	8	0	0.052527	-1.145763	-0.109224
2	6	0	-1.323108	-0.829684	0.166240
3	6	0	-1.484039	0.678088	-0.079708
4	6	0	-0.066021	1.199110	0.188922
5	6	0	0.804905	0.053910	-0.387324
6	6	0	2.171364	-0.063720	0.176831
7	1	0	-1.538915	-1.093004	1.210712
8	1	0	-1.962145	-1.440520	-0.481454
9	1	0	-2.241880	1.130370	0.567237
10	1	0	-1.769280	0.871677	-1.120226
11	1	0	0.118440	1.297167	1.264968
12	1	0	0.150445	2.160122	-0.286173
13	1	0	0.869091	0.184109	-1.481832
14	1	0	2.325218	-0.611143	1.100615
15	1	0	3.010200	0.441104	-0.289822

Version=AM64L-G03RevE.01\State=2-A\HF=-271.1201629\S2=0.753834\S2-1=0.\
S2A=0.75001\RMSD=4.547e-09\RMSF=7.534e-07\ZeroPoint=0.1294895\Thermal=
0.1360879\Dipole=0.6334341,-0.0681858,0.5155249\PG=C01 [X(C5H9O1)]\\@

(*ii*) BHandHLYP/6-31+G**//BHandHLYP/6-31+G**

Standard orientation:

Center Number	Atomic Number	Atomic Type	Coordinates (Angstroms) X	Y	Z
1	8	0	0.052199	-1.128943	-0.089913
2	6	0	-1.313638	-0.826027	0.151690
3	6	0	-1.472137	0.676163	-0.074941
4	6	0	-0.062085	1.188057	0.192697
5	6	0	0.791376	0.049041	-0.383533
6	6	0	2.160680	-0.066891	0.162400
7	1	0	-1.551553	-1.103001	1.177736
8	1	0	-1.933801	-1.421275	-0.513854
9	1	0	-2.223063	1.117753	0.573147
10	1	0	-1.757363	0.880130	-1.104730
11	1	0	0.121682	1.278502	1.261237
12	1	0	0.154975	2.143727	-0.274076
13	1	0	0.843701	0.173006	-1.470439
14	1	0	2.333416	-0.662542	1.041971
15	1	0	2.969236	0.503186	-0.261565

Version=AM64L-G03RevE.01\State=2-A\HF=-270.9557763\S2=0.755247\S2-1=0.\
S2A=0.750018\RMSD=5.353e-09\RMSF=2.900e-07\ZeroPoint=0.1343445\Thermal=
0.1407878\Dipole=0.6451734,-0.0555184,0.5012758\PG=C01[X(C5H9O1)]\
NImag=0\\@

(*iii*) BHandHLYP/6-311G**//BHandHLYP/6-311G**

Standard orientation:

Center Number	Atomic Number	Atomic Type	Coordinates (Angstroms) X	Y	Z
1	8	0	0.051487	-1.128320	-0.118038
2	6	0	-1.301808	-0.825179	0.170428
3	6	0	-1.472004	0.669627	-0.076173
4	6	0	-0.065801	1.189006	0.188069
5	6	0	0.791325	0.052794	-0.388114
6	6	0	2.151995	-0.066860	0.174530
7	1	0	-1.505460	-1.078327	1.209299
8	1	0	-1.945118	-1.433081	-0.458371
9	1	0	-2.225553	1.115560	0.563244
10	1	0	-1.752548	0.856770	-1.109087
11	1	0	0.117018	1.280566	1.255392
12	1	0	0.147268	2.143674	-0.278919
13	1	0	0.856643	0.188992	-1.471421
14	1	0	2.313681	-0.691304	1.034150
15	1	0	2.959934	0.527386	-0.212421

Version=AM64L-G03RevE.01\State=2-A\HF=-271.0036263\S2=0.755332\S2-1=0.\
S2A=0.750018\RMSD=2.634e-09\RMSF=2.162e-07\ZeroPoint=0.1338352\Thermal=
0.1402611\Dipole=0.5829622,-0.0744891,0.4608763\PG=C01 [X(C5H9O1)]\
NImag=0\\@

A8.5 Methoxyl Radical Addition to Propene

A8.5.1 Methoxyl radical (Ik)

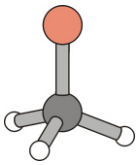

Figure A134. Ball-and-stick model of computed equilibrium structure of the methoxyl radical (**Im**).

(*i*) B3LYP/6-31+G**//B3LYP/6-31+G**

Standard orientation:

Center Number	Atomic Number	Atomic Type	Coordinates (Angstroms) X	Y	Z
1	8	0	-0.011028	0.793737	0.000000
2	6	0	-0.011028	-0.577119	0.000000
3	1	0	1.060625	-0.867662	0.000000
4	1	0	-0.453118	-1.009759	0.911434
5	1	0	-0.453118	-1.009759	-0.911434

```
Version=AM64L-G03RevE.01\State=2-A'\HF=-115.0632975\S2=0.753499\S2-1=0.\
S2A=0.750009\RMSD=0.000e+00\RMSF=5.714e-06\ZeroPoint=0.0363109\ Thermal=
0.0393505\Dipole=0.092549,0.,0.8822571\ PG=CS [SG(C1H1O1),X(H2)]\NImag=0\\@
```

(*ii*) BHandHLYP/6-31+G**//BHandHLYP/6-31+G**

Standard orientation:

Center Number	Atomic Number	Atomic Type	Coordinates (Angstroms) X	Y	Z
1	8	0	-0.008725	0.791541	0.000000
2	6	0	-0.008725	-0.579110	0.000000
3	1	0	1.048205	-0.870123	0.000000
4	1	0	-0.463024	-0.993773	0.900153
5	1	0	-0.463024	-0.993773	-0.900153

```
Version=AM64L-G03RevE.01\State=2-A'\HF=-115.0001926\S2=0.754977\S2-1=0.\
S2A=0.750019\RMSD=0.000e+00\RMSF=5.596e-06\ZeroPoint=0.0381938\ Thermal=
0.0411873\Dipole=0.0777085,0.,0.852451\ PG=CS [SG(C1H1O1),X(H2)]\NImag=0\\@
```

(*iii*) BHandHLYP/6-311G**//BHandHLYP/6-311G**

Standard orientation:

Center Number	Atomic Number	Atomic Type	Coordinates (Angstroms) X	Y	Z
1	8	0	-0.009067	0.789824	0.000000
2	6	0	-0.009067	-0.576052	0.000000
3	1	0	1.046992	-0.869045	0.000000
4	1	0	-0.460025	-0.996617	0.898929
5	1	0	-0.460025	-0.996617	-0.898929

```
Version=AM64L-G03RevE.01\State=2-A'\HF=-115.0231817\S2=0.754332\S2-1=0.\S2A
=0.750014\RMSD=0.000e+00\RMSF=7.207e-06\ZeroPoint=0.038019\ Thermal=
0.0410064\Dipole=0.0716673,0.,0.7884664\ PG=CS
[SG(C1H1O1),X(H2)]\NImag=0\\@
```

A8.5.2 Propene

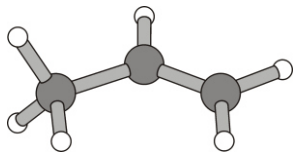

Figure A135. Ball-and-stick model showing the computed equilibrium of propene.

(*i*) B3LYP/6-31+G**//B3LYP/6-31+G**

Standard orientation:

Center Number	Atomic Number	Atomic Type	Coordinates (Angstroms) X	Y	Z
1	6	0	-1.285471	0.220790	0.000000
2	6	0	-0.132616	-0.455269	-0.000001
3	6	0	1.236630	0.163272	0.000000
4	1	0	-2.244615	-0.288910	0.000004
5	1	0	-1.308206	1.308661	-0.000001
6	1	0	-0.164982	-1.545627	0.000001
7	1	0	1.811424	-0.151766	-0.880247
8	1	0	1.183715	1.256617	-0.000023
9	1	0	1.811405	-0.151729	0.880274

```
Version=AM64L-G03RevE.01\State=1-A\HF=-117.9227982\RMSD=2.970e-09\RMSF=
1.478e-06\ZeroPoint=0.0795432\Thermal=0.0836416\Dipole=0.0634245,
0.0000044,0.1625806\PG=C01 [X(C3H6)]\NImag=0\\@
```

(*ii*) BHandHLYP/6-31+G**//BHandHLYP/6-31+G**

Standard orientation:

Center Number	Atomic Number	Atomic Type	Coordinates (Angstroms) X	Y	Z
1	6	0	-1.275050	0.220283	0.000000
2	6	0	-0.133510	-0.453067	0.000000
3	6	0	1.228770	0.161772	0.000000
4	1	0	-2.227580	-0.284092	0.000001
5	1	0	-1.294308	1.299828	-0.000001
6	1	0	-0.167753	-1.534660	0.000000
7	1	0	1.797085	-0.150868	-0.874490
8	1	0	1.174223	1.246710	-0.000013
9	1	0	1.797074	-0.150846	0.874505

```
Version=AM64L-G03RevE.01\State=1-A\HF=-117.8377786\RMSD=8.955e-09\RMSF=
1.350e-06\ZeroPoint=0.0823352\Thermal=0.0863587\Dipole=0.0586603,
0.0000021,0.156776\PG=C01 [X(C3H6)]\NImag=0\\@
```

(*iii*) BHandHLYP/6-311G**//BHandHLYP/6-311G**

Standard orientation:

Center Number	Atomic Number	Atomic Type	Coordinates (Angstroms) X	Y	Z
1	6	0	-1.270865	0.220030	0.000000
2	6	0	-0.135388	-0.451678	0.000000
3	6	0	1.226329	0.160971	0.000000
4	1	0	-2.223283	-0.281976	0.000001
5	1	0	-1.288706	1.298445	-0.000001
6	1	0	-0.169537	-1.532055	0.000000
7	1	0	1.793922	-0.152523	-0.873439
8	1	0	1.173235	1.244677	-0.000012
9	1	0	1.793912	-0.152505	0.873452

Version=AM64L-G03RevE.01\State=1-A\HF=-117.8573314\RMSD=2.797e-09\RMSF=
1.918e-06\ZeroPoint=0.0819904\Thermal=0.0860096\Dipole=0.0443792,
0.0000019,0.1390108\PG=C01 [X(C3H6)]\NImag=0\\@

A8.5.3 Transition structure for methoxyl addition to the terminal carbon of propene

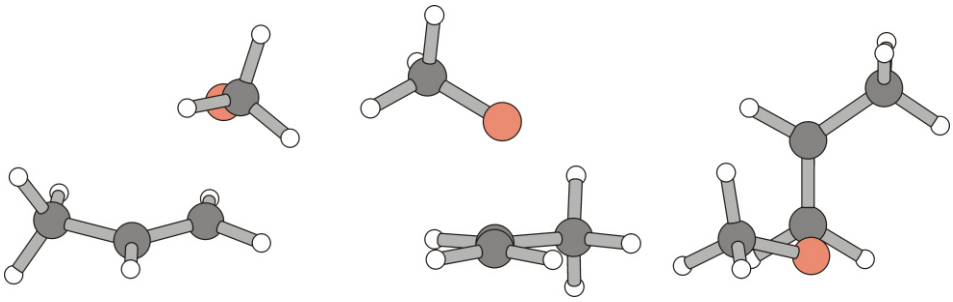

Figure A136. Ball-and-stick models showing different projections of computed transition structure TS[1]-**VII** (left: side-on view; center: end-on view (center); right: top view.

(*i*) B3LYP/6-31+G**//B3LYP/6-31+G**

Standard orientation:

Center Number	Atomic Number	Atomic Type	Coordinates (Angstroms) X	Y	Z
1	6	0	0.316309	1.130301	0.022919
2	6	0	1.131378	0.175308	0.561792
3	6	0	2.128631	-0.623748	-0.214665
4	8	0	-1.280498	0.023485	-0.715246
5	6	0	-2.087098	-0.491704	0.298377
6	1	0	-0.316406	1.742376	0.656781
7	1	0	0.478857	1.490485	-0.986756
8	1	0	1.005579	-0.086248	1.612374
9	1	0	3.124514	-0.563914	0.244098
10	1	0	1.852788	-1.686996	-0.225646
11	1	0	2.200385	-0.282374	-1.251139
12	1	0	-2.991923	-0.876333	-0.201905
13	1	0	-1.630314	-1.335965	0.838245
14	1	0	-2.414817	0.270148	1.025377

```
Version=AM64L-G03RevE.01\State=2-A\HF=-232.9827193\S2=0.774311\S2-1=0.\
S2A=0.750115\RMSD=4.084e-09\RMSF=1.701e-07\ZeroPoint=0.1191318\Thermal=
0.1265417\Dipole=-0.4009503,0.3081397,0.5377889\PG=C01 [X(C4H9O1)]\
NImag=1\\@
```

(*ii*) BHandHLYP/6-31+G**//BHandHLYP/6-31+G**

Standard orientation:

Center Number	Atomic Number	Atomic Type	Coordinates (Angstroms) X	Y	Z
1	6	0	0.274893	1.122975	0.084931
2	6	0	1.093930	0.147113	0.569442
3	6	0	2.074735	-0.608451	-0.257929
4	8	0	-1.282751	0.142741	-0.695486
5	6	0	-1.980704	-0.571630	0.267018
6	1	0	-0.331257	1.706655	0.756639
7	1	0	0.457626	1.552216	-0.884709
8	1	0	0.971012	-0.171544	1.595241
9	1	0	3.065313	-0.588385	0.194625
10	1	0	1.787437	-1.656698	-0.340229
11	1	0	2.144935	-0.200954	-1.261643
12	1	0	-2.895357	-0.914057	-0.221360
13	1	0	-1.443276	-1.451504	0.622386
14	1	0	-2.271552	0.042305	1.122172

Version=AM64L-G03RevE.01\State=2-A\HF=-232.8273665\S2=0.821343\S2-1=0.\
S2A=0.750641\RMSD=8.780e-09\RMSF=4.567e-07\ZeroPoint=0.1235929\Thermal=
0.1307706\Dipole=-0.4122284,0.226645,0.5381189\PG=C01
[X(C4H9O1)]\NImag=1\\@

(*ii*) BHandHLYP/6-311G**//BHandHLYP/6-311G**

Standard orientation:

Center Number	Atomic Number	Atomic Type	Coordinates (Angstroms) X	Y	Z
1	6	0	0.265742	1.121707	0.064261
2	6	0	1.088274	0.164506	0.571075
3	6	0	2.058335	-0.613462	-0.245122
4	8	0	-1.254006	0.111231	-0.700976
5	6	0	-1.974250	-0.554528	0.274897
6	1	0	-0.338803	1.720035	0.722616
7	1	0	0.454835	1.535229	-0.909374
8	1	0	0.968091	-0.131382	1.602464
9	1	0	3.050890	-0.594975	0.200651
10	1	0	1.760651	-1.659142	-0.306999
11	1	0	2.125959	-0.225824	-1.255502
12	1	0	-2.877430	-0.918914	-0.217430
13	1	0	-1.453120	-1.419381	0.686054
14	1	0	-2.287624	0.095168	1.094657

Version=AM64L-G03RevE.01\State=2-A\HF=-232.8698526\S2=0.822071\S2-1=0.\
S2A=0.750607\RMSD=8.678e-09\RMSF=2.587e-07\ZeroPoint=0.1229893\Thermal=
0.1301643\Dipole=-0.3853017,0.2110959,0.4576732\PG=C01[X(C4H9O1)]
\NImag=1\\@

A8.5.4 Transition structure for methoxyl addition to the inner carbon of propene

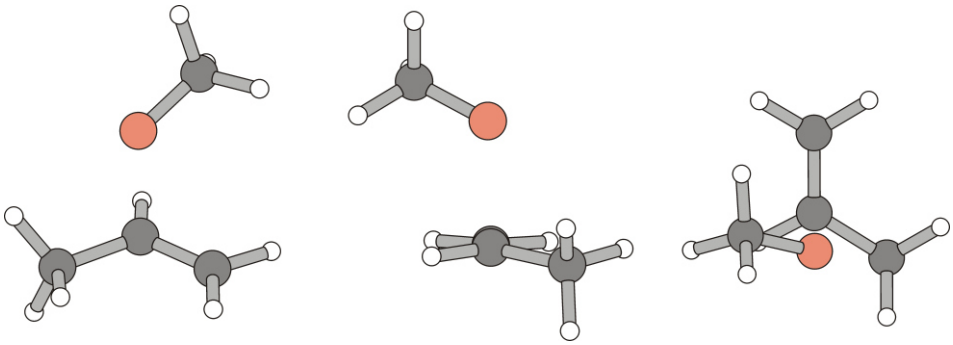

Figure A137. Ball-and-stick models showing different projections of computed transition structure TS^2-**VII** (left: side-on view; center: end-on view (center); right: top view.

(*i*) B3LYP/6-31+G**//B3LYP/6-31+G**

Standard orientation:

Center Number	Atomic Number	Atomic Type	Coordinates (Angstroms) X	Y	Z
1	6	0	2.097983	-0.076794	0.098252
2	8	0	0.900994	-0.634797	-0.352539
3	6	0	-0.802703	0.215154	0.436027
4	6	0	-0.705437	1.444261	-0.162410
5	6	0	-1.743882	-0.856040	-0.032811
6	1	0	2.122808	0.074250	1.190544
7	1	0	2.357878	0.866531	-0.405212
8	1	0	2.886180	-0.807395	-0.148716
9	1	0	-0.114690	2.243185	0.274420
10	1	0	-1.147380	1.627186	-1.137832
11	1	0	-0.424115	0.106823	1.450471
12	1	0	-2.003185	-0.722332	-1.086916
13	1	0	-1.292000	-1.843203	0.092665
14	1	0	-2.669214	-0.826154	0.556542

```
Version=AM64L-G03RevE.01\State=2-A\HF=-232.9815166\S2=0.775952\S2-1=0.\
S2A=0.750124\RMSD=6.870e-09\RMSF=2.181e-07\ZeroPoint=0.1190836\Thermal=
0.1263569\Dipole=0.5128292,-0.0592211,-0.2007177\PG=C01 [X(C4H9O1)]
\NImag=1\\@
```

(*ii*) BHandHLYP/6-31+G**//BHandHLYP/6-31+G**

Standard orientation:

Center Number	Atomic Number	Atomic Type	Coordinates (Angstroms) X	Y	Z
1	6	0	2.055773	-0.071552	0.061157
2	8	0	0.862390	-0.692415	-0.278150
3	6	0	-0.770947	0.216838	0.429501
4	6	0	-0.650864	1.443917	-0.158469
5	6	0	-1.734477	-0.819567	-0.051067
6	1	0	2.115081	0.175905	1.123369
7	1	0	2.255994	0.822201	-0.529323
8	1	0	2.842141	-0.798163	-0.153076
9	1	0	-0.061725	2.226492	0.289592
10	1	0	-1.067257	1.632890	-1.134857
11	1	0	-0.432985	0.110770	1.449395
12	1	0	-1.939379	-0.699048	-1.110343
13	1	0	-1.333556	-1.813961	0.111661
14	1	0	-2.674347	-0.735589	0.492056

Version=AM64L-G03RevE.01\State=2-A\HF=-232.8266952\S2=0.823151\S2-1=0.\
S2A=0.750651\RMSD=7.433e-09\RMSF=2.658e-07\ZeroPoint=0.1234463\Thermal=
0.1304837\Dipole=0.4593215,0.0043118,-0.2735085\PG=C01[X(C4H9O1)]\
NImag=1\\@

(*iii*) BHandHLYP/6-311G**//BHandHLYP/6-311G**

Standard orientation:

Center Number	Atomic Number	Atomic Type	Coordinates (Angstroms) X	Y	Z
1	6	0	2.046021	-0.074618	0.069507
2	8	0	0.854424	-0.674234	-0.298562
3	6	0	-0.758496	0.214630	0.427061
4	6	0	-0.660215	1.441454	-0.158357
5	6	0	-1.719663	-0.827457	-0.042618
6	1	0	2.101662	0.142687	1.138139
7	1	0	2.264420	0.833343	-0.491389
8	1	0	2.829355	-0.799715	-0.157227
9	1	0	-0.077855	2.229959	0.284975
10	1	0	-1.087561	1.625504	-1.129452
11	1	0	-0.415753	0.113813	1.444546
12	1	0	-1.918155	-0.720750	-1.103328
13	1	0	-1.316054	-1.816699	0.134380
14	1	0	-2.661330	-0.738324	0.494295

Version=AM64L-G03RevE.01\State=2-A\HF=-232.8695677\S2=0.823321\S2-1=0.\
S2A=0.750616\RMSD=5.379e-09\RMSF=2.567e-07\ZeroPoint=0.122879\Thermal=
0.1298972\Dipole=0.0166082,0.3860869,0.3017036\Polar=65.3333003,10.4831885,
50.7814032,12.8518568,0.7358499,60.3796669\PG=C01 [X(C4H9O1)] \NImag=1\\@

A8.5.5 1-Methoxprop-2-yl radical *iso*-(VIII)

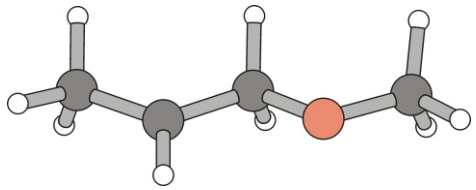

Figure A138. Ball-and-stick models showing computed equilibrium structure of carbon radical *iso*-**VIII**.

(*i*) B3LYP/6-31+G**//B3LYP/6-31+G**

Standard orientation:

Center Number	Atomic Number	Atomic Type	Coordinates (Angstroms) X	Y	Z
1	6	0	2.398331	-0.185298	-0.003971
2	8	0	1.170099	0.513232	-0.069710
3	6	0	0.040462	-0.336825	0.056502
4	6	0	-1.206907	0.471671	0.015015
5	6	0	-2.542907	-0.188782	-0.038361
6	1	0	3.194974	0.554823	-0.106478
7	1	0	2.514721	-0.707985	0.958606
8	1	0	2.487346	-0.923085	-0.816865
9	1	0	0.038741	-1.095663	-0.750946
10	1	0	0.113692	-0.908494	1.008165
11	1	0	-1.119743	1.531554	0.235286
12	1	0	-3.331779	0.522124	-0.302674
13	1	0	-2.564094	-1.006304	-0.772512
14	1	0	-2.828525	-0.637433	0.929991

Version=AM64L-G03RevE.01\State=2-A\HF=-233.0135496\S2=0.753954\S2-1=0.\
S2A=0.750011\RMSD=6.031e-09\RMSF=1.492e-07\ZeroPoint=0.1209638\Thermal=
0.1284394\Dipole=0.5185199,0.0604196,-0.2626168\PG=C01[X(C4H9O1)]\
NImag=0\\@

(*ii*) BHandHLYP/6-31+G**//BHandHLYP/6-31+G**

Standard orientation:

Center Number	Atomic Number	Atomic Type	Coordinates (Angstroms) X	Y	Z
1	6	0	2.378423	-0.182097	0.000409
2	8	0	1.161879	0.504734	-0.051788
3	6	0	0.043170	-0.334716	0.037830
4	6	0	-1.197143	0.473861	-0.005410
5	6	0	-2.525954	-0.189500	-0.023337
6	1	0	3.170451	0.553941	-0.073926
7	1	0	2.488092	-0.728332	0.939910
8	1	0	2.472766	-0.889426	-0.826424
9	1	0	0.051254	-1.066865	-0.780684
10	1	0	0.095282	-0.920469	0.969595
11	1	0	-1.107841	1.527324	0.202226
12	1	0	-3.314573	0.507687	-0.290378
13	1	0	-2.553005	-1.014731	-0.735228
14	1	0	-2.788429	-0.612280	0.952263

Version=AM64L-G03RevE.01\State=2-A\HF=-232.8672925\S2=0.755624\S2-1=0.\
S2A=0.750023\RMSD=2.485e-09\RMSF=1.626e-07\ZeroPoint=0.1255586\Thermal=
0.1329041\Dipole=0.5187985,0.0504959,-
0.2788378\PG=C01[X(C4H9O1)]\NImag=0\\@

(*iii*) BHandHLYP/6-311G**//BHandHLYP/6-311G**

Standard orientation:

Center Number	Atomic Number	Atomic Type	Coordinates (Angstroms) X	Y	Z
1	6	0	2.373235	-0.180650	0.002185
2	8	0	1.159560	0.504751	-0.057538
3	6	0	0.045321	-0.335320	0.038657
4	6	0	-1.194145	0.471393	-0.007543
5	6	0	-2.523181	-0.187804	-0.024110
6	1	0	3.166372	0.552122	-0.076382
7	1	0	2.483659	-0.720170	0.944886
8	1	0	2.471617	-0.895235	-0.817194
9	1	0	0.050597	-1.073877	-0.773145
10	1	0	0.096371	-0.915287	0.973689
11	1	0	-1.103514	1.517943	0.225704
12	1	0	-3.303666	0.498615	-0.335527
13	1	0	-2.538567	-1.041470	-0.699612
14	1	0	-2.806727	-0.566369	0.962750

Version=AM64L-G03RevE.01\State=2-A\HF=-232.9093502\S2=0.755667\S2-1=0.\
S2A=0.750023\RMSD=4.869e-09\RMSF=4.236e-07\ZeroPoint=0.1250554\Thermal=
0.1323703\Dipole=0.4609028,0.047443,-0.2628264\PG=C01[X
(C4H9O1)]\NImag=0\\@

A8.5.6 The 2-Methoxprop-1-yl radical (VIII)

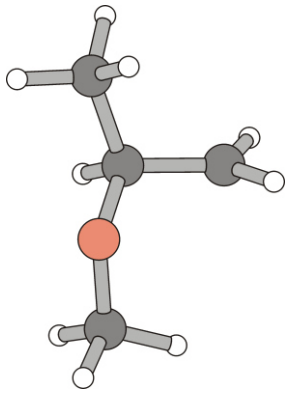

Figure A139. Ball-and-stick models showing computed equilibrium structure of carbon radical **VIII**.

(*i*) B3LYP/6-31+G**//B3LYP/6-31+G**

Standard orientation:

Center Number	Atomic Number	Atomic Type	Coordinates (Angstroms) X	Y	Z
1	6	0	-0.588502	1.477054	-0.110997
2	6	0	-0.437818	0.051278	0.314670
3	6	0	-1.673492	-0.794321	-0.029833
4	8	0	0.670388	-0.587305	-0.329518
5	6	0	1.938925	-0.111571	0.090994
6	1	0	-0.402172	1.748249	-1.146192
7	1	0	-1.033427	2.214627	0.549447
8	1	0	-0.283322	0.012127	1.407917
9	1	0	-1.521603	-1.826296	0.302623
10	1	0	-2.564752	-0.390203	0.459611
11	1	0	-1.838119	-0.795607	-1.111591
12	1	0	2.076909	0.953565	-0.141252
13	1	0	2.079831	-0.256809	1.173532
14	1	0	2.688874	-0.695851	-0.446966

```
Version=AM64L-G03RevE.01\State=2-A\HF=-233.0118568\S2=0.753661\S2-1=0.\
S2A=0.750008\RMSD=4.273e-09\RMSF=5.654e-07\ZeroPoint=0.1211087\Thermal=
0.128218\Dipole=-0.0156316,0.3308128,0.3590719\PG=C01[X(C4H9O1)]\
NImag=0\\@
```

(ii) BHandHLYP/6-31+G**//BHandHLYP/6-31+G**

Standard orientation:

Center Number	Atomic Number	Atomic Type	Coordinates (Angstroms) X	Y	Z
1	6	0	-0.585808	1.467636	-0.104568
2	6	0	-0.430636	0.044896	0.311448
3	6	0	-1.656868	-0.791589	-0.033267
4	8	0	0.665950	-0.573105	-0.327815
5	6	0	1.920855	-0.111333	0.091301
6	1	0	-0.360155	1.749880	-1.120081
7	1	0	-1.092341	2.175229	0.530148
8	1	0	-0.277326	0.002994	1.395512
9	1	0	-1.507953	-1.817089	0.292921
10	1	0	-2.542127	-0.391417	0.452663
11	1	0	-1.818647	-0.789716	-1.107280
12	1	0	2.057868	0.947829	-0.126387
13	1	0	2.060137	-0.267652	1.163169
14	1	0	2.667689	-0.682878	-0.447627

Version=AM64L-G03RevE.01\State=2-A\ HF=-232.8663428\S2=0.754984\S2-1=0.\
S2A=0.750016\RMSD=5.787e-09\RMSF=8.737e-08\ZeroPoint=0.1255823\ Thermal=
0.132513\Dipole=-0.1952881,-0.4069541,-0.225176\PG=C01 [X(C4H9O1)]
\NImag=0\\@

(ii) BHandHLYP/6-311G**//BHandHLYP/6-311G**

Standard orientation:

Center Number	Atomic Number	Atomic Type	Coordinates (Angstroms) X	Y	Z
1	6	0	-0.590567	1.466672	-0.103174
2	6	0	-0.428183	0.045627	0.310696
3	6	0	-1.650259	-0.795962	-0.031477
4	8	0	0.665001	-0.566255	-0.334013
5	6	0	1.916406	-0.111130	0.094302
6	1	0	-0.351886	1.749053	-1.114202
7	1	0	-1.116215	2.167042	0.521710
8	1	0	-0.273065	0.003868	1.393536
9	1	0	-1.493559	-1.818807	0.295224
10	1	0	-2.538448	-0.401926	0.451452
11	1	0	-1.807757	-0.796662	-1.104921
12	1	0	2.053182	0.951834	-0.100833
13	1	0	2.057707	-0.287474	1.162173
14	1	0	2.665655	-0.668128	-0.454116

Version=AM64L-G03RevE.01\State=2-A\HF=-232.9087648\S2=0.755082\S2-1=0.\
S2A=0.750016\RMSD =1.461e-09\RMSF=7.103e-08\ZeroPoint=0.1250384\ Thermal=
0.1319545\Dipole=-0.1968934,-0.3672109,-0.2047589\PG=C01 [X(C4H9O1)]\
NImag=0\\@

A8.6 Transition structure models for 2-allylcyclohexyl-1-oxyl radical cyclizations

A8.6.1 2,4-Cis-cyclization of the *cis*-2-(propen-3-yl)-cyclohexyl-1-oxyl radical *cis*-Ic– favored conformer of transition structure *TS*^{1}-*cis*-Ic

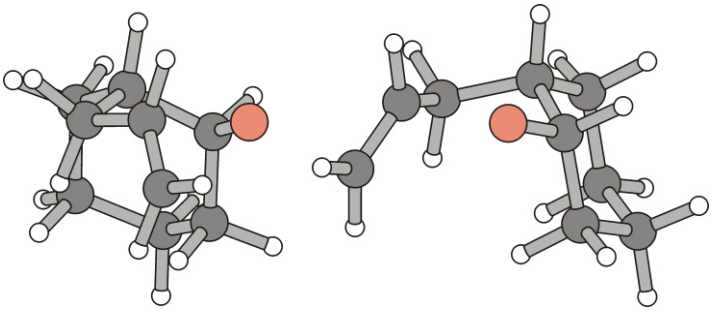

Figure A140. Projections of the ball-and-stick model for computed transition structure TS^1-*cis*-**Ic**.

(*i*) B3LYP/6-31+G**//B3LYP/6-31+G**

Standard orientation:

Center Number	Atomic Number	Atomic Type	Coordinates (Angstroms) X	Y	Z
1	6	0	-0.152681	0.855917	-0.716508
2	6	0	-1.588435	1.312485	-0.395685
3	6	0	-2.254587	0.491401	0.722134
4	6	0	-2.174757	-1.015597	0.431410
5	6	0	-0.717547	-1.466123	0.240561
6	6	0	-0.016814	-0.677503	-0.880928
7	8	0	1.335368	-0.985644	-1.029507
8	6	0	0.907085	1.250061	0.338490
9	6	0	2.191283	0.507672	0.072012
10	6	0	2.833373	-0.239530	1.033785
11	1	0	-1.591479	2.380869	-0.141900
12	1	0	-2.193735	1.214350	-1.307714
13	1	0	-3.299893	0.804889	0.832785
14	1	0	-1.768761	0.699249	1.685629
15	1	0	-2.751467	-1.239407	-0.478570
16	1	0	-2.644141	-1.585998	1.242101
17	1	0	-0.658990	-2.535332	0.007035
18	1	0	-0.160043	-1.323413	1.175608
19	1	0	-0.486720	-0.956687	-1.844858
20	1	0	0.155999	1.306019	-1.669182
21	1	0	1.087278	2.331963	0.291459
22	1	0	0.555903	1.026975	1.351859
23	1	0	2.760985	0.817409	-0.799230
24	1	0	3.803853	-0.686126	0.845070
25	1	0	2.346753	-0.482306	1.974333

Zero-point correction=	0.222220	(Hartree/Particle)
Thermal correction to Energy=	0.231299	
Thermal correction to Enthalpy=	0.232244	
Thermal correction to Gibbs Free Energy=	0.187914	
Sum of electronic and zero-point Energies=		-426.939071
Sum of electronic and thermal Energies=		-426.929991
Sum of electronic and thermal Enthalpies=		-426.929047
Sum of electronic and thermal Free Energies=		-426.973376

```
Version=AM64L-G03RevE.01\State=2-A\HF=-427.1612907\S2=0.778927\S2-1=0.\
S2A=0.750149\RMSD=3.650e-09\RMSF=7.905e-07\Dipole=-0.137655,0.5613339,
0.6226988\PG=C01 [X(C9H15O1)]\NImag=1\\@
```

(*ii*) BHandHLYP/6-31+G**//BHandHLYP/6-31+G**

```
Standard orientation:
---------------------------------------------------------------------
Center     Atomic         Atomic           Coordinates (Angstroms)
Number     Number          Type           X           Y           Z
---------------------------------------------------------------------
   1          6              0       -0.158957    0.859034   -0.707305
   2          6              0       -1.587306    1.297945   -0.382552
   3          6              0       -2.236148    0.468841    0.724678
   4          6              0       -2.142917   -1.024276    0.423063
   5          6              0       -0.691569   -1.453166    0.225974
   6          6              0       -0.016670   -0.656278   -0.887260
   7          8              0        1.333381   -0.946677   -1.033782
   8          6              0        0.888373    1.240000    0.345333
   9          6              0        2.161648    0.494101    0.071337
  10          6              0        2.803833   -0.243517    1.032443
  11          1              0       -1.597754    2.356008   -0.122567
  12          1              0       -2.190942    1.200841   -1.285686
  13          1              0       -3.276206    0.768316    0.840419
  14          1              0       -1.751949    0.672364    1.680205
  15          1              0       -2.715336   -1.244787   -0.480235
  16          1              0       -2.599317   -1.601763    1.224657
  17          1              0       -0.622125   -2.512386   -0.011270
  18          1              0       -0.136446   -1.308726    1.152234
  19          1              0       -0.476790   -0.936801   -1.842628
  20          1              0        0.144457    1.319500   -1.647073
  21          1              0        1.074017    2.312749    0.313783
  22          1              0        0.538646    1.006903    1.347895
  23          1              0        2.734780    0.816934   -0.782184
  24          1              0        3.767578   -0.684834    0.844502
  25          1              0        2.318615   -0.487014    1.963935
---------------------------------------------------------------------

Zero-point correction=                          0.230391 (Hartree/Particle)
Thermal correction to Energy=                   0.239135
Thermal correction to Enthalpy=                 0.240079
Thermal correction to Gibbs Free Energy=        0.196369
Sum of electronic and zero-point Energies=           -426.660375
Sum of electronic and thermal Energies=              -426.651630
Sum of electronic and thermal Enthalpies=            -426.650686
Sum of electronic and thermal Free Energies=         -426.694397

Version=AM64L-G03RevE.01\State=2-A\HF=-426.8907654\S2=0.827049\S2-1=0.\
S2A=0.750736\RMSD=1.004e-09\RMSF=3.563e-07\ Dipole=-0.1224624,
0.5154782,0.6274927\PG=C0 1 [X(C9H15O1)]\NImag=1\\@
```

(*iii*) BHandHLYP/6-311G**//BHandHLYP/6-311G**

Standard orientation:

Center Number	Atomic Number	Atomic Type	Coordinates (Angstroms) X	Y	Z
1	6	0	-0.161510	0.864551	-0.703166
2	6	0	-1.589369	1.297132	-0.374888
3	6	0	-2.234130	0.459018	0.726440
4	6	0	-2.136286	-1.030719	0.415247
5	6	0	-0.684602	-1.452655	0.216908
6	6	0	-0.011146	-0.648020	-0.890450
7	8	0	1.336895	-0.930297	-1.034634
8	6	0	0.886091	1.240080	0.349639
9	6	0	2.155543	0.489400	0.073303
10	6	0	2.790414	-0.251624	1.032812
11	1	0	-1.603503	2.351969	-0.108263
12	1	0	-2.192615	1.203928	-1.277082
13	1	0	-3.273630	0.753927	0.844943
14	1	0	-1.750478	0.657520	1.681782
15	1	0	-2.705800	-1.246283	-0.489483
16	1	0	-2.591941	-1.613949	1.211040
17	1	0	-0.609671	-2.508756	-0.025844
18	1	0	-0.131455	-1.310885	1.143203
19	1	0	-0.468170	-0.925427	-1.846755
20	1	0	0.140289	1.329321	-1.639561
21	1	0	1.076716	2.310509	0.320240
22	1	0	0.536507	1.006145	1.350514
23	1	0	2.735195	0.822071	-0.770038
24	1	0	3.753930	-0.691778	0.848653
25	1	0	2.299442	-0.498921	1.958654

```
Zero-point correction=                          0.229641 (Hartree/Particle)
Thermal correction to Energy=                   0.238379
Thermal correction to Enthalpy=                 0.239323
Thermal correction to Gibbs Free Energy=        0.195648
Sum of electronic and zero-point Energies=                -426.734639
Sum of electronic and thermal Energies=                   -426.725901
Sum of electronic and thermal Enthalpies=                 -426.724957
Sum of electronic and thermal Free Energies=              -426.768631

Version=AM64L-G03RevE.01\State=2-A \HF=-426.9642794\S2=0.826958\S2-1=0.\
S2A=0.750702\RMSD=4.351e-09\RMSF=2.866e-07\Dipole=-0.1243078, 0.4861921,
0.5485657\PG=C01 [X(C9H15O1)]\NImag=1\\@
```

A8.6.2 2,4-Cis-cyclization of the *cis*-2-(propen-3-yl)-cyclohexyl-1-oxyl radical *cis*-Ic – disfavored conformer of transition structure TS^1-*cis*-Ic

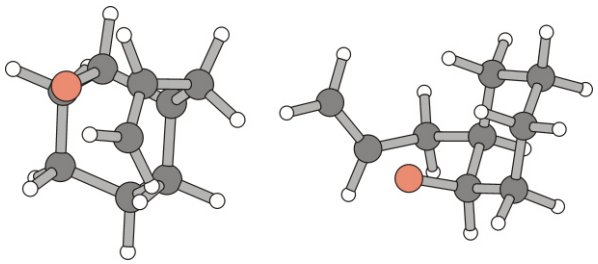

Figure A141. Projections of the ball-and-stick model for computed transition structure TS^1-*cis*-**Ic**.

(*i*) B3LYP/6-31+G**//B3LYP/6-31+G**

Standard orientation:

Center Number	Atomic Number	Atomic Type	Coordinates (Angstroms) X	Y	Z
1	6	0	-2.046643	1.184906	-0.327709
2	6	0	-2.283368	-0.273147	-0.747359
3	6	0	-1.712915	-1.246677	0.290844
4	6	0	-0.224975	-0.980989	0.621945
5	6	0	0.047994	0.505673	0.955760
6	6	0	-0.551640	1.451674	-0.098665
7	8	0	0.566770	-1.330381	-0.472855
8	6	0	1.591252	0.616896	1.051610
9	6	0	2.251327	-0.263390	0.007633
10	6	0	2.665339	0.210287	-1.217290
11	1	0	-3.355859	-0.463524	-0.878522
12	1	0	-1.804950	-0.455667	-1.717119
13	1	0	-1.815630	-2.284175	-0.045419
14	1	0	-2.273571	-1.159063	1.233031
15	1	0	0.044536	-1.587883	1.508851
16	1	0	-0.401861	0.740666	1.931171
17	1	0	-0.019753	1.320765	-1.048825
18	1	0	-0.390517	2.490707	0.218039
19	1	0	-2.436698	1.870603	-1.089877
20	1	0	-2.604537	1.395338	0.597352
21	1	0	1.902641	1.660436	0.922569
22	1	0	1.921036	0.302450	2.047829
23	1	0	2.682195	-1.197670	0.354372
24	1	0	3.190765	-0.432032	-1.916451
25	1	0	2.409820	1.210702	-1.554773

```
Zero-point correction=                          0.222239 Hartree/Particle)
Thermal correction to Energy=                   0.231425
Thermal correction to Enthalpy=                 0.232370
Thermal correction to Gibbs Free Energy=        0.187773
Sum of electronic and zero-point Energies=           -426.935676
Sum of electronic and thermal Energies=              -426.926490
Sum of electronic and thermal Enthalpies=            -426.925545
Sum of electronic and thermal Free Energies=         -426.970142

Version=AM64L-G03RevE.01\State=2-A\HF=-427.1579149\S2=0.783393\S2-1=0.\
S2A=0.750174\RMSD=9.577e-09\RMSF=3622e-07\Dipole=0.2271718,0.083556,-
0.6967465\ PG=C01 [X(C9H15O1)]\NImag=1\\@
```

(*ii*) BHandHLYP/6-31+G**//BHandHLYP/6-31+G**

Standard orientation:

Center Number	Atomic Number	Atomic Type	Coordinates (Angstroms) X	Y	Z
1	6	0	-2.039282	1.158194	-0.348558
2	6	0	-2.259198	-0.299096	-0.740395
3	6	0	-1.687892	-1.240534	0.312647
4	6	0	-0.220484	-0.949676	0.638503
5	6	0	0.041868	0.526794	0.945343
6	6	0	-0.557854	1.440542	-0.122708
7	8	0	0.563063	-1.300327	-0.456441
8	6	0	1.571749	0.647320	1.027813
9	6	0	2.218623	-0.270710	0.017669
10	6	0	2.663106	0.168290	-1.202997
11	1	0	-3.320911	-0.500489	-0.872212
12	1	0	-1.777097	-0.492996	-1.696653
13	1	0	-1.778155	-2.277225	-0.002766
14	1	0	-2.252353	-1.141519	1.241305
15	1	0	0.064351	-1.544585	1.514948
16	1	0	-0.404376	0.778409	1.908585
17	1	0	-0.025073	1.294423	-1.060718
18	1	0	-0.407307	2.479078	0.170704
19	1	0	-2.431153	1.820726	-1.118205
20	1	0	-2.596950	1.377558	0.564503
21	1	0	1.881360	1.676184	0.856529
22	1	0	1.909695	0.373321	2.024341
23	1	0	2.637536	-1.189128	0.394351
24	1	0	3.190132	-0.492001	-1.870543
25	1	0	2.421986	1.154112	-1.566543

```
Zero-point correction=                          0.230385 Hartree/Particle)
Thermal correction to Energy=                   0.239244
Thermal correction to Enthalpy=                 0.240189
Thermal correction to Gibbs Free Energy=        0.196165
Sum of electronic and zero-point Energies=           -426.657211
Sum of electronic and thermal Energies=              -426.648351
Sum of electronic and thermal Enthalpies=            -426.647407
Sum of electronic and thermal Free Energies=         -426.691431

Version=AM64L-G03RevE.01\State=2-A\HF=-426.8875955\S2=0.837039\S2-1=0.\
S2A=0.750851\RMSD=2.340e-09\RMSF=7.723e-08\ Dipole=0.2566768,0.1
270104,-0.636262\ PG=C01 [X(C9H15O1)]\NImag=1\\@
```

(*iii*) BHandHLYP/6-311G**//BHandHLYP/6-311G**

Standard orientation:

Center Number	Atomic Number	Atomic Type	Coordinates (Angstroms) X	Y	Z
1	6	0	-2.025971	1.162331	-0.345471
2	6	0	-2.246112	-0.291362	-0.745992
3	6	0	-1.688134	-1.237340	0.308171
4	6	0	-0.222046	-0.952131	0.637143
5	6	0	0.044988	0.519627	0.957138
6	6	0	-0.546887	1.440787	-0.107446
7	8	0	0.554644	-1.289130	-0.462566
8	6	0	1.574492	0.626376	1.036160
9	6	0	2.204342	-0.279309	0.004676
10	6	0	2.639209	0.180110	-1.209072
11	1	0	-3.305112	-0.488694	-0.892493
12	1	0	-1.751273	-0.483191	-1.694455
13	1	0	-1.778296	-2.271127	-0.011936
14	1	0	-2.257600	-1.139906	1.232363
15	1	0	0.062909	-1.555381	1.506429
16	1	0	-0.398450	0.768160	1.920572
17	1	0	-0.009939	1.298772	-1.041796
18	1	0	-0.396832	2.476199	0.191902
19	1	0	-2.409817	1.828554	-1.113906
20	1	0	-2.589857	1.378040	0.563048
21	1	0	1.893739	1.653557	0.883319
22	1	0	1.912722	0.329299	2.024369
23	1	0	2.630903	-1.198968	0.364825
24	1	0	3.160004	-0.468006	-1.891180
25	1	0	2.396462	1.171192	-1.552380

```
Zero-point correction=                           0.229626 Hartree/Particle)
Thermal correction to Energy=                    0.238470
Thermal correction to Enthalpy=                  0.239414
Thermal correction to Gibbs Free Energy=         0.195476
Sum of electronic and zero-point Energies=           -426.731832
Sum of electronic and thermal Energies=              -426.722988
Sum of electronic and thermal Enthalpies=            -426.722044
Sum of electronic and thermal Free Energies=         -426.765981

Version=AM64L-G03RevE.01\State=2-A\HF=-426.9614577\S2=0.837013\S2-1=0.\
S2A=0.750816\RMSD=3.002e-09\RMSF=1.890e-07\ Dipole=0.2596675,0.0672917,
-0.5929465\PG=C01 [X(C9H15O1)]\NImag=1\\@
```

A8.6.3 2,4-Trans-cyclization of the *cis*-2-(propen-3-yl)-cyclohexyl-1-oxyl radical *cis*-Ic – favored conformer of transition structure TS^2-*cis*-Ic

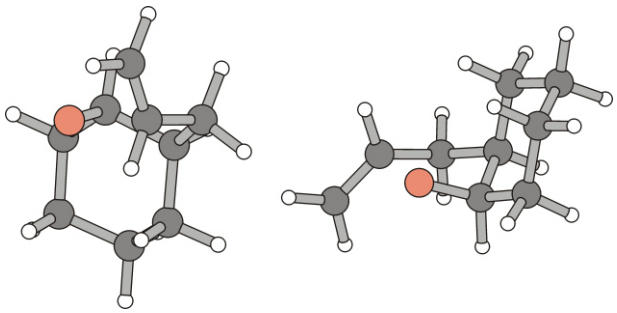

Figure A142. Projections of the ball-and-stick model for computed transition structure of TS^2-*cis*-**Ic**.

(*i*) B3LYP/6-31+G**//B3LYP/6-31+G**

Standard orientation:

Center Number	Atomic Number	Atomic Type	Coordinates (Angstroms) X	Y	Z
1	6	0	-2.340459	0.863904	-0.318391
2	6	0	-2.344848	-0.659723	-0.510351
3	6	0	-1.486153	-1.354278	0.554071
4	6	0	-0.047767	-0.785489	0.643937
5	6	0	-0.018969	0.756756	0.732773
6	6	0	-0.906893	1.414595	-0.339413
7	8	0	0.657474	-1.168164	-0.500942
8	6	0	1.475025	1.118915	0.574153
9	6	0	2.099240	0.292563	-0.526021
10	6	0	3.209084	-0.493536	-0.324268
11	1	0	-3.370134	-1.047236	-0.462311
12	1	0	-1.957984	-0.903217	-1.507389
13	1	0	-1.425036	-2.432223	0.370363
14	1	0	-1.944270	-1.221706	1.544801
15	1	0	0.420420	-1.208518	1.552061
16	1	0	-0.373565	1.076100	1.723853
17	1	0	-0.475948	1.235569	-1.332652
18	1	0	-0.911132	2.501839	-0.187017
19	1	0	-2.940132	1.349126	-1.098198
20	1	0	-2.815976	1.113000	0.642373
21	1	0	1.588828	2.187412	0.347812
22	1	0	2.006374	0.927932	1.514137
23	1	0	1.838621	0.550549	-1.547952
24	1	0	3.695250	-1.004282	-1.148738
25	1	0	3.575328	-0.701275	0.677453

```
Zero-point correction=                          0.222461 (Hartree/Particle)
Thermal correction to Energy=                   0.231577
Thermal correction to Enthalpy=                 0.232521
Thermal correction to Gibbs Free Energy=        0.188147
Sum of electronic and zero-point Energies=           -426.939500
Sum of electronic and thermal Energies=              -426.930385
Sum of electronic and thermal Enthalpies=            -426.929440
Sum of electronic and thermal Free Energies=         -426.973815

Version=AM64L-G03RevE.01\State=2-A\HF=-427.1619615\S2=0.77813\S2-1=0.\
S2A=0.75014\RMSD=3.597e-09\RMSF=5.468e-07\Dipole=0.2770511,0.1469996,
-0.6333259\PG=C01 [X(C9H15O1)]\NImag=1\\@
```

(*ii*) BHandHLYP/6-31+G**//BHandHLYP/6-31+G**

Standard orientation:

Center Number	Atomic Number	Atomic Type	Coordinates (Angstroms) X	Y	Z
1	6	0	-2.325483	0.845823	-0.316652
2	6	0	-2.316711	-0.667520	-0.504806
3	6	0	-1.461448	-1.345882	0.558762
4	6	0	-0.045209	-0.768451	0.644984
5	6	0	-0.020791	0.759406	0.728571
6	6	0	-0.906159	1.403221	-0.339000
7	8	0	0.651963	-1.139501	-0.502145
8	6	0	1.458868	1.119031	0.560039
9	6	0	2.068449	0.273562	-0.525401
10	6	0	3.183148	-0.493644	-0.314657
11	1	0	-3.330921	-1.060730	-0.461478
12	1	0	-1.925165	-0.907296	-1.491789
13	1	0	-1.393375	-2.416155	0.380308
14	1	0	-1.923386	-1.215047	1.538508
15	1	0	0.438030	-1.184355	1.535403
16	1	0	-0.371677	1.079317	1.711108
17	1	0	-0.476209	1.225331	-1.323746
18	1	0	-0.917815	2.482467	-0.190585
19	1	0	-2.924314	1.320575	-1.091765
20	1	0	-2.799031	1.090654	0.636511
21	1	0	1.575966	2.174843	0.318346
22	1	0	1.992030	0.940393	1.491697
23	1	0	1.819177	0.526433	-1.542434
24	1	0	3.664428	-1.012036	-1.126194
25	1	0	3.548575	-0.681660	0.682223

```
Zero-point correction=                          0.230582 (Hartree/Particle)
Thermal correction to Energy=                   0.239372
Thermal correction to Enthalpy=                 0.240316
Thermal correction to Gibbs Free Energy=        0.196530
Sum of electronic and zero-point Energies=           -426.661020
Sum of electronic and thermal Energies=              -426.652230
Sum of electronic and thermal Enthalpies=            -426.651286
Sum of electronic and thermal Free Energies=         -426.695072

Version=AM64L-G03RevE.01\State=2-A\HF=-426.8916022\S2=0.825906\S2-1=0.\
S2A=0.750706\RMSD=2.398e-09\RMSF=6.920e-07\ Dipole=0.2868565,0.1732445,
-0.6016817\PG=C01 [X(C9H15O1)]\NImag=1\\@
```

(iii) BHandHLYP/6-311G**//BHandHLYP/6-311G**

Standard orientation:

Center Number	Atomic Number	Atomic Type	Coordinates (Angstroms) X	Y	Z
1	6	0	-2.320750	0.838495	-0.320322
2	6	0	-2.304577	-0.674158	-0.504201
3	6	0	-1.453505	-1.344449	0.566021
4	6	0	-0.040832	-0.761990	0.647523
5	6	0	-0.020009	0.764923	0.732268
6	6	0	-0.905333	1.402729	-0.337459
7	8	0	0.644376	-1.124511	-0.505384
8	6	0	1.458183	1.122022	0.555690
9	6	0	2.059040	0.268105	-0.527803
10	6	0	3.166049	-0.503993	-0.313467
11	1	0	-3.316017	-1.071157	-0.469190
12	1	0	-1.902295	-0.914631	-1.485092
13	1	0	-1.379204	-2.413384	0.390764
14	1	0	-1.918610	-1.212144	1.542572
15	1	0	0.448951	-1.177776	1.532745
16	1	0	-0.367954	1.087416	1.713143
17	1	0	-0.471710	1.225389	-1.319037
18	1	0	-0.923179	2.480761	-0.191497
19	1	0	-2.917108	1.307670	-1.098676
20	1	0	-2.799868	1.083165	0.628572
21	1	0	1.576509	2.174557	0.307129
22	1	0	1.994445	0.947273	1.484554
23	1	0	1.819855	0.527932	-1.543818
24	1	0	3.647024	-1.023953	-1.122434
25	1	0	3.524553	-0.695131	0.683846

```
Zero-point correction=                          0.229847 (Hartree/Particle)
Thermal correction to Energy=                   0.238622
Thermal correction to Enthalpy=                 0.239566
Thermal correction to Gibbs Free Energy=        0.195836
Sum of electronic and zero-point Energies=           -426.735746
Sum of electronic and thermal Energies=              -426.726971
Sum of electronic and thermal Enthalpies=            -426.726027
Sum of electronic and thermal Free Energies=         -426.769757

Version=AM64L-G03RevE.01\State=2-A\HF=-426.9655932\S2=0.825796\S2-1=0.\
S2A=0.750672\RMSD=9.647e-09\RMSF=2.600e-07\ Dipole=0.289737,0.1225767,-
0.5574019\PG=C01 [X(C9H15O1)]\NImag=1\\@
```

A8.6.4 2,4-Trans-cyclization of the *cis*-2-(propen-3-yl)-cyclohexyl-1-oxyl radical *cis*-Ic– disfavored conformer of transition structure TS^2-*cis*-Ic

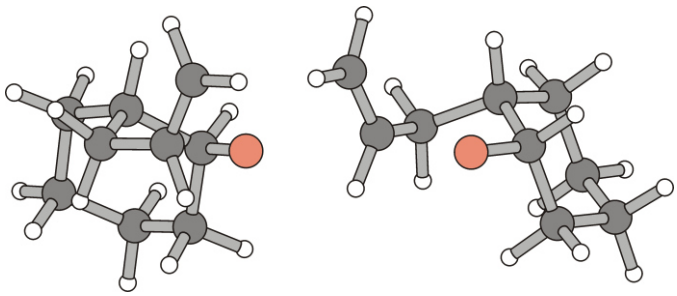

Figure A143. Projections of the ball-and-stick model for computed transition structure of TS^2-*cis*-**Ic**.

(*i*) B3LYP/6-31+G**//B3LYP/6-31+G**

Standard orientation:

Center Number	Atomic Number	Atomic Type	Coordinates (Angstroms) X	Y	Z
1	6	0	-0.080694	-0.688968	-0.549603
2	6	0	1.281062	-1.404981	-0.601757
3	6	0	2.322540	-0.820227	0.367024
4	6	0	2.465835	0.696411	0.172446
5	6	0	1.113062	1.403655	0.345828
6	6	0	0.043968	0.860041	-0.624932
7	8	0	-1.209798	1.416959	-0.372150
8	6	0	-0.939900	-0.994974	0.697431
9	6	0	-2.150899	-0.091197	0.692258
10	6	0	-3.217110	-0.299271	-0.149539
11	1	0	1.138218	-2.477067	-0.412040
12	1	0	1.673647	-1.325833	-1.625030
13	1	0	3.286521	-1.320366	0.213208
14	1	0	2.031118	-1.026442	1.406261
15	1	0	2.862032	0.897176	-0.834046
16	1	0	3.197317	1.106023	0.879630
17	1	0	1.210622	2.483435	0.185365
18	1	0	0.753786	1.275315	1.375305
19	1	0	0.340400	1.109213	-1.660951
20	1	0	-0.667064	-0.995535	-1.425263
21	1	0	-1.247855	-2.047791	0.677143
22	1	0	-0.364791	-0.845988	1.615914
23	1	0	-2.287264	0.579431	1.534192
24	1	0	-4.095539	0.335727	-0.109118
25	1	0	-3.179948	-1.045893	-0.938315

```
Zero-point correction=                          0.222155 (Hartree/Particle)
Thermal correction to Energy=                   0.231375
Thermal correction to Enthalpy=                 0.232319
Thermal correction to Gibbs Free Energy=        0.187557
Sum of electronic and zero-point Energies=           -426.936270
Sum of electronic and thermal Energies=              -426.927050
Sum of electronic and thermal Enthalpies=            -426.926105
Sum of electronic and thermal Free Energies=         -426.970867

Version=AM64L-G03RevE.01\State=2-A\HF=-427.1584244\S2=0.778523\S2-1=0.\
S2A=0.750143\RMSD=3.844e-09\RMSF=1.157e-06\ Dipole=-0.285087,0.5675337,
0.6335652\\PG=C01 [X(C9H15O1)]\NImag=1\\@
```

(*ii*) BHandHLYP/6-31+G**//BHandHLYP/6-31+G**

Standard orientation:

Center Number	Atomic Number	Atomic Type	Coordinates (Angstroms) X	Y	Z
1	6	0	-0.067174	-0.690357	-0.561013
2	6	0	1.291641	-1.390129	-0.599293
3	6	0	2.306269	-0.799870	0.377787
4	6	0	2.434088	0.708480	0.189453
5	6	0	1.079942	1.393555	0.346369
6	6	0	0.045286	0.839954	-0.632643
7	8	0	-1.215235	1.381004	-0.406643
8	6	0	-0.921173	-0.995161	0.674864
9	6	0	-2.107950	-0.069296	0.679072
10	6	0	-3.208051	-0.302670	-0.102561
11	1	0	1.158085	-2.455407	-0.413790
12	1	0	1.693963	-1.305092	-1.609329
13	1	0	3.270754	-1.284201	0.236593
14	1	0	2.005972	-1.009773	1.404745
15	1	0	2.835974	0.914262	-0.804590
16	1	0	3.146900	1.121119	0.900761
17	1	0	1.165294	2.467001	0.192511
18	1	0	0.712296	1.257273	1.363140
19	1	0	0.343342	1.105692	-1.652839
20	1	0	-0.642704	-1.003619	-1.431076
21	1	0	-1.248339	-2.032729	0.649757
22	1	0	-0.345970	-0.864309	1.586405
23	1	0	-2.214715	0.607212	1.509763
24	1	0	-4.073764	0.334642	-0.047796
25	1	0	-3.202481	-1.067153	-0.863325

```
Zero-point correction=                          0.230229 (Hartree/Particle)
Thermal correction to Energy=                   0.239133
Thermal correction to Enthalpy=                 0.240077
Thermal correction to Gibbs Free Energy=        0.195773
Sum of electronic and zero-point Energies=           -426.657300
Sum of electronic and thermal Energies=              -426.648396
Sum of electronic and thermal Enthalpies=            -426.647452
Sum of electronic and thermal Free Energies=         -426.691756

Version=AM64L-G03RevE.01\State=2-A \HF=-426.8875294\S2=0.831067\S2-1=0.\
S2A=0.750779\RMSD=1.057e-09\RMSF=6.016e-07\ Dipole=-0.2447059,0.5226366,
0.6258052\ PG=C01 [X(C9H15O1)]\NImag=1\\@
```

(*iii*) BHandHLYP/6-311G**//BHandHLYP/6-311G**

Standard orientation:

Center Number	Atomic Number	Atomic Type	Coordinates (Angstroms) X	Y	Z
1	6	0	-0.072995	-0.691850	-0.548277
2	6	0	1.282852	-1.393849	-0.591531
3	6	0	2.305213	-0.799464	0.372881
4	6	0	2.435651	0.705568	0.170442
5	6	0	1.085900	1.393737	0.334989
6	6	0	0.037811	0.837680	-0.627541
7	8	0	-1.213219	1.381447	-0.376521
8	6	0	-0.921218	-0.984752	0.692152
9	6	0	-2.113542	-0.067504	0.675616
10	6	0	-3.188505	-0.305311	-0.133198
11	1	0	1.149098	-2.456274	-0.398656
12	1	0	1.677382	-1.315995	-1.603797
13	1	0	3.265891	-1.287370	0.229451
14	1	0	2.011489	-0.999291	1.402348
15	1	0	2.827102	0.901114	-0.828366
16	1	0	3.156065	1.121733	0.869646
17	1	0	1.170689	2.464684	0.173599
18	1	0	0.727543	1.264898	1.354538
19	1	0	0.321071	1.098918	-1.651606
20	1	0	-0.653214	-1.008237	-1.412165
21	1	0	-1.240962	-2.023439	0.686004
22	1	0	-0.348272	-0.832093	1.599996
23	1	0	-2.248657	0.594730	1.511471
24	1	0	-4.062686	0.319040	-0.092159
25	1	0	-3.153782	-1.059536	-0.901332

```
Zero-point correction=                          0.229526 (Hartree/Particle)
Thermal correction to Energy=                   0.238410
Thermal correction to Enthalpy=                 0.239354
Thermal correction to Gibbs Free Energy=        0.195181
Sum of electronic and zero-point Energies=           -426.731636
Sum of electronic and thermal Energies=              -426.722752
Sum of electronic and thermal Enthalpies=            -426.721808
Sum of electronic and thermal Free Energies=         -426.765981

Version=AM64L-G03RevE.01\State=2-A\HF=-426.9611614\S2=0.830117\S2-1=0.\
S2A=0.750727\RMSD=2.042e-09\RMSF=5.079e-07\ Dipole=-0.2518872, 0.4899384,
0.5523471\ PG=C01 [X(C9H15O1)]\NImag=1\\@
```

A8.6.5 2,4-Cis-cyclization of the *trans*-2-(propen-3-yl)-cyclohexyl-1-oxyl radical *trans*-Ic – transition structure TS[1]-*trans*-Ic

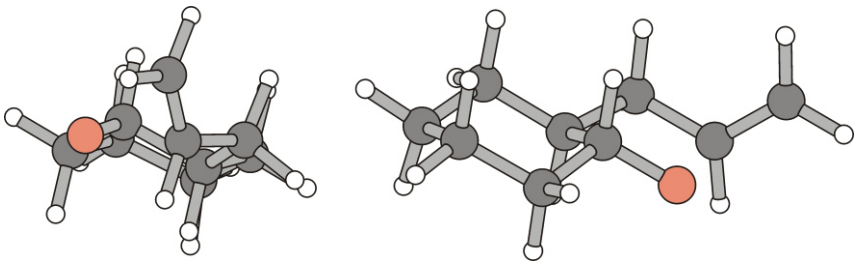

Figure A144. Projections of the ball-and-stick model for computed transition structure TS[1]-*trans*-**Ic**.

(*i*) B3LYP/6-31+G**//B3LYP/6-31+G**

Standard orientation:

Center Number	Atomic Number	Atomic Type	Coordinates (Angstroms) X	Y	Z
1	6	0	-1.269145	1.487036	0.191899
2	6	0	-0.066135	0.707719	-0.345332
3	6	0	-0.017982	-0.722780	0.211324
4	6	0	-1.298352	-1.492988	-0.166465
5	6	0	-2.532278	-0.729697	0.354086
6	6	0	-2.572456	0.730549	-0.132374
7	1	0	-1.300613	2.498149	-0.234002
8	1	0	-1.172356	1.607490	1.281142
9	1	0	-0.166065	0.615574	-1.437641
10	6	0	1.329759	1.280757	-0.043101
11	8	0	1.113224	-1.354020	-0.303831
12	1	0	0.024979	-0.673029	1.318137
13	1	0	-1.259981	-2.504525	0.251664
14	1	0	-1.338705	-1.592597	-1.258768
15	1	0	-2.526488	-0.743939	1.453181
16	1	0	-3.444647	-1.252881	0.042670
17	1	0	-3.430181	1.249246	0.312879
18	1	0	-2.730332	0.743507	-1.220271
19	6	0	2.367299	0.236186	-0.385517
20	6	0	3.325808	-0.183773	0.513203
21	1	0	1.513288	2.194384	-0.623147
22	1	0	1.405447	1.545838	1.019472
23	1	0	2.547147	0.059920	-1.442106
24	1	0	4.124277	-0.853530	0.212033
25	1	0	3.249340	0.060495	1.569065

```
Zero-point correction=                          0.222307 (Hartree/Particle)
Thermal correction to Energy=                   0.231434
Thermal correction to Enthalpy=                 0.232378
Thermal correction to Gibbs Free Energy=        0.187942
Sum of electronic and zero-point Energies=           -426.941556
Sum of electronic and thermal Energies=              -426.932430
Sum of electronic and thermal Enthalpies=            -426.931485
Sum of electronic and thermal Free Energies=         -426.975921

Version=AM64L-G03RevE.01\State=2-A\HF=-427.163863 8\S2=0.779033\S2-1=0.\
S2A=0.750145\RMSD=3.631e-09\RMSF=6.053e-07\ Dipole=-0.4920779,-0.2430848,-
0.6047289\PG=C01 [X(C9H15O1)]\NImag=1\\@
```

(*ii*) BHandHLYP/6-31+G**//BHandHLYP/6-31+G**

Standard orientation:

Center Number	Atomic Number	Atomic Type	Coordinates (Angstroms) X	Y	Z
1	6	0	-1.262342	1.475193	0.189203
2	6	0	-0.067331	0.705187	-0.349589
3	6	0	-0.017679	-0.711211	0.203832
4	6	0	-1.281367	-1.482448	-0.162170
5	6	0	-2.507316	-0.729377	0.360264
6	6	0	-2.554291	0.719074	-0.128116
7	1	0	-1.297811	2.478341	-0.233470
8	1	0	-1.162215	1.594206	1.269887
9	1	0	-0.169533	0.613649	-1.433327
10	6	0	1.316529	1.273966	-0.049912
11	8	0	1.108010	-1.333382	-0.316657
12	1	0	0.041179	-0.660461	1.299402
13	1	0	-1.238758	-2.485952	0.253773
14	1	0	-1.328475	-1.582872	-1.245941
15	1	0	-2.493790	-0.738867	1.451070
16	1	0	-3.413455	-1.251766	0.059624
17	1	0	-3.406766	1.231409	0.313998
18	1	0	-2.712855	0.727280	-1.207484
19	6	0	2.342311	0.222706	-0.378296
20	6	0	3.295727	-0.180819	0.523586
21	1	0	1.508520	2.176048	-0.628981
22	1	0	1.389348	1.541319	1.003711
23	1	0	2.533174	0.048224	-1.424505
24	1	0	4.086004	-0.852318	0.234845
25	1	0	3.215914	0.075195	1.567833

```
Zero-point correction=                          0.230395 (Hartree/Particle)
Thermal correction to Energy=                   0.239204
Thermal correction to Enthalpy=                 0.240148
Thermal correction to Gibbs Free Energy=        0.196275
Sum of electronic and zero-point Energies=           -426.662633
Sum of electronic and thermal Energies=              -426.653825
Sum of electronic and thermal Enthalpies=            -426.652880
Sum of electronic and thermal Free Energies=         -426.696754

Version=AM64L-G03RevE.01\State=2-A\HF=-426.8930281\S2=0.82674\S2-1=0.\
S2A=0.750716\RMSD=1.834e-09\RMSF=4.142e-07\Dipole=-0.4556083,
-0.2385617, -0.6033449\PG=C01 [X(C9H15O1)]\NImag=1\\@
```

(iii) BHandHLYP/6-311G**//BHandHLYP/6-311G**

Standard orientation:

Center Number	Atomic Number	Atomic Type	Coordinates (Angstroms) X	Y	Z
1	6	0	-1.264157	1.473962	0.191220
2	6	0	-0.069204	0.708078	-0.348916
3	6	0	-0.012951	-0.707690	0.202645
4	6	0	-1.273044	-1.482038	-0.162735
5	6	0	-2.500655	-0.734505	0.359555
6	6	0	-2.552499	0.713674	-0.126178
7	1	0	-1.304250	2.476100	-0.229589
8	1	0	-1.163657	1.591771	1.270643
9	1	0	-0.173324	0.614040	-1.430850
10	6	0	1.314793	1.275546	-0.053913
11	8	0	1.109663	-1.323005	-0.322037
12	1	0	0.045548	-0.657109	1.297250
13	1	0	-1.225354	-2.484582	0.251237
14	1	0	-1.317339	-1.581086	-1.245458
15	1	0	-2.485971	-0.745064	1.448969
16	1	0	-3.404515	-1.258160	0.059706
17	1	0	-3.405851	1.221309	0.315997
18	1	0	-2.710715	0.722755	-1.204216
19	6	0	2.336818	0.219269	-0.376922
20	6	0	3.281797	-0.183662	0.529553
21	1	0	1.509221	2.172237	-0.637777
22	1	0	1.389112	1.547850	0.996868
23	1	0	2.538039	0.051585	-1.420704
24	1	0	4.073742	-0.853345	0.246180
25	1	0	3.192625	0.069947	1.572197

```
Zero-point correction=                          0.229616 (Hartree/Particle)
Thermal correction to Energy=                   0.238423
Thermal correction to Enthalpy=                 0.239367
Thermal correction to Gibbs Free Energy=        0.195515
Sum of electronic and zero-point Energies=                -426.736508
Sum of electronic and thermal Energies=                   -426.727701
Sum of electronic and thermal Enthalpies=                 -426.726757
Sum of electronic and thermal Free Energies=              -426.770609


Version=AM64L-G03RevE.01\State=2-A\HF=-426.9661239\S2=0.826469\S2-1=0.\
S2A=0.75068\RMSD=4.126e-09\RMSF=2.859e-07\ Dipole=-0.4301163,
-0.2379023,-0.5309277\PG=C01 [X(C9H15O1)]\NImag=1\\@
```

A8.6.6 2,4-Trans-cyclization of the *trans*-2-(propen-3-yl)-cyclohexyl-1-oxyl radical *trans*-Ic – transition structure TS^2-*trans*-Ic

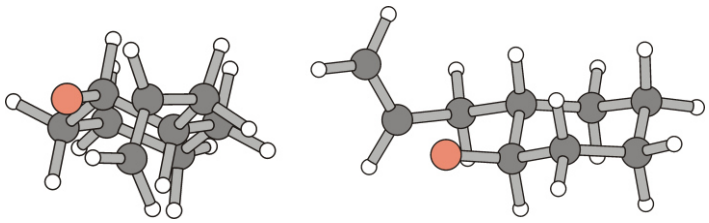

Figure A145. Projections of the ball-and-stick model for computed transition structure TS^2-*trans*-**Ic**.

(i) B3LYP/6-31+G**//B3LYP/6-31+G**

Standard orientation:

Center Number	Atomic Number	Atomic Type	Coordinates (Angstroms) X	Y	Z
1	6	0	1.215797	1.501487	-0.128538
2	6	0	-0.046238	0.670926	0.116799
3	6	0	0.092562	-0.751700	-0.463683
4	6	0	1.287423	-1.472635	0.184374
5	6	0	2.576392	-0.659417	-0.039600
6	6	0	2.447691	0.789408	0.464002
7	1	0	1.107902	2.501398	0.311393
8	1	0	1.355404	1.646505	-1.209799
9	1	0	-0.183616	0.552596	1.201933
10	6	0	-1.361282	1.213424	-0.470822
11	8	0	-1.109155	-1.426734	-0.267398
12	1	0	0.298614	-0.643904	-1.549473
13	1	0	1.385307	-2.478393	-0.238993
14	1	0	1.084634	-1.591222	1.256786
15	1	0	2.814512	-0.648620	-1.112850
16	1	0	3.418628	-1.155520	0.457855
17	1	0	3.357876	1.353000	0.225602
18	1	0	2.362204	0.783529	1.560055
19	6	0	-2.422500	0.141233	-0.325700
20	6	0	-3.079884	-0.074217	0.866698
21	1	0	-1.667299	2.130457	0.047315
22	1	0	-1.220049	1.465992	-1.528137
23	1	0	-2.867135	-0.255699	-1.232381
24	1	0	-3.872608	-0.810493	0.944637
25	1	0	-2.760900	0.413191	1.784067

```
Zero-point correction=                          0.222034 (Hartree/Particle)
Thermal correction to Energy=                   0.231254
Thermal correction to Enthalpy=                 0.232199
Thermal correction to Gibbs Free Energy=        0.187429
Sum of electronic and zero-point Energies=                -426.938864
Sum of electronic and thermal Energies=                   -426.929644
Sum of electronic and thermal Enthalpies=                 -426.928699
Sum of electronic and thermal Free Energies=              -426.973469

Version=AM64L-G03RevE.01\State=2-A\HF=-427.1608981\S2=0.780578\S2-1=0.\
S2A=0.750155\RMSD=2.934e-09\RMSF=6.527e-07\Dipole=-0.621196,
-0.1364414,-0.5910704\PG=C01 [X(C9H15O1)]\NImag=1\\@
```

(ii) BHandHLYP/6-31+G**//BHandHLYP/6-31+G**

Standard orientation:

Center Number	Atomic Number	Atomic Type	Coordinates (Angstroms) X	Y	Z
1	6	0	1.215713	1.490569	-0.123185
2	6	0	-0.038993	0.669253	0.128272
3	6	0	0.092405	-0.735954	-0.448360
4	6	0	1.276049	-1.463973	0.177940
5	6	0	2.557309	-0.660407	-0.052488
6	6	0	2.438184	0.776250	0.456725
7	1	0	1.115720	2.483173	0.313935
8	1	0	1.348040	1.633205	-1.197319
9	1	0	-0.171566	0.553711	1.205923
10	6	0	-1.343838	1.209878	-0.451594
11	8	0	-1.100347	-1.408625	-0.228930
12	1	0	0.277588	-0.639348	-1.528034
13	1	0	1.365922	-2.460597	-0.247564
14	1	0	1.085186	-1.584823	1.243770
15	1	0	2.782921	-0.644328	-1.119817
16	1	0	3.396011	-1.157688	0.430826
17	1	0	3.343457	1.331734	0.218952
18	1	0	2.357906	0.764342	1.544698
19	6	0	-2.387891	0.125546	-0.337316
20	6	0	-3.097891	-0.069437	0.821072
21	1	0	-1.664487	2.106306	0.075110
22	1	0	-1.199065	1.480350	-1.495604
23	1	0	-2.796776	-0.272724	-1.250310
24	1	0	-3.883907	-0.802979	0.873791
25	1	0	-2.820453	0.428313	1.736696

```
Zero-point correction=                          0.230126 (Hartree/Particle)
Thermal correction to Energy=                   0.239044
Thermal correction to Enthalpy=                 0.239988
Thermal correction to Gibbs Free Energy=        0.195687
Sum of electronic and zero-point Energies=                -426.659649
Sum of electronic and thermal Energies=                   -426.650731
Sum of electronic and thermal Enthalpies=                 -426.649787
Sum of electronic and thermal Free Energies=              -426.694088


Version=AM64L-G03RevE.01\State=2-A\HF=-426.8897755\S2=0.833209\S2-1=0.\
S2A=0.750804\RMSD=1.350e-09\RMSF=5.612e-07\Dipole=-0.5568576,
-0.1484082,-0.589441\PG=C01 [X(C9H15O1)]\NImag=1\\@
```

(iii) BHandHLYP/6-311G**//BHandHLYP/6-311G**

Standard orientation:

Center Number	Atomic Number	Atomic Type	Coordinates (Angstroms) X	Y	Z
1	6	0	1.215024	1.489608	-0.126243
2	6	0	-0.041572	0.672312	0.118676
3	6	0	0.088826	-0.731586	-0.459365
4	6	0	1.262312	-1.463609	0.177185
5	6	0	2.547807	-0.666130	-0.041387
6	6	0	2.429827	0.771484	0.462767
7	1	0	1.116745	2.481602	0.308971
8	1	0	1.354568	1.630375	-1.198285
9	1	0	-0.177014	0.554638	1.194335
10	6	0	-1.344879	1.208583	-0.463400
11	8	0	-1.106034	-1.398181	-0.257969
12	1	0	0.288374	-0.629469	-1.535204
13	1	0	1.350710	-2.459549	-0.246681
14	1	0	1.058788	-1.583080	1.239511
15	1	0	2.782195	-0.652979	-1.105475
16	1	0	3.379949	-1.163892	0.449310
17	1	0	3.337951	1.321906	0.230987
18	1	0	2.341354	0.762381	1.548782
19	6	0	-2.386027	0.125233	-0.325103
20	6	0	-3.055325	-0.073138	0.852973
21	1	0	-1.663320	2.111890	0.049771
22	1	0	-1.203853	1.460713	-1.511010
23	1	0	-2.828604	-0.259772	-1.226053
24	1	0	-3.843955	-0.799949	0.927366
25	1	0	-2.741573	0.414089	1.760807

```
Zero-point correction=                          0.229373 (Hartree/Particle)
Thermal correction to Energy=                   0.238275
Thermal correction to Enthalpy=                 0.239219
Thermal correction to Gibbs Free Energy=        0.195020
Sum of electronic and zero-point Energies=           -426.733601
Sum of electronic and thermal Energies=              -426.724700
Sum of electronic and thermal Enthalpies=            -426.723755
Sum of electronic and thermal Free Energies=         -426.767955

Version=AM64L-G03RevE.01\State=2-A\HF=-426.9629744\S2=0.832289\S2-1=0.\
S2A=0.750755\RMSD=3.158e-09\RMSF=6.183e-07\ Dipole=-0.5402038,
-0.1407461,-0.5158939\PG=C01 [X(C9H15O1)]\NImag=1\\@


TWO ROADS DIVERGED IN A WOOD, AND I--
I TOOK THE ONE LESS TRAVELED BY,
AND THAT HAS MADE ALL THE DIFFERENCE.
           -- ROBERT FROST
```

A9 Crystallography

The applied model for solving the crystal structure uses restraints for fixing carbons 2 and 4, nitrogen N3/N3a, and oxygen 1/1a in a plane. Treating residual electron density as systematic disordering leads to a 78/22-ratio of diastereomers of 3-[(1-methylcyclohex-1-en-4-yl)-methyloxy]-4-methylthiazole-2(3*H*)-thione (**1g**) at crystallographic independent positions. The diastereomers differ in configuration at C8 and C8a with respect to configuration at the stereogenic N,O-bond. The minor diastereomer (population of 22%) is depicted in Figure A146 and the major (population of 78%) in Figure 2 of the associated article.

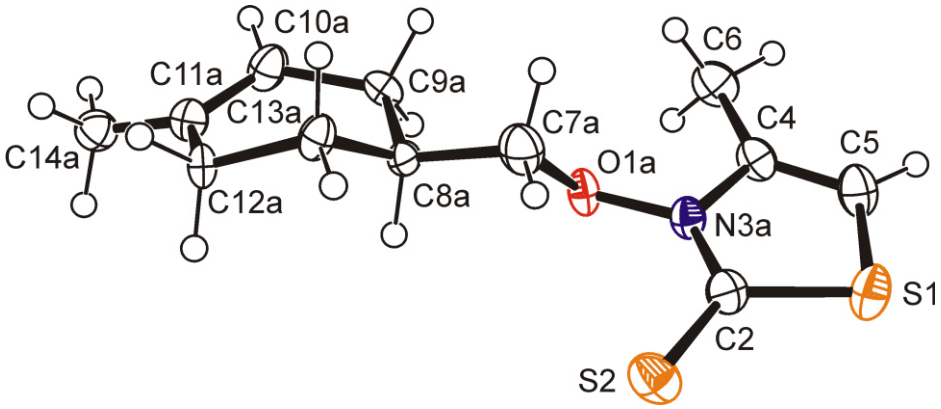

Figure A146. Ellipsoid graphic of (*S*,*P*)/(*R*,*M*)-3-[(1-methylcyclohex-1-en-4-yl)-methoxy]-4-methylthiazole-2(3*H*)-thione (*S*,*P*)/(*R*,*M*)-(**1g**) in the solid state [minor diastereomer at 150 K; the (*S*,*P*)-isomer was arbitrarily chosen from the racemate for presentation (50% probability level); hydrogen atoms are drawn as circles of an arbitrary radius; oxygen is depicted in red, nitrogen in blue, and sulfur in orange; for depiction of the minor diastereomer see the ESI].

A10 References

[1] J. Flügge, *Grundlagen der Polarimetrie*, Bd. 88, Zeiss, Oberkochen/Württemberg, **1965**, S. 62.

[2] D. D. Perrin, W. L. F. Armarego and D. R. Perin, *Purification of Laboratory Chemicals* 2nd ed.; Pergamon Press: Oxford, 1980.

[3] D. H. R. Barton, D. Crich and G. Kretzschmar, *J. Chem. Soc., Perkin Trans. I*, 1986, 39−53.

[4] J. Hartung, T. Gottwald and K. Spehar, *Synlett* 2003, **2**, 227−229.

[5] H. J. Pyun, R. M. Coates, K. C. Wagschal, P. McGeady and R. B. Croteau, *J. Org. Chem*., 1993, **58**, 3998−4009.

[6] J. C. Kauer, *Org. Synth*. Coll. Vol., 1963, **4**, 411–414.

[7] M. H. Norman, G. C. Rigdon, F. Navas III and B. R. Cooper, *J. Med. Chem. Soc*., 1994, **37**, 2552–2563.

[8] R. M. Borzilleri, S. M. Weinreb and M. Parvez, *J. Am. Chem. Soc*., 1995, **117**, 10905–10913.

[9] A. Berkessel, K. Glaubitz and J. Lex, *Eur. J. Org. Chem*., 2002, 2948–2952.

[10] S. Baskaran, I. Islam and S. Chandrasekaran, *J. Org. Chem.,* 1990, ***55***, 891–895.

[11] D. P. Curran and H.J. Liu, *J. Chem. Soc., Perkin Trans. 1,* 1994, 1377–1393.

[12] L. S. Hegedus and J. M. McKearin, *J. Am. Chem. Soc.,* 1982, ***104***, 2444–2451.

[13] L. Streinz and M. Romaňuk, *Coll. Czech. Chem. Comm.,* 1978, **43**, 647–654.

[14] J. M. Schomaker, B. R. Travis and B. Borhan, *Org. Lett*., 2003, **5** (17), 3089–3092.

[15] V. Spezialé, M. Armat and A. Lattes, *J. Heterocycl. Chem.,* 1976, **13**, 349–356.

[16] B. D. Kelly, J. M. Allen, R. E. Tundel and T. H. Lambert, *Org. Lett*., 2009, **11**, 1381–1383.

[17] R. Kuhn and I. Butula, *Liebigs Ann. Chem*., 1968, **718**, 50–77.

[18] I. J. Jakovac, H. B. Goodbrand, K. P. Lok and J. B. Jones, *J. Am. Chem. Soc*., 1982, **104** (7), 4659–4665.

[19] R. M. Borzilleri and S. M. Weinreb, *J. Am. Chem. Soc*., 1994, **116**, 9789–9790.

[20] A. Segre, R. Viterbo and G. Parisi, *J. Am. Chem. Soc*., 1957, **79** (13), 3503–3505.

[21] G. E. Gream, A. K. Serelis and T. I. Stoneman, *Aust. J. Chem*., 1974, **27**, 1711–1729.

[22] T. Inukai and M. Kasai, *J. Org. Chem*., 1965, **30**, 3567–3569.

[23] S. A. Monti and G. L. White, *J. Org. Chem*., 1975, **40**, 215–217.

[24] R. K. Guy and R. A. DiPietro, *Synth.Commun*., 1992, **22**, 687–692.

[25] X. Wei, J. C. Lorenz, S. Kapadia, A. Saha, N. Haddad, C. A. Busacca and C. H. Senanayake, *J. Org. Chem.,* 2007, **72**, 4250–4253.

[26] P. A. Grieco, J. D. Clark, and C. T. Jagoe, *J. Am. Chem. Soc.,* 1991, **113**, 5488–5489.

[27] M. T. Reetz and A. Gansäuer, *Tetrahedron*, 1993, **49**, 6025–6030.

[28] M. Tycho, A. Kirschning, C. Beier, N. Bräuer, E. Schaumann and G. Adiwidjaja, *Liebigs Ann*., 1996, **11**, 1811–1822.

[29] S. Young-Ger, K. Soon-Ai, C. Hyun-Uk, C and Youn-Sang, *Chem. Lett*., 1994, **1**, 63–66.

[30] R. G. Salomon, S. Ghosh, M. G. Zagorski, M. Reitz, *J. Org. Chem*., 1982, **47**, 829836.

[31] Gaussian 03, Revision E.01, M. J. Frisch, G.W. Trucks, H.B. Schlegel, G.E. Scuseria, M. A. Robb, J. R. Cheeseman, J. A. Montgomery, Jr., T. Vreven, K. N. Kudin, J.C. Burant, J. M. Millam, S. S. Iyengar, J. Tomasi, V. Barone, B. Mennucci, M. Cossi, G. Scalmani, N. Rega, G.A. Petersson, H. Nakatsuji, M. Hada, M. Ehara, K. Toyota, R. Fukuda, J. Hasegawa, M. Ishida, T. Nakajima, Y. Honda, O. Kitao, H. Nakai, M. Klene, X. Li, J. E. Knox, H. P. Hratchian, J. B. Cross, V. Bakken, C. Adamo, J. Jaramillo, R. Gomperts, R. E. Stratmann, O. Yazyev, A. J. Austin, R. Cammi, C. Pomelli, J. W. Ochterski, P. Y. Ayala, K. Morokuma, G. A. Voth, P. Salvador, J. J. Dannenberg, V. G. Zakrzewski, S. Dapprich, A. D. Daniels, M. C. Strain, O. Farkas, D. K. Malick, A. D. Rabuck, K. Raghavachari, J. B. Foresman, J. V. Ortiz, Q. Cui, A.G. Baboul, S. Clifford, J. Cioslowski, B. B. Stefanov, G. Liu, A. Liashenko, P. Piskorz, I. Komaromi, R. L. Martin, D. J. Fox, T. Keith, M. A. Al-Laham, C. Y. Peng, A. Nanayakkara, M. Challacombe, P. M. W. Gill, B. Johnson, W. Chen, M. W. Wong, C. Gonzalez, J. A. Pople, Gaussian, Inc., Wallingford CT, 2004.

[32] G. Schaftenaar and J. H. Noordik, *Comput.-Aided Mol. Des*., 2000, **14**, 123–134.

Anhang B

Supplementary data for:

Tertiary Alkoxyl Radicals from 3-Alkoxythiazole-2(3*H*)-thiones

Christine Schur,[a] Nina Becker,[a] Uwe Bergsträßer,[a] Thomas Gottwald,[b] and Jens Hartung*[a]

[a] *Fachbereich Chemie, Organische Chemie, Technische Universität Kaiserslautern, Erwin-Schrödinger-Straße, D-67663 Kaiserslautern, Germany*

[b] *Institut für Organische Chemie, Universität Würzburg, Am Hubland, 97074 Würzburg, Germany*

Contents

B1 General Remarks: (i) The compound numbering in the Supplementary data is consistent with that of the associated publication. (ii) References refer exclusively to the Supplementary data. (iii) All compounds used in this study were racemic.

B2 Instrumentation

Melting points [°C] were determined on an *Electrothermal* 9100 instrument. Values were not corrected.

^{1}H and ^{13}C NMR spectra were recorded with FT-NMR DPX 200, DPX 400 and DMX 600 instruments (*Bruker*). Chemical shifts refer to the δ-scale. The resonances of residual protons and those of carbons of deuterated solvent molecules $CDCl_3$ (δ_H 7.26, δ_C 77.0), C_6D_6 (δ_H 7.16, δ_C 128.06) served as internal standard.

Mass spectra (EI, 70 eV) were recorded with a Mass Selective Detector HP 6890 (*Hewlett Packard*).

UV/Vis spectra were recorded with a Perkin Elmer UV/Vis 330 spectrometer and a Cary 100 Conc spectrometer (VARIAN).

Reaction progress was monitored via thin layer chromatography (tlc) on aluminum sheets coated with silica gel (60 F_{254}, *Merck*). Compounds were detected on developed tlc sheets via UV-light absorption (254 nm) or staining with a solution of Ekkert's reagent, prepared from anisaldehyde (15 g), EtOH (250 mL), and conc. H_2SO_4 (2.5 mL).[1]

Combustion analysis was performed with a Carlo Erba 1106 instrument (analytical laboratory, Universität Würzburg) and a vario Micro cube (analytical laboratory, Technische Universität Kaiserslautern).

Photochemical reactions were performed in a Southern New England Rayonet® chamber reactor equipped with 12 light bulbs (λ = 350 nm). The photoreactor was ventilated from the bottom in order to maintain approximately 25 °C inside the cavity. Stirring was achieved with a micro magnetic stirring device.

B3 Reagents

Copper(I)-chloride (Stem Chemicals, anhydrous, 97%+), DIC (Aldrich Chemicals, 99%), 2-methylpropan-2-ol (**3a**) (Riedel-de Haen 99%), 2-methylbutan-2-ol (**3b**) (Merck Chemicals, 99%) and 2-phenylpropan-2-ol (**3d**) (Acros Chemicals 99%) were commercially available. 2-Methyl-5-phenylpentan-2-ol (**3c**),[2] 2-(4-chlorophenyl)-2-propanol (**3e**),[3,4] and 2-phenylhex-5-en-2-ol (**3f**)[5,6] were prepared according to published procedures. Column chromatography was performed on SiO_2 (Fluka, 0.04–0.063 mm) as stationary phase. Petroleum ether referred to the fraction boiling between 40–55°C. All solvents were purified according to standard procedures.[7]

B4 3-Alkoxythiazole-2(3*H*)-thione Reactions

B4.1 Thermal decomposition of 3-cumyloxythiazolethione 1d. A solution of 3-cumyloxythiazolethione **1d** (185 mg, 0.50 mmol) in dry toluene (6 mL) was heated under reflux for 1 h. The solution was subjected to GC-analysis for identification of volatile products. *α-Methylstyrene* **6**. Yield: 46.1 mg (78%). *Phenyl methyl ketone* (**7**). Yield: 1.8 mg (3%). Concentration of the solution under reduced pressure (100 → 20 mbar, 40 °C) afforded an oil that was purified by column chromatography [elution gradient *tert*-butyl methyl ether:pentane = 1:1 → *tert*-butyl methyl ether:acetone = 1:1 (*v*/*v*)]. 1,2-Bis-[5-(4-methoxyphenyl)-4-methylthiaz-3-yl]-disulfane (**5**).[8] Yield: 65.0 mg (27%), yellow solid, mp 87 °C. R_f = 0.30 for *tert*-butyl methyl ether:pentane = 1:1 (*v*/*v*). ^{1}H NMR ($CDCl_3$, 400 MHz) δ 2.44 (s, 6H), 3.83 (s, 6H), 6.93 (d, 4H, *J* = 9.0 Hz), 7.32 (d, 4H, *J* = 8.7 Hz), ^{13}C NMR ($CDCl_3$, 101 MHz) δ 16.1, 55.3, 114.2, 123.5, 130.4, 136.0, 149.0, 159.6, 160.4. *5-(p-Methoxyphenyl)-4-methylthiazole-2(3H)-thione* **8**.[9] Yield 6.6 mg (6%), colorless crystals. R_f = 0.53 for *tert*-butyl methyl ether:acetone = 1:1 (*v*/*v*). ^{1}H NMR ($CDCl_3$, 400 MHz) δ 2.18 (s, 3H), 3.82 (s, 3H), 6.91 (d, 2H, *J* = 8.6 Hz), 7.25 (d, 2H, *J* = 6.6 Hz), 9.98 (s, 1H). ^{13}C NMR ($CDCl_3$, 101 MHz) δ 12.7, 55.3, 113.9, 114.2, 124.1, 124.8, 129.9, 159.1, 174.2.

B4.2 Thermal conversion of 3-(2-methyl-5-phenylpent-2-oxy)-thiazole-2(3*H*)-thione 1c. An oxygen-free solution of 3-alkoxythiazolethione **1c** (207 mg, 500 µmol), $BrCCl_3$ (988 mg, 5.00 mmol, 0.49 mL), and AIBN (spatula tip) in C_6H_6 (6.0 mL) was boiled under reflux in an atmosphere of Ar. AIBN was added in small portions (spatula tip) until complete

consumption of starting material **1c** had occurred (tlc). The reaction mixture was allowed to cool to 20 °C and was concentrated under reduced pressure (100 → 20 mbar, 40 °C). The residue was purified by column chromatography using pentane:Et_2O = 10:1 (*v*/*v*) as eluent. *2,2-Dimethyl-5-phenyltetrahydrofuran* (**10**).[10] Yield: 53.6 mg (61%), colorless liquid. R_f = 0.80 for pentane:Et_2O = 10:1 (*v*/*v*).

B4.3 Analytical scale reactions (NMR analysis)

B4.3.1 Photochemical conversion. A solution of 3-alkoxythiazolethione **1c** (16.9 mg, 40.9 µmol) and $BrCCl_3$ (169 mg, 0.85 mmol) in C_6D_6 (0.50 mL) was prepared as described in section 4.3.1 of the associated publication. The solution was photolyzed for 45 min at 25 °C and left for additional 48 h at that temparature. It was checked in intervals for changes in **9**/**10**-ratios (^{1}H NMR) using *p*-bromobenzaldehyde (δ = 9.41) as internal standard: *2,2-Dimethyl-5-phenyltetrahydrofuran* (**10**).[10] Yield: 1.6 mg (22%, after 2 h), 3.3 mg (46%, after 48 h). ^{1}H NMR (C_6D_6, 400 MHz) δ 1.24 (s, 3H), 1.28 (s, 3H), 1.46–1.58 (m, 2H), 1.62–1.72 (m, 1H), 1.96–2.03 (m, 1H), 4.88 (t, 1H, *J* = 7.5 Hz), 7.09–7.13 (m, 1H), 7.20–7.24 (m, 2H), 7.39–7.40 (m, 2H). ^{13}C NMR (C_6D_6, 151 MHz) δ 28.5, 29.2, 35.9, 39.1, 80.4, 80.9, 126.0, 127.2, 128.5, 144.7. *5-Bromo-2-methyl-5-phenylpentan-2-ol* (**9**). Yield: 4.3 mg (44%, after 2 h), 0.5 mg (5%, after 48 h). ^{1}H NMR (C_6D_6, 600 MHz) δ 0.92 (s, 3H), 0.93 (s, 3H), 1.14–1.19 (m, 1H), 1.44–1.49 (m, 1H), 2.10–2.18 (m, 1H), 2.26–2.32 (m, 1H), 4.73 (t, 1H, *J* = 7.6 Hz), 7.0–7.08 (m, 3H), 7.20–7.21 (m, 2H). ^{13}C NMR (C_6D_6, 151 MHz) δ 29.3, 29.5, 35.3, 43.6, 56.3, 69.7, 127.6, 128.3, 128.8, 142.7.

B4.3.2 Thermal conversion. A solution of 3-alkoxythiazolethione **1c** (20.7 mg, 50.0 µmol) and $BrCCl_3$ (98.8 mg, 500 µmol, 0.05 mL) in C_6D_6 (0.60 mL) was prepared and treated as described in procedure 4.2. *2,2-Dimethyl-5-phenyltetrahydrofuran* (**10**).[10] Yield: 7.40 mg (84%), determined via ^{1}H NMR versus anisole (δ = 3.29) as internal standard.

B4.4 Thermally conversion of 3-(1-methyl-1-phenylpent-4-enyl-1-oxy)-thiazole-thione 1f.

A solution of thiazolethione **1f** (90.0 mg, 219 µmol) and $BrCCl_3$ (434 mg, 2.19 mmol, 0.22 mL) was prepared and treated as described in procedure 4.2. Reaction time: 30 min. Products identified from the reaction mixture (GC/MS versus authentic references and *n*-decane as

internal standard). *Phenyl methyl ketone* (**7**). Yield: 2.71 mg (10%). *2-Phenyl-5-hexene-2-ol* (**3f**).[4,5] Yield: 8.37 mg (21%). MS (EI) *m*/*z* 176 (<1), 158 (32), 143 (93), 129 (94), 121 (93), 115 (100), 105 (28)]. Eluent used for chromatographic purification: pentane:Et_2O = 10:1 (*v*/*v*). *2-Methyl-2-phenyl-5-bromomethyl-tetrahydrofuran* (**13**).[11] Yield: 35.1 mg (63%), yellowish liquid, 73/27-mixture of cis/trans-isomers. R_f = 0.50 for pentane:Et_2O = 10:1 (*v*/*v*).

B4.5 Conversion of 3-cumyloxythiazolethione 1d in the presence of norbornene 14. 3-cumyloxythiazolethione **1d** (190 mg, 510 μmol) was treated as described in procedure 4.3.1 of the associated publication. *2-Bromo-3-trichloro-methylbicyclo[2.2.1]heptane* (**17**). Yield: 1.38g (92%), colorless oil, 5/95-mixture of 2-*exo*-3-*exo*/2-*endo*-3-*exo*-isomers.[12] *2-Bromo-3-(2-phenyl-prop-2-oxy)-bicyclo[2.2.1]heptane* (**16d**). Yield: 73.5 mg (46%), pale yellow oil, 28/72-mixture of 2-exo-3-exo/2-endo-3-exo-isomers. R_f = 0.47 for pentane:Et_2O = 20:1 (*v*/*v*). Anal. Calcd. for $C_{16}H_{21}OBr$ (309.24): C, 62.14; H, 6.84; Found: C, 61.78; H, 6.97. *2-endo-3-exo-*(**16d**). ^{1}H NMR ($CDCl_3$, 400 MHz) δ 0.93–0.99 (m, 1H), 1.31–1.34 (m, 1H), 1.36–1.49 (m, 2H), 1.54 (s, 3H), 1.59 (s, 3H), 1.73–1.83 (m, 2H), 2.05–2.06 (m, 1H), 2.36–2.39 (m, 1H), 3.20–3.22 (m, 1H), 3.99–4.01 (m, 1H), 7.23–7.27 (m, 1H), 7.32–7.36 (m, 2H), 7.45–7.46 (m, 2H). ^{13}C NMR ($CDCl_3$, 151 MHz) δ 24.0, 24.6, 29.1, 29.6, 34.5, 42.8, 44.2, 63.1, 77.3, 84.4, 126.1, 126.9, 128.1, 146.6. MS (EI) *m*/*z* 229 (6), 175 (4), 120 (43), 119 (100), 103 (9). *2-exo-3-exo-*(**16d**). ^{1}H NMR ($CDCl_3$, 400 MHz) δ 0.85–0.92 (m, 1H), 0.99–1.06 (m, 1H), 1.12–1.15 (m, 1H), 1.32–1.41 (m, 1H), 1.47–1.53 (m, 1H), 1.58 (s, 3H), 1.59 (s, 3H), 2.05–2.06 (m, 1H), 2.13–2.14 (m, 1H), 2.47–2.48 (m, 1H), 3.11 (dd, 1H, *J* = 5.6, 1.2 Hz), 3.93 (dd, 1H, *J* = 6.4, 1.9 Hz), 7.23–7.26 (m, 1H), 7.32–7.36 (m, 2H), 7.52–7.55 (m, 2H). ^{13}C NMR ($CDCl_3$, 150 MHz) δ 25.5, 27.0, 28.7, 33.6, 44.2, 46.5, 61.6, 76.5, 78.6, 126.4, 126.8, 128.0, 147.0. MS (EI) *m*/*z* 229 (6), 175 (4), 120 (43), 119 (100), 103 (9).

B4.6 Conversion of 3-(4-chlorocumyloxy)-thiazolethione 1e in the presence norbornene 14. 3-(*p*-Chlorocumyloxy)-thiazolethione **1e** (207 mg, 510 μmol) was treated as described in procedure 4.3.1 of the associated publication. *2-Bromo-3-trichloro-methylbicyclo-[2.2.1]heptane* (**17**). Yield: 1.43 g (93%), colorless oil, 7/93-mixture of 2-*exo*-3-*exo*/2-*endo*-3-*exo*-isomers.[12] *2-endo-3-exo-2-Bromo-3-[2-(4-chlorophenyl)-prop-2-oxy]-bicyclo[2.2.1]-heptane 2-endo-3-exo-*(**16e**). Yield: 49.2 mg (28%), colorless oil. R_f = 0.46 for pentane:Et_2O = 20:1 (*v*/*v*). *2-Bromo-3-[2-(4-chlorophenyl)-prop-2-oxy]-bicyclo-[2.2.1]heptane* (**16e**). Yield:

27.7 mg (16%), colorless oil, 75/25-mixture of 2-*exo*-3-*exo*/2-*endo*-3-*exo*-isomers. R_f = 0.45 for pentane:Et_2O = 20:1 (*v*/*v*). Anal. Calcd. for $C_{16}H_{20}OBrCl$ (343.68): C, 55.92; H, 5.87; Found: C, 56.04; H, 5.98. *2-endo-3-exo*-(**16e**). ^{1}H NMR ($CDCl_3$, 400 MHz) δ 0.94–1.00 (m, 1H), 1.31–1.34 (m, 1H), 1.37–1.48 (m, 2H), 1.51 (s, 3H), 1.55 (s, 3H), 1.73–1.81 (m, 2H), 2.04 (d, 1H, *J* = 4.7 Hz), 2.38–2.40 (m, 1H), 3.18 (t, 1H, *J* = 2.0 Hz), 3.97–3.98 (m, 1H), 7.29–7.31 (m, 2H), 7.37–7.39 (m, 2H). ^{13}C NMR ($CDCl_3$, 151 MHz) δ 23.9, 24.6, 29.2, 29.5, 34.5, 42.7, 44.2, 62.8, 84.6, 127.6, 128.2, 132.7, 145.3. ^{13}C NMR (C_6D_6, 151 MHz) δ 24.2, 24.6, 28.9, 29.7, 34.5, 43.0, 44.5, 63.0, 77.0, 84.8, 127.8, 128.2, 133.1, 145.6. MS (EI) *m*/*z* 309 (1) 307 (1), 175 (2), 155 (63), 137 (3), 125 (34), 115 (6). *2-exo-3-exo*-(**16e**). ^{1}H NMR ($CDCl_3$, 400 MHz) δ 0.83–0.97 (m, 1H), 1.01–1.08 (m, 1H), 1.13–1.16 (m, 1H), 1.55 (s, 3H), 1.56 (s, 3H), 1.36–1.50 (m, 2H), 2.02–2.05 (m, 1H), 2.11–2.12 (m, 1H), 2.48–2.49 (m, 1H), 3.09 (dd, 1H, *J* = 6.1, 1.0 Hz), 3.92 (dd, 1H, *J* = 6.3, 2.0 Hz), 7.29–7.31 (m, 2H), 7.46–7.48 (m, 2H). ^{13}C NMR ($CDCl_3$, 151 MHz) δ 25.4, 27.0, 28.5, 28.6, 33.6, 44.2, 46.5, 61.4, 76.5, 78.1, 127.8, 128.2, 132.6, 145.7. MS (EI) *m*/*z* 309 (1), 307 (1), 175 (2), 155 (63), 137 (3), 125 (34), 115 (6).

B4.7 2-(3-Chlorobicyclo[2.2.1]hept-2-ylsulfanyl)-5-(*p*-methoxyphenyl)-4-methylthiazole (18)

. Colorless oil. R_f = 0.16 for pentane:Et_2O = 20:1 (*v*/*v*). ^{1}H NMR ($CDCl_3$, 400 MHz) δ 1.43–1.53 (m, 3H), 1.70–1.74 (m, 1H), 1.78–1.81 (m, 1H), 1.98–2.06 (m, 1H), 2.43 (s, 3H), 2.46–2.50 (m, 2H), 3.36 (dd, 1H, J_d = 3.8, 3.1 Hz), 3.83 (s, 3H), 4.08 (dt, 1H, J_d = 4.1 Hz, J_t = 1.6 Hz), 6.92–7.00 (m, 2H), 7.30–7.42 (m, 2H). ^{13}C NMR ($CDCl_3$, 101 MHz) δ 16.0, 21.7, 28.7, 35.9, 44.2, 44.3, 55.3, 60.3, 66.4, 114.2, 124.0, 130.3, 133.6, 147.9, 158.1, 159.4. MS (EI) *m*/*z* 365 (14), 330 (3), 288 (3), 264 (2), 237 (100), 222 (5), 178 (4), 163 (5), 151 (5), 129 (3).

B5 Application of the p-Chlorocumyloxyl-"Radical Clock"

B5.1 Kinetic model

Formation of products **15** and **16e** from 3-(*p*-chlorocumyloxy)-thiazole-2(3*H*)-thione **1e**, bicyclohept[2.2.1]heptene (**14**), and $BrCCl_3$ according to a general mechanistic model[13] was assumed to occur via elementary reactions described in equations 1–4 (An = 4-H_3CO-C_6H_4, CP = 4-Cl-C_6H_4).

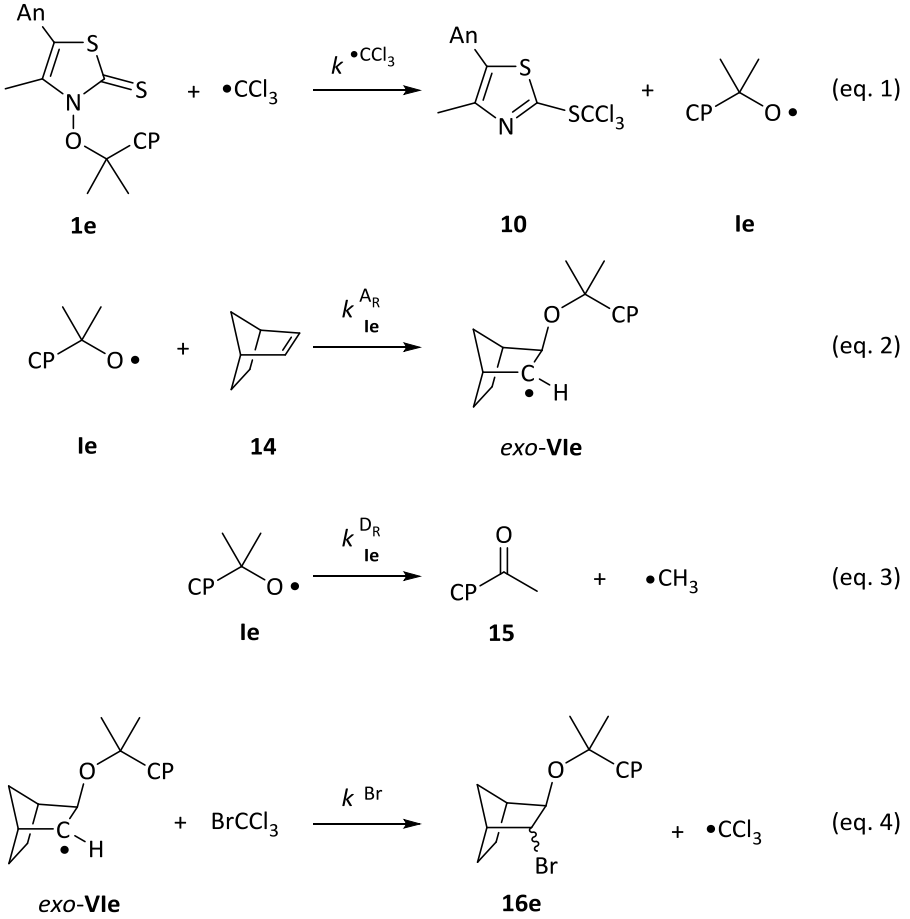

Formation of *p*-chlorocumyoxyl radical-derived products **15** and **16e** for analysis (GC), according to the model, was expressed by eqs. 5–6. Application of Bodenstein's quasi-stationary principle[14] allowed us to transform eq. 6 by replacing [*exo*-**VIe**] via eq. 7a into eq. 6a. Division eq. 6a by eq. 5, and integration of differential eq. 8a provided analytical expression eq. 8b used for determining $k^{AR}_{\mathbf{Ie}}$ on the basis of known value $k^{DR}_{\mathbf{Ie}} = 1.1 \times 10^6\ s^{-1}$ (in CH_3CN, 23 °C)[15] in section 5.2.

$$\frac{d[\mathbf{15}]}{dt} = k_{\mathbf{Ie}}^{D_R}[\mathbf{Ie}] \qquad \text{(eq. 5)}$$

$$\frac{d[\mathbf{16e}]}{dt} = k^{Br}[\textit{exo}\text{-}\mathbf{VIe}][BrCCl_3] \qquad \text{(eq. 6)}$$

$$\frac{d[\textit{exo}\text{-}\mathbf{VIe}]}{dt} = k_{\mathbf{Ie}}^{A_R}[\mathbf{Ie}][\mathbf{14}] - k^{Br}[\textit{exo}\text{-}\mathbf{VIe}][BrCCl_3] = 0 \qquad \text{(eq. 7)}$$

$$[\textit{exo}\text{-}\mathbf{VIe}] = \frac{k_{\mathbf{Ie}}^{A_R}[\mathbf{Ie}][\mathbf{14}]}{k^{Br}[BrCCl_3]} \qquad \text{(eq. 7a)}$$

eq. 7a ⟶ eq. 6

$$\frac{d[\mathbf{16e}]}{dt} = k^{Br}[BrCCl_3]\,\frac{k_{\mathbf{Ie}}^{A_R}[\mathbf{Ie}][\mathbf{14}]}{k^{Br}[BrCCl_3]} = k_{\mathbf{Ie}}^{A_R}[\mathbf{Ie}][\mathbf{14}] \qquad \text{(eq. 6a)}$$

eq. 6a : eq. 5

$$\frac{d[\mathbf{16e}]\,dt}{d[\mathbf{15}]\,dt} = \frac{k_{\mathbf{Ie}}^{A_R}[\mathbf{Ie}][\mathbf{14}]}{k_{\mathbf{Ie}}^{D_R}[\mathbf{Ie}]} \qquad \text{(eq. 8)}$$

$$d[\mathbf{16e}] = \frac{k_{\mathbf{Ie}}^{A_R}}{k_{\mathbf{Ie}}^{D_R}}[\mathbf{14}]\,d[\mathbf{15}] \qquad \text{(eq. 8a)}$$

$$\frac{[\mathbf{16e}]}{[\mathbf{15}]} = \frac{k_{\mathbf{Ie}}^{A_R}}{k_{\mathbf{Ie}}^{D_R}}[\mathbf{14}] \qquad \text{(eq. 8b)}$$

B5.2 Rate constant for *p*-Chlorocumyloxyl radical addition to norbornene 14

Table B1. Products formed from *p*-chlorocumyloxythiazolethione **1e** and $BrCCl_3$ at different norbornene concentrations

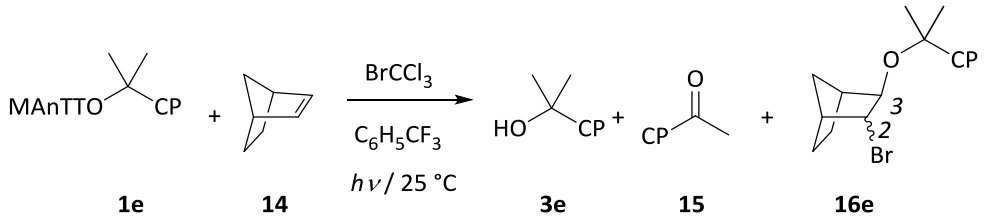

1e **14** **3e** **15** **16e**

entry	c_{14} / M	**3e** /%	**15** /%	**16e** (2-*exo*:2-*endo*) [a] /%	**16e**:**15**
1	0.210	27.0	18.5	36.0 (30:70)	1.95
2	0.105	29.5	29.5	29.5 (24:76)	1.00
3	0.050	37.5	26.5	12.0 (22:78)	0.45

[a] 3-*exo*-configuration for both stereoisomers.

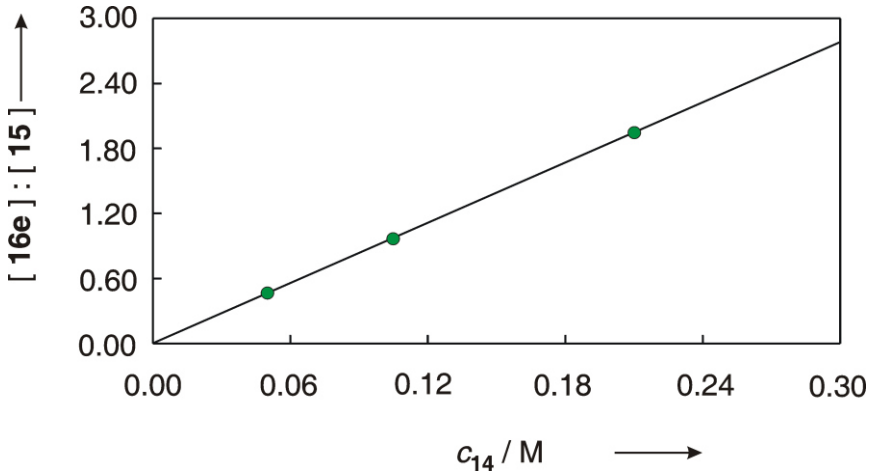

Figure B1. Plot of product ratio **16e**:**15** vs. norbornene concentration {[**16e**]:[**15**] = (9.331 M^{-1})[**14**] – 0.002; correlation coefficient (R^2) = 0.9997}.

Rate constant $k^{A_R cis}_{\mathbf{1e}}$ was calculated from the slope of the correlation obtained in Figure B1 on the basis of eq. 8b.

$$k^{A_R}_{\mathbf{1e}} = 9.331\ M^{-1} \qquad k^{D_R}_{\mathbf{1e}} = 1.03 \times 10^7\ M^{-1}s^{-1}$$

B6 Variable Temperature NMR Spectroscopy – Barrier to N,O-Rotation

B6.1 Experimental

A solution of *p*-chlorocumyloxythiazolethione **1e** (35–40 mg) in $CDCl_3$ (0.5 mL, 99.8 atom%, filtrated through basic Al_2O_3) was thermostated (15 min) at a preselected temperature, chosen at the instrument panel of the NMR spectrometer. The temperature inside the cavity was measured with a MeOH NMR–thermometer.[16,17]

Table B2. Temperaturedependent chemical shifts of selected protons in *p*-chlorocumyl ester **1e** (600.13 MHz, $CDCl_3$).

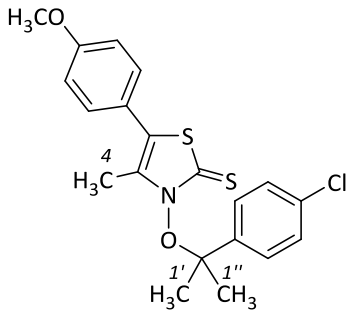

1e

entry	*T* / °C [a]	$\delta_{1'\text{-}CH_3}$	$\delta_{1''\text{-}CH_3}$	$\delta_{4\text{-}CH_3}$
1	–62	2.11	1.89	1.55
2	–13	2.08	1.88	1.60
3	–7	2.07	1.89	1.60
4 [b]	–3	2.03	1.93	1.62
5	3	1.99		1.63
6	10	1.99		1.63
7	20	1.99		1.65

[a] referenced versus the MeOH NMR thermometer. [b] signal coalescence

B6.2 Barrier to N,O-Rotation

The rate constant k^c for exchange of nuclei from two equally populated positions at coalescence temperature T_c can be approximated with eq. 9, whereby ν_a and ν_b denote resonance frequencies of associated nuclei at slow exchange.[18]

$$k^c = \frac{\pi\,(\nu_a - \nu_b)}{\sqrt{2}} \qquad \text{(eq. 9)}$$

k^c = rate of topomerization at T_c

$(\nu_a - \nu_b) = \Delta\delta 600.13\ s^{-1} = 132.1\ s^{-1}$

$k^c = 293.4\ s^{-1}$

The Gibbs free energy of activation of the process can be derived from the rate constant k^c of topomerization at coalescence temperature T_c via the Eyring equation (eq. 10).

$$\Delta G^{\ddagger}_{T_c} = -RT\,ln\ \frac{k_c\,h}{k^b\,\kappa\,T_c} \qquad \text{(eq. 10)}$$

κ = transmission coefficient ~ 1

k^b = Boltzmann constant = 1.381×10^{-23} J K^{-1}

h = Planck constant = 6.626×10^{-34} J s

T_c = 270 K

$$\Delta G^{\ddagger}_{T_c} = -2.24\ \text{kJ mol}^{-1}\ ln\ \frac{1.94 \cdot 10^{-31}}{3.73 \cdot 10^{-21}}$$

$$\Delta G^{\ddagger}_{T_c} = 53\ \text{kJ mol}^{-1}$$

B7 N–O/C=S Bond Length Correlation – Solid State Chemistry

Table B3. N–O and C=S bond lengths of thiazole-derived cyclic thiohydroxamates (X-ray diffraction).[19,20]

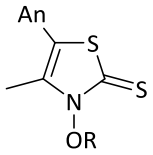

entry	number	R	$d_{N–O}$ / Å	$d_{C=S}$ / Å
1	–	Li	1.354(2)	1.701(2)
2	–	Li	1.367(2)	1.685(2)
3	**2**	H	1.373(3)	1.676(3)
4	– [a]	CH_3	1.391(3)	1.650(3)
5	– [a]	*n*-C_5H_{11}	1.370(6)	1.671(7)
6	– [a]	$CH(CH_3)_2$	1.389(2)	1.657(2)
7	– [a]	$(CH_2)_4C_6H_5$	1.381(2)	1.663(3)
8	**1d**	$C(CH_3)_2C_6H_5$	1.376(3)	1.649(3)
9	**1e**	$C(CH_3)_2$(*p*-ClC_6H_4)	1.382(2)	1.666(3)
10	– [a]	$C(O)C_6H_5$	1.389(2)	1.662(2)

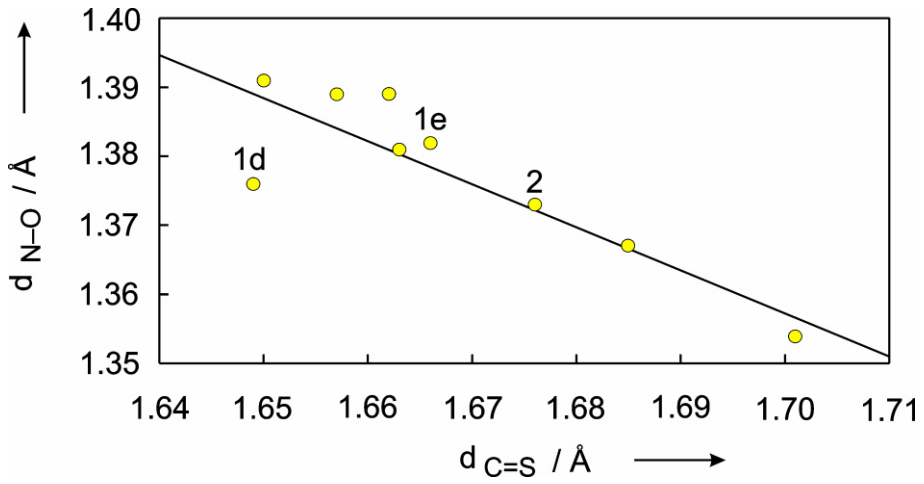

Figure B2. Plot of distances N–O versus C=S from the data provided in Table B3 [including **1e**: $d_{N–O} = – 0.62 d_{C=S} + 2.42$ Å; R2 = 0.86; without **1e**: $d_{N–O} = – 0.62 d_{C=S} + 2.41$ Å; $R^2 = 0.869$].

B8 Computational Chemistry

B8.1 Computational Details

All calculations were carried out with Gaussian03[21], using the density functional/Hartee-Fock hybrid models B3LYP and BHandHLYP, and split valance double-ζ basis set 6-31+G(d,p), and split valence triple-ζ basis set 6-311G(d,p). No symmetry or internal coordinate constraints were applied during energy function minimization. The ultrafine grid in combination with the tight option for energy function minimization was used. The absence of imaginary modes of vibration characterized computed structures as minima (for radicals **I** and **VII**). Transition structures *exo*/*endo*-**VI** were located with the Berny algorithm. Hessian matrices of transition structures had exactly one negative stretching mode (Table 4 of the associated manuscript). Animations of eigenvector coordinates using Molden[22] were performed to verify that the imaginary mode correlated with the trajectory of C,O bond formation. Approximate Gibbs free energies ($G_{298.15}$) were obtained through thermochemical analysis for 298.15 K by unscaled frequency calculation from the thermal correction reported by Gaussian03. Likewise obtained Gibbs free energies took into account zero-point correction, thermal correction, and entropy. All transition structures were maxima on electronic potential energy hypersurface, which may not correspond to maxima on the free energy surface.

B3LYP- and BHandHLYP-calculated equilibrium and transition structures differed slightly but not notably. For presentation, Ball-and-stick models of B3LYP-structures were selected in the following sections. Oxygen atoms are depicted in red, carbons in gray and hydrogens in white.

Table B4. Calculated zero-point vibrational energy (ZPVE)-corrected electronic energies (*E*, 0 K), expectation values of the spin operator $\langle S^2 \rangle$ (for radicals), and Gibbs free energies (*G*, 298.15K) for alkoxyl radical additions to norbornene **14**

method	**I** / R	parameter	**14**	**I**	*exo*-**VI**	*endo*-**VI**	*exo*-**VII**	*endo*-**VII**
B3LYP	**Ia** / *t*Bu	*E* + ZPVE / a.u. [a]	–272.597449	–232.907367	–505.530192	–505.530320	–505.499163	–505.493238
/6-31+G**		$\langle S^2 \rangle$	–	0.753498	0.75414	0.754067	0.777249	0.777507
		$G_{298.15}$ / a.u. [a]	–272.625980	–232.936930	–505.569029	–505.569257	–505.538594	–505.532554
BHandHLYP	**Ia** / *t*Bu	*E* + ZPVE / a.u. [a]	–272.415746	–232.760321	–505.204600	–505.204763	–505.163884	–505.156925
/6-31+G**		$\langle S^2 \rangle$	–	0.754915	0.755849	0.755732	0.8276	0.83058
		$G_{298.15}$ / a.u. [a]	–272.444168	–232.789724	–505.243003	–505.243120	–505.202675	–505.195687
BHandHLYP	**Ia** / *t*Bu	*E* + ZPVE / a.u. [a]	-272.460359	-232.803110	–505.292648	–505.293025	–505.252737	–505.245947
/6-311G**		$\langle S^2 \rangle$	–	0.754343	0.755884	0.755764	0.826274	0.829193
		$G_{298.15}$ / a.u. [a]	-272.488778	-232.832555	–505.331066	–505.331497	–505.291558	–505.284662
B3LYP	**Ig** / CH_3	*E* + ZPVE / a.u. [a]	–272.597449	–115.026937	–387.655063	–387.654399	–387.621461	–387.616656
/6-31+G**		$\langle S^2 \rangle$	–	0.753503	0.754029	0.754051	0.771286	0. 774342
		$G_{298.15}$ / a.u. [a]	–272.625980	–115.049881	–387.688595	–387.687957	–387.656581	–387.651046
BHandHLYP	**Ig** / CH_3	*E* + ZPVE / a.u. [a]	–272.415746	–114.961953	–387.411175	–387.410588	–387.368331	–387.362486
/6-31+G**		$\langle S^2 \rangle$	–	0.754978	0.755669	0.755729	0.823516	0.825317
		$G_{298.15}$ / a.u. [a]	–272.444168	–114.984871	–387.444475	–387.443913	–387.402773	–387.396585
BHandHLYP	**Ig** / CH_3	*E* + ZPVE / a.u. [a]	-272.460359	–114.985134	–387.479184	–387.478787	–387.437198	–387.431272
/6-311G**		$\langle S^2 \rangle$	–	0.75434	0.755705	0.755758	0.824633	0.825411
		$G_{298.15}$ / a.u. [a]	-272.488778	–115.008043	–387.512476	–387.512157	–387.471493	–387.465355

[a] 1 a.u. = 1 Hartree = 2625.5 kJ mol^{-1}

B8.2 Bicyclo[2.2.1]heptene (14)

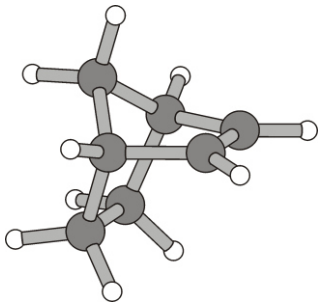

Figure B3. Equilibrium structure of olefin **14**.

B8.2.1 B3LYP/6-31+G**//B3LYP/6-31+G**

Standard orientation:

Center Number	Atomic Number	Atomic Type	Coordinates (Angstroms) X	Y	Z
1	6	0	1.192153	0.781430	-0.516665
2	6	0	1.192493	-0.781046	-0.516588
3	6	0	-0.088341	1.129424	0.323046
4	6	0	-0.087968	-1.129473	0.322992
5	6	0	-1.279449	-0.671914	-0.507989
6	6	0	-1.279742	0.671564	-0.507847
7	6	0	-0.041104	-0.000048	1.381048
8	1	0	1.147686	1.207409	-1.522986
9	1	0	2.087968	1.178725	-0.026514
10	1	0	2.088453	-1.177943	-0.026378
11	1	0	1.148226	-1.207117	-1.522878
12	1	0	-0.120506	2.158254	0.688878
13	1	0	-0.119837	-2.158328	0.688776
14	1	0	-1.923370	-1.328362	-1.084625
15	1	0	-1.923919	1.327860	-1.084369
16	1	0	-0.911736	-0.000218	2.043775
17	1	0	0.878779	0.000095	1.978333

```
Version=IA32L-G03RevC.01\State=1-A\HF=-272.750159\RMSD=5.182e-
09\RMSF=8.526e- 06\Dipole=-0.1278744,-0.0791881,0.0000053\PG=C01 [X(C7H10)]
\NImag=0\\@
```

B8.2.2 BHandHLYP/6-31+G**//BHandHLYP/6-31+G**

Standard orientation:

Center Number	Atomic Number	Atomic Type	Coordinates (Angstroms) X	Y	Z
1	6	0	-1.181443	-0.775938	-0.515108
2	6	0	-1.181283	0.776100	-0.515176
3	6	0	0.084867	-1.120795	0.320661
4	6	0	0.085048	1.120789	0.320641
5	6	0	1.272693	0.665456	-0.501571
6	6	0	1.272537	-0.665656	-0.501623
7	6	0	0.035979	0.000014	1.370520
8	1	0	-1.135634	-1.197813	-1.514213
9	1	0	-2.072892	-1.168742	-0.031764
10	1	0	-2.072675	1.169110	-0.031894
11	1	0	-1.135364	1.197889	-1.514312
12	1	0	0.117350	-2.141860	0.684073
13	1	0	0.117675	2.141858	0.684031
14	1	0	1.917380	1.316230	-1.068153
15	1	0	1.917086	-1.316538	-1.068240
16	1	0	0.896936	-0.000052	2.032078
17	1	0	-0.880243	0.000097	1.958328

Version=IA32L-G03RevC.01\State=1-A\HF=-272.5741559\RMSD=5.992e-09\RMSF=4.582
e-05\Dipole=-0.121767,-0.0712408,0.0000069\PG=C01 [X(C7H10)] \NImag=0\\@

B8.2.3 BHandHLYP/6-311G**//BHandHLYP/6-311G**

Standard orientation:

Center Number	Atomic Number	Atomic Type	Coordinates (Angstroms) X	Y	Z
1	6	0	-1.179838	-0.775457	-0.515057
2	6	0	-1.179681	0.775617	-0.515122
3	6	0	0.084576	-1.119656	0.321328
4	6	0	0.084754	1.119649	0.321310
5	6	0	1.270875	0.662729	-0.501841
6	6	0	1.270723	-0.662924	-0.501893
7	6	0	0.035941	0.000012	1.370618
8	1	0	-1.132163	-1.196247	-1.512813
9	1	0	-2.071119	-1.167333	-0.034072
10	1	0	-2.070905	1.167695	-0.034198
11	1	0	-1.131898	1.196323	-1.512909
12	1	0	0.118346	-2.139045	0.683699
13	1	0	0.118663	2.139040	0.683662
14	1	0	1.913785	1.312897	-1.068296
15	1	0	1.913498	-1.313197	-1.068383
16	1	0	0.896729	-0.000053	2.029658
17	1	0	-0.879039	0.000094	1.957586

Version=IA32L-G03RevC.01\State=1-A\HF=-272.6182395\RMSD=6.963e-09\
RMSF=5.004e-05\Dipole=-0.0965901,-0.0409814,0.0000031\PG=C01 [X(C7H10)]
\NImag=0\\@

B8.3 2-Methylprop-2-oxyl radical (Ia)

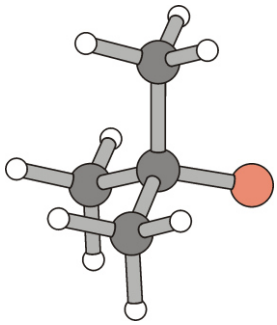

Figure B4. Presentation of computed equilibrium structure of *tert*-butoxyl radical **Ia**.

B8.3.1 B3LYP/6-31+G**//B3LYP/6-31+G**

Standard orientation:

Center Number	Atomic Number	Atomic Type	Coordinates (Angstroms) X	Y	Z
1	6	0	1.278236	-0.793405	-0.314685
2	6	0	-0.000001	-0.027353	0.080468
3	8	0	0.000006	0.263630	1.432455
4	6	0	-1.278269	-0.793352	-0.314685
5	6	0	0.000029	1.390203	-0.579731
6	1	0	1.308521	-0.975097	-1.394541
7	1	0	2.166591	-0.224815	-0.025433
8	1	0	1.308620	-1.761352	0.195649
9	1	0	-1.308568	-0.975032	-1.394542
10	1	0	-1.308686	-1.761303	0.195639
11	1	0	-2.166601	-0.224732	-0.025421
12	1	0	0.000021	1.255817	-1.666266
13	1	0	-0.890766	1.950479	-0.286461
14	1	0	0.890852	1.950438	-0.286468

```
Version=IA32L-G03RevC.01\State=2-A\HF=-233.0294646\S2=0.753498\S2-1=0\
S2A=0.75001\RMSD=0.000e+00\RMSF=5.737e-07\Dipole=-0.8567359,0.1107579,
-0.2639248\PG=C01 [X(C4H9O1)] \NImag=0\\@
```

B8.3.2 BHandHLYP/6-31+G**//BHandHLYP/6-31+G**

Standard orientation:

Center Number	Atomic Number	Atomic Type	Coordinates (Angstroms) X	Y	Z
1	6	0	1.264438	-0.781094	-0.323382
2	6	0	0.000000	-0.019375	0.067323
3	6	0	0.000010	1.387237	-0.555045
4	8	0	0.000001	0.229315	1.432123
5	6	0	-1.264449	-0.781076	-0.323383
6	1	0	1.297638	-0.950544	-1.396799
7	1	0	2.147477	-0.222159	-0.028920
8	1	0	1.291518	-1.747685	0.172572
9	1	0	-1.297650	-0.950528	-1.396800
10	1	0	-1.291543	-1.747666	0.172573
11	1	0	-2.147480	-0.222127	-0.028922
12	1	0	0.000009	1.290356	-1.637265
13	1	0	-0.883222	1.940847	-0.253251
14	1	0	0.883251	1.940834	-0.253253

Version=IA32L-G03RevC.01\State=2- A\HF=-232.8869029\S2=0.754915\S2-1=0.\
S2A=0.750019\RMSD=4.955e-09\RMSF =3.623e-06\Dipole=0.3969308,0.709421,
-0.2580331\PG=C01 [X(C4H9O1)] \NImag=0\\@

B8.3.3 BHandHLYP/6-311G**//BHandHLYP/6-311G**

Standard orientation:

Center Number	Atomic Number	Atomic Type	Coordinates (Angstroms) X	Y	Z
1	6	0	1.263815	-0.780220	-0.323488
2	6	0	-0.000001	-0.019492	0.067770
3	6	0	0.000026	1.386296	-0.553717
4	8	0	0.000013	0.228039	1.428215
5	6	0	-1.263850	-0.780168	-0.323479
6	1	0	1.302188	-0.948570	-1.395863
7	1	0	2.143997	-0.221824	-0.023884
8	1	0	1.289122	-1.746046	0.171718
9	1	0	-1.302242	-0.948512	-1.395854
10	1	0	-1.289190	-1.745994	0.171724
11	1	0	-2.144008	-0.221738	-0.023864
12	1	0	0.000019	1.294166	-1.635120
13	1	0	-0.881884	1.937877	-0.248547
14	1	0	0.881961	1.937840	-0.248554

Version=IA32L-G03RevC.01\State=2 -A\HF=-232.9290535\S2=0.754343\S2-1=0.\
S2A=0.750014\RMSD=4.054e-09\RMS F=9.270e-07\Dipole=0.3663205,0.6401794,
-0.2298882\PG=C01 [X(C4H9O1)] \NImag=0\\ @

B8.4 Methoxyl radical (Ig)

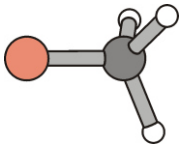

Figure B5. View onto calculated equilibrium structure of radical (**Ig**).

B8.4.1 B3LYP/6-31+G**//B3LYP/6-31+G**

Standard orientation:

Center Number	Atomic Number	Atomic Type	Coordinates (Angstroms) X	Y	Z
1	8	0	-0.011097	0.793492	0.000000
2	6	0	-0.011097	-0.576802	0.000000
3	1	0	1.060636	-0.867581	0.000000
4	1	0	-0.452637	-1.009771	0.911583
5	1	0	-0.452637	-1.009771	-0.911583

```
Version=IA32L-G03RevC.01\State=2-A'\HF=-115.0632982\S2=0.753503\S2-1=0.\
S2A=0.750009\RMSD=0.000e+00\RMSF=1.257e-04\Dipole=0.0927509, 0.,0.8822137\
PG=CS[SG(C1H1O1),X(H2)] \NImag=0\\@
```

B8.4.2 BHandHLYP/6-31+G**//BHandHLYP/6-31+G**

Standard orientation:

Center Number	Atomic Number	Atomic Type	Coordinates (Angstroms) X	Y	Z
1	8	0	-0.008715	0.791526	0.000000
2	6	0	-0.008715	-0.579044	0.000000
3	1	0	1.048158	-0.870214	0.000000
4	1	0	-0.463072	-0.993864	0.900138
5	1	0	-0.463072	-0.993864	-0.900138

```
Version=IA32L-G03RevC.01\State=2-A'\HF=-115.000193\S2=0.754978\
S2-1=0.\S2A=0.750019\RMSD=6.510e-09\RMSF=4.143e-05\Dipole=0.0777554,
0.,0.8523819\PG=CS [SG(C1H1O1),X(H2)] \NImag=0\\@
```

B8.4.3 BHandHLYP/6-311G**//BHandHLYP/6-311G**

Standard orientation:

Center Number	Atomic Number	Atomic Type	Coordinates (Angstroms) X	Y	Z
1	8	0	-0.009151	0.789657	0.000000
2	6	0	-0.009151	-0.575754	0.000000
3	1	0	1.046955	-0.868803	0.000000
4	1	0	-0.459417	-0.996965	0.898948
5	1	0	-0.459417	-0.996965	-0.898948

```
Version=IA32L-G03RevC.01\State=2-A'\HF=-115.0231824\S2=0.75434\S2-1=0\
S2A=0.750014\RMSD=5.253e-09\RMSF=1.197e-04\Dipole=0.0772223,0,0.7878534\
PG=CS [SG(C1H1O1),X(H2)] \NImag=0\\@
```

B8.5 Transition structures for *exo*-addition to norbornene

B8.5.1 *tert*-Butoxyl radical addition

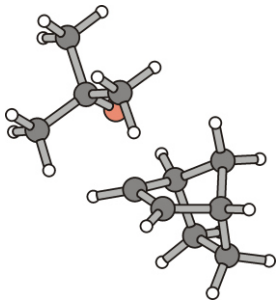

Figure B6. Presentation of computed transition structure *exo*-**VIIa**.

B8.5.1.1 B3LYP/6-31+G**//B3LYP/6-31+G**

Standard orientation:

Center Number	Atomic Number	Atomic Type	Coordinates (Angstroms) X	Y	Z
1	6	0	1.650133	0.026508	-1.348892
2	6	0	1.535070	-1.082415	-0.277665
3	6	0	0.610975	-0.405543	0.719710
4	6	0	0.948185	0.930901	0.712354
5	6	0	2.029777	1.126894	-0.326799
6	6	0	3.323644	0.491320	0.300862
7	6	0	2.967931	-1.030256	0.353153
8	8	0	-1.165375	-0.672127	-0.377550
9	6	0	-2.346949	-0.006317	-0.010138
10	6	0	-2.343067	1.462526	-0.477405
11	6	0	-3.450017	-0.788001	-0.773580
12	6	0	-2.614406	-0.098198	1.505440
13	1	0	0.616986	1.684072	1.419731
14	1	0	0.137098	-0.925869	1.541347
15	1	0	1.210354	-2.068722	-0.610891
16	1	0	3.664898	-1.622256	-0.249446
17	1	0	2.988148	-1.435085	1.369813
18	1	0	4.184047	0.680214	-0.350969
19	1	0	3.555239	0.910353	1.284619
20	1	0	2.165600	2.143811	-0.701376
21	1	0	2.442601	-0.162871	-2.081907
22	1	0	0.701336	0.210960	-1.854466
23	1	0	-3.468077	-1.832741	-0.450910
24	1	0	-3.259340	-0.759090	-1.850137
25	1	0	-4.429424	-0.337368	-0.576599
26	1	0	-1.859811	0.460798	2.069066
27	1	0	-2.588834	-1.142535	1.833203
28	1	0	-3.595577	0.320065	1.757223
29	1	0	-1.559916	2.025965	0.039442
30	1	0	-3.305182	1.948883	-0.276947
31	1	0	-2.144796	1.513915	-1.552634

Version=IA32L-G03RevC.01\State=2-A\HF=-505.7754284\S2=0.777249\S2-1=0.\
S2A=0.750136\RMSD=6.787e-09\RMSF=3.762e-07\Dipole=0.1307209,-0.5624869,
0.110702\PG=C01 [X(C11H19O1)] \NImag=1\\@

B8.5.1.2 BHandHLYP/6-31+G**//BHandHLYP/6-31+G**

Standard orientation:

Center Number	Atomic Number	Atomic Type	Coordinates (Angstroms) X	Y	Z
1	6	0	2.925839	-1.016879	0.350032
2	6	0	1.508200	-1.077630	-0.279212
3	6	0	1.615986	0.027819	-1.337982
4	6	0	1.985291	1.118479	-0.320369
5	6	0	3.269845	0.496910	0.300517
6	6	0	0.907146	0.914450	0.711875
7	6	0	0.575945	-0.417219	0.710038
8	8	0	-1.140167	-0.705621	-0.352547
9	6	0	-2.302362	-0.004661	-0.010626
10	6	0	-2.551923	-0.022300	1.496518
11	6	0	-2.271222	1.427114	-0.542275
12	6	0	-3.410205	-0.794747	-0.722754
13	1	0	0.576479	1.655371	1.419818
14	1	0	0.129707	-0.939451	1.535715
15	1	0	1.194024	-2.057510	-0.615731
16	1	0	3.625096	-1.598689	-0.244978
17	1	0	2.945496	-1.418724	1.359187
18	1	0	4.125306	0.687753	-0.343451
19	1	0	3.496406	0.911507	1.278364
20	1	0	2.110590	2.129561	-0.691258
21	1	0	2.405808	-0.153593	-2.063856
22	1	0	0.675978	0.206607	-1.844582
23	1	0	-3.445260	-1.814854	-0.352807
24	1	0	-3.226478	-0.822343	-1.792605
25	1	0	-4.374886	-0.323997	-0.547825
26	1	0	-1.792716	0.548192	2.024934
27	1	0	-2.538081	-1.043004	1.869456
28	1	0	-3.519229	0.415906	1.731209
29	1	0	-1.485699	1.999836	-0.058546
30	1	0	-3.219283	1.931289	-0.365899
31	1	0	-2.077154	1.423096	-1.611350

Version=IA32L-G03RevC.01\State=2-A\HF=-505.450111\S2=0.8276\S2-1=0.\
S2A=0.75076\RMSD=6.406e-09\RMSF=2.101e-07\Dipole=0.0918505,-0.3767342,
-0.3405594\PG=C01 [X(C11H19O1)] \NImag=1\\@

B8.5.1.3 BHandHLYP/6-311G**//BHandHLYP/6-311G**

Standard orientation:

Center Number	Atomic Number	Atomic Type	Coordinates (Angstroms) X	Y	Z
1	6	0	2.916769	-1.016474	0.356053
2	6	0	1.502178	-1.076189	-0.276014
3	6	0	1.613108	0.023568	-1.338772
4	6	0	1.983802	1.116644	-0.325791
5	6	0	3.264748	0.495215	0.299644
6	6	0	0.905765	0.918796	0.706606
7	6	0	0.570296	-0.408562	0.707672
8	8	0	-1.123776	-0.672276	-0.368890
9	6	0	-2.295740	-0.003669	-0.009489
10	6	0	-2.557028	-0.082037	1.492724
11	6	0	-2.286264	1.446482	-0.486139
12	6	0	-3.382396	-0.785827	-0.759864
13	1	0	0.579603	1.661219	1.412563
14	1	0	0.125068	-0.926218	1.534958
15	1	0	1.183332	-2.054239	-0.607078
16	1	0	3.615630	-1.602250	-0.232590
17	1	0	2.931995	-1.411837	1.366167
18	1	0	4.120917	0.679845	-0.342587
19	1	0	3.489898	0.913033	1.274688
20	1	0	2.111079	2.124210	-0.699878
21	1	0	2.401985	-0.162133	-2.062267
22	1	0	0.673611	0.200093	-1.842548
23	1	0	-3.396114	-1.818909	-0.430528
24	1	0	-3.187491	-0.768083	-1.826643
25	1	0	-4.357617	-0.343924	-0.576118
26	1	0	-1.815293	0.484760	2.047071
27	1	0	-2.521211	-1.114549	1.826112
28	1	0	-3.534880	0.323855	1.736257
29	1	0	-1.517236	2.013456	0.027224
30	1	0	-3.244095	1.926717	-0.302470
31	1	0	-2.080395	1.485475	-1.550993

Version=IA32L-G03RevC.01\State=2-A\HF=-505.5378831\S2=0.826274\S2-1=0.\
S2A=0.750717\RMSD=8.987e-09\RMSF=2.276e-07\Dipole=0.0524465,-0.3505709,
-0.3231135\PG=C01 [X(C11H19O1)] \NImag=1\\@

B8.5.2 Methoxyl radical addition

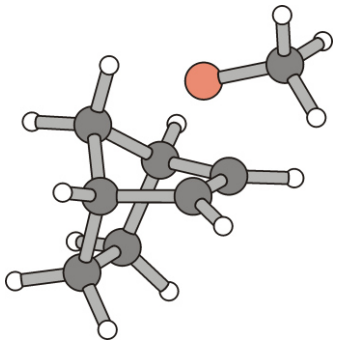

Figure B7. Projection of computed transition structure *exo*-**VIIg**.

B8.5.2.1 B3LYP/6-31+G**//B3LYP/6-31+G**

Standard orientation:

Center Number	Atomic Number	Atomic Type	Coordinates (Angstroms) X	Y	Z
1	6	0	-1.965429	-0.923210	-0.582552
2	6	0	-0.540487	-1.080663	0.052041
3	6	0	0.386170	-0.206235	-0.773147
4	6	0	-2.338019	0.557684	-0.249011
5	6	0	-1.066349	1.070847	0.520270
6	6	0	0.045556	1.091482	-0.507079
7	6	0	-0.691334	-0.203661	1.317692
8	1	0	-2.664619	-1.624167	-0.114197
9	1	0	-1.964830	-1.128614	-1.657418
10	1	0	-0.208817	-2.110248	0.192438
11	1	0	0.956095	-0.556505	-1.625067
12	1	0	-3.215553	0.612532	0.404770
13	1	0	-2.550944	1.155735	-1.139982
14	1	0	-1.223335	1.993457	1.083071
15	1	0	0.412563	1.976700	-1.016302
16	1	0	0.245592	-0.107493	1.868592
17	1	0	-1.494520	-0.541048	1.982953
18	8	0	2.240308	-0.480723	0.399437
19	6	0	3.311678	0.202960	-0.160349
20	1	0	3.438163	0.010977	-1.239667
21	1	0	3.279243	1.289900	0.016202
22	1	0	4.217781	-0.180667	0.341919

```
Version=IA32L-G03RevC.01\State =2-A\HF=-387.8133082\S2=0.771286\S2-1=0.\
S2A=0.750103\RMSD=6.112e-09\R MSF=3.213e-07\Dipole=0.3839915,0.1219603,
-0.4942681\PG=C01 [X(C8H13O1)] \NImag=1\\@
```

B8.5.2.2 BHandHLYP/6-31+G**//BHandHLYP/6-31+G**

Standard orientation:

Center Number	Atomic Number	Atomic Type	Coordinates (Angstroms) X	Y	Z
1	6	0	-1.917876	-0.914779	-0.584881
2	6	0	-0.515365	-1.070934	0.062898
3	6	0	0.425090	-0.209574	-0.747184
4	6	0	-2.294326	0.555859	-0.257731
5	6	0	-1.043050	1.066359	0.514604
6	6	0	0.072883	1.086024	-0.498032
7	6	0	-0.677880	-0.195189	1.313279
8	1	0	-2.619692	-1.610419	-0.131956
9	1	0	-1.902544	-1.116883	-1.652099
10	1	0	-0.188200	-2.092341	0.211837
11	1	0	0.951756	-0.556276	-1.618401
12	1	0	-3.173034	0.606483	0.381040
13	1	0	-2.499199	1.147425	-1.145051
14	1	0	-1.202467	1.983237	1.070675
15	1	0	0.432487	1.960627	-1.013205
16	1	0	0.243805	-0.100166	1.873801
17	1	0	-1.483416	-0.528210	1.964424
18	8	0	2.165772	-0.537912	0.347057
19	6	0	3.208057	0.236082	-0.132865
20	1	0	3.350418	0.133837	-1.211209
21	1	0	3.107039	1.292203	0.119371
22	1	0	4.111669	-0.139307	0.353795

```
Version=IA32L-G03Rev C.01\State=2-A\HF=-387.5674795\S2=0.823516\S2-1=0.\
S2A=0.750695\RMSD=3 .233e-09\RMSF=1.720e-07\Dipole=0.4277155,0.1430398,
-0.3918539\PG=C01 [X(C8H13O1)] \NImag=1\\@
```

B8.5.2.3 BHandHLYP/6-311G**//BHandHLYP/6-311G**

Standard orientation:

Center Number	Atomic Number	Atomic Type	Coordinates (Angstroms) X	Y	Z
1	6	0	-1.917032	-0.911948	-0.572525
2	6	0	-0.512583	-1.071007	0.065782
3	6	0	0.426252	-0.217888	-0.754156
4	6	0	-2.285121	0.560597	-0.248821
5	6	0	-1.026697	1.068972	0.510499
6	6	0	0.079184	1.077994	-0.511999
7	6	0	-0.659642	-0.188815	1.312210
8	1	0	-2.618386	-1.601665	-0.113655
9	1	0	-1.908993	-1.117125	-1.637661
10	1	0	-0.186184	-2.090317	0.216630
11	1	0	0.936893	-0.569921	-1.631024
12	1	0	-3.157745	0.616801	0.395221
13	1	0	-2.493684	1.148081	-1.136067
14	1	0	-1.176804	1.987932	1.062061
15	1	0	0.434445	1.946384	-1.037257
16	1	0	0.268353	-0.095618	1.858399
17	1	0	-1.458804	-0.514393	1.972328
18	8	0	2.142080	-0.548497	0.328304
19	6	0	3.182532	0.241829	-0.118374
20	1	0	3.338502	0.173276	-1.197051
21	1	0	3.081068	1.290094	0.162185
22	1	0	4.083343	-0.143960	0.363768

Version=IA32L-G03RevC.01\State=2-A\HF=-387.6356399\S2=0.824633\S2-1=0.\
S2A=0.750669\RMSD =8.700e-09\RMSF=1.897e-07\Dipole=0.4155684,0.122025,
-0.3354518\PG=C01 [X(C8H13O1)] \NImag=1\\@

B8.6 Transition structure for *endo*-addition to norbornene

B8.6.1 *tert*-Butoxyl radical addition

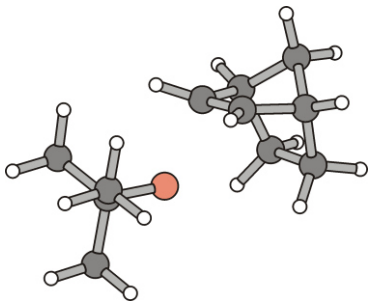

Figure B8. Projection of computed transition structure *endo*-**VIIa**.

B8.6.1.1 B3LYP/6-31+G**//B3LYP/6-31+G**

Standard orientation:

Center Number	Atomic Number	Atomic Type	Coordinates (Angstroms) X	Y	Z
1	6	0	2.955127	-0.552211	0.637645
2	6	0	1.681688	0.161399	1.171742
3	6	0	0.604481	-0.759384	0.597635
4	6	0	1.098565	-1.227715	-0.603291
5	6	0	2.442950	-0.575260	-0.829549
6	6	0	2.201450	0.957956	-1.078476
7	6	0	1.738854	1.469256	0.320019
8	8	0	-0.931347	0.519417	-0.059309
9	6	0	-2.254723	0.037431	-0.020747
10	6	0	-3.086080	1.211512	-0.597976
11	6	0	-2.434847	-1.203080	-0.919378
12	6	0	-2.722625	-0.259658	1.419226
13	1	0	0.592481	-1.889973	-1.295808
14	1	0	-0.167446	-1.223365	1.193663
15	1	0	1.618350	0.330212	2.248628
16	1	0	2.480051	2.146146	0.758759
17	1	0	0.776190	1.975939	0.284745
18	1	0	3.133417	1.434319	-1.402511
19	1	0	1.447602	1.126230	-1.851061
20	1	0	3.076371	-1.056229	-1.578156
21	1	0	3.866959	0.042497	0.773262
22	1	0	3.105961	-1.553181	1.054004
23	1	0	-3.487658	-1.504668	-0.964050
24	1	0	-2.089778	-0.986313	-1.934933
25	1	0	-1.860769	-2.052032	-0.532915
26	1	0	-3.791036	-0.503376	1.447198
27	1	0	-2.182879	-1.110318	1.850019
28	1	0	-2.548478	0.612581	2.057075
29	1	0	-4.150334	0.949288	-0.610981
30	1	0	-2.953765	2.108126	0.014663
31	1	0	-2.763506	1.437305	-1.618228

Version=IA32L-G03RevC.01\State=2-A\HF=-505.7695819\S2=0.777507\S2-1=0.\
S2A= 0.750135\RMSD=5.730e-09\RMSF=5.796e-07\Dipole=0.1468195,0.2770078,
-0.3475227\PG=C01 [X(C11H19O1)] \NImag=1\\@

B8.6.1.2 BHandHLYP/6-31+G**//BHandHLYP/6-31+G**

Standard orientation:

Center Number	Atomic Number	Atomic Type	Coordinates (Angstroms) X	Y	Z
1	6	0	1.726481	1.462411	0.301391
2	6	0	1.648593	0.176249	1.159790
3	6	0	2.911336	-0.547474	0.649638
4	6	0	2.416413	-0.583479	-0.809963
5	6	0	2.187430	0.931934	-1.079079
6	6	0	1.072865	-1.226391	-0.588255
7	6	0	0.571280	-0.736660	0.592221
8	8	0	-0.916500	0.537082	-0.027549
9	6	0	-2.225844	0.037375	-0.022264
10	6	0	-2.712667	-0.267010	1.395467
11	6	0	-3.047380	1.194545	-0.606232
12	6	0	-2.365394	-1.190929	-0.920464
13	1	0	0.578255	-1.897707	-1.267312
14	1	0	-0.186340	-1.200952	1.191792
15	1	0	1.578353	0.356712	2.226312
16	1	0	2.471364	2.127451	0.731928
17	1	0	0.781996	1.984187	0.255350
18	1	0	3.114145	1.399464	-1.403390
19	1	0	1.442502	1.093949	-1.850633
20	1	0	3.049174	-1.076580	-1.539392
21	1	0	3.819151	0.037877	0.786579
22	1	0	3.050081	-1.537249	1.075409
23	1	0	-3.407047	-1.494972	-0.995467
24	1	0	-1.995903	-0.970036	-1.917647
25	1	0	-1.802539	-2.031842	-0.523789
26	1	0	-3.771925	-0.514548	1.398126
27	1	0	-2.181509	-1.109686	1.830982
28	1	0	-2.558970	0.597768	2.034831
29	1	0	-4.100795	0.926155	-0.642749
30	1	0	-2.937642	2.083821	0.007417
31	1	0	-2.709038	1.426105	-1.611449

Version=IA32L-G03RevC.01\State=2-A\HF=-505.4432472\S2=0.83058 1\S2-1=0.\
S2A=0.7508\RMSD=8.479e-09\RMSF=3.298e-07\Dipole=0.1511735,-0.1364009,
0.3610895\PG=C01 [X(C11H19O1)] \NImag=1\\@

B8.6.1.3 BHandHLYP/6-311G**//BHandHLYP/6-311G**

Standard orientation:

Center Number	Atomic Number	Atomic Type	Coordinates (Angstroms) X	Y	Z
1	6	0	1.710456	1.460363	0.308337
2	6	0	1.646807	0.171293	1.160313
3	6	0	2.909008	-0.542338	0.638162
4	6	0	2.402680	-0.575993	-0.816599
5	6	0	2.156029	0.937243	-1.078677
6	6	0	1.066964	-1.229361	-0.585511
7	6	0	0.570528	-0.743742	0.594593
8	8	0	-0.902465	0.524708	-0.035064
9	6	0	-2.212226	0.036166	-0.021181
10	6	0	-2.697929	-0.245116	1.400510
11	6	0	-3.023593	1.192193	-0.618651
12	6	0	-2.364051	-1.201165	-0.903144
13	1	0	0.573908	-1.904898	-1.258927
14	1	0	-0.180009	-1.213448	1.196466
15	1	0	1.582231	0.345064	2.226373
16	1	0	2.457234	2.125354	0.731985
17	1	0	0.764357	1.975635	0.275953
18	1	0	3.070929	1.414958	-1.416246
19	1	0	1.396867	1.092114	-1.835217
20	1	0	3.032130	-1.060258	-1.551988
21	1	0	3.812751	0.047495	0.770049
22	1	0	3.055514	-1.531823	1.057777
23	1	0	-3.407276	-1.496115	-0.976358
24	1	0	-1.990889	-0.995480	-1.900836
25	1	0	-1.809610	-2.041056	-0.495766
26	1	0	-3.759495	-0.477072	1.412463
27	1	0	-2.176003	-1.088674	1.842528
28	1	0	-2.527706	0.624355	2.027040
29	1	0	-4.078422	0.934398	-0.654091
30	1	0	-2.904834	2.085996	-0.015563
31	1	0	-2.679998	1.408538	-1.624044

```
Version=IA32L-G03RevC.01\State=2-A\HF=-505.5312054\S2=0.829193\S2-1=0.\
S2A=0.750754\RMSD=4.045e-09\RMSF=3.893e-07\Dipole=0.1416015,-0.1366442,
0.3617564\PG=C01 [X(C11H19O1)] \NImag=1\\@
```

B8.6.2 Methoxyl radical addition

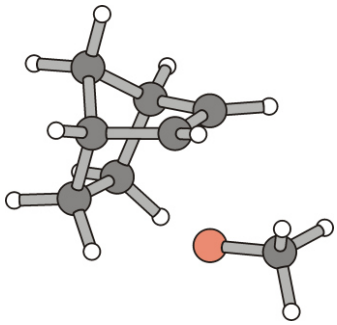

Figure B9. Depiction of calcuated transition structure *endo*-**VIIg**.

B8.6.2.1 B3LYP/6-31+G**//B3LYP/6-31+G**

Standard orientation:

Center Number	Atomic Number	Atomic Type	Coordinates (Angstroms) X	Y	Z
1	6	0	-1.969425	-0.651849	-0.550604
2	6	0	-1.351305	-0.641754	0.874462
3	6	0	-1.175860	0.903639	1.104504
4	6	0	-0.837020	1.432655	-0.322778
5	6	0	-0.777930	0.125169	-1.176568
6	6	0	0.385583	-0.728817	-0.677866
7	6	0	0.009461	-1.218125	0.552744
8	8	0	1.900368	0.606970	-0.016694
9	6	0	3.107277	-0.071056	0.130183
10	1	0	3.414565	-0.626165	-0.773548
11	1	0	3.878045	0.694792	0.320985
12	1	0	3.119910	-0.758515	0.992297
13	1	0	0.100866	1.984805	-0.354077
14	1	0	-1.637325	2.073609	-0.708298
15	1	0	-2.108850	1.330360	1.488967
16	1	0	-0.381523	1.116344	1.823394
17	1	0	-1.901103	-1.153161	1.667636
18	1	0	0.607758	-1.834668	1.214383
19	1	0	1.175703	-1.106146	-1.312833
20	1	0	-0.800444	0.291793	-2.255364
21	1	0	-2.096328	-1.660880	-0.955318
22	1	0	-2.918910	-0.107096	-0.619140

Version=IA32L-G03RevC.01\State=2-A\HF=-387.8088563\S2=0.774342\S2-1=0.\
S2A=0.750115\RMSD=4.527e-09\RMSF=6.655e-07\Dipole=-0.5510019,0.2038605,
-0.0931718\PG=C01 [X(C8H13O1)] \NImag=1\\@

B8.6.2.2 BHandHLYP/6-31+G**//BHandHLYP/6-31+G**

Standard orientation:

Center Number	Atomic Number	Atomic Type	Coordinates (Angstroms) X	Y	Z
1	6	0	-1.939796	-0.623668	-0.577690
2	6	0	-1.333575	-0.678885	0.838114
3	6	0	-1.162768	0.838062	1.141857
4	6	0	-0.831655	1.435095	-0.248876
5	6	0	-0.758211	0.181571	-1.155174
6	6	0	0.404465	-0.685159	-0.697752
7	6	0	0.022287	-1.239479	0.495185
8	8	0	1.875401	0.620105	-0.077154
9	6	0	3.043395	-0.078732	0.174948
10	1	0	3.369443	-0.687914	-0.672049
11	1	0	3.816089	0.671662	0.357120
12	1	0	2.980724	-0.708233	1.064296
13	1	0	0.088668	2.000929	-0.252610
14	1	0	-1.636014	2.077214	-0.599677
15	1	0	-2.086459	1.244855	1.546558
16	1	0	-0.372759	1.016565	1.863133
17	1	0	-1.882379	-1.227642	1.595229
18	1	0	0.607196	-1.894771	1.117029
19	1	0	1.168296	-1.054225	-1.355847
20	1	0	-0.777203	0.397241	-2.217166
21	1	0	-2.059688	-1.605451	-1.026999
22	1	0	-2.883971	-0.083894	-0.625457

```
Version=IA32L-G03RevC.01\State=2-A\HF=-387.5618926\S2=0.825317\S2-1=0.\
S2A=0.750716\RMSD=8.707e-09\RMSF=6.097e-07\Dipole=-
0.5353475,0.0890887,0.0246542\PG=C01 [X(C8H13O1)] \NImag=1\\@
```

B8.6.2.3 BHandHLYP/6-311G**//BHandHLYP/6-311G**

Standard orientation:

Center Number	Atomic Number	Atomic Type	Coordinates (Angstroms) X	Y	Z
1	6	0	-1.940607	-0.619523	-0.564697
2	6	0	-1.324274	-0.669428	0.845846
3	6	0	-1.135544	0.846825	1.138837
4	6	0	-0.820404	1.433522	-0.258737
5	6	0	-0.759333	0.174454	-1.155135
6	6	0	0.402477	-0.693863	-0.697548
7	6	0	0.023266	-1.242614	0.495140
8	8	0	1.850554	0.609558	-0.081527
9	6	0	3.023896	-0.072499	0.172378
10	1	0	3.359213	-0.683549	-0.669135
11	1	0	3.788350	0.686759	0.347932
12	1	0	2.975471	-0.696486	1.065746
13	1	0	0.099855	1.995000	-0.277075
14	1	0	-1.627068	2.073428	-0.603851
15	1	0	-2.046265	1.265555	1.556474
16	1	0	-0.331174	1.019995	1.842723
17	1	0	-1.870603	-1.207765	1.609533
18	1	0	0.605192	-1.901719	1.112978
19	1	0	1.157445	-1.072767	-1.357949
20	1	0	-0.783560	0.381192	-2.216898
21	1	0	-2.067799	-1.602445	-1.005450
22	1	0	-2.880355	-0.074920	-0.609319

```
Version=IA32L-G03RevC01\State=2-A\HF=-387.6299408\S2=0.825411\S2-1=0.\
S2A=0.750681\RMSD=4.886e-09\RMSF=6.304e-07\Dipole=-0.5066365,0.0273559,
0.0297472\PG=C01 [X(C8H13O1)] \NImag=1\\@
```

B8.7 *exo*-Alkoxyl radical addition products

B8.7.1 *exo*-2-(2-Methylprop-2-yl)-bicyclo[2.2.1]hept-3-yl radical *exo*-(VIa)

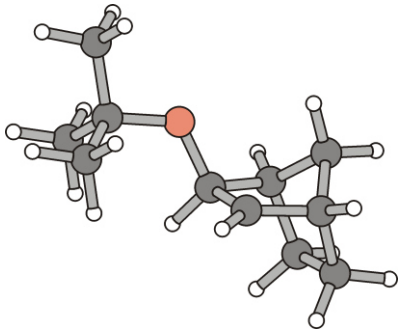

Figure B10. Presentation of computed equilibrium structure of addition product *exo*-**VIa**.

B8.7.1.1 B3LYP/6-31+G**//B3LYP/6-31+G**

Standard orientation:

Center Number	Atomic Number	Atomic Type	Coordinates (Angstroms) X	Y	Z
1	6	0	1.931420	-0.135063	1.392386
2	6	0	1.326917	0.953506	0.476092
3	6	0	0.229320	0.156894	-0.271392
4	6	0	0.931659	-1.166195	-0.471778
5	6	0	2.263708	-1.097864	0.220330
6	6	0	3.187224	-0.181906	-0.648463
7	6	0	2.495926	1.215365	-0.511906
8	8	0	-0.932327	0.049846	0.579729
9	6	0	-2.246955	0.016234	-0.021608
10	6	0	-2.589602	1.382726	-0.642302
11	6	0	-2.364734	-1.105785	-1.067207
12	6	0	-3.176739	-0.268828	1.163439
13	1	0	-0.049406	0.649184	-1.212549
14	1	0	0.935182	1.847783	0.965881
15	1	0	3.184090	1.959975	-0.098743
16	1	0	2.142275	1.602736	-1.474239
17	1	0	4.203861	-0.169411	-0.236703
18	1	0	3.254012	-0.525524	-1.685137
19	1	0	2.710509	-2.061760	0.477950
20	1	0	2.822747	0.203470	1.933156
21	1	0	1.208098	-0.547377	2.100437
22	1	0	0.587523	-1.971435	-1.111335
23	1	0	-3.392525	-1.166757	-1.441201
24	1	0	-1.711492	-0.930580	-1.928219
25	1	0	-2.101765	-2.070769	-0.623169
26	1	0	-4.222515	-0.294060	0.839191
27	1	0	-2.926850	-1.232210	1.618064
28	1	0	-3.066146	0.507920	1.926227
29	1	0	-3.620998	1.386794	-1.011859
30	1	0	-2.488044	2.173525	0.107488
31	1	0	-1.938800	1.625237	-1.488620

Version=IA32L-G03RevC.01\State=2-A\HF=-505.8083172\S2=0.75414\S2-1=0.\
S2A=0.750012\RMSD=5.776e-09\RMSF=5.794e-07\Dipole=0.1269521,-0.2805339,
0.2934444\PG=C01 [X(C11H19O1)] \NImag=0\\@

B8.7.1.2 BHandHLYP/6-31+G**// BHandHLYP/6-31+G**

Standard orientation:

Center Number	Atomic Number	Atomic Type	Coordinates (Angstroms) X	Y	Z
1	6	0	2.479772	1.199762	-0.511757
2	6	0	1.316820	0.952220	0.468406
3	6	0	1.908209	-0.128959	1.382829
4	6	0	2.238735	-1.089081	0.225490
5	6	0	3.159400	-0.191436	-0.638073
6	6	0	0.912866	-1.154784	-0.466712
7	6	0	0.221018	0.168816	-0.269795
8	8	0	-0.923535	0.078671	0.566866
9	6	0	-2.221532	0.015174	-0.019672
10	6	0	-3.142697	-0.257811	1.160386
11	6	0	-2.582137	1.354059	-0.661348
12	6	0	-2.326036	-1.118847	-1.036584
13	1	0	-0.044668	0.654436	-1.207997
14	1	0	0.933966	1.844764	0.950458
15	1	0	3.166296	1.937212	-0.104947
16	1	0	2.132637	1.580715	-1.469679
17	1	0	4.167717	-0.179311	-0.228590
18	1	0	3.226839	-0.537534	-1.665404
19	1	0	2.673480	-2.047982	0.487780
20	1	0	2.792067	0.205467	1.921951
21	1	0	1.185575	-0.531760	2.084691
22	1	0	0.589044	-1.936424	-1.131967
23	1	0	-3.346892	-1.199989	-1.401379
24	1	0	-1.683231	-0.950941	-1.896674
25	1	0	-2.049005	-2.064420	-0.579343
26	1	0	-4.180036	-0.304043	0.838536
27	1	0	-2.880535	-1.201342	1.630062
28	1	0	-3.043536	0.529487	1.902015
29	1	0	-3.608178	1.337625	-1.020824
30	1	0	-2.485855	2.154348	0.067067
31	1	0	-1.943909	1.585648	-1.509708

Version=IA32L-G03RevC.01\State=2-A\HF=-505.4930388\S2=0.755849\S2-1=0.\
S2A=0.750024\RMSD=9.960e-09\RMSF=4.579e-07\Dipole=-0.2479711,-0.2461896,
-0.2824854\PG=C01 [X(C11H19O1)] \NImag=0\\@

B8.7.1.3 BHandHLYP/6-311G**// BHandHLYP/6-311G**

Standard orientation:

Center Number	Atomic Number	Atomic Type	Coordinates (Angstroms) X	Y	Z
1	6	0	0.221485	0.172998	-0.280017
2	6	0	1.314127	0.955581	0.460521
3	6	0	2.483703	1.194944	-0.511245
4	6	0	3.160424	-0.197537	-0.625257
5	6	0	2.228781	-1.089157	0.230718
6	6	0	0.911476	-1.150295	-0.474851
7	6	0	1.890275	-0.126048	1.382292
8	8	0	-0.918408	0.082172	0.560325
9	6	0	-2.216769	0.014861	-0.019696
10	6	0	-2.323253	-1.114673	-1.039582
11	6	0	-3.128119	-0.265643	1.164471
12	6	0	-2.584627	1.353860	-0.653983
13	1	0	-0.044261	0.657550	-1.217146
14	1	0	0.929511	1.848342	0.936281
15	1	0	3.168914	1.931644	-0.105164
16	1	0	2.144399	1.570071	-1.472461
17	1	0	4.162803	-0.186099	-0.205449
18	1	0	3.237505	-0.547100	-1.649028
19	1	0	2.656578	-2.047404	0.498993
20	1	0	2.767632	0.203383	1.931664
21	1	0	1.154780	-0.522576	2.071366
22	1	0	0.588615	-1.931760	-1.137945
23	1	0	-3.345312	-1.200668	-1.396318
24	1	0	-1.688106	-0.939506	-1.902432
25	1	0	-2.036921	-2.058876	-0.588095
26	1	0	-4.167412	-0.311913	0.853172
27	1	0	-2.858337	-1.209602	1.625904
28	1	0	-3.021082	0.517075	1.907920
29	1	0	-3.610982	1.337382	-1.009046
30	1	0	-2.486324	2.149732	0.077176
31	1	0	-1.949768	1.589604	-1.502227

Version=IA32L-G03RevC.01\State=2-A\HF=-505.5799994\S2=0.755884\S2-1=0.\
S2A=0.750024\RMSD=4.505e-09\RMSF=3.983e-07\Dipole=0.345931,0.1509597,
-0.2041926\PG=C01 [X(C11H19O1)] \NImag=0\\@

B8.7.2 *exo*-2-Methoxybicyclo[2.2.1]hept-3-yl radical *exo*-(VIg)

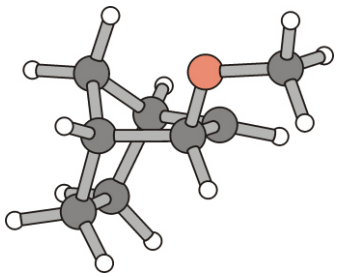

Figure B11. Projection of calculated equilibrium structure of addition product *exo*-**VIg**.

B8.7.2.1 B3LYP/6-31+G**//B3LYP/6-31+G**

Standard orientation:

Center Number	Atomic Number	Atomic Type	Coordinates (Angstroms) X	Y	Z
1	6	0	-1.661698	-1.022423	-0.675955
2	6	0	-0.427216	-1.045731	0.264783
3	6	0	-0.864246	-0.064971	1.377081
4	6	0	-1.139067	1.105621	0.396497
5	6	0	-2.194183	0.443706	-0.551479
6	6	0	0.710808	-0.255438	-0.416700
7	6	0	0.158402	1.151558	-0.360169
8	8	0	1.917192	-0.446722	0.345805
9	6	0	3.054402	0.186096	-0.213455
10	1	0	0.503835	1.989083	-0.957658
11	1	0	0.903398	-0.602743	-1.446819
12	1	0	-1.466555	2.055008	0.828461
13	1	0	-0.112903	-2.042767	0.581297
14	1	0	-2.410370	-1.746232	-0.338553
15	1	0	-1.398860	-1.286379	-1.706401
16	1	0	-3.187796	0.473472	-0.088052
17	1	0	-2.263729	0.956052	-1.515860
18	1	0	-1.762886	-0.394073	1.911109
19	1	0	-0.068704	0.147518	2.095663
20	1	0	2.955371	1.280865	-0.220858
21	1	0	3.239800	-0.159633	-1.243080
22	1	0	3.908646	-0.086905	0.410691

Version=IA32L-G03RevC.01\State=2-A\HF=-387.8496843\S2=0.754029\S2-1=0.\
S2A=0.750011\RMSD=2.375e-09\RMSF=2.092e-06\Dipole=0.0167779,-0.3171147,
-0. 3960057 \PG=C01 [X(C8H13O1)] \NImag=0\\@

B8.7.2.2 BHandHLYP/6-31+G**//BHandHLYP/6-31+G**

Standard orientation:

Center Number	Atomic Number	Atomic Type	Coordinates (Angstroms) X	Y	Z
1	6	0	-0.852446	-0.065401	1.366672
2	6	0	-1.130116	1.095994	0.396174
3	6	0	0.161821	1.143842	-0.359376
4	6	0	0.710076	-0.259429	-0.414276
5	6	0	-0.422387	-1.039308	0.261415
6	6	0	-2.176508	0.443352	-0.542165
7	6	0	-1.648374	-1.011934	-0.670872
8	8	0	1.898374	-0.446197	0.334133
9	6	0	3.022958	0.188963	-0.205354
10	1	0	0.485595	1.964706	-0.977151
11	1	0	0.892872	-0.602722	-1.437589
12	1	0	-1.450187	2.038190	0.828746
13	1	0	-0.113030	-2.030155	0.574478
14	1	0	-2.391838	-1.730605	-0.337692
15	1	0	-1.388960	-1.270981	-1.694716
16	1	0	-3.162397	0.469228	-0.082196
17	1	0	-2.247930	0.953545	-1.498446
18	1	0	-1.742001	-0.393473	1.899924
19	1	0	-0.060348	0.144845	2.077533
20	1	0	2.915707	1.273910	-0.205636
21	1	0	3.214070	-0.144894	-1.228030
22	1	0	3.871307	-0.078493	0.414411

Version=IA32L-G03RevC.01\State=2-A\HF=-387.6805774\S2=0.755705\S2-1=0.\
S2A=0.750023\RMSD=5.186e-09\RMSF=5.330e-07\Dipole=0.006409,0.1447087,
0.4622867\PG=C01 [X(C8H13O1)] \NImag=0\\@

B8.7.2.3 BHandHLYP/6-311G**//BHandHLYP/6-311G**

Standard orientation:

Center Number	Atomic Number	Atomic Type	Coordinates (Angstroms) X	Y	Z
1	6	0	-0.836548	-0.067454	1.365334
2	6	0	-1.122787	1.094769	0.399514
3	6	0	0.159271	1.141115	-0.369885
4	6	0	0.708645	-0.260894	-0.422449
5	6	0	-0.421049	-1.040267	0.255122
6	6	0	-2.178557	0.445372	-0.528596
7	6	0	-1.651935	-1.008367	-0.667661
8	8	0	1.890283	-0.444988	0.332447
9	6	0	3.014881	0.189227	-0.201482
10	1	0	0.476235	1.959420	-0.991739
11	1	0	0.893103	-0.604840	-1.443715
12	1	0	-1.436835	2.035056	0.836016
13	1	0	-0.108578	-2.029663	0.562810
14	1	0	-2.393132	-1.727208	-0.335003
15	1	0	-1.398481	-1.261065	-1.692914
16	1	0	-3.157983	0.468875	-0.058474
17	1	0	-2.259991	0.957989	-1.480957
18	1	0	-1.718233	-0.392742	1.909849
19	1	0	-0.033073	0.139466	2.061409
20	1	0	2.909553	1.273602	-0.205265
21	1	0	3.213135	-0.144524	-1.222159
22	1	0	3.860490	-0.075464	0.421183

```
Version=IA32L-G03RevC.01\State=2-A\HF=-387.6805645\S2=0.755709\S2-1=0.\
S2A=0.750023\RMSD=9.218e-09\RMSF=6.124e-06\Dipole=-0.177376,0.3724172,
-0.252896\PG=C01 [X(C8H13O1)] \NImag=0\\@
```

B8.8. *endo*-Addition products

B8.8.2 *endo*-2-(2-Methylprop-2-yl)-bicyclo[2.2.1]hept-3-yl radical *endo*-(VIa)

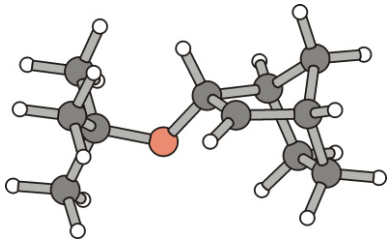

Figure B12. View onto calculated equilibrium structure of addition product *endo*-**VIa**.

B8.8.1.1 B3LYP/6-31+G**//B3LYP/6-31+G**

Standard orientation:

Center Number	Atomic Number	Atomic Type	Coordinates (Angstroms) X	Y	Z
1	6	0	-2.509104	0.441242	1.110581
2	6	0	-1.353811	-0.571875	0.958040
3	6	0	-0.224590	0.351505	0.414692
4	6	0	-1.011561	1.261161	-0.501983
5	6	0	-2.462161	0.898786	-0.372494
6	6	0	-2.665253	-0.471628	-1.103809
7	6	0	-1.872082	-1.467322	-0.195955
8	8	0	0.799093	-0.398159	-0.248637
9	6	0	2.185141	-0.033898	-0.046470
10	6	0	2.437677	1.432150	-0.436074
11	6	0	2.609240	-0.300572	1.408806
12	6	0	2.944517	-0.970499	-0.992579
13	1	0	0.214064	0.905118	1.258718
14	1	0	-1.060224	-1.123241	1.855406
15	1	0	-2.528378	-2.248844	0.201589
16	1	0	-1.049969	-1.955793	-0.723213
17	1	0	-3.732704	-0.722037	-1.145213
18	1	0	-2.289809	-0.445531	-2.131041
19	1	0	-3.173780	1.670704	-0.678173
20	1	0	-3.457792	-0.033528	1.386156
21	1	0	-2.296931	1.250719	1.817692
22	1	0	-0.571507	1.795395	-1.337517
23	1	0	3.682650	-0.119499	1.531782
24	1	0	2.085590	0.349468	2.117103
25	1	0	2.401589	-1.341039	1.677521
26	1	0	4.023783	-0.798190	-0.924775
27	1	0	2.741086	-2.014777	-0.736509
28	1	0	2.627418	-0.803864	-2.026475
29	1	0	3.502212	1.671905	-0.341035
30	1	0	2.138031	1.608206	-1.474000
31	1	0	1.883849	2.125803	0.204555

Version=IA32L-G03RevC.01\State=2-A\HF=-505.8086376\S2=0.754067\S2-1=0.\
S2A=0.750012\RMSD=3.741e-09\RMSF=6.828e-07\Dipole=0.1503416,0.310807,
-0.0262525\PG=C01 [X(C11H19O1)] \NImag=0\\@

B8.8.1.2 BHandHLYP/6-31+G**// BHandHLYP/6-31+G**

Standard orientation:

Center Number	Atomic Number	Atomic Type	Coordinates (Angstroms) X	Y	Z
1	6	0	-1.859512	-1.453957	-0.200021
2	6	0	-1.349398	-0.573301	0.953670
3	6	0	-2.491343	0.439143	1.098708
4	6	0	-2.433838	0.895266	-0.370929
5	6	0	-2.636687	-0.457437	-1.101867
6	6	0	-0.985374	1.247206	-0.491105
7	6	0	-0.217906	0.333605	0.429633
8	8	0	0.794096	-0.415221	-0.208696
9	6	0	2.159706	-0.034109	-0.047350
10	6	0	2.913603	-0.974986	-0.975352
11	6	0	2.385045	1.414149	-0.473768
12	6	0	2.612036	-0.255967	1.394807
13	1	0	0.206138	0.884888	1.270731
14	1	0	-1.070545	-1.127238	1.844407
15	1	0	-2.517585	-2.228442	0.185652
16	1	0	-1.042400	-1.940259	-0.719991
17	1	0	-3.696007	-0.703552	-1.150592
18	1	0	-2.258083	-0.430523	-2.119378
19	1	0	-3.131075	1.669494	-0.674496
20	1	0	-3.437289	-0.026927	1.365430
21	1	0	-2.280505	1.239668	1.804004
22	1	0	-0.539789	1.749104	-1.333174
23	1	0	3.678474	-0.066593	1.488915
24	1	0	2.102042	0.404233	2.090845
25	1	0	2.417954	-1.282703	1.692321
26	1	0	3.982997	-0.785077	-0.931911
27	1	0	2.732394	-2.007384	-0.690593
28	1	0	2.577254	-0.841079	-1.999328
29	1	0	3.439837	1.666753	-0.401028
30	1	0	2.070455	1.558844	-1.503633
31	1	0	1.834966	2.110888	0.152828

Version=IA32L-G03RevC.01\State=2-A\HF=-505.4934696\S2=0.755732\S2-1=0.\
S2A=0.750024\RMSD=7.169e-09\RMSF=2.960e-07\Dipole=-0.0279848,-0.0496281,
0.3485412\PG=C01 [X(C11H19O1)] \NImag=0\\@

B8.8.1.3 BHandHLYP/6-311G**// BHandHLYP/6-311G**

Standard orientation:

Center Number	Atomic Number	Atomic Type	Coordinates (Angstroms) X	Y	Z
1	6	0	-2.490589	0.441345	1.095280
2	6	0	-1.343228	-0.563913	0.957630
3	6	0	-0.218469	0.344202	0.424071
4	6	0	-0.991505	1.248354	-0.498597
5	6	0	-2.435885	0.887624	-0.376676
6	6	0	-2.628262	-0.470497	-1.098224
7	6	0	-1.843616	-1.454560	-0.190916
8	8	0	0.790230	-0.404570	-0.215504
9	6	0	2.155520	-0.033781	-0.046595
10	6	0	2.392660	1.413752	-0.464902
11	6	0	2.599435	-0.265598	1.395228
12	6	0	2.904374	-0.974868	-0.976203
13	1	0	0.206430	0.902650	1.258438
14	1	0	-1.060357	-1.108525	1.850520
15	1	0	-2.493286	-2.233751	0.195082
16	1	0	-1.019828	-1.931209	-0.705216
17	1	0	-3.683974	-0.725515	-1.144737
18	1	0	-2.250215	-0.446806	-2.114270
19	1	0	-3.137791	1.653240	-0.684652
20	1	0	-3.432540	-0.027549	1.364583
21	1	0	-2.283994	1.247305	1.793079
22	1	0	-0.549467	1.756882	-1.336497
23	1	0	3.665919	-0.086999	1.496296
24	1	0	2.091021	0.395214	2.089991
25	1	0	2.393608	-1.290730	1.685889
26	1	0	3.973953	-0.792988	-0.933145
27	1	0	2.714712	-2.005320	-0.694875
28	1	0	2.566678	-0.834970	-1.997528
29	1	0	3.447572	1.659330	-0.387505
30	1	0	2.082533	1.564083	-1.494098
31	1	0	1.844566	2.109864	0.162113

```
Version=IA32L-G03RevC.01\State=2-A\HF=-505.5806208\S2=0.755764\S2-1=0.\
S2A=0.750024\RMSD=7.224e-09\RMSF=3.523e-07\Dipole=0.1916781,0.2966779,
-0.0478412\PG=C01 [X(C11H19O1)] \NImag=0\\@
```

B8.8.2 *endo*-2-Methoxybicyclo[2.2.1]hept-3-yl radical *endo*-(VIg)

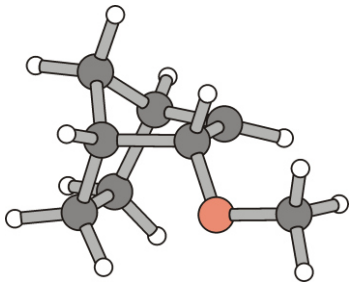

Figure B13. Presentation of calculated equilibrium structure of addition product *endo*-**VIg**.

B8.8.2.1 B3LYP/6-31+G**//B3LYP/6-31+G**

Standard orientation:

Center Number	Atomic Number	Atomic Type	Coordinates (Angstroms) X	Y	Z
1	6	0	1.573266	-0.525040	1.065917
2	6	0	1.394296	-0.980084	-0.407762
3	6	0	-0.084063	-1.237459	-0.436465
4	6	0	-0.735487	-0.266727	0.523064
5	6	0	0.486191	0.569491	0.984691
6	6	0	1.644961	0.371219	-1.160001
7	6	0	0.991789	1.423841	-0.206195
8	8	0	-1.743490	0.572936	-0.048210
9	6	0	-2.992463	-0.070004	-0.227994
10	1	0	-0.610565	-1.777191	-1.216758
11	1	0	-1.181376	-0.783813	1.394103
12	1	0	2.025410	-1.802123	-0.756165
13	1	0	0.293203	1.140637	1.896240
14	1	0	1.730717	2.152047	0.144558
15	1	0	0.176878	1.974650	-0.680136
16	1	0	2.722382	0.541907	-1.276594
17	1	0	1.198683	0.371349	-2.158822
18	1	0	2.569212	-0.118368	1.274874
19	1	0	1.351216	-1.315708	1.790771
20	1	0	-3.382901	-0.459562	0.725198
21	1	0	-3.684712	0.680989	-0.615985
22	1	0	-2.931168	-0.899730	-0.947136

```
Version=IA32L-G03RevC.01\State=2-A\HF=-387.8490635\S2=0.754051\S2-1=0.\
S2A=0.750012\RMSD=8.800e-09\RMSF=1.094e-06\Dipole=0.0504018,-0.3307045,
0.0387918\PG=C01 [X(C8H13O1)] \NImag=0\\@
```

B8.8.2.2 BHandHLYP/6-31+G**//BHandHLYP/6-31+G**

Standard orientation:

Center Number	Atomic Number	Atomic Type	Coordinates (Angstroms) X	Y	Z
1	6	0	1.558898	-0.511950	1.063129
2	6	0	1.386282	-0.974636	-0.395294
3	6	0	-0.086881	-1.230921	-0.426775
4	6	0	-0.733457	-0.256662	0.524014
5	6	0	0.480004	0.574076	0.972382
6	6	0	1.634261	0.355836	-1.152883
7	6	0	0.981231	1.409761	-0.218506
8	8	0	-1.729868	0.564083	-0.043019
9	6	0	-2.962534	-0.071964	-0.230591
10	1	0	-0.607772	-1.739040	-1.220808
11	1	0	-1.167263	-0.769560	1.391364
12	1	0	2.011185	-1.796233	-0.729897
13	1	0	0.290018	1.151115	1.871189
14	1	0	1.712640	2.138209	0.121785
15	1	0	0.171789	1.949379	-0.695894
16	1	0	2.702791	0.529081	-1.267298
17	1	0	1.194686	0.346553	-2.145890
18	1	0	2.546833	-0.106920	1.269943
19	1	0	1.336729	-1.290787	1.788675
20	1	0	-3.357720	-0.454625	0.712749
21	1	0	-3.649652	0.667487	-0.625999
22	1	0	-2.892149	-0.898562	-0.938619

Version=IA32L-G03RevC.01\State=2-A\HF=-387.6127583\S2=0.755729\S2-1=0.\
S2A=0.750023\RMSD=2.434e-09\RMSF=6.704e-07\Dipole=0.0738833,-0.3431338,
0.0527005\PG=C01 [X(C8H13O1)] \NImag=0\\@

B8.8.2.3 BHandHLYP/6-311G**//BHandHLYP/6-311G**

Standard orientation:

Center Number	Atomic Number	Atomic Type	Coordinates (Angstroms) X	Y	Z
1	6	0	1.562791	-0.515379	1.056477
2	6	0	1.387550	-0.967385	-0.404151
3	6	0	-0.082601	-1.231001	-0.432242
4	6	0	-0.731461	-0.264980	0.523464
5	6	0	0.479154	0.564731	0.978101
6	6	0	1.624911	0.369389	-1.151851
7	6	0	0.967848	1.411454	-0.208707
8	8	0	-1.723081	0.560779	-0.038310
9	6	0	-2.954716	-0.069891	-0.230764
10	1	0	-0.602570	-1.749009	-1.218222
11	1	0	-1.165049	-0.785751	1.384795
12	1	0	2.015281	-1.781219	-0.746328
13	1	0	0.288329	1.132674	1.880159
14	1	0	1.692796	2.144842	0.129769
15	1	0	0.149896	1.942223	-0.677016
16	1	0	2.690367	0.551002	-1.267245
17	1	0	1.183099	0.364165	-2.142121
18	1	0	2.548235	-0.108318	1.262787
19	1	0	1.345736	-1.300184	1.774641
20	1	0	-3.353301	-0.457931	0.708217
21	1	0	-3.640239	0.671708	-0.621638
22	1	0	-2.888791	-0.892060	-0.943277

Version=IA32L-G03RevC.01\State=2-A\HF=-387.6802129\S2=0.755758\S2-1=0.\
S2A=0.750023\RMSD=3.764e-09\RMSF=8.677e-07\Dipole=0.1088815,-0.3286462,
0.057588\PG=C01 [X(C8H13O1)] \NImag=0\\@

B9 ^{1}H and ^{13}C NMR-Spectra of Selected Thiazole Derivatives

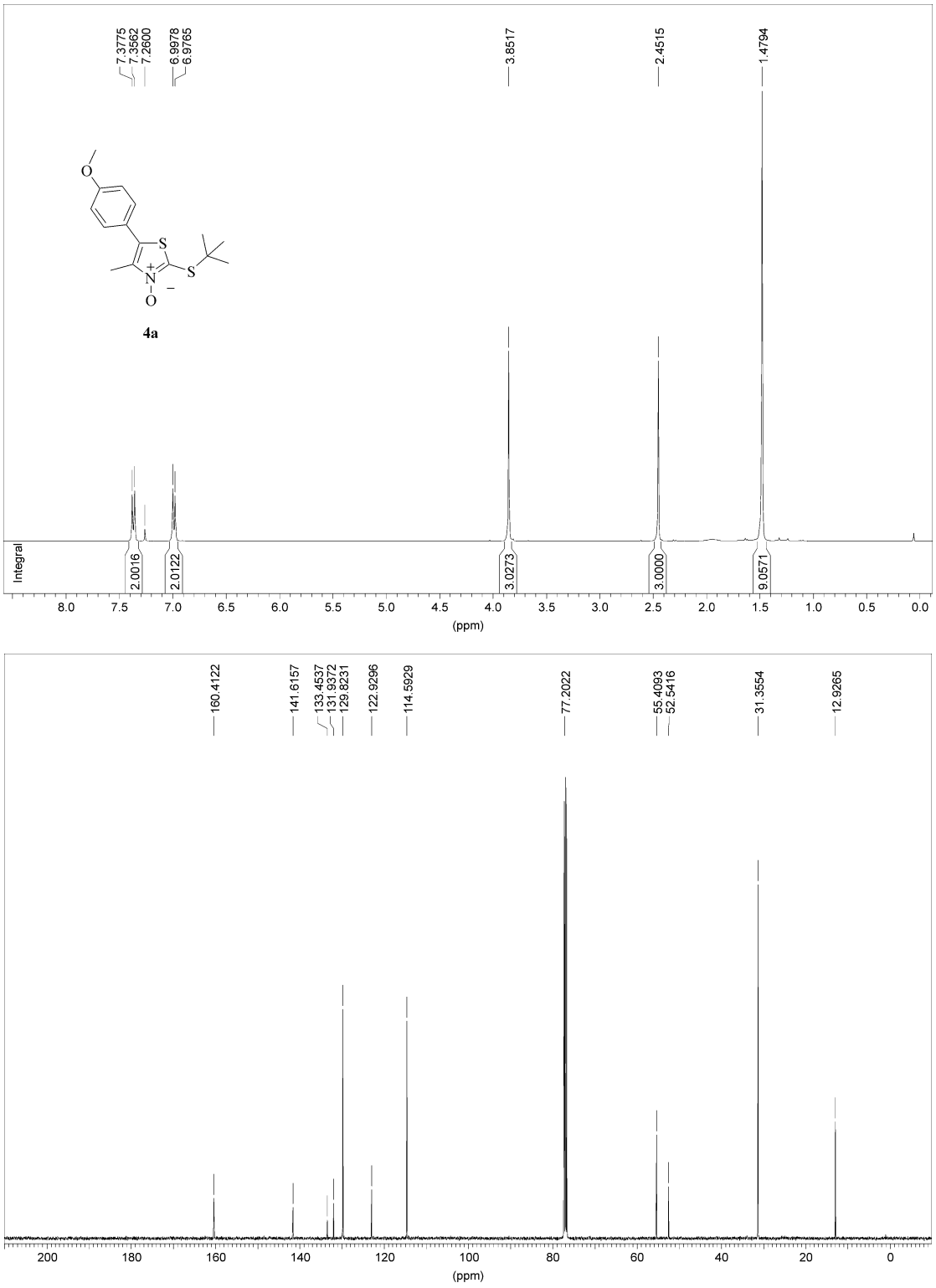

Figure B14. ^{1}H (400 MHz; top) and ^{13}C NMR spectra (101 MHz; bottom) of 2-(2-methyl-propyl-2-sulfanyl)-5-(4-methoxyphenyl)-4-methylthiazole *N*-Oxide (**4a**) in $CDCl_3$.[23]

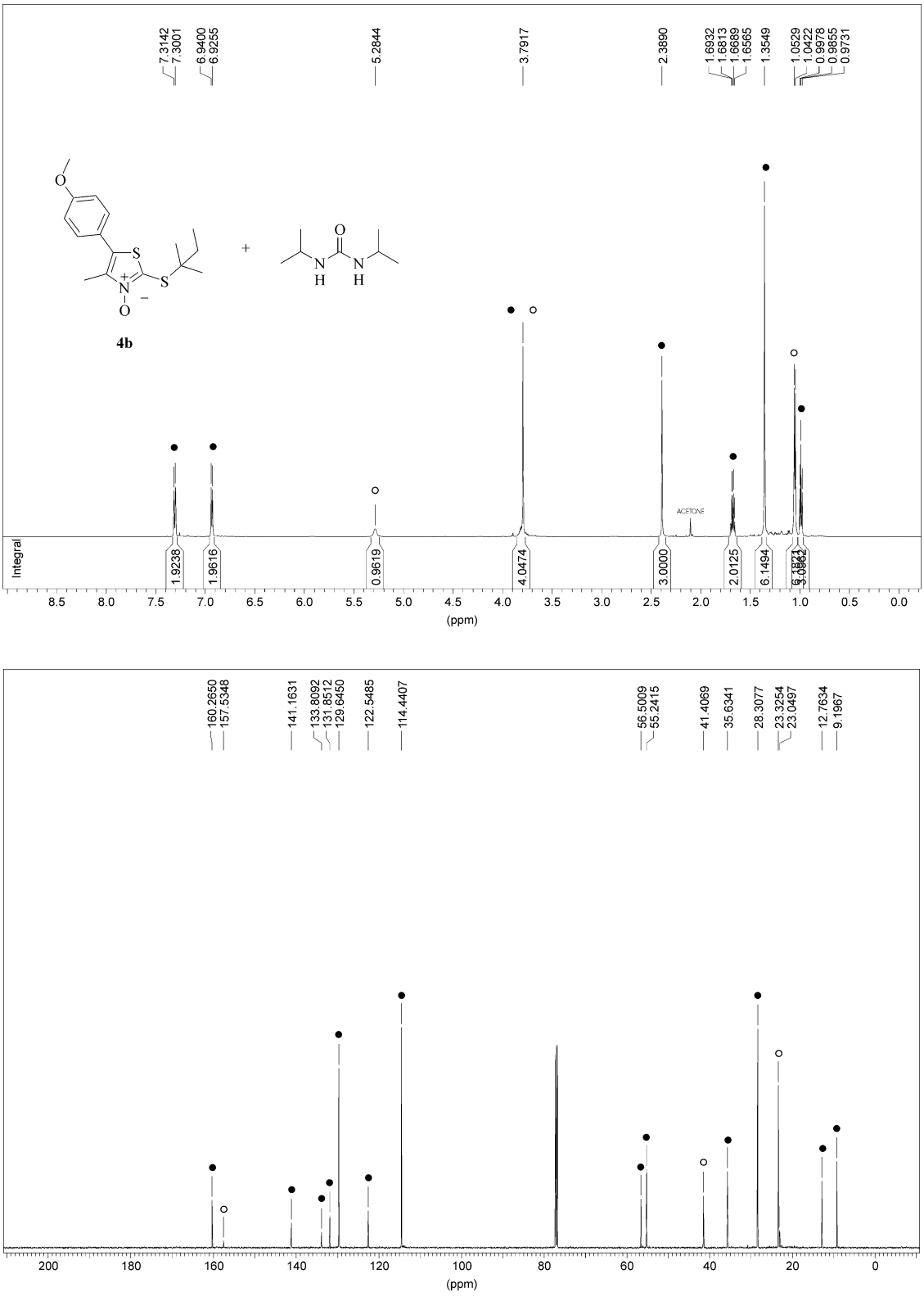

Figure B15. ^{1}H (600 MHz; top) and ^{13}C NMR spectra (151 MHz; bottom) of 2-(2-methyl-butyl-2-sulfanyl)-5-(4-methoxyphenyl)-4-methylthiazole *N*-Oxide (**4b**) (●) and isopropyl urea (○) in $CDCl_3$.

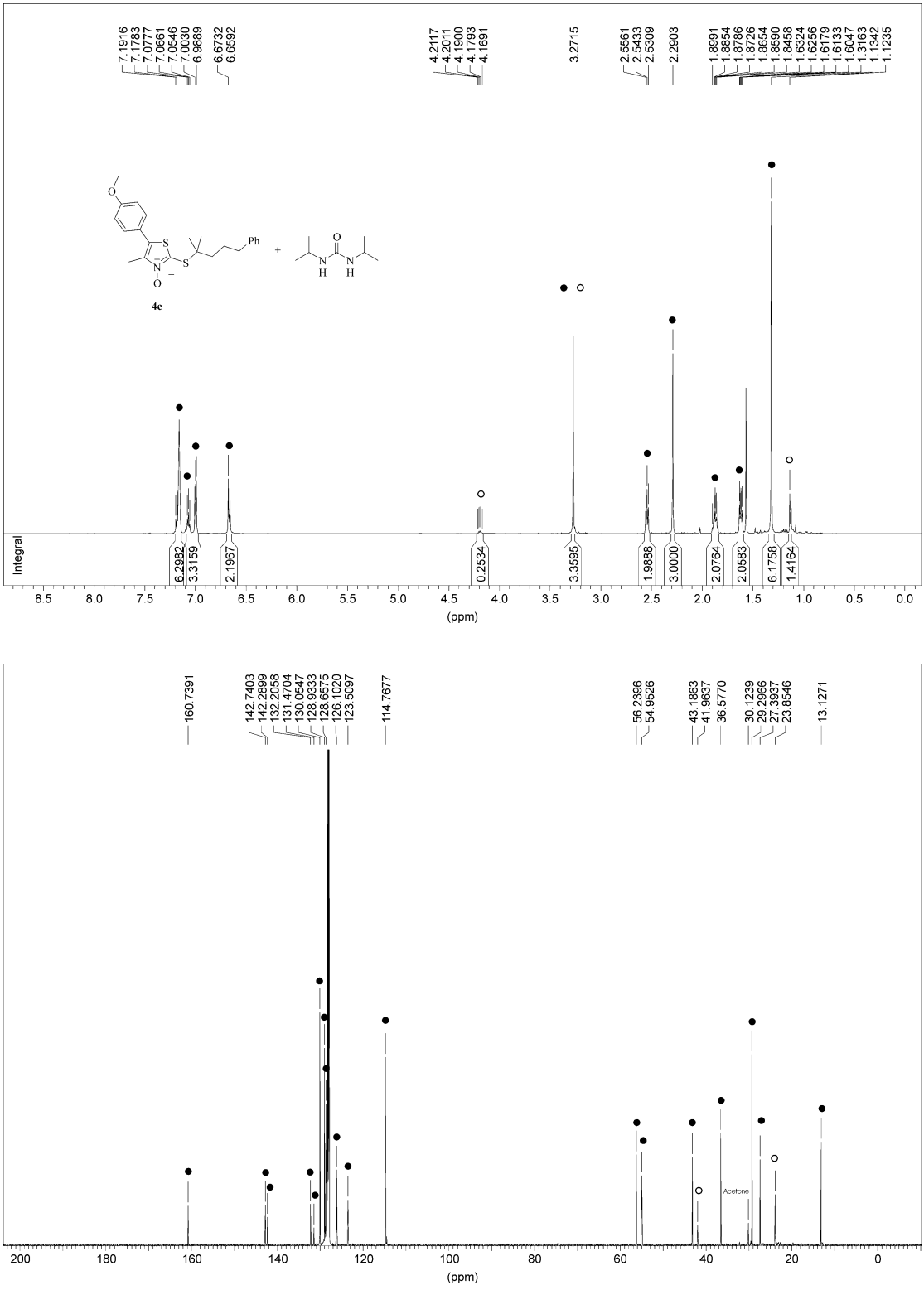

Figure B16. ^{1}H (400 MHz; top) and ^{13}C NMR spectra (101 MHz; bottom) of 2-(2-methyl-5-phenylsulfanyl)-5-(4-methoxyphenyl)-4-methylthiazole *N*-Oxide (**4c**) (●) and isopropyl urea (○) in C_6D_6.

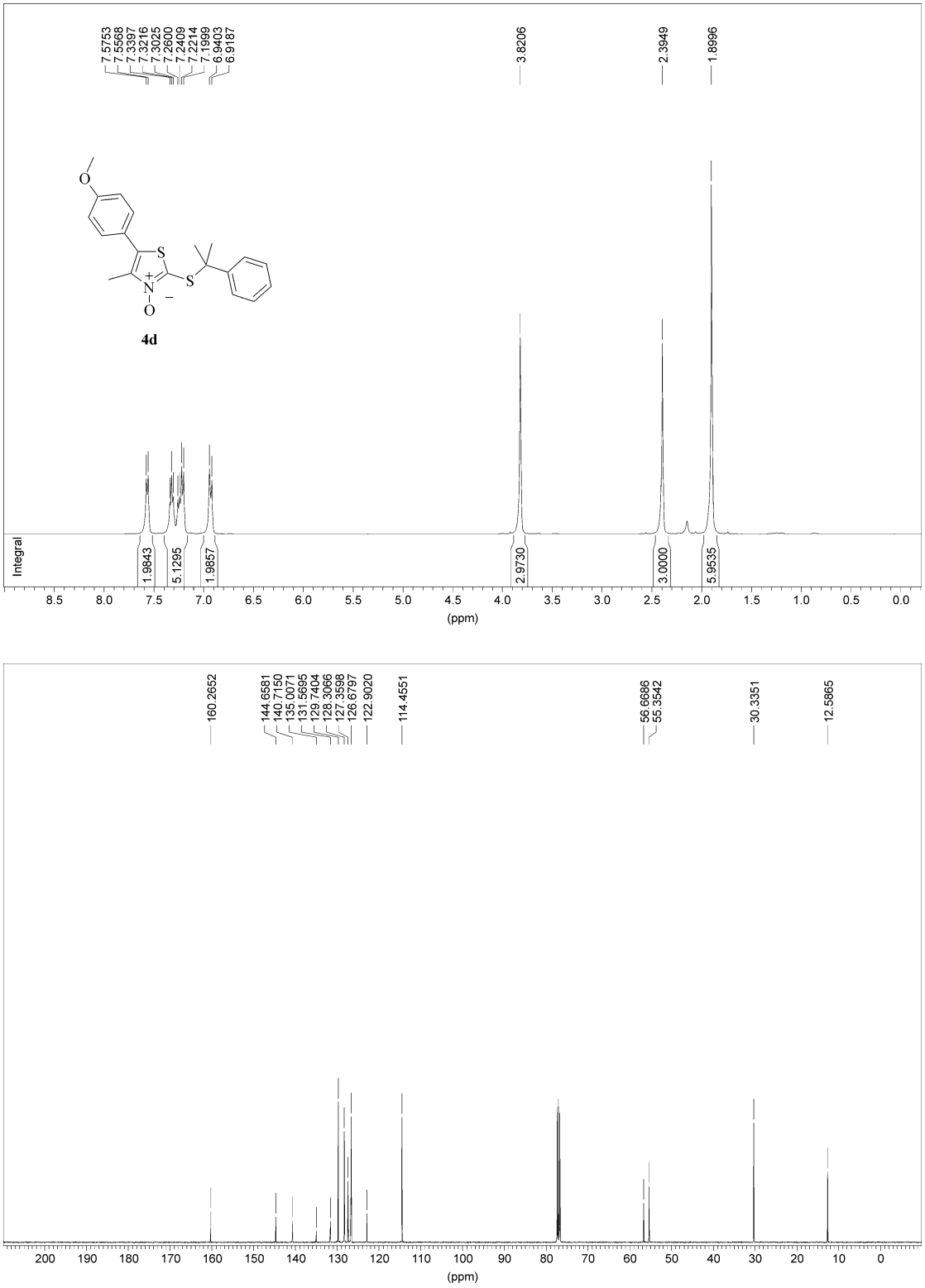

Figure B17. ^{1}H (400 MHz; top) and ^{13}C NMR spectra (101 MHz; bottom) of 2-(2-phenyl-propyl-2-sulfanyl)-5-(4-methoxyphenyl)-4-methylthiazole *N*-Oxide (**4d**) in $CDCl_3$.

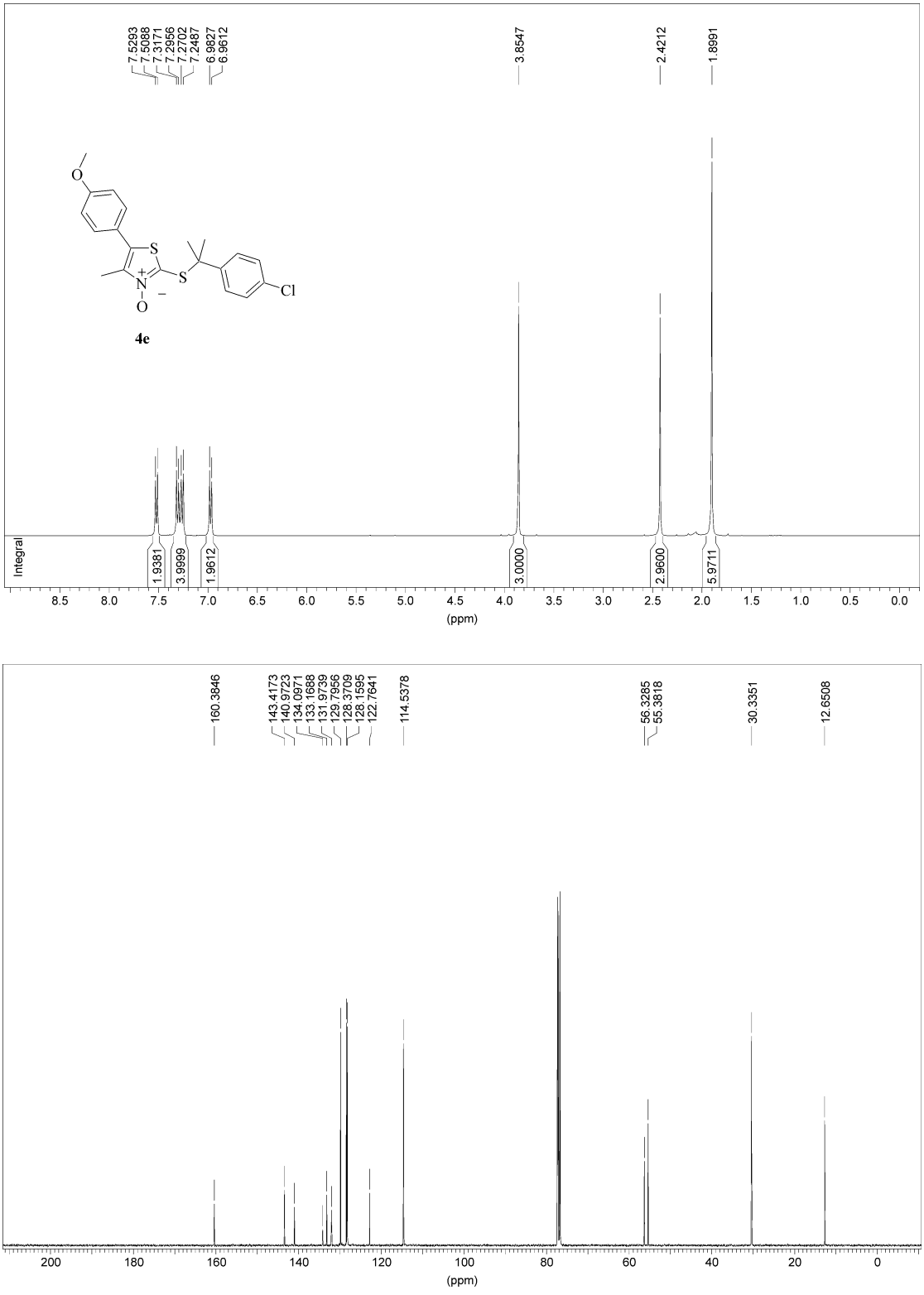

4e

Figure B18. ^{1}H (400 MHz; top) and ^{13}C NMR spectra (101 MHz; bottom) of 2-[2-(4-chloro-phenyl)-propyl -2-sulfanyl]-5-(4-methoxyphenyl)-4-methylthiazole *N*-Oxide (**4e**) in $CDCl_3$.

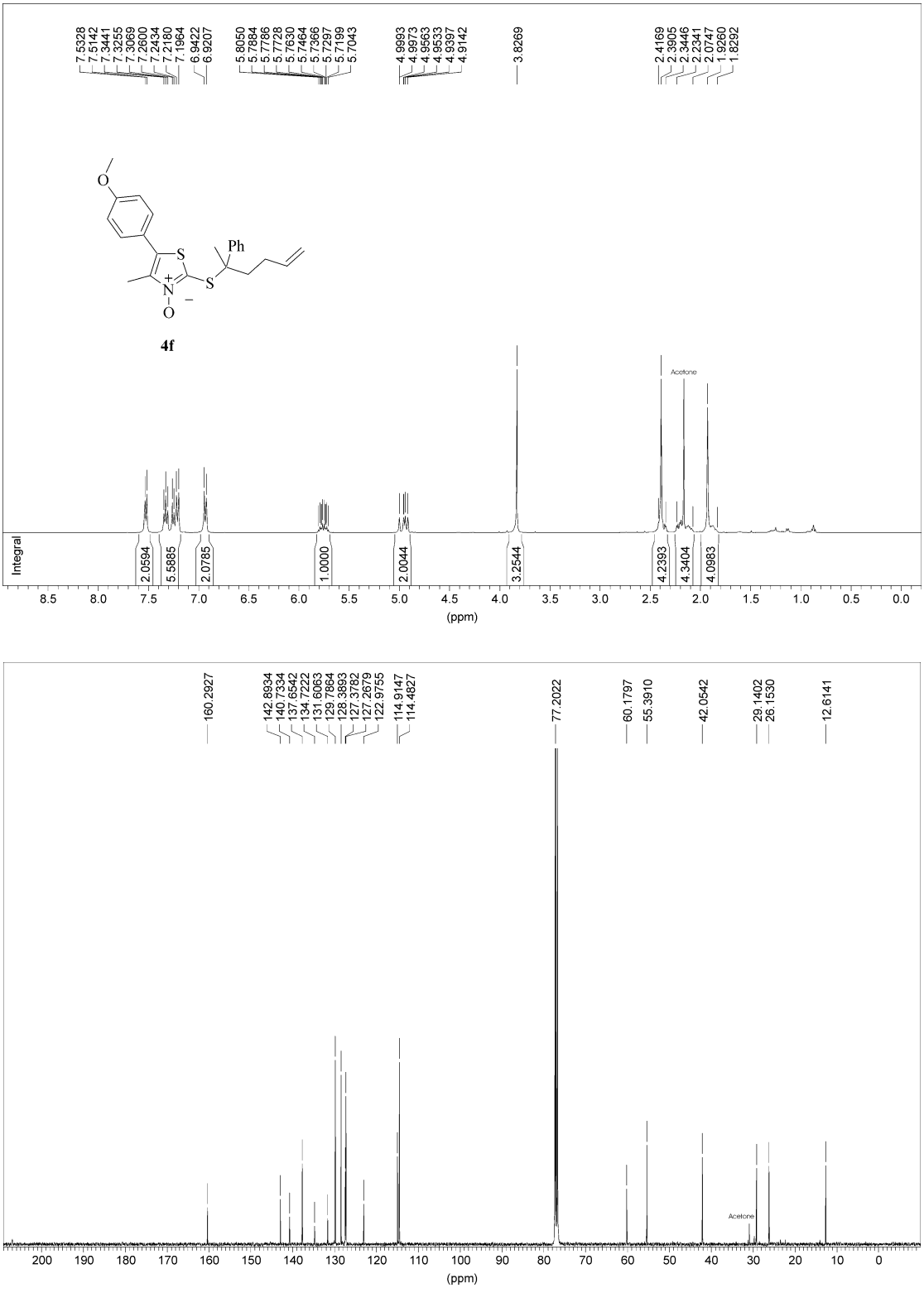

Figure B19. ^{1}H (400 MHz; top) and ^{13}C NMR spectra (151 MHz; bottom) of 2-(1-methyl-1-phenylpent-4-enyl-2-sulfanyl]-5-(4-methoxyphenyl)-4-methylthiazole *N*-Oxide (**4f**) in $CDCl_3$.

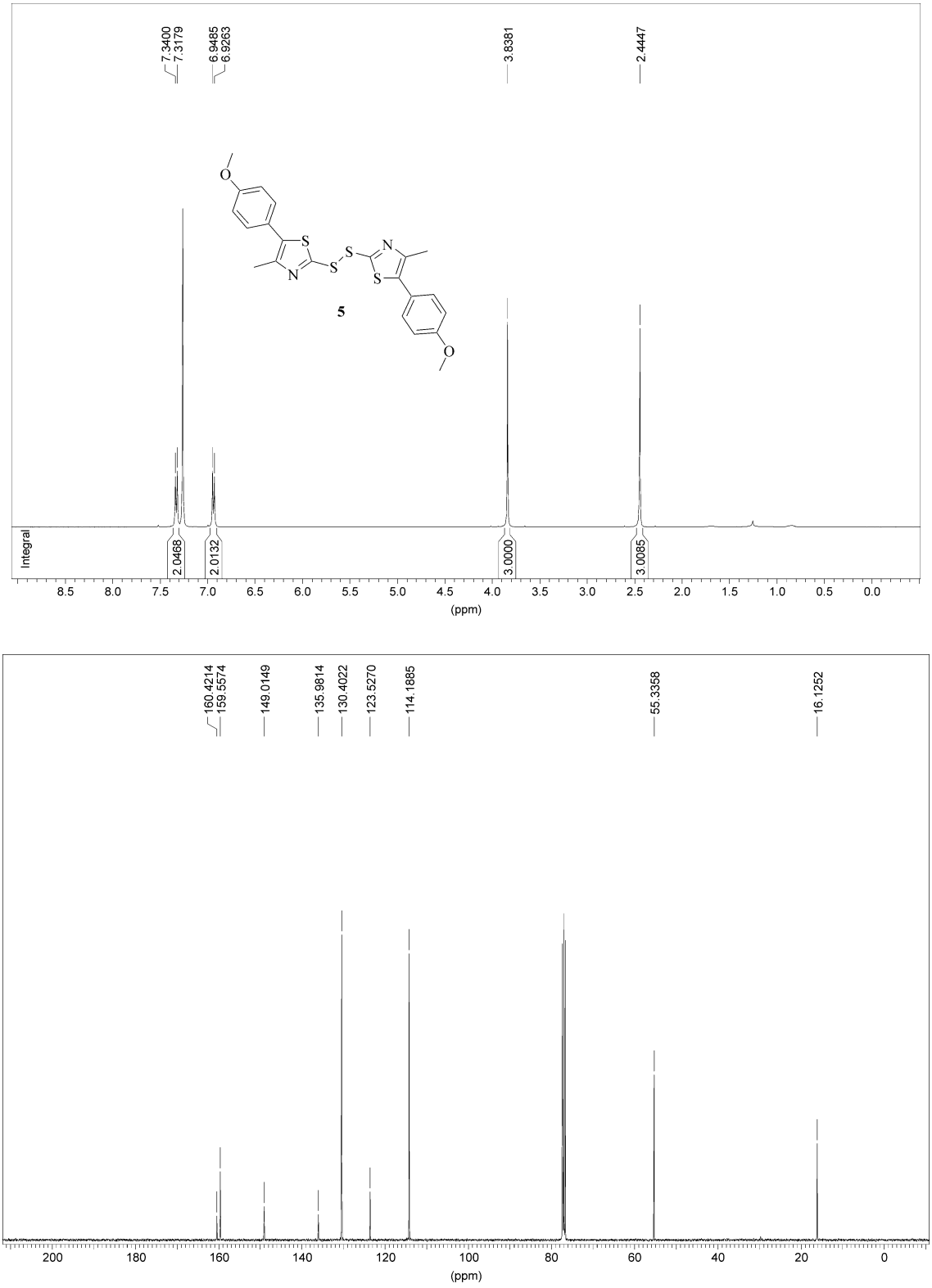

Figure B20. ^{1}H (400 MHz; top) and ^{13}C NMR spectra (101 MHz; bottom) of 1,2-bis-[5-(4-methoxyphenyl)-4-methylthiaz-3-yl]-disulfane (**5**) in $CDCl_3$.

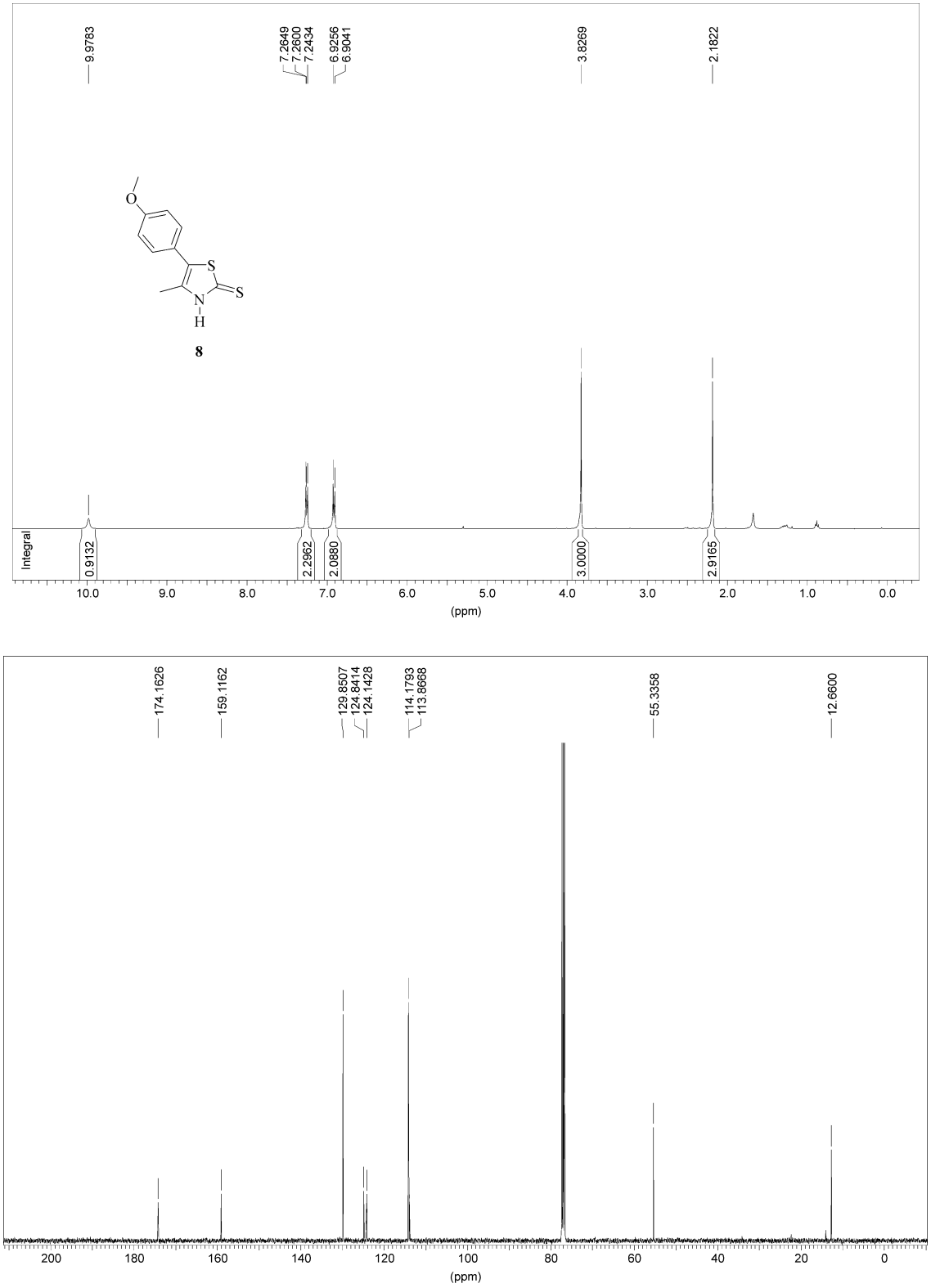

Figure B21. ^{1}H (400 MHz; top) and ^{13}C NMR spectra (101 MHz; bottom) of 5-(*p*-methoxyphenyl)-4-methylthiazole-2(3*H*)-thione (**8**) in $CDCl_3$.

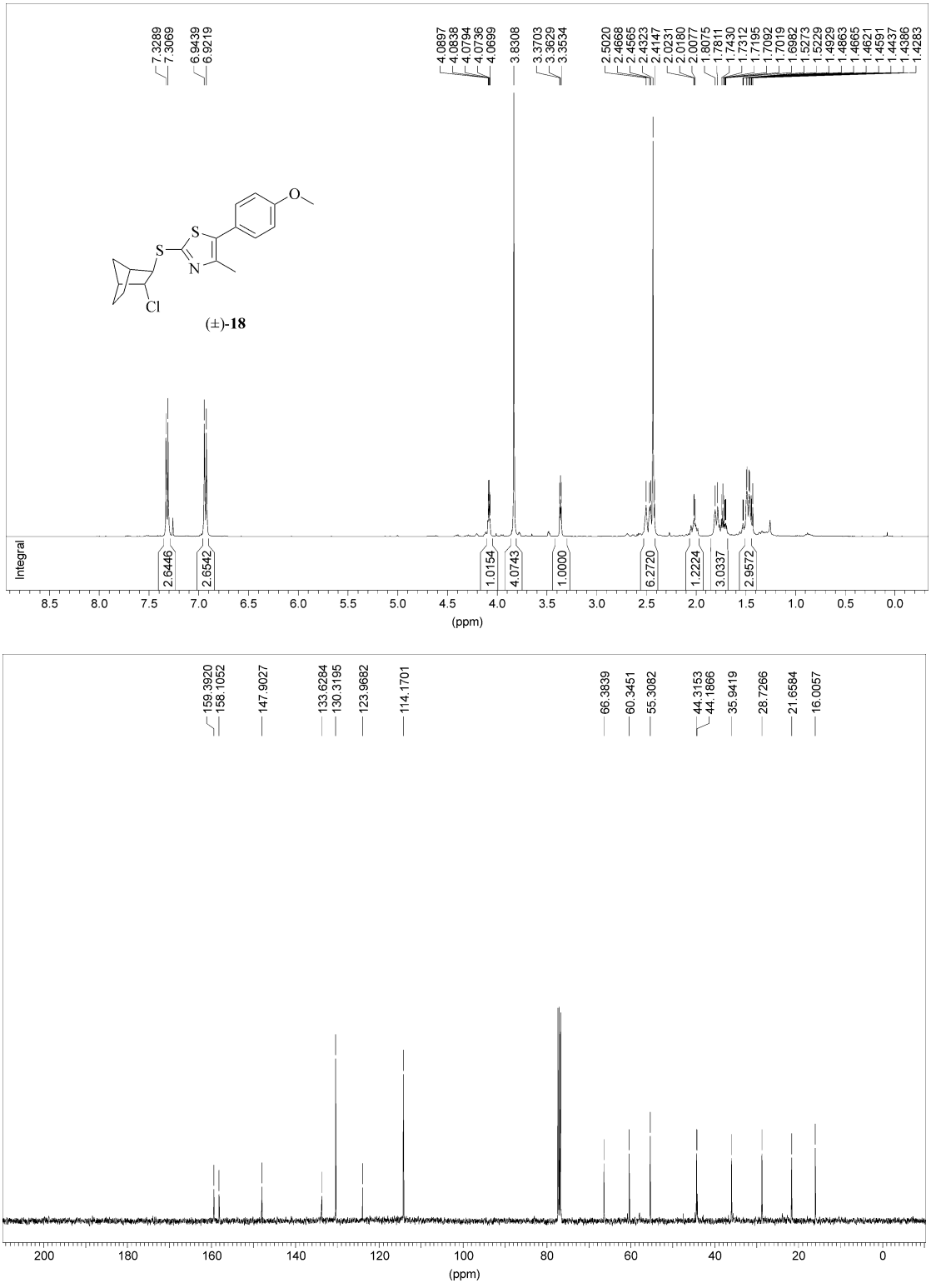

Figure B22. ^{1}H NMR (400 MHz; top) and ^{13}C NMR spectra (101 MHz; bottom) of 2-(3-chloro-bicyclo[2.2.1]hept-2-ylsulfanyl)-5-(*p*-methoxyphenyl)-4-methylthiazole (**18**) (bottom) in $CDCl_3$.

B10 References

[1] Jork, H; Funk, W.; Fischer, W.; Wimmer, H. *Dünnschichtchromatographie: Reagenzien und Nachweismethoden*; Wiley-VCH: Weinheim 1993, Vol. 1b.

[2] Braude, E.A.; Jackman, L.M.; Linstead, R.P.; Lowe, G. *J. Chem. Soc*. **1960**, 3123–3132.

[3] Alcohol **2e** was prepared in extension to a general procedure reported in Tietze, L.F.; Eicher, T. in *Reaktionen und Synthesen im organisch chemischen Grundpraktikum*, Thieme: Stuttgart, 1991, p 209 (2nd edition).

[4] Norikazu, M.; Tsuyoshi, M.; Makoto, W. *Eur. J. Org. Chem*. **2005**, 4253–4255.

[5] Menéndez Pérez, B.; Schuch, D.; Hartung J. *Org Biomol. Chem*. **2008**, *6*, 3532–3541.

[6] Rawal, V.H.; Singh, S.P.; Dufour, C.; Michoud, C. *J. Org. Chem*. **1993**, *58*, 7718–7727.

[7] Armarego, W. L. F.; Perrin, D. D. *Purification of Laboratory Chemicals* fourth ed.; The Bath Press: Bath, 1996.

[8] Hartung, J.; Daniel, K.; Schmidt, P.; Laug, S.; Svoboda, I.; Fuess, H. *Acta Cryst*. **2005**, *E61*, o3971–o3973.

[9] Hartung, J.; Daniel, K.; Svoboda, I.; Fuess, H. *Acta Cryst*. **2005**, *E61*, o1744-o1746.

[10] Kundu, R.; Ball, Z.T.; *Org. Lett*. **2010**, *12*, 2460–2463.

[11] Zhao, P.; Incarvito, C.D.; Hartwig, J.F. *J. Am. Chem. Soc*. **2006**, *128*, 9642–9643.

[12] Giese, B.; Jay, K. *Angew. Chem*., *Int. Ed. Engl*. **1977**, *16*, 466–467.

[13] Hartung, J.; Schur, C.; Kempter, I.; Gottwald, T. *Tetrahedron* **2010**, *66*, 1365–1374

[14] Bodenstein, M. *Z. Phys. Chem.* **1913**, *85*, 329–397.

[15] Baciocchi, E.; Bietti, M.; Salamone M.; Steenken, S. *J. Org. Chem*., **2002**, *67*, 2266–2270.

[16] Van Geet, A.L. *Anal. Chem*. **1970**, *42*, 679–680.

[17] Hansen, E.W. *Anal. Chem*. **1985**, *57*, 2993–2994.

[18] Günther, H, *NMR-Spektroskopie*; Thieme: Stuttgart, 1974, ch. VIII, pp. 240–257.

[19] Hartung, J.; Bergsträßer, U.; Daniel, K.; Schneiders, N.; Svoboda, I.; Fuess, H.; *Tetrahedron* **2009**, *65*, 2567–2573.

[20] Hartung, J. Altermann, S. Svoboda, I. Fuess, H. *Acta Cryst*. **2005**, *E61*, o1738–o1740.

[21] Gaussian 03, Revision C.01, Frisch, M. J.; Trucks, G. W.; Schlegel, H. B.; Scuseria, G. E.; Robb, M. A.; Cheeseman, J. R.; Montgomery, Jr., J. A.; Vreven, T.; Kudin, K. N.; Burant, J. C.; Millam, J. M.; Iyengar, S. S.; Tomasi, J.; Barone, V.; Mennucci, B.; Cossi, M.; Scalmani, G.; Rega, N.; Petersson, G. A.; Nakatsuji, H.; Hada, M.; Ehara, M.; Toyota,

K.; Fukuda, R.; Hasegawa, J.; Ishida, M.; Nakajima, T.; Honda, Y.; Kitao, O.; Nakai, H.; Klene, M.; Li, X.; Knox, J.E.; Hratchian, H.P.; Cross, J.B.; Adamo, C.; Jaramillo, J.; Gomperts, R.; Stratmann, R. E.; Yazyev, O.; Austin, A.J.; Cammi, R.; Pomelli, C.; Ochterski, J. W.; Ayala, P. Y.; Morokuma, K.; Voth, G. A.; Salvador, P.; Dannenberg, J.J.; Zakrzewski, V.G.; Dapprich, S.; Daniels, A.D.; Strain, M.C.; Farkas, O.; Malick, D. K.; Rabuck, A.D.; Raghavachari, K.; Foresman, J. B.; Ortiz, J.V.; Cui, Q.; Baboul, A. G.; Clifford, S.; Cioslowski, J.; Stefanov, B. B.; Liu, G.; Liashenko, A.; Piskorz, P.; Komaromi, I.; Martin, R. L.; Fox, D. J.; Keith, T.; Al-Laham, M. A.; Peng, C. Y. Nanayakkara, A.; Challacombe, M.; Gill, P. M. W.; Johnson, B.; Chen, W.; Wong, M. W.; Gonzalez, C.; Pople, J. A., Gaussian, Inc., Wallingford CT, 2004.

[22] Schaftenaar, G.; Noordik, J.H.; *Comput.-Aided Mol. Des*. **2000**, *14*, 123–134.

[23] An analytically pure sample of 2-(2-methyl-propyl-2-sulfanyl)-5-(4-methoxyphenyl)-4-methyl-thiazole *N*-Oxide (**4a**) was isolated by column-chromatography from a mixture obtained from a reaction between DCC (22 mmol), *t*BuOH (22 mmol), CuCl (2 mol%) and MAnTTOH (4 mmol).

Anhang C

Supporting Information for:

Heterocyclic *O*-(*tert*-Butyl) Thiohydroxamates

Christine Schur,[a] Manuel Zimmer,[b] Harald Kelm,[c] Markus Gerhards,[b] and Jens Hartung*[a]

[a] *Fachbereich Chemie, Organische Chemie, Technische Universität Kaiserslautern, Erwin-Schrödinger-Straße, D-67663 Kaiserslautern, Germany*

[b] *Fachbereich Chemie, Physikalische Chemie & Research Center Optimas, Technische Universität Kaiserslautern, Erwin-Schrödinger-Straße, D-67663 Kaiserslautern, Germany*

[c] *Fachbereich Chemie, Anorganische Chemie, Technische Universität Kaiserslautern, Erwin-Schrödinger-Straße, D-67663 Kaiserslautern, Germany*

Contents

C1 General Remarks

C1.1 Numbering of compounds: Numbering of compounds in the *Electronic Supporting Information* and the accompanying publication are consistent.

C1.2 References: References refer exclusively to the *Electronic Supporting Information*.

C2 Instrumentation

C2.1 Nuclear magnetic resonance (NMR)-spectroscopy: Proton- and carbon-13-NMR spectra were measured with Avance I 200, DPX 400, Avance I 600 instruments (*Bruker*). Chemical shifts refer to the δ-scale. Proton resonances of residual non-deuterated solvents and carbon chemical shifts of $CDCl_3$ (δ_H 7.26, δ_C 77.0), C_6D_6 (δ_H 7.16, δ_C 128.06), DMSO[d_6] (δ_H 2.50, δ_C 39.52) were used as internal standards.

C2.2 Infrared (IR)-spectroscopy: All spectra were measured with a Bruker Vertex 80v FTIR spectrometer with a vacuum tight liquid cell (Bruker A140). The cell is composed of housing, KBr-windows, separated by two Mylar® spacers with a variable thickness of 0.006 to 0.5 millimeters and several seal rings. The sample cell with a path length of 0.075 millimeters is filled with a millimolar solution of the respective substance dissolved in acetonitrile and positioned inside the argon purged sample compartment. An average of 50 spectra at a resolution of 4 cm^{-1} is recorded. A spectrum of acetonitrile is measured and used as background that is subtracted from the sample spectrum to yield the final transmission spectrum.

C2.3 Electron impact (EI)-mass spectrometry: Mass spectra (EI, 70 eV) were recorded with a Mass Selective Detector HP 6890 (*Hewlett Packard*).

C2.4 High resolution mass spectrometry (HRMS) were measured with a GCT Premier Micromass instrument (*Waters*).

C2.5 Ultraviolet/visible light (UV/Vis)-spectra were recorded in 1-centimeter quartz cuvettes with a Cary 100 Conc UV/Vis spectrophotometer (Varian).

C2.6 Combustion analysis were performed with a vario Micro cube (analytical laboratory, Technische Universität Kaiserslautern).

C2.7 Melting points [°C] were determined on a Koffler hot-plate melting point microscope

(*Reichert*) and are not corrected.

C3 Reagents and Chromatography

C3.1 Reagents: Benzene, dimethyl formamide, dichloromethane, and diethyl ether were purified and dried according to standard procedures.[1] All other reagents were used as received from commercial suppliers (Sigma Aldrich, Acros Organics, Fisher Scientific, Merck), unless otherwise indicated. 3-Hydroxy-4-methylthiazole-2(3*H*)thione,[2] *N*-hydroxy-4-methyl-thiazole-2(3*H*)thione tetraethylammonium salt,[3] were prepared according to published procedures.

C3.2 Thin layer chromatography: Reaction progress was monitored via thin layer chromatography (tlc) on aluminum sheets coated with silica gel (60 F_{254}, *Merck*). Compounds on developed tlc-sheets were detected with the aid of the UV-VIS indicator commercially disposed on the sheets, becoming apparent for example by a hand lamp emitting 254 nm light. As alternative method for detecting compounds, developed tlc-sheets were stained by Ekkert´s reagent and subsequently heated, leading to blue-green spots for organobromines, blue spots for alcohols and yellow spots for alkoxyl radical precursors.

C3.3 Column chromatography: Column chromatography (flash chromatography) was performed using Geduran Si60 silica gel (40–63 μm) as stationary phase.

C3.4 Gas chromatography coupled to mass spectrometry: Mass spectra (EI, 70 eV) were recorded with a Mass Selective Detector HP 6890 (*Hewlett Packard*) connected to an Agilent-gaschromatograph.

C4 Supplementary *O*-Alkyl Thiohydroxamate Chemistry

C4.1 *O*-Pentyl 2-pyridylsulfenate (10c). A solution of 1-pentoxy-pyridine-2(1*H*)-thione (376 mg, 1.91 mmol) was dissolved in deaerated perdeuterobenzene (4.0 mL) and placed into a water bath (18–20 °C). The reaction mixture is photolyzed for 15 min at 18–20 °C with 150 W tungsten light. A fraction of the solution is immediately analyzed by NMR-spectroscopy, showing resonances from 1-pentanol, pentanal, *O*-pentyl 2-pyridylsulfenate (**10c**), and 4-(pyridyl-2-sulfanyl)pentan-1-ol (**11**). *1-Pentanol*. ^{13}C NMR (C_6D_6, 100 MHz) δ 14.3, 22.8, 28.1, 32.9, 62.6. *Pentanal*. ^{13}C NMR (C_6D_6, 100 MHz) δ 13.8, 22.4, 24.2, 43.5, 200.9. 4-(pyridyl-2-sulfanyl)pentan-1-ol (**11**).[4] ^{1}H NMR (C_6D_6, 400 MHz) δ 1.32 (d, J = 6.9 Hz, 3 H), 1.42–1.52 (m, 2 H), 1.59–1.66 (m, 2 H), 2.71 (br s, 1 H), 3.57 (t, J = 5.3 Hz, 2 H), 4.18 (sxt, J = 6.8 Hz, 1 H), 6.37–6.40 (m, 1 H), 7.36 (dt, J_d = 8.1, J_t = 1.0 Hz, 1 H), 8.17 (ddd, J_d = 4.9, 1.9, 0.9 Hz, 1 H). 8.26 (ddd, J_d = 5.0, 1.8, 0.9 Hz, 1 H). ^{13}C NMR (C_6D_6, 100 MHz) δ 20.8, 30.1, 33.8, 38.7, 61.9, 119.1, 122.7, 135.8, 149.5, 160.2. For isolating *O*-pentyl 2-pyridylsulfenate (**10c**), the content of the NMR-tube was added to the rest of the reaction mixture, which was concentrated under reduced pressure. The remaining oil was purified by chromatography using a 1/1-mixture (*v*/*v*) of diethyl ether/pentane as eluent. *O-Pentyl 2-pyridylsulfenate* (**10c**). Yield: 43%, colorless oil. R_f = 0.78 [diethyl ether/pentane = 1:1 (*v*/*v*)]. ^{1}H NMR (C_6D_6, 400 MHz) δ 0.76–0.81 (m, 3 H), 1.10–1.18 (m, 4 H), 1.44–1.51 (m, 2H), 3.66 (t, J = 6.7 Hz, 2 H), 6.38 (ddd, J_d = 7.4, 4.8, 1.1 Hz, 1 H), 7.03 (td, J_t = 7,8 J_d= 1.8 Hz, 1 H), 7.13 (dt, J_d = 8.1, J_t = 0.9 Hz, 1 H), 8.28–8.30 (ddd, J_d = 4.9, 1.8, 1,1 Hz, 1 H). ^{13}C NMR (C_6D_6, 100 MHz) δ 14.0, 22.6, 28.0, 30.4, 79.5, 116.0, 119.0, 136.3, 149.8, 166.0. ^{1}H NMR ($CDCl_3$, 400 MHz) δ 0.88–0.94 (m, 3 H), 1.30–1.42 (m, 4 H), 1.71–1.78 (m, 2H), 3.94 (t, J = 6.7 Hz, 2 H), 6.97 (ddd, J_d = 7.5, 4.9, 1.1 Hz, 1 H), 7.28 (dt, J_d = 8.1, J_t = 0.9 Hz, 1 H), 7.66 (td, J_t = 7,8 J_d= 1.8 Hz, 1 H), 8.44–8.46 (ddd, J_d = 4.8, 1.8, 0,9 Hz, 1 H). ^{13}C NMR ($CDCl_3$, 100 MHz) δ 14.0, 22.4, 27.8, 30.1, 79.7, 116.2, 119.3, 136.8, 149.4, 165.0. Anal. Calcd. for $C_{10}H_{15}NOS$ (197.27): C, 60.89; H, 7.66; N, 7.10; S, 16.25 Found: C, 60.64; H, 7.41; N, 7.02; S, 16.17.

When referenced versus the yield of isolated sulfenate **10c**, the yields of the remaining products observed via NMR-spectroscopy in the crude reaction mixture calculate as follows: 10% of 1-pentanol, 3% of pentanal, 43% of *O*-pentyl 2-pyridylsulfenate (**10c**), and 12% of 4-(pyridyl-2-sulfanyl)pentan-1-ol (**11**).

C4.2 4-(Pyridyl-2-sulfanyl)pentan-1-ol (11). A solution of 1-(1-pentoxy)pyridine-2(1*H*)thione (**4c**) (68.30 mg, 346 μmol) and deaerated perdeuterobenzene (0.7 mL) and photolyzed at 20 °C with 150 W-tungsten light for 5 minutes. The products are immediately analyzed by NMR-spectrosocopy and purified by preparative thin layer chromatography using a 1/1-mixture of diethyl ether/pentane as eluent, to afford *O*-pentyl pyridine-2-sulfenate (**10c**) (51%; R_f = 0.78) and 4-(pyridyl-2-sulfanyl)pentan-1-ol (**11**) (32%; R_f = 0.35).

C5 Supplementary Infrared Data of Thiohydroxamic Acids and *O*-Alkyl Thiohydroxamates

C5.1 3-Hydroxy-5-(4-methoxyphenyl)-4-methylthiazole-2(3*H*)-thione (**1a**): IR (CCl_4) ν_{max} / cm^{-1} 3006, 2960, 2838, 1514, 1361, 1292, 1274, 1253, 1178, 1146, 1038.

C5.2 3-(*tert*-Butoxy)-5-(4-methoxyphenyl)-4-methylthiazole-2(3*H*)-thione (1b): IR (CCl_4) ν_{max} / cm^{-1} 2981, 2935, 2838, 1605, 1510, 1464, 1441, 1393, 1381, 1371, 1333, 1294, 1271, 1251, 1177, 1133, 1037, 1030, 985. IR (MeCN) ν_{max} / cm^{-1} 2984, 2936, 2846, 1512, 1336, 1291, 1272, 1251, 1181, 1132, 1028, 988, 837.

C5.3 3-Hydroxy-4-methylthiazole-2(3*H*)-thione (**2a**): IR (CCl_4) ν_{max} / cm^{-1} 3125, 2969, 1508, 1440, 1360, 1302, 1188, 1142, 1023, 869.

C5.4 1-Hydroxypyridin-2(1*H*)-thione (4a): IR (CCl_4) ν_{max} / cm^{-1} 3115, 1612, 1563, 1485, 1456, 1414, 1265, 1193, 1171, 1141, 1076, 859, 834, 826.

C6 Archive of Selected NMR-Spectra

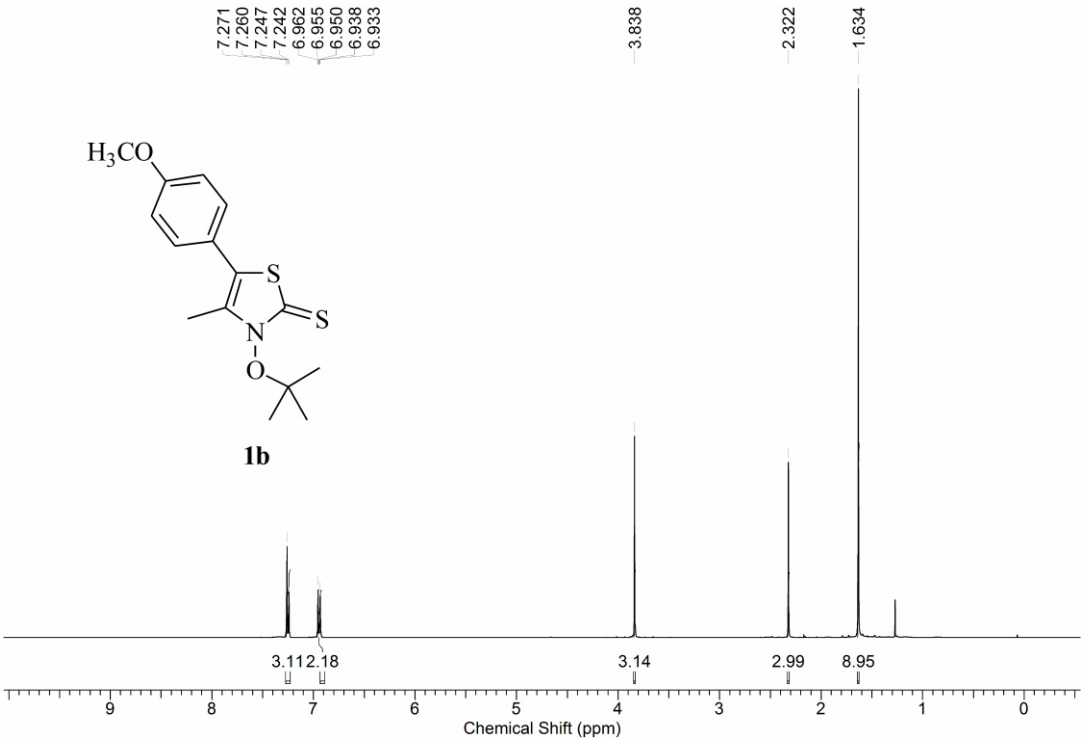

Figure C1. Proton-1 NMR-spectrum of 3-(2-methylprop-2-oxy)-5-(4-methoxyphenyl)-4-methylthiazol-2(3*H*)-thione (**1b**) (400MHz, $CDCl_3$, 23 °C).

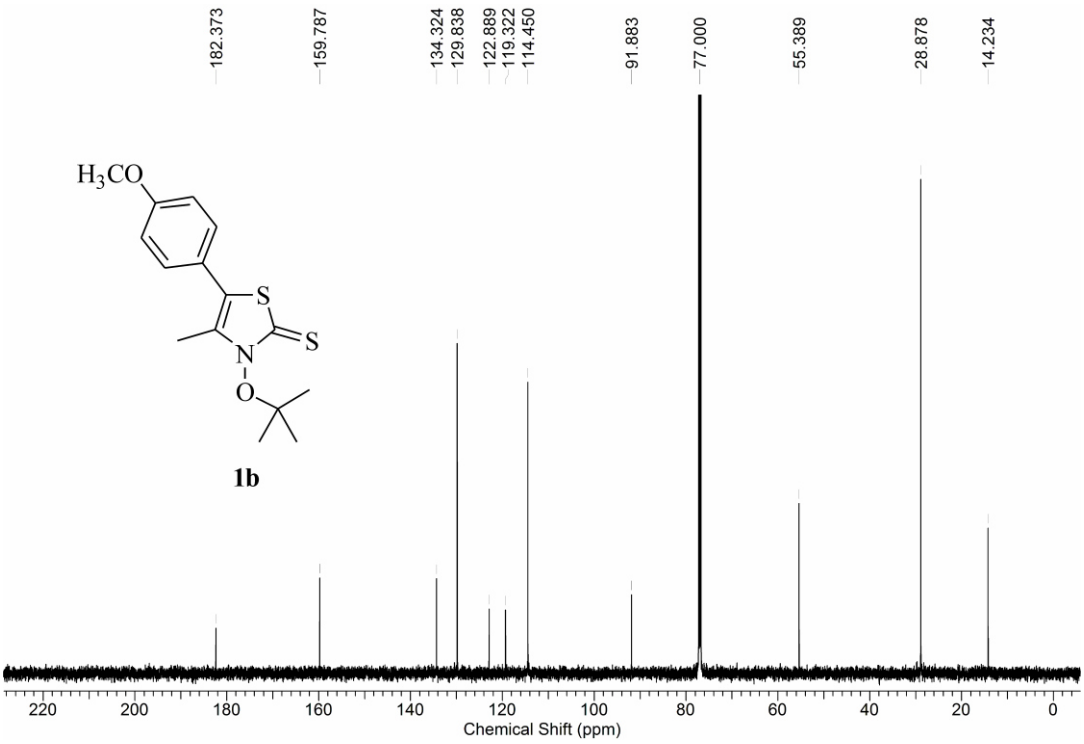

Figure C2. Carbon-13 NMR-spectrum of 3-(2-methylprop-2-oxy)-5-(4-methoxyphenyl)-4-methylthiazol-2(3*H*)-thione (**1b**) (150MHz, $CDCl_3$, 23 °C).

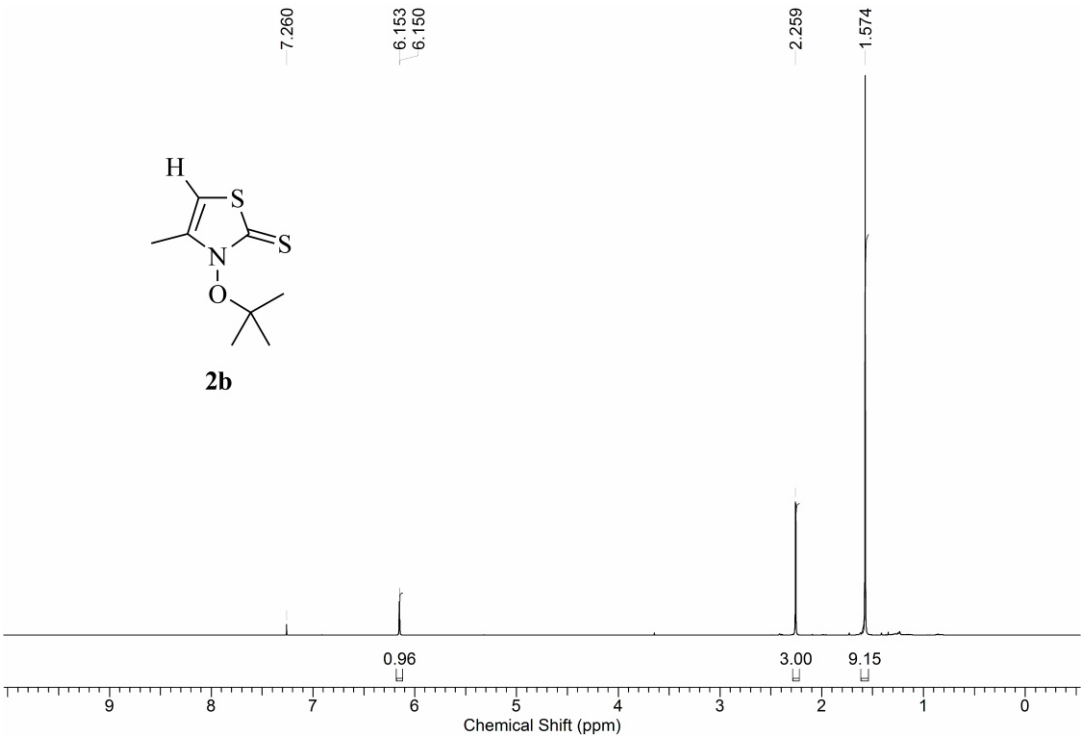

Figure C3. Proton-1 NMR-spectrum of 3-(2-methylprop-2-oxy)-4-methylthiazol-2(3*H*)-thione (**2b**) (400MHz, $CDCl_3$, 23 °C).

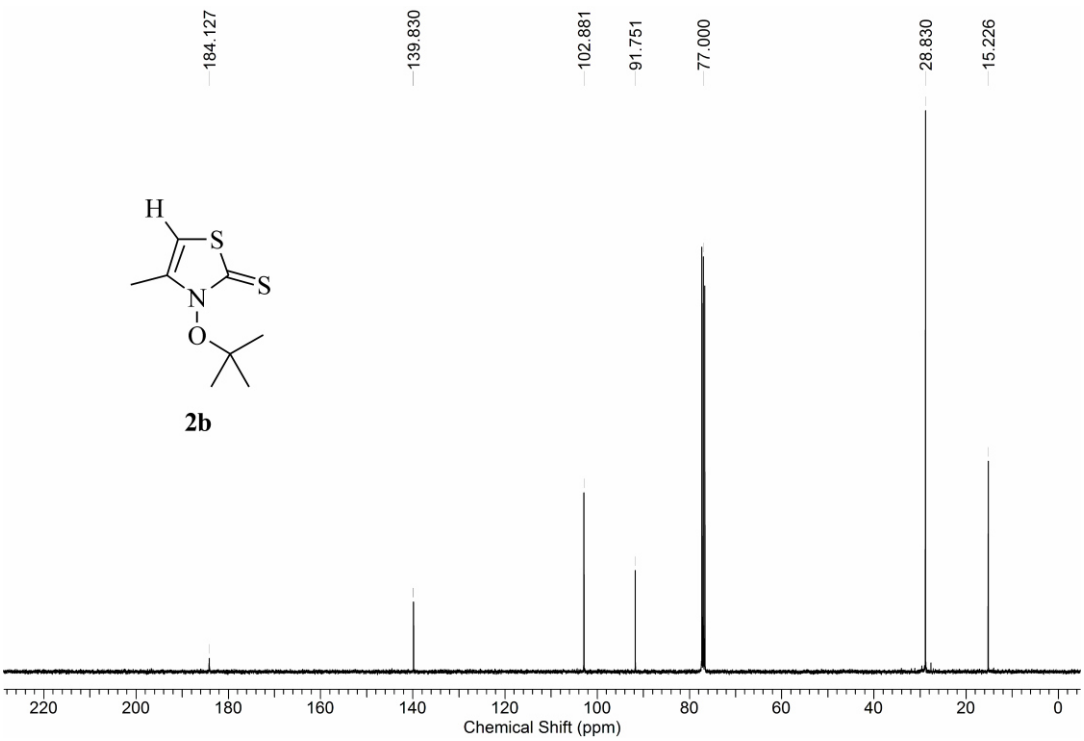

Figure C4. Carbon-13 NMR-spectrum of 3-(2-methylprop-2-oxy)-4-methylthiazol-2(3*H*)-thione (**2b**) (100MHz, $CDCl_3$, 23 °C).

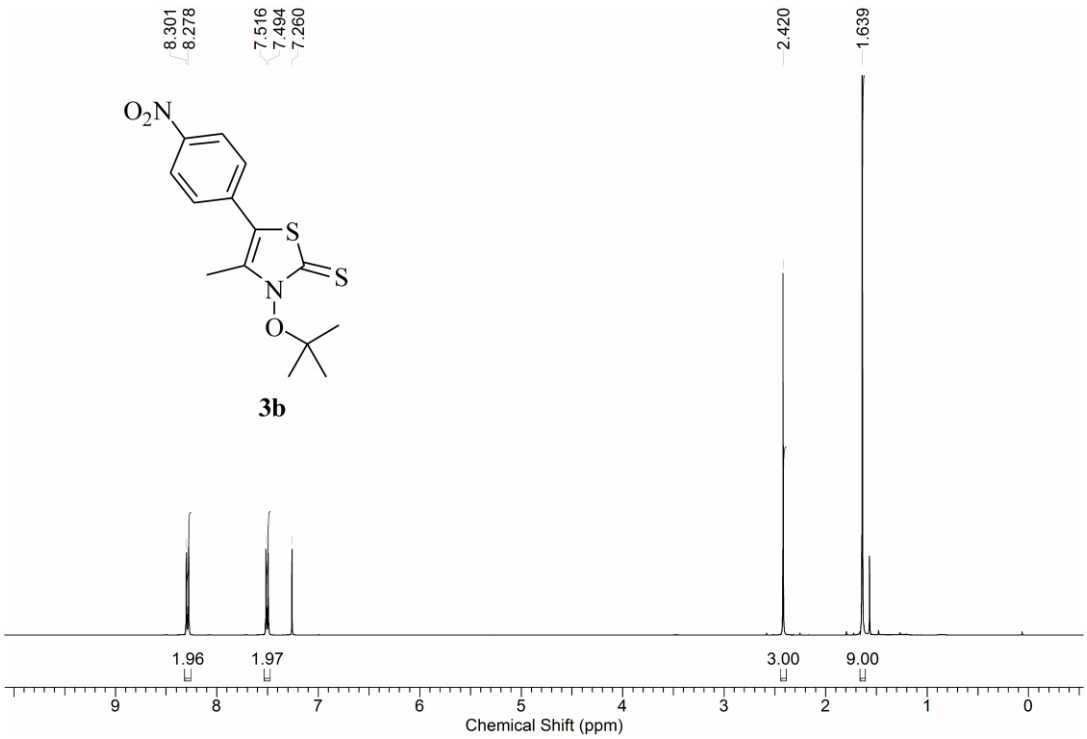

Figure C5. Proton-1 NMR-spectrum of 3-(2-methylprop-2-oxy)-4-methyl-5-(4-nitrophenyl)thiazol-2(3*H*)-thione (**3b**) (400MHz, $CDCl_3$, 23 °C).

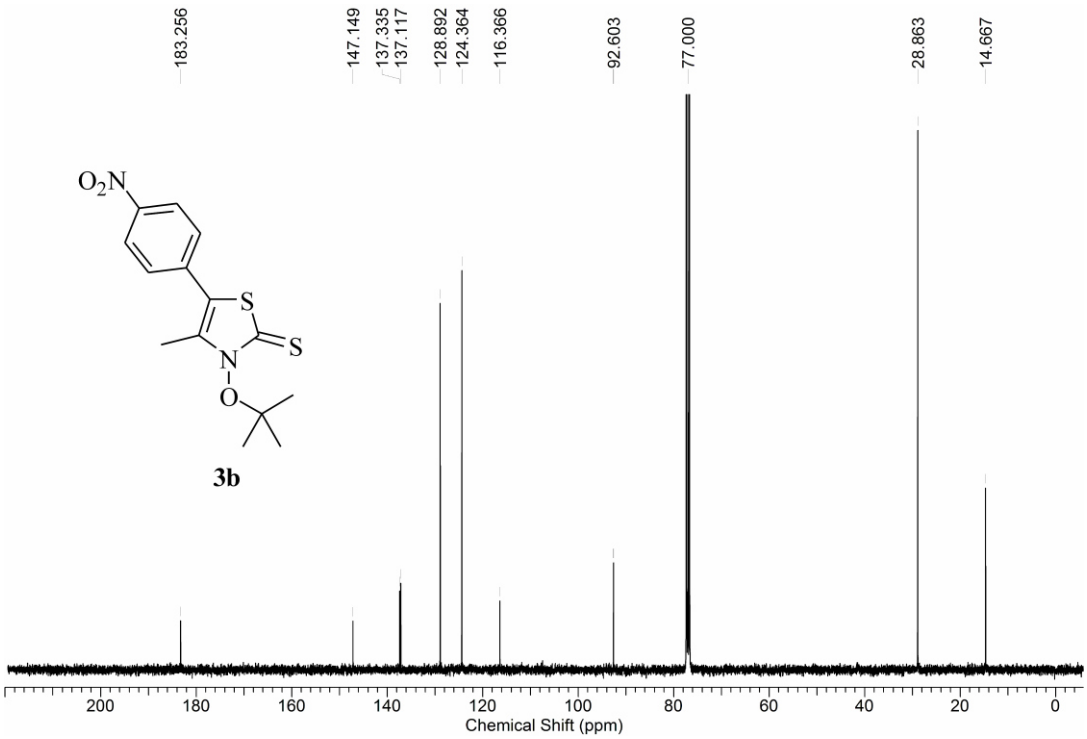

Figure C6. Carbon-13 NMR-spectrum of 3-(2-methylprop-2-oxy)-4-methyl-5-(4-nitrophenyl)thiazol-2(3*H*)-thione (**3b**) (100MHz, $CDCl_3$, 23 °C).

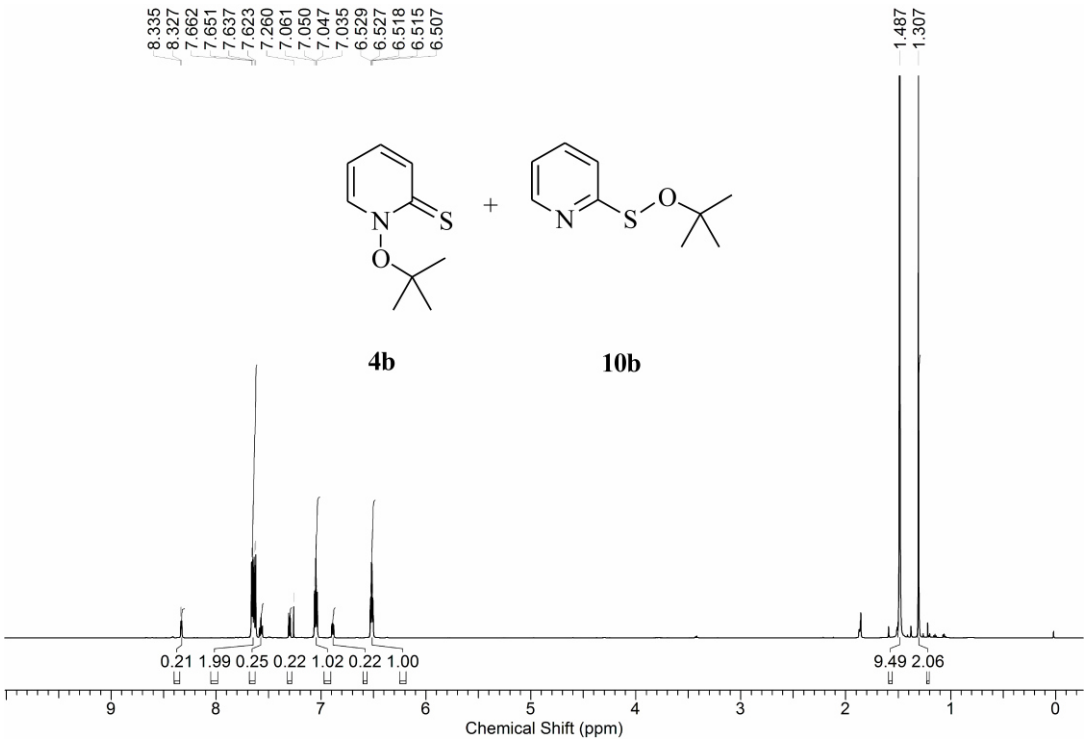

Figure C7. Proton-1 NMR-spectrum of a 83/17-mixture of 1-(2-methylprop-2-oxy)-pyridine-2(1*H*)-thione (**4b**) and *O*-(2-methylprop-2-yl)pyridine-2-sulfenate (**10b**) (600MHz, $CDCl_3$, 23 °C).

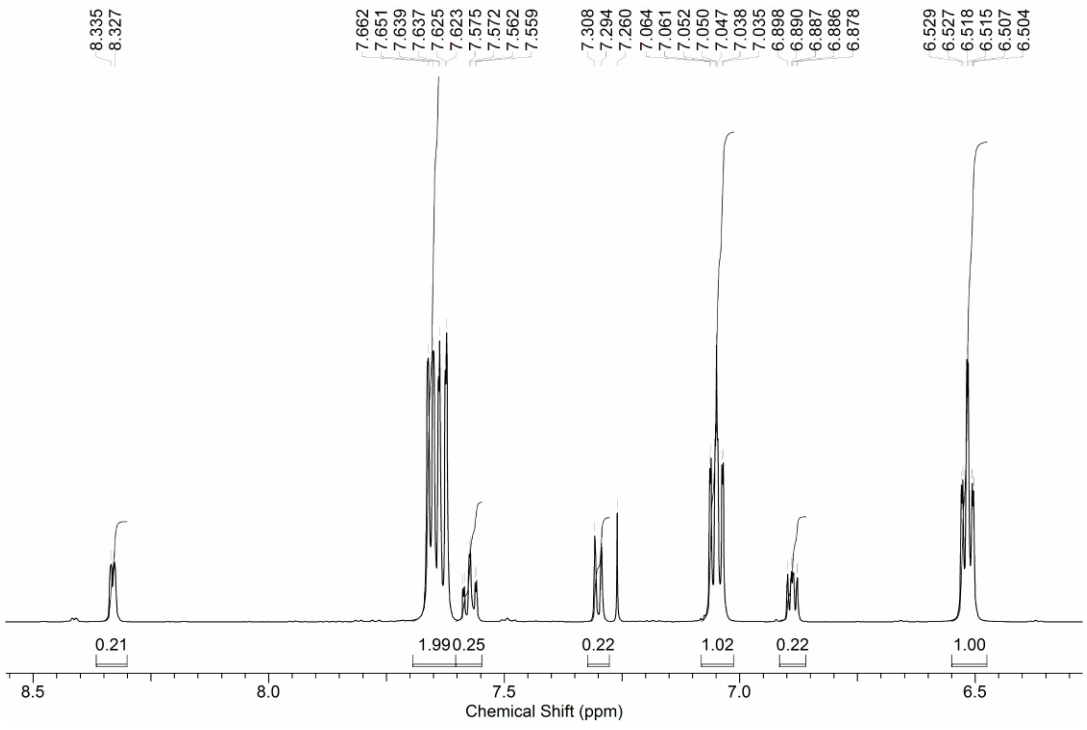

Figure C8. Enhancement of the proton-1 NMR-spectrum of a 83/17-mixture of 1-(2-methylprop-2-oxy)-pyridine-2(1*H*)-thione (**4b**) and *O*-(2-methylprop-2-yl)pyridine-2-sulfenate (**10b**) (600MHz, $CDCl_3$, 23 °C).

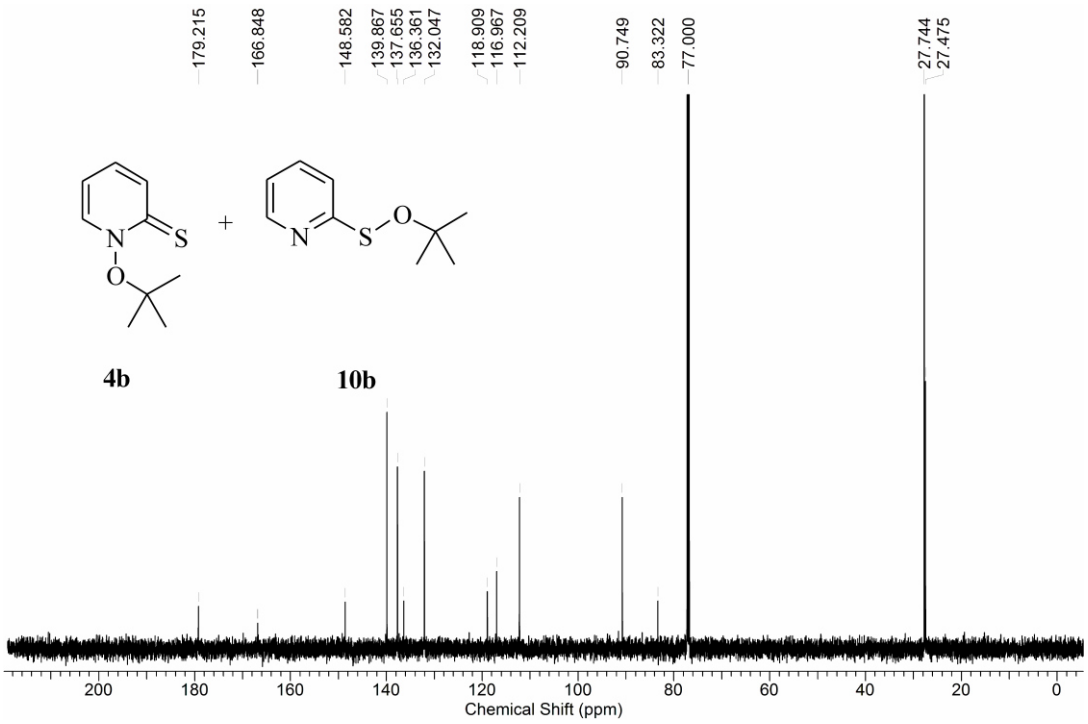

Figure C9. Carbon-13 NMR-spectrum of a 83/17-mixture of 1-(2-methylprop-2-oxy)-pyridine-2(1*H*)-thione (**4b**) and *O*-(2-methylprop-2-yl)pyridine-2-sulfenate (**10b**) (150MHz, $CDCl_3$, 23 °C).

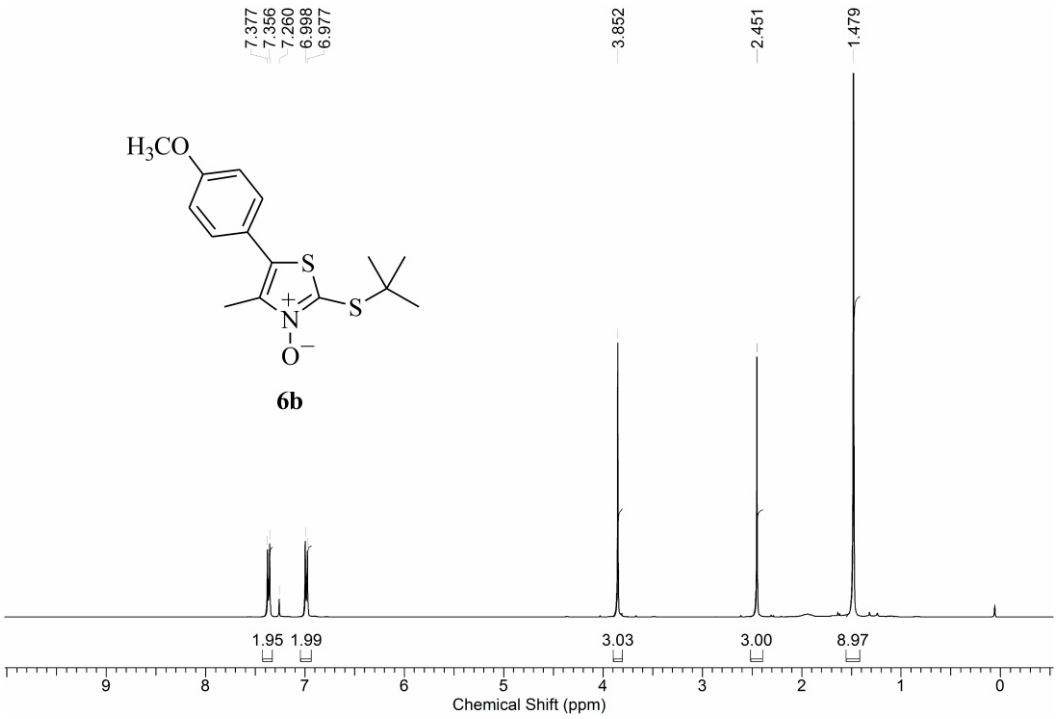

Figure C10. Proton-1 NMR-spectrum of a mixture of 2-(2-methylpropyl-2-sulfanyl)-5-(4-methoxyphenyl)-4-methylthiazole *N*-oxide (**6b**) (400MHz, $CDCl_3$, 23 °C).

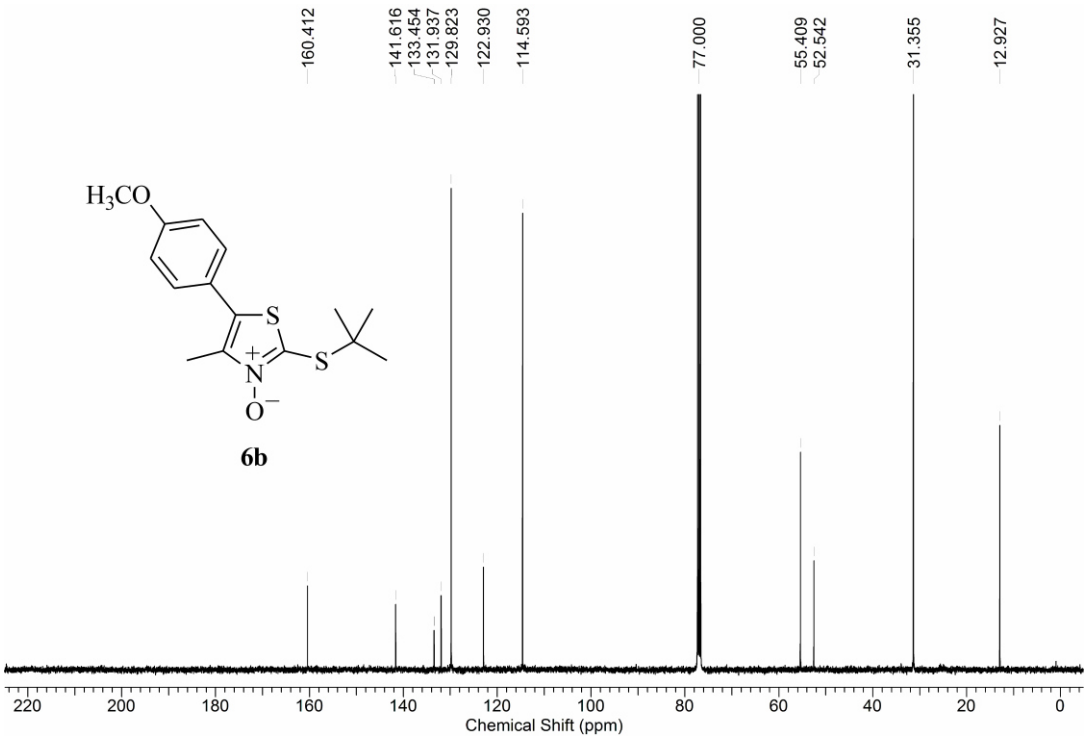

Figure C11. Carbon-13 NMR-spectrum of a mixture of 2-(2-methylpropyl-2-sulfanyl)-5-(4-methoxyphenyl)-4-methylthiazole *N*-oxide (**6b**) (100MHz, $CDCl_3$, 23 °C).

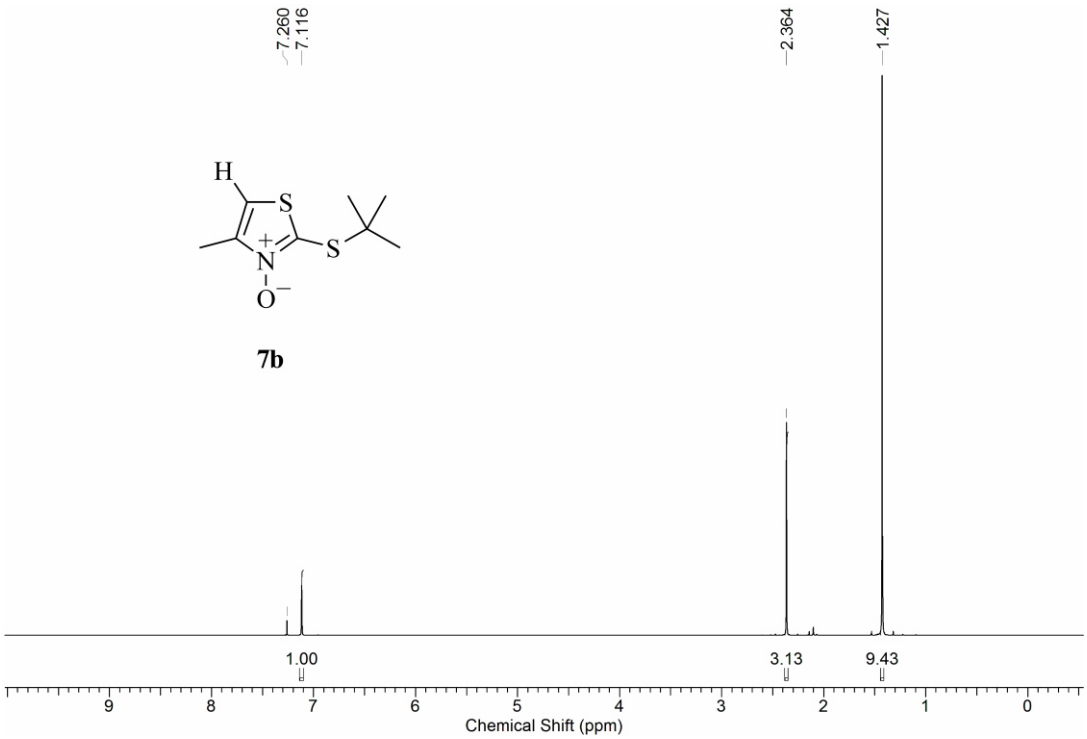

Figure C12. Proton-1 NMR-spectrum of 2-(2-methylpropyl-2-sulfanyl)-4-methylthiazole *N*-oxide (**7b**) (600MHz, $CDCl_3$, 23 °C).

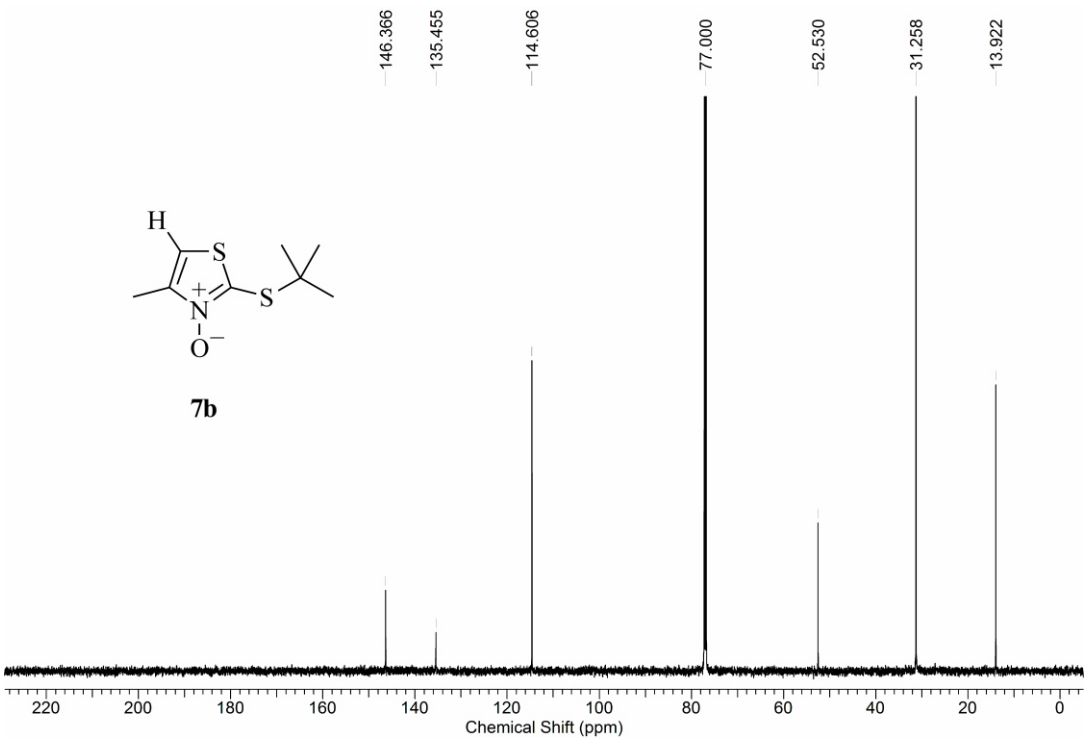

Figure C13. Carbon-13 NMR-spectrum of 2-(2-methylpropyl-2-sulfanyl)-4-methylthiazole *N*-oxide (**7b**) (150MHz, $CDCl_3$, 23 °C).

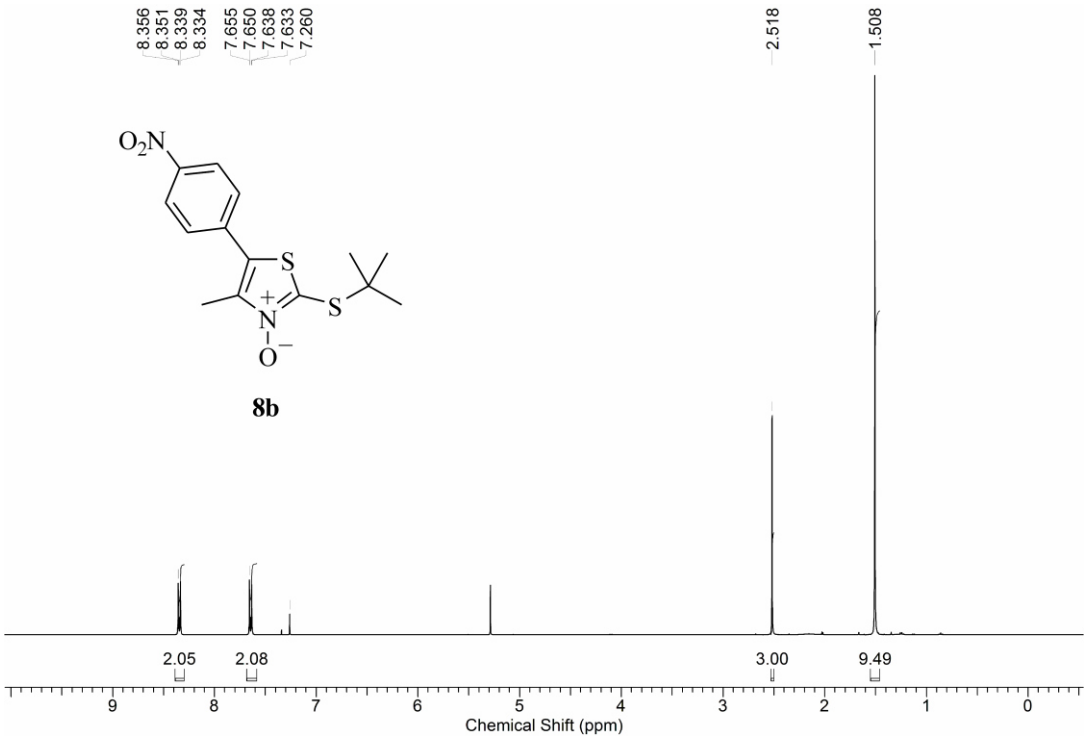

Figure C14. Proton-1 NMR-spectrum of 2-(2-methylpropyl-2-sulfanyl)-5-(4-nitrophenyl)-4-methylthiazole *N*-oxide (**8b**) (400MHz, $CDCl_3$, 23 °C).

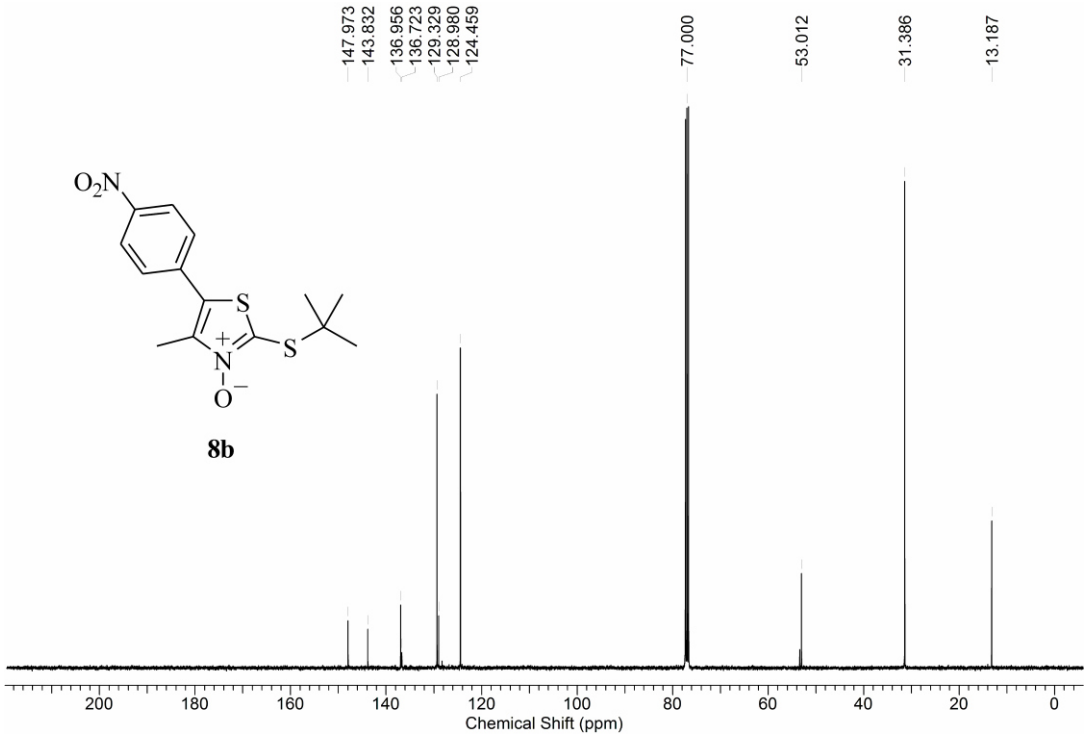

Figure C15. Carbon-13 NMR-spectrum of 2-(2-methylpropyl-2-sulfanyl)-5-(4-nitrophenyl)-4-methylthiazole *N*-oxide (**8b**) (100MHz, $CDCl_3$, 23 °C).

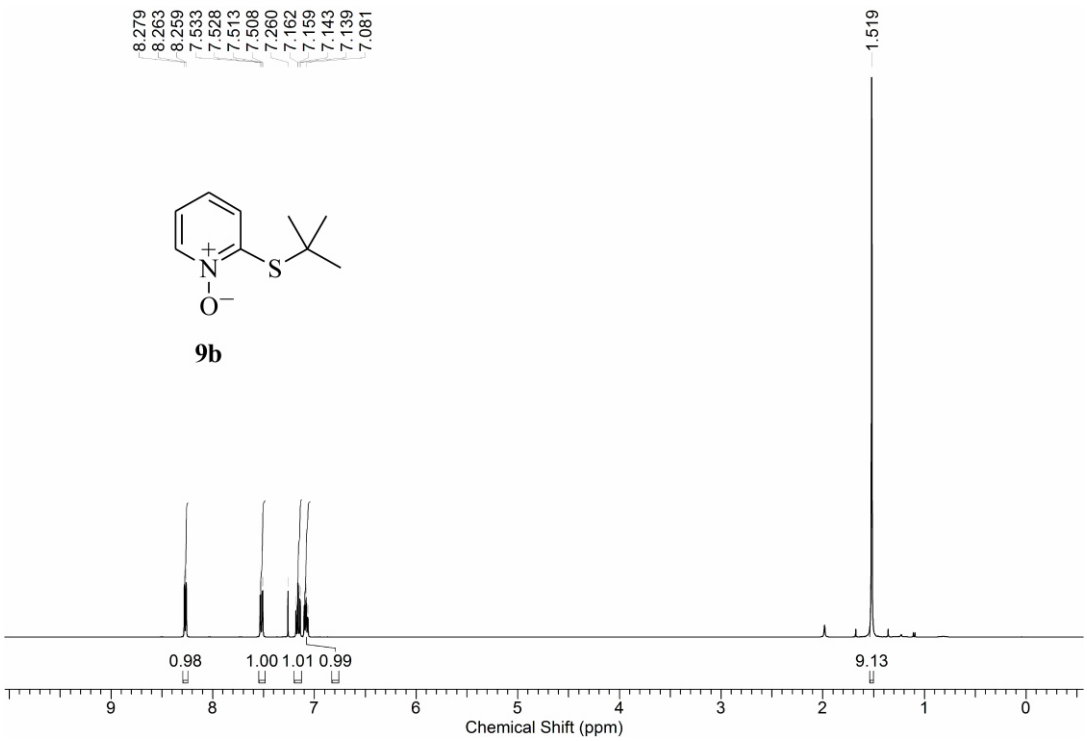

Figure C16. Proton-1 NMR-spectrum of 2-(2-methylpropyl-2-sulfanyl)pyridine *N*-oxide (**9b**) (400MHz, $CDCl_3$, 23 °C).

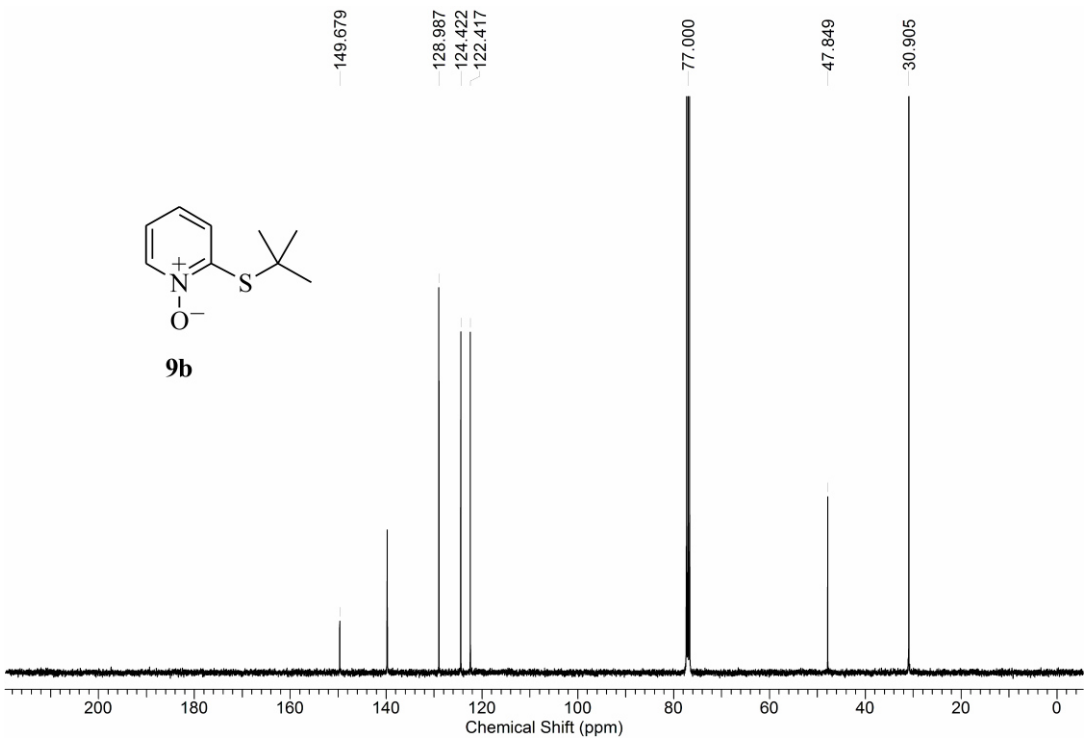

Figure C17. Carbon-13 NMR-spectrum of 2-(2-methylpropyl-2-sulfanyl)pyridine *N*-oxide (**9b**) (100MHz, $CDCl_3$, 23 °C).

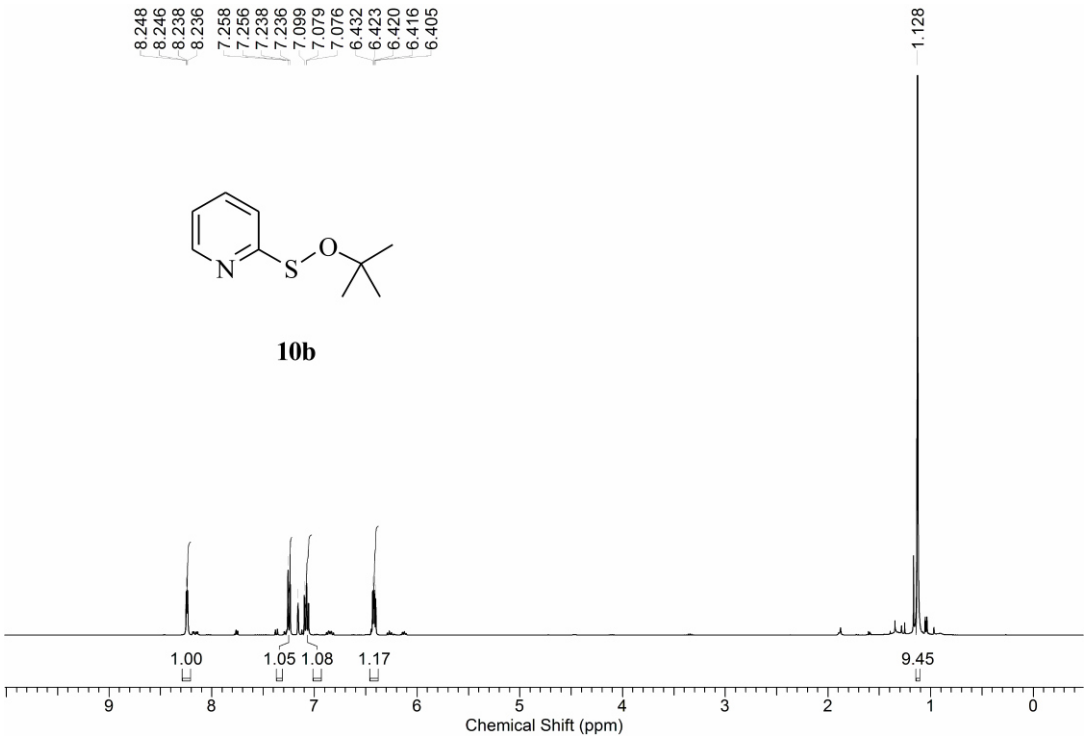

Figure C18. Proton-1 NMR-spectrum of *O*-(2-methylprop-2-yl)pyridine-2-sulfenate (**10b**) (400MHz, C_6D_6, 23 °C).

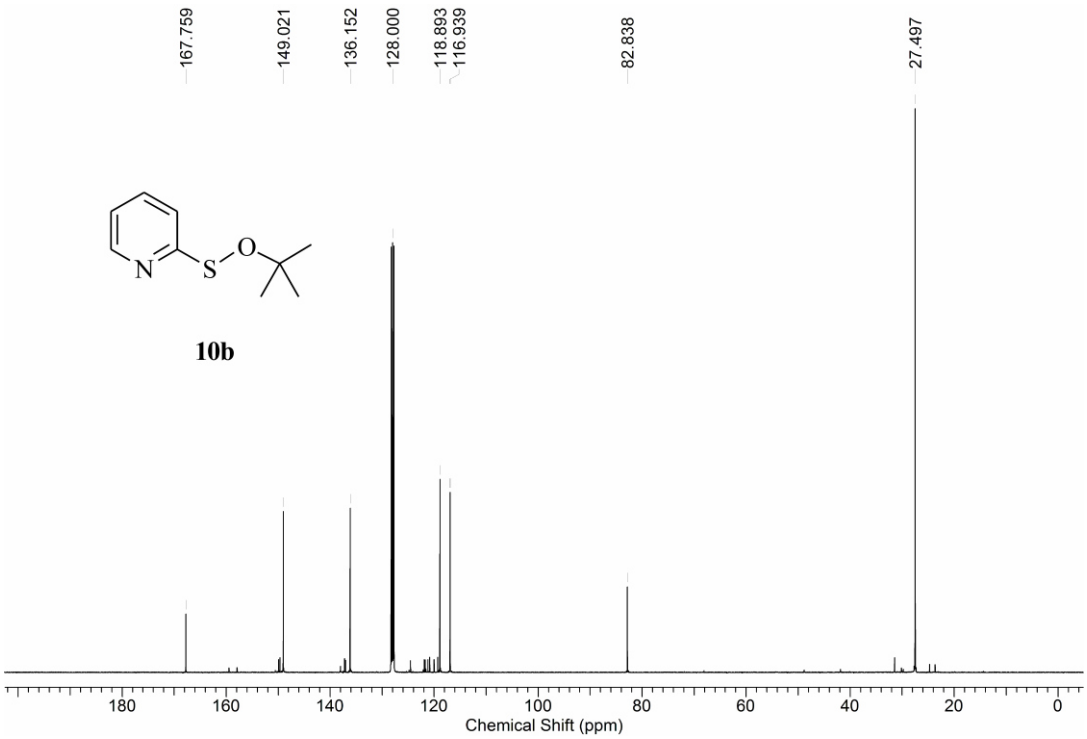

Figure C19. Proton-1 NMR-spectrum of *O*-(2-methylprop-2-yl)pyridine-2-sulfenate (**10b**) (100MHz, C_6D_6, 23 °C).

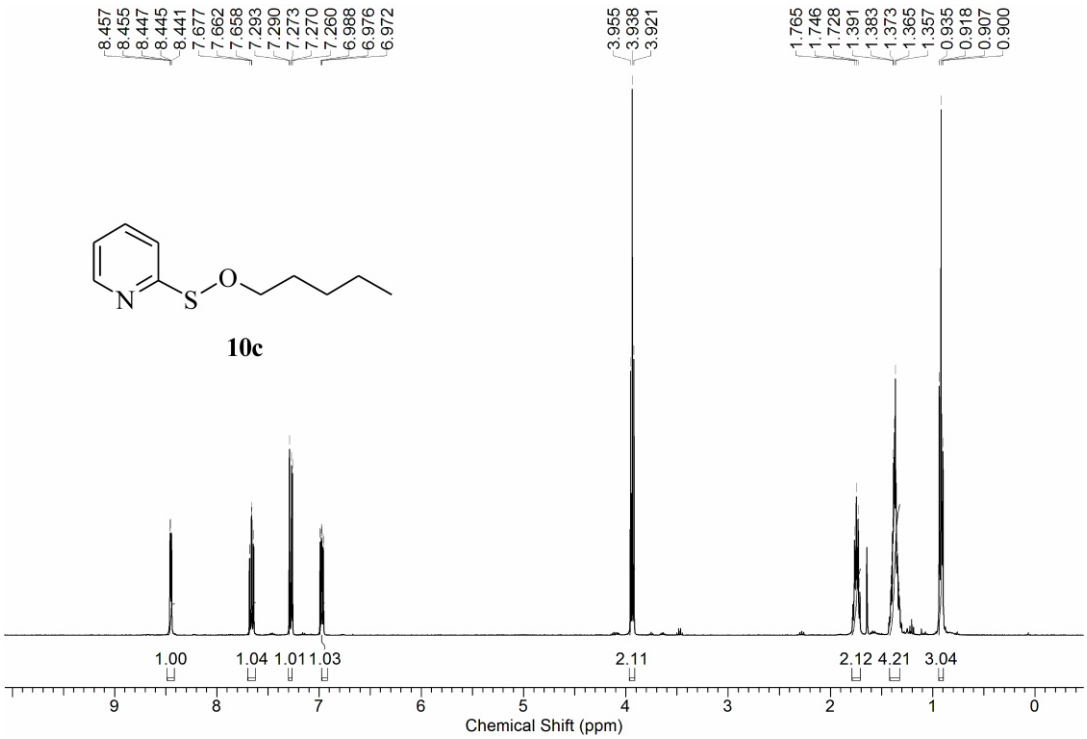

Figure C20. Proton-1 NMR-spectrum of *O*-pentyl 2-pyridylsulfenate (**10c**) (400MHz, $CDCl_3$, 23 °C).

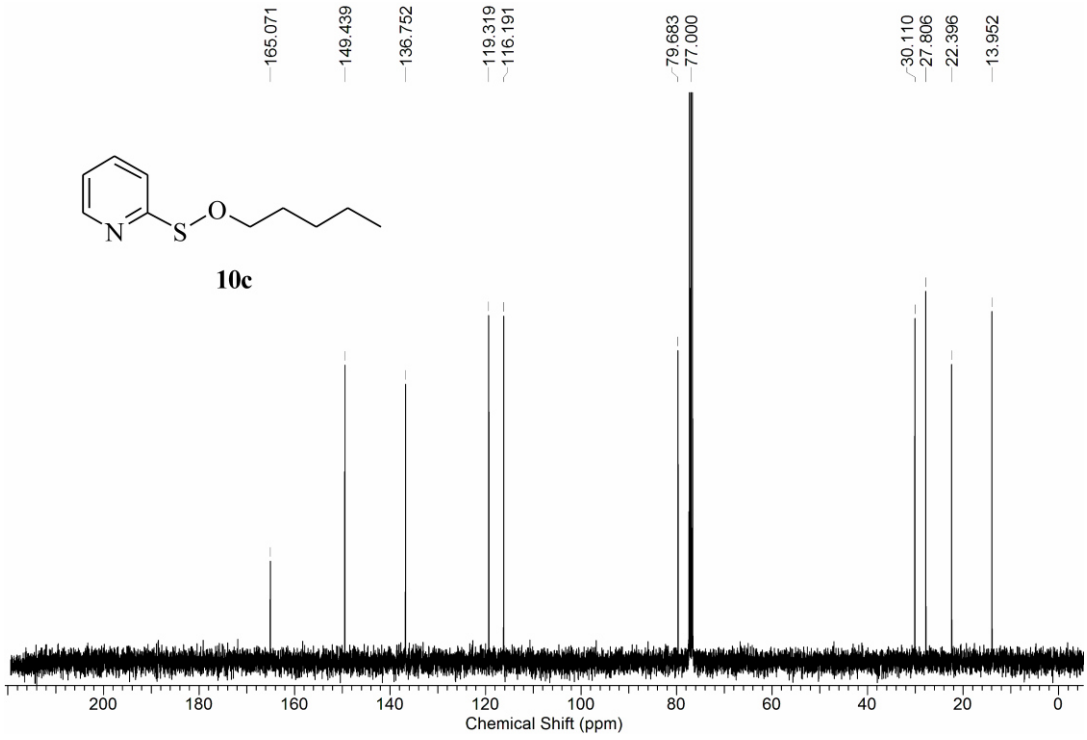

Figure C21. Carbon-13 NMR-spectrum of *O*-pentyl 2-pyridylsulfenate (**10c**) (100MHz, $CDCl_3$, 23 °C).

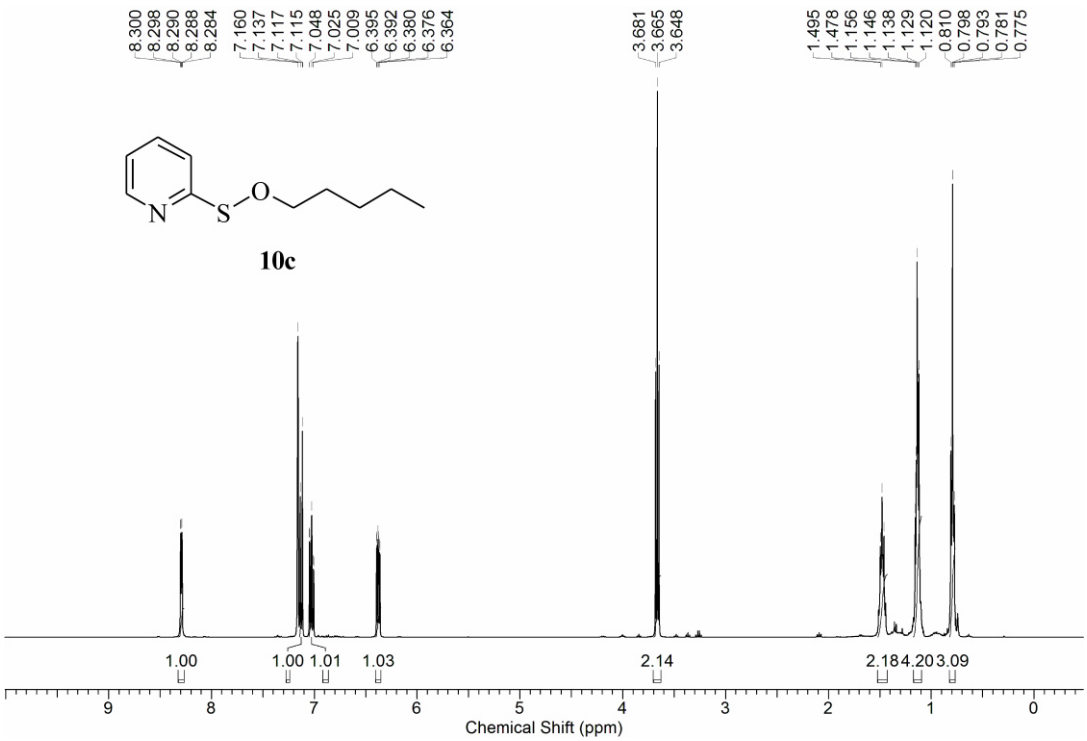

Figure C22. Proton-1 NMR-spectrum of *O*-pentyl 2-pyridylsulfenate (**10c**) (400MHz, C_6D_6, 23 °C).

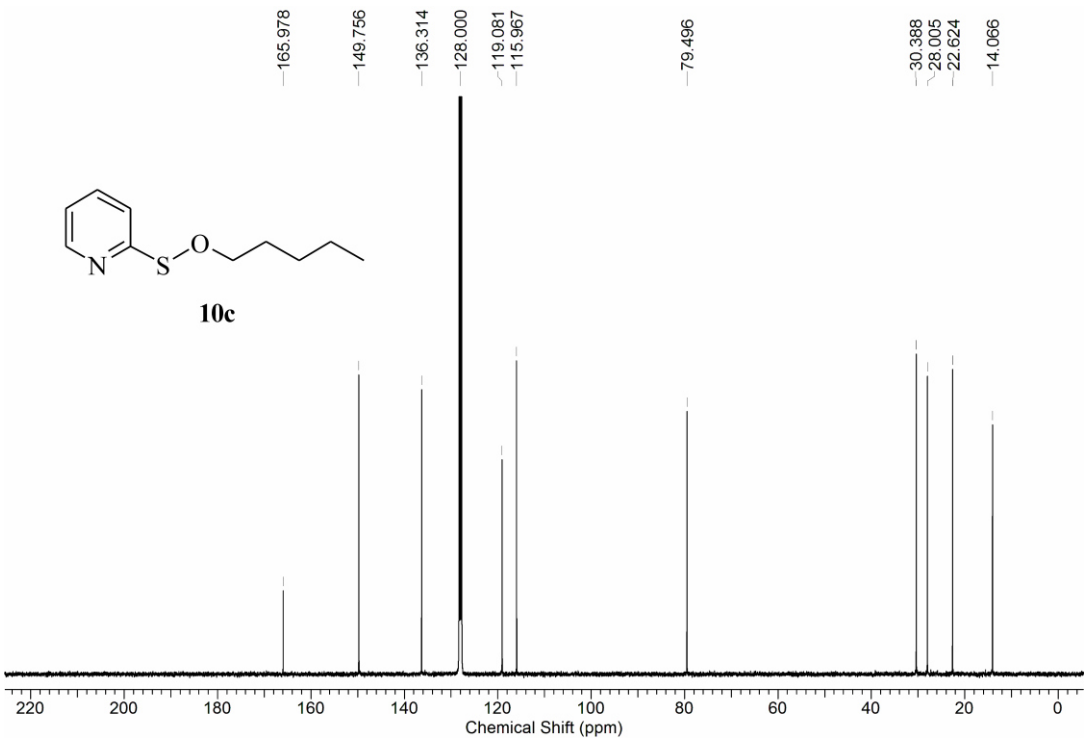

Figure C23. Carbon-13 NMR-spectrum of *O*-pentyl 2-pyridylsulfenate (**10c**) (100MHz, C_6D_6, 23 °C).

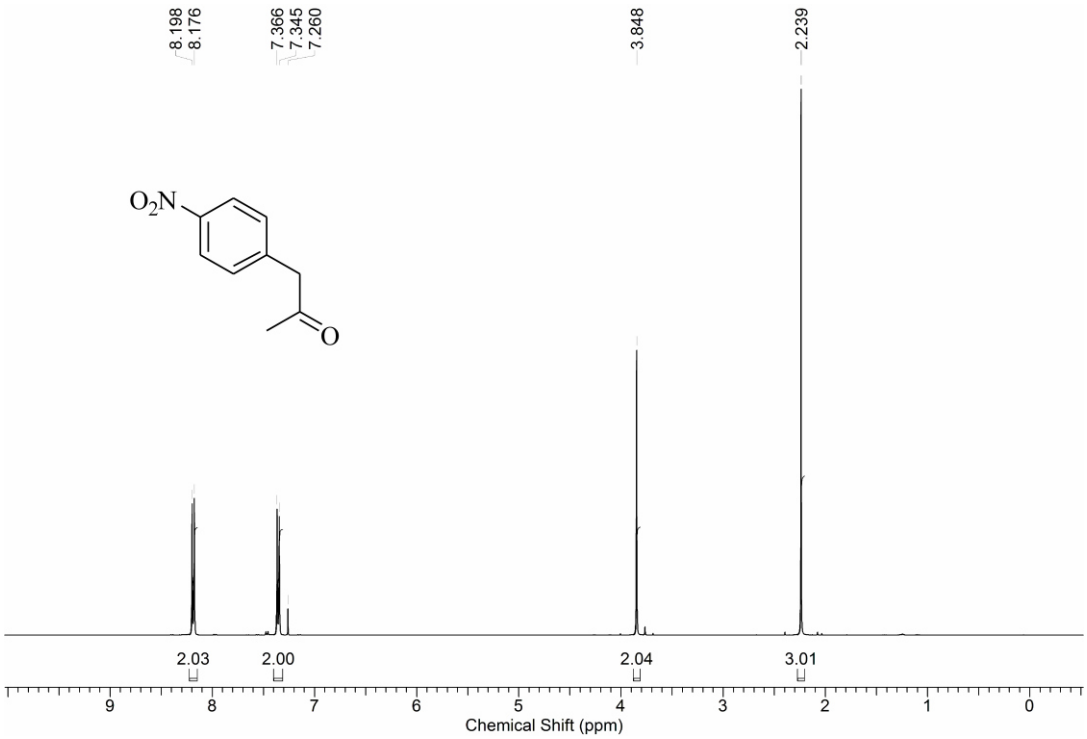

Figure C24. Proton-1 NMR-spectrum of 1-(4-nitrophenyl)propan-2-one (400MHz, $CDCl_3$, 23 °C).

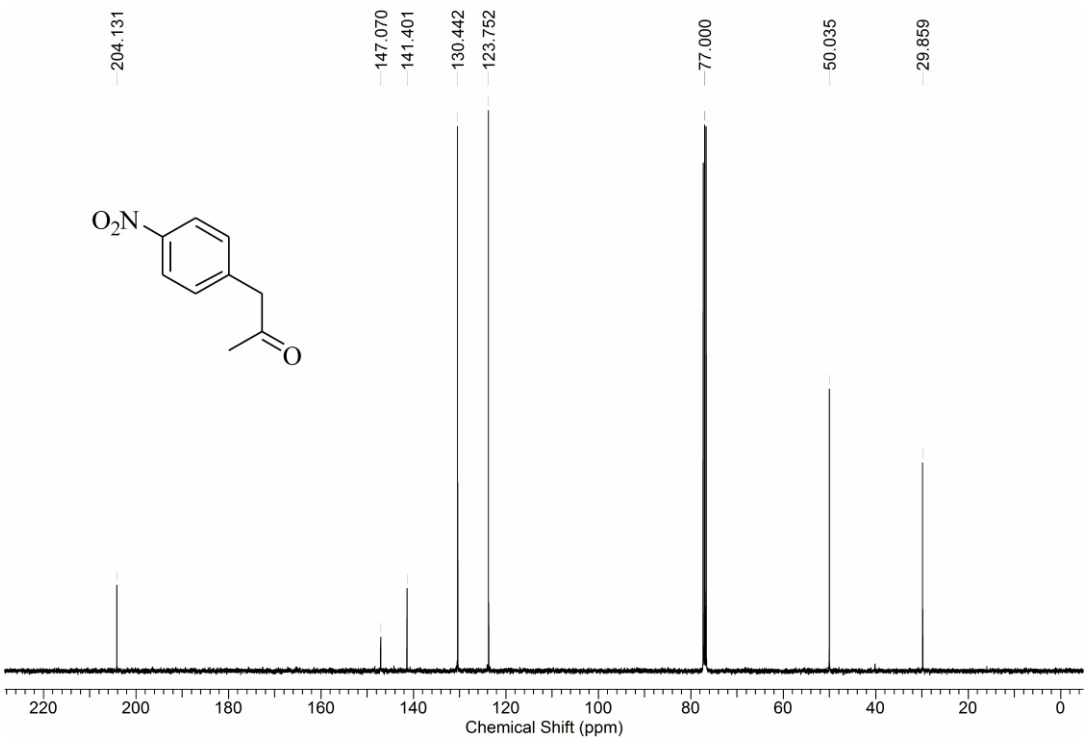

Figure C25. Carbon-13 NMR-spectrum of 1-(4-nitrophenyl)propan-2-one (100MHz, $CDCl_3$, 23 °C).

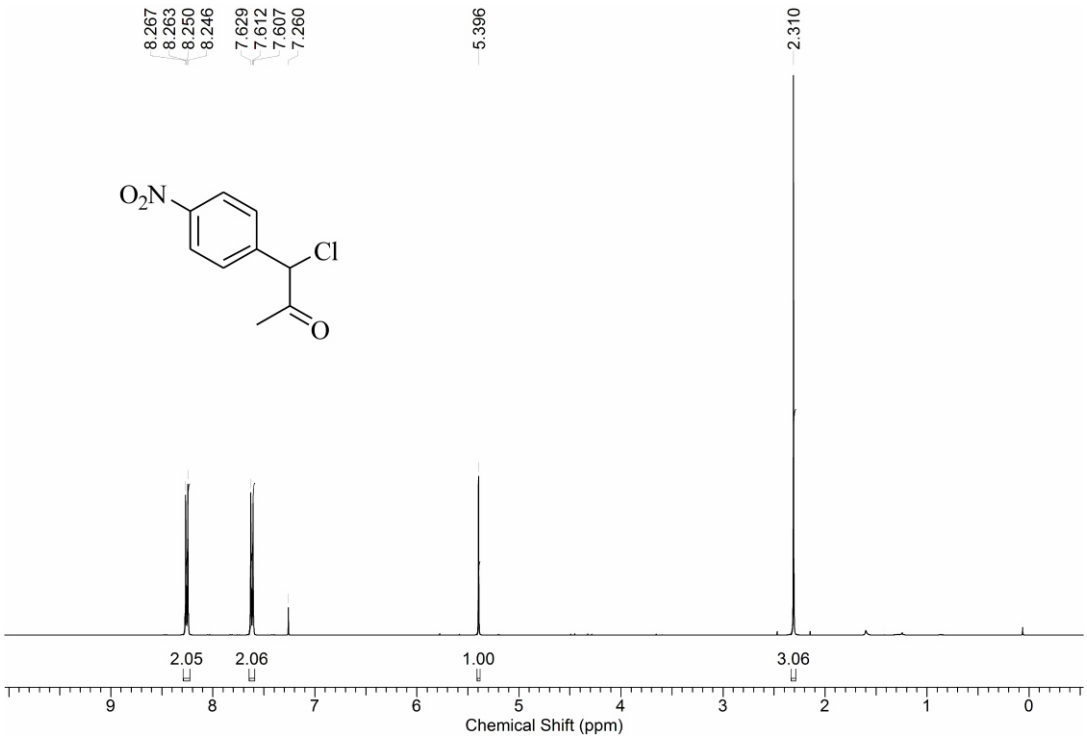

Figure C26. Proton-1 NMR-spectrum of 1-chloro-1-(4-nitrophenyl)propan-2-one (400MHz, $CDCl_3$, 23 °C).

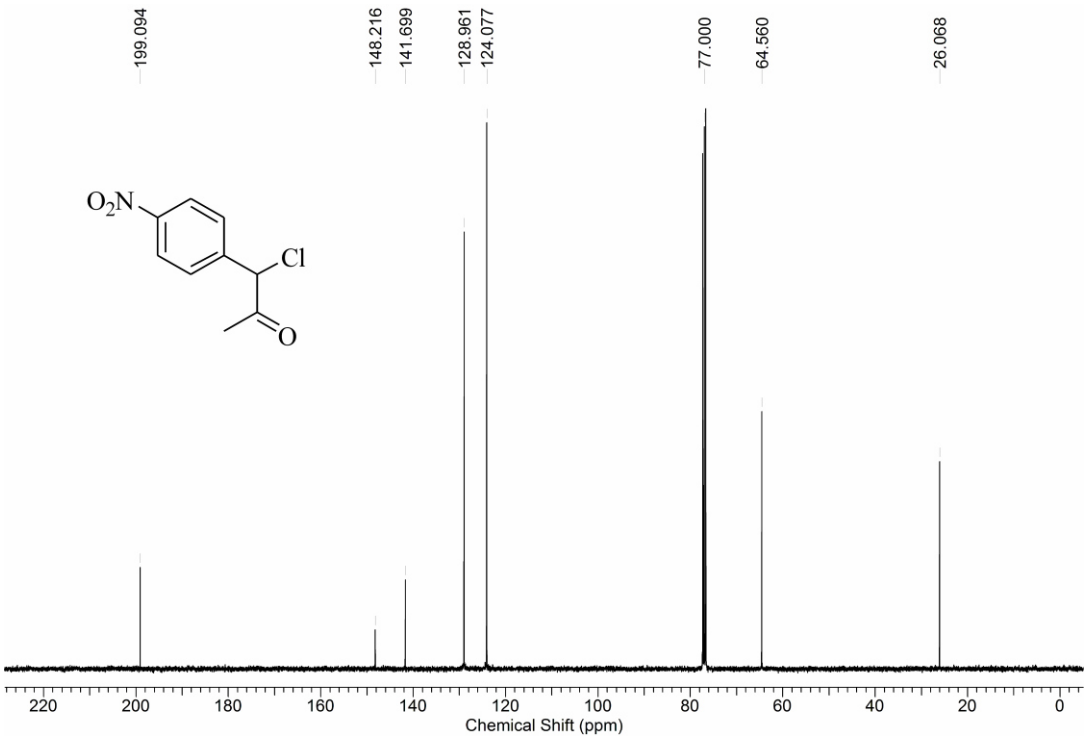

Figure C27. Carbon-13 NMR-spectrum of 1-chloro-1-(4-nitrophenyl)propan-2-one (100MHz, $CDCl_3$, 23 °C).

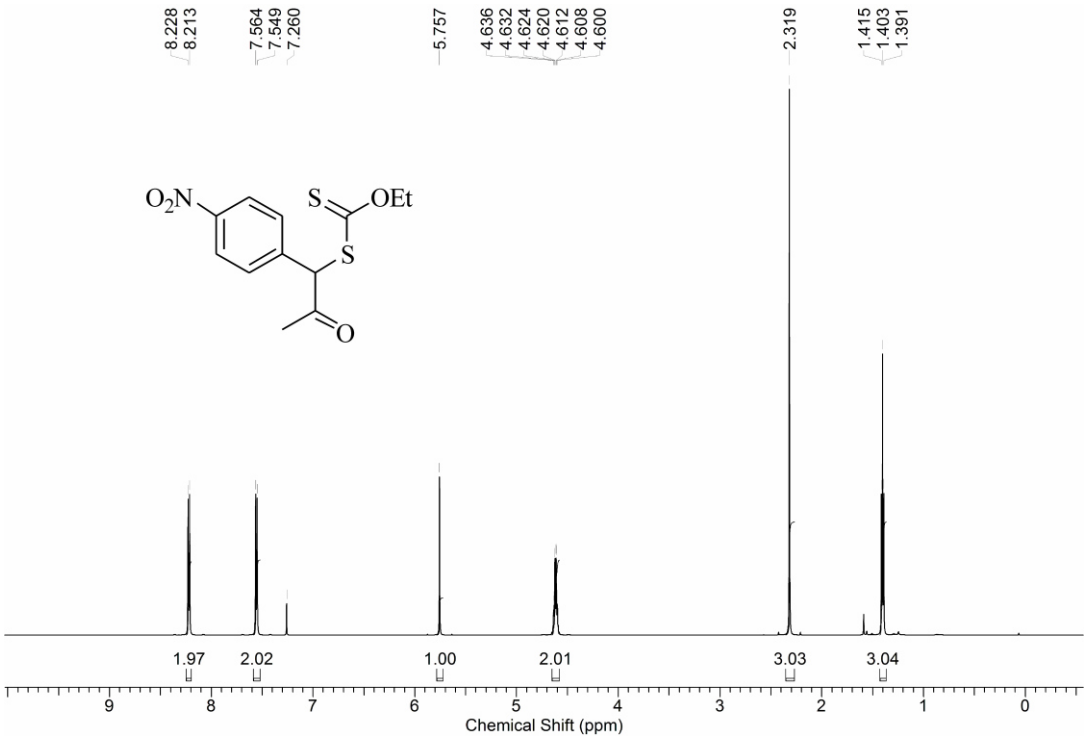

Figure C28. Proton-1 NMR-spectrum of 1-(ethoxythiocarbonylsulfanyl)-1-(4-nitrophenyl)propan-2-one (600MHz, $CDCl_3$, 23 °C).

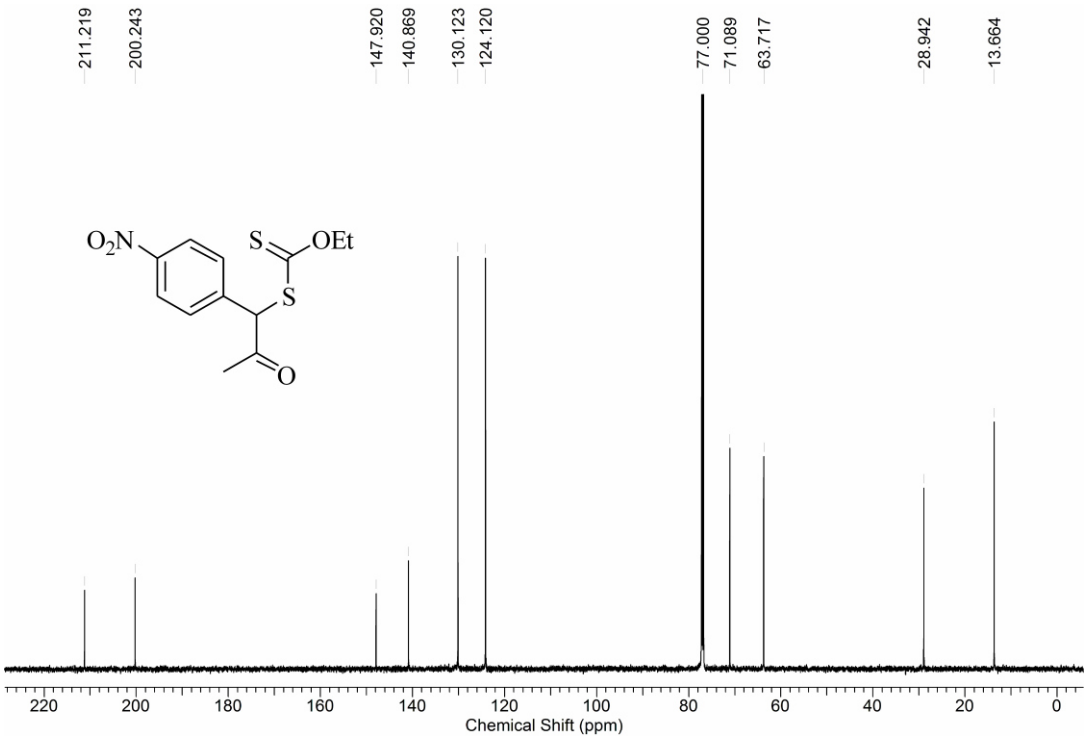

Figure C29. Carbon-13 NMR-spectrum of 1-(ethoxythiocarbonylsulfanyl)-1-(4-nitrophenyl)propan-2-one (150MHz, $CDCl_3$, 23 °C).

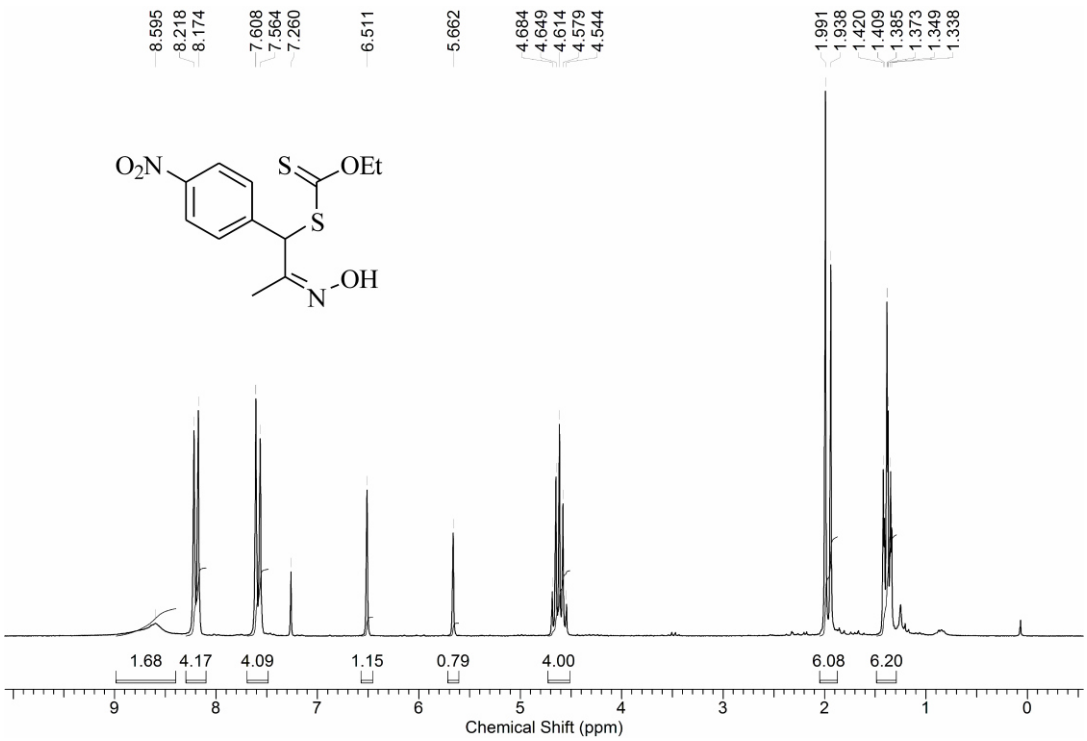

Figure C30. Proton-1 NMR-spectrum of a 60/40-mixture of *E*/*Z*-isomers of (ethoxythiocarbonylsulfanyl)-1-(4-nitrophenyl)propan-2-one oxime (200MHz, $CDCl_3$, 23 °C).

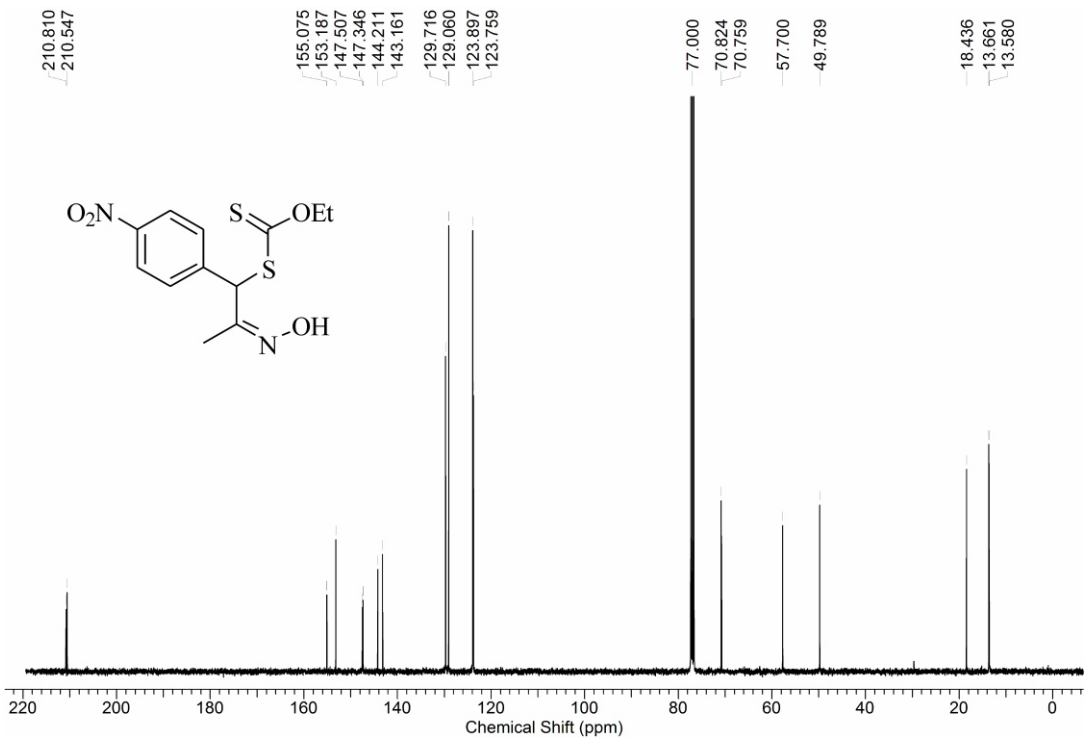

Figure C31. Carbon-13 NMR-spectrum of a 60/40-mixture of *E*/*Z*-isomers of (ethoxythiocarbonylsulfanyl)-1-(4-nitrophenyl)propan-2-one oxime (100MHz, $CDCl_3$, 23 °C).

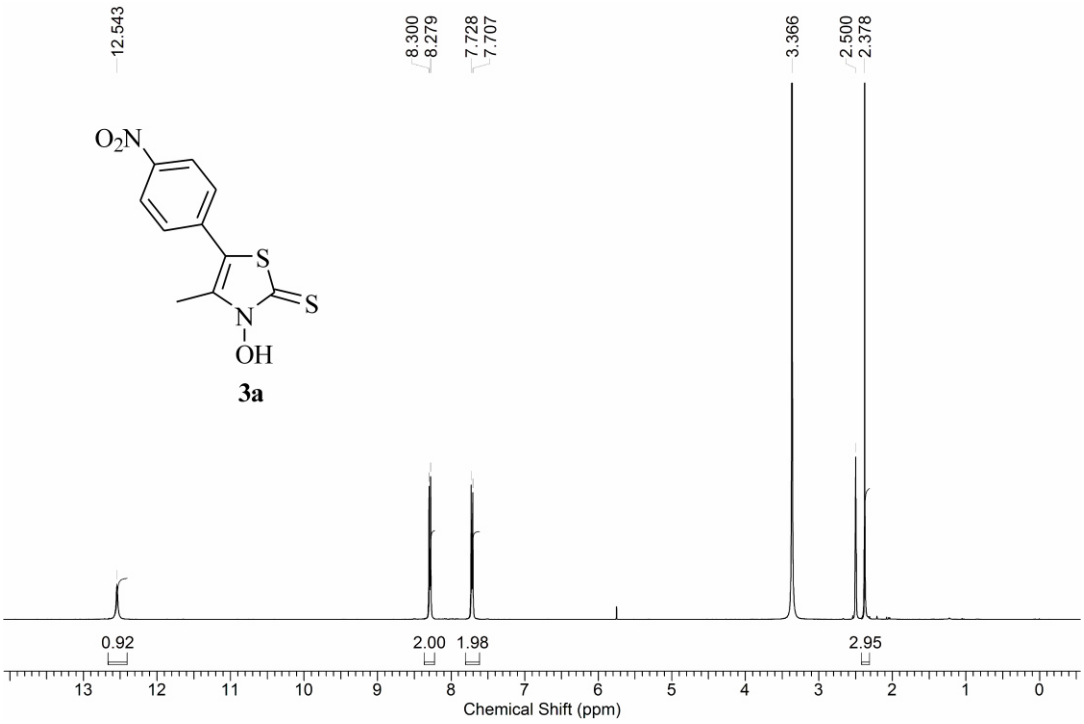

Figure C32. Proton-1 NMR-spectrum of 3-hydroxy-4-methyl-5-(4-nitrophenyl)thiazole-2(3*H*)-thione (**3a**) (400MHz, $CDCl_3$, 23 °C).

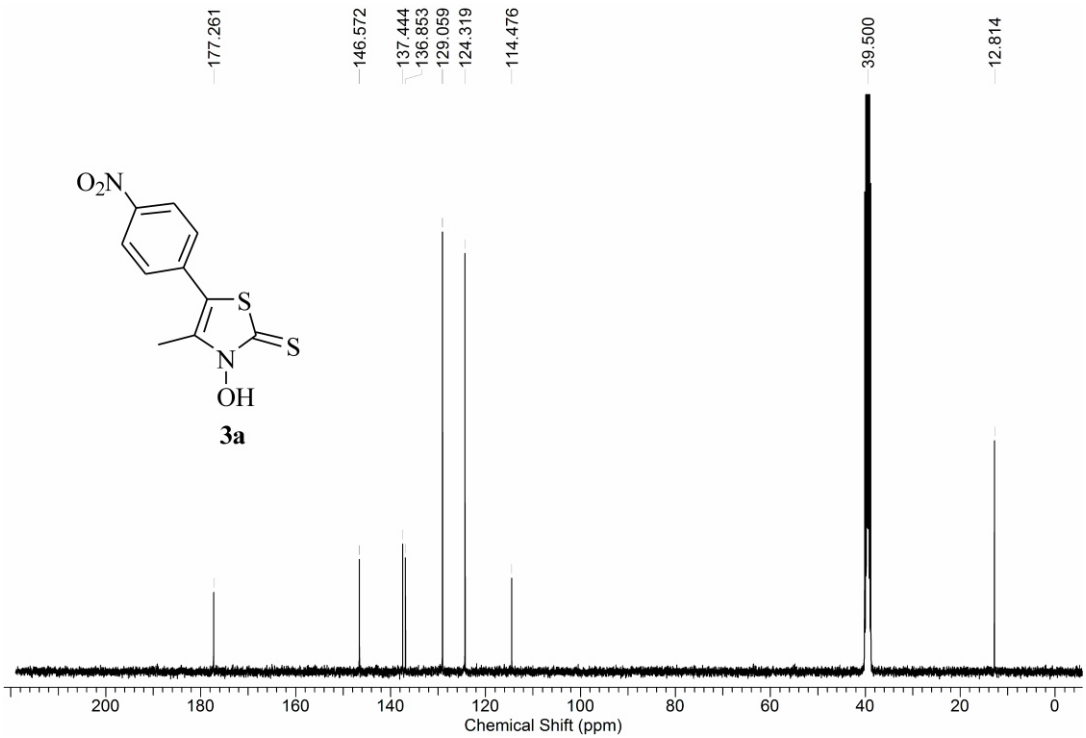

Figure C33. Carbon-13 NMR-spectrum of 3-hydroxy-4-methyl-5-(4-nitrophenyl)thiazole-2(3*H*)-thione (**3a**) (100MHz, $CDCl_3$, 23 °C).

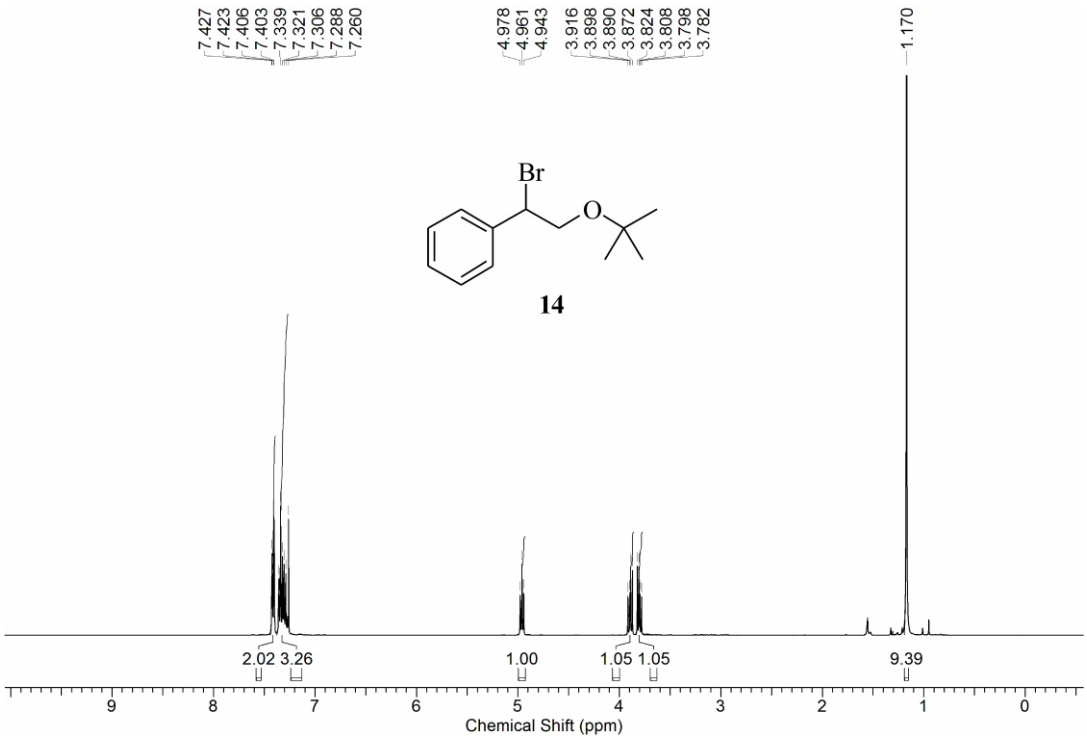

Figure C34. Proton-1 NMR-spectrum of 2-brom-2-phenyl-1-(2-methyl-2-propoxy)ethan (**14**) (400MHz, $CDCl_3$, 23 °C).

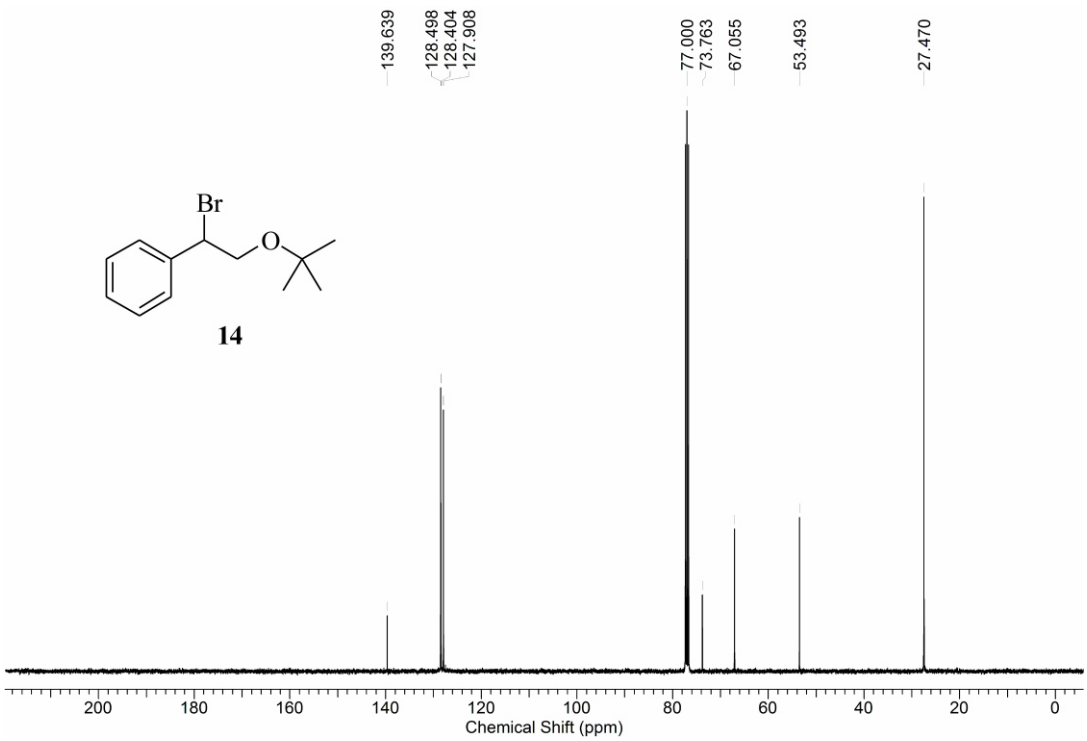

Figure C35. Carbon-13 NMR-spectrum of 2-brom-2-phenyl-1-(2-methyl-2-propoxy)ethan (**14**) (100MHz, $CDCl_3$, 23 °C).

C7 Computational Chemistry

C7.1 Computational Details

Calculations were performed with the Gaussian03[5] suite of program, using density functional/Hartree-Fock hybrid models B3LYP and BHandHLYP, and Møller-Plesset second order pertubation theory MP2 in combination with the split valance double-ζ basis set 6-31+G(d,p). No symmetry or internal coordinate constraints were applied during energy function minimization. All energy fuction minimizations were conducted using ultrafine grid in combination with the tight option. Absence of an imaginary mode of vibration served as evidence for assigning computed structures as minimum on the potential energy surface. Approximate Gibbs free energies ($G^{298.15}$) were obtained through thermochemical analysis for 298.15 K by unscaled frequency calculation from the thermal correction reported by Gaussian03. Likewise obtained Gibbs free energies take into account zero-point correction, thermal correction, and entropy. All transition structures were maxima on electronic potential energy hypersurface, which may not correspond to maxima on the free energy surface.

All NBO-calculations[6] were performed with the density functional/Hartree-Fock hybrid model B3LYP and split valance double-ζ basis sets 6-31G(d) using input coordinates from B3LYP/6-31+G(d,p)-energy minimized structures.

Vibrational analysis of 3-(*tert*-butoxy)thiazolethiones were performed from B3LYP-energy-minimized structures, considering corrections from Grimme (D3 dispersion parameters), and using the TZVP-basis set. For energy minimizing structures we used the Berny algorithm implemented in GAUSSIAN, and energies and gradients from TURBOMOLE, for shortening computing time. Computed harmonic vibrational frequencies were scaled by factor 0.99, since calculated vibrational frequencies disregarding anharmonicities generally are larger than experimental values. For comparing computed to experimental spectra, we transformed line spectra usign Lorentzian-functions with full width at half maximum (FWHM) of 15 cm^{-1} into simulated spectra.

C7.2 Ball-and-Stick Presentations of Computed Structures

Graphics displaying computed equilibrium structures in the succeeding sections were generated from B3LYP-calculated atomic coordinates, which were file-converted with OpenBabel[7] for generating presentation graphics with ChemPlus-add on (release 1.6) for HyperChem 4.5[8] MP2-calculated geometries differed insignificantly with respect to bond lengths, bond angles and torsion angles, but showed similar conformations for energy-minimized structures and therefore were presented separately. In succeeding depictions of modelled compounds, oxygen is displayed in red, carbon in gray, nitrogen in blue, sulfur in yellow, and hydrogen in white.

C7.3 3-(*tert*-Butoxy)-4-methylthiazole-2(3*H*)thione (2b)

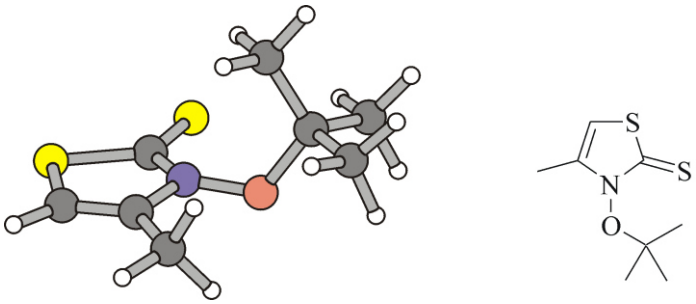

Figure C36. Computed minimum structure of 3-(*tert*-butoxy)thiazolethione **2b**.

(*i*) B3LYP/6-31+G**//B3LYP/6-31+G**

Standard orientation:

Center Number	Atomic Number	Atomic Type	Coordinates (Angstroms) X	Y	Z
1	7	0	0.321658	0.303111	-0.253638
2	6	0	1.146446	-0.794600	-0.119921
3	16	0	2.747954	-0.174657	0.300137
4	6	0	2.222647	1.489461	0.155528
5	6	0	0.911935	1.575584	-0.159847
6	6	0	0.114582	2.813080	-0.414434
7	16	0	0.777878	-2.403366	-0.295891
8	8	0	-0.940035	0.184397	-0.788242
9	6	0	-2.092845	-0.071540	0.156217
10	6	0	-3.037235	1.119401	-0.031528
11	6	0	-2.740284	-1.355931	-0.363685
12	6	0	-1.628992	-0.205116	1.602919
13	1	0	2.906701	2.313056	0.299403
14	1	0	0.786625	3.673607	-0.441188
15	1	0	-0.416389	2.748192	-1.368395
16	1	0	-0.629091	2.986969	0.369503
17	1	0	-3.987758	0.920501	0.474470
18	1	0	-2.620721	2.040775	0.383533
19	1	0	-3.245051	1.277825	-1.093967
20	1	0	-3.647822	-1.572063	0.210644
21	1	0	-3.019609	-1.240468	-1.415447
22	1	0	-2.048740	-2.195348	-0.280606
23	1	0	-2.510545	-0.367162	2.231234
24	1	0	-0.959261	-1.058007	1.733213
25	1	0	-1.130502	0.701497	1.959557

```
Zero-point correction=                          0.200656 (Hartree/Particle)
Thermal correction to Energy=                   0.214231
Thermal correction to Enthalpy=                 0.215176
Thermal correction to Gibbs Free Energy=        0.160853
Sum of electronic and zero-point Energies=          -1238.810630
Sum of electronic and thermal Energies=             -1238.797055
Sum of electronic and thermal Enthalpies=           -1238.796111
Sum of electronic and thermal Free Energies=        -1238.850433

Version=AM64L-G03RevE.01\State=1-A\HF=-1239.0112861\RMSD=7.748e-09\
RMSF=1.276e-06\Dipole=0.6346478,0.5918876,-2.080593\PG=C01
[X(C8H13N1O1S2)]\NImag=0\\\@
```

(*ii*) BHandHLYP/6-31+G**//BHandHLYP/6-31+G**

Standard orientation:

Center Number	Atomic Number	Atomic Type	Coordinates (Angstroms) X	Y	Z
1	6	0	0.888687	1.564171	-0.162414
2	7	0	0.315141	0.295414	-0.259282
3	6	0	1.141518	-0.775866	-0.121166
4	16	0	2.717535	-0.156782	0.299510
5	6	0	2.185283	1.492112	0.155707
6	8	0	-0.930582	0.166145	-0.776802
7	6	0	-2.060453	-0.080085	0.151804
8	6	0	-1.602254	-0.181970	1.593188
9	16	0	0.791023	-2.379744	-0.295659
10	6	0	0.080124	2.785285	-0.415325
11	6	0	-3.014306	1.087218	-0.052013
12	6	0	-2.699798	-1.369975	-0.333298
13	1	0	2.855198	2.316502	0.300701
14	1	0	0.738709	3.645221	-0.455040
15	1	0	-0.455960	2.706400	-1.355488
16	1	0	-0.648529	2.952631	0.372080
17	1	0	-3.952532	0.888062	0.458685
18	1	0	-2.609828	2.014590	0.339113
19	1	0	-3.225859	1.220287	-1.108902
20	1	0	-3.600340	-1.572124	0.241408
21	1	0	-2.975649	-1.279539	-1.380007
22	1	0	-2.012316	-2.199641	-0.231400
23	1	0	-2.477677	-0.340312	2.216579
24	1	0	-0.929291	-1.019330	1.739639
25	1	0	-1.116988	0.729280	1.931506

```
Zero-point correction=                          0.208528 (Hartree/Particle)
Thermal correction to Energy=                   0.221583
Thermal correction to Enthalpy=                 0.222527
Thermal correction to Gibbs Free Energy=        0.169280
Sum of electronic and zero-point Energies=          -1238.486397
Sum of electronic and thermal Energies=             -1238.473342
Sum of electronic and thermal Enthalpies=           -1238.472398
Sum of electronic and thermal Free Energies=        -1238.525645

Version=AM64L-G03RevE.01\State=1-A\HF=-1238.6949249\RMSD=4.918e-09\
RMSF=1.068e-06\Dipole=-1.4646342,0.6603484,-1.7280528\PG=C01
[X(C8H13N1O1S2)]\NImag=0\\\@
```

(*iii*) MP2/6-31+G**

Standard orientation:

Center Number	Atomic Number	Atomic Type	Coordinates (Angstroms) X	Y	Z
1	6	0	0.878595	1.569826	-0.180808
2	7	0	0.311148	0.298922	-0.266303
3	6	0	1.142899	-0.792100	-0.125947
4	16	0	2.711128	-0.158673	0.320024
5	6	0	2.190342	1.483061	0.161206
6	8	0	-0.941852	0.150516	-0.816567
7	6	0	-2.053047	-0.077295	0.165837
8	6	0	-1.532926	-0.154565	1.586945
9	16	0	0.765111	-2.384408	-0.318138
10	6	0	0.068018	2.789841	-0.444217
11	6	0	-3.005278	1.091882	-0.025402
12	6	0	-2.704910	-1.373560	-0.280573
13	1	0	2.862862	2.310646	0.312030
14	1	0	0.736928	3.642881	-0.533416
15	1	0	-0.497783	2.681971	-1.367262
16	1	0	-0.632513	2.990141	0.364713
17	1	0	-3.929338	0.903423	0.521138
18	1	0	-2.576378	2.021652	0.339663
19	1	0	-3.247914	1.205301	-1.081085
20	1	0	-3.590938	-1.563438	0.326042
21	1	0	-3.010543	-1.293090	-1.322920
22	1	0	-2.009708	-2.201179	-0.184023
23	1	0	-2.385482	-0.302320	2.249746
24	1	0	-0.851451	-0.992857	1.715150
25	1	0	-1.032954	0.767052	1.884471

```
Zero-point correction=                           0.205682 (Hartree/Particle)
Thermal correction to Energy=                    0.219051
Thermal correction to Enthalpy=                  0.219995
Thermal correction to Gibbs Free Energy=         0.166112
Sum of electronic and zero-point Energies=          -1236.416853
Sum of electronic and thermal Energies=             -1236.403484
Sum of electronic and thermal Enthalpies=           -1236.402540
Sum of electronic and thermal Free Energies=        -1236.456423

Version=AM64L-G03RevE.01\State=1-A\HF=-1234.7955932\MP2=-1236.6225353\
RMSD=7.039e-09\RMSF=3.838e-06\Dipole=-1.3427588,0.6728942,-1.6501606\
PG=C01 X(C8H13N1O1S2)]\NImag=0\\\@
```

Table C1. Calculated parameters and energies of conformers associated with rotation about the N,O-bond in MTTO*t*Bu (**2b**)

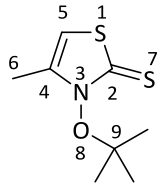

$\omega_{C2,N3,O8,C9}$ / deg	$\alpha_{N3,O8,C9}$ / deg	E / a.u. [a]	E_{rel} / kJ mol^{-1}	$d_{N3,O8}$ / Å	$d_{N3,C2}$ / Å	$d_{C2,S7}$ / Å	$E_{n1(O)}$ / a.u. [b]	$E_{n2(O)}$ / a.u. [b]	$E_{n1(N)}$ / a.u. [b]
0	129.0	–1238.9930907	47.8	1.4091	1.3725	1.6740	–0.61044	–0.32691	–0.28811
15	128.5	–1238.9940060	45.4	1.4068	1.3736	1.6733	–0.61068	–0.32717	–0.28829
30	126.8	–1238.9967176	38.2	1.4003	1.3744	1.6713	–0.61179	–0.32776	–0.28871
45	124.3	–1239.0009268	27.2	1.3914	1.3755	1.6683	–0.61474	–0.32802	–0.28904
60	121.8	–1239.0057168	14.6	1.3824	1.3761	1.6651	–0.62037	–0.32707	–0.28890
75	119.6	–1239.0096020	4.4	1.3765	1.3768	1.6624	–0.62808	–0.32447	–0.28809
90	118.2	–1239.0112750	0.03	1.3753	1.3792	1.6600	–0.63401	–0.32226	–0.28675
105	117.6	–1239.0099428	3.5	1.3786	1.3839	1.6576	–0.63280	–0.32349	–0.30140
120	118.0	–1239.0054471	15.3	1.3846	1.3902	1.6553	–0.63028	–0.32301	–0.31067
135	119.6	–1238.9980818	34.7	1.3934	1.3964	1.6539	–0.62683	–0.31978	–0.31780
150	122.8	–1238.9891114	58.2	1.4033	1.3989	1.6542	–0.61865	–0.31842	–0.31658
165	127.2	–1238.9810731	79.3	1.4089	1.3940	1.6569	–0.60565	–0.31996	–0.30201
180	130.2	–1238.9771589	89.6	1.4074	1.3869	1.6595	–0.59573	–0.32022	–0.28197
91.3	118.3	–1239.0112861	0.0	1.3754	1.3795	1.6598	–0.63423	–0.32227	–0.28662

[a] 1 atom unit = 1 Hartree. 1 Hartree/particle = 2625.5 kJ mol^{-1} or [b] 1. a.u. = 27.211 eV; [e] *n*N(X) = non-bonding electron pair number N at heteroatom X

Table C2. Calculated parameters and energies associated with angle variation at thiohydroxmate oxygen in MTTO*t*Bu (**2b**)

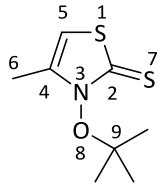

$\alpha_{N3,O8,C9}$ / deg	$\omega_{C2,N3,O8,C9}$ / deg	E / a.u. [a]	E_{rel} / kJ mol^{-1}	$d_{N3,O8}$ / Å	$d_{N3,C2}$ / Å	$d_{C2,S7}$ / Å	$E_{n1(O)}$ / a.u. [b]	$E_{n2(O)}$ / a.u. [b]	$E_{n1(N)}$ / a.u. [b]
90	108.1	–1238.9661922	110.5	1.4446	1.3949	1.6514	–0.76494	–0.32172	–0.32754
100	98.3	–1238.9935442	46.6	1.4062	1.3814	1.6586	–0.72634	–0.32288	–0.30421
110	94.6	–1239.0080007	8.6	1.3871	1.3804	1.6591	–0.67449	–0.32358	–0.28658
120	90.4	–1239.0111254	0.4	1.3731	1.3793	1.6600	–0.62503	–0.32181	–0.28660
130	85.4	–1239.0056229	14.9	1.3634	1.3776	1.6612	–0.57445	–0.32094	–0.28625
118.3	91.3	–1239.0112861	0.0	1.3754	1.3795	1.6598	–0.63423	–0.32227	–0.28662
129.0	0.0	–1238.9930907	47.8	1.4091	1.3733	1.6740	–0.61044	–0.32691	–0.28811
130.2	180.0	–1238.9771589	89.6	1.4074	1.3869	1.6595	–0.59573	–0.32022	–0.28197

[a] 1 a.u. = 1 Hartree. 1 Hartree/particle = 2625.5 kJ mol^{-1}. [b] 1. a.u. = 27.211 eV; [e] *n*N(X) = non-bonding electron pair number N at heteroatom X.

Table C3. Calculated parameters and energies associated with angle variation at thiohydroxmate oxygen in MTTO*t*Bu (**2b**)

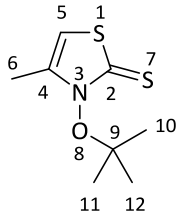

$\alpha_{N3,O8,C9}$ / deg	$E_{\pi 1(N3,O8)}$ [a] / kJ mol^{-1}	$E_{\pi 2(N3,O8)}$ [b] / kJ mol^{-1}	$E_{\pi 3(N3,O8)}$ [c] / kJ mol^{-1}	$E_{\pi 4(N3,C4)}$ [d] / kJ mol^{-1}	$E_{\pi 5(N3,C2)}$ [e] / kJ mol^{-1}	$\sigma_{N3,O8}$ / %p(O)	$\sigma_{C9,O8}$ / %p(O)	$n1(O)$ [f] / %p	$n2(O)$ [f] / %p
90	40.7	36.4	36.4	97.4	92.7	87.11	80.64	32.25	99.50
100	43.0	47.0	50.4	123.9	219.9	83.88	78.98	36.89	99.75
110	66.2	53.8	68.3	139.6	256.2	81.32	74.97	43.37	99.85
120	71.2	56.8	77.9	141.5	257.4	78.93	71.44	49.26	99.92
130	76.3	57.4	82.6	142.4	266.4	76.43	68.19	55.48	99.49
118.3	70.2	56.4	76.4	141.2	256.5	79.39	72.07	48.17	99.91
129.0	46.7	35.3	– [e]	134.9	299.3	80.92	66.64	52.29	99.95
130.2	66.3	35.1	– [e]	143.8	245.9	80.71	67.17	51.84	99.86

[a] [σ(C4,C5)→σ*(N3,O8)] + [σ(S1,C2)→σ*(N3,O8)] + [σ(C9,C10–12)→σ*(N3,O8)]. [b] [n1/2(O)→σ*(N3,C2)] + [n1/2(O)→σ*(N3,C4)]. [c] n1(N)→σ*(O8,C9). [d] n1(N)→π*(N3,C2). [e] n1(N)→π*(N3,C4). [e] nN(X) = non-bonding electron pair number N at heteroatom X. [f] Below default threshhold of 2.1 kJ mol^{-1}.

C7.4 3-Methoxy-4-methylthiazole-2(3*H*)thione (2d)

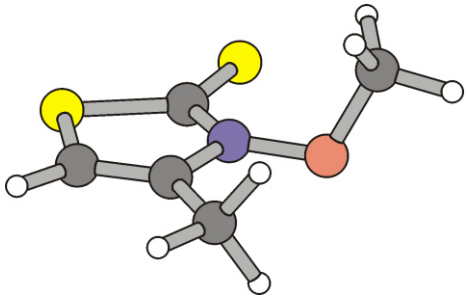

Figure C37. Computed minimum structure of 3-(methoxy)thiazolethione **2d**.

(*i*) B3LYP/6-31+G**//B3LYP/6-31+G**

Standard orientation:

Center Number	Atomic Number	Atomic Type	Coordinates (Angstroms) X	Y	Z
1	7	0	0.338230	0.352259	-0.139329
2	6	0	-0.892744	-0.255615	-0.066257
3	16	0	-0.569006	-1.976246	0.208161
4	6	0	1.167696	-1.740595	0.127168
5	6	0	1.489047	-0.442867	-0.070794
6	6	0	2.839263	0.177954	-0.230358
7	16	0	-2.389193	0.448486	-0.197219
8	8	0	0.460804	1.683632	-0.482366
9	6	0	0.262410	2.550573	0.658991
10	1	0	1.853523	-2.569414	0.224453
11	1	0	3.605536	-0.597337	-0.165484
12	1	0	2.927370	0.681375	-1.198105
13	1	0	3.036083	0.923064	0.547729
14	1	0	0.396223	3.555520	0.256317
15	1	0	-0.749018	2.432056	1.052060
16	1	0	1.013411	2.347310	1.429693

```
Zero-point correction=                          0.117026 (Hartree/Particle)
Thermal correction to Energy=                   0.126677
Thermal correction to Enthalpy=                 0.127621
Thermal correction to Gibbs Free Energy=        0.081829
Sum of electronic and zero-point Energies=          -1120.936373
Sum of electronic and thermal Energies=             -1120.926723
Sum of electronic and thermal Enthalpies=           -1120.925779
Sum of electronic and thermal Free Energies=        -1120.971571

Version=AM64L-G03RevE.01\State=1-A\HF=-1121.0533999\RMSD=1.064e-09\
RMSF=6.227e-07\Dipole=1.1379247,0 .5088277,-1.8860428\PG=C01
[X(C5H7N1O1S2)]\NImag=0
```

(*ii*) BHandHLYP/6-31+G**//BHandHLYP/6-31+G**

Standard orientation:

Center Number	Atomic Number	Atomic Type	Coordinates (Angstroms) X	Y	Z
1	7	0	0.338168	0.343415	-0.143887
2	6	0	-0.885378	-0.237286	-0.066627
3	16	0	-0.608340	-1.940864	0.207485
4	6	0	1.121347	-1.746975	0.128776
5	6	0	1.464328	-0.469921	-0.072177
6	6	0	2.817085	0.125483	-0.233247
7	16	0	-2.360219	0.492029	-0.194972
8	8	0	0.483954	1.652429	-0.475029
9	6	0	0.329949	2.511780	0.655169
10	1	0	1.785720	-2.582570	0.227291
11	1	0	3.564887	-0.656215	-0.168933
12	1	0	2.907454	0.621974	-1.194693
13	1	0	3.021837	0.862001	0.538965
14	1	0	0.477782	3.509106	0.261725
15	1	0	-0.667303	2.416086	1.066044
16	1	0	1.083774	2.289170	1.405475

```
Zero-point correction=                          0.121946 (Hartree/Particle)
Thermal correction to Energy=                   0.131258
Thermal correction to Enthalpy=                 0.132202
Thermal correction to Gibbs Free Energy=        0.087120
Sum of electronic and zero-point Energies=          -1120.694149
Sum of electronic and thermal Energies=             -1120.684837
Sum of electronic and thermal Enthalpies=           -1120.683893
Sum of electronic and thermal Free Energies=        -1120.728975

Version=AM64L-G03RevE.01\State=1-A\HF=-1120.8160947\RMSD=2.341e-09\
RMSF=2.283e-07\ Dipole=1.0675398,0.5669794,-2.0492517\PG=C01
[X(C5H7N1O1S2)]\NImag=0\\\@
```

(*iii*) MP2/6-31+G**

Standard orientation:

Center Number	Atomic Number	Atomic Type	Coordinates (Angstroms) X	Y	Z
1	7	0	0.338349	0.352166	-0.109540
2	6	0	-0.888806	-0.269179	-0.058319
3	16	0	-0.550060	-1.967209	0.210158
4	6	0	1.164322	-1.732372	0.116492
5	6	0	1.489403	-0.427510	-0.074372
6	6	0	2.825298	0.209752	-0.234576
7	16	0	-2.370976	0.434731	-0.205941
8	8	0	0.440061	1.677795	-0.488643
9	6	0	0.231902	2.527317	0.664326
10	1	0	1.854360	-2.554616	0.202234
11	1	0	3.593346	-0.558761	-0.194594
12	1	0	2.890774	0.730207	-1.187942
13	1	0	3.017175	0.932510	0.557316
14	1	0	0.313089	3.534561	0.268639
15	1	0	-0.759444	2.356860	1.073082
16	1	0	1.005635	2.343321	1.408416

```
Zero-point correction=                          0.119657 (Hartree/Particle)
Thermal correction to Energy=                   0.129297
Thermal correction to Enthalpy=                 0.130242
Thermal correction to Gibbs Free Energy         0.084448
Sum of electronic and zero-point Energies=          -1118.917497
Sum of electronic and thermal Energies=             -1118.907856
Sum of electronic and thermal Enthalpies=           -1118.906912
Sum of electronic and thermal Free Energies=        -1118.952706

Version=AM64L-G03RevE.01\State=1-A\HF=-1117.680086\MP2=-1119.0371538\
RMSD=2.050e-09\RMSF=9.396e-08\Dipole=1.0015761,0.5714922,-1.8953686\ PG=C01
[X(C5H7N1O1S2)]\NImag=0\\\@
```

Table C4. Calculated parameters and energies of conformers associated with rotation about the N,O-bond in $MTTOCH_3$ (**2d**)

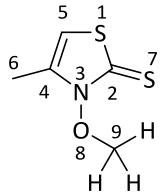

$\omega_{C2,N3,O8,C9}$ / deg	$\alpha_{N3,O8,C9}$ / deg	E / a.u. [a]	E_{rel} / kJ mol^{-1}	$d_{N3,O8}$ / Å	$d_{N3,C2}$ / Å	$d_{C2,S7}$ / Å	$E_{n1(O)}$ / a.u. [b]	$E_{n2(O)}$ / a.u. [b]	$E_{n1(N)}$ / a.u. [b]
0	120.4	–1121.0396277	36.2	1.4021	1.3698	1.6720	–0.64033	–0.33915	–0.29358
15	119.5	–1121.0408610	32.9	1.4002	1.3706	1.6709	–0.64091	–0.33915	–0.29381
30	117.7	–1121.0438894	25.0	1.3951	1.3716	1.6686	–0.64170	–0.33982	–0.29432
45	115.8	–1121.0475578	15.3	1.3890	1.3722	1.6659	–0.64329	–0.34121	–0.29475
60	113.9	–1121.0509333	6.5	1.3842	1.3729	1.6634	–0.64772	–0.34175	–0.29485
75	112.3	–1121.0530641	0.9	1.3809	1.3737	1.6606	–0.65411	–0.34021	–0.29431
90	111.5	–1121.0532003	0.5	1.3806	1.3761	1.6577	–0.65947	–0.33736	–0.29328
105	111.5	–1121.0513886	5.3	1.3835	1.3802	1.6551	–0.65848	–0.33741	–0.30598
120	112.1	–1121.0480320	14.1	1.3886	1.3852	1.6531	–0.65505	–0.33798	–0.31305
135	113.5	–1121.0432673	26.6	1.3941	1.3895	1.6518	–0.65015	–0.33627	–0.31801
150	115.3	–1121.0377083	41.2	1.3984	1.3902	1.6519	–0.64339	–0.33504	–0.31716
165	117.6	–1121.0323206	55.3	1.4021	1.3877	1.6534	–0.63777	–0.33483	–0.30914
180	119.6	–1121.0293940	63.0	1.3994	1.3802	1.6566	–0.63407	–0.33560	–0.29058
83.4	111.7	–1121.0533999	0.0	1.3803	1.3748	1.6590	–0.65759	–0.33845	–0.29377

[a] 1 a.u. = 1 Hartree. 1 Hartree/particle = 2625.5 kJ mol^{-1}. [b] 1. a.u. = 27.211 eV; *n*N(X) = non-bonding electron pair number N at heteroatom X.

Table C5. Calculated parameters and energies associated with angle variation at thiohydroxmate oxygen in $MTTOCH_3$ (**2d**)

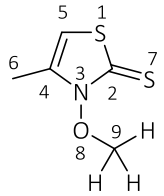

$\alpha_{N3,O8,C9}$ / deg	$\omega_{C2,N3,O8,C9}$ / deg	E / a.u. [a]	E_{rel} / kJ mol^{-1}	$d_{N3,O8}$ / Å	$d_{N3,C2}$ / Å	$d_{C2,S7}$ / Å	$E_{n1(O)}$ / a.u. [b]	$E_{n2(O)}$ / a.u. [b]	$E_{n1(N)}$ / a.u. [b]
90	93.0	–1121.0294988	62.8	1.4340	1.3762	1.6569	–0.75831	–0.33644	–0.29798
100	88.3	–1121.0471247	16.5	1.4026	1.3753	1.6582	–0.71007	–0.33824	–0.29553
110	84.1	–1121.0532805	0.3	1.3828	1.3749	1.6589	–0.66512	–0.33843	–0.29400
120	79.4	–1121.0508055	6.8	1.3705	1.3741	1.6596	–0.61950	–0.33940	–0.29278
130	73.5	–1121.0419043	30.2	1.36121	1.3726	1.6605	–0.56522	–0.34576	–0.29197
111.7	83.4	–1121.0533999	0.0	1.3803	1.3748	1.65899	–0.65759	–0.33845	–0.29377
120.4	0.0	–1121.0396277	36.2	1.4022	1.3698	1.6720	–0.64033	–0.33195	–0.29358
119.6	180.0	–1121.029394	63.0	1.3994	1.3802	1.6560	–0.63407	–0.33560	–0.29058

[a] 1 a.u. = 1 Hartree. 1 Hartree/particle = 2625.5 kJ mol^{-1}. [b] 1. a.u. = 27.211 eV; *n*N(X) = non-bonding electron pair number N at heteroatom X.

Table C6. Calculated parameters and energies associated with angle variation at thiohydroxmate oxygen in $MTTOCH_3$ (**2d**)

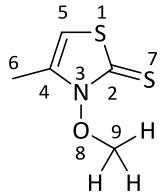

$\alpha_{N3,O8,C9}$ / deg	$E_{\pi 1(N3,O8)}$ [a] / kJ mol^{-1}	$E_{\pi 2(N3,O8)}$ [b] / kJ mol^{-1}	$E_{\pi 3(N3,O8)}$ [c] / kJ mol^{-1}	$E_{\pi 4(N3,C4)}$ [d] / kJ mol^{-1}	$E_{\pi 5(N3,C2)}$ [e] / kJ mol^{-1}	$\sigma_{N3,O8}$ / %p(O)	$\sigma_{C9,O8}$ / %p(O)	$n1(O)$ [f] / %p	$n2(O)$ [f] / %p
90	58.3	43.0	– [f]	136.5	253.1	86.24	79.06	34.20	99.90
100	64.2	49.2	4.1	141.5	269.8	83.26	76.01	40.29	99.87
110	69.7	52.8	10.5	143.3	273.3	80.67	73.42	45.66	99.71
120	77.8	52.2	16.2	143.6	275.7	78.24	70.94	51.17	99.16
130	85.0	52.6	19.5	143.3	277.7	75.61	68.10	58.48	97.38
111.7	71.1	53.2	11.3	143.4	273.7	80.26	73.01	46.55	99.66
120.4	73.9	30.8	– [f]	138.2	294.1	80.75	69.54	49.34	59.93
119.6	71.0	30.3	– [f]	146.4	257.2	80.75	79.53	48.53	99.90

[a] [σ(C4,C5)→σ*(N3,O8)] + [(σ(S1,C2)→σ*(N3,O8)] + [σ(C9,H)→σ*(N3,O8)]. [b] [n1/2(O)→σ*(N3,C2)] + [n1/2(O)→σ*(N3,C4)]. [c] n1(N)→σ*(O8,C9). [d] n1(N)→π*(N3,C2). [e] n1(N)→π*(N3,C4). [e] nN(X) = non-bonding electron pair number N at heteroatom X. [f] Below a threshhold of 2.1 kJ mol^{-1}.

C7.5 1-(*tert*-Butoxy)pyridine-2(1*H*)thione (4b)

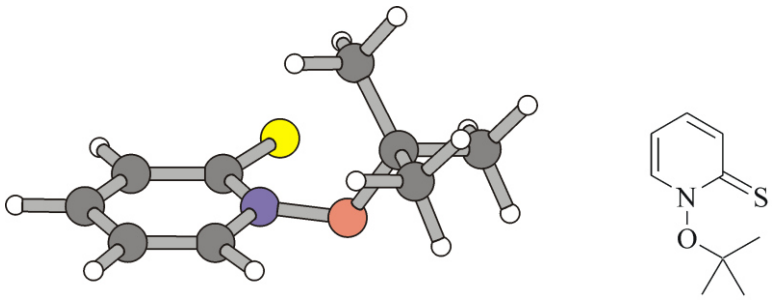

Figure C38. Computed minimum structure of 3-(*tert*-butoxy)pyridinethione **4b**.

(*i*) B3LYP/6-31+G**//B3LYP/6-31+G**

Standard orientation:

Center Number	Atomic Number	Atomic Type	Coordinates (Angstroms) X	Y	Z
1	7	0	-0.432242	-0.346152	-0.371886
2	6	0	-1.221234	0.773394	-0.078013
3	6	0	-2.568810	0.425737	0.288234
4	6	0	-3.037185	-0.862574	0.291542
5	6	0	-2.183589	-1.932567	-0.088530
6	6	0	-0.894681	-1.631930	-0.429707
7	16	0	-0.658765	2.352612	-0.149274
8	8	0	0.844568	-0.144117	-0.855177
9	6	0	1.976689	-0.267073	0.124003
10	6	0	2.534960	-1.690165	0.007971
11	6	0	2.967339	0.765584	-0.413023
12	6	0	1.546435	0.048688	1.554683
13	1	0	-3.211283	1.257658	0.549883
14	1	0	-4.067924	-1.062849	0.568651
15	1	0	-2.527861	-2.958529	-0.131585
16	1	0	-0.169792	-2.358655	-0.768943
17	1	0	3.465363	-1.772381	0.579988
18	1	0	1.838470	-2.433719	0.408866
19	1	0	2.752556	-1.934889	-1.036064
20	1	0	3.891024	0.737623	0.174226
21	1	0	3.216200	0.550913	-1.456851
22	1	0	2.532150	1.765828	-0.358368
23	1	0	2.428673	-0.010086	2.200213
24	1	0	1.125853	1.053144	1.628453
25	1	0	0.816418	-0.674412	1.931581

```
Zero-point correction=                          0.206324 (Hartree/Particle)
Thermal correction to Energy=                   0.218542
Thermal correction to Enthalpy=                 0.219486
Thermal correction to Gibbs Free Energy=        0.167888
Sum of electronic and zero-point Energies=           -878.719310
Sum of electronic and thermal Energies=              -878.707092
Sum of electronic and thermal Enthalpies=            -878.706148
Sum of electronic and thermal Free Energies=         -878.757745

Version=AM64L-G03RevE.01\State=1-A\HF=-878.9256335\RMSD=9.335e-09\
RMSF=8.494e-07\Dipole=1.1693885,0.6737474,-1.7626555\PG=C01
[X(C9H13N1O1S1)]\NImag=0\\\@
```

(*ii*) BHandHLYP/6-31+G**//BHandHLYP/6-31+G**

Standard orientation:

Center Number	Atomic Number	Atomic Type	Coordinates (Angstroms) X	Y	Z
1	6	0	-0.882364	-1.614530	-0.431991
2	7	0	-0.425279	-0.336646	-0.375371
3	6	0	-1.201889	0.762975	-0.081834
4	6	0	-2.542449	0.423092	0.289402
5	6	0	-3.004636	-0.853326	0.293081
6	6	0	-2.155698	-1.917930	-0.090471
7	8	0	0.835473	-0.139410	-0.842484
8	6	0	1.946046	-0.265329	0.119936
9	6	0	1.515147	0.021150	1.546523
10	16	0	-0.647436	2.334033	-0.150739
11	6	0	2.512587	-1.672382	-0.011942
12	6	0	2.932350	0.771964	-0.385401
13	1	0	-3.176749	1.249302	0.553502
14	1	0	-4.025804	-1.053551	0.573062
15	1	0	-2.497292	-2.935919	-0.133430
16	1	0	-0.161368	-2.332965	-0.771044
17	1	0	3.435727	-1.753591	0.555885
18	1	0	1.826147	-2.421080	0.374713
19	1	0	2.730837	-1.898824	-1.051578
20	1	0	3.842790	0.738947	0.207058
21	1	0	3.189949	0.575273	-1.422155
22	1	0	2.494586	1.761592	-0.321117
23	1	0	2.391823	-0.042081	2.185168
24	1	0	1.091549	1.014022	1.637289
25	1	0	0.795392	-0.707950	1.908118

```
Zero-point correction=                          0.214337 (Hartree/Particle)
Thermal correction to Energy=                   0.226075
Thermal correction to Enthalpy=                 0.227020
Thermal correction to Gibbs Free Energy=        0.176471
Sum of electronic and zero-point Energies=           -878.391182
Sum of electronic and thermal Energies=              -878.379444
Sum of electronic and thermal Enthalpies=            -878.378499
Sum of electronic and thermal Free Energies=         -878.429049

Version=AM64L-G03RevE.01\State=1-A\HF=-878.6055191\RMSD=8.469e-09\
RMSF=1.885e-06\Dipole=-0.7006301,0.7957221,-2.0824223\PG=C01
[X(C9H13N1O1S1)]\NImag=0\\\@
```

(*iii*) MP2/6-31+G**

Standard orientation:

Center Number	Atomic Number	Atomic Type	Coordinates (Angstroms) X	Y	Z
1	6	0	-0.889300	-1.611970	-0.491754
2	7	0	-0.424964	-0.330213	-0.414351
3	6	0	-1.182410	0.797417	-0.089347
4	6	0	-2.509666	0.446008	0.331033
5	6	0	-2.994160	-0.839694	0.329356
6	6	0	-2.170904	-1.904539	-0.105432
7	8	0	0.855381	-0.126066	-0.890823
8	6	0	1.926225	-0.286701	0.137104
9	6	0	1.413802	-0.032945	1.542300
10	16	0	-0.591443	2.347426	-0.170963
11	6	0	2.484690	-1.694692	-0.001935
12	6	0	2.935618	0.759053	-0.296028
13	1	0	-3.136785	1.272599	0.632863
14	1	0	-4.009897	-1.031118	0.649001
15	1	0	-2.525263	-2.922524	-0.163511
16	1	0	-0.181404	-2.327748	-0.877309
17	1	0	3.377726	-1.797586	0.614842
18	1	0	1.764926	-2.442115	0.329421
19	1	0	2.753996	-1.891384	-1.038615
20	1	0	3.824571	0.694668	0.331319
21	1	0	3.229178	0.589299	-1.331104
22	1	0	2.499030	1.750973	-0.212155
23	1	0	2.256068	-0.120188	2.228453
24	1	0	0.991897	0.964719	1.629599
25	1	0	0.667384	-0.770012	1.837865

```
Zero-point correction=                          0.210491 (Hartree/Particle)
Thermal correction to Energy=                   0.222595
Thermal correction to Enthalpy=                 0.223539
Thermal correction to Gibbs Free Energy=        0.172453
Sum of electronic and zero-point Energies=           -876.752491
Sum of electronic and thermal Energies=              -876.740387
Sum of electronic and thermal Enthalpies=            -876.739442
Sum of electronic and thermal Free Energies=         -876.790529

Version=AM64L-G03RevE.01\State=1-A\HF=-875.1556496\MP2=-876.9629812\
RMSD=5.243e-09\RMSF=6.155e-06\Dipole=-0.6320188,0.8291699,-1.9060322\
PG=C01 [X(C9H13N1O1S1)]\NImag=0\\\@
```

Table C7. Parameters and energies of conformers associated with rotation about the nitrogen-oxygen bond in PTO*t*Bu (**4b**)

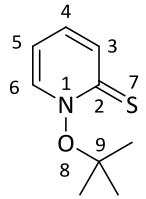

$\omega_{C2,N1,O8,C9}$ / deg	$\alpha_{N1,O8,C9}$ / deg	E / a.u. [a]	E_{rel} / kJ mol^{-1}	$d_{N1,O8}$ / Å	$d_{N1,C2}$ / Å	$d_{C2,S7}$ / Å	$E_{n1(O)}$ / a.u. [b]	$E_{n2(O)}$ / a.u. [b]	$E_{n1(N)}$ / a.u. [b]
0	132.47	–878.9019267	62.2	1.4241	1.3959	1.6885	–0.60507	–0.32213	–0.28894
15	131.6	–878.9029294	59.6	1.4212	1.3963	1.6881	–0.60533	–0.32330	–0.28919
30	129.2	–878.9059314	51.7	1.4132	1.3971	1.6869	–0.60540	–0.32711	–0.28981
45	125.9	–878.9107133	39.2	1.4022	1.3980	1.6848	–0.60388	–0.33400	–0.29044
60	122.6	–878.9164603	24.1	1.3913	1.3987	1.6823	–0.60176	–0.34220	–0.29069
75	119.9	–878.9217159	10.3	1.3829	1.3992	1.6801	–0.60721	–0.34240	–0.29041
90	118.0	–878.9249872	1.7	1.3790	1.3998	1.6787	–0.63342	–0.32054	–0.28969
105	117.0	–878.9254663	0.4	1.3820	1.4015	1.6773	–0.61955	–0.33807	–0.28867
120	117.3	–878.9227425	7.6	1.3870	1.4034	1.6762	–0.60664	–0.35051	–0.28742
135	119.1	–878.9179230	20.2	1.3875	1.4037	1.6762	–0.60054	–0.34905	–0.29819
150	121.2	–878.9135870	31.6	1.3893	1.4049	1.6767	–0.60536	–0.33901	–0.28699
165	123.2	–878.9104378	39.9	1.3911	1.4058	1.6777	–0.60996	–0.32934	–0.28745
180	124.2	–878.9092635	43.0	1.3917	1.4061	1.6783	–0.61168	–0.32522	–0.28773
99.9	117.2	–878.9256335	0.0	1.3800	1.4008	1.6779	–0.62704	–0.32930	–0.28906

[a] 1 a.u. = 1 Hartree. 1 Hartree/particle = 2625.5 kJ mol^{-1}. [b] 1. a.u. = 27.211 eV; *n*N(X) = non-bonding electron pair number N at heteroatom X.

Table C8. Calculated parameters and energies associated with angle variation at thiohydroxmate oxygen in PTO*t*Bu (**4b**)

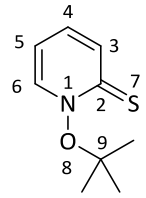

$\alpha_{N1,O8,C9}$ / deg	$\omega_{C2,N1,O8,C9}$ / deg	E / a.u. [a]	E_{rel} / kJ mol^{-1}	$d_{N1,O8}$ / Å	$d_{N1,C2}$ / Å	$d_{C2,S7}$ / Å	$E_{n1(O)}$ / a.u. [b]	$E_{n2(O)}$ / a.u. [b]	$E_{n1(N)}$ / a.u. [b]
90	108.3	–878.8854896	105.4	1.4433	1.4079	1.6730	–0.76688	–0.32179	–0.31768
100	105.9	–878.9106856	39.2	1.4158	1.4045	1.6750	–0.71463	–0.32636	–0.30574
110	102.9	–878.9232101	6.4	1.3921	1.4018	1.6773	–0.66352	–0.32891	–0.28911
120	98.9	–878.9252977	0.9	1.3765	1.4007	1.6780	–0.61256	–0.32982	–0.28900
130	94.8	–878.9040269	16.4	1.3665	1.4003	1.6785	–0.54621	–0.34623	–0.28856
117.2	99.9	–878.9256335	0.0	1.3800	1.4008	1.6779	–0.62704	–0.32930	–0.28906
132.5	0.0	–878.9019267	62.2	1.4241	1.3959	1.6885	–0.60507	–0.32213	–0.28894
124.2	180.0	–878.9092635	43.0	1.3917	1.4061	1.6783	–0.61168	–0.32522	–0.28773

[a] 1 a.u. = 1 Hartree. 1 Hartee/particle = 2625.5 kJ mol^{-1}. [b] 1. a.u. = 27.211 eV; *n*N(X) = non-bonding electron pair number N at heteroatom X.

Table C9. Calculated parameters and energies associated with angle variation at thiohydroxmate oxygen in PTO*t*Bu (**4b**)

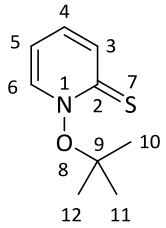

$\alpha_{N1,O8,C9}$ / deg	$E_{\pi 1(N1,O8)}$ [a] / kJ mol^{-1}	$E_{\pi 2(N1,O8)}$ [b] / kJ mol^{-1}	$E_{\pi 3(N1,O8)}$ [c] / kJ mol^{-1}	$E_{\pi 4(N1,C2)}$ [d] / kJ mol^{-1}	$E_{\pi 5(N1,C6)}$ [e] / kJ mol^{-1}	$\sigma_{N1,O8}$ / %p(O)	$\sigma_{C9,O8}$ / %p(O)	$n1(O)$ [f] / %p	$n2(O)$ [f] / %p
90	36.7	32.8	– [g]	134.7	188.6	87.29	81.39	31.47	99.34
100	41.5	37.5	– [g]	148.8	208.4	84.89	76.98	38.34	99.27
110	52.8	44.9	11.5	165.9	237.9	82.08	74.14	44.41	98.86
120	58.6	48.2	19.0	166.0	240.7	79.49	71.24	50.45	98.36
130	65.1	48.1	24.1	165.5	242.0	76.92	68.31	59.31	95.03
117.2	55.0	47.5	17.2	166.1	240.3	80.19	72.07	48.71	98.55
132.5	63.1	31.8	– [g]	155.9	266.5	81.35	66.04	52.28	99.95
124.2	56.6	26.7	– [g]	176.7	227.8	80.23	68.49	50.91	99.92

[a] [σ(C5,C6)→σ^*(N1,O8)] + [σ(C2,C3)→σ^*(N1,O8)] + [σ(C9,C10–12)→σ^*(N1,O8)]. [b] [$n1/2$(O)→σ^*(N1,C2)] + [$n1/2$(O)→σ^*(N1,C6)]. [c] $n1$(N)→σ^*(O8,C9). [d] $n1$(N)→π^*(N1,C2). [e] $n1$(N)→π^*(N1,C6). [f] nN(X) = non-bonding electron pair number N at heteroatom X. [g] Below default threshhold of 2.1 kJ mol^{-1}.

C7.6 1-(Methoxy)pyridine-2(1*H*)thione (4d)

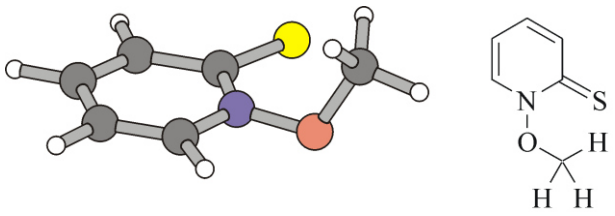

Figure C39. Computed minimum structure of 1-(methoxy)pyridinethione **4d**.

(*i*) B3LYP/6-31+G**//B3LYP/6-31+G**

Standard orientation:

Center Number	Atomic Number	Atomic Type	Coordinates (Angstroms) X	Y	Z
1	6	0	-1.122884	-1.376638	-0.222781
2	7	0	0.008573	-0.612111	-0.213724
3	6	0	0.053218	0.773840	-0.039048
4	6	0	-1.247259	1.339521	0.204033
5	6	0	-2.397471	0.593088	0.221157
6	6	0	-2.346865	-0.809369	-0.003005
7	8	0	1.166503	-1.298115	-0.549439
8	6	0	1.958695	-1.611380	0.618647
9	16	0	1.471355	1.667369	-0.108865
10	1	0	-1.269273	2.411260	0.360502
11	1	0	-3.352600	1.077952	0.399685
12	1	0	-3.237592	-1.425154	-0.010784
13	1	0	-0.955396	-2.427474	-0.421771
14	1	0	2.826908	-2.135363	0.216969
15	1	0	2.272039	-0.695031	1.122347
16	1	0	1.397595	-2.268761	1.292464

```
Zero-point correction=                          0.122753 (Hartree/Particle)
Thermal correction to Energy=                   0.130951
Thermal correction to Enthalpy=                 0.131896
Thermal correction to Gibbs Free Energy=        0.089446
Sum of electronic and zero-point Energies=           -760.843853
Sum of electronic and thermal Energies=              -760.835655
Sum of electronic and thermal Enthalpies=            -760.834711
Sum of electronic and thermal Free Energies=         -760.877160

Version=AM64L-G03RevE.01\State=1-A\HF=-760.9666061\RMSD=3.083e-09\
RMSF=1.936e-06\Dipole=-0.4508162,0.6744546,-2.0158804\PG=C01
[X(C6H7N1O1S1)]\NImag=0\\\@
```

(*ii*) BHandHLYP/6-31+G**//BHandHLYP/6-31+G**

Standard orientation:

Center Number	Atomic Number	Atomic Type	Coordinates (Angstroms) X	Y	Z
1	7	0	0.012091	-0.601048	-0.218378
2	6	0	0.057666	0.762571	-0.041754
3	6	0	-1.231528	1.335006	0.202766
4	6	0	-2.371652	0.597517	0.221212
5	6	0	-2.325131	-0.798949	-0.004214
6	6	0	-1.113648	-1.358374	-0.226185
7	16	0	1.467664	1.649331	-0.104341
8	8	0	1.151920	-1.277144	-0.542310
9	6	0	1.916212	-1.619581	0.613251
10	1	0	-1.248171	2.397933	0.360440
11	1	0	-3.318122	1.080046	0.401694
12	1	0	-3.210746	-1.407401	-0.011203
13	1	0	-0.948009	-2.400705	-0.426806
14	1	0	2.785615	-2.131607	0.222177
15	1	0	2.218839	-0.725626	1.143960
16	1	0	1.346460	-2.286598	1.255862

```
Zero-point correction=                          0.127840 (Hartree/Particle)
Thermal correction to Energy=                   0.135746
Thermal correction to Enthalpy=                 0.136691
Thermal correction to Gibbs Free Energy=        0.094814
Sum of electronic and zero-point Energies=           -760.597565
Sum of electronic and thermal Energies=              -760.589660
Sum of electronic and thermal Enthalpies=            -760.588715
Sum of electronic and thermal Free Energies=         -760.630591

Version=AM64L-G03RevE.01\State=1-A\HF=-760.7254059\RMSD=1.848e-09\
RMSF=5.084e-07\Dipole=1.5194656,0.631643,-1.6211776\ PG=C01
[X(C6H7N1O1S1)]\NImag=0\\\@
```

(*iii*) MP2/6-31+G**

Standard orientation:

Center Number	Atomic Number	Atomic Type	Coordinates (Angstroms) X	Y	Z
1	7	0	-0.006341	-0.608908	-0.211580
2	6	0	0.080724	0.772203	-0.040311
3	6	0	-1.205082	1.352262	0.230482
4	6	0	-2.377336	0.636248	0.232046
5	6	0	-2.359983	-0.756624	-0.017364
6	6	0	-1.149209	-1.353077	-0.249040
7	16	0	1.509948	1.613647	-0.127579
8	8	0	1.142868	-1.313685	-0.548837
9	6	0	1.890260	-1.613542	0.652528
10	1	0	-1.207599	2.419110	0.401843
11	1	0	-3.313756	1.142408	0.425050
12	1	0	-3.260985	-1.350066	-0.044352
13	1	0	-0.998545	-2.399528	-0.465708
14	1	0	2.785170	-2.108266	0.289975
15	1	0	2.148952	-0.692591	1.166076
16	1	0	1.312796	-2.282400	1.290087

```
Zero-point correction=                          0.124436 (Hartree/Particle)
Thermal correction to Energy=                   0.132726
Thermal correction to Enthalpy=                 0.133670
Thermal correction to Gibbs Free Energy=        0.091086
Sum of electronic and zero-point Energies=           -759.252615
Sum of electronic and thermal Energies=              -759.244325
Sum of electronic and thermal Enthalpies=            -759.243380
Sum of electronic and thermal Free Energies=         -759.285965

Version=AM64L-G03RevE.01\State=1-A\HF=-758.0379884\MP2=-759.3770505\
RMSD=1.238e-09\RMSF=7.020e-08\Dipole=1.3669221,0.6581288,-1.4614683\ PG=C01
[X(C6H7N1O1S1)]\NImag=0\\\@
```

Table C10. Parameters and energies of conformers associated with rotation about the nitrogen-oxygen bond in $PTOCH_3$ (**4d**)

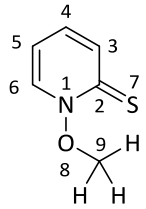

$\omega_{C2,N1,O8,C9}$ / deg	$\alpha_{N1,O8,C9}$ / deg	E / a.u. [a]	E_{rel} / kJ mol^{-1}	$d_{N1,O8}$ / Å	$d_{N1,C2}$ / Å	$d_{C2,S7}$ / Å	$E_{n1(O)}$ / a.u. [b]	$E_{n2(O)}$ / a.u. [b]	$E_{n1(N)}$ / a.u. [b]
0	123.3	–760.9500436	43.5	1.4129	1.3940	1.6894	–0.63392	–0.33516	–0.29505
15	121.6	–760.9516878	39.2	1.4096	1.3946	1.6889	–0.63600	–0.33627	–0.29517
30	119.1	–760.9553543	29.5	1.4030	1.3950	1.6872	–0.63608	–0.34000	–0.29580
45	116.7	–760.9596174	18.3	1.3964	1.3954	1.6848	–0.63405	–0.34638	–0.29637
60	114.4	–760.9635276	8.1	1.3920	1.3963	1.6825	–0.63426	–0.35239	–0.29665
75	112.4	–760.9661483	1.2	1.3883	1.3972	1.6794	–0.63874	–0.35302	–0.29631
90	111.4	–760.9666061	0.5	1.3868	1.3979	1.6766	–0.65254	–0.34182	–0.29546
105	111.4	–760.9645194	5.5	1.3879	1.3986	1.6746	–0.65860	–0.33498	–0.30077
120	112.2	–760.9614952	13.4	1.3905	1.3998	1.6734	–0.64533	–0.34580	–0.30275
135	113.6	–760.9582394	22.0	1.3921	1.4010	1.6733	–0.63708	–0.34940	–0.30240
150	115.11	–760.9558568	28.2	1.3923	1.4012	1.6741	–0.63740	–0.34605	–0.29947
165	116.3	–760.9544952	31.8	1.3935	1.4032	1.6749	–0.64148	–0.34185	–0.29558
180	116.7	–760.9540381	33.0	1.3940	1.4038	1.6753	–0.64322	–0.34023	–0.29583
83.9	111.7	–760.9666061	0.0	1.3871	1.3976	1.6776	–0.64575	–0.34790	–0.29584

[a] 1 a.u. = 1 Hartree. 1 Hartree/particle = 2625.5 kJ mol^{-1}. [b] 1. a.u. = 27.211 eV; *n*N(X) = non-bonding electron pair number N at heteroatom X.

Table C11. Calculated parameters and energies associated with angle variation at thiohydroxmate oxygen in $PTOCH_3$ (**4d**)

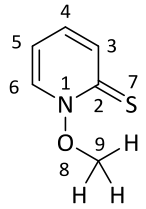

$\alpha_{N1,O8,C9}$ / deg	$\omega_{C2,N1,O8,C9}$ / deg	E / a.u. [a]	E_{rel} / kJ mol^{-1}	$d_{N1,O8}$ / Å	$d_{N1,C2}$ / Å	$d_{C2,S7}$ / Å	$E_{n1(O)}$ / a.u. [b]	$E_{n2(O)}$ / a.u. [b]	$E_{n1(N)}$ / a.u. [b]
90	92.0	–760.9428847	62.3	1.4402	1.3975	1.6757	–0.75676	–0.33605	–0.30818
100	88.3	–760.9604724	16.1	1.4090	1.3974	1.6768	–0.70582	–0.33977	–0.29738
110	84.6	–760.9664944	0.3	1.3895	1.3976	1.6775	–0.65474	–0.34612	–0.29603
120	79.9	–760.9640764	6.6	1.3776	1.3972	1.6783	–0.59526	–0.36202	–0.29496
130	73.1	–760.9555394	29.1	1.3696	1.3962	1.6792	–0.52645	–0.38448	–0.29496
111.7	83.9	–760.9666061	0.0	1.3871	1.3976	1.6776	–0.64574	–0.34790	–0.29584
123.3	0.0	–760.9500436	43.5	1.4129	1.3940	1.6894	–0.63392	–0.33516	–0.29505
116.7	180.0	–760.9540381	33.0	1.3940	1.4038	1.6753	–0.64322	–0.34023	–0.29583

[a] 1 a.u. = 1 Hartree. 1 Hartree/particle = 2625.5 kJ mol^{-1}. [b] 1. a.u. = 27.211 eV; *n*N(X) = non-bonding electron pair number N at heteroatom X.

Table C12. Calculated parameters and energies associated with angle variation at thiohydroxmate oxygen in $PTOCH_3$ (**4d**)

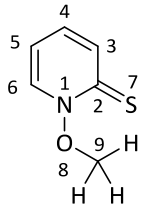

$\alpha_{N1,O8,C9}$ / deg	$E_{\pi 1(N1,O8)}$ [a] / kJ mol^{-1}	$E_{\pi 2(N1,O8)}$ [b] / kJ mol^{-1}	$E_{\pi 3(N1,O8)}$ [c] / kJ mol^{-1}	$E_{\pi 4(N1,C2)}$ [d] / kJ mol^{-1}	$E_{\pi 5(N1,C6)}$ [e] / kJ mol^{-1}	$\sigma_{N1,O8}$ / %p(O)	$\sigma_{C9,O8}$ / %p(O)	$n1(O)$ [f] / %p	$n2(O)$ [f] / %p
90	42.6	34.9	– [g]	152.8	224.7	86.74	79.10	34.10	99.99
100	47.0	41.3	4.1	164.6	238.9	83.79	76.05	40.57	99.99
110	58.2	42.0	10.0	165.9	240.8	81.27	73.45	47.01	97.73
120	66.9	43.5	15.3	165.7	242.3	78.92	71.05	55.09	94.50
130	74.5	42.7	18.3	164.8	243.8	76.35	68.80	65.29	89.71
118.3	53.8	42.4	11.0	165.9	241.0	80.88	73.05	48.18	97.36
129.0	66.9	27.9	– [g]	159.0	260.0	81.08	68.69	49.64	99.40
130.2	60.8	23.5	– [g]	174.6	223.8	80.56	79.42	48.21	99.89

[a] $[\sigma(C5,C6)\rightarrow\sigma^*(N1,O8)] + [\sigma_{C2,C3}\rightarrow\sigma^*(N1,O8)] + [\sigma(C9,C10–12)\rightarrow\sigma^*(N1,O8)]$. [b] $[n1/2(O)\rightarrow\sigma^*(N1,C2)] + [n1/2(O)\rightarrow\sigma^*(N1,C6)]$. [c] $n1(N)\rightarrow\sigma^*(O8,C9)$. [d] $n1(N)\rightarrow\pi^*(N1,C2)$. [e] $n1(N)\rightarrow\pi^*(N1,C6)$. [f] nN(X) = non-bonding electron pair number N at heteroatom X. [g] Below default threshhold of 2.1 kJ mol^{-1}.

C7.7 Isomers of *O*-Alkyl Thiohydroxamates

C7.7.1 2-(2-Methylpropyl-2-sulfanyl)-4-methylthiazole 3-oxide (7b)

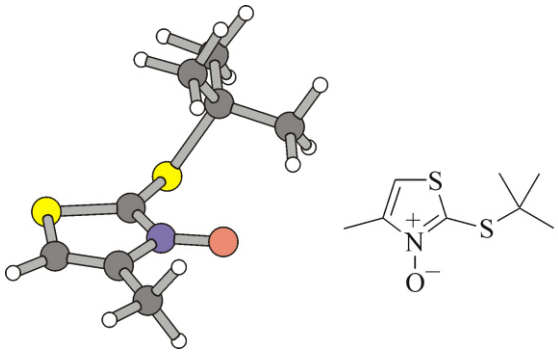

Figure C40. Computed minimum structure of (*tert*-butylsulfanyl)thiazole 3-oxide **7b**.

(*i*) B3LYP/6-31+G**//B3LYP/6-31+G**

Standard orientation:

Center Number	Atomic Number	Atomic Type	Coordinates (Angstroms) X	Y	Z
1	6	0	2.491009	0.458365	0.117647
2	7	0	1.143996	0.633738	-0.275129
3	6	0	0.440973	-0.519384	-0.347627
4	16	0	1.428212	-1.885572	0.091907
5	6	0	2.794774	-0.847227	0.336561
6	8	0	0.668511	1.804489	-0.516691
7	16	0	-1.178294	-0.699249	-0.961073
8	6	0	-2.333914	0.217313	0.252880
9	6	0	-2.613051	1.621584	-0.298772
10	6	0	3.350923	1.670345	0.218925
11	6	0	-3.613173	-0.634087	0.254765
12	6	0	-1.713015	0.277972	1.649559
13	1	0	3.754799	-1.249356	0.627211
14	1	0	3.386304	2.195129	-0.741012
15	1	0	2.937166	2.374090	0.948344
16	1	0	4.363529	1.391023	0.518483
17	1	0	-4.380037	-0.129035	0.854698
18	1	0	-4.016178	-0.760080	-0.756188
19	1	0	-3.437094	-1.626106	0.680984
20	1	0	-2.439668	0.726737	2.338206
21	1	0	-1.461182	-0.718155	2.026452
22	1	0	-0.815871	0.902367	1.660134
23	1	0	-3.309602	2.141771	0.372131
24	1	0	-1.689403	2.197417	-0.377059
25	1	0	-3.074670	1.569977	-1.289936

```
Zero-point correction=                          0.200010 (Hartree/Particle)
Thermal correction to Energy=                   0.213818
Thermal correction to Enthalpy=                 0.214762
Thermal correction to Gibbs Free Energy=        0.159453
Sum of electronic and zero-point Energies=          -1238.805177
Sum of electronic and thermal Energies=             -1238.791369
Sum of electronic and thermal Enthalpies=           -1238.790425
Sum of electronic and thermal Free Energies=        -1238.845734

Version=AM64L-G03RevE.01\State=1-A\HF=-1239.0051869\RMSD=5.112e-09\
RMSF=3.192e-07\Dipole=0.6773932,0.4879701,-0.9055555\PG=C01
[X(C8H13N1O1S2)]\NImag=0 \\\@
```

(*ii*) BHandHLYP/6-31+G**//BHandHLYP/6-31+G**

Standard orientation:

Center Number	Atomic Number	Atomic Type	Coordinates (Angstroms) X	Y	Z
1	6	0	2.785807	-0.807087	0.328353
2	6	0	2.448662	0.476964	0.107685
3	7	0	1.108729	0.611134	-0.272875
4	6	0	0.445812	-0.536154	-0.332147
5	16	0	1.451720	-1.866906	0.098789
6	6	0	3.271533	1.706790	0.196311
7	8	0	0.608150	1.762000	-0.513591
8	16	0	-1.173727	-0.755659	-0.914833
9	6	0	-2.294749	0.215186	0.238333
10	6	0	-1.652536	0.389249	1.605582
11	6	0	-2.611821	1.564129	-0.397359
12	6	0	-3.555385	-0.640878	0.337129
13	1	0	3.751131	-1.177677	0.613208
14	1	0	3.285147	2.220308	-0.760273
15	1	0	2.844471	2.395247	0.919425
16	1	0	4.285090	1.456785	0.488963
17	1	0	-4.306646	-0.103275	0.912452
18	1	0	-3.977678	-0.846064	-0.643787
19	1	0	-3.356724	-1.588637	0.828326
20	1	0	-2.374402	0.861057	2.270044
21	1	0	-1.369232	-0.564606	2.041918
22	1	0	-0.781983	1.034100	1.550164
23	1	0	-3.295640	2.112190	0.250159
24	1	0	-1.707337	2.143168	-0.535965
25	1	0	-3.094337	1.435317	-1.362397

```
Zero-point correction=                          0.207753 (Hartree/Particle)
Thermal correction to Energy=                   0.220996
Thermal correction to Enthalpy=                 0.221940
Thermal correction to Gibbs Free Energy=        0.168222
Sum of electronic and zero-point Energies=          -1238.475182
Sum of electronic and thermal Energies=             -1238.461939
Sum of electronic and thermal Enthalpies=           -1238.460995
Sum of electronic and thermal Free Energies=        -1238.514713

Version=AM64L-G03RevE.01\State=1-A\HF=-1238.6829351\RMSD=3.099e-09\
RMSF=2.411e-06\Dipole=-0.6456957,0.6165469,-0.9357354\PG=C01
[X(C8H13N1O1S2)]\NImag=0\\\@
```

(*iii*) MP2/6-31+G**

Standard orientation:

Center Number	Atomic Number	Atomic Type	Coordinates (Angstroms) X	Y	Z
1	6	0	2.698025	-0.884092	0.365152
2	6	0	2.436908	0.436800	0.134333
3	7	0	1.123015	0.636179	-0.313504
4	6	0	0.395233	-0.527519	-0.402924
5	16	0	1.340017	-1.885358	0.071472
6	6	0	3.312221	1.628536	0.260947
7	8	0	0.667327	1.803533	-0.561383
8	16	0	-1.202848	-0.624094	-1.034662
9	6	0	-2.243692	0.209565	0.268294
10	6	0	-1.499283	0.287249	1.592766
11	6	0	-2.615428	1.605393	-0.223980
12	6	0	-3.491418	-0.659409	0.407793
13	1	0	3.635407	-1.298971	0.697412
14	1	0	3.388279	2.140658	-0.696688
15	1	0	2.887604	2.334104	0.973298
16	1	0	4.302459	1.326650	0.593594
17	1	0	-4.194110	-0.172553	1.086490
18	1	0	-3.991502	-0.791733	-0.552299
19	1	0	-3.244003	-1.642861	0.805207
20	1	0	-2.176721	0.699722	2.343203
21	1	0	-1.176841	-0.697064	1.932535
22	1	0	-0.636050	0.947678	1.522681
23	1	0	-3.255444	2.088376	0.518050
24	1	0	-1.722465	2.205778	-0.378392
25	1	0	-3.166429	1.550787	-1.162741

```
Zero-point correction=                           0.204888 (Hartree/Particle)
Thermal correction to Energy=                    0.218458
Thermal correction to Enthalpy=                  0.219402
Thermal correction to Gibbs Free Energy=         0.164911
Sum of electronic and zero-point Energies=          -1236.418744
Sum of electronic and thermal Energies=             -1236.405174
Sum of electronic and thermal Enthalpies=           -1236.404230
Sum of electronic and thermal Free Energies=        -1236.458721

Version=AM64L-G03RevE.01\State=1-A\HF=-1234.772648\MP2=-1236.6236319\
RMSD=7.556e-09\RMSF=9.365e-07\Dipole=-0.7986379,0.5782972,-0.975035\ PG=C01
[X(C8H13N1O1S2)]\NImag=0\\\@
```

C7.7.2 O-(2-Methylprop-2-yl) 4-methyl-1,3-thiazole-2-sulfenate (12b)

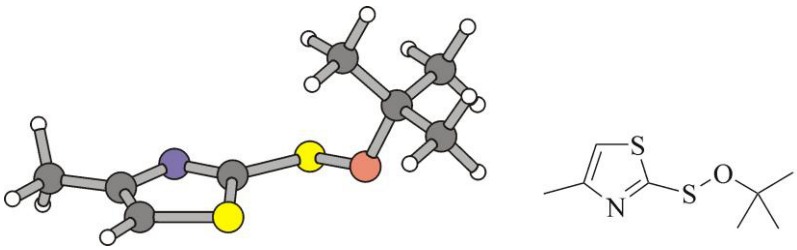

Figure C41. Computed minimum structure of *O*-(*tert*-butyl) sulfenate **12b**.

(*i*) B3LYP/6-31+G**//B3LYP/6-31+G**

Standard orientation:

Center Number	Atomic Number	Atomic Type	Coordinates (Angstroms) X	Y	Z
1	6	0	3.096219	-0.120819	0.234674
2	7	0	2.042023	-1.006474	0.072458
3	6	0	0.957780	-0.389077	-0.292918
4	16	0	1.113054	1.353978	-0.484609
5	6	0	2.781363	1.187714	-0.006813
6	16	0	-0.509987	-1.285710	-0.698219
7	8	0	-1.623289	-0.025291	-0.791117
8	6	0	-2.623473	0.123238	0.294481
9	6	0	-1.941636	0.347775	1.645170
10	6	0	4.431451	-0.652192	0.663349
11	6	0	-3.393286	1.366936	-0.155627
12	6	0	-3.528385	-1.111849	0.315593
13	1	0	3.417330	2.057053	0.087255
14	1	0	4.349327	-1.171593	1.624318
15	1	0	4.809373	-1.375701	-0.067273
16	1	0	5.162733	0.153907	0.764162
17	1	0	-4.198229	1.585015	0.553754
18	1	0	-2.728941	2.234370	-0.205467
19	1	0	-3.833055	1.209478	-1.144622
20	1	0	-4.332525	-0.978729	1.046872
21	1	0	-3.979300	-1.274053	-0.668173
22	1	0	-2.967182	-2.008642	0.597091
23	1	0	-2.701341	0.495188	2.419894
24	1	0	-1.333897	-0.514938	1.933443
25	1	0	-1.301401	1.233649	1.618282

```
Zero-point correction=                          0.199374 (Hartree/Particle)
Thermal correction to Energy=                   0.213412
Thermal correction to Enthalpy=                 0.214357
Thermal correction to Gibbs Free Energy=        0.157847
Sum of electronic and zero-point Energies=          -1238.844909
Sum of electronic and thermal Energies=             -1238.830870
Sum of electronic and thermal Enthalpies=           -1238.829926
Sum of electronic and thermal Free Energies=        -1238.886436

Version=AM64L-G03RevE.01\State=1-A\HF=-1239.0442829\RMSD=1.709e-09\
RMSF=8.848e-07\Dipole=0.459962,-0.7485897,-0.2117358\PG=C01
[X(C8H13N1O1S2)]\NImag=0\\\@
```

(*ii*) BHandHLYP/6-31+G**//BHandHLYP/6-31+G**

Standard orientation:

Center Number	Atomic Number	Atomic Type	Coordinates (Angstroms) X	Y	Z
1	6	0	3.074498	-0.103301	0.218072
2	7	0	2.035460	-0.995924	0.068516
3	6	0	0.951525	-0.396379	-0.276723
4	16	0	1.079155	1.325565	-0.464580
5	6	0	2.744319	1.187616	-0.016710
6	16	0	-0.505497	-1.300354	-0.640525
7	8	0	-1.586685	-0.053185	-0.769054
8	6	0	-2.592545	0.129257	0.271850
9	6	0	-1.943757	0.369992	1.624869
10	6	0	4.412631	-0.620031	0.624226
11	6	0	-3.337927	1.363740	-0.206051
12	6	0	-3.508096	-1.084894	0.300290
13	1	0	3.370396	2.055529	0.060030
14	1	0	4.346871	-1.135775	1.578709
15	1	0	4.780798	-1.334102	-0.107876
16	1	0	5.132226	0.186841	0.713915
17	1	0	-4.144897	1.601955	0.481709
18	1	0	-2.666896	2.215487	-0.261194
19	1	0	-3.760013	1.194121	-1.191801
20	1	0	-4.320879	-0.924307	1.003524
21	1	0	-3.934216	-1.261370	-0.683198
22	1	0	-2.970571	-1.976110	0.612600
23	1	0	-2.714628	0.541801	2.371360
24	1	0	-1.358403	-0.487489	1.942758
25	1	0	-1.296954	1.241004	1.594998

```
Zero-point correction=                          0.207041 (Hartree/Particle)
Thermal correction to Energy=                   0.220585
Thermal correction to Enthalpy=                 0.221529
Thermal correction to Gibbs Free Energy=        0.166145
Sum of electronic and zero-point Energies=          -1238.521748
Sum of electronic and thermal Energies=             -1238.508205
Sum of electronic and thermal Enthalpies=           -1238.507260
Sum of electronic and thermal Free Energies=        -1238.562644

Version=AM64L-G03RevE.01\State=1-A\HF=-1238.7287892\RMSD=2.328e-09\
RMSF=5.298e-07\Dipole=0.4911796,-0.7358279,-0.2411372\PG=C01
[X(C8H13N1O1S2)]\NImag=0\\\@
```

(*iii*) MP2/6-31+G**

Standard orientation:

Center Number	Atomic Number	Atomic Type	Coordinates (Angstroms) X	Y	Z
1	6	0	2.726784	0.582366	-0.085537
2	7	0	1.623618	0.725304	0.714939
3	6	0	0.831869	-0.333453	0.620331
4	16	0	1.399495	-1.565680	-0.455817
5	6	0	2.754325	-0.590613	-0.818391
6	16	0	-0.665388	-0.508861	1.510363
7	8	0	-1.731283	-0.802205	0.229201
8	6	0	-2.381364	0.364152	-0.392406
9	6	0	-1.348615	1.313207	-0.978517
10	6	0	3.755431	1.666680	-0.118078
11	6	0	-3.205641	-0.294325	-1.484472
12	6	0	-3.267464	1.058270	0.627698
13	1	0	3.494369	-0.896211	-1.540885
14	1	0	3.301100	2.612210	-0.408935
15	1	0	4.197783	1.797078	0.868246
16	1	0	4.546698	1.426191	-0.825236
17	1	0	-3.769233	0.461751	-2.030947
18	1	0	-2.553614	-0.819708	-2.180316
19	1	0	-3.903138	-1.008200	-1.049987
20	1	0	-3.824871	1.863082	0.148130
21	1	0	-3.975247	0.347579	1.052240
22	1	0	-2.672385	1.490445	1.430512
23	1	0	-1.859304	2.102923	-1.530631
24	1	0	-0.744282	1.777444	-0.201677
25	1	0	-0.690606	0.780874	-1.665208

```
Zero-point correction=                           0.204353 (Hartree/Particle)
Thermal correction to Energy=                    0.218130
Thermal correction to Enthalpy=                  0.219074
Thermal correction to Gibbs Free Energy=         0.162748
Sum of electronic and zero-point Energies=          -1236.456977
Sum of electronic and thermal Energies=             -1236.443200
Sum of electronic and thermal Enthalpies=           -1236.442256
Sum of electronic and thermal Free Energies=        -1236.498582

Version=AM64L-G03RevE.01\State=1-A\HF=-1234.8290054\MP2=-1236.6613298\
RMSD=7.069e-09\RMSF=1.966e-08\Dipole=0.1029303,-0.628734,-0.7373158\ PG=C01
[X(C8H13N1O1S2)]\NImag=0\\\@
```

C7.7.3 2-(Methylsulfanyl)-4-methylthiazole 3-oxide (7d)

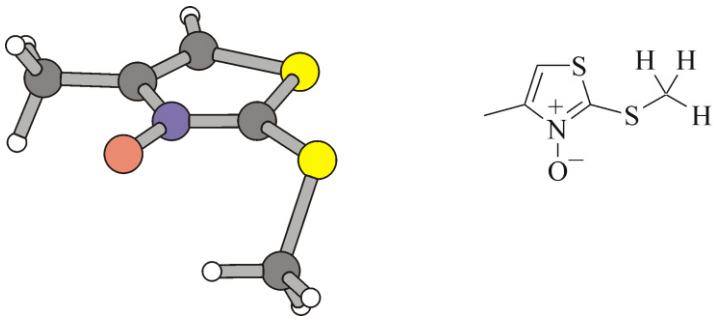

Figure C42. Computed minimum structure of 2-(methylsulfanyl)thiazole 3-oxide **7d**.

(*i*) B3LYP/6-31+G**//B3LYP/6-31+G**

Standard orientation:

Center Number	Atomic Number	Atomic Type	Coordinates (Angstroms) X	Y	Z
1	6	0	1.778581	-0.289818	0.047575
2	7	0	0.431598	-0.668948	-0.160467
3	6	0	-0.430828	0.370568	-0.160432
4	16	0	0.389440	1.879929	0.111253
5	6	0	1.914304	1.053646	0.189309
6	8	0	0.096450	-1.900894	-0.326733
7	16	0	-2.140302	0.232896	-0.476061
8	6	0	-2.654724	-0.947591	0.836451
9	6	0	2.810168	-1.363937	0.060533
10	1	0	2.834138	1.602289	0.332186
11	1	0	2.598355	-2.088018	0.853841
12	1	0	2.797440	-1.917252	-0.883813
13	1	0	3.801898	-0.933970	0.217329
14	1	0	-3.703277	-1.175417	0.631595
15	1	0	-2.049750	-1.851945	0.760004
16	1	0	-2.562809	-0.488309	1.822300

```
Zero-point correction=                          0.115771 (Hartree/Particle)
Thermal correction to Energy=                   0.125556
Thermal correction to Enthalpy=                 0.126500
Thermal correction to Gibbs Free Energy=        0.080412
Sum of electronic and zero-point Energies=          -1120.936432
Sum of electronic and thermal Energies=             -1120.926647
Sum of electronic and thermal Enthalpies=           -1120.925703
Sum of electronic and thermal Free Energies=        -1120.971791

Version=AM64L-G03RevE.01\State=1-A\HF=-1121.0522032\RMSD=7.771e-09\
RMSF=2.599e-07\Dipole=0.5803008,-0.4965862,-1.0052083\PG=C01
[X(C5H7N1O1S2)]\NImag=0\\\@
```

(*ii*) BHandHLYP/6-31+G**//BHandHLYP/6-31+G**

Standard orientation:

Center Number	Atomic Number	Atomic Type	Coordinates (Angstroms) X	Y	Z
1	6	0	1.756810	-0.291205	0.045344
2	7	0	0.419938	-0.652943	-0.159029
3	6	0	-0.420650	0.372301	-0.156106
4	16	0	0.395476	1.864170	0.110142
5	6	0	1.903554	1.038611	0.187724
6	8	0	0.083565	-1.874767	-0.327053
7	16	0	-2.125664	0.244206	-0.459663
8	6	0	-2.616938	-0.955332	0.814690
9	6	0	2.773202	-1.369972	0.055504
10	1	0	2.822402	1.572332	0.332654
11	1	0	2.554599	-2.085925	0.842191
12	1	0	2.752723	-1.914742	-0.883500
13	1	0	3.760791	-0.950801	0.211342
14	1	0	-3.660757	-1.177054	0.622857
15	1	0	-2.017578	-1.850431	0.710114
16	1	0	-2.513133	-0.525073	1.803376

```
Zero-point correction=                          0.120480 (Hartree/Particle)
Thermal correction to Energy=                   0.129911
Thermal correction to Enthalpy=                 0.130855
Thermal correction to Gibbs Free Energy=        0.085516
Sum of electronic and zero-point Energies=          -1120.688968
Sum of electronic and thermal Energies=             -1120.679537
Sum of electronic and thermal Enthalpies=           -1120.678592
Sum of electronic and thermal Free Energies=        -1120.723932

Version=AM64L-G03RevE.01\State=1-A\HF=-1120.8094477\RMSD=2.077e-09\
RMSF=8.463e-07\Dipole=0.6537234,-0.5072127,-1.0577043\PG=C01
[X(C5H7N1O1S2)]\NImag=0\\\@
```

(*iii*) MP2/6-31+G**

Standard orientation:

Center Number	Atomic Number	Atomic Type	Coordinates (Angstroms) X	Y	Z
1	6	0	1.765820	-0.262534	0.053573
2	7	0	0.443386	-0.672746	-0.177061
3	6	0	-0.451738	0.368592	-0.187533
4	16	0	0.332689	1.871214	0.097720
5	6	0	1.856552	1.092039	0.195364
6	8	0	0.133782	-1.902376	-0.339781
7	16	0	-2.134945	0.151359	-0.504530
8	6	0	-2.551717	-0.896772	0.915492
9	6	0	2.818402	-1.308161	0.076491
10	1	0	2.759320	1.657244	0.357678
11	1	0	2.610840	-2.032858	0.861952
12	1	0	2.830436	-1.848488	-0.868408
13	1	0	3.790065	-0.851887	0.249164
14	1	0	-3.595674	-1.179543	0.800254
15	1	0	-1.929222	-1.787143	0.900007
16	1	0	-2.427538	-0.349243	1.845661

```
Zero-point correction=                          0.118333 (Hartree/Particle)
Thermal correction to Energy=                   0.128102
Thermal correction to Enthalpy=                 0.129046
Thermal correction to Gibbs Free Energy=        0.082993
Sum of electronic and zero-point Energies=          -1118.924986
Sum of electronic and thermal Energies=             -1118.915218
Sum of electronic and thermal Enthalpies=           -1118.914274
Sum of electronic and thermal Free Energies=        -1118.960326

Version=AM64L-G03RevE.01\State=1-A\HF=-1117.662358\MP2=-1119.0433193\
RMSD=1.822e-09\RMSF=3.560e-08\Dipole=0.6374972,-0.5550871,-1.1177471\
PG=C01 [X(C5H7N1O1S2)]\NImag=0\\\@
```

C7.7.4 O-Methyl 4-methyl-1,3-thiazole-2-sulfenate (12d)

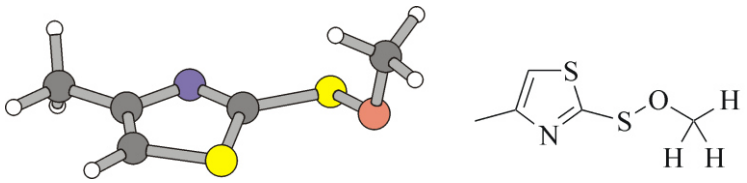

Figure C43. Computed minimum structure of *O*-methyl sulfenate **12d**.

(*i*) B3LYP/6-31+G**//B3LYP/6-31+G**

Standard orientation:

Center Number	Atomic Number	Atomic Type	Coordinates (Angstroms) X	Y	Z
1	6	0	2.223754	-0.175929	0.145839
2	7	0	1.121601	-1.014238	0.078332
3	6	0	0.034877	-0.346126	-0.169065
4	16	0	0.243462	1.393589	-0.346407
5	6	0	1.941387	1.149352	-0.039062
6	16	0	-1.514841	-1.162341	-0.416772
7	8	0	-2.567937	0.146186	-0.291639
8	6	0	-3.062376	0.404527	1.038586
9	6	0	3.571882	-0.769517	0.426476
10	1	0	2.619323	1.990363	0.007073
11	1	0	4.342396	0.004508	0.468594
12	1	0	3.564753	-1.308096	1.380252
13	1	0	3.844061	-1.489504	-0.352979
14	1	0	-3.736204	1.257685	0.931904
15	1	0	-3.612876	-0.459277	1.424213
16	1	0	-2.244240	0.660705	1.719955

```
Zero-point correction=                          0.115734 (Hartree/Particle)
Thermal correction to Energy=                   0.125834
Thermal correction to Enthalpy=                 0.126778
Thermal correction to Gibbs Free Energy=        0.078999
Sum of electronic and zero-point Energies=          -1120.964752
Sum of electronic and thermal Energies=             -1120.954652
Sum of electronic and thermal Enthalpies=           -1120.953708
Sum of electronic and thermal Free Energies=        -1121.001487

Version=AM64L-G03RevE.01\State=1-A\HF=-1121.080486\RMSD=5.831e-09\
RMSF=3.483e-07\Dipole=0.2754156,-0.6620024,-0.5065611\PG=C01
[X(C5H7N1O1S2)]\NImag=0\\\@
```

(*ii*) BHandHLYP/6-31+G**//BHandHLYP/6-31+G**

Standard orientation:

Center Number	Atomic Number	Atomic Type	Coordinates (Angstroms) X	Y	Z
1	6	0	2.211971	-0.155839	0.133006
2	7	0	1.126576	-1.003315	0.077092
3	6	0	0.040754	-0.354256	-0.148599
4	16	0	0.218925	1.365298	-0.320419
5	6	0	1.913101	1.151776	-0.044550
6	16	0	-1.494278	-1.180925	-0.348922
7	8	0	-2.516115	0.120339	-0.325287
8	6	0	-3.063554	0.449380	0.947459
9	6	0	3.562177	-0.733330	0.389163
10	1	0	2.579133	1.992519	-0.019955
11	1	0	4.319455	0.042778	0.420022
12	1	0	3.572761	-1.268450	1.335077
13	1	0	3.824170	-1.443545	-0.390779
14	1	0	-3.707333	1.304052	0.776622
15	1	0	-3.646562	-0.378043	1.340710
16	1	0	-2.279779	0.714838	1.651545

```
Zero-point correction=                          0.120562 (Hartree/Particle)
Thermal correction to Energy=                   0.130320
Thermal correction to Enthalpy=                 0.131265
Thermal correction to Gibbs Free Energy=        0.084375
Sum of electronic and zero-point Energies=          -1120.723499
Sum of electronic and thermal Energies=             -1120.713741
Sum of electronic and thermal Enthalpies=           -1120.712797
Sum of electronic and thermal Free Energies=        -1120.759686

Version=AM64L-G03RevE.01\State=1-A\HF=-1120.8440618\RMSD=2.865e-09\
RMSF=3.721e-07\Dipole=0.3334568,-0.6748417,-0.5106903\PG=C01
[X(C5H7N1O1S2)]\NImag=0\\\@
```

(*iii*) MP2/6-31+G**

Standard orientation:

Center Number	Atomic Number	Atomic Type	Coordinates (Angstroms) X	Y	Z
1	6	0	1.910489	0.590956	0.066667
2	7	0	0.642145	0.767577	0.539942
3	6	0	-0.083380	-0.338849	0.385673
4	16	0	0.771441	-1.646145	-0.358985
5	6	0	2.160857	-0.670034	-0.455085
6	16	0	-1.774517	-0.480293	0.797300
7	8	0	-2.469639	0.111827	-0.628944
8	6	0	-2.494383	1.552283	-0.694806
9	6	0	2.894580	1.713257	0.155457
10	1	0	3.089222	-1.036469	-0.863752
11	1	0	3.858983	1.413787	-0.249489
12	1	0	2.535294	2.576805	-0.401603
13	1	0	3.029022	2.015459	1.192448
14	1	0	-2.976356	1.780081	-1.641283
15	1	0	-3.070833	1.964156	0.132475
16	1	0	-1.483004	1.955854	-0.677316

```
Zero-point correction=                          0.118386 (Hartree/Particle)
Thermal correction to Energy=                   0.128385
Thermal correction to Enthalpy=                 0.129329
Thermal correction to Gibbs Free Energy=        0.081509
Sum of electronic and zero-point Energies=          -1118.955559
Sum of electronic and thermal Energies=             -1118.945561
Sum of electronic and thermal Enthalpies=           -1118.944617
Sum of electronic and thermal Free Energies=        -1118.992437

Version=AM64L-G03RevE.01\State=1-A\HF=-1117.7059446\MP2=-1119.0739454\
RMSD=9.299e-09\RMSF=5.266e-08\Dipole=-0.4807682,-0.236794,-0.9596591\
PG=C01 [X(C5H7N1O1S2)]\NImag=0\\\@
```

C7.7.5 2-(2-Methylpropyl-2-sulfanyl)-pyridine 1-oxide (9b)

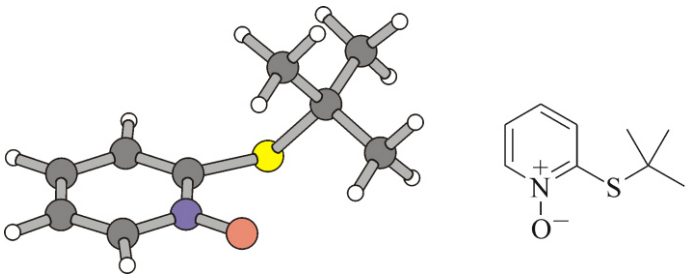

Figure C44. Computed structure of 2-(*tert*-butylsulfanyl)pyridine 1-oxide **9b**.

(*i*) B3LYP/6-31+G**//B3LYP/6-31+G**

Standard orientation:

Center Number	Atomic Number	Atomic Type	Coordinates (Angstroms) X	Y	Z
1	6	0	2.549521	1.132981	0.125215
2	7	0	1.239921	0.893494	-0.208986
3	6	0	0.790884	-0.415496	-0.307049
4	6	0	1.687413	-1.460340	-0.055583
5	6	0	3.019308	-1.221011	0.268970
6	6	0	3.445329	0.107619	0.358274
7	8	0	0.453099	1.887587	-0.411469
8	16	0	-0.821870	-0.772014	-0.929477
9	6	0	-2.119271	-0.013694	0.241779
10	6	0	-2.659386	1.286011	-0.368610
11	6	0	-3.224633	-1.082583	0.291606
12	6	0	-1.532163	0.219818	1.636188
13	1	0	1.302700	-2.471331	-0.125403
14	1	0	3.700191	-2.043659	0.457150
15	1	0	4.468640	0.360735	0.614335
16	1	0	2.790599	2.186295	0.177256
17	1	0	-4.069798	-0.697644	0.875393
18	1	0	-3.597909	-1.325447	-0.709298
19	1	0	-2.871513	-2.006186	0.759439
20	1	0	-2.336357	0.550745	2.305316
21	1	0	-1.104284	-0.696715	2.054446
22	1	0	-0.769539	1.001830	1.618606
23	1	0	-3.443658	1.692755	0.283409
24	1	0	-1.863606	2.023243	-0.476071
25	1	0	-3.101805	1.102613	-1.353030

```
Zero-point correction=                          0.205836 (Hartree/Particle)
Thermal correction to Energy=                   0.218131
Thermal correction to Enthalpy=                 0.219075
Thermal correction to Gibbs Free Energy=        0.167753
Sum of electronic and zero-point Energies=           -878.721280
Sum of electronic and thermal Energies=              -878.708985
Sum of electronic and thermal Enthalpies=            -878.708041
Sum of electronic and thermal Free Energies=         -878.759363

Version=AM64L-G03RevE.01\State=1-A\HF=-878.9271159\RMSD=2.530e-09\
RMSF=4.988e-07\Dipole=0.953838,0.6006566,-0.7849452\PG=C01
[X(C9H13N1O1S1)]\NImag=0\\\@
```

(*ii*) BHandHLYP/6-31+G**//BHandHLYP/6-31+G**

Standard orientation:

Center Number	Atomic Number	Atomic Type	Coordinates (Angstroms) X	Y	Z
1	6	0	2.509445	1.126652	0.124374
2	7	0	1.221108	0.878021	-0.212792
3	6	0	0.784000	-0.410284	-0.311110
4	6	0	1.674198	-1.448055	-0.060654
5	6	0	2.992485	-1.204091	0.268503
6	6	0	3.407460	0.116813	0.360772
7	8	0	0.436603	1.860664	-0.418266
8	16	0	-0.821364	-0.772266	-0.921745
9	6	0	-2.085190	-0.015586	0.237923
10	6	0	-2.630068	1.273491	-0.366609
11	6	0	-3.189498	-1.069788	0.310353
12	6	0	-1.493494	0.226711	1.618345
13	1	0	1.296365	-2.452251	-0.134242
14	1	0	3.672230	-2.016912	0.456547
15	1	0	4.419714	0.374654	0.620076
16	1	0	2.740735	2.173549	0.177604
17	1	0	-4.020035	-0.676675	0.893767
18	1	0	-3.569871	-1.319198	-0.677386
19	1	0	-2.838388	-1.983382	0.780480
20	1	0	-2.288172	0.559210	2.284246
21	1	0	-1.066374	-0.680777	2.036442
22	1	0	-0.737504	1.003472	1.589067
23	1	0	-3.401022	1.677740	0.288747
24	1	0	-1.841724	2.004623	-0.485686
25	1	0	-3.080736	1.085566	-1.337450

```
Zero-point correction=                          0.213621 (Hartree/Particle)
Thermal correction to Energy=                   0.225423
Thermal correction to Enthalpy=                 0.226367
Thermal correction to Gibbs Free Energy=        0.176111
Sum of electronic and zero-point Energies=           -878.387922
Sum of electronic and thermal Energies=              -878.376121
Sum of electronic and thermal Enthalpies=            -878.375177
Sum of electronic and thermal Free Energies=         -878.425432

Version=AM64L-G03RevE.01\State=1-A\HF=-878.6015435\RMSD=2.528e-09\
RMSF=3.627e-07\Dipole=1.0816778,0.5799746,-0.9337406\PG=C01
[X(C9H13N1O1S1)]\NImag=0\\\@
```

(*iii*) MP2/6-31+G**

Standard orientation:

Center Number	Atomic Number	Atomic Type	Coordinates (Angstroms) X	Y	Z
1	6	0	2.513102	1.111460	0.175272
2	7	0	1.206146	0.911598	-0.226896
3	6	0	0.733069	-0.395213	-0.372287
4	6	0	1.602242	-1.459424	-0.123458
5	6	0	2.923132	-1.261983	0.265538
6	6	0	3.369201	0.055374	0.409904
7	8	0	0.448757	1.914816	-0.425915
8	16	0	-0.858719	-0.649967	-1.043217
9	6	0	-2.037363	-0.039814	0.262980
10	6	0	-2.643059	1.290207	-0.174615
11	6	0	-3.124444	-1.111614	0.340175
12	6	0	-1.343352	0.093987	1.611018
13	1	0	1.199287	-2.455679	-0.240854
14	1	0	3.577719	-2.100445	0.453944
15	1	0	4.382289	0.277642	0.715480
16	1	0	2.771844	2.155006	0.264692
17	1	0	-3.906242	-0.780045	1.025987
18	1	0	-3.583387	-1.281493	-0.634323
19	1	0	-2.720051	-2.057007	0.699051
20	1	0	-2.093684	0.355050	2.360011
21	1	0	-0.874169	-0.841857	1.914832
22	1	0	-0.597429	0.886670	1.595721
23	1	0	-3.368821	1.615249	0.574333
24	1	0	-1.872023	2.047052	-0.283220
25	1	0	-3.164059	1.181737	-1.125752

```
Zero-point correction=                          0.209923 (Hartree/Particle)
Thermal correction to Energy=                   0.222102
Thermal correction to Enthalpy=                 0.223046
Thermal correction to Gibbs Free Energy=        0.172108
Sum of electronic and zero-point Energies=           -876.760849
Sum of electronic and thermal Energies=              -876.748669
Sum of electronic and thermal Enthalpies=            -876.747725
Sum of electronic and thermal Free Energies=         -876.798663

Version=AM64L-G03RevE.01\State=1-A\HF=-875.1423675\MP2=-876.9707712\
RMSD=1.097e-09\RMSF=2.687e-07\Dipole=0.9488324,0.6536964,-0.8493964\ PG=C01
[X(C9H13N1O1S1)]\NImag=0\\\@
```

C7.7.6 O-(2-Methylprop-2-yl)pyridine-2-sulfenate (10b)

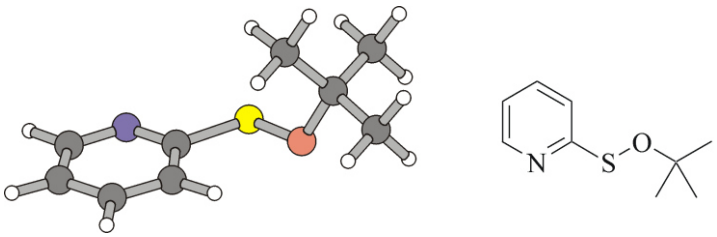

Figure C45. Computed minimum structure of *O*-(*tert*-butyl) sulfenate **10b**.

(*i*) B3LYP/6-31+G**//B3LYP/6-31+G**

Standard orientation:

Center Number	Atomic Number	Atomic Type	Coordinates (Angstroms) X	Y	Z
1	6	0	3.462243	-0.628061	0.418880
2	7	0	2.262135	-1.192639	0.230814
3	6	0	1.265050	-0.406602	-0.184189
4	6	0	1.403809	0.964221	-0.441838
5	6	0	2.657446	1.532811	-0.230462
6	6	0	3.713395	0.728902	0.210820
7	16	0	-0.247621	-1.317442	-0.439499
8	8	0	-1.334225	-0.084285	-0.825745
9	6	0	-2.375329	0.271674	0.162819
10	6	0	-1.747664	0.764959	1.468797
11	6	0	-3.127424	1.396558	-0.552922
12	6	0	-3.288382	-0.935762	0.398785
13	1	0	0.561402	1.540756	-0.803490
14	1	0	2.811177	2.592297	-0.416192
15	1	0	4.703128	1.138048	0.384197
16	1	0	4.252789	-1.295774	0.754074
17	1	0	-3.958889	1.746655	0.067457
18	1	0	-2.462553	2.242930	-0.749889
19	1	0	-3.528507	1.042910	-1.507083
20	1	0	-4.121493	-0.658367	1.053217
21	1	0	-3.698704	-1.296072	-0.549555
22	1	0	-2.744237	-1.755078	0.878824
23	1	0	-2.535294	1.049129	2.174511
24	1	0	-1.143169	-0.016876	1.937660
25	1	0	-1.113717	1.639083	1.294387

```
Zero-point correction=                          0.205241 (Hartree/Particle)
Thermal correction to Energy=                   0.217840
Thermal correction to Enthalpy=                 0.218784
Thermal correction to Gibbs Free Energy=        0.165954
Sum of electronic and zero-point Energies=           -878.759656
Sum of electronic and thermal Energies=              -878.747057
Sum of electronic and thermal Enthalpies=            -878.746113
Sum of electronic and thermal Free Energies=         -878.798943

Version=AM64L-G03RevE.01\State=1-A\HF=-878.9648968\RMSD=2.471e-09\
RMSF=5.919e-07\Dipole=0.9391718,-0.6259661,-0.350359\PG=C01
[X(C9H13N1O1S1)]\NImag=0\\\@
```

(*ii*) BHandHLYP/6-31+G**//BHandHLYP/6-31+G**

Standard orientation:

Center Number	Atomic Number	Atomic Type	Coordinates (Angstroms) X	Y	Z
1	6	0	3.670164	0.727039	0.209465
2	6	0	3.422655	-0.618881	0.422331
3	7	0	2.235543	-1.180534	0.233333
4	6	0	1.245111	-0.410447	-0.185993
5	6	0	1.379110	0.949201	-0.447454
6	6	0	2.621012	1.518992	-0.236420
7	16	0	-0.253115	-1.313119	-0.439763
8	8	0	-1.313797	-0.091684	-0.808671
9	6	0	-2.337627	0.271227	0.159202
10	6	0	-3.258940	-0.916821	0.393619
11	6	0	-1.713814	0.753744	1.459305
12	6	0	-3.077228	1.397605	-0.543413
13	1	0	0.542365	1.516470	-0.811250
14	1	0	2.770859	2.569852	-0.425435
15	1	0	4.650513	1.136263	0.382855
16	1	0	4.207409	-1.276739	0.762116
17	1	0	-3.897170	1.751792	0.075704
18	1	0	-2.408491	2.230889	-0.738696
19	1	0	-3.480419	1.052791	-1.490635
20	1	0	-4.084243	-0.629392	1.039712
21	1	0	-3.667033	-1.270279	-0.549058
22	1	0	-2.730280	-1.735986	0.872617
23	1	0	-2.496115	1.049905	2.153157
24	1	0	-1.128220	-0.029586	1.930612
25	1	0	-1.070416	1.611173	1.286706

```
Zero-point correction=                          0.213031 (Hartree/Particle)
Thermal correction to Energy=                   0.225169
Thermal correction to Enthalpy=                 0.226113
Thermal correction to Gibbs Free Energy=        0.174221
Sum of electronic and zero-point Energies=           -878.434280
Sum of electronic and thermal Energies=              -878.422142
Sum of electronic and thermal Enthalpies=            -878.421198
Sum of electronic and thermal Free Energies=         -878.473090

Version=AM64L-G03RevE.01\State=1-A\HF=-878.647311\RMSD=6.457e-09\
RMSF=2.940e-06\Dipole=0.165655,-0.6659316,-0.987366\ PG=C01
[X(C9H13N1O1S1)]\NImag=0\\\@
```

(*iii*) MP2/6-31+G**

Standard orientation:

Center Number	Atomic Number	Atomic Type	Coordinates (Angstroms) X	Y	Z
1	6	0	3.578330	0.757803	0.265291
2	6	0	3.327443	-0.577803	0.576450
3	7	0	2.149735	-1.185405	0.341708
4	6	0	1.187852	-0.451553	-0.237964
5	6	0	1.344622	0.885876	-0.619616
6	6	0	2.563124	1.499560	-0.343686
7	16	0	-0.290388	-1.369348	-0.559202
8	8	0	-1.357016	-0.102599	-0.881837
9	6	0	-2.260891	0.300216	0.211373
10	6	0	-3.216081	-0.841339	0.516812
11	6	0	-1.479462	0.722592	1.444327
12	6	0	-2.990123	1.478778	-0.408044
13	1	0	0.536686	1.406128	-1.113187
14	1	0	2.724022	2.534704	-0.615924
15	1	0	4.539113	1.198672	0.491693
16	1	0	4.087714	-1.194166	1.039878
17	1	0	-3.725280	1.872328	0.293664
18	1	0	-2.284526	2.270389	-0.655796
19	1	0	-3.502119	1.168168	-1.317044
20	1	0	-3.958459	-0.521117	1.247971
21	1	0	-3.730126	-1.149082	-0.392560
22	1	0	-2.681482	-1.696002	0.928677
23	1	0	-2.175085	1.052763	2.216142
24	1	0	-0.898072	-0.105797	1.845922
25	1	0	-0.807088	1.546442	1.210878

```
Zero-point correction=                           0.209563 (Hartree/Particle)
Thermal correction to Energy=                    0.222012
Thermal correction to Enthalpy=                  0.222956
Thermal correction to Gibbs Free Energy=         0.170479
Sum of electronic and zero-point Energies=           -876.797130
Sum of electronic and thermal Energies=              -876.784681
Sum of electronic and thermal Enthalpies=            -876.783737
Sum of electronic and thermal Free Energies=         -876.836214

Version=AM64L-G03RevE.01\State=1-A\HF=-875.2030604\MP2=-877.0066928\
RMSD=7.290e-09\RMSF=2.660e-06\Dipole=-0.0146822,-0.7130791,-0.9856979\
PG=C01 [X(C9H13N1O1S1)]\NImag=0\\\@
```

C7.7.7 2-(Methylsulfanyl)pyridine 1-oxide (9d)

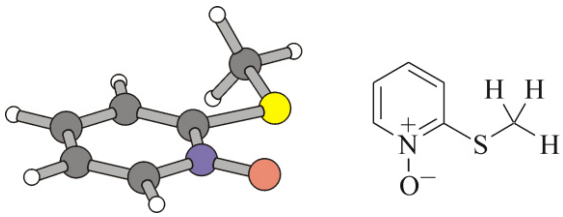

Figure C46. Computed minimum structure of 2-(methylsulfanyl)pyridine-*N*-oxide **9d**.

(*i*) B3LYP/6-31+G**//B3LYP/6-31+G**

Standard orientation:

Center Number	Atomic Number	Atomic Type	Coordinates (Angstroms) X	Y	Z
1	6	0	-2.098583	0.675616	0.000010
2	7	0	-0.761969	0.958928	0.000001
3	6	0	0.162198	-0.067576	-0.000014
4	6	0	-0.278722	-1.391810	-0.000012
5	6	0	-1.641919	-1.684959	-0.000006
6	6	0	-2.558228	-0.629410	0.000004
7	8	0	-0.336987	2.176552	0.000014
8	16	0	1.812441	0.545792	-0.000022
9	6	0	2.749158	-1.024635	0.000032
10	1	0	0.449458	-2.193032	-0.000017
11	1	0	-1.978180	-2.716002	-0.000004
12	1	0	-3.628007	-0.806427	0.000010
13	1	0	-2.727239	1.556067	0.000021
14	1	0	3.799875	-0.726271	0.000051
15	1	0	2.555621	-1.617619	0.897663
16	1	0	2.555667	-1.617655	-0.897584

```
Zero-point correction=                          0.121649 (Hartree/Particle)
Thermal correction to Energy=                   0.129849
Thermal correction to Enthalpy=                 0.130793
Thermal correction to Gibbs Free Energy=        0.088472
Sum of electronic and zero-point Energies=           -760.855507
Sum of electronic and thermal Energies=              -760.847307
Sum of electronic and thermal Enthalpies=            -760.846363
Sum of electronic and thermal Free Energies=         -760.888684

Version=AM64L-G03RevE.01\State=1-A\HF=-760.9771558\RMSD=1.821e-09\
RMSF=3.983e-07\Dipole=1.9202163,-0.0002549,-0.6353599\PG=C01
[X(C6H7N1O1S1)]\NImag=0\\\@
```

(*ii*) BHandHLYP/6-31+G**//BHandHLYP/6-31+G**

Standard orientation:

Center Number	Atomic Number	Atomic Type	Coordinates (Angstroms) X	Y	Z
1	6	0	2.077413	0.666486	0.000001
2	7	0	0.757850	0.946853	0.000000
3	6	0	-0.158195	-0.058567	-0.000001
4	6	0	0.271753	-1.377208	-0.000002
5	6	0	1.622543	-1.673005	-0.000001
6	6	0	2.535677	-0.628632	0.000001
7	8	0	0.345729	2.157884	0.000001
8	16	0	-1.800392	0.542404	-0.000002
9	6	0	-2.721902	-1.013617	0.000003
10	1	0	-0.454256	-2.168663	-0.000003
11	1	0	1.952951	-2.697376	-0.000001
12	1	0	3.596764	-0.806205	0.000002
13	1	0	2.702512	1.539348	0.000002
14	1	0	-3.766643	-0.723743	0.000003
15	1	0	-2.529780	-1.602814	-0.890404
16	1	0	-2.529779	-1.602807	0.890414

```
Zero-point correction=                          0.126426 (Hartree/Particle)
Thermal correction to Energy=                   0.134311
Thermal correction to Enthalpy=                 0.135255
Thermal correction to Gibbs Free Energy=        0.093527
Sum of electronic and zero-point Energies=           -760.603514
Sum of electronic and thermal Energies=              -760.595630
Sum of electronic and thermal Enthalpies=            -760.594685
Sum of electronic and thermal Free Energies=         -760.636413

Version=AM64L-G03RevE.01\State=1-A\HF=-760.72994\RMSD=5.183e-09\
RMSF=3.125e-07\Dipole=2.0785861,-0.0002837,-0.7694504\PG=C01
[X(C6H7N1O1S1)]\NImag=0\\\@
```

(*iii*) MP2/6-31+G**

Standard orientation:

Center Number	Atomic Number	Atomic Type	Coordinates (Angstroms) X	Y	Z
1	6	0	2.095499	0.681026	0.000009
2	7	0	0.749873	0.966639	0.000001
3	6	0	-0.176724	-0.069360	-0.000006
4	6	0	0.273343	-1.387099	-0.000012
5	6	0	1.635553	-1.682442	-0.000004
6	6	0	2.547146	-0.624326	0.000006
7	8	0	0.326237	2.171783	-0.000001
8	16	0	-1.812266	0.542196	-0.000008
9	6	0	-2.702548	-1.031018	0.000016
10	1	0	-0.449149	-2.188900	-0.000022
11	1	0	1.971123	-2.709378	-0.000008
12	1	0	3.613659	-0.799445	0.000012
13	1	0	2.718125	1.561814	0.000015
14	1	0	-3.756967	-0.765726	0.000035
15	1	0	-2.496593	-1.617470	-0.892385
16	1	0	-2.496561	-1.617456	0.892419

```
Zero-point correction=                          0.122691 (Hartree/Particle)
Thermal correction to Energy=                   0.131258
Thermal correction to Enthalpy=                 0.132202
Thermal correction to Gibbs Free Energy=        0.088869
Sum of electronic and zero-point Energies=           -759.268005
Sum of electronic and thermal Energies=              -759.259438
Sum of electronic and thermal Enthalpies=            -759.258494
Sum of electronic and thermal Free Energies=         -759.301827

Version=AM64L-G03RevE.01\State=1-A\HF=-758.0324339\MP2=-759.3906962\
RMSD=3.004e-09\RMSF=7.716e-08\Dipole=1.8480736,-0.0002237,-0.6381227\
PG=C01 [X(C6H7N1O1S1)]\NImag=0\\\@
```

C7.7.8 O-Methyl pyridine-2-sulfenate (10d)

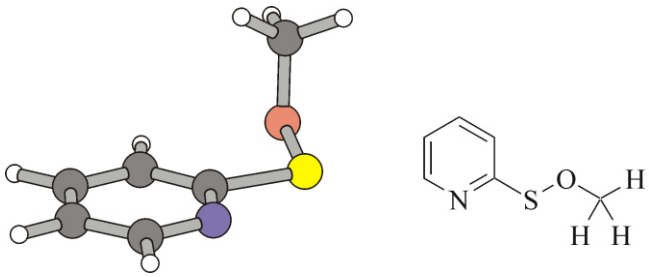

Figure C47. Computed minimum structure of *O*-methyl pyridine-2-sulfenate (**10d**).

(*i*) B3LYP/6-31+G**//B3LYP/6-31+G**

Standard orientation:

Center Number	Atomic Number	Atomic Type	Coordinates (Angstroms) X	Y	Z
1	6	0	-2.482408	-0.824768	0.317517
2	7	0	-1.212967	-1.239717	0.212757
3	6	0	-0.288090	-0.329254	-0.099803
4	6	0	-0.564837	1.025938	-0.326731
5	6	0	-1.889395	1.438330	-0.200019
6	6	0	-2.873976	0.501549	0.129408
7	16	0	1.344550	-1.039318	-0.242990
8	8	0	2.295008	0.336019	-0.474492
9	6	0	2.866610	0.878799	0.730362
10	1	0	0.227873	1.710397	-0.604624
11	1	0	-2.151704	2.479674	-0.364971
12	1	0	-3.915275	0.787381	0.233988
13	1	0	-3.212517	-1.591232	0.567309
14	1	0	3.470468	1.730513	0.407169
15	1	0	2.087019	1.216864	1.422438
16	1	0	3.504623	0.141801	1.228775

```
Zero-point correction=                          0.121643 (Hartree/Particle)
Thermal correction to Energy=                   0.130287
Thermal correction to Enthalpy=                 0.131231
Thermal correction to Gibbs Free Energy=        0.087231
Sum of electronic and zero-point Energies=           -760.879825
Sum of electronic and thermal Energies=              -760.871181
Sum of electronic and thermal Enthalpies=            -760.870237
Sum of electronic and thermal Free Energies=         -760.914236

Version=AM64L-G03RevE.01\State=1-A\HF=-761.0014676\RMSD=9.174e-09\
RMSF=5.522e-07\Dipole=0.8310156,0.6280341,-0.6492255\PG=C01
[X(C6H7N1O1S1)]\NImag=0\\\@
```

(*ii*) BHandHLYP/6-31+G**//BHandHLYP/6-31+G**

Standard orientation:

Center Number	Atomic Number	Atomic Type	Coordinates (Angstroms) X	Y	Z
1	6	0	-2.456115	-0.818450	0.316916
2	7	0	-1.198684	-1.228687	0.212580
3	6	0	-0.279108	-0.331475	-0.099716
4	6	0	-0.552320	1.013239	-0.327413
5	6	0	-1.866799	1.424707	-0.202995
6	6	0	-2.845170	0.497179	0.126467
7	16	0	1.339672	-1.031394	-0.240818
8	8	0	2.261288	0.329106	-0.462565
9	6	0	2.818086	0.883010	0.721806
10	1	0	0.235138	1.690716	-0.603836
11	1	0	-2.125945	2.457919	-0.369155
12	1	0	-3.878220	0.781326	0.229428
13	1	0	-3.180965	-1.577062	0.567870
14	1	0	3.408666	1.734478	0.402947
15	1	0	2.038256	1.211569	1.404679
16	1	0	3.457346	0.162063	1.223227

```
Zero-point correction=                          0.126571 (Hartree/Particle)
Thermal correction to Energy=                   0.134916
Thermal correction to Enthalpy=                 0.135860
Thermal correction to Gibbs Free Energy=        0.092484
Sum of electronic and zero-point Energies=           -760.636439
Sum of electronic and thermal Energies=              -760.628095
Sum of electronic and thermal Enthalpies=            -760.627151
Sum of electronic and thermal Free Energies=         -760.670526

Version=AM64L-G03RevE.01\State=1-A\HF=-760.7630106\RMSD=2.394e-09\
RMSF=4.765e-07\Dipole=0.8473303,0.639576,-0.7038308\PG=C01
[X(C6H7N1O1S1)]\NImag=0\\\@
```

(*iii*) MP2/6-31+G**

Standard orientation:

Center Number	Atomic Number	Atomic Type	Coordinates (Angstroms) X	Y	Z
1	6	0	-2.429489	-0.825029	0.391439
2	7	0	-1.159348	-1.249517	0.265319
3	6	0	-0.250410	-0.348867	-0.137161
4	6	0	-0.547260	0.985545	-0.436220
5	6	0	-1.862530	1.409111	-0.265522
6	6	0	-2.827172	0.489692	0.151952
7	16	0	1.373221	-1.031482	-0.316144
8	8	0	2.277190	0.386502	-0.426199
9	6	0	2.669333	0.908586	0.859909
10	1	0	0.227954	1.649789	-0.790139
11	1	0	-2.133664	2.435602	-0.475290
12	1	0	-3.859325	0.780248	0.288919
13	1	0	-3.144211	-1.574582	0.707389
14	1	0	3.249133	1.800818	0.641597
15	1	0	1.792665	1.167183	1.454081
16	1	0	3.279001	0.185038	1.397713

```
Zero-point correction=                          0.123482 (Hartree/Particle)
Thermal correction to Energy=                   0.132173
Thermal correction to Enthalpy=                 0.133118
Thermal correction to Gibbs Free Energy=        0.089010
Sum of electronic and zero-point Energies=           -759.295265
Sum of electronic and thermal Energies=              -759.286574
Sum of electronic and thermal Enthalpies=            -759.285629
Sum of electronic and thermal Free Energies=         -759.329737

Version=AM64L-G03RevE.01\State=1-A\HF=-758.0812251\MP2=-759.4187471\
RMSD=3.011e-09\RMSF=4.872e-07\Dipole=0.7957081,0.655688,-0.7735054\ PG=C01
[X(C6H7N1O1S1)]\NImag=0 \\\@
```

C7.8 Nitrogen-Oxygen Bond Order Analysis

C7.8.1 Hydroxylamine

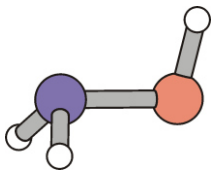

Figure C48. Computed minimum structure of hydroxylamine.

B3LYP/6-31+G//B3LYP/6-31+G****

Standard orientation:

Center Number	Atomic Number	Atomic Type	Coordinates (Angstroms) X	Y	Z
1	7	0	0.691217	-0.000002	0.153413
2	8	0	-0.725498	0.000003	-0.140189
3	1	0	1.045271	-0.816158	-0.346120
4	1	0	1.045281	0.816162	-0.346101
5	1	0	-1.125088	-0.000012	0.739839

```
Zero-point correction=                          0.040336 (Hartree/Particle)
Thermal correction to Energy=                   0.043530
Thermal correction to Enthalpy=                 0.044474
Thermal correction to Gibbs Free Energy=        0.017875
Sum of electronic and zero-point Energies=           -131.690099
Sum of electronic and thermal Energies=              -131.686905
Sum of electronic and thermal Enthalpies=            -131.685961
Sum of electronic and thermal Free Energies=         -131.712559

Version=AM64L-G03RevE.01\State=1-A\HF=-131.7304345\RMSD=2.187e-09\
RMSF=2.094e-06\Dipole=0.0491956,-0.0048473,-0.2587995\PG=C01
[X(H3N1O1)]\NImag=0\\\@
```

C7.8.2 O-(2-Methylprop-2-yl)-N,N-(dimethyl)hydroxylamine

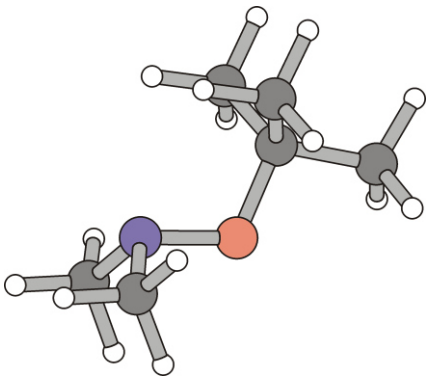

Figure C49. Computed minimum structure of O-(*tert*-butyl)dimethylhydroxylamine **12c**.

B3LYP/6-31+G//B3LYP/6-31+G****

Standard orientation:

Center Number	Atomic Number	Atomic Type	Coordinates (Angstroms) X	Y	Z
1	7	0	-1.306421	-0.000002	-0.227759
2	8	0	-0.180315	-0.000005	0.681743
3	6	0	1.102188	-0.000001	-0.008280
4	6	0	1.253181	-1.263765	-0.865161
5	6	0	1.253176	1.263771	-0.865148
6	6	0	2.105822	-0.000005	1.148946
7	6	0	-2.074726	-1.206054	0.080893
8	6	0	-2.074713	1.206059	0.080891
9	1	0	2.238988	-1.283987	-1.342445
10	1	0	1.154860	-2.162594	-0.247538
11	1	0	0.492979	-1.288709	-1.650786
12	1	0	2.238983	1.284001	-1.342434
13	1	0	0.492973	1.288721	-1.650772
14	1	0	1.154853	2.162594	-0.247516
15	1	0	3.129942	-0.000003	0.761818
16	1	0	1.970754	0.887124	1.775342
17	1	0	1.970755	-0.887139	1.775335
18	1	0	-2.961813	-1.221444	-0.560591
19	1	0	-1.470838	-2.088452	-0.137359
20	1	0	-2.390971	-1.241895	1.136215
21	1	0	-2.961799	1.221457	-0.560592
22	1	0	-2.390956	1.241906	1.136214
23	1	0	-1.470815	2.088450	-0.137364

```
Zero-point correction=                          0.207915 (Hartree/Particle)
Thermal correction to Energy=                   0.218331
Thermal correction to Enthalpy=                 0.219275
Thermal correction to Gibbs Free Energy=        0.173650
Sum of electronic and zero-point Energies=                -367.419696
Sum of electronic and thermal Energies=                   -367.409279
Sum of electronic and thermal Enthalpies=                 -367.408335
Sum of electronic and thermal Free Energies=              -367.453960

Version=AM64L-G03RevE.01\State=1-A\HF=-367.6276101\RMSD=1.685e-09\
RMSF=8.044e-07\Dipole=0.1136067,-0.0001985,-0.2208686\PG=C01
[X(C6H15N1O1)]\NImag=0\\\@
```

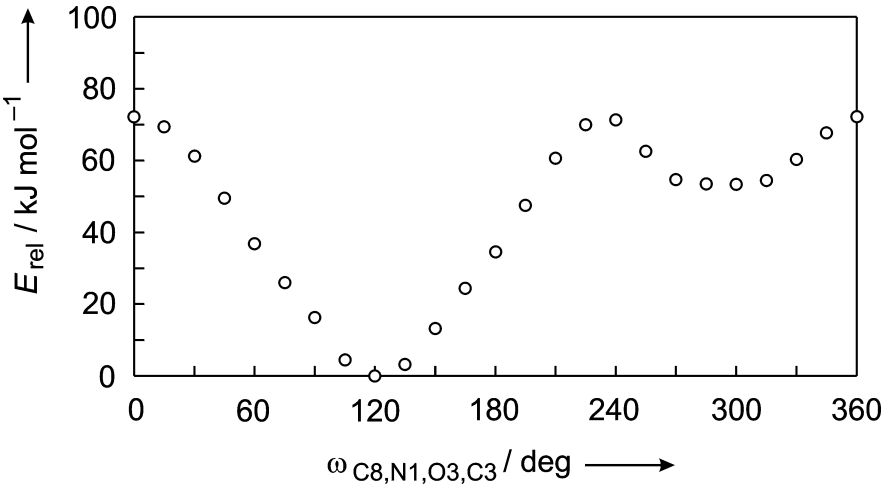

Figure C50. Computed energies of rotamers associcated with topomerization of the *tert*-butyl group about the nitrogen-oxygen bond in *O*-(2-methylprop-2-yl)-*N*,*N*-dimethyl-hydroxylamine.

Table C13. Energies and structural paramaters of conformers associated with rotation about the nitrogen-oxygen bond in *O*-(2-methylprop-2-yl)-*N*,*N*-dimethylhydroxylamine

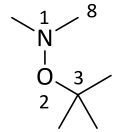

$\omega_{C8,N1,O2,C3}$ / deg	$\alpha_{N1,O2,C3}$ / deg	E /a.u. [a]	E_{rel} / kJ mol^{-1}	$d_{N3,O8}$ / Å	$E_{n1(O)}$ / eV [b]	$E_{n2(O)}$ / eV [b]	$E_{n1(N)}$ / eV [b]
0	126.6	–367.6000545	72.3	1.473	–16.04	–7.77	–8.39
15	125.6	–367.6011785	69.4	1.477	–16.13	–7.80	–8.42
30	123.9	–367.6042867	61.2	1.476	–16.24	–7.90	–8.50
45	121.5	–367.6087436	49.5	1.470	–16.36	–8.01	–8.60
60	119.2	–367.6135933	36.8	1.462	–16.49	–8.10	–8.17
75	117.2	–367.6177258	26.0	1.454	–16.63	–8.11	–8.81
90	116.3	–367.6214072	16.3	1.451	–16.81	–8.07	–8.80
105	113.8	–367.625883	4.5	1.447	–17.07	–7.98	–8.89
120	112.8	–367.6276045	0.01	1.447	–17.20	–7.94	–9.03
135	113.4	–367.6263908	3.2	1.451	–17.17	–7.97	–9.21
150	115.3	–367.6225706	13.2	1.456	–17.01	–8.04	–9.37
165	117.0	–367.6183073	24.4	1.457	–16.74	–8.10	–9.21
180	118.5	–367.6144355	34.6	1.466	–16.64	–8.09	–9.28
118.4	112.8	–367.6276101	0.0	1.448	–16.62	–7.57	–8.84

[a] 1 a.u. = 1 Hartree. 1 Hartree/particle = 2625.5 kJ mol^{-1}. [b] 1. a.u. = 27.211 eV; *n*N = non-bonding electron pair number N.

Table C14. Energies and structural paramaters of conformers associated with rotation about the nitrogen-oxygen bond in *O*-(2-methylprop-2-yl)-*N*,*N*-dimethylhydroxylamine

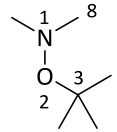

$\omega_{C8,N1,O2,C3}$ / deg	$\alpha_{N1,O2,C3}$ / deg	E /a.u. [a]	E_{rel} / kJ mol^{-1}	$d_{N3,O8}$ / Å	$E_{n1(O)}$ / eV [b]	$E_{n2(O)}$ / eV [b]	$E_{n1(N)}$ / eV [b]
180	118.5	–367.6144355	34.6	1.466	–16.64	–8.09	–9.28
195	120.9	–367.6094856	47.6	1.475	–16.51	–8.01	–9.25
210	123.7	–367.6045157	60.6	1.482	–16.33	–7.90	–9.07
225	126.0	–367.6009659	70.0	1.481	–16.14	–7.79	–8.85
240	126.3	–367.6004628	71.3	1.465	–16.03	–7.79	–8.06
255	124.1	–367.6037616	62.6	1.442	–16.11	–7.89	–7.46
270	123.4	–367.6067665	54.7	1.430	–16.18	–7.88	–7.41
285	124.4	–367.6071945	53.6	1.427	–16.13	–7.87	–7.63
300	123.7	–367.6072765	53.4	1.424	–16.18	–7.88	–7.42
315	124.5	–367.6068355	54.5	1.444	–16.12	–7.86	–7.81
330	125.4	–367.6046242	60.3	1.450	–16.05	–7.84	–8.13
345	126.3	–367.6018292	67.7	1.463	–16.02	–7.81	–8.35
360	126.6	–367.6000545	72.3	1.473	–16.04	–7.77	–8.39
118.4	112.8	–367.6276101	0.0	1.448	–16.62	–7.57	–8.84

[a] 1 a.u. = 1 Hartree. 1 Hartree/particle = 2625.5 kJ mol^{-1}. [b] 1. a.u. = 27.211 eV; *n*N = non-bonding electron pair number N.

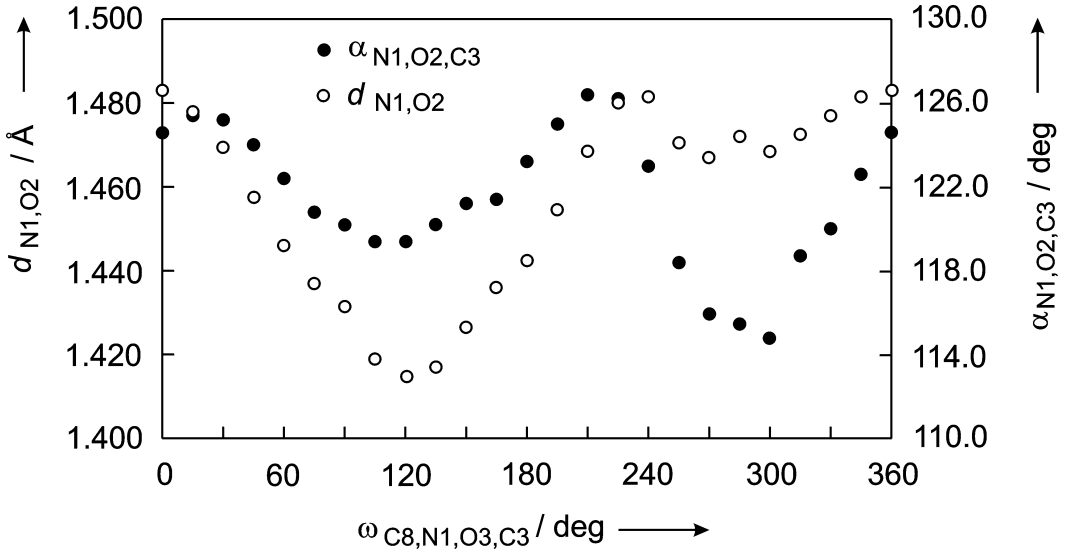

Figure C51. Nitrogen-oxygen bond length/torsion angle correlation for *O*-(2-methylprop-2-yl)-*N*,*N*-dimethylhydroxylamine.

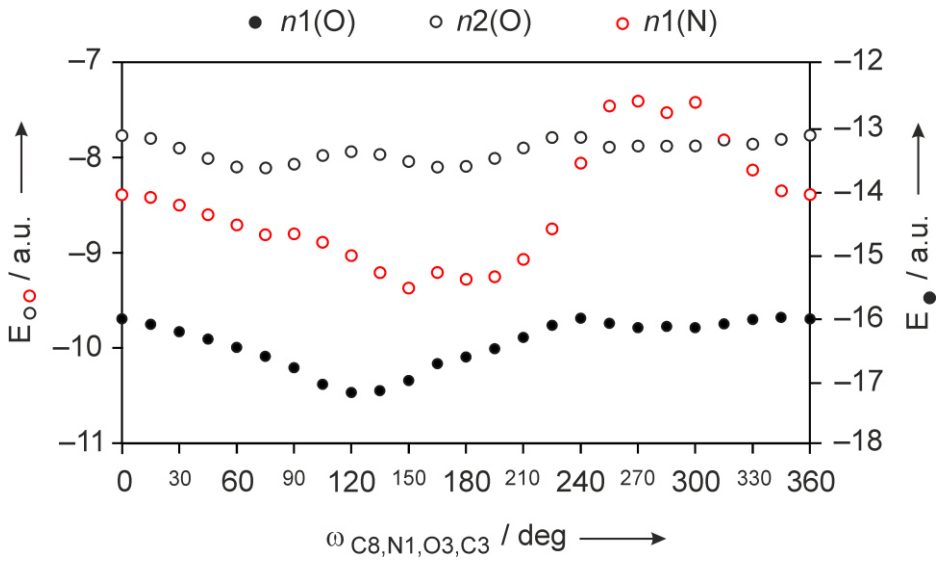

Figure C52. Calcuated energies (NBO; B3LYP/6-31+G**) of non bonding orbitals for rotamers of *O*-(2-methylprop-2-yl)-*N*,*N*-dimethylhydroxylamine.

C7.8.3 Nitrogen monoxide

Figure C53. Computed minimum structure of nitrogen monoxide.

B3LYP/6-31+G**//B3LYP/6-31+G**

Standard orientation:

Center Number	Atomic Number	Atomic Type	Coordinates (Angstroms) X	Y	Z
1	7	0	0.000000	0.000000	-0.617420
2	8	0	0.000000	0.000000	0.540242

```
Zero-point correction=                           0.004513 (Hartree/Particle)
Thermal correction to Energy=                    0.006874
Thermal correction to Enthalpy=                  0.007818
Thermal correction to Gibbs Free Energy=        -0.015491
Sum of electronic and zero-point Energies=           -129.890964
Sum of electronic and thermal Energies=              -129.888603
Sum of electronic and thermal Enthalpies=            -129.887658
Sum of electronic and thermal Free Energies=         -129.910967

Version=AM64L-G03RevE.01\HF=-129.8954762\S2=0.753016\S2-1=0.\
S2A=0.750006\RMSD=2.545e-09\RMSF=1.289e-06\Dipole=0.,0.,0.034451\PG=C*V
[C*(N1O1)]\NImag=0\\\@
```

C7.8.4 Nitrosyl Cation

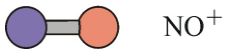

Figure C54. Computed minimum structure of the nitrosyl cation.

B3LYP/6-31+G//B3LYP/6-31+G****

```
Standard orientation:
---------------------------------------------------------------------
 Center     Atomic     Atomic              Coordinates (Angstroms)
 Number     Number      Type              X           Y           Z
---------------------------------------------------------------------
   1          7             0        0.000000    0.000000   -0.572090
   2          8             0        0.000000    0.000000    0.500578
---------------------------------------------------------------------

Zero-point correction=                          0.005650 (Hartree/Particle)
Thermal correction to Energy=                   0.008011
Thermal correction to Enthalpy=                 0.008955
Thermal correction to Gibbs Free Energy=  -0.013555
Sum of electronic and zero-point Energies=           -129.526503
Sum of electronic and thermal Energies=              -129.524142
Sum of electronic and thermal Enthalpies=            -129.523198
Sum of electronic and thermal Free Energies=         -129.545708

Version=AM64L-G03RevE.01\State=1-SG\HF=-129.5321532\RMSD=1.978e-09\
RMSF=7.224e-10\Dipole=0.,0.,-0.1697337\PG=C*V [C*(N1O1)]\NImag=0\\\@
```

C7.8.5 Singlet Nitrosyl Anion

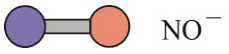

Figure C55. Computed minimum structure of the singlet nitrosyl anion.

B3LYP/6-31+G//B3LYP/6-31+G****

```
Standard orientation:
---------------------------------------------------------------------
 Center     Atomic     Atomic              Coordinates (Angstroms)
 Number     Number      Type              X           Y           Z
---------------------------------------------------------------------
    1          7             0        0.000000    0.000000   -0.669277
    2          8             0        0.000000    0.000000    0.585617
---------------------------------------------------------------------

Zero-point correction=                          0.003325 (Hartree/Particle)
Thermal correction to Energy=                   0.005691
Thermal correction to Enthalpy=                 0.006635
Thermal correction to Gibbs Free Energy=   -0.016177
Sum of electronic and zero-point Energies=           -129.860025
Sum of electronic and thermal Energies=              -129.857658
Sum of electronic and thermal Enthalpies=            -129.856714
Sum of electronic and thermal Free Energies=         -129.879527

Version=AM64L-G03RevE.01\HF=-129.8633495\RMSD=1.980e-09\RMSF=2.894e-07\
Dipole=0.,0.,0.6380828\PG=C*V [C*(N1O1)]\NImag=0\\\@
```

C7.8.6 Triplet Nitrosyl Anion

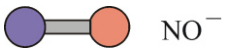

Figure C56. Ball-and-stick presentation of computed minimum structure of the triplet nitrosyl anion.

B3LYP/6-31+G//B3LYP/6-31+G****

```
Standard orientation:
---------------------------------------------------------------------
 Center     Atomic     Atomic              Coordinates (Angstroms)
 Number     Number      Type              X           Y           Z
---------------------------------------------------------------------
   1          7             0        0.000000    0.000000   -0.677745
   2          8             0        0.000000    0.000000    0.593027
---------------------------------------------------------------------

Zero-point correction=                          0.003246 (Hartree/Particle)
Thermal correction to Energy=                   0.005614
Thermal correction to Enthalpy=                 0.006558
Thermal correction to Gibbs Free Energy=       -0.017317
Sum of electronic and zero-point Energies=           -129.907578
Sum of electronic and thermal Energies=              -129.905211
Sum of electronic and thermal Enthalpies=            -129.904267
Sum of electronic and thermal Free Energies=         -129.928141


Version=AM64L-G03RevE.01\State=3-SG\HF=-129.9108243\S2=2.011964\
S2-1=0.\S2A=2.000075\RMSD=7.451e-09\RMSF=6.277e-07\
Dipole=0.,0.,0.3882382\PG=C*V [C*(N1O1)]\NImag=0\\\@
```

C7.8.7 2-Methyl-2-nitrosopropane

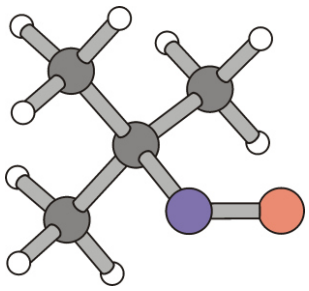

Figure C57. Computed minimum structure of 2-methyl-2-nitrosopropane.

B3LYP/6-31+G//B3LYP/6-31+G****

Standard orientation:

Center Number	Atomic Number	Atomic Type	Coordinates (Angstroms) X	Y	Z
1	7	0	0.940092	0.238967	-0.772537
2	8	0	1.980210	0.056176	-0.183571
3	6	0	-0.317547	-0.012145	0.038453
4	6	0	-1.068914	1.331605	-0.014365
5	6	0	-1.074170	-1.083568	-0.768906
6	6	0	-0.030486	-0.459518	1.469001
7	1	0	-2.060850	1.214863	0.434150
8	1	0	-0.529985	2.105959	0.541118
9	1	0	-1.193000	1.670210	-1.047399
10	1	0	-2.066073	-1.238964	-0.332294
11	1	0	-1.198265	-0.773323	-1.810795
12	1	0	-0.539070	-2.038628	-0.753803
13	1	0	-0.974693	-0.622679	1.998343
14	1	0	0.541217	-1.391888	1.487704
15	1	0	0.545096	0.294026	2.014201

```
Zero-point correction=                          0.127849 (Hartree/Particle)
Thermal correction to Energy=                   0.135386
Thermal correction to Enthalpy=                 0.136330
Thermal correction to Gibbs Free Energy=        0.097065
Sum of electronic and zero-point Energies=           -287.642141
Sum of electronic and thermal Energies=              -287.634604
Sum of electronic and thermal Enthalpies=            -287.633660
Sum of electronic and thermal Free Energies=         -287.672925

Version=AM64L-G03RevE.01\State=1-A\HF=-287.7699899\RMSD=8.486e-09\
RMSF=1.893e-05\Dipole=0.8433761,-0.0004917,-0.6875585\PG=C01
[X(C4H9N1O1)]\NImag=0\\\@
```

Table C15. Survey of computed and experimentally determined nitrogen-oxygen bond lengths and associated bond orders (BO) from molecular orbital theory

compound	BO [a]	$d_{N,O}$ / Å (*calc.*) [b]	$d_{N,O}$ / Å (*exptl.*)
H_2N–OH	1	1.447	1.453(3) [c]
$(H_3C)_2N$–O*t*Bu	1	1.448	– [d]
*t*BuN=O	2	1.209	– [d]
NO^- (singlet)	2	1.255	– [d]
NO^- (triplet)	2	1.271	1.271 [e]
•NO	2.5	1.158	1.151 [e]
NO^+	3	1.073	1.063 [e]

[a] BO = bond order from MO-theory: BO = $[n(e^-)^{bonding} - n(e^-)^{antibonding}]/2$; $n(e^-)$ = number of electrons; bonding = in bonding orbitals; antibonding = in antibonding orbitals. [b] B3LYP/6-31+G**. [c] X-ray diffraction.[9] [d] Not available. [e] Microwave spectroscopy.[10]

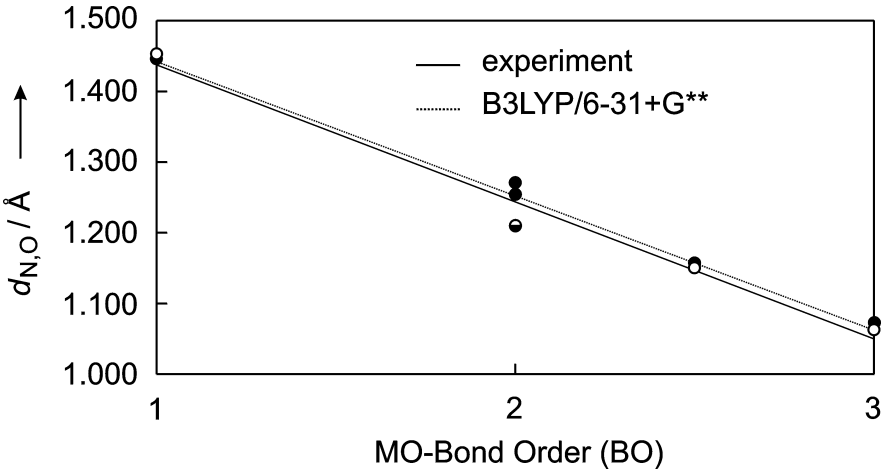

Figure C58. Bond order/distance-correlation for bonding between nitrogen and oxygen [correlation analysis for computed data: $d_{N,O}$ = 1.6316 – 0.1897 × BO (R2 = 0.9900), based on N,O-distances $d_{N,O}^{calc}$ in Table C15; correlation analysis for experimental data: $d_{N,O}$ = 1.6490 – 0.1966 × BO (correlation coefficient R2 = 0.9996), based on N,O-distances $d_{N,O}^{exp}$ in Table C15].

C7.9 Supplementary Structural Data of O-Alkyl Thiohydroxamates

C7.9.1 3-(*tert*-Butoxy)-4-methyl-5-(4-nitrophenyl)-thiazole-2(3*H*)thione (3b)

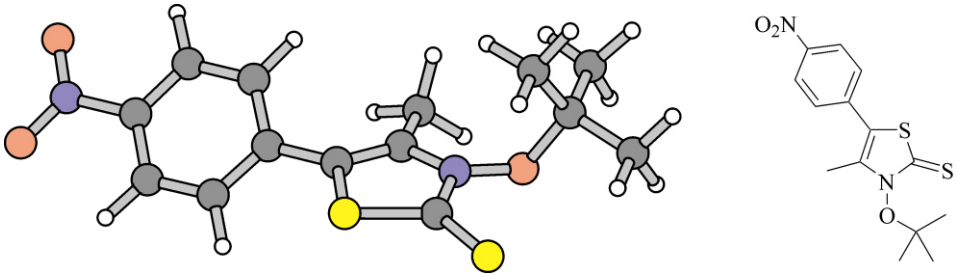

Figure C59. Computed minimum structure of 3-(*tert*-butoxy)thiazolethione **3b**.

(*i*) B3LYP/6-31+G**//B3LYP/6-31+G**

Standard orientation:

Center Number	Atomic Number	Atomic Type	Coordinates (Angstroms) X	Y	Z
1	6	0	-2.218759	-1.011942	0.436904
2	6	0	-1.664403	0.197145	-0.032737
3	6	0	-2.543618	1.222176	-0.441419
4	6	0	-3.921881	1.044295	-0.404552
5	6	0	-4.432900	-0.173130	0.047427
6	6	0	-3.595679	-1.205452	0.471122
7	6	0	-0.213244	0.404959	-0.072567
8	16	0	0.483303	1.980462	0.338952
9	6	0	2.126035	1.449975	-0.016528
10	7	0	2.045996	0.106331	-0.324530
11	6	0	0.771541	-0.469469	-0.428300
12	16	0	3.463345	2.424862	0.045752
13	8	0	3.135085	-0.559816	-0.830844
14	6	0	4.060228	-1.256571	0.146576
15	6	0	5.443676	-0.699495	-0.189543
16	6	0	0.630344	-1.853829	-0.977806
17	7	0	-5.888349	-0.370742	0.085599
18	8	0	-6.309752	-1.461279	0.478123
19	6	0	3.668031	-0.990738	1.596047
20	6	0	3.976232	-2.745371	-0.200253
21	8	0	-6.604652	0.564219	-0.278323
22	1	0	0.827420	-2.621313	-0.221302
23	1	0	1.339911	-2.005376	-1.794360
24	1	0	-0.382916	-2.002059	-1.354095
25	1	0	-2.140590	2.159933	-0.810229
26	1	0	-4.599914	1.824969	-0.726596

Standard orientation of **3b** (continued):

Center Number	Atomic Number	Atomic Type	Coordinates (Angstroms) X	Y	Z
27	1	0	-4.026563	-2.130314	0.834391
28	1	0	-1.566845	-1.795491	0.806082
29	1	0	2.660884	-1.354096	1.822545
30	1	0	3.731552	0.071103	1.843053
31	1	0	4.366295	-1.531277	2.242720
32	1	0	4.758465	-3.293026	0.335546
33	1	0	4.129652	-2.898694	-1.272591
34	1	0	3.011828	-3.176286	0.080939
35	1	0	5.484418	0.372218	0.010241
36	1	0	5.672933	-0.863918	-1.246796
37	1	0	6.204497	-1.210991	0.409830

Zero-point correction= 0.284019 (Hartree/Particle)
Thermal correction to Energy= 0.304914
Thermal correction to Enthalpy= 0.305858
Thermal correction to Gibbs Free Energy= 0.233140
Sum of electronic and zero-point Energies= -1674.306623
Sum of electronic and thermal Energies= -1674.285729
Sum of electronic and thermal Enthalpies= -1674.284785
Sum of electronic and thermal Free Energies= -1674.357503

Version=AM64L-G03RevE.01\State=1-A\HF=-1674.5906424\ RMSD=4.789e-09\
RMSF=1.588e-06\Dipole=-2.0291962,-0.5279989,-0.939038\PG=C01
[X(C14H16N2O3S2)]\NImag=0\\\@

(*ii*) BHandHLYP/6-31+G**//BHandHLYP/6-31+G**

Standard orientation:

Center Number	Atomic Number	Atomic Type	Coordinates (Angstroms) X	Y	Z
1	16	0	0.491392	1.964460	0.353457
2	6	0	2.110502	1.432758	-0.005780
3	16	0	3.441667	2.400694	0.064858
4	7	0	2.033032	0.111983	-0.322977
5	6	0	0.764337	-0.455763	-0.426849
6	6	0	0.620155	-1.834528	-0.968331
7	1	0	0.833425	-2.589844	-0.216533
8	1	0	1.309281	-1.983055	-1.791815
9	1	0	-0.392269	-1.985306	-1.321398
10	6	0	-0.204034	0.408810	-0.066754
11	6	0	-1.652983	0.201166	-0.028301
12	6	0	-2.519667	1.198075	-0.486095
13	1	0	-2.117430	2.113111	-0.887129
14	6	0	-3.889093	1.019441	-0.452264
15	1	0	-4.561618	1.777646	-0.809770
16	6	0	-4.393601	-0.169474	0.045492
17	6	0	-3.566527	-1.173586	0.516867
18	1	0	-3.994713	-2.076793	0.911732
19	6	0	-2.198761	-0.978632	0.484785
20	1	0	-1.549790	-1.738396	0.883993
21	8	0	3.104012	-0.547931	-0.823286
22	6	0	4.008248	-1.247677	0.124905
23	6	0	3.609606	-1.018424	1.569271
24	1	0	2.609739	-1.387949	1.779401
25	1	0	3.666615	0.030055	1.838760
26	1	0	4.301833	-1.566675	2.201814
27	6	0	3.936039	-2.720552	-0.246999
28	1	0	4.709277	-3.270316	0.282561
29	1	0	4.099400	-2.849952	-1.312842
30	1	0	2.977659	-3.157400	0.012929
31	6	0	5.389022	-0.692771	-0.178549
32	1	0	5.432849	0.365443	0.045270
33	1	0	5.625797	-0.831806	-1.229429
34	1	0	6.134515	-1.219061	0.412211
35	7	0	-5.836599	-0.367535	0.080681
36	8	0	-6.538152	0.532276	-0.325852
37	8	0	-6.249360	-1.421389	0.513501

```
Zero-point correction=                          0.295561 (Hartree/Particle)
Thermal correction to Energy=                   0.315704
Thermal correction to Enthalpy=                 0.316648
Thermal correction to Gibbs Free Energy=        0.245498
Sum of electronic and zero-point Energies=          -1673.722938
Sum of electronic and thermal Energies=             -1673.702796
Sum of electronic and thermal Enthalpies=           -1673.701852
Sum of electronic and thermal Free Energies=        -1673.773002

Version=AM64L-G03RevE.01\State=1-A\HF=-1674.0184995\RMSD=6.940e-09\
RMSF=2.462e-07\Dipole=-1.2716226,0.6644919,1.6625505\PG=C01
[X(C14H16N2O3S2)]\NImag=0\\\@
```

Table C16. Computed parameters of 3-(*tert*-butoxy)-4-methylthiazole-2(3*H*)thione (**2b**)

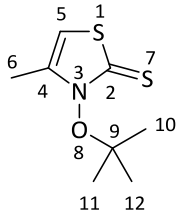

Parameter	B3LYP [a]	BHandHLYP [a]	MP2 [a]
N3,C2 / Å	1.380	1.360	1.379
C2,S1 / Å	1.768	1.745	1.749
S1,C5 / Å	1.751	1.739	1.730
C4,C5 / Å	1.351	1.337	1.358
C4,N3 / Å	1.406	1.396	1.395
N3,O8 / Å	1.375	1.355	1.378
C2,S7 / Å	1.660	1.651	1.648
C4,N3,C2 / deg	117.6	117.3	118.0
N3,C2,S1 / deg	106.6	107.1	106.3
C2,S1,C5 / deg	92.4	92.3	92.9
S1,C5,C4 / deg	111.8	111.6	112.0
C5,C4,N3 / deg	111.4	111.5	110.5
N3,O8,C9 / deg	118.1	118.5	115.4
O8,C9,C10[syn b] / deg	112.1	112.1	111.6
O8,C9,C11[ac c] / deg	105.2	105.4	105.4
O8,C9,C12 [ac c] / deg	104.6	105.2	104.8
C2,N3,O8,C9 / deg	91.3	91.3	93.2

[a] in combination with the 6-31+G** split valence double zeta-basis set. [b] *syn* = synperiplanar.

[c] *ac* = anticline.

Table C17. Computed parameters of 3-methoxy-4-methylthiazole-2(3*H*)thione (**2d**)

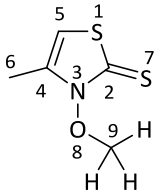

Parameter	B3LYP [a]	BHandHLYP [a]	MP2 [a]
N3,C2 / Å	1.375	1.357	1.376
C2,S1 / Å	1.772	1.748	1.752
S1,C5 / Å	1.755	1.743	1.733
C4,C5 / Å	1.351	1.338	1.358
C4,N3 / Å	1.400	1.391	1.391
N3,O8 / Å	1.380	1.358	1.383
C2,S7 / Å	1.659	1.656	1.647
C4,N3,C2 / deg	118.8	118.5	118.9
N3,C2,S1 / deg	105.9	106.5	105.7
C2,S1,C5 / deg	92.5	92.4	93.0
S1,C5,C4 / deg	111.8	111.6	112.0
C5,C4,N3 / deg	110.9	111.0	110.1
N3,O8,C9 / deg	111.7	112.1	109.5
O8,C9,H[sc b] / deg	110.5	110.4	110.1
O8,C9,H[sc b] / deg	110.3	110.3	109.8
O8,C9,H[anti c] / deg	104.1	104.6	104.1
C2,N3,O8,C9 / deg	83.4	84.1	85.6

[a] in combination with the 6-31+G** split valence double zeta-basis set. [b] *sc* = syncline. [c] *anti* = antiperiplanar.

Table C18. Computed and experimental parameters of 3-(*tert*-butoxy)-4-methyl-5-(4-nitrophenyl)-thiazole-2(3*H*)thione (**3b**) [a]

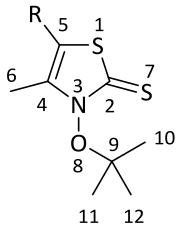

Parameter	B3LYP [b]	BHandHLYP [b]	MP2 [b]	X-ray [c]
N3,C2 / Å	1.381	1.361	1.379	1.363(2)
C2,S1 / Å	1.762	1.742	1.751	1.728(2)
S1,C5 / Å	1.771	1.755	1.744	1.743(2)
C4,C5 / Å	1.364	1.347	1.368	1.355(2)
C4,N3 / Å	1.402	1.394	1.392	1.395(2)
N3,O8 / Å	1.373	1.354	1.375	1.378(2)
C2,S7 / Å	1.656	1.647	1.645	1.656(2)
C4,N3,C2 / deg	118.0	117.8	118.3	117.9(1)
N3,C2,S1 / deg	106.5	106.9	106.1	107.0(1)
C2,S1,C5 / deg	93.0	92.8	93.2	93.4(1)
S1,C5,C4 / deg	110.3	110.4	111.0	110.3(1)
C5,C4,N3 / deg	111.9	111.9	110.9	111.4(1)
N3,O8,C9 / deg	118.0	118.4	115.1	116.8(1)
O8,C9,C10[syn d] / deg	112.1	112.1	111.6	111.6(2)
O8,C9,C11[ac e] / deg	105.5	105.7	105.5	105.8(2)
O8,C9,C12[ac e] / deg	104.1	104.7	104.5	103.0(2)
C2,N3,O8,C9 / deg	92.2	91.3	94.6	93.6(2)

[a] R = *p*$C_6H_4(NO_2)$. [b] In combination with the 6-31+G** split valence double zeta-basis set. [c] Crystal structure determined at 160 K. [d] *syn* = synperiplanar. [e] *ac* = anticline.

Table C19. Computed parameters of 1-(*tert*-butoxy)-pyridine-2(1*H*)thione (**4b**)

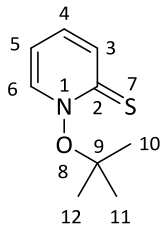

Parameter	B3LYP [a]	BHandHLYP [a]	MP2 [a]
N1,C2 / Å	1.401	1.378	1.397
C2,C3 / Å	1.439	1.432	1.436
C3,C4 / Å	1.371	1.358	1.374
C4,C5 / Å	1.421	1.415	1.414
C5,C6 / Å	1.367	1.353	1.370
C6,N1 / Å	1.368	1.358	1.365
N1,O8 / Å	1.380	1.359	1.381
C2,S7 / Å	1.678	1.667	1.661
C6,N1,C2 / deg	124.7	124.8	125.9
N1,C2,C3 / deg	112.8	113.2	111.8
C2,C3,C4 / deg	123.2	122.9	123.7
C3,C4,C5 / deg	120.1	120.2	120.0
C4,C5,C6 / deg	117.9	117.7	118.0
C5,C6,N1 / deg	121.0	121.1	120.2
N1,O8,C9 / deg	117.2	117.5	114.3
O8,C9,C10[syn b] / deg	112.4	112.6	112.2
O8,C9,C11[ac c] / deg	107.5	107.6	107.5
O8,C9,C12[ac c] / deg	101.8	102.3	101.9
C2,N1,O8,C9 / deg	99.9	99.7	98.9

[a] in combination with the 6-31+G** split valence double zeta-basis set. [b] *syn* = synperiplanar.

[c] *ac* = anticline.

Table C20. Computed parameters of 1-methoxy-pyridine-2(1*H*)thione (**4d**)

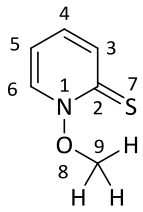

Parameter	B3LYP [a]	BHandHLYP [a]	MP2 [a]
N1,C2 / Å	1.398	1.376	1.394
C2,C3 / Å	1.439	1.432	1.436
C3,C4 / Å	1.372	1.358	1.374
C4,C5 / Å	1.421	1.415	1.415
C5,C6 / Å	1.367	1.353	1.369
C6,N1 / Å	1.366	1.357	1.364
N1,O8 / Å	1.387	1.364	1.390
C2,S7 / Å	1.678	1.667	1.661
C6,N1,C2 / deg	125.6	125.6	126.6
N1,C2,C3 / deg	112.6	112.9	111.5
C2,C3,C4 / deg	123.1	122.8	123.6
C3,C4,C5 / deg	120.4	120.4	120.2
C4,C5,C6 / deg	117.8	117.6	118.0
C5,C6,N1 / deg	120.6	120.8	119.9
N1,O8,C9 / deg	111.7	112.0	109.3
O8,C9,H[sc b] / deg	110.4	110.4	109.9
O8,C9,H[sc b] / deg	110.3	110.2	109.8
O8,C9,H[anti c] / deg	104.0	104.5	104.1
C2,N1,O8,C9 / deg	83.9	85.1	83.9

[a] in combination with the 6-31+G** split valence double zeta-basis set. [b] *sc* = syncline. [c] *anti* = antiperiplanar.

C8 Vibrational Analysis

C8.1 General remarks

For assigning N,O- and C=S-vibrations, harmonic frequencies of isotopomeric compounds were computed starting from atomic coordinates of B3LYP/6-31+G**- and B3LYP/TZVP-energy minimized structures.[5] Isotopes considered are the following pairs: C^{12}/C^{13}, N^{14}/N^{15}, O^{16}/O^{18} and S^{32}/S^{34}. Vibrational modes were characterized from animations using the program Molden.[11]

C8.2 Hydroxylamine

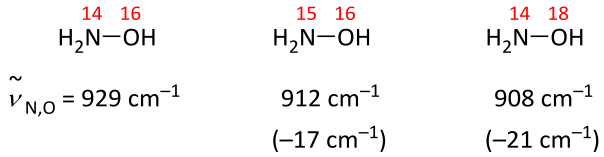

Figure C60. Calculated (B3LYP/6-31+G**) wavenumbers for the nitrogen-oxygen stretching mode of hydroxylamine.

C8.3 Thioformaldehyde

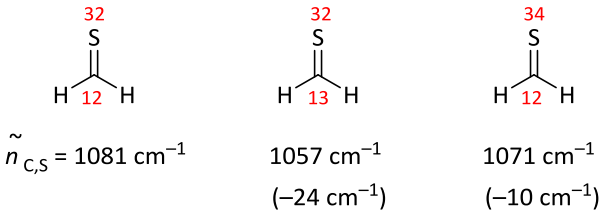

Figure C61. Calculated (B3LYP/6-31+G**) wavenumbers for the nitrogen-oxygen stretching mode of hydroxylamine.

C8.4 Methanethiocarboxamide

Table C21. Computed fundamental vibrations of thioformamide

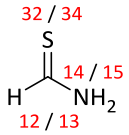

isotopes / wavenumbers in cm^{-1} [shift in cm^{-1}]			
C^{12} / S^{32} / N^{14}	C^{13} / S^{32} / N^{14}	C^{12} / S^{34} / N^{14}	C^{12} / S^{32} / N^{15}
384	384 [0]	384 [0]	382 [–2]
435	431 [–4]	432 [–3]	431 [–4]
618	614 [–4]	618 [0]	617 [–1]
879	869 [–10]	872 [–7]	875 [–4]
956	947 [–9]	956 [0]	956 [0]
1143	1136 [–9]	1142 [–1]	1140 [–3]
1316	1298 [–18]	1316 [0]	1304 [–8]
1460	1438 [–22]	1460 [0]	1457 [–3]
1645	1642 [–3]	1645 [0]	1635 [–10]
3110	3100 [–10]	3110 [0]	3110 [0]
3565	3565 [0]	3565 [0]	3561 [–4]
3706	3706 [0]	3706 [0]	3695 [–11]

C8.5 Methanethiohydroxamic acid

Table C22. Computed fundamental vibrations of N-hydroxythioformamide

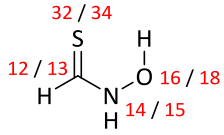

isotopes / wavenumbers in cm^{-1} [shift in cm^{-1}]				
N^{14} / O^{16} / C^{12} / S^{32}	N^{14} / O^{16} / C^{13} / S^{32}	N^{14} / O^{18} / C^{12} / S^{32}	N^{14} / O^{16} / C^{12} / S^{34}	N^{15} / O^{16} / C^{12} / S^{32}
243	243 [0]	243 [0]	243 [0]	240 [–3]
252	251 [–1]	245 [–7]	249 [–3]	252 [0]
440	438 [–2]	437 [–3]	440 [0]	439 [–1]
492	489 [–3]	492 [0]	491 [–1]	491 [–1]
687	681 [–6]	683 [–4]	682 [–5]	677 [–10]
879	871 [–8]	879 [0]	879 [0]	879 [0]
917	897 [–10]	908 [–9]	912 [–5]	916 [–1]
1024	1019 [–5]	1007 [–14]	1023 [–1]	1015 [–9]
1271	1270 [–1]	1266 [–5]	1271 [0]	1268 [–3]
1418	1413 [–5]	1417 [–1]	1418 [0]	1407 [–11]
1457	1433 [–24]	1456 [–1]	1457 [0]	1450 [–7]
1590	1582 [–2]	1585 [–5]	1590 [0]	1577 [–13]
3144	3134 [–10]	3144 [0]	3144 [0]	3144 [0]
3382	3382 [0]	3371 [–11]	3382 [0]	3381 [–1]
3664	3664 [0]	3664 [0]	3664 [0]	3655 [–9]

C8.5 3-(*tert*-Butyloxy)-4-methylthiazole-2(*H*)thione

Table C23. Computed fundamental vibrations of 3-*tert*-butyloxy-4-methylthiazole-2(*H*)thione

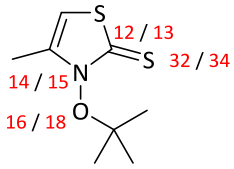

isotopes / wavenumbers in cm^{-1} [shift in cm^{-1}]				
N^{14} / O^{16} / C^{12} / S^{32}	N^{14} / O^{16} / C^{13} / S^{32}	N^{14} / O^{18} / C^{12} / S^{32}	N^{14} / O^{16} / C^{12} / S^{34}	N^{15} / O^{16} / C^{12} / S^{32}
664	661 [–3]	651 [–13]	664 [0]	659 [–5]
714	714 [0]	710 [–4]	714 [0]	714 [0]
727	725 [–2]	715 [–12]	727 [0]	726 [–1]
814	813 [–1]	811 [–3]	814 [0]	814 [0]
838	838 [0]	837 [–1]	838 [0]	838 [0]
894	885 [–9]	880 [–14]	894 [0]	890 [–4]
923	923 [0]	923 [0]	923 [0]	923 [0]
935	935 [0]	934 [–1]	935 [0]	934 [–1]
971	957 [–17]	971 [0]	971 [0]	969 [–2]
974	971 [0]	972 [–2]	974 [0]	971 [–3]
1031	1028 [–3]	1030 [–1]	1030 [–1]	1028 [–4]
1048	1048 [0]	1047 [–1]	1048 [0]	1048 [0]
1056	1056 [0]	1056 [0]	1056 [0]	1056 [0]
1065	1065 [0]	1065 [0]	1065 [0]	1065 [0]
1161	1153 [–8]	1159 [–2]	1160 [–1]	1155 [–6]
1183	1183 [0]	1181 [–2]	1183 [0]	179 [–4]
1216	1213 [–3]	1211 [–5]	1216 [0]	1207 [–9]
1264	1263 [–1]	1264 [0]	1264 [0]	1263 [–1]
1291	1286 [–5]	1291 [0]	1291 [0]	1290 [–1]
1310	1294 [–16]	1308 [–2]	1310 [0]	1295 [–5]
1352	1350 [–2]	1351 [–1]	1352 [0]	1339 [–13]
1407	1407 [0]	1407 [0]	1407 [0]	1407 [0]
1411	1411 [0]	1411 [0]	1411 [0]	1411 [0]
1423	1423 [0]	1423 [0]	1423 [0]	1423 [0]
1435	1435 [0]	1435 [0]	1435 [0]	1435 [0]
1474	1474 [0]	1474 [0]	1474 [0]	1474 [0]
1477	1477 [0]	1477 [0]	1477 [0]	1477 [0]
1486	1486 [0]	1486 [0]	1486 [0]	1486 [0]
1493	1493 [0]	1493 [0]	1493 [0]	1492 [–1]
1497	1497 [0]	1497 [0]	1497 [0]	1497 [0]
1504	1504 [0]	1504 [0]	1504 [0]	1504 [0]
1510	1510 [0]	1510 [0]	1510 [0]	1510 [0]
1527	1527 [0]	1527 [0]	1527 [0]	1527 [0]
1651	1651 [0]	1651 [0]	1651 [0]	1650 [–1]

C8.6 3-(*tert*-Butoxy)-5-(4-methoxyphenyl)-4-methylthiazole-2(3*H*)thione (1b)

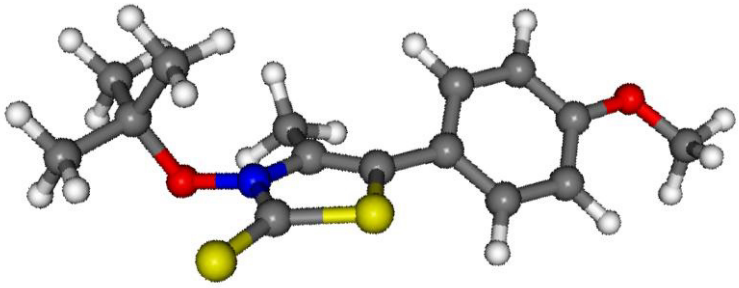

Figure C61. DFT-D3/B3LYP/TZVP-energy-minimized structure of *tert*-butyl ester **1b**.

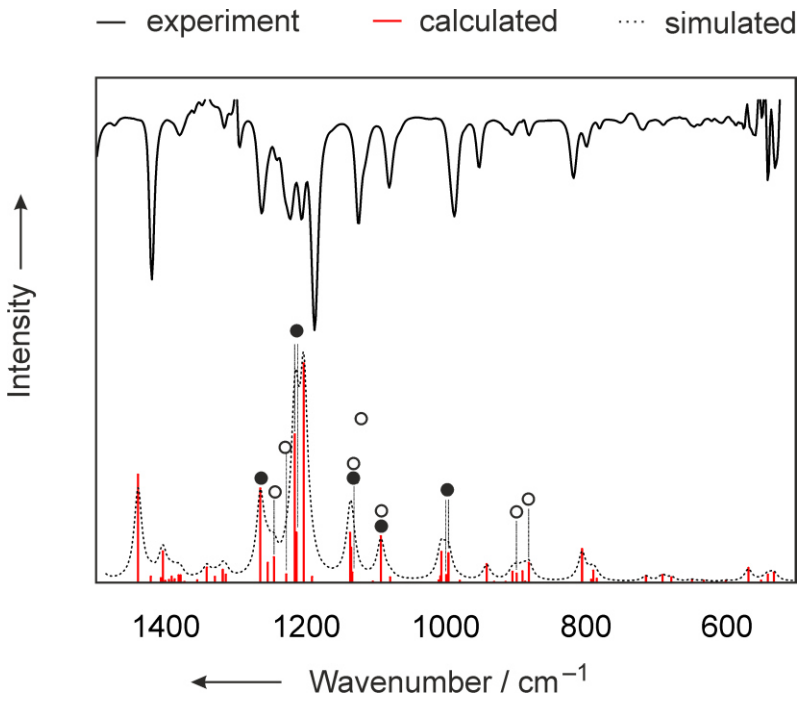

Figure C62. Experimental infrared spectrum of 3-(*tert*-butoxy)-5-(4-methoxyphenyl)-4-methylthiazolethione **1b** (top; 20 °C in CH_3CN) and computed harmonic frequencies (DFT-D3/B3LYP/TZVP; bottom). Computed ground state structure from which the frequencies are calculated shown in the middle (● = contribution from C=S-stretching vibration; ○ contribution from N,O-elongation in the vibrational mode).

Due to the complexity of the molecule and the generally strong overlap of vibrations in the fingerprint region all of the vibrations with contributions from a C=S elongation (1040, 1043, 1147, 1192, 1280, 1283 and 1338 cm^{-1} computed, scaling factor 0.99) have also

contributions of bending, torsional, skeletal and deformation modes (Figure C62). Vibrations with contribution from a N,O-elongation are calculated at 921, 932, 1147, 1192, 1297 and 1316 cm^{-1} (scaling factor 0.99).

C8.7 3-(*tert*-Butoxy)-5-(4-nitrophenyl)-4-methylthiazole-2(3*H*)thione (3b)

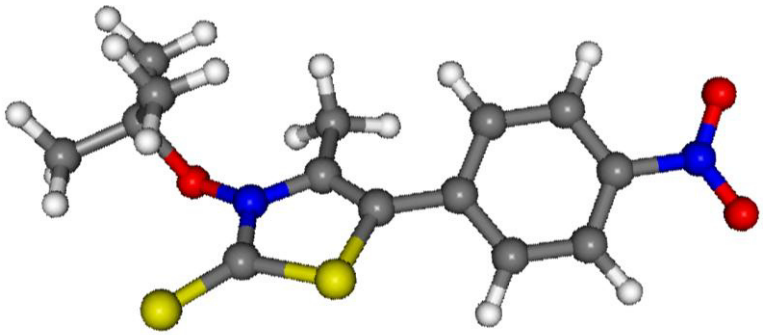

Figure C63. DFT-D3/B3LYP/TZVP-energy-minimized structure of *tert*-butyl ester **3b**.

Due to the complexity of the molecule and the generally strong overlap of vibrations in the fingerprint region all of the vibrations with contributions from a C=S elongation (1039, 1043, 1147, 1191, 1331 and 1346 cm^{-1} computed, scaling factor 0.99) have also contributions of bendng, torsional, skeletal and deformation modes (Figure C64). Vibrations with contribution from a N,O-elongation are calculated at 914, 935, 1147, 1191 and 1304 cm^{-1} (scaling factor 0.99).

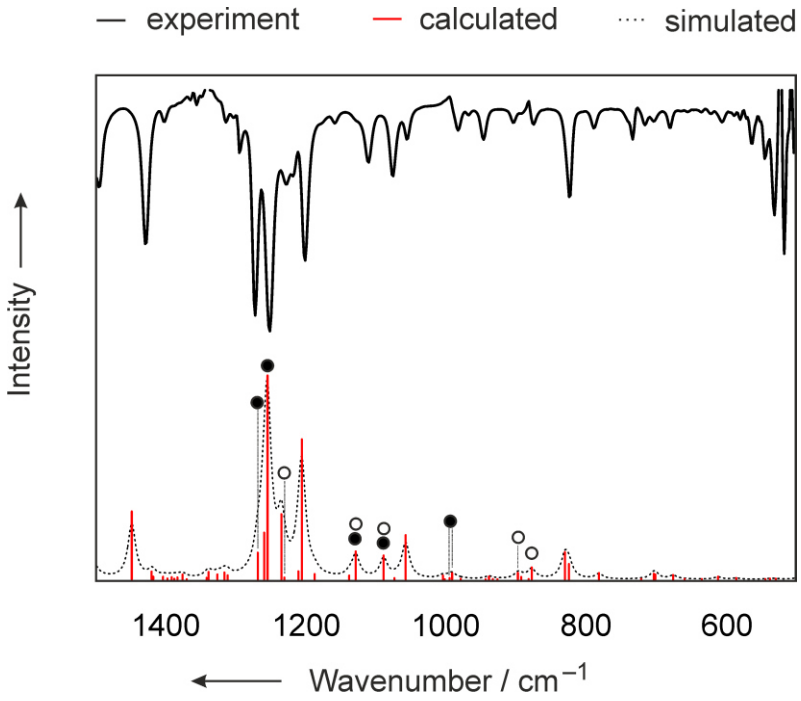

Figure C64. Experimental infrared spectrum of 3-(*tert*-butoxy)-5-(4-nitrophenyl)-4-methyl-thiazolethione **3b** (top; 20 °C in CH_3CN) and computed harmonic frequencies (DFT-D3/B3LYP/TZVP; bottom). Computed ground state structure from which the frequencies are calculated shown in the middle (● = contribution from C=S-stretching vibration; ○ contribution from N,O-elongation in the vibrational mode).

C9 References

[1] D. D. Perrin, W. L. F. Armarego, D.R. Perin, *Purification of Laboratory Chemicals* 2nd Ed., Pergamon Press, Oxford, 1980.

[2] D. H. R. Barton, D. Crich, G. Kretzschmar, *J. Chem. Soc., Perkin Trans. I*, 1986, 39–53.

[3] J. Hartung, T. Gottwald, K. Spehar, *Synlett*, 2003, **2**, 227–229.

[4] J. Hartung, T. Gottwald, K. Špehar, *Synthesis*, 2002, **11**, 1469−1498.

[5] Gaussian 03, Revision E.01, M. J. Frisch, G.W. Trucks, H.B. Schlegel, G.E. Scuseria, M.A. Robb, J.R. Cheeseman, J.A. Montgomery, Jr., T. Vreven, K.N. Kudin, J.C. Burant, J.M. Millam, S.S. Iyengar, J. Tomasi, V. Barone, B. Mennucci, M. Cossi, G. Scalmani, N. Rega, G.A. Petersson, H. Nakatsuji, M. Hada, M. Ehara, K. Toyota, R. Fukuda, J. Hasegawa, M. Ishida, T. Nakajima, Y. Honda, O. Kitao, H. Nakai, M. Klene, X. Li, J.E. Knox, H.P. Hratchian, J.B. Cross, V. Bakken, C. Adamo, J. Jaramillo, R. Gomperts, R. E. Stratmann, O. Yazyev, A. J. Austin, R. Cammi, C. Pomelli, J.W. Ochterski, P.Y. Ayala, K. Morokuma, G.A. Voth, P. Salvador, J.J. Dannenberg, V. G. Zakrzewski, S. Dapprich, A.D. Daniels, M.C. Strain, O. Farkas, D.K. Malick, A.D. Rabuck, K. Raghavachari, J.B. Foresman, J.V. Ortiz, Q. Cui, A.G. Baboul, S. Clifford, J. Cioslowski, B.B. Stefanov, G. Liu, A. Liashenko, P. Piskorz, I. Komaromi, R.L. Martin, D.J. Fox, T. Keith, M.A. Al-Laham, C.Y. Peng, A. Nanayakkara, M. Challacombe, P.M.W. Gill, B. Johnson, W. Chen, M.W. Wong, C. Gonzalez, J.A. Pople, Gaussian, Inc., Wallingford CT, 2004.

[6] NBO 5.9, E.D. Glendening, J.K. Badenhoop, A.E. Reed, J.E. Carpenter, J.A. Bohmann, C.M. Morales, F. Weinhold, Theoretical Chemistry Institute, University of Wisconsin, Madison, WI, 2009, http://www.chem.wisc.edu/~nbo5.

[7] N. M O'Boyle, M. Banck, C.A. James, C. Morley, T. Vandermeersch, G.R. Hutchison, *J. Cheminform.*, 2011, **3**, 33.

[8] HyperChem Professional 4.5 in combination with ChemPlus 1.6, Hypercube, Inc., 419 Phillip St., Waterloo, Ontario, Canada, 1995.

[9] K. L. Shi, R.Q-Wang, T. C. W. Mak, *J. Mol. Struc.*, 1987, **160**, 109−116.

[10] K. P. Huber, G. Herzberg, in Molecular Spectra and Molecular Structure IV. Constants of Diatomic Molecules, Van Nostrand, New York, N.Y. 1979, pp. 466–484.

[11] G. Schaftenaar, J.H. Noordik, *Comput.-Aided Mol. Des*., 2000, **14**, 123–134.

Anhang D

Posterpräsentationen

TECHNISCHE UNIVERSITÄT KAISERSLAUTERN

Tertiary Alkoxyl Radicals from 3-Alkoxythiazole-2(3*H*)-thiones

Christine Schur[a], Nina Becker[a], Uwe Bergsträßer[a], Thomas Gottwald[b], Jens Hartung[a,*]

[a] Fachbereich Chemie, Organische Chemie, Technische Universität Kaiserslautern, Erwin-Schrödinger-Straße, D-67663 Kaiserslautern, Germany
[b] Institut für Organische Chemie, Universität Würzburg, Am Hubland, 97074 Würzburg, Germany

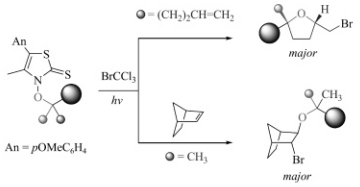

Abstract: *O*-Alkyl thiohydroxamates are useful compounds to serve as alkoxyl radical precursors in organic chemistry. Synthesis of primary and secondary derivatives thereof are already established[1], while preparation of the corresponding *tert*-alkoxyl thiohydroxamates remained difficult. Using the isourea-method preparation of 3-(*tert*-alkoxy)-thiazole-2(3*H*)-thiones was verified from 3-hydroxy-5-(*p*-methoxyphenyl)-4-methylthiazole-2(3*H*)-thione (MAnTTOH), *tert*-alcohols, diisopropylcarbodiimide (DIC), and copper(I)-chloride under nonoxidative, pH-neutral conditions. Radical precursor formation was feasible in up to 64 % yield. On activation, the molecules liberated *tert*-alkoxyl radicals, which were investigated in mechanistic studies to determine rate constances of (a) radical substitution, (b) intramolecular and (c) intermolecular addition. For the first time 2,2,5-substituted tetrahydrofurans and 2-bromo-3-alkoxynorbornanes were isolated via an alkoxyl radical route leading to unexpected and synthetically useful selectivities as outlined in this contribution.[2]

Background

tert-Alkoxyl radicals undergo fast uni- and bimolecular reactions to leave diagnostic product mixtures. Chemical changes thereby follow distinct patterns of homolytic substitution, *β*-C-C-homolysis, and *π*-bond addition, to mention the most important elementary reactions.[3] This combination of reactivity and selectivity explains the significance that *tert*-alkoxyl radicals have gained for elucidating reaction mechanisms in physical organic chemistry[4], atmospheric science[5], biochemistry[6] and macromolecular chemistry[7].

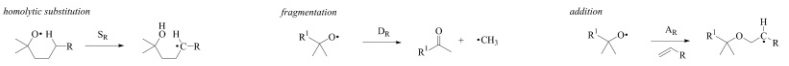

nomenclature: S = substitution, D = dissociative step, A = associative step, R = radical-based transformation

Results

Synthesis of radical precursors

Table 1: Alkylation products formed from of 3-hydroxy-5-(*p*-methoxyphenyl)-4-methylthiazole-2(3*H*)-thione.

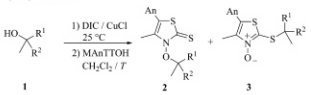

1–3	R^1	R^2	*T* / °C	**2** / %	**3** / %
a	CH_3	CH_3	24	58–64 [a]	25 [c]
b	C_2H_5	CH_3	0	45–47 [b]	33 [c]
c	CH_3	$(CH_2)_3C_6H_5$	0	44	11 [c]
d	CH_3	C_6H_5	–30	15	38
e	CH_3	*p*-ClC_6H_4	–30	13	33
f	$(CH_2)_2CH=CH_2$	C_6H_5	–30	18	27 [c]

[a] mean value from five experiments, [b] mean value from three experiments, [c] determined via ^{1}H and ^{13}C NMR; An = *p*$OMeC_6H_4$

Radical reactions

(a) Substitution

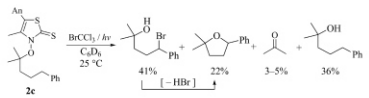

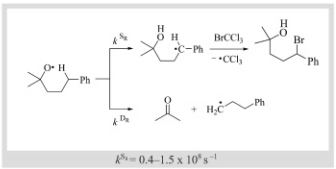

Scheme 1: Products formed by photochemical activation (350 nm) of 3-(5-phenyl-2-methylpentoxy)-thiazolethione **2c** and $BrCCl_3$ in a NMR experiment (left) and proposed scheme for mechanistic discussion of 2-methyl-5-phenyl-pent-2-oxyl radical reactivity (right).

(b) Intramolecular addition

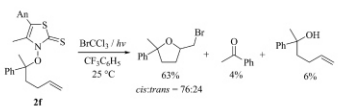

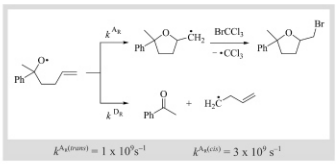

Scheme 2: Product distribution after photolysis (350 nm) of 3-(5-phenyl-2-methylpentoxy)-thiazolethione **2f** with $BrCCl_3$ (left) and reaction scheme for kinetic analysis of 2-phenylhex-5-en-2-oxyl radical reactivity (right).

(c) Intermolecular addition

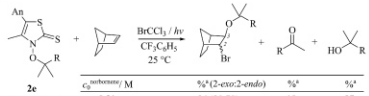

$c_0^{norbornene}$ / M	%[a] (2-*exo*:2-*endo*)	%[a]	%[a]
0.21	36 (30:70)	19	27
0.11	29 (24:76)	30	30
0.05	12 (22:78)	26	38

[a] determined via GC/MS-analysis

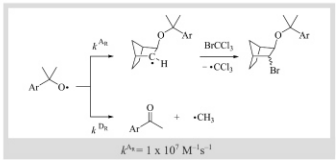

Scheme 3: Products formed by photolysis (350 nm) 3-(5-phenyl-2-methylpentoxy)-thiazolethione **2e**, norbornene and $BrCCl_3$ (left) and elementary reactions of intermolecular alkoxyl radical addition (right).

Conclusions

O-Alkyl isoureas are suprisingly selective reagents to convert thiohydroxamic acids into derived *O*-alkyl esters. The latter compounds, in this study, were successfully applied to generate *tert*-alkoxyl radicals for synthesis of 2,2,5-substituted terahydrofurans and 2-bromo-3-alkoxynorboranes.

The study also shows that chemical reactivity of *tert*-alkoxyl radicals is similar to their secondary and primary congener, in spite of higher steric encroachment in proximity of the O-radical center.

References:

[1] J. Hartung, C. Schur, I. Kempter, T. Gottwald *Tetrahedron* **2010**,1365–1374.
[2] C. Schur, N. Becker, U. Bergsträßer, T. Gottwald, J. Hartung *Tetrahedron* **2011**, *67*, 2338–2347.
[3] J. Hartung, T. Gottwald, K. Špehar *Synthesis* **2002**, 1469–1498.
[4] E. Baciocchi, M. Bietti, M. Salamone, S. Steenken *J. Org. Chem.* **2002**, *67*, 2266–2270.
[5] R. Atkinson *Atmos. Environ.* **2007**, *41*, 8468–8485.
[6] B. Halliwell, J.M.C. Gutteridge *Free Radicals in Biology and Medicine*, 3rd ed.; Oxford University: Oxford, 1999, Chapter 2, pp 36–104.
[7] P.G. Griffiths, E. Rizzardo, D.H.J. Solomon *Macromol. Sci.* **1982**, *A17*, 45–50.

TECHNISCHE UNIVERSITÄT KAISERSLAUTERN

Tertiary alkoxyl radicals from 3-alkoxythiazole-2(3*H*)-thiones

Christine Schur, Nina Becker, Uwe Bergsträßer, Jens Hartung*
Department of Organic Chemistry, Technische Universität Kaiserslautern, Erwin-Schrödinger-Straße, 67663 Kaiserslautern, Germany

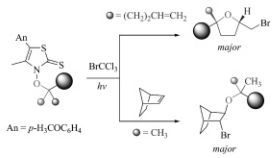

Abstract

Since generation of *tert*-alkoxyl radicals under nonoxidative, pH-neutral conditions remaind difficult, we developed in this project a practical method for synthesis of 3-(*tert*-alkoxy)-thiazole-2(3*H*)-thiones from 3-hydroxy-5-(*p*-methoxyphenyl)-4-methylthiazole-2(3*H*)-thione (MAnTTOH), selected *tert*-alcohols, diisopropylcarbodiimid (DIC) and copper (I) chloride. Radical precursor formation was feasible in up to 64 % yield. If activated, the molecules liberate *tert*-alkoxyl radicals, which were applied in mechanistic studies to determine rate constants of (a) radical substitution (1,5-H-atom shift), (b) intramolecular and (c) intermolecular addition. These reactions represent key steps in synthesis of 2,2,5-substituted tetrahydrofurans and 2-bromo-3-alkoxybicyclo[2.2.1]heptanes.

Background

tert-Alkoxy radicals undergo fast uni- and bimolecular reactions to leave diagnostic product mixtures. Chemical changes thereby follow distinct patterns of homolytic substitution, *β*-C-C-homolysis, and *π*-bond addition, to mention the most important elementary reactions.[2] This combination of reactivity and selectivity explains the significance that *tert*-alkoxyl radicals have gained for elucidating reaction mechanisms in physical organic chemistry[3], atmospheric science[4], biochemistry[5] and macromolecular chemistry.[6]

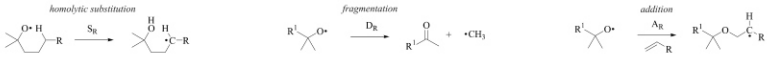

nomenclature: S = substitution, D = dissociative step, A = associative step, R = radical-based transformation

Results

Synthesis of radical precursors

Table 1 Alkylation products of 3-hydroxy-5-(*p*-methoxyphenyl)-4-methylthiazole-2(3*H*)-thione.

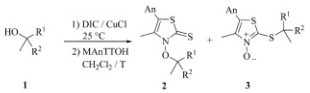

1/2/3	R^1	R^2	T / °C	**2** / %	**3** / %
a	CH_3	CH_3	24	58–64 [a]	25 [c]
b	C_2H_5	CH_3	0	45–47 [b]	33 [c]
c	CH_3	$(CH_2)_3C_6H_5$	0	44	11 [c]
d	CH_3	C_6H_5	–30	15	38
e	CH_3	*p*-ClC_6H_4	–30	13	33
f	$(CH_2)_2CH=CH_2$	C_6H_5	–30	18	27 [c]

[a] mean value from five experiments,
[b] mean value from three experiments,
[c] determined via ^1H and ^{13}C NMR;
An = *p*$OMeC_6H_4$

Radical reactions

(a) Substitution

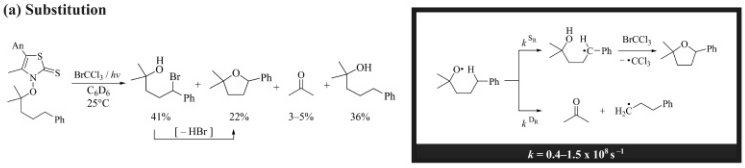

Scheme 1 Products formed from photochemical activation of 3-(5-phenyl-2-methylpent-2-oxy)-thiazolethione and $BrCCl_3$ in a NMR experiment (left) and proposed scheme for mechanistic discussion of 2-methyl-5-phenylpent-2-oxyl radical reactivity (right).

(b) Intramolecular addition

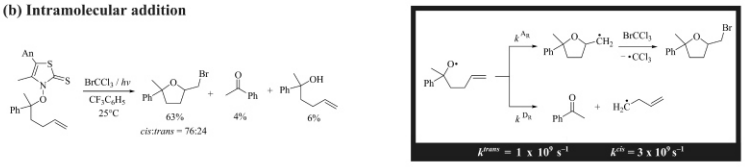

Scheme 2 Product distribution after photolysis of 3-(2-phenylhex-5-en-2-oxy)-thiazolethione with $BrCCl_3$ (left) and reaction scheme for kinetic analysis of 2-phenylhex-5-en-2-oxyl radical reactivity (right).

(c) Intermolecular addition

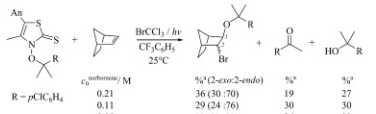

R = *p*ClC_6H_4	$c_0^{norbornene}$ / M	%[a] (2-*exo*:2-*endo*)	%[a]	%[a]
	0.21	36 (30 :70)	19	27
	0.11	29 (24 :76)	30	30
	0.05	12 (22 :78)	26	38

[a] determined via GC/MS-analysis

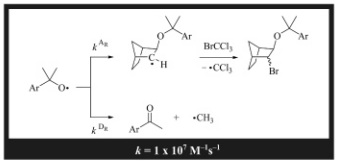

Scheme 3 Liberated products of 3-[2-(*p*-chlorophenyl)-prop-2-oxy]-thiazolethione with norbornene and BrCCl3 (left) and elementary reactions of intermolecular alkoxyl radical addition (right).

Conclusion

By means of using the isourea pathway, it was for the first time possible to obtain *tert*-alkoxyl radical precursors from thiohydroxamic acids. These compounds were successfully converted in radical substitutions as well as additions, to get 2,2,5-substituted tetrahydrofurans and 2-bromo-3-alkoxynorbornanes. Especially intermolecular addition becomes more and more important, as the knowledge about this reaction increases.

Rate constants, from the mechanistic part of the study, show that *tert*-alkyl substitution near oxygen does not reduce alkoxyl radical reactivity, at least in the investigatet cases.

References:

[1] Schur, C.; Becker, N.; Bergsträßer, U.; Gottwald, T.; Hartung, J. *Tetrahedron* **2011**, *67*, 2338–2347.
[2] Hartung, J.; Gottwald, T.; Špehar, K. *Synthesis* **2002**, 1469–1498.
[3] Baciooccchi, E.; Bietti, M.; Salamone, M.; Steenken, S. *J. Org. Chem.* **2002**, *67*, 2266–2270.
[4] Atkinson, R. *Atmos. Environ.* **2007**, *41*, 8468–8485.
[5] Halliwell, B.; Gutteridge, J.M.C. *Free Radikal in Biology and Medicine*, 3rd ed.; Oxford University: Oxford, 1999, Chapter 2, pp 36–104.
[6] Griffiths, P.G.; Rizzardo, E.; Solomon, D.H.J. *Macromol. Sci.* **1982**, *A17*, 45–50.

Acknowledgements:

We thank Dipl.-Chem. Steffen Danner for helpful discussions on computational chemistry.

TECHNISCHE UNIVERSITÄT KAISERSLAUTERN

Annulated and Bridged Tetrahydrofurans from Alkenoxyl Radical Cyclization

Christine Schur[a], Jens Hartung[a,*]

[a] Fachbereich Chemie, Organische Chemie, Technische Unversität Kaiserslautern, Erwin-Schrödinger-Straße, D-67663 Kaiserslautern, Germany

Abstract

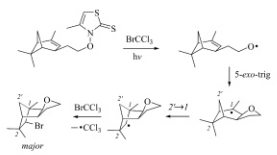

Cycloalkyl-annulated and bridged 4-penten-1-oxyl radicals cyclize stereoselectively in solutions of bromotrichloromethane to obtain tetrahydrofuran-derived bicyclic and tricyclic *β*-bromohydrin ethers in up to 95 % yield. Stereocontrol in synthesis of bicyclic tetrahydrofurans thereby arises from steric substituent effects, becoming more effective as the distance of the substituents to the C,C−double bond shortens. Endocyclic double bonds are intramolecularly attacked by the oxygen radical from the direction where the side chain is attached to the alicyclic subunit. Model calculations on a density functional level of theory show that the intrinsic barrier, reflecting strain effects in 5-*exo*-additions, is similar for 2,3-cis-cyclization of the 2-(cyclohexen-3-yl)ethyloxyl radical and the 4-penten-1-oxyl radical. The results of the calculation were exemplified in synthesis of a diastereomerically pure tricyclic brominated tetrahydrofuran from a verbenylethyloxyl radical.

Background

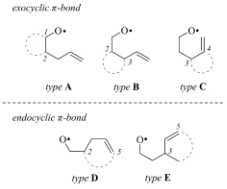

Cyclization reactions of 4-penten-1-oxyl radicals, generated from thiohydroxamate derived radical precursors, are well known in current literature.[1,2] Selectivities of products gained from these compounds follow systematic patterns depending on substituent effects as described below. In position 1 or 3 substituted 4-pentenoxyl radicals, with exception of 1-aryl-substituted compounds, preferentially cyclize 5-*exo*-trans selectiv, whereas substituents in positon 2 predominatly provide cis-substituted tetrahydrofurans. Regioselectivity is changed by substituents in position 4. In this case the 6-*endo* product ist enhanced, especially for phenyl groups. Alkyl- and aryl-groups in position 5 increase reactivity and selectivity of 5-*exo*-trig cyclizations, in doing so the effect of two substituents is higher than the effect of one. To explore new aspects of stereocontrol in intramolekular alkenoxyl-radical addition reactions of more complex structures than monocyclic tetrahydrofurans, we investigated in this study stereochemical guidelines for synthesis of bicyclic and tricyclic tetrahydrofuran derived compounds. The basic structures investigated are type **A**−**C** cycloalkyl-annulated 4-pentenoxyl radicals and type **D** and **E** cycloalkenylalkoxyl radicals.

Results and Conclusion

Chain reaction for intramolekular addition

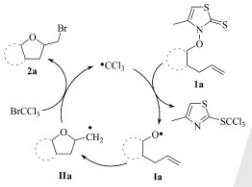

Conditions (cond.): **(i)** hν/ 25°C; **(ii)** AIBN/ 80°C

✓ stereoselectivity ***correlates*** with 4-penten-1-oxyl radical cyclization

X stereoselectivity ***differs*** from 4-penten-1-oxyl radical cyclization

induction (main product ratio):
(++) very high (85−99)
(+) high (75−84)
(-) low (< 75)

● major inductor for types **A**−**C**

— major inductor for types **D** and **E**

MTTOR =

type **A**

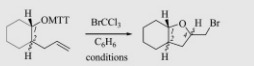

1a	cond.	2a / % (1,4-*cis*:1,4-*trans*)
1,2-*cis*-**1a**	i	*cis*-**2a**: 45 (89:11)
1,2-*trans*-**1a**	i	*trans*-**2a**: 49 (8:92)
1,2-*cis*-**1a**	ii	*cis*-**2a**: 61 (68:32)
1,2-*trans*-**1a**	ii	*trans*-**2a**: 70 (13:87)

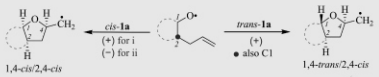

X ✓

type **B**

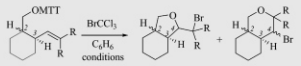

1e-d	R	cond.	2e-d / % (3,4-*cis*:3,4-*trans*)	3e-d/ % (3,4-*cis*:3,4-*trans*)
2,3-*cis*-**1d**	H	i−ii	*cis*-**2d**: 70−81(20:80)	**3d**: 3−5 (>99:1)
2,3-*trans*-**1d**	H	i−ii	*trans*-**2d**: 57−70 (9:91)	**3d**: 10−17 (50:50)
2,3-*cis*-**1e**	CH_3	i−ii	*cis*-**2e**: 80−95 (1:99)	**3e**: –
2,3-*trans*-**1e**	CH_3	i−ii	*trans*-**2e**: 81−94 (1:99)	**3e**: –

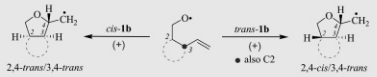

X ✓

type **C**

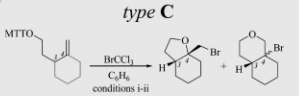

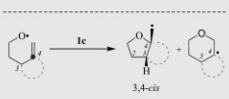

for stereoselectivity X

for regioselectivity ✓

type **D**

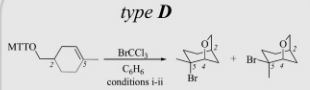

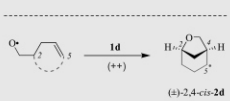

X

type **E**

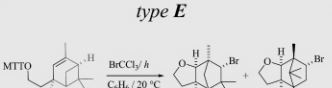

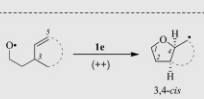

X

For simplification, atom count refers in all cases to alkoxyl radical convention and not to heterocycle convention for cyclic compounds.

References

[1] Hartung, J. *Eur. J. Org. Chem.* **2001**, 619-632.
[2] Hartung, J.; Gottwald, T.; Špehar, K. *Synthesis* **2002**, *11*, 1469-1498.
[3] Schur, C.; Gottwald, T.; Kneuer, R.; Hartung, J. manuscript in preparation.

GDCh-Wissenschaftsforum Chemie
Darmstadt, September 2013

Danksagung

Meinen ersten Dank möchte ich an Prof. Dr. *Jens Hartung* richten, der mich sehr herzlich in seinem Arbeitskreis aufgenommen und während der gesamten Promotion bei wissenschaftlichen Fragestellungen, der Anfertigung von Manuskripten, Postern, Buchbeiträgen und der vorliegenden Doktorarbeit stets unterstützt hat. Ohne sein Engagement hätten diese Werke nie die Form erlangt, in der sie heute vorliegen. *Vielen Dank*!

Dem gesamten Arbeitskreis danke ich für die gute Stimmung, Hilfsbereitschaft, für viele hilfreiche Diskussionen, chemischer und nicht-chemischer Natur, sowie für schöne Aktivitäten nach Laborende. Insbesondere danke ich dabei *Georg* für die Einführung der heute noch existierenden und über Promotionen hinaus geltenden Wurstmarkt-Tradition, sowie für meine ersten Erfahrungen mit dem „Betzen"…ich weiß, es heißt „Betze"!!! *Domi* danke ich für den Präfix „Mega" und *Barbara* für den wohl lustigsten Diskussionsauftakt einer Promotion. *Heiko* danke ich für all seine "todesgeilen" Gründe gemeinsam ein Fläschchen Sekt zu köpfen und *Mario* für seine ansteckend ruhige und sehr angenehme Art. Meinen Thizolthion-„Eltern" *Nina* und *Andreas* danke ich für all die hilfreichen Tipps und Tricks rund um Thiohydroxamsäuren und Andreas darüber hinaus für die sehr angenehme und freundliche Betreuung meines ersten FPs. *Olli* danke ich für seinen alljährlichen „Rückblick", seine wertvollen Hilfestellungen und natürlich das übelst geile Handballspiel.

Irina danke ich für viele schöne Stunden im Labor, die zahlreichen Lästereien und die unzähligen Taxi-Dienste. Nicht zu vergessen die massenhaften NMR-Messungen und die gemeinsamen Nächte in der "Vilsmaier-Residenz". *Diana* danke ich für ihre mehr als aufmunternde Art Leistungen Studierender in Klausuren zu bewerten und Patrick für die „Einladung" zur Mikrowellentagung nach Düsseldorf, sowie der Auffrischung meiner russisch Kenntnisse. Matthias danke ich für die Beantwortung jeder(!) Frage, sowie für jegliche Art von technischer Unterstützung an PC und Auto.

Auch *Maike* möchte ich für viele, viele Kutschierfahrten und NMR-Messungen danken, aber insbesondere für ihr strahlendes Lächeln und ihre liebenswürdige Art, die selbst bei übelster Laune aufmunternd wirkt. *Madlen* danke ich für die Überprüfung jeder „Milchmädchenrechnung" und die „Audienz im fernen Osten". *Alexander H*. danke ich für seine konstruktive Kritik und fachliche Bewertung chemischer Fragestellungen sowie für viele schnelle Korrekturen. Den tatkräftigen Nachfolgern der Radikal-Szene *Alexander K*.,

Benny, *Swen*, *Britta* und *Katharina* danke ich für die Unterstützung und Diskussionsbereitschaft bei neuen Thiazolthion-Herausforderungen. *Alexandra* danke ich für ihren absolut unkomplizierten und coolen Charakter! Melanie danke ich für die bereitwillige Übernahme all meiner Dienste und Mark für seine offene Art, die zum Vorschein kommt sobald man ihn angesprochen hat.

Luki und *Jürgen* danke ich für die Teilnahme an der morgendlichen Kaffepause und dem damit verbundenen frischen Wind in Kombination mit äußerst interessanten Frühstücksgewohnheiten (@ Luki). *Frank* danke ich für den stets charmanten Empfang in der Chemikalienausgabe und für das zügige Erfüllen zahlreicher technischer Wünsche. Den Mitgliedern der Analytik-Abteilung *Birgitt*, *Ruth*, *E. Biehl*, *Jana* und *Patrick* danke ich für unzählige CHN- und HRMS-Messungen, sowie für diverse Tipps und die Leihgabe analytischer Instrumente. *Uwe* danke ich für Hilfe jeglicher Art. Angefangen von Kristallstruktur- oder HRMS-Messungen und deren Auswertungen, für Literaturrecherchen, Synthesetipps aber auch für die Organisation von Wandertagen, die Beteiligung am Praktikum und und und…..Uwe du bist einfach unser „Mädchen für Alles“ und wir danken dir viel zu selten dafür. *Vielen, vielen lieben Dank* !!!!! Ein Dank für bürokratische und organisatorische Erledigungen geht an *Edith* und *Susanne.*

Meinen Praktikantinnen und Praktikanten *Alexander Ganß*, *Julia Becker*, *Patrick Unger*, *Jennifer Mohrbach* und *Benjamin Erb* danke ich für die Beiträge die sie zu meiner Forschung geleistet haben. Für spezifische Messungen danke ich *Dr. Harald Kelm* (NMR / X-Ray), *Christiane Müller* (NMR), *Dr. Reinhard Philipp* (ESR) und *Manuel Zimmer* (FTIR).

Der wichtigste Dank gilt meinen Eltern, Schwestern und Philip! Ich danke euch von ganzem Herzen für eure unendliche Unterstützung während der gesamten Promotion, für grenzenloses Zuhören, Trösten, Motivieren und Aufmuntern, aber insbesondere dafür, dass Ihr mir immer das Gefühl gegeben habt euch niemals enttäuschen zu können. ***Danke!!!***

Lebenslauf

Christine Schur

Ausbildung

02.2009–05.2015	**Promotion** TU Kaiserlautern/ Fachbereich Organische Chemie Betreuer: Prof. Dr.-Ing. Jens Hartung Titel der Dissertation: Reaktivität und Selektivität anellierter, verbrückter und tertiärer Sauerstoffradikale Promotion mit der Gesamtnote: „sehr gut“
10.2003–12.2008	**Diplom-Chemiestudium** TU Kaiserlautern/ Fachbereich Organische Chemie Diplomarbeit in der Gruppe von Prof. Dr.-Ing. Jens Hartung Titel der Diplomarbeit: Synthese *O*-Alkyl- und *O*-Acyl-substituierter Thiohydroxamsäuren zur Untersuchung neuer Selektivitäten in Sauerstoffradikalreaktionen Diplom mit der Gesamtnote: „sehr gut“
	Forschungspraktika
08.2007–09.2007	Synthese eines Cyclohexapeptidtrithiols Arbeitsgruppe von Prof. Dr. Stefan Kubik
01.2007–02.2007	Synthese und Evaluierung des Radikalvorläufers 3-Hydroxy-4-methyl-5-(4-acetimidophenyl)thiazol-2(3*H*)-thion Arbeitsgruppe von Prof. Dr.-Ing. Jens Hartung
	Wahlfachpraktikum
11.2006 (3 Wochen)	Synthese von 5-Carboxyindirubin und Umsetzung zu Indirubin-5-carbonsäurepentafluorphenylester Arbeitsgruppe von Prof. Dr. med., Dr. rer. nat. Dieter Schrenk

Schulbildung

02.1995–03.2003	Integrierte Gesamtschule Rockenhausen Abitur mit der Gesamtnote: „gut“ Leistungskurse: Gesundheit, Biologie, Englisch
09.1994–02.1995	Integrierte Gesamtschule Kaiserslautern Bertha von Suttner

Veröffentlichungen

Übersichtsartikel

- *Annulated and Bridged Tetrahydrofurans from Alkenoxyl Radical Cyclization.* C. Schur, H. Kelm., T. Gottwald, A. Ludwig, R. Kneuer, J. Hartung, *Org. Biomol. Chem.* **2014**, *12*, 8288–8307.
- *Discussion Addendum for: N-Hydroxy-4-(p-chlorphenyl)thiazole-2(3H)-thione*. C. Schur, I. Kempter, J. Hartung, *Org. Synth*. **2012**, *89*, 409–419.
- *Tertiary Alkoxyl Radicals from 3-Alkoxythiazole-2(3H)-thiones.* C. Schur, N. Becker, U. Bergsträßer, T. Gottwald, J. Hartung, *Tetrahedron* **2011**, *67*, 2338–2347.
- *Efficiency of alkoxyl radical product formation from 5-substituted 3-alkoxy-4-methylthiazole-2(3H)-thiones*. J. Hartung, C. Schur, I. Kempter, T. Gottwald, *Tetrahedron* **2010**, *66*, 1365–1374.
- *A Practical Method for O-Acylation of N-Hydroxythiazole-2(3H)-thiones.* C. Schur, A. Groß, J. Hartung, *Synthesis* **2010**, 3, 538–542.
- *Hindered rotation in N-acyloxy-4-methylthiazole-2(3H)-thiones*. J. Hartung, C. Schur, I. Kempter, S. Altermann, G. Stapf, U. Bergsträßer, T. Gottwald, M. Heubes, *Tetrahedron* **2009**, *65*, 7527–7532.

Buchbeitrag

- *Propylphosphonic Anhydride*. C. Millbanks, M. Bonnekessel, C. Schur, J. Hartung, *e-EROS Encyclopedia of Reagents for Organic Synthesis,* **2012**, Wiley VCH.

Patent

- *Tageslichtaktive Substanzen zur Vermittlung von Polymerisationsreaktionen.* H. Ritter, G. Maatz, J. Hartung, C. Schur, **2009**, PCT/EP2009/006617.

Posterpräsentationen

- Annulated and Bridged Tetrahydrofurans from Alkenoxyl Radical Cyclization
  - *GDCh-Wissenschaftsforum Chemie **2013**, Darmstadt*

- Tertiary Alkoxyl Radicals from 3-Alkoxythiazole-2(3*H*)thiones
  - *ISOFR-11, **2012**, Bern, Schweiz und*
  - *GDCh-Wissenschaftsforum Chemie **2011**, Bremen*